

AAPS Advances in the Pharmaceutical Sciences Series 1

Holly H.C. Kimko
Carl C. Peck
Editors

Clinical Trial Simulations

Applications and Trends

 **aapspress**

 **Springer**

AAPS Advances in the Pharmaceutical Sciences Series

Volume I: Clinical Trial Simulations: Applications and Trends
Holly H.C. Kimko and Carl C. Peck

Holly H. C. Kimko • Carl C. Peck
Editors

Clinical Trial Simulations

Applications and Trends



Editors

Holly H.C. Kimko
Johnson & Johnson Pharmaceutical
Research & Development, LLC
Advanced Modeling & Simulation
Raritan, NJ
USA
hkimko@its.jnj.com

Carl C. Peck
Center for Drug Development Science
Department of Bioengineering
and Therapeutic Sciences
Schools of Pharmacy and Medicine
University of California
San Francisco, CA
USA
carl@carlpeck.com

ISSN 2210-7371

e-ISSN 2210-738X

ISBN 978-1-4419-7414-3

e-ISBN 978-1-4419-7415-0

DOI 10.1007/978-1-4419-7415-0

Springer New York Dordrecht Heidelberg London

© American Association of Pharmaceutical Scientists 2011

All rights reserved. This work may not be translated or copied in whole or in part without the written permission of the publisher (Springer Science+Business Media, LLC, 233 Spring Street, New York, NY 10013, USA), except for brief excerpts in connection with reviews or scholarly analysis. Use in connection with any form of information storage and retrieval, electronic adaptation, computer software, or by similar or dissimilar methodology now known or hereafter developed is forbidden.

The use in this publication of trade names, trademarks, service marks, and similar terms, even if they are not identified as such, is not to be taken as an expression of opinion as to whether or not they are subject to proprietary rights.

Printed on acid-free paper

Springer is part of Springer Science+Business Media (www.springer.com)

Preface

During the seven years following the inaugural publication of *Simulation for Designing Clinical Trials: A Pharmacokinetic-Pharmacodynamic Modeling Perspective*, acceptance and application of clinical trials modeling and simulation (M&S) in drug development and regulation have greatly expanded. Biopharmaceutical companies have employed M&S in all phases of drug development to achieve greater efficiency and dosage optimization. The food and Drug Administration's (FDA) visionary 2004 Critical Path Initiative highlighted clinical trial simulations (CTS) in "model based drug development" to facilitate efficient development. In the meantime, FDA and the European Medicines Agency have encouraged use of CTS via regulatory guidances, and have employed M&S for labeling and approval decisions. On the backdrop of these developments, the title of this edition has been chosen to reflect how CTS is being employed in drug development and regulation, and trends for expanded applications in the future.

This edition includes updates, new uses, and issues concerning CTS, along with case studies on how clinical trial simulations are being applied in various therapeutic and application areas. Importantly, the book expands on the use of CTS for informing decisions during drug development and regulatory review. Each chapter author was selected on the basis of demonstrated expertise in state-of-the-art application of CTS.

Editors' opinions on advances and impactful trends of CTS in model-based drug development and regulation are introduced (Chap. 1). Regulatory agencies have been proactive in promoting use of CTS, and Chaps. 2 and 3 present the perspectives and experiences of FDA and European regulatory agencies by the authors working in these agencies.

Methods to facilitate decision making in drug development are discussed by pointing out the importance of assessing uncertainty of predicted trial performance and outcomes in planning of prospective trials (Chap. 4). For quantitative decision-making, constructing clinical utility curves (Chap. 5) can be useful. Adaptive trial design has gained attention as a method for more efficient and informative drug development, and its current status is reviewed in Chap. 6. Chapter 7 illustrates an M&S application case where personnel from biostatistics, clinical research and clinical PK-PD could collaborate to make better informed decisions on trial designs

throughout a clinical development. Chapter 8 illustrates how preclinical data can be integrated in a model-based drug development program to optimize early stage development, using CTS to simulate a first-in-human study.

Many successful cases employing CTS in guiding drug development decisions have been published in the literature and presented at conferences. Representative cases in selected therapeutic areas provide a general background on how to beneficially employ CTS, followed by the authors' experiences. Applications of CTS in eight therapeutic areas (Chaps. 9–16) are covered: diabetes, cardiovascular diseases, viral infections, antimicrobial chemotherapy, cancer, hematology, anxiety disorder, and epilepsy.

Chapter 17 discusses how CTS can be used in therapeutic biologics development. Designing ethical and informative pediatric studies requires integrating all available information, while gaining pediatric specific knowledge from a limited number of observations. The factors to consider in using CTS for pediatrics studies are described in Chap. 18.

The final section of the book includes chapters that describe evolving methodologies in CTS. The importance of incorporation of disease progression elements in CTS models is emphasized, especially when the evolution of disease during a trial is considered in evaluating treatment effects attributable to the drug (Chap. 19). The systems biology approach incorporates high resolution mechanistic models, involving fundamental dynamics of cells and biological signaling systems. Using such models, predictions of clinical responses may ultimately be made by simulations (Chap. 20). Recent advances in *in vitro*, *ex vivo*, and *in silico* methods to provide input variable information have significantly increased the applicability of the traditional whole-body physiology-based pharmacokinetic modeling approach, and its practical implementation is reviewed in the Chap. 21. Simulating drug responses in a virtual patient population and how to collect and utilize datasets for construction of covariate distribution models are presented (Chap. 22).

The target audience for this volume, *Clinical Trial Simulations* includes researchers and scientists who wish to consider use of simulations in the design, analysis, or regulatory review and guidance of clinical trials. This book does not embrace all aspects of trial design, nor is it intended as a complete recipe for using computers to design trials. Rather, it is an information source that enables the reader to gain understanding of essential background and knowledge for practical applications of simulation for clinical trial design and analysis. It is assumed that the reader has a working understanding of pharmacokinetics and pharmacodynamics, modeling, pharmacometric analyses, and the drug development and regulatory processes.

We express our sincere gratitude to all the authors who have contributed to this book. Many thanks go to the Springer publication team. Lastly, on behalf of all the contributors of this book, we appreciate the reader's interest in the application of clinical trial simulations in order to improve the way we develop useful drugs.

Raritan, NJ
San Francisco, CA

Holly H.C. Kimko
Carl C. Peck

Contents

1 Clinical Trial Simulation and Quantitative Pharmacology	1
Carl C. Peck and Holly H. C. Kimko	

Part I Application of M&S in Regulatory Decisions

2 Contribution of Modeling and Simulation Studies in the Regulatory Review: A European Regulatory Perspective	15
Siv Jönsson, Anja Henningsson, Monica Edholm, and Tomas Salmonson	
3 Contribution of Modeling and Simulation in the Regulatory Review and Decision-Making: U.S. FDA Perspective	37
Christine E. Garnett, Joo-Yeon Lee, and Jogarao V.S. Gobburu	

Part II Strategic Applications of M&S in Drug Development

4 Decision-Making in Drug Development: Application of a Model Based Framework for Assessing Trial Performance.....	61
Mike K. Smith, Jonathan L. French, Kenneth G. Kowalski Matthew M. Hutmacher, and Wayne Ewy	
5 Decision-Making in Drug Development: Application of a Clinical Utility IndexSM	85
Timothy J. Carrothers, F. Lee Hodge, Robert J. Korsan, William B. Poland, and Kevin H. Dykstra	
6 Adaptive Trial Designs.....	109
José C. Pinheiro, Frank Bretz, and Chyi-Hung Hsu	

7	Keys of Collaboration to Enhance Efficiency and Impact of Modeling and Simulation	131
	Anthe S. Zandvliet, Rik de Greef, Anton F.J. de Haan, Pieta C. IJzerman-Boon, Maya Z. Marintcheva-Petrova, Bernadette M.J.L. Mannaerts, and Thomas Kerbusch	
8	Leveraging Pharmacometrics in Early Phase Anti-inflammatory Drug Development	149
	Ene I. Ette and Christopher J. Godfrey	
Part III Application of M&S in Selected Therapeutic Areas		
9	The Application of Drug-Disease Models in the Development of Anti-Hyperglycemic Agents	175
	Jenny Y. Chien and Vikram P. Sinha	
10	Modeling and Simulation in the Development of Cardiovascular Agents	199
	Diane R. Mould, Bill Frame, and Timothy Taylor	
11	Viral Dynamic Modeling and Simulations in HIV and Hepatitis C	227
	Philippe Jacqmin and Eric Snoeck	
12	A Model-Based PK/PD Antimicrobial Chemotherapy Drug Development Platform to Simultaneously Combat Infectious Diseases and Drug Resistance	251
	N. L'ntshotsholé “Shasha” Jumble and George L. Drusano	
13	PKPD and Disease Modeling: Concepts and Applications to Oncology	281
	Oscar E. Della Pasqua	
14	Application of Pharmacokinetic–Pharmacodynamic Modeling and Simulation for Erythropoietic Stimulating Agents	311
	Juan José Pérez-Ruixo, Sameer Doshi, and Andrew Chow	
15	Model Based Development of an Agent for the Treatment of Generalized Anxiety Disorder	329
	Peter A. Lockwood and Jaap W. Mandema	
16	Balancing Efficacy and Safety in the Clinical Development of an Atypical Antipsychotic, Paliperidone Extended-Release	345
	Filip De Ridder and An Vermeulen	

Part IV Expanded Applications of M&S

- 17 Application of Modeling and Simulation in the Development of Protein Drugs** 365
Lorin K. Roskos, Song Ren, and Gabriel Robbie
- 18 Modeling and Simulation in Pediatric Research and Development** 401
Jeffrey S. Barrett

Part V Evolving Methodologies in M&S

- 19 Disease Progression Analysis: Towards Mechanism-Based Models**..... 437
Stephan Schmidt, Teun M. Post, Massoud A. Boroujerdi, Charlotte van Kesteren, Bart A. Ploeger
Oscar E. Della Pasqua, and Meindert Danhof
- 20 Using a Systems Biology Approach to Explore Hypotheses Underlying Clinical Diversity of the Renin Angiotensin System and the Response to Antihypertensive Therapies**..... 461
Arthur Lo, Jennifer Beh, Hector De Leon, Melissa K. Hallow, Ramprasad Ramakrishna, Manoj Rodrigo, Anamika Sarkar, Ramesh Sarangapani, and Anna Georgieva
- 21 Recent Developments in Physiologically Based Pharmacokinetic Modeling** 487
Vikash Sinha and Holly H.C. Kimko
- 22 Covariate Distribution Models in Simulation** 505
Peter L. Bonate
- Index**..... 527

Contributors

Jeffrey S. Barrett

Department of Pediatrics, The Children's Hospital of Philadelphia,
Division of Clinical Pharmacology and Therapeutics,
University of Pennsylvania Medical School, Philadelphia, PA, USA

Jennifer Beh

Entelos, Inc., Foster City, CA, USA

Peter L. Bonate

Clinical Pharmacology, Modeling, and Simulation, GlaxoSmithKline,
Research Triangle Park, NC, USA

Massoud A. Boroujerdi

Leiden/Amsterdam Center for Drug Research, Division of Pharmacology,
Leiden University, 2300 RA, Leiden, The Netherlands

Frank Bretz

Statistical Methodology/IIS, Novartis Pharma AG, Basel, Switzerland

Timothy J. Carrothers

Pharsight Consulting Services, Pharsight – A Certara Company,
100 Mathilda Place, Suite 160, Sunnyvale, CA 94086, USA

Jenny Y. Chien

Lilly Research Laboratories, Eli Lilly and Co., Lilly Corporate Center,
Indianapolis, IN 46285, USA

Andrew T. Chow

Pharmacokinetics and Drug Metabolism, Amgen Inc, Thousand Oaks, CA, USA

Meindert Danhof

Leiden-Amsterdam Center for Drug Research, Division of Pharmacology,
Leiden University, Leiden, The Netherlands

Oscar E. Della Pasqua

Division of Pharmacology, Leiden-Amsterdam Center for Drug Research,
Gorlaeus Laboratories, Einsteinweg 55, 2300 RA Leiden, The Netherlands
and

Clinical Pharmacology & Discovery Medicine, GlaxoSmithKline
R & D, 1-3 Ironbridge Road Stockley Park, UB11 1BT Uxbridge, United Kingdom

Sameer Doshi

Pharmacokinetics and Drug Metabolism, Amgen Inc, Thousand Oaks, CA, USA

George L. Drusano

Ordway Research Institute, Albany, NY, USA

Kevin H. Dykstra

Pharsight Consulting Services, Pharsight – A Certara Company,
100 Mathilda Place, Suite 160, Sunnyvale, CA 94086, USA

Monica Edholm

Medical Products Agency, Uppsala, Sweden

Ene I. Ette

Anoixis Corporation, Natick, MA, USA

Wayne Ewy

Pharmacometrics, Pfizer Inc. (Retired), Ann Arbor, MI, USA

Bill Frame

Wolverine Pharmacometrics Corporation, Projections Research Inc.,
Phoenixville, PA, USA

Jonathan L. French

Pharmacometrics, Pfizer Ltd., Groton, CT, USA

Christine E. Garnett

Center for Drug Evaluation and Research, Food and Drug Administration,
Silver Spring, MD, USA

Anna Georgieva

Novartis Pharmaceuticals, East Hanover, NJ, USA

Jogarao V.S. Gobburu

Center for Drug Evaluation and Research, Food and Drug Administration,
Silver Spring, MD, USA

Christopher J. Godfrey

Anoixis Corporation, Natick, MA, USA

Rik de Greef

Pharmacokinetics, Pharmacodynamics & Pharmacometrics (P3),
Global Drug Metabolism and Pharmacokinetics, Merck Research Labs,
Merck Sharp and Dohme, AP1110, 5340 BH, Oss, The Netherlands

Anton F.J. de Haan

Biostatistics and Research Decision Sciences (BARDS),
Early Development Statistics, Merck Research Labs,
Merck Sharp & Dohme, Oss, The Netherlands

Melissa K. Hallow

Novartis Pharmaceuticals, East Hanover, NJ, USA

Anja Henningsson

Medical Products Agency, Uppsala, Sweden

F. Lee Hodge

Pharsight Consulting Services, Pharsight – A Certara Company, 100 Mathilda
Place, Suite 160, Sunnyvale, CA 94086, USA

Chyi-Hung Hsu

Statistical Methodology / IIS, Novartis Pharmaceuticals Corporation,
East Hanover, NJ, USA

Matthew M. Hutmacher

Ann Arbor Pharmacometrics Group, Ann Arbor, MI, USA

Pieta C. IJzerman-Boon

Biostatistics and Research Decision Sciences (BARDS),
Late Development Statistics, Women's Health & Endocrine,
Merck Research Labs, Merck Sharp & Dohme, Oss, The Netherlands

Philippe Jacqmin

Exprimo NV, Mechelen, Belgium

Siv Jönsson

Medical Products Agency, Uppsala, Sweden

N. L'ntshotsholé “Shasha” Jumbe

Roche, Palo Alto, CA, USA

Thomas Kerbusch

Pharmacokinetics, Pharmacodynamics & Pharmacometrics (P3),
Global Drug Metabolism & Pharmacokinetics, Merck Research Labs,
Merck Sharp & Dohme, Oss, The Netherlands

Charlotte van Kesteren

Leiden/Amsterdam Center for Drug Research, Division of Pharmacology,
Leiden University, 2300 RA, Leiden, The Netherlands

Holly H.C. Kimko

Johnson & Johnson Pharmaceutical Research & Development, LLC,
Advanced Modeling & Simulation, Raritan, NJ, USA

Robert J. Korsan

Decisions, Decisions!, 1966 Tice Valley Blvd, Walnut Creek, CA 94595, USA

Kenneth G. Kowalski

Ann Arbor Pharmacometrics Group, Ann Arbor, MI, USA

Joo Yeon Lee

Center for Drug Evaluation and Research, Food and Drug Administration,
Silver Spring, MD, USA

Hector De Leon

Entelos, Inc., Foster City, CA, USA

Arthur Lo

Entelos, Inc., 110 Marsh Drive, Foster City, CA, USA

Peter A. Lockwood

Pfizer Global Research and Development, Clinical Pharmacology,
Primary Care Business Unit, New London, CT, USA

Jaap W. Mandema

Quantitative Solutions, Menlo Park, CA, USA

Bernadette M.J.L. Mannaerts

Global Clinical Research, Women's Health & Endocrine,
Merck Research Labs, Merck Sharp & Dohme, Oss, The Netherlands

Maya Z. Marintcheva-Petrova

Biostatistics and Research Decision Sciences (BARDS),
Late Development Statistics, Women's Health & Endocrine,
Merck Research Labs, Merck Sharp & Dohme, Oss, The Netherlands

Diane R. Mould

Projections Research Inc., 535 Springview Lane, Phoenixville, PA 19460, USA

Carl C. Peck

Center for Drug Development Science, Department of Bioengineering
and Therapeutic Sciences, Schools of Pharmacy and Medicine,
University of California at San Francisco, 5955 Balm Ridge Way,
San Luis Obispo, CA 93401, USA

Juan José Pérez-Ruixo

Pharmacokinetics and Drug Metabolism, Amgen Inc., Thousand Oaks, CA, USA

José C. Pinheiro

Adaptive Designs, Johnson & Johnson Pharmaceutical Research & Development,
Raritan, NJ, USA

Bart A. Ploeger

Leiden/Amsterdam Center for Drug Research, Division of Pharmacology,
Leiden University, 2300 RA, Leiden, The Netherlands

William B. Poland

Pharsight Consulting Services, Pharsight – A Certara Company,
100 Mathilda Place, Suite 160, Sunnyvale, CA 94086, USA

Teun M. Post

Pharmacokinetics, Pharmacodynamics & Pharmacometrics (P3),
Global Drug Metabolism & Pharmacokinetics, Merck Research Labs,
Merck Sharp & Dohme, Oss, The Netherlands

Ramprasad Ramakrishna

Novartis Pharmaceuticals, East Hanover, NJ, USA

Song Ren

Pharmacokinetics, Pharmacodynamics & Bioanalysis,
Translational Sciences, MedImmune, Gaithersburg, MD, USA

Filip De Ridder

Janssen Research & Development, a division of Janssen Pharmaceutica NV,
Advanced Modeling & Simulation, Beerse, Belgium

Gabriel Robbie

Pharmacokinetics, Pharmacodynamics & Bioanalysis,
Translational Sciences, MedImmune, Gaithersburg, MD, USA

Manoj Rodrigo

Entelos, Inc, Foster City, CA, USA

Lorin K. Roskos

Pharmacokinetics, Pharmacodynamics & Bioanalysis,
Translational Sciences, MedImmune, One MedImmune Way,
Gaithersburg, MD 20878, USA

Tomas Salmonson

Medical Products Agency, Uppsala, Sweden

Ramesh Sarangapani

Novartis Pharmaceuticals, East Hanover, NJ, USA

Anamika Sarkar

Novartis Pharmaceuticals, East Hanover, NJ, USA

Stephan Schmidt

Division of Pharmacology, Leiden-Amsterdam Center for Drug Research,
Leiden, The Netherlands

Vikash Sinha

Janssen Research & Development, a division of Janssen
Pharmaceutica NV, Beerse, Belgium

Vikram P. Sinha

Lilly Research Laboratories, Eli Lilly & Co, Indianapolis, IN, USA

Mike K. Smith

Pharmacometrics, Pfizer Ltd., Sandwich, Kent, CT, USA

Eric Snoeck

Exprimov NV, Mechelen, Belgium

Timothy Taylor

Taylor Pharmaceutical Consulting, Projections Research Inc.,
Phoenixville, PA, USA

An Vermeulen

Janssen Research & Development, a division of Janssen
Pharmaceutica NV, Advanced Modeling & Simulation, Beerse, Belgium

Anthe S. Zandvliet

Pharmacokinetics, Pharmacodynamics & Pharmacometrics (P3),
Global Drug Metabolism & Pharmacokinetics, Merck Research Labs,
Merck Sharp & Dohme, Oss, The Netherlands

Chapter 1

Clinical Trial Simulation and Quantitative Pharmacology

Carl C. Peck and Holly H. C. Kimko

Abstract Clinical trial simulation (CTS) concepts and techniques comprise a specialized niche in the field of quantitative pharmacology, enabled by advanced pharmacostatistical data analytic and simulation techniques. Since the first demonstrations of the value of CTS in drug development programs, these techniques have been embraced and advanced by both biopharmaceutical developers and regulatory agencies. In this introductory chapter, the editors discuss important trends that have been impacted by CTS, elaborated in more detail in subsequent chapters.

1.1 Introduction

Although pharmacology, the science of drugs and their effects in animals and humans, may in some ancient time have been purely qualitative in concept, it has long employed counts and measures. The German-Swiss alchemist Paracelsus (Philippus Theophrastus Aureolus Bombastus von Hohenheim, 1493–1541), however, is often credited with first emphasizing the concept of the dose-response relationship with his famous quote – “Sola dosis facit venenum!” – “All drugs are poisons; it is only a matter of dose!”

As applied to the subject matter of this book, a broad definition of *quantitative pharmacology* is *the science of describing, analyzing, interpreting, and forecasting pharmacology in a quantitative fashion, using mathematical-statistical models*. Quantitative pharmacology encompasses concepts of systems biology, genetics, anatomy, physiology, and pathophysiology to generate causal theories of drug action and experimental designs to test them. Resulting data observations can be analyzed using a broad array of pharmacostatistical procedures, by which drug

C.C. Peck (✉)

Center for Drug Development Science, Department of Bioengineering and Therapeutic Sciences, Schools of Pharmacy and Medicine, University of California at San Francisco, 5955 Balm Ridge Way, San Luis Obispo, CA 93401, USA
e-mail: ccpeck@mac.com

disposition and pharmacological effects in animals and humans can be interpreted and utilized according to pharmacometric concepts and techniques (*e.g.*, pharmacokinetics [PK], pharmacodynamics [PD], statistics, and modeling and simulation [M&S]). Quantitative pharmacology can be extensively applied in translational science, clinical pharmacology, drug development, and regulation.

Clinical trial simulation (CTS) comprises a specialized niche of quantitative pharmacology. Modified slightly from the book titled *Simulation for Designing Clinical Trials* (Kimko and Duffull 2003), a technical definition of CTS is the generation of biomarker or clinical responses in virtual subjects that take into account (a) the trial design and execution, (b) pathophysiological changes in subjects during the trial (disease progress model), and (c) pharmacology (drug intervention model), using mathematical, statistical and numerical methods and models. Figure 1.1 depicts information sources that can inform the models underlying generation of virtual trial subjects' responses in CTS. CTS can be applied in the design, analysis, and interpretation of human clinical drug trials in order to facilitate key decisions in drug development management and regulatory approval (Peck 1997; Holford *et al.* 2000).

In the aforementioned book by Kimko and Duffull (2003), basic concepts of CTS model structure, development and diagnostics, virtual trial execution, and examples of applications by drug developers and regulators were presented.

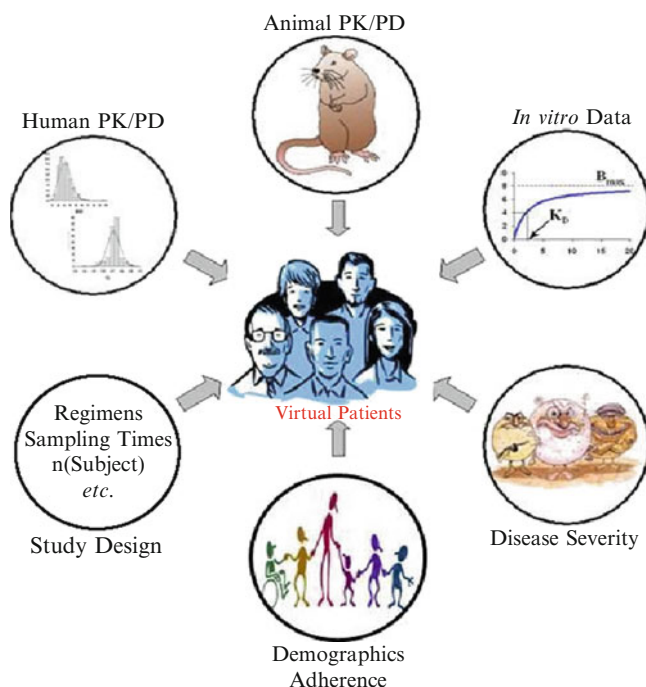


Fig. 1.1 Information sources for a model used in generation of responses in virtual trial subjects by Monte-Carlo simulations

In the 7 years since its publication, significant uptake of CTS by scientists in the pharmaceutical industry and regulatory agencies has taken place. Previously described and expanded applications of CTS have increasingly contributed to pivotal strategic and tactical development and regulatory decisions. Discussed in this introductory chapter is, according to our view, the most important trends that have been impacted by CTS; these advances are described in detail in the remaining chapters of our book. Also commented here are advances concerning a significant source of variability that should always be considered when constructing a realistic CTS platform – *i.e.*, variable adherence with the assigned treatment regimen.

1.2 Encouragement by EMA and FDA

In Chaps. 2 and 3, notable and novel contributions of CTS in regulatory review and decision-making in Europe and the United States are presented. The European Medicines Agency (EMA) and the Center for Drug Evaluation and Research (CDER) in the U.S. Food and Drug Administration (FDA) have each issued a number of guidances for drug developers that pertain to role of CTS in development and regulation. Although not solely focused on CTS, these guidances describe standards and expectations concerning regulatory submission that include quantitative pharmacology data on population PK and PD, exposure-response, drug metabolism, drug–drug interaction studies, effects of extrinsic factors (*e.g.*, concurrent exposure to drugs, herbal products, variations of diet, smoking, and alcohol use) and intrinsic factors affecting PK/PD (*e.g.*, age (emphasizing pediatrics and elderly influences), gender, race, weight, height, disease, genetic polymorphisms, pregnancy, and organ dysfunction).

Interestingly, in 2008 the EMA sponsored a Workshop on Modeling in Pediatric Medicines (European Medicines Agency 2008) that facilitated a public discussion of pharmacometric methods for efficient pediatric drug development, including CTS and physiologically-based pharmacokinetic modeling (PBPK, see below and Chap. 21) for pediatric dose finding. The EMA endorsement of CTS for support of the required Pediatric Investigation Plan (PIP, Chap. 2), as well as its receptivity to pharmacometric analyses included in its review of submissions for marketing authorization, confirms the value of this evolving technology in international regulatory circles.

The US FDA has taken a strong leadership role by aggressively applying pharmacometrics in a number of ways. As described in Chap. 3 and previously (Powell and Gobburu 2007), the Office of Clinical Pharmacology (OCP) in CDER has advanced a strategy for beneficial employment of CTS and related methods. To this end, in 2009 OCP established a Division of Pharmacometrics to facilitate implementation of its goals. The Pharmacometrics Webpage (FDA 2010a) presents its visionary “FDA Pharmacometrics 2020 Strategic Goals” plan, which is explained in more detail by Gobburu (2010). FDA’s Pharmacometrics 2020 goals include rationale for the training of 500 pharmacometricians, industry-wide employment of CTS in all clinical trials, and FDA development and publication

of data analysis standards for drug products to treat 15 disease conditions and 250 case studies employing advanced pharmacometric methods. In addition to the Pharmacometrics 2020 plan, the FDA pharmacometrics website includes staff publications, guidance on model and pharmacometric data formatting, and a disease model library.

Involved in essentially all aspects of medical product regulation, from preclinical guidance and generic drug policy development to IND and NDA product guidance, reviews, and approvals, FDA clinical pharmacologists and pharmacometricians are making valuable contributions to drug development and regulation. For drug industry pharmacometricians and drug developers, FDA-derived practical tools and regulatory procedures of specific relevance to CTS include the clinical pharmacology question-based review template (QBR), which describes the quantitative pharmacology data expected by the FDA in an NDA (FDA 2004). The QBR implicitly encourages modeling by inclusion of specific questions concerning exposure-response modeling of both safety and effectiveness trial outcomes, as well as rationalization of clinical pharmacology study designs – both queries that are well served by CTS procedures. The other key regulatory procedure is the opportunity to meet with FDA scientists and pharmacometricians after the completion of phase 1 trials and the first set of exposure-response trials in patients, and prior to commencement of phase 2B (*i.e.*, patient dose-ranging trial) and phase 3 clinical efficacy-safety trials – the so-called End-of-Phase 2A meeting (EOP2A) (FDA 2009). The stated purpose of this voluntary meeting is to “facilitate interaction between FDA and sponsors who seek guidance related to clinical trial design employing clinical trial simulation and quantitative modeling of prior knowledge.” Sponsors accepted by FDA for an EOP2A meeting are expected to “. . . perform these modeling analyses and include them in the meeting package so that FDA can review this information in planning subsequent work.”

Described in Chap. 3 are the key roles of pharmacometrics used by FDA in provision of guidances, (especially, QT and pediatric study design and analyses, and disease-specific models). The authors highlight the positive impacts of pharmacometrics on sponsors’ drug labels and regulatory decisions, which are encouraging for greater uptake by industry. FDA’s own publications cited in Chap. 3 confirm the large number of IND and NDA programs that have been positively impacted (since 2000, more than 52 pediatric and 198 adult NDAs). These impacts have included trial design and analysis enhancements, approved dosage regimens that were not directly evaluated in phase 3 trials, endorsement of model-based primary clinical trial endpoints and NDA approval decisions. A few of these impacts were pioneered in 1990s, such as the FDA-requested CTS of a proposed randomized concentration controlled trial of mycophenolate mofetil (Hale *et al.* 1998), and the 1991 (Toradol[®] (Dobin 2000; Gobburu 2010)) and 1996 (Remifentanyl (Egan *et al.* 2001; Gobburu 2010)) FDA approvals of dosing regimens of new drugs based on data-informed M&S without clinical trial confirmation. It important to recognize that the increase in FDA acceptance and utility of pharmacometrics, M&S and CTS in the last decade marks a major shift from reliance solely on empirical data to acceptance of mechanistic evidence of effectiveness and safety.

Although not mentioned in Chap. 3, physiologically based PK modeling (PBPK, Chap. 21) has also gained traction in regulatory agencies and industry (Rowland *et al.* 2011). The first application of PBPK by FDA concerned the review and approval of the highly teratogenic topical “wrinkle cream” active ingredient, tretinoin (Renova[®]) (Clewell *et al.* 1997; Rowland *et al.* 2004). In consideration of the potential risk of fetal exposure and birth defects, FDA requested PBPK simulation to assess risk of fetal exposure, from which FDA concluded that the risk is de minimus (FDA 2000). In 2002, a workshop was held on PBPK in drug development and regulation, which revealed little regulatory application of this technique (Rowland *et al.* 2004). Nonetheless, 8 years later, it is evident that FDA has been employing PBPK modeling in both new drug review and the development of generic drug policy and standards. CDER new drug review scientists are employing PBPK to (a) evaluate mechanisms and the potential for multiple comedications that may affect each other’s metabolism, leading to adverse effects and (b) to guide drug–drug interaction trial designs (Oo and Chen 2009; Zhao *et al.* 2009, 2010; Zhang *et al.* 2010; Duan *et al.* 2010). In addition, use of PBPK is encouraged in the FDA clinical lactation study guidance (FDA 2005).

Interestingly, the Office of Generics Drugs (OGD) review section of FDA is also employing PBPK M&S for challenging generic drug testing policy conundrums (Lionberger 2008, 2009). For example, PBPK models of drug absorption (Huang *et al.* 2009) are being employed to rationalize for regulatory policies on biowaivers for certain BCS Class drugs, oral drug products exhibiting multiple concentrations peaks, locally acting GI drugs, and drugs applied topically on skin and in the lung. Other PBPK applications by OGD include evaluation of (1) methods for characterizing complex drug delivery systems, substances, and products, (2) drug release profile criteria and improved *in vitro*–*in vivo* correlation methods, (3) prediction of alcohol induced dose-dumping, and (4) bioequivalence testing procedures of nonsmall molecule products, such as liposomes, nanotechnology, multiple-component mixtures.

1.3 Clinical Trial Protocol Deviations and Adherence

The book, *Simulation for Designing Clinical Trials* (Kimko and Duffull 2003), included chapters concerning trial protocol deviations (Kastrissios and Girard 2003) and pharmacodynamic consequences of unintended irregular dosing (“adherence”) (Urquhart 2003). Variable adherence has been identified previously as one of the largest sources of variability in drug response in drug therapy and clinical trials (Harter and Peck 1991; Urquhart 1991). References to these realities of clinical trial execution are sparse in the remainder of this book (Chap. 11), despite growing published literature documenting negative impacts of unappreciated variable adherence on PK (Vrijens and Goetghebeur 1999) and PK/PD analyses (Vrijens *et al.* 2005a, b, c), and clinical trial results and interpretation (Vrijens *et al.* 2005a, b, c), using objective adherence monitoring techniques such as electronic medication

event monitoring systems (Vrijens *et al.* 2005a, b, c). Therefore, key advances in adherence science (termed “pharmionics” (Urquhart and Vrijens 2005)) are discussed here in order to emphasize the need for intensified attention to the special problem of the confounding effects of variable adherence on analysis and interpretation of clinical trial results.

The taxonomy of variable adherence phenomena has been refined with the aim of comprising the most important characteristics of an intended dosage regimen; *i.e.*, prescription, initiation, and quality of execution, discontinuation(s) (including “drug holidays”), persistence, and termination (Urquhart and Vrijens 2005). Lack of consensus on precise definition and utility of these terms have motivated a concerted effort to resolve and finalize a rigorous taxonomy. As of the writing of this chapter, a project commissioned by the Seventh Framework Program of the European Commission (European Commission: Seventh Framework Programme 2010), “Ascertaining Barriers for Compliance: policies for safe, effective and cost effective use of medicines in Europe” is under way, which will be informed by a “Consensus Report on European Taxonomy and Terminology of Patient Compliance.”

In a 2008 conference on “Improving Drug Development Using Patient Adherence Data in Clinical Trials (UCSF-CDDS-DIA 2008),” the extent and negative consequences of objectively documented variable adherence in clinical trials were presented. For example, in a summary analysis of electronically monitored adherence in 21 short and long-term antihypertension trials, almost 50% of subjects had terminated their assigned long-term treatment regimen by the end of 1 year, mostly in the first 3 months. Eight to ten percent of patients omitted their dose on any given day, whereas 43% of subjects engaged in multiday dosing omissions (“holidays”) (Vrijens *et al.* 2008). Not confined to antihypertensive trials, variable adherence is a ubiquitous phenomena in clinical trials that can seriously dilute estimates of both drug effectiveness and safety when statistical analyses ignore this sometimes large source of variability according to the “intention to treat” (ITT) policy (Sheiner 1991, 1997). Variable adherence in clinical trials is not only a nuisance source of variability and contributor to bias and misinterpretation of trials results; it can lead to serious harm to both the patient and the community, as illustrated by the emergence of resistance to HIV therapy when patients do not adhere to prescribed antiretroviral therapy (Vrijens *et al.* 2005a, b, c). Indeed, safety of dosing recommendations in regulatory agency approved labels that are based on ITT may be misleading for the fully compliant patient (Lasagna and Hutt 1991; Peck 1999). An exception to the almost complete lack of label information on what a patient should do when one or more prescribed doses are missed is that of low dose oral contraceptive pills (LDOC). Because nearly perfect adherence according to labeled dosing instructions is associated with the maximum contraceptive protection, the FDA approved drug label provides both prescriber and patient with detailed directions on what to do when one or more LDOC’s are missed (FDA 2008).

Given the implications of variable compliance in clinical trials described above, it is surprising that drug developers and regulatory authorities have so rarely

incorporated scientific evaluations of temporal dosing patterns or employed objective adherence monitoring to improve efficiency and informativeness of clinical trials and accuracy of approved drug labels. To proactively provide knowledge of the potential influence of typical adherence deviations of a new drug, small dose-response trials employing a “minimum cassette of temporal patterns of drug input for robust modeling” were rationally proposed by Urquhart (Urquhart 2003), but there are few published reports using this approach. Nonetheless, in an illustrative recent example, investigators evaluated the effects on bone density and turnover of discontinuing and restarting treatment with denosumab, which is a recently approved human monoclonal antibody that inhibits osteoclast formation (Miller *et al.* 2008). In this 3-year osteoporosis treatment trial in 412 postmenopausal women with low bone mass, reversible effects on bone turnover biomarkers, correlated with bone mineral density changes, which provided sound data on the consequences of stopping and restarting therapy for inclusion in the FDA approved drug label (FDA 2010b). Finally, solution to the long-standing concerns of frequentist statisticians to ITT-violative analysis of adherence-informed clinical trial outcomes has recently been advanced by demonstration of the application of structural mean models to estimation of treatment efficacy in the presence of variable adherence (Comté *et al.* 2009).

1.4 CTS-Supported Strategic Decisions in Drug Development

Further evidence of the emerging value of CTS in drug development is presented in Chaps. 4–16. Although numerous simulation-based evaluations of sample size requirements of simple, ITT analyzed, hypothesis-testing clinical trial designs have been undertaken in the past, simulation evaluations of model-based trial designs and analysis procedures are of more recent origin (Pharsight Reference Library 2010). Early examples of model-based simulations of trial design compared dose-ranging designs (Sheiner *et al.* 1991), and evaluated statistical power and sample size requirements of randomized dose-controlled and concentration-controlled trials (Sanathanan and Peck 1991). The novel leap from simulation-based evaluation of a trial design’s statistical power to the likelihood of achieving the target treatment effect, along with assessment of the probability of making a correct decision are described in Chap. 4. Chapter 6 also presents application of CTS for evaluation of operating characteristics of the growingly popular class of adaptive clinical trial designs. In Chap. 5, the principles of the multiattribute utility modeling theory are explained, along with an example of application in a model-based drug development program, illustrating how a CTS-informed reformulation decision of a new drug candidate supported a “go decision” for continued development.

CTS-supported development decisions sometimes present internal organizational tensions and conflicts because of the challenge of a potentially disruptive, philosophical shift from reliance on empirical data to the more assumption-rich,

mechanistic/causal quality of model-based information. Bridging such a gap requires leadership, motivation and incentives to overcome inevitable barriers. In Chap. 7, opportunities are identified for resolution of common internecine challenges among drug developers with various backgrounds – especially, biostatistics, clinical research and clinical PK/PD – along with description of an example of successful accomplishment of productive collaboration. Philosophy and overall procedures in pharmacometrics-based drug development paradigms are described in Chap. 8, and application to efficient decision making in early development is illustrated.

The increasing complexity and richness of disease and drug intervention models applied in CTS, supporting model-based drug development programs, are illustrated in Chaps. 9 (diabetes), 10 (cardiovascular), 11 (viral infections), 12 (antimicrobial chemotherapy), 13 (cancer), 14 (hematological conditions), 15 (anxiety disorders), and 16 (psychoses). Biomarkers reflecting disordered biological effects of disease and drugs (both efficacy and toxicity), informed by concepts of mechanism-based disease progression and systems biology (Chaps. 19 and 20), are emerging to identify drug targets, PK/PD covariates (Chap. 21), and elements of disease progress and drug intervention model components in CTS models. Drug resistance elements are being incorporated into CTS models in viral, bacterial and oncology development projects (Chaps. 11–13). Current CTS models involving biological therapeutic interventions (Chap. 17) must integrate the elements that differ uniquely from conventional small molecule drugs, including target-mediated drug disposition and drug-mediated target disposition, immunogenic and complex inflammatory and biological systems control mechanisms. Chapter 10 describes two cases in which pharmacogenomic information was included in CTS.

Many chapters in this book briefly address applications of CTS in pediatric drug development programs, which are fully considered in Chap. 18. Stimulated by United States and European government derived economic incentives and regulatory requirements, and much enhanced by availability of pharmacometric and CTS procedures, pediatric dosage regimens and indications are being greatly expanded.

1.5 Conclusion

Within just a few years after the first employment of CTS in drug development programs, it has become a frequently used tool in quantitative pharmacology investigations in academia, regulatory and the biopharmaceutical industry. This has resulted from a combination of recognition of the urgent need for more cost-effective drug development procedures, and advances in quantitative pharmacology and pharmacometrics. Previously, clinical trials were designed using ad hoc empirical approaches, unaided by a systematic clinical pharmacology orientation or a quantitative PK/PD framework, leading to highly inefficient drug development

programs. The advent of modern CTS is transforming clinical drug development from empiricism to a mechanistic scientific discipline.

References

- Clewell HJ, Andersen ME, Wills RJ, Latriano L (1997) A physiologically based pharmacokinetic model for retinoic acid and its metabolites. *J Am Acad Dermatol* 36:S77–S85
- Comté L, Vansteelandt S, Tousset E, Baxter G, Vrijens B (2009) Linear and loglinear structural mean models to evaluate the benefits of an on-demand dosing regimen. *Clin Trials* 6:403–415
- Dobin RE (2000) Regulation of the medical use of psychedelics and marijuana. PhD, Harvard University, pp 168–169
- Duan J, Jackson A, Zhao P (2010) Bioavailability considerations in evaluating drug-drug interactions using the population pharmacokinetic approach. *J Clin Pharmacol*. Published online before print September 23, 2010 doi: 10.1177/0091270010377200
- Egan TD, Muir K, Hermann DJ, Stanski DR, Shafer SL (2001) The electroencephalogram (EEG) and clinical measures of opioid potency: defining the EEG-clinical potency relationship ('fingerprint') with application to remifentanyl. *Int J Pharm Med* 15(1–2):8–13
- European Commission: Seventh Framework Programme (2010) Ascertaining barriers for compliance: policies for safe, effective and cost-effective use of medicines in Europe. Available from <http://abcproject.eu/index.php?page=project>. Accessed June 2010
- European Medicines Agency (2008) EMEA workshop on modeling in paediatric medicines. Available from <http://www.ema.europa.eu/meetings/conferences/1415apr08.htm>. Accessed June 2010
- FDA (2000) Clinical pharmacology and biopharmaceutics review: NDA 21-108 0.02% Tretinoin emollient cream (RENOVA[®]). Available from http://www.accessdata.fda.gov/drugsatfda_docs/nda/2000/21-108_Renova_BioPharmr.pdf, p 19. Accessed June 2010
- FDA (2004) Clinical pharmacology and biopharmaceutics review template. Available from <http://www.fda.gov/downloads/AboutFDA/CentersOffices/CDER/ManualofPoliciesProcedures/UCM073007.pdf>. Accessed June 2010
- FDA (2005) Guidance for industry clinical lactation studies – study design, data analysis, and recommendations for labeling. Available from <http://www.fda.gov/downloads/RegulatoryInformation/Guidances/ucm127505.pdf>. Accessed June 2010
- FDA (2008) FDA approved label: ORTHO TRI-CYCLEN[®] Lo Tablets (norgestimate/ethinyl estradiol) Raritan. Ortho Womens Health and Urology, New Jersey
- FDA (2009) Guidance for industry end-of-phase 2A meetings. Available from <http://www.fda.gov/downloads/Drugs/GuidanceComplianceRegulatoryInformation/Guidances/ucm079690.pdf>. Accessed June 2010
- FDA (2010a) Pharmacometrics at FDA. Available from <http://www.fda.gov/AboutFDA/CentersOffices/CDER/ucm167032.htm>. Accessed June 2010
- FDA (2010b). FDA approved drug label: Prolia[®], prescribing information. Available from http://www.accessdata.fda.gov/drugsatfda_docs/label/2010/125320s00001b1.pdf. Accessed June 2010
- Gobburu JV (2010) Pharmacometrics (2020) *J Clin Pharmacol* 50(Supp 9):151S–157S, doi: 10.1177/0091270010376977
- Hale MD, Nicholls AJ, Bullingham RE, Hené R, Hoitsma A, Squifflet JP, Weimar W, Vanrenterghem Y, Van de Woude FJ, Verpooten GA (1998) The pharmacokinetic-pharmacodynamic relationship for mycophenolate mofetil in renal transplantation. *Clin Pharmacol Ther* 64:672–683
- Harter JG, Peck CC (1991) Chronobiology. Suggestions for integrating it into drug development. *Ann N Y Acad Sci* 618:563–571

- Holford NHG, Kimko H, Monteleone JP, Peck CC (2000) Simulation of Clinical Trials. *Annu Rev Pharmacol Toxicol* 40:209–234
- Huang W, Lee SL, Yu LX (2009) Mechanistic approaches to predicting oral drug absorption. *AAPS J* 11(2):217–224
- Kastrissios H, Girard P (2003) Protocol deviations and execution models. In: Kimko H, Duffell SB (eds) *Simulation for designing clinical trials – a pharmacokinetic-pharmacodynamic modeling perspective*. Marcel Dekker, New York
- Kimko H, Duffell SB (2003) *Simulation for designing clinical trials – a pharmacokinetic-pharmacodynamic modeling perspective*. Marcel Dekker, New York
- Lasagna L, Hutt BB (1991) Health care, research, and regulatory impact of noncompliance. In: Cramer JA, Spilker B (eds) *Patient compliance in medical practice and clinical trials*. Raven, New York, p 401
- Lionberger R (2008) FDA critical path initiatives: opportunities for generic drug development. *AAPS J* 10(1):103–109
- Lionberger R (2009) Regulatory applications of modelling and simulations at FDA. Presented at Conference of Physiologically Based Pharmacokinetic Modeling in Drug Development and Regulation, Arlington VA, April 6. http://www.thehamner.org/docs/pbpbk_09/Day1.Lionberger.pdf. Accessed June 2010
- Miller PD, Bolognese MA, Lewiecki EM, McClung MR, Ding B, Austin M, Liu Y, San Martin J, and for the AMG 162 Bone Loss Study Group (2008) Effect of denosumab on bone density and turnover in postmenopausal women with low bone mass after long-term continued, discontinued, and restarting of therapy: a randomized blinded phase 2 clinical trial. *Bone* 43(2):222–229
- Oo C, Chen YC (2009) The need for multiple doses of 400 mg Ketoconazole as a Precipitant Inhibitor of a CYP3A Substrate in an In Vivo Drug-Drug Interaction Study. *J Clin Pharmacol* 49(3):368–369
- Peck CC (1997) Drug development: improving the process. *Food Drug Law J* 52(2):163–167
- Peck CC (1999) Noncompliance and clinical trials: regulatory perspective. In: Metry JM, Meyer UA (eds) *Drug regimen compliance: issues in clinical trials and patient management*. Wiley, Chichester, pp 97–102
- Pharsight Reference Library (2010) Bibliography for computer-assisted trial design. Available from http://www.pharsight.com/library/soln_catd_bibliography.pdf. Accessed June 2010
- Powell JR, Gobburu JV (2007) Pharmacometrics at FDA: evolution and impact on decisions. *Clin Pharmacol Ther* 82(1):97–102
- Rowland M, Balant L, Peck C (2004) Physiologically based pharmacokinetics in drug development and regulatory science: a workshop report. *AAPS J* 6(1):6–10
- Rowland M, Peck C, Tucker G (2011) Physiologically-based pharmacokinetics in drug development and regulatory science. *Annu Rev of Pharmacol and Toxicol* 51:45–73
- Sanathanan L, Peck C (1991) The randomized concentration-controlled trial: an evaluation of its sample size efficiency. *Control Clin Trials* 12:780–794
- Sheiner LB (1991) The intellectual health of clinical drug evaluation. *Clin Pharmacol Ther* 50(1):4–9
- Sheiner LB (1997) Learning versus confirming in clinical drug development. *Clin Pharmacol Ther* 61(3):275–291
- Sheiner LB, Hashimoto Y, Beal SL (1991) A simulation study comparing designs for dose ranging. *Stat Med* 10(3):303–321
- UCSF-CDDSD-DIA (2008) Conference: improving drug development using patient adherence data in clinical trials. Available from http://bts.ucsf.edu/cdds/pdfs/dia_patient_adherence.pdf. Accessed June 2010
- Urquhart J (1991) Compliance and clinical trials. *Lancet* 337(8751):1224–1225
- Urquhart J (2003) History-informed perspectives on the modeling and simulation of therapeutic drug actions. In: Kimko H, Duffell SB (eds) *Simulation for designing clinical trials - a pharmacokinetic-pharmacodynamic modeling perspective*. Marcel Dekker, New York

- Urquhart J, Vrijens B (2005) New findings about patient adherence to prescribed drug dosing regimens: an introduction to pharmionics. *Eur J Hosp Pharm Sci* 11(5):103–106
- Vrijens B, Goetghebeur E (1999) The impact of compliance in pharmacokinetic studies. *Stat Methods Med Res* 8:247–262
- Vrijens B, Goetghebeur E, de Klerk E, Rode R, Mayer S, Urquhart J (2005a) Modelling the association between adherence and viral load in HIV-infected patients. *Stat Med* 24(17):2719–2731
- Vrijens B, Gross R, Urquhart J (2005b) The odds that clinically unrecognized poor or partial adherence confuses population pharmacokinetic/pharmacodynamic analyses. *Basic Clin Pharmacol* 96(3):225–227
- Vrijens B, Tousset E, Rode R, Bertz R, Mayer S, Urquhart J (2005c) Successful projection of the time course of drug concentration in plasma during a 1-year period from electronically compiled dosing-time data used as input to individually parameterized pharmacokinetic models. *J Clin Pharmacol* 45:461–467
- Vrijens B, Vincze G, Kristanto P, Urquhart J, Burnier M (2008) Adherence to prescribed antihypertensive drug treatments: longitudinal study of electronically compiled dosing histories. *Br Med J* 336:1114–1117
- Zhang L, Reynolds KS, Zhao P, Huang SM (2010) Drug interactions evaluation: an integrated part of risk assessment of therapeutics. *Toxicol Appl Pharmacol* 243(2):134–145
- Zhao P, Ragueneau-Majlessi I, Zhang L, Strong JM, Reynolds KS, Levy RH, Thummel KE, Huang SM (2009) Quantitative evaluation of pharmacokinetic inhibition of CYP3A substrates by ketoconazole: a simulation study. *J Clin Pharmacol* 49(3):351–359
- Zhao P, Zhang L, Lesko J, Huang S (2010) Utility of physiologically-based pharmacokinetic modeling and simulation in drug development and challenges for regulatory reviews. *Clin Pharmacol Ther* 87:S72

Part I
Application of M&S in
Regulatory Decisions

Chapter 2

Contribution of Modeling and Simulation Studies in the Regulatory Review: A European Regulatory Perspective¹

Siv Jönsson, Anja Henningson, Monica Edholm, and Tomas Salmonson

Abstract Modeling and simulation of pharmacokinetic and pharmacodynamic/response data has been increasingly advocated during drug development, to allow more efficient utilization of collected clinical data and to support informed decision making, *e.g.*, regarding future study designs and dosing strategies in subpopulations. This chapter reflects the view of the Swedish Medical Products Agency, one of the European regulatory bodies, on how M&S studies contribute in the regulatory review. The availability of European guidelines related to modeling and simulation is discussed and some insight is provided into the types of recommendations given, together with a few examples.

2.1 Introduction

Modeling and simulation (M&S) of pharmacokinetic (PK) and pharmacodynamic (PD)/response data has been increasingly advocated during drug development, to allow more efficient utilization of collected clinical data and to support informed decision making regarding future studies and study designs including dose selection (Sheiner 1997; Breimer and Danhof 1997; Minto and Schnider 1998; Derendorf and Meibohm 1999; Balant and Gex-Fabry 2000; Holford *et al.* 2000; Bonate 2000; Sheiner and Steimer 2000; Aarons *et al.* 2001; Meibohm and Derendorf 2002; Stanski *et al.* 2005). The application of M&S has been found beneficial in clinical drug development in terms of time and cost savings as well as being influential on the direction of the development program (Chaikin *et al.* 2000; Reigner *et al.* 1997; Gieschke and Steimer 2000; Olson *et al.* 2000; Blesch *et al.* 2003; Veyrat-Follet *et al.* 2000; Lockwood *et al.* 2006). From the regulatory side, several European

¹This chapter reflects the view of the Swedish Medical Products Agency and may not be the view of the European Medicines Agency or any other European regulatory agency.

S. Jönsson (✉)
Medical Products Agency, Uppsala, Sweden
e-mail: siv.jonsson@mpa.se

guidelines recommend M&S as a useful tool to support dose selection and establish dose recommendations in special populations and some specific proposals have been described (Edholm *et al.* 2008; Manolis and Pons 2009). Moreover, the US Food and Drug Administration (FDA) has emphasized this technology in its discussion of the critical path from laboratory concept to commercial product (Food and Drug Administration 2004, 2006; Lesko 2007) and proposed that computer-based predictive modeling is one opportunity to improve predictability and efficiency during drug development. Recent publications describe the implementation of model-based drug development in large pharmaceutical companies (e.g., Miller *et al.* 2005; Chien *et al.* 2005; Zhang *et al.* 2006; Lalonde *et al.* 2007; Grasela *et al.* 2007) and the FDA has been active in reporting the use of M&S in regulatory decision making (Gobburu and Marroum 2001; Gobburu and Sekar 2002; Bhattaram *et al.* 2005, 2007; Powell and Gobburu 2007; Wang *et al.* 2008; Jadhav *et al.* 2009). FDA's views on this technology are described as a separate chapter within this book (Chap. 3). As a consequence of the increased usage, applications submitted to regulatory agencies increasingly contain reports where M&S has been employed. Thus, regulatory agencies must be resourced with capabilities to assess and understand this type of documentation.

The European regulatory system is based on collaboration between the national regulatory agencies allocated in the 30 member states of the European Union (EU) and EEA-EFTA (European Economic Area–European Free Trade Association). In general, the marketing authorization of a new medicinal product requires the cooperation between member states through various regulated procedures according to Directive 2001/83/EC (EU Legislation – Eudralex 2001), *i.e.*, the Centralised, Decentralised and Mutual Recognition Procedures (EU Legislation – Eudralex, Volume 2A). These procedures have their foundation via Rapporteurs or Reference Member States who are appointed with the main responsibility to thoroughly review submitted applications. Their initial review is subjected to secondary assessment by the other member states, eventually leading to a common decision for each marketing authorization application. European regulatory guidance is developed in various areas through joint efforts by Working Parties composed of delegates from several member states. The websites of the European commission and the European Medicines Agency provide further reading on European pharmaceutical legislation (European Commission; European Medicines Agency).

The experience with use and application of M&S documentation in regulatory decision making is limited among European regulators. Accordingly, common European views are currently not settled but are under development. However, generally, the use of M&S during drug development is accepted and encouraged, for the reasons stated above. This chapter will focus on how M&S studies contribute to the regulatory review process from the perspective of one European regulatory agency, the Swedish Medical Product Agency. Thus, the views given here may not reflect the European community overall. It should also be noted that the focus of this chapter is not on clinical trial simulation specifics but rather on how models and their simulation results can be useful in making regulatory decisions.

2.2 Regulatory Guidance

2.2.1 Available Guidelines

At present, there is one European guideline that specifically deals with population pharmacokinetic modeling, namely the Guideline on reporting the results of population pharmacokinetic analyses (CHMP 2007). This guideline does not explicitly state views on when and how M&S should be used from a regulatory perspective but describes what is expected to be *reported* by the applicant when submitting a population pharmacokinetic analysis. These expectations should be considered applicable to other types of modeling, *e.g.*, exposure-response modeling. The contents of this guideline describe what the regulatory assessor needs to know to be able to make an assessment of the developed model. Thus, the aim of the model, the assumptions and methodology used during model development, and the qualification of the model are main topics discussed in the guideline. Using the guideline, drug developers can understand what is expected and how the model is assessed by the regulators. Apart from this document, there are several other European guidance texts that refer to M&S or exposure-response modeling as summarized in Table 2.1.

One guideline that advocates the use of modeling in more general terms is the internationally adopted guideline ICH Topic E 4: Note for guidance on dose response information to support drug registration (CPMP/ICH/378/95). The ICH guideline states that regulators, as well as developers, should be open to new approaches and statistical/pharmacometric techniques, *e.g.*, Bayesian and population methods and pharmacokinetic-pharmacodynamic modeling, which may increase information extraction and interpretability of the data.

Guidelines with encouraging wording concerning the use of modeling and/or the evaluation of exposure-response relationships include the Clinical investigation of pharmacokinetics of therapeutic proteins (CHMP/EWP/89249/04) and the development of medicinal products in pediatric patients (CHMP/EWP/147013/04 and EMEA/536810/08). The pediatric guidelines emphasize the importance of taking into account organ maturation and physiology, as well as body size, to predict systemic exposure in pediatric patients and suggest the use of physiologically-based pharmacokinetic models to predict characteristics in the pediatric population. Furthermore, it is also pointed out that pharmacokinetic data alone may be of limited value for the extrapolation of efficacy and safety from other age patient groups. In general, there is also a need for PD data to elucidate whether the exposure-response relationship is different in children compared with other sub-populations (*e.g.*, older children and adults).

The usefulness of simulation is specifically mentioned in the guidance documents on evaluation of pharmacokinetics in organ impairment (CHMP/EWP/225/02 and CPMP/EWP/2339/02) and in pediatric patients (CHMP/EWP/147013/04) as a valuable mean to establish adequate dosing recommendations.

Finally, a therapeutic area where the modeling approach has clearly won acceptance is anti-infectives (CPMP/EWP/2655/99, CHMP/EWP/4713/03, CHMP/

Table 2.1 Examples of European guidance documents touching on M&S and/or exposure-response^a

Name of guideline (date for adoption by CHMP)	Excerpts from guideline. (The heading of the sub-section in each document is given and text not included in a section is denoted by.....)
Clinical Pharmacology and Pharmacokinetics	
Note for guidance on the investigation of drug interactions. CPMP/EWP/560/95 (December 1997)	<p>5.2. Population studies</p> <p>It is often valuable to include a population approach in Phase II/III clinical trials to screen for pharmacokinetic drug interactions. Valuable additional information is then obtained from studies that are performed for other reasons</p>
Points to consider on pharmacokinetics and pharmacodynamics in the development of antibacterial medicinal products. CPMP/EWP/2655/99 (July 2000)	<p>I Introduction</p> <p>..... Based on the current status of scientific investigations in this field, the CPMP is of the opinion that there seems to be sufficient evidence to support a recommendation that the PK/PD relationship for an antibacterial medicinal product should be investigated during the drug development programme. Although, the CPMP currently takes the position that data on the PK/PD relationship cannot replace confirmatory clinical trials of efficacy, but rather complement them to arrive more quickly at better dose recommendations, there may be areas in which detailed study of the PK/PD relationship might potentially impact on the content of the clinical programme (<i>e.g.</i> with reference to certain types of infections, patients, and medicinal products, see below). At present there is a lack of published studies that have sought to prospectively validate the correlation between the PK/PD relationship and clinical and bacteriological outcomes. In principle, the CPMP encourages attempts to validate and confirm the PK/PD concept during the clinical development programme.</p> <p>III Aspects of characterising PK/PD relationships</p> <p>..... PK and PD data from preclinical, early Phase I and Phase II studies could be used to build models that can then be used to help design Phase III trials. Through simulation, the influence of certain aspects of the planned Phase III trial can be assessed, and, the design (for example, with respect to dose or dosing interval) subsequently modified if needed.</p>
Note for guidance on the evaluation of the pharmacokinetics of medicinal products in patients with impaired renal function. CHMP/EWP/225/02 (June 2004)	<p>IV.2 Presentation of data</p> <p>..... Mathematical models may be constructed to evaluate the relationship between renal function and pharmacokinetic parameters. The intended result is a model that can successfully predict the pharmacokinetics behaviour, given information about renal function.</p> <p>IV.3 Development of dosing recommendations</p> <p>..... Study results including the graphical description and the model for the relationships between renal function and relevant pharmacokinetic parameters should be used to construct specific dosing recommendations, Simulations can be used to identify doses and dosing intervals that achieve that goal for patients with different degrees of renal</p>

<p>Guideline on the evaluation of the pharmacokinetics of medicinal products in patients with impaired hepatic function. CPMP/EWP/2339/02 (February 2005)</p>	<p>function impairment Another approach is to estimate appropriate cut-offs and doses given the information on pharmacokinetic parameters and distribution of renal function in the population.</p> <p>3.6 Physiological based pharmacokinetic models The use of Physiological based pharmacokinetic models, may be used as a tool.</p> <p>4.2 Presentation of data Modelling of the relationship (linear or nonlinear) between measures of hepatic function and pharmacokinetic parameters should be considered if a relevant marker is found.</p> <p>4.3 Evaluation of Results and Development of Dosing Recommendations Study results including the graphical description and a potential model for the relationships between hepatic function and relevant pharmacokinetic parameters should be used to construct specific dosing recommendations. Simulations can be used as a tool to identify doses and dosing intervals that achieve the target criteria for patients with different degrees of hepatic impairment. Simulations of the steady state exposure at the resulting recommended dose(s) could also be provided. The simulations may include graphical description of (total and, when relevant, unbound) concentration over time, also showing the predicted variability in the population. Graphical description of relevant steady state pharmacokinetic parameters versus hepatic function including appropriate measures for variability could also be supplied.</p>
<p>Guideline on the role of pharmacokinetics in the development of medicinal products in the paediatric population. CHMP/EWP/147013/04 Corrigendum (June 2006)</p>	<p>4.2.6 Population pharmacokinetics Population pharmacokinetic analysis, using nonlinear mixed effects models, is an appropriate methodology for obtaining pharmacokinetic information in paediatric trials both from a practical and ethical point of view. Simulations or theoretical optimal design approaches, based on prior knowledge (see Sect 2.2), should be considered as tools for the selection of sampling times and number of subjects Adult data may be used as prior information and may be included in the analysis as long as the predictions in children are satisfactory.</p> <p>4.2.7 Interactions Such studies may be of conventional design but may also be model-based using sparse sampling.</p> <p>4.3.1 Parameter Estimation The parameters can be estimated using either noncompartmental analysis or a model-dependent approach, for example nonlinear mixed effects models.</p> <p>4.3.2 Presentation of results If population pharmacokinetic analysis has been undertaken, a prospectively defined analysis plan, a detailed description of the data, the methodology used, the model selection criteria and an overview of the main model development steps (run record) should be included. Proper graphical diagnostics (goodness of fit, parameter</p>

(continued)

Table 2.1 (continued)

Name of guideline (date for adoption by CHMP)	Excerpts from guideline. (The heading of the sub-section in each document is given and text not included in a section is denoted by....)
Guideline on the clinical investigation of the pharmacokinetics of therapeutic proteins. CHMP/EWP/89249/04 (January 2007)	<p>distributions, etc.) should be included wherein any stratification by age/maturation, relevant descriptors of size, etc, should be visible. Proper model validation should be undertaken.</p> <p>3.2.7. Data analysis</p> <p>..... Population pharmacokinetic analysis of Phase II/III using a sparse sample approach is recommended for characterising the pharmacokinetics and possible covariate relationships.</p> <p>3.3 PK/PD relationships</p> <p>It is recommended that the relationship between drug concentration and pharmacodynamic response (PK/PD) is evaluated. If feasible, markers for both efficacy and safety should be measured, preferably in the same study. Given that the pharmacodynamic response as well as the pharmacokinetics may be altered because of modifications of the molecule or the expression system for its production, binding to blood components, or formation of antidrug antibodies, evaluation of the exposure-response relationship is considered an important tool in the drug development. PK/PD models may allow extrapolation from volunteers to target population given that suitable assumptions have been made, e.g. regarding pathological factors. These models may provide guidance for dose selection and are helpful when interpreting changes in the pharmacokinetics in important subpopulations (Section 3.2.6) or when evaluating comparability (Section 2.2).</p>
Reflection paper on the use of pharmacogenetics in the pharmacokinetic evaluation of medicinal products EMEA/128517/06 (May 2007)	<p>5 STUDY DESIGN AND METHODOLOGY</p> <p>..... The investigation of the effect of PG on the PK of a drug substance may be performed using a population PK approach in genotyped subjects and patients, or in a conventional PK study.</p>
Clinical in various therapeutic areas Appendix to the Committee for Proprietary Medicinal Products (CPMP) Note for Guidance on the Clinical Investigation of Medicinal Products in the Treatment of Schizophrenia, on the Methodology of Clinical	<p>III. Pharmacokinetics</p> <p>..... Data on release rate over time, residues in the injection site and accumulation may be estimate by using adequate pharmacokinetic modelling with the use of pharmacokinetic data after oral administration and data after single dose with the depot formulation.</p>

Trials concerning the Development of Depot Preparations of Approved Medicinal Products in Schizophrenia. CPMP/EWP/49/01 (February 2003)
 Guideline on the clinical evaluation of medicinal products intended for treatment of Hepatitis B. CPMP/EWP/6172/03 (February 2006)

4.2.1 Pharmacodynamics

It is desirable that the PK/PD relationship should be further explored during both the early and confirmatory clinical studies in infected patients to verify the conclusions drawn from the preclinical observations and pharmacokinetic data in healthy volunteers. (As suggested in CHMP/EWP/2655/99, these investigations may constitute sub-studies within larger trials or may be the studies that are specifically designed to address PK/PD relationships.) It is recommended that the relationship between drug exposure and safety and efficacy is explored also in confirmatory studies e.g. by means of population pharmacokinetics/pharmacodynamics.

4.2.3 Exploratory studies

..... Data derived from these studies may also provide important bridging pharmacokinetics/pharmacodynamics (PK/PD) documentation. Monotherapy studies are needed to characterise the relationship between anti-HBV activity and dose/concentration. In the dose ranging studies, a treatment arm with established anti-HBV agents could be included to assist selection of an optimal dose. Appropriate modelling might also provide information on pharmacokinetic markers of importance for efficacy in relation to virus with different degrees of reduced susceptibility *in vitro*. Early and repeated determinations of viral load and drug concentrations are recommended and PK/PD modelling may be a useful tool for dose selection. Dose selection for the phase III confirmatory trials of efficacy should be based on the considerations outlined above and should be preceded by well-planned dose ranging comparative studies.

3.1 Efficacy criteria in exploratory studies

..... Population PK/PD modelling is encouraged.

3.2.2. Secondary efficacy endpoints

..... Population PK/PD modelling may provide additional insight as regards, e.g. the temporal dynamics of the underlying condition and the activity of the experimental compound.

4.1.2 Pharmacokinetics

..... The relationship between drug exposure and efficacy as well as safety should also be explored in confirmatory studies, e.g. by means of population pharmacokinetics. An understanding of these relations is a prerequisite for assessing the relevance of alterations in drug exposure, e.g. because of impaired hepatic function or drug-drug interactions.

Guideline on clinical investigation of medicinal products for the treatment of sepsis. CPMP/EWP/4713/03 (June 2006)

Guideline on the clinical development of medicinal products for the treatment of HIV infection. CPMP/EWP/

(continued)

Table 2.1 (continued)

Name of guideline (date for adoption by CHMP)	Excerpts from guideline. (The heading of the sub-section in each document is given and text not included in a section is denoted by)
633/02 Revision 2 (November 2008)	<p>4.1.3 Exploratory studies in HIV-infected individuals</p> <p>Monotherapy studies</p> <p>.... Early and repeated determinations of viral load and drug concentrations are recommended, and PK/PD modelling may be a useful tool for dose selection. Appropriate modelling might also provide information on pharmacokinetic markers of importance for efficacy, in relation to virus with different degrees of <i>in vitro</i> susceptibility.</p>
Guideline on the clinical evaluation of antifungal agents for the treatment and prophylaxis of invasive fungal disease. CPMP/EWP/1343/01 Rev. 1 (April 2010)	<p>4.1. Assessment of antifungal activity</p> <p>.... During the conduct of clinical studies of efficacy it is expected that: ... Clinical and mycological outcomes should be analysed in the light of <i>in-vitro</i> susceptibility and patient pharmacokinetic data to further assess the PK/PD relationship.</p> <p>4.2.3. Treatment regimens</p> <p>Combination therapy</p> <p>.... Consideration should also be given to the potential for significant drug-drug pharmacokinetic or pharmacodynamic interactions to occur, which may preclude co-administration or may indicate a need for dose adjustment of one or both agents. An extensive evaluation of pharmacokinetics in patients and population PK and PK/PD analyses may be indicated in these circumstances.</p>
Multidisciplinary Guideline on clinical trials in small populations. CHMP/EWP/83561/05 (July 2006)	<p>3. PHARMACOLOGICAL CONSIDERATIONS</p> <p>.... The credibility of study results may be enhanced if a dose-response relationship is seen or in cases where a chain of events can be identified (for example, drug exposure to target occupancy, to pharmacodynamic measures, to clinical outcome). Cases where no such clear chain of events exists are much less convincing and will increase the data requirements regarding robustness and persuasiveness of study results. In very rare disorders, it is important that every patient participating in a study contributes as much information as possible to make a benefit-risk assessment possible. Therefore, the well-planned use of the best available techniques to obtain and analyse information is crucial. This applies throughout the study process from pharmacokinetic and pharmacodynamic modelling to handling and analyses of biopsy material.</p>
Guideline on the investigation of medicinal products in the term and preterm neonate.	<p>7 DOSE-FINDING</p> <p>.... PK/PD modelling techniques, using age appropriate and validated biomarkers, need to be considered to find the optimal dose. For a new medicinal product, the optimal dose has to be clinically verified. Existing physiologically based pharmacokinetic models to predict pharmacokinetic characteristics in the neonatal population may be</p>

EMA/536810/08
(June 2009)

considered if appropriate. The modelling of the influence of maturation on PK and on the PK / PD relationship may be considered to predict the changes in dosing as a function of age. Applicability of these models would need to be justified and new models might need to be developed. Allometric scaling should be considered for drug clearance when it is predicted from sparse data in neonates or extrapolated from data in older infants.

8 PHARMACOKINETIC STUDIES AND PK/PD STUDIES

.... However, pharmacokinetics alone is of limited value for extrapolating efficacy and safety from other patient groups, and extrapolation of efficacy will in general need pharmacodynamic data and PK/PD monitoring. A population PK approach is preferable because of the importance of finding covariates related to dose-individualisation between individuals and over time in the maturing individual. The analysis can be made on rich and/or sparse data depending on the number of patients available and the possibility of developing highly sensitive analytical methods where very small sample volumes could be used. The initial model could be based on rich data of a limited number of individuals and/or on data available in older children, as well as on other prior information, followed preferably by a population PK approach. It should be noted that population PK and modelling of oral administration require extra cautious consideration in the neonatal population as there may be marked absorption differences in neonates as compared to other age groups as well as very prolonged absorption in a subgroup of individuals....

ICH guidelines

ICH Topic E 4. Note for guidance on dose response information to support drug registration.
CPMP/ICH/378/95
(May 1994)

3. STUDY DESIGNS FOR ASSESSING DOSE-RESPONSE

.... Placebo-controlled individual subject titration designs typical of many early drug development studies, for example, properly conducted and analyzed (quantitative analysis that models and estimates the population and individual dose-response relationships), can give guidance for more definitive parallel, fixed dose, dose-response studies or may be definitive on their own.

4.1. GUIDANCE AND ADVICE

.... 4.6 Regulatory agencies and drug developers should be open to new approaches and to the concept of reasoned and well documented exploratory data analysis of existing or future databases in search of dose-response data. Agencies should also be open to the use of various statistical and pharmacometric techniques such as Bayesian and population methods, modeling, and pharmacokinetic-pharmacodynamic approaches. However, these approaches should not subvert the requirement for dose-response data from prospective, randomized, multi-dose-level clinical trials. Posthoc explanatory data analysis in search of dose-response information from databases generated to meet other objectives will often generate new hypotheses, but will only occasionally provide definitive assessment of dose-response relationships. A variety of data analytical techniques, including increased use of retrospective population-type analyses, and novel designs (*e.g.*, sequential designs) may help define the dose-response relationship. For example, fixed dose designs can be reanalyzed as a continuum of dose levels if doses are refigured on a mg/kg basis,

(continued)

Table 2.1 (continued)

Name of guideline (date for adoption by CHMP)	Excerpts from guideline. (The heading of the sub-section in each document is given and text not included in a section is denoted by...)
ICH Topic E 7. Note for guidance on studies in support of special populations: geriatrics. CPMP/ICH/379/95 (September 1993)	<p>or adjusted for renal function, lean body mass, etc. Similarly, blood levels taken during a dose-response study may allow estimates of concentration-response relationships. Adjustment of drug exposure levels might be made on the basis of reliable information on drug taking compliance. In all of these cases, one should always be conscious of confounding, <i>i.e.</i>, the presence of a factor that alters both the refuged dose and response or that alters both blood level and response, compliance and response, etc.</p> <p>B: Pharmacokinetic Screening Approach</p> <p>.... Sponsors may opt, instead of conducting a separate PK evaluation of the elderly, to utilize a Pharmacokinetic Screen in conjunction with the main Phase 3 (and Phase 2, if the sponsor wishes) clinical trials program. This screening procedure involves obtaining, under steady-state conditions, a small number (one or two) of drug blood level determinations at "trough" (<i>i.e.</i>, just prior to the next dose) or other defined times from sufficient numbers of Phase 2/3 clinical trials patients, geriatric and younger, to detect age-associated differences in pharmacokinetic behaviour, if they are present.</p>
ICH Topic E 11. Note for guidance on clinical investigation of medicinal products in the paediatric population. CPMP/ICH/271/99 (July 2000)	<p>2.4.1 Pharmacokinetics</p> <p>.... Several approaches can be used to minimize the amount of blood drawn and/or the number of venipunctures: use of population pharmacokinetics and sparse sampling based on optimal sampling theory to minimize the number of samples obtained from each patient. Techniques include: • sparse sampling approaches where each patient contributes as few as 2 to 4 observations at predetermined times to an overall "population area-under-the-curve" • population pharmacokinetic analysis using the most useful sampling time points derived from modeling of adult data.</p>
ICH Topic E 14. The Clinical Evaluation of QT/QTc Interval Prolongation and Proarrhythmic Potential for Non-Antiarrhythmic Drugs. CHMP/ICH/2/04 (May 2005)	<p>3.2.3 Analysis of Relationship Between Drug Exposure and QT/QTc Interval Changes</p> <p>Establishing the relationship of drug concentrations to changes in QT/QTc interval may provide additional information to assist the planning and interpretation of studies assessing cardiac repolarization. This area is under active investigation.</p>

^a All guidelines mentioned in the table can be found at the website of the European Medicines Agency (European Medicines Agency, Scientific guidelines for human medicinal products. Clinical efficacy and safety guidelines; European Medicines Agency. Scientific guidelines for human medicinal products. Multidisciplinary guidelines)
 CPMP and CHMP = Committee for medicinal products for human use

EWP/6172/03, EMEA/CPMP/EWP/633/02, CPMP/EWP/1343/01). Here, the use of pharmacodynamic measurements is highly encouraged and exploration of exposure-response by means of modeling is recommended, both in dose-response and confirmatory studies to support dose selection.

Thus, it can be concluded from the available guidance documents that there is impetus and encouragement from the European regulatory agencies for an increased use of M&S methodologies, to better understand and interpret the collected data, to improve study designs and to move toward adequate dosing recommendations resulting in safe and efficacious treatment in all subpopulations.

2.2.2 Would a Specific European Guideline on M&S Be of Value?

As stated in the previous section, there is currently only one specific guideline concerning modeling, *i.e.*, the Guideline on reporting the results of population pharmacokinetic analyses. There are several reasons for the limited availability of more specific guidance in this area. One major reason is that the methodology used for M&S involves advanced and rapidly evolving techniques. Consequently, there is a risk that the guideline, when adopted, is already outdated. Accordingly, in order not to constrain science and innovation, any guidance will have to be very general, and may therefore not provide specialized assistance, but merely provide a confirmation of the regulatory agencies' acceptance of M&S in drug development.

So, can such a document still be of value? We think that the answer to this question is "Yes" and that it is time to reconsider the development of a new guidance. The production and adoption of such a guidance document would, in addition to extensive discussions, lead to training sessions for regulators, thereby increasing the awareness among regulators of the potential for using this type of information. Eventually, the guidance would describe the common European view and serve as a support for regulatory assessors as well as encouragement for drug developers.

2.3 Regulatory Decisions: When and Impact

In Europe, regulatory assessors may encounter M&S documentation at several time points during drug development. For example, a decision or view based on this type of documentation can be made early during drug development in the assessment of Pediatric Investigation Plans and Clinical Trial Applications or when giving Scientific Advice. Hence, regulators may influence the choices made and approaches taken during the drug development path. However, so far, the main focus of the regulatory assessment has been during the approval phase of the

marketing authorization application of new medicinal products. Here, M&S reports are a basis for efficient utilization and interpretation of the collected data and eventually the knowledge/information may be translated into dosing recommendations. Some insights into the type of recommendations given are outlined below.

2.3.1 Pediatric Investigation Plan

The Pediatric Investigation Plan is a newly required document based on the recently enacted European Pediatric Regulation 1901/2006 ([EU Legislation – Eudralex 2006](#)). According to this regulation, a Pediatric Investigation Plan must be generated for new drugs under development. This plan should describe in detail how and when the new medicinal product will be developed for use in the pediatric population. The Pediatric Investigation Plan is reviewed and adopted by the Pediatric Committee (PDCO), one of the Scientific Committees at the European Medicines Agency, and drug developers need to justify any deviations from the approved plan.

For new active substances, the Pediatric Investigation Plan should be submitted for regulatory review during early drug development, *i.e.*, at the initiation of Phase 2, but may be updated when more knowledge is gained. The proposed selection of dose or approach to establish the dose to be investigated in pediatric patients is commonly based on modeling principles and the regulatory assessor has the opportunity to provide a regulatory view on this issue at an early stage. Because limited data are available at this time, the Pediatric Investigation Plan should preferably include a general description of the future modeling strategy and any regulatory comments given should not pose a hindrance to the further development. Thus, the regulatory assessment is, and should be, broad and provides a general opinion concerning concepts and suitability of using M&S in pediatric drug development. Regulatory experience in this area is growing, and general recommendations on how to use prior information concerning the relation between ontogeny and pharmacokinetic characteristics are often provided. Furthermore, the drug developer is usually advised to carefully consider the similarity of pharmacodynamics in children compared with adults, *i.e.*, whether it is scientifically justified to aim for similar systemic exposure as in adults, and that exposure-response relationships in the pediatric population should be elucidated as much as possible. Because of the typical nature of pediatric data, *i.e.*, sparse sampling, the general advice is to employ a population modeling approach. Even deterministic simulations, in combination with known distributions of body size for given ages, are considered valuable tools to predict the average systemic exposure in children.

2.3.2 Clinical Trial Application

M&S documentation is regularly available as part of the background documentation in clinical trial applications. In early clinical trials, predictions of exposure

levels for the doses proposed to be studied can be made on the basis of modeling using previous preclinical or clinical data. This is helpful information in the regulatory assessment of safety for the planned study. At later clinical stages, e.g., dose-response studies, the choice of dose level may be justified by clinical trial simulations originated from exposure-response models. This type of M&S approach is highly encouraged, because such exploration offers an efficient use of already collected data resulting in well-founded decisions for the drug developer. This also facilitates the regulatory understanding of the dose selection from both efficacy and safety perspectives. By the use of simulations, the drug developer also has the opportunity to evaluate alternative study designs. Eventually this may lead to fewer failed studies.

2.3.3 *Scientific Advice*

The drug developers can at any stage of drug development request scientific advice from the regulatory agencies. The companies have the option to seek scientific advice: (1) at the national level through each national agency or (2) at the community level via the European Medicines Agency. The national advice is often provided in an informal discussion setting, in comparison to the more formal community advice, which is mainly provided in written format. Drug developers often choose a combination of the two types of scientific advice.

The ultimate goal of scientific advice is to ensure that appropriate investigations are performed, so that no major objections regarding the used methodology are likely to be raised during evaluation of the marketing authorization application. Thus, scientific advice is prospective in nature and focuses on development strategies rather than pre-evaluation of data to support a marketing authorization application. The responsibility of the agencies is to provide the advice by answering the prespecified questions posed by the company on the basis of the provided documentation and considering the current regulatory framework and scientific knowledge. Thus, the role of the regulators is *not* to substitute the industry's responsibility for the development of their products.

A scientific advice may be particularly useful when there appears to be no or insufficient applicable regulatory guidance available or where the company chooses to deviate from the available guidance in its development plan. For example, answers to many questions pertaining to what is and what is not regarded adequate in M&S activities cannot be found in a guideline at present, and the number of such questions is steadily increasing. Questions related to the suitability of using population modeling for identification of important covariates or for the estimation of drug interactions are often posed. Furthermore, M&S of exposure-response data is frequently used as a basis for justifying the choice of dose for use in Phase 3. Then, developers usually wish to obtain the regulators' view on the strategy used for dose selection. As for Pediatric Investigational Plans, the advice is usually a general recommendation concerning M&S concepts and suitability of these methods.

In some cases, the advice may be quite detailed and, although not legally binding for either party, the applicant is recommended to justify deviations from the advice in a future application.

2.3.4 Approval for Marketing Authorization

The main review of the M&S documentation takes place during the drug approval procedure. Nowadays, M&S analyses are increasingly performed as an integrated part of the drug development by many companies and accordingly, applications for new medicinal products typically contain at least one modeling report. The reports usually concern pharmacokinetic data but there is a trend of an increasing number of exposure-response analyses of both clinical endpoints and adverse effects in recent applications. Exposure-response analyses put systemic exposure into a clinical utility perspective and help answer the following key questions:

1. Within which range of exposure will the drug treatment result in sufficient efficacy and with tolerable side effects?
2. What deviations in exposure can be allowed but still result in a positive benefit/risk balance for the drug treatment?

Currently, the regulatory assessors in Europe do not redevelop models or build new models based on raw data but rather evaluate and interpret the analyses submitted in the application. Based on the assessment of the models and the “whole picture” of the drug under evaluation, an overall judgment of the relevance of the information gained by the modeling is made. If the M&S documentation is critical for drawing conclusions on dosing recommendations or the overall benefit/risk assessment, then this material is very thoroughly assessed and the applicant is frequently requested to provide supplementary information. On the other hand, if the model is considered of little value as basis for dosing recommendations or for labeling purposes, then the analyses (which may be of poor quality) are not given any weight in the overall assessment. The requests to the applicant may vary in detail as exemplified below:

- Clarification on how models were developed, *e.g.*, procedures for model building
- Supplementary analyses, *e.g.*, additional evaluation of alternative structural models
- Additional information on the model’s capability to describe and predict the observed data, *e.g.*, additional goodness-of-fit plots or predictive checks
- Model predictions of studied and nonstudied situations, *e.g.*,
 - Drug–drug interactions
 - Subpopulations
 - Effect of concomitant food intake
 - Worst-case scenarios

At present, the models are rarely used as a main basis for assessment of overall benefit–risk from a regulatory perspective but rather for the following:

- (a) As a general description of pharmacokinetic and exposure-response (pharmacokinetic–pharmacodynamic relationship) in the target population
- (b) As an aid in judging the clinical relevance of changes in pharmacokinetics and for evaluation of
 - Dose recommendations in special populations
 - Dose adjustments with concomitant medications

2.4 Examples of Contribution of M&S Documentation in the Regulatory Review

In the following sections, a few examples are given on how modeling documentation was accepted and used during the approval phase. The product-related information is publicly available in European Public Assessment Reports (EPAR) for these products (European Medicines Agency 2007, 2008, 2009). Other examples where M&S and/or PKPD information has been considered useful can be found in EPARs of Baraclude, Inovelon, Invega, Ivemend and in the assessment of compassionate use of IV zanamivir (European Medicines Agency).

2.4.1 *Keppra (levetiracetam)*

Keppra contains the antiepileptic agent levetiracetam. Levetiracetam has been shown to have uncomplicated pharmacokinetic features: rapid and almost complete absorption after oral administration, formulations studied demonstrated to be bio-equivalent, no relevant food interaction, eliminated mainly by renal excretion (2/3), and dose proportional pharmacokinetic properties.

In 2008, the marketing authorization holder (MAH) for Keppra applied to extend the indication to include children from 1 month to 4 years old in the indication of adjunctive treatment of partial onset seizures with or without secondary generalization. The main concern with this application from a regulatory perspective was the limited information in very young children. For the age group 1 month to 4 years, one pivotal efficacy study was performed and longer term open-label follow up data were also submitted. Overall, 226 children between 1 month and 4 years were exposed to Keppra, but the actual numbers in the youngest age groups were relatively small, with only 8 children aged <6 months (the youngest subject being 2.3 months old) and 15 children aged from 6 to 12 months. Short-term efficacy was convincingly shown in the pivotal study and the open long-term study indicated maintained effect over time. However, there was limited safety information gathered for patients <1 year old and a lack of long-term safety data in this new population.

For this application, a population pharmacokinetic model was developed using data from several clinical studies in 197 children aged from 0.19 to 17 years, weighing 5.5–93 kg of which 112 and 85 were male and female, respectively.

The data was described with a one-compartment model with first-order absorption and first-order elimination and the final model included body weight, concomitant antiepileptic drugs and age through a maturation factor on oral clearance, and age on apparent volume of distribution. This model was considered to describe the observed data sufficiently well and a visual predictive check stratified for body weight and age demonstrated adequate predictive properties of the model with respect to both central tendency and variability.

The dose recommendation suggested by the MAH aimed at obtaining similar systemic exposure in children younger than 4 years as that obtained in a 4-year-old patient when given a dose of 10 mg/kg.

Suggested dose recommendation by MAH, including dose titration levels		
Age range (months)	1–6	Above 6
Recommended starting dose (mg/kg b.i.d.)	7	10
Recommended dose titration level 2 (mg/kg b.i.d.)	14	20
Recommended dose titration level 3 (mg/kg b.i.d.)	21	30

Simulations of systemic exposure in children from 1 month to 4 years, in combination with actually observed data, were used as a support that this dosing regimen would result in the expected systemic exposure. The simulations covered worst-case scenarios, *i.e.*, a 1-month child with a very low body weight and a 6-month child with a high body weight. The calculated fraction of the dose required to achieve the same exposure as a 4-year-old was 0.58 for a 1-month-old child, which substantially exceeded the minimum threshold established by the applicant prior to simulations, *i.e.*, a change of 20%, necessitating a dose adjustment. The proposed cut-off for dose adjustment, *i.e.*, 6 months, was found reasonable because the fraction of the reference dose was equal to 0.8 at this age and considering that the maturation of glomerular filtration is essentially complete by the age of 6–12 months. The 30% reduction of the dose (*e.g.*, 7 vs. 10 mg) in children 1–6 months was a compromise resulting in systemic exposure similar to or slightly lower compared to a 4-year-old and was considered reasonable from a safety point of view. From an efficacy point of view this dose was deemed sufficient because the dosing involves an up-titration and the dose recommendation in children 1–6 months was also consistent with the dose used in this age group in the pivotal efficacy study.

In conclusion, although there was limited pharmacokinetic data in infants below 1 year of age the modeling of the pharmacokinetic data, in conjunction with a priori information on maturation of renal function and body weight distributions for children, contributed in making relevant predictions of systemic exposure of levetiracetam in the youngest children where actual data were missing. These efforts strengthened the view that the proposed dose titration schedule was adequate and served as a significant regulatory aid for the assessment of safety and efficacy in very young children. However, this pharmacokinetic M&S exercise assumed that the same exposure-response relation was valid for children from 1 month to 4 years of age as compared to older children and adults. This assumption was not proven

but because there was sufficient evidence of efficacy this was not further pursued. Both from an efficacy and safety point of view the limited number of patients <1 year old was of concern, in particular because of the heterogeneity of epileptic syndromes in this age group and the limited long-term safety data available. Therefore, the MAH committed to further assess the long-term efficacy and safety in this age range postapproval through an observational sentinel site study. The MAH also committed to submit specific safety reports every 6 months for children <4 years old. The limitation of data in children from 1 month to 4 years of age was also reflected in the product information.

2.4.2 *Celsentri (Maraviroc)*

Celsentri (Maraviroc) is a CCR5 antagonist used in combination with other antiretroviral agents in treatment of HIV-1. Maraviroc has relatively complex pharmacokinetic behavior with highly variable absorption, dose-dependent oral bioavailability and food effect, likely because of saturation of efflux at higher doses and a combination of more efficient efflux because of slower absorption (less saturation) and to some extent complex formation when administered with food. Moreover, being a substrate for CYP3A4 and P-gp, the interaction potential with other antiretroviral drugs is high. Although the contribution of renal elimination is low when maraviroc is administered as a single drug, the importance of this elimination pathway increases significantly when administered together with CYP3A4 enzyme inhibitors.

Sophisticated pharmacokinetic-pharmacodynamic models have been applied during the development of maraviroc (Rosario *et al.* 2005, 2006, 2008; Jacqmin *et al.* 2008). Both pharmacokinetic and pharmacokinetic/pharmacodynamic models were presented in the submitted application for marketing authorization. For example, the probability of failure, where failure was defined as a patient having HIV-1 RNA (>50 copies/ml), in the Phase 2b/3 studies has been related to average exposure.

Because of its relatively complex pharmacokinetic behavior and interactions with other antiretrovirals, it was not reasonable to clinically study all possible scenarios. Simulations of the systemic exposure of maraviroc have therefore been used in the assessment and these were evaluated in combination with the suggested exposure-response relationship to answer questions such as:

1. What happens with the exposure if maraviroc is administered with inhibitors of various potency in combination with food?
2. What is the effect of impaired renal function when maraviroc is administered in combination with potent inhibitors of CYP3A4/P-gp?

M&Ss together with observed data from Phase 2b/3, where maraviroc had been administered with or without food in combination with various antiretroviral agents, resulted in dose recommendations that were expected to yield sufficient exposure regardless of food intake. Because of some uncertainties in the model, a study in subjects with renal impairment was requested as a follow-up measure. Based on the result of this study and further simulations the dose recommendations have been amended.

2.4.3 *Bridion (sugammadex)*

Bridion contains sugammadex, which reverses neuromuscular block induced by the nondepolarizing neuromuscular blockers rocuronium and vecuronium by forming complexes with these drugs. The assessment of safety issues related to drug–drug interactions because of the mode of action was greatly enhanced by the use of population model predictions as follows: the mechanism of interactions may be due to the possibility of (1) sugammadex’s binding to other molecules, reducing their effect or (2) displacement of the neuromuscular blocking agent from sugammadex, resulting in reduced reversal of the neuromuscular blockade or reoccurrence of neuromuscular blockade. Because investigating all interactions *in vivo* is not feasible, the applicant developed a strategy to screen for the interaction potential. In this strategy the knowledge from two major data sources was combined:

1. Binding affinity to sugammadex for several drugs estimated as the association constant determined by isothermal titration calorimetry
2. Predictions of systemic exposure and pharmacodynamic effects using a population pharmacokinetic–pharmacodynamic interaction model, including pharmacokinetics of rocuronium and sugammadex, the complex binding interaction and pharmacodynamic effects of rocuronium (with and without sugammadex).

Although several assumptions were made in the model predictions, the approach was considered acceptable from a regulatory perspective. One important reason for this opinion was that the model, which was developed using data from healthy volunteers and patients, exhibited adequate predictive properties as demonstrated by external validation, independent of the data used to build the model. Furthermore, model predictions for worst case scenarios were performed, and drugs that were identified with a risk for interaction were included in the product information. Model predictions of pharmacodynamic outcome also supported clinical recommendations concerning duration of surveillance for re-occurrence of blockade because of concomitant administration of a drug potentially being able to displace rocuronium from sugammadex. In addition, model predictions of pharmacodynamic outcome, such as time to recovery from neuromuscular blockade, supported the use in patients with renal impairment, which at the time for approval of marketing authorization was based on limited clinical data.

2.5 Future Perspectives and Summary

Obtaining a complete description of the population intended for treatment within the clinical development program is usually not feasible. Hence, the collected clinical trial data do not represent the entire target population and there is a need for better approaches to extrapolate efficacy and safety data to various subpopulations. M&S of pharmacokinetic, pharmacodynamic and clinical endpoints offer such a tool and the contribution in regulatory decision making by this type of

documentation is predicted to increase. It is anticipated that the use of M&S will increase in pharmaceutical development. Accordingly, the regulatory agencies will need to increase their capability to assess and utilize this type of information. Moreover, discussion and cooperation among regulatory agencies is necessary to provide more unified guidance to drug developers. The demand for collaboration is not limited to a European level, but should also be placed in a global perspective.

Thus, an increased awareness of the utilities of M&S at the European agencies is essential. To move forward, it is crucial to spread knowledge within regulatory authorities about the use and possible gains of M&S. Moreover, there is a need for more regulatory pharmacometricians, *i.e.*, assessors of M&S documentation. These assessors should, in addition to technical skills (Holford and Karlsson 2007), have the knowledge to determine the importance of model deficiencies, to recognize when M&S may be useful and to judge the appropriateness of endpoints used. The latter points toward the multidisciplinary aspects of pharmacometrics (Barrett *et al.* 2008), which demand frequent communication between clinical and pharmacometric assessors.

From a short-term perspective, it is likely that the type of regulatory requests forwarded to applicants today will continue and that results from model-based analyses will constitute a larger part of the critical knowledge prior to marketing approval compared with the present situation. Moreover, physiology-based models and software are readily available tools for predicting (1) the effect of varying renal function or (2) drug interaction potential based on *in vitro* data, etc. It is envisaged that the usage will increase (Rowland *et al.* 2010). For example, it is of particular interest to forecast systemic exposure in the paediatric population. For simple cases, such as intravenous administration of drugs that are purely eliminated by glomerular filtration, limited pharmacokinetic data would be sufficient when combined with model predictions.

From a long-term perspective, it would be of great value to have a European regulatory forum or discussion group, *e.g.*, a pharmacometric network for assessors, where continuous dialogue on the use of M&S in drug applications can take place to form consensus among the member states. Organizing a formal network will permit better priority ranking of issues and the creation of an agenda. The network should preferably include regulatory statisticians and should have good communication with relevant Working Parties that develop guidelines in the clinical area.

In summary, drug development needs appropriate tools for more efficient interpretation of collected data and for extrapolation of knowledge to the entire target population. M&S is considered to be useful in this respect and European regulatory agencies will promote and encourage the increased use of these methodologies. The contribution in regulatory decision making by this type of documentation may gradually increase. To assist drug developers and provide more unified guidance, an interactive process among regulatory agencies is needed on a global level.

Acknowledgment Dr Monique Wakelkamp is gratefully acknowledged for providing linguistic review.

References

- Aarons L, Karlsson MO, Mentre F, Rombout F, Steimer JL, van Peer A (2001) Role of modelling and simulation in phase I drug development. *Eur J Pharm Sci* 13:115–122
- Balant LP, Gex-Fabry M (2000) Modelling during drug development. *Eur J Pharm Biopharm* 50:13–26
- Barrett JS, Fossler MJ, Cadieu KD, Gastonguay MR (2008) Pharmacometrics: a multidisciplinary field to facilitate critical thinking in drug development and translational research settings. *J Clin Pharmacol* 48:632–649
- Bhattaram VA, Booth BP, Ramchandani RP, Beasley BN, Wang Y, Tandon V, Duan JZ, Baweja RK, Marroum PJ, Uppoor RS, Rahman NA, Sahajwalla CG, Powell JR, Mehta MU, Gobburu JV (2005) Impact of pharmacometrics on drug approval and labeling decisions: a survey of 42 new drug applications. *AAPS J* 7:E503–E512
- Bhattaram VA, Bonapace C, Chilukuri DM, Duan JZ, Garnett C, Gobburu JV, Jang SH, Kenna L, Lesko LJ, Madabushi R, Men Y, Powell JR, Qiu W, Ramchandani RP, Tornøe CW, Wang Y, Zheng JJ (2007) Impact of pharmacometric reviews on new drug approval and labeling decisions—a survey of 31 new drug applications submitted between 2005 and 2006. *Clin Pharmacol Ther* 81:213–221
- Blesch KS, Gieschke R, Tsukamoto Y, Reigner BG, Burger HU, Steimer JL (2003) Clinical pharmacokinetic/pharmacodynamic and physiologically based pharmacokinetic modeling in new drug development: the capecitabine experience. *Invest New Drugs* 21:195–223
- Bonate PL (2000) Clinical trial simulation in drug development. *Pharm Res* 17:252–256
- Breimer DD, Danhof M (1997) Relevance of the application of pharmacokinetic-pharmacodynamic modelling concepts in drug development. The ‘wooden shoe’ paradigm. *Clin Pharmacokinet* 32:259–267
- Chaikin P, Rhodes GR, Bruno R, Rohatagi S, Natarajan C (2000) Pharmacokinetics/pharmacodynamics in drug development: an industrial perspective. *J Clin Pharmacol* 40:1428–1438
- Chien JY, Friedrich S, Heathman MA, de Alwis DP, Sinha V (2005) Pharmacokinetics/pharmacodynamics and the stages of drug development: role of modeling and simulation. *AAPS J* 7:E544–E559
- Committee for Medicinal Products for Human Use (CHMP) (2007) Guideline on reporting the results of population pharmacokinetic analyses. CHMP/EWP/185990/06. Available for http://www.ema.europa.eu/docs/en_GB/document_library/Scientific_guideline/2009/09/WC500003067.pdf. Accessed 10 October 2010
- Derendorf H, Meibohm B (1999) Modeling of pharmacokinetic/pharmacodynamic (PK/PD) relationships: concepts and perspectives. *Pharm Res* 16:176–185
- Edholm M, Gil Berglund E, Salmonson T (2008) Regulatory aspects of pharmacokinetic profiling in special populations: a European perspective. *Clin Pharmacokinet* 47:693–701
- EU Legislation – Eudralex, Directive 2001/83/EC of the European Parliament and of the Council of 6 November 2001 on the Community code relating to medicinal products for human use (Consolidated version: 30/12/2008). http://ec.europa.eu/health/files/eudralex/vol-1/dir_2001_83_cons/dir2001_83_cons_20081230_en.pdf. Accessed 10 October 2010
- EU Legislation – Eudralex, Regulation (EC) No 1902/2006 of the European Parliament and of the Council of 20 December 2006 amending Regulation 1901/2006 on medicinal products for paediatric use. http://ec.europa.eu/health/files/eudralex/vol-1/reg_2006_1901/reg_2006_1901_en.pdf. Accessed 10 October 2010
- EU Legislation – Eudralex, The rules governing medicinal products in the European Union Volume 2A: Notice to applicants and regulatory guidelines for medicinal products for human use. http://ec.europa.eu/health/documents/eudralex/vol-2/index_en.htm#h2-volume-2a—procedures-for-marketing-authorisation. Accessed 10 October 2010
- European Commission. <http://ec.europa.eu/health/documents/eudralex/>. Accessed 10 October 2010

- European Medicines Agency (2007) European public assessment report for Celsentri, procedure no. EMEA/H/C/811. http://www.ema.europa.eu/docs/en_GB/document_library/EPAR_-_Scientific_Discussion/human/000811/WC500022194.pdf. Accessed 10 October 2010
- European Medicines Agency (2008) European public assessment report for Bridion, procedure no. EMEA/H/C/000885. http://www.ema.europa.eu/docs/en_GB/document_library/EPAR_-_Public_assessment_report/human/000885/WC500052309.pdf. Accessed 10 October 2010
- European Medicines Agency (2009) European public assessment report for Keppra, procedure no. EMEA/H/C/000277/II/0097. http://www.ema.europa.eu/docs/en_GB/document_library/EPAR_-_Assessment_Report_-_Variation/human/000277/WC500041557.pdf. Accessed 10 October 2010
- European Medicines Agency. <http://www.ema.europa.eu>. Accessed 2 May 2010
- European Medicines Agency. Scientific guidelines for human medicinal products. Clinical efficacy and safety guidelines. http://www.ema.europa.eu/ema/index.jsp?curl=pages/regulation/general/general_content_000085.jsp&murl=menus/regulations/regulations.jsp&mid=WC0b01ac0580027549. Accessed 10 October 2010
- European Medicines Agency. Scientific guidelines for human medicinal products. Multidisciplinary guidelines. http://www.ema.europa.eu/ema/index.jsp?curl=pages/regulation/general/general_content_000086.jsp&murl=menus/regulations/regulations.jsp&mid=WC0b01ac058002754a. Accessed 10 October 2010
- Food and Drug Administration (2004) Innovation or stagnation: challenge and opportunity on the critical path to new medical products. <http://www.fda.gov/ScienceResearch/SpecialTopics/CriticalPathInitiative/CriticalPathOpportunitiesReports/ucm077262.htm>. Accessed 2 May 2010
- Food and Drug Administration (2006) Innovation or stagnation: Critical path opportunities report. <http://www.fda.gov/downloads/ScienceResearch/SpecialTopics/CriticalPathInitiative/CriticalPathOpportunitiesReports/UCM077254.pdf>. Accessed 2 May 2010
- Gieschke R, Steimer JL (2000) Pharmacometrics: modelling and simulation tools to improve decision making in clinical drug development. *Eur J Drug Metab Pharmacokinet* 25:49–58
- Gobburu JV, Marroum PJ (2001) Utilisation of pharmacokinetic-pharmacodynamic modelling and simulation in regulatory decision-making. *Clin Pharmacokinet* 40:883–892
- Gobburu JV, Sekar VJ (2002) Application of modeling and simulation to integrate clinical pharmacology knowledge across a new drug application. *Int J Clin Pharmacol Ther* 40:281–288
- Grasela TH, Dement CW, Kolterman OG, Fineman MS, Grasela DM, Honig P, Antal EJ, Bjornsson TD, Loh E (2007) Pharmacometrics and the transition to model-based development. *Clin Pharmacol Ther* 82:137–142
- Holford N, Karlsson MO (2007) Time for quantitative clinical pharmacology: a proposal for a pharmacometrics curriculum. *Clin Pharmacol Ther* 82:103–105
- Holford NH, Kimko HC, Monteleone JP, Peck CC (2000) Simulation of clinical trials. *Annu Rev Pharmacol Toxicol* 40:209–234
- Jacqmin P, McFadyen L, Wade JR (2008) A receptor theory-based semimechanistic PD model for the CCR5 noncompetitive antagonist maraviroc. *Br J Clin Pharmacol* 65(suppl 1):95–106
- Jadhav PR, Zhang J, Gobburu JV (2009) Leveraging prior quantitative knowledge in guiding pediatric drug development: a case study. *Pharm Stat* 8:216–224
- Lalonde RL, Kowalski KG, Hutmacher MM, Ewy W, Nichols DJ, Milligan PA, Corrigan BW, Lockwood PA, Marshall SA, Benincosa LJ, Tensfeldt TG, Parivar K, Amantea M, Glue P, Koide H, Miller R (2007) Model-based drug development. *Clin Pharmacol Ther* 82:21–32
- Lesko LJ (2007) Paving the critical path: how can clinical pharmacology help achieve the vision? *Clin Pharmacol Ther* 81:170–177
- Lockwood P, Ewy W, Hermann D, Holford N (2006) Application of clinical trial simulation to compare proof-of-concept study designs for drugs with a slow onset of effect; an example in Alzheimer's disease. *Pharm Res* 23:2050–2059
- Manolis E, Pons G (2009) Proposals for model-based paediatric medicinal development within the current European Union regulatory framework. *Brit J Clin Pharmacol* 68:493–501

- Meibohm B, Derendorf H (2002) Pharmacokinetic/pharmacodynamic studies in drug product development. *J Pharm Sci* 91:18–31
- Miller R, Ewy W, Corrigan BW, Ouellet D, Hermann D, Kowalski KG, Lockwood P, Koup JR, Donevan S, El-Kattan A, Li CS, Werth JL, Feltner DE, Lalonde RL (2005) How modeling and simulation have enhanced decision making in new drug development. *J Pharmacokinet Pharmacodyn* 32:185–197
- Minto C, Schnider T (1998) Expanding clinical applications of population pharmacodynamic modelling. *Br J Clin Pharmacol* 46:321–333
- Olson SC, Bockbrader H, Boyd RA, Cook J, Koup JR, Lalonde RL, Siedlik PH, Powell JR (2000) Impact of population pharmacokinetic-pharmacodynamic analyses on the drug development process: experience at Parke-Davis. *Clin Pharmacokinet* 38:449–459
- Powell JR, Gobburu JV (2007) Pharmacometrics at FDA: evolution and impact on decisions. *Clin Pharmacol Ther* 82:97–102
- Reigner BG, Williams PE, Patel IH, Steimer JL, Peck C, van Brummelen P (1997) An evaluation of the integration of pharmacokinetic and pharmacodynamic principles in clinical drug development. Experience within Hoffmann La Roche. *Clin Pharmacokinet* 33:142–152
- Rosario MC, Jacqmin P, Dorr P, van der Ryst E, Hitchcock C (2005) A pharmacokinetic-pharmacodynamic disease model to predict in vivo antiviral activity of maraviroc. *Clin Pharmacol Ther* 78:508–519
- Rosario MC, Poland B, Sullivan J, Westby M, van der Ryst E (2006) A pharmacokinetic-pharmacodynamic model to optimize the phase IIa development program of maraviroc. *J Acquir Immune Defic Syndr* 42:183–191
- Rosario MC, Jacqmin P, Dorr P, James I, Jenkins TM, Abel S, van der Ryst E (2008) Population pharmacokinetic/pharmacodynamic analysis of CCR5 receptor occupancy by maraviroc in healthy subjects and HIV-positive patients. *Br J Clin Pharmacol* 65(suppl 1):86–94
- Rowland M, Tucker G, Peck C (2011) Physiologically based pharmacokinetics in drug development and regulatory science. *Annu Rev Pharmacol Toxicol* 51 (expected, Epub ahead of print 18 January 2010)
- Sheiner LB (1997) Learning versus confirming in clinical drug development. *Clin Pharmacol Ther* 61:275–291
- Sheiner LB, Steimer JL (2000) Pharmacokinetic/pharmacodynamic modeling in drug development. *Annu Rev Pharmacol Toxicol* 40:67–95
- Stanski DR, Rowland M, Sheiner LB (2005) Getting the dose right: Report from the Tenth European Federation of Pharmaceutical Sciences (EUFEPS) conference on optimizing drug development. *J Pharmacokinet Pharmacodyn* 32:199–211
- Veyrat-Follet C, Bruno R, Olivares R, Rhodes GR, Chaikin P (2000) Clinical trial simulation of docetaxel in patients with cancer as a tool for dosage optimization. *Clin Pharmacol Ther* 68:677–687
- Wang Y, Bhattaram AV, Jadhav PR, Lesko LJ, Madabushi R, Powell JR, Qiu W, Sun H, Yim DS, Zheng JJ, Gobburu JV (2008) Leveraging prior quantitative knowledge to guide drug development decisions and regulatory science recommendations: impact of FDA pharmacometrics during 2004–2006. *J Clin Pharmacol* 48:146–156
- Zhang L, Sinha V, Fargue ST, Callies S, Ni L, Peck R, Allerheiligen SR (2006) Model-based drug development: the road to quantitative pharmacology. *J Pharmacokinet Pharmacodyn* 33:369–393

Chapter 3

Contribution of Modeling and Simulation in the Regulatory Review and Decision-Making: U.S. FDA Perspective

Christine E. Garnett, Joo Yeon Lee, and Jogarao V.S. Gobburu

Abstract The Division of Pharmacometrics at the U.S. FDA engages in regulatory reviews, research and policy development. During 2000–2008, over 50% of pharmacometric reviews of 198 NDA and BLA applications influenced approval and safety decisions. During this time, pharmacometric analyses were used in pediatric dose selection, and approval of doses not directly studied in effectiveness trials. Additionally, pharmacometrics has been used in FDA advice on protocol design to optimize dosing regimens based on benefit-risk for clinical testing, and to provide confirmatory evidence of effectiveness. Current research projects aim to solve drug development challenges and develop policies grounded in pharmacometric principles and methodologies.

3.1 History of Pharmacometrics at FDA

On the backdrop of population pharmacokinetic and pharmacodynamic concepts evolving in academia, pharmacometric work at the Food and Drug Administration (FDA) began in 1991 when Carl Peck, MD, as Director of the Center for Drug Evaluation and Research (CDER), appointed Thomas Ludden, PhD, to lead the Biopharmaceutics Division and organize the first pharmacometrics group. This team influenced the focus in drug development by changing emphasis from interpreting dose–response information to analyzing exposure–response data (Peck *et al.* 1992). The FDA issued a number of Guidances for Industry to clarify to sponsors how to implement the exposure–response paradigm. The 1999 Guidance for Industry on Population Pharmacokinetics discusses how to design and execute

The opinions and information in this review article are those of the authors, and do not represent the views and/or policies of the U.S. Food and Drug Administration.

C.E. Garnett (✉)
Center for Drug Evaluation and Research, Food and Drug Administration,
Silver Spring, MD, USA
e-mail: Christine.Garnett@fda.gov

collection of sparse pharmacokinetic (PK) data from late-phase clinical trials, as well as how to analyze population pharmacokinetic data using modeling applications (Food and Drug Administration 1999). The value of understanding the exposure–response relationship has been acknowledged in several regulatory documents, such as the ICH E4: Dose Response Information to Support Drug Registration (ICH 1994), and the Guidance on Clinical Evidence of Effectiveness (Food and Drug Administration 1998). However, it was not until 2003 that the FDA stressed the importance of exposure–response trials in regulatory decision-making by issuing the Guidance for Industry on Exposure–Response Relationships (Food and Drug Administration 2003). Moreover, in a landmark report describing challenges and opportunities on the critical path to new medical products (the Critical Path Initiative), the FDA recognized the importance of model-based drug development as a way to improve decision-making for effectiveness and safety (Food and Drug Administration 2004). In 2005, Lawrence Lesko, PhD, as Director of the Office of Clinical Pharmacology (OCP) appointed J. Robert Powell, PharmD, to lead a centralized Pharmacometrics Group that reviewed regulatory submissions across all therapeutic areas. In 2009, this group was elevated to its own formal Division of Pharmacometrics, led by Jogarao Gobburu, PhD.

3.2 Division of Pharmacometrics

3.2.1 Vision and Strategic Goals

FDA pharmacometricians serve three primary functions: regulatory review, research, and policy development. As reviewers, they support drug approval, labeling, and trial design decisions. Dose selection based on quantitative benefit-risk assessments is another major area of focus. This requires quantitative methods to determine dosing adjustments based on age, liver or renal function, changes in bioavailability, concomitant administration of other drugs, and so forth. Pharmacometricians advise sponsors on trial designs to maximize the possibility of successful outcomes with optimal dosing regimens. As researchers, FDA pharmacometricians create or confirm quantitative disease, drug, and trial models. Such models help determine the value of biomarkers across clinical trials for given diseases or drug classes to reflect changes in primary disease endpoints. An important byproduct of this research is the training of postdoctoral fellows and graduate students as future pharmacometricians. An important consequence of pharmacometric research is the development of regulatory policy on matters related to effectiveness, safety, and bioequivalence.

3.2.2 Pharmacometric Reviews

Pharmacometric reviews are quantitative analyses of exposure, response, and disease data. The four primary types of pharmacometric reviews are NDA/BLA

Table 3.1 Types of pharmacometric reviews

NDA or BLA Submissions	Optimize dosing regimen based on exposure–response analysis of effectiveness and safety endpoints Use exposure–response relationship as evidence of effectiveness
QT Studies	Characterize concentration–QT relationship for dose selection, risk assessment in specific populations with high exposure, and ECG monitoring in late-stage trials
Pediatric Studies	Design trial to obtain precise estimates of PK and PD parameters in different age groups Justify trial design using exposure–response data from adults and prior observations in pediatric population Exposure–response is standard analysis
EOP2a Meetings	Exposure–response modeling and clinical trial simulation are used for dose selection and design of late-stage trials

submissions, QT studies, and protocol designs for late-phase clinical trials, including pediatric trials, and End-of-Phase 2a (EOP2a) meetings (Table 3.1).

3.2.2.1 NDA and BLA Submissions

The twenty-first Century Review is a CDER initiative to integrate and organize the review process for new drugs by identifying key scientific and regulatory issues early in the review and ensuring that differing opinions from decision-makers are addressed (www.fda.gov/AboutFDA/CentersOffices/CDER/WhatWeDo/Initiatives/). Emphasis is placed on quantitative methods under this initiative. OCP is charged with evaluating the exposure–response analyses to support effectiveness and appropriateness of the dosing regimen, in addition to evaluating other key clinical pharmacology issues. The Division of Pharmacometrics is notified when OCP receives a submission for a new molecular entity or for a pediatric indication. The submission is evaluated for the need for a pharmacometric review based on availability of appropriate data and whether the pharmacometric analysis can potentially influence dose, approval, or labeling. Key review questions are identified at an interdisciplinary “Scoping Meeting” held during the first 2 months after the filing of the NDA/BLA. The pharmacometric and clinical pharmacology reviewers write a collaborative assessment of the NDA/BLA with final recommendations on the key questions presented to the OCP senior leadership team for scientific and regulatory consensus.

The impact of pharmacometric reviews of NDA/BLA submissions from 2000 to 2006 has been previously published with 13 regulatory case studies (Bhattaram *et al.* 2005, 2007). These, as well as additional examples from 2007 to 2008, are extensively discussed in Sect. 3.3.

3.2.2.2 QT Study Design and Analysis

In 2006, a centralized interdisciplinary review team within CDER was formed following the FDA’s implementation of ICH E14 guidelines (ICH 2005). The team includes pharmacometric, statistical, clinical, and pharmacologic reviewers

who collaboratively provide expert advice both to the FDA's review divisions and to the sponsors on the design, analysis, and interpretation of thorough QT (TQT) studies. Moreover, this QT team strives to develop the science of evaluating drug effects on cardiac repolarization by refining the methods recommended in ICH E14. Contributions have included (1) using concentration–QT modeling to evaluate the proarrhythmic potential of new drugs (Garnett *et al.* 2008; Wang and Garnett 2010); (2) assessing the proarrhythmic potential of drugs when TQT studies are not feasible (Rock *et al.* 2009); (3) evaluating TQT study design features on moxifloxacin response (Florian *et al.* 2010; Yan *et al.* 2010); and (4) developing a QT knowledge management system to increase efficiency of QT reviews and leveraging knowledge from previous experiences (Tornoe *et al.* 2010).

The criterion for assessing whether a drug prolongs QT interval as described in ICH E14 does not explicitly account for individual drug concentrations. Experience with reviewing QT studies indicates that understanding the relationship, if any, between individual drug concentration and QT change provides important additional information to support regulatory decision making (Garnett *et al.* 2008). Therefore, regulatory reviews of TQT studies routinely include evaluation of the concentration–QT relationship. Published examples illustrate how exposure–response modeling has been used to (1) project QT prolongation at doses not directly studied in the TQT study; (2) support lack of QT prolongation when the TQT study was positive based on primary statistical criteria; and (3) confirm assay sensitivity with reduced moxifloxacin exposure. There is a recently described multivariate concentration–QT model to assess the pharmacokinetic and potential pharmacodynamic interaction between an investigational drug and its metabolic inhibitor (Zhu *et al.* 2010).

3.2.2.3 Protocol Design

The FDA encourages sponsors to use quantitative approaches in planning clinical trials for dose selection, sample size justification, and endpoint evaluation. Improving early dose selection and trial design increases the likelihood of successful trials. Such quantitative approaches are used in the design of pediatric trials and EOP2a meetings.

Pediatric Trials

About 50% of pediatric trials for drugs used in adults fail to provide evidence of effectiveness (Benjamin *et al.* 2008). Clinical studies in children are challenging in drug development programs because of the complexities of disease and drug effects (Jadhav *et al.* 2010b). There is urgent need to improve the design of pediatric clinical trials to improve the usefulness of labeled drug dosing information to the benefit of the pediatric population. Current practices for deciding critical trial design elements, such as dose range and sample size, are inconsistent and unclear. Therefore, pharmacometric reviews of pediatric submissions focus on three elements.

- Number of trial subjects. There is need for sufficient numbers of patients enrolled in each age group to obtain meaningful PK and response data. A quality metric has been proposed to increase the value of data collected: the 95% confidence interval of the geometric mean estimate of the PK or PD parameter (*e.g.*, CL or EC50) is between 60 and 140% (Jadhav *et al.* 2010a). The sample size within each age group should be computed to meet this criterion. Accordingly, traditional statistical and clinical trial simulation procedures can be used to identify appropriate sample sizes.
- Informed clinical trial design. The design of these trials should be based on prior knowledge of the exposure–response in adult or pediatric patients. For example, sample size and dose range for a pediatric trial of a confidential antihypertensive were justified by clinical trial simulations. These simulations employed exposure–response and drop-out data for placebo, and a related antihypertensive agent for which this information was already available, in order to evaluate various design features and statistical analysis of the primary endpoint for the confidential drug (Jadhav *et al.* 2009).
- Exposure–response orientation. Data from pediatric trials are routinely analyzed using exposure–response approaches due to the extreme variation in body size, maturation of eliminating organs, and sensitivity of target tissues.

End-of-Phase 2a Meetings

The EOP2a meeting provides a powerful opportunity to sponsors to engage with FDA on the design of key late-phase clinical trials. The Division of Pharmacometrics has been active in this new regulatory initiative (Wang *et al.* 2008). Under a pilot program starting in 2004, the FDA conducted 11 EOP2a meetings focusing on using exposure–response modeling and clinical trial simulation for dose selection and trial design decisions. The FDA often performed the modeling analyses for the pilot program, but it is now expected that sponsors will perform these analyses and include them in the meeting information package. In addition, the FDA may use in-house modeling to address particular problems or independently assess the sponsor’s model.

3.2.2.4 Knowledge Management

Although the application of modeling and simulation continues to significantly impact regulatory decisions, the efficiency of such quantitative analyses during the review process needs improvement. The time-limiting steps in these analyses are the tedious but necessary tasks of formatting clinical trial data, creating disease databases, programming modeling code, and generating analysis reports. To increase efficiency, the Division of Pharmacometrics has developed a knowledge management system to streamline pharmacometric analysis. The goals of knowledge management are to archive input data, models, and output data in a

manner that allows pharmacometricians to readily access data and rapidly execute standard analyses as new data become available. This strategy intends to alleviate the bottleneck of accessing and formatting prior trial data, allowing more time to explore innovative trial designs and analyses.

Data from late-phase clinical trials for diseases with active drug development programs are being used to create the databases. Templates and tools for data formatting, analyses, and reporting of routine functions are also under development. Automatic tools for population analysis and TQT studies are routinely used for regulatory reviews. Results from the standardized processes may then lead to learning more about disease progression and drug responses. The division has thus far initiated disease databases for Parkinson's disease, nonsmall cell lung cancer, pulmonary arterial hypertension, drug-induced QT prolongation, and hepatitis C infection.

3.2.3 *Research and Policy Development*

The Division of Pharmacometrics has an active research program. The primary goals of these projects are to contribute to the solution of drug development challenges and develop policies rooted in pharmacometric methodologies. The group has been working on projects related to the application of concentration–QT modeling to regulatory decision making (see [Sect. 3.2.2.2](#)), building quantitative disease–drug–trial models as a drug development aid to the industry (Gobburu and Lesko 2009), and establishing bioequivalence criteria for novel dosage forms.

The building of disease–drug–trial models is a goal consistent with the FDA's Critical Path Initiative. Pharmacometric reviews of regulatory submissions are the primary source of identifying drug development challenges. Lessons learned from previous trials in a disease area can guide future development and regulatory decisions. Parkinson's disease and nonsmall lung cancer (NSCLC) disease models are examples of this effort.

- *Parkinson's disease*: Pharmaceutical companies are attempting to develop drugs to slow the progression of Parkinson's disease, referred to as disease modification. There is currently no FDA-approved drug that has a claim for Parkinson's disease modification. The Division of Pharmacometrics has developed disease–drug–trial models to separate competing trial endpoints and discern between symptomatic relief versus an actual disease-modifying effect using a delayed-start study design (Bhattaram *et al.* 2009). The main goal of this clinical trial simulation was to explore appropriate analysis methods and endpoints to demonstrate disease modification.
- *NSCLC*: Over the last decade, lung cancer has exhibited the highest cancer-related death rate, exceeding that from colon, breast, and prostate cancers combined. Despite the significant unmet medical need for more effective new cancer treatments, oncology drugs have one of the lowest rates of successful drug development (Kola and Landis 2004). The purpose of the NSCLC model

was to leverage prior quantitative knowledge to facilitate future drug development of other NSCLC regimens. A tumor size (biomarker) – survival (clinical outcome) model across NSCLC trials was developed (Wang *et al.* 2009). The model may facilitate clinical screening of novel compounds and provides a tool to perform clinical trial simulations to improve the design of future trials.

Other disease–drug–trial model projects underway include human immunodeficiency virus, hepatitis C, Alzheimer’s disease, pulmonary arterial hypertension, and cardiovascular safety. These projects provide training grounds for pharmacometricians.

3.3 Impact of Pharmacometric Analyses on Regulatory Decisions from 2000 to 2008

3.3.1 Summary of Regulatory Impact

From January 2000 to December 2008, the FDA performed pharmacometric reviews for 198 NDA/BLA submissions. The majority of these reviews were of population pharmacokinetic analyses (57%), followed by exposure–response analyses (50%), and of pediatric submissions (26%). Therapeutic areas were primarily neurology (16%), cardiovascular–renal (15%), and oncology (13%). Pharmacometric reviews in other therapeutic areas were each less than 10%, but the numbers have been increasing after the centralization of pharmacometrics in 2005.

Each pharmacometrician was asked to complete a standardized questionnaire to determine the impact of the pharmacometric analysis in regulatory decisions. Other disciplines were not queried for this questionnaire because in previous surveys there was a good correlation in responses between pharmacometric, clinical pharmacology, and clinical reviewers (Bhattaram *et al.* 2005, 2007). An analysis was considered to have influenced approval if the results supported effectiveness and safety, or were used to derive the dosing regimen. For labeling, a pharmacometric analysis was considered influential if the results supported the clinical pharmacology, dosing and administration, or safety sections (*e.g.*, Warnings and Precautions, or Contraindications).

Of the 198 reviews, pharmacometrics influenced approval decisions in 64% and contributed to labeling in 67%. Figure 3.1 shows that the proportion of pharmacometric-based reviews affecting regulatory decisions increased during 2000–2008. The percentage affecting approval decisions increased from 40% during 2000–2004 to 75% during 2007–2008. A similar trend was observed for labeling decisions, with 56% of analyses during 2000–2004 influencing labeling, compared to 79% during 2007–2008.

Figure 3.2 illustrates the types of approval (a) and labeling (b) decisions influenced by pharmacometric analyses. One hundred twenty-six pharmacometric reviews influenced drug approval decisions, the analyses in which provided insight into the product’s effectiveness or dosing regimen in over 50%. Impact on safety

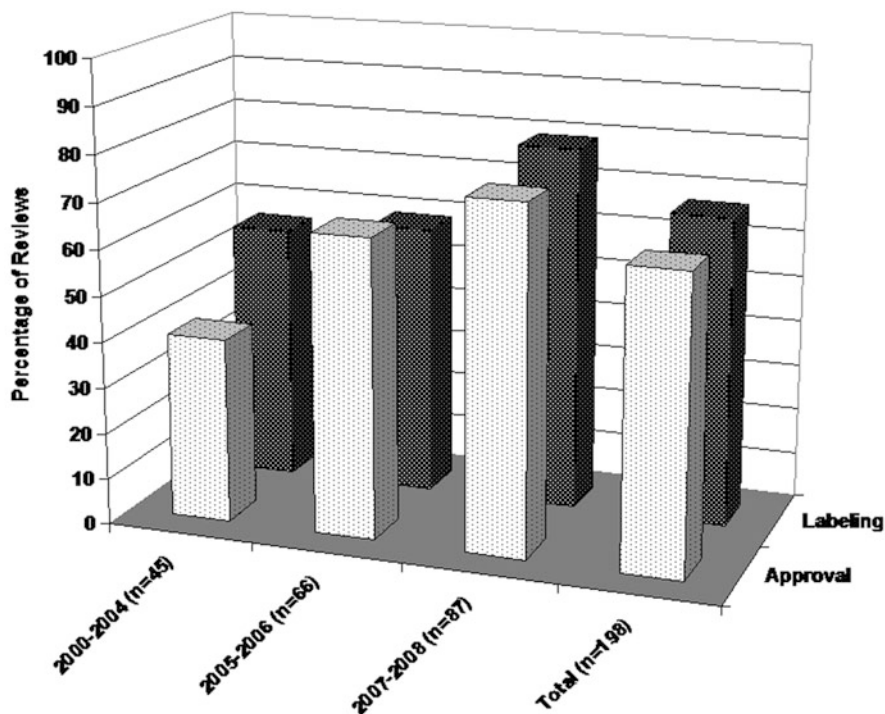


Fig. 3.1 Percentage of pharmacometric reviews influencing approval or labeling decisions during 2000–2008 as reported by the pharmacometric reviewer

assessment was exerted in 43% of the analyses. Of the 133 reviews in which pharmacometrics affected labeling decisions, 41% of analyses contributed to statements in the Dosage and Administration section, 11% in the safety sections, and 80% in the Clinical Pharmacology section. The role of pharmacometric analyses has increased over time within all decision types, especially in approving dosing regimens. The impact of these analyses on labeling decisions has also noticeably increased across all sections of the drug label.

3.3.2 Scope of Pharmacometric Reviews

3.3.2.1 Published Case Examples

Table 3.2 summarizes key review questions and the impact of pharmacometric analyses on specific regulatory decisions in 13 published cases (Bhattaram *et al.* 2005, 2007). Overall, the examples illustrate that exposure–response analyses usually influence the following approval or labeling decisions:

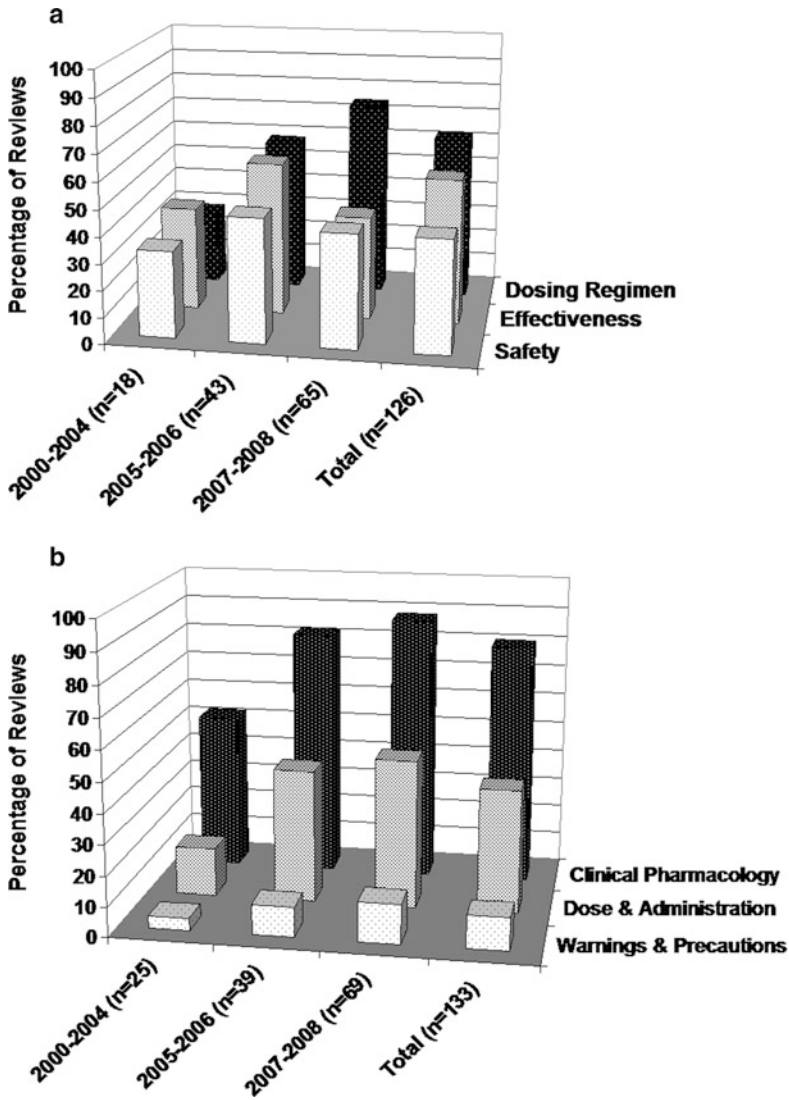


Fig. 3.2 Type of approval decisions (a) and labeling sections (b) influenced by pharmacometric reviews during 2000–2008. Percentage of reviews is computed from the subset of pharmacometric reviews influencing approval ($n = 126$) and labeling ($n = 133$) decisions. Each review could contribute to more than one decision category

- Optimizing dosing regimen for labeling (cases 2, 3, 4, 5, 10, 11)
- Selecting doses for further clinical testing (cases 1, 6, 9, 12)
- Improving trial design (case 13)
- Providing evidence of effectiveness (cases 7, 8)

Table 3.2 Previously published cases showing regulatory impact of pharmacometric analyses

FDA case example	Regulatory question	Effect of pharmacometric analysis on regulatory decision
<i>Case 1</i> Natrecor [®] (Nesiritide) for decompensated heart failure	What is the optimal dosing regimen of nesiritide to optimize benefit–risk profile?	Alternative dosing regimens were explored using the exposure–response relationship for blood pressure effects. A new dosing regimen was selected based on pharmacometric analyses and evaluated in an additional clinical trial. Nesiritide was approved by FDA in 2001
<i>Case 2</i> Apokyn [™] (Apomorphine HCl) for Parkinson’s disease	Is the proposed dosing regimen appropriate for Parkinson’s patients with normal and impaired renal function?	Exposure–response modeling for UPDRS and blood pressure was performed to assess proposed dosing regimen. Results showed no additional benefit at doses >6 mg and titration to higher dose should not be sooner than 90 min. For patients with mild-moderate renal impairment, the starting dose should be reduced to 1 mg
<i>Case 3</i> Zometa [®] (zoledronic acid) for hypercalcemia and osteolytic metastases	Is there a need to adjust dose in renal impaired patients?	The risk of renal deterioration based on increased drug exposure formed basis for dose adjustments in patients with reduced renal function. Recommended Zometa doses for patients with mild-moderate renal impairment were calculated to achieve the same AUC as in patients with creatinine clearance of 75 mL/min
<i>Case 4</i> Busulfex [®] (busulfan) Injection for chronic myelogenous leukemia	What is the appropriate dosing strategy in pediatric patients?	Based on population PK modeling and simulation, a 2-step dosing regimen was included in label with instructions on drug monitoring. (Booth <i>et al.</i> 2007) This dosing strategy was never directly tested in a clinical trial
<i>Case 5</i> Betapace [®] (sotalol) for arrhythmias	Is the proposed pediatric dosing regimen acceptable?	Dosing recommendations based on FDA’s modified exposure–response analysis for QT and heart rate were included in label. Label also included specific dosing instructions for patients <2 years, which were never directly studied in a clinical trial

(continued)

Table 3.2 (continued)

FDA case example	Regulatory question	Effect of pharmacometric analysis on regulatory decision
<i>Case 6</i> Confidential drug	Is the dose and biomarker predictive of clinical outcome?	Model for dose–biomarker–outcome relationship was developed. Simulations estimated reduction in biomarker needed to achieve clinical benefit. Doses based on simulation were selected for future clinical studies
<i>Case 7</i> Trileptal® (oxcarbazepine) for epilepsy	Is there adequate evidence to approve oxcarbazepine in pediatric patients without a need for additional clinical trials?	Approval of oxcarbazepine monotherapy in pediatrics was based on demonstrating similar exposure–response relationship for seizure frequency in pediatrics and adults using data from adjunctive therapy trials. Drug effect in pediatrics was 85% the effect in adults
<i>Case 8</i> Xenazine® (tetraabenazine) for Huntington’s chorea	Is there adequate evidence of effectiveness in current clinical trial database?	A significant dose–response relationship for Total Chorea Score provided confirmatory evidence of effectiveness to support a single successful controlled clinical trial. (Drug Approval Package 2008c)
<i>Case 9</i> Afinitor® (everolimus) for heart and renal transplant rejection	What is the optimal dosing regimen of everolimus to optimize benefit–risk profile?	Exposure–response relationships for organ rejection (effectiveness) and creatinine clearance (safety) were developed. Simulations explored alternative dosing regimens to optimize benefit–risk profile. Pharmacometric analyses were presented to Cardio-Renal Advisory Committee in 2005 with recommendations to conduct another clinical study using an optimized dosing regimen
<i>Case 10</i> Mycamine® (micafungin) for esophageal candidiasis	What is the optimal dosing regimen of micafungin to optimize benefit–risk profile?	Dose–response relationships for endoscopic response (effectiveness) and alkaline phosphatase (safety) were developed. Analysis supported the 150-mg micafungin dose, with label including statement indicating greater potential for liver toxicity at higher doses

(continued)

Table 3.2 (continued)

FDA case example	Regulatory question	Effect of pharmacometric analysis on regulatory decision
<i>Case 11</i> Chantix® (varenicline) for smoking cessation	What is the optimal dosing regimen of varenicline to optimize benefit–risk profile?	Exposure–response analyses for both efficacy and safety were basis for dose selection. Lower dose for patients who cannot tolerate adverse effects was included in label
<i>Case 12</i> Confidential drug	What is the optimal dosing strategy to avoid the majority of clinical failures?	Based on exposure–response analysis, the sponsor committed to conduct a phase IV study evaluating therapeutic advantages of monitoring plasma concentrations and adjusting dose accordingly
<i>Case 13</i> Confidential drug	What is the reason for inconsistent results across three registration trials?	Pharmacometric dose–response analysis identified the proportion of mildly diseased nonresponders was the primary cause of equivocal evidence. FDA’s approvable letter suggested that sponsor conduct a future study including patients with moderate and severe disease

Cases 1–7 are from (Bhattaram *et al.* 2005) and Cases 8–13 are from (Bhattaram *et al.* 2007)

Additional cases are presented in the following sections to show how pharmacometrics has been used to select pediatric dosing regimens, approve dosing regimens not directly studied in clinical trials, and provide evidence of effectiveness as a primary endpoint or to support a single successful effectiveness trial.

3.3.2.2 Pediatric Dosing Regimen

From 2000 to 2008 FDA pharmacometricians reviewed 52 submissions for pediatric indications. Thirty-eight resulted in labeling with pediatric dosing information. Figure 3.3 shows that these dosing recommendations were primarily driven by an effectiveness study in children (41%), by matching drug exposures in children to adults (37%), or by a combination of both (11%). Fewer cases were based on pharmacodynamic endpoints (*e.g.*, QT prolongation or aPTT) or a combination of all data types. Pharmacometric reviews of pediatric indications evaluate the appropriateness of a dosing regimen in all age groups using exposure–response modeling approaches. Examples of pediatric dosing regimens based solely on pharmacometric analyses are presented in Table 3.3.

When disease progression and exposure–response relationships in pediatrics are similar to adults, then PK data alone can support approval and labeling for pediatric

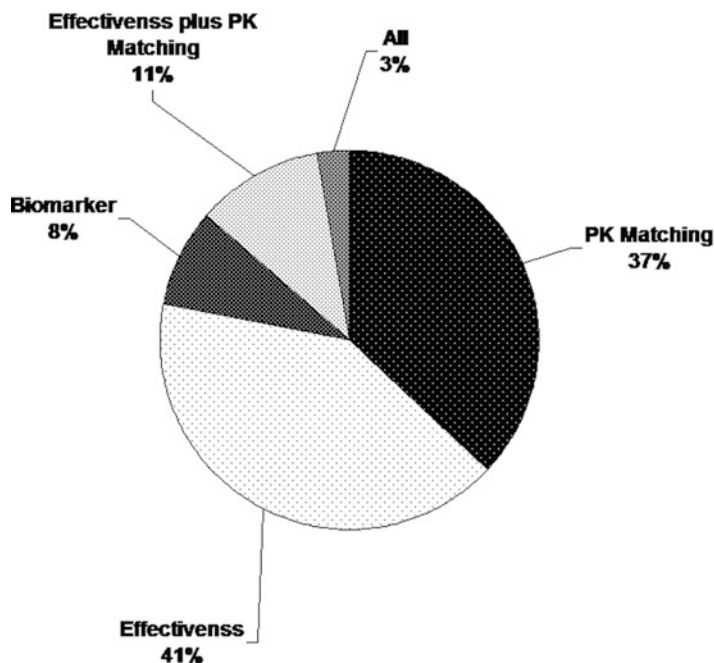


Fig. 3.3 Approaches used to optimize pediatric dosing regimens in 38 submissions with dosing information in label

Table 3.3 Pediatric dosing regimens based on modeling and simulation

Approaches for dosing regimen	Examples of specific drugs ^a
Matching drug exposure in children to adult exposure at labeled-dose	Busulfex [®] (busulfan) Injection, Zosyn [®] (piperacillin/tazobactam), Lovaquin [®] (levofloxacin), Videx [®] (didanosine), Xyzal [®] (levocetirizine dihydrochloride), and Digoxin Elixir
Exposure–response of biomarker or clinical endpoint data	Trileptal [®] (oxcarbazepine), Betapace [®] (sotalol) and Argatroban Injection [®] (argatroban)
Effectiveness study plus matching drug exposures	Celebrex [®] (celecoxib), Humira [®] (adalimumab), Ilaris [®] (canakinumab), and Corlopam [®] (fenoldopam)

^aRefer to drug approval package (Drugs@FDA) and product label for specific details

indications. The objective of dose selection is to match drug exposures in pediatrics with those in adults. PK modeling was used to select optimal dosing regimens of Zosyn[®] (piperacillin/tazobactam) in pediatrics (Tornoe *et al.* 2007). The pharmacokinetic analysis was based on data collected from 53 hospitalized pediatric patients (age 2 months to 17 years) with intra-abdominal infections in two clinical trials. The analysis showed that dosing in children under 2 years needed to be reduced by an age-related factor due to reduced renal clearance. This finding was consistent with what is known about maturation of renal function in children. Optimal dosing based on the modeling and simulation approach was 100 mg

piperacillin/12.5 mg tazobactam q8h for children ≥ 9 months and 80 mg piperacillin/10 mg tazobactam q8h for children 2–9 months. A similar pediatric dose selection strategy was implemented for the labeling of levofloxacin for anthrax following inhalational exposure (Li *et al.* 2010).

When disease progression is considered to be similar between pediatrics and adults, appropriate pediatric doses may be derived by comparing the exposure–response relationships in the two populations. For this approach, both clinical endpoints and qualified biomarkers have been used to define the exposure–response relationship. The approval of Trileptal[®] (oxcarbazepine) monotherapy stemmed from demonstrating similar exposure–response for seizure frequency, a clinical endpoint, in pediatrics and adults using data from adjunctive-therapy trials. The analysis showed that the same trough concentrations in pediatrics have 85% of the effect in adults. The pediatric dose was selected by matching target concentrations in adults that were shown to be effective in the exposure–response model.

Pediatric dosing information for Argatroban Injection[®] (argatroban) was based on exposure–analysis of a biomarker, activated partial thromboplastin times (aPTT), obtained from 15 patients (birth to 16 years) in an open-label study (Madabushi *et al.* 2010). There was a concentration-dependent increase in aPTT, which was similar in pediatric patients and healthy adults. Simulations using the exposure–response relationship indicated that 0.75 $\mu\text{g}/\text{kg}/\text{min}$ was a reasonable starting dose in pediatrics and gave comparable aPPT levels as the approved 2.0- $\mu\text{g}/\text{kg}/\text{min}$ dose in adults. Furthermore, a dose increment step size of 0.25 $\mu\text{g}/\text{kg}/\text{min}$ was suitable for titration.

If the disease process is unique to pediatrics, an effectiveness and safety trial is conducted. Dose selection for clinical trials or product labels is often based on PK and exposure–response data. For example, approval of Celebrex[®] (celecoxib) for juvenile rheumatoid arthritis was based on an effectiveness study in pediatrics patients (age 2 to <17 years) who received an oral suspension of celecoxib at doses of 3 and 6 mg/kg BID (Advisory Committee Meeting 2006). Population PK modeling and simulation bridged the investigational suspension formulation to the marketed oral capsules by integrating pediatric and historical adult data. Doses were selected to obtain celecoxib peak concentrations that did not exceed those observed in the effectiveness study, whereas achieving a similar overall exposure that was shown to be effective. From the results of the modeling approach, dosing recommendations were based on body weight cut-off values: 50 mg BID for children 10–25 kg and 100 mg BID for children >25 kg.

3.3.2.3 Drugs with Approved Doses Not Directly Evaluated in Phase 3 Trials

In 21 (11%) of the 198 NDA/BLA submissions reviewed by FDA pharmacometricians, the labeled dose was based on pharmacometric analyses, rather than being evaluated in effectiveness trials. Of the 21 submissions, 13 were for pediatric indications listed in Table 3.3. For adult indications, Table 3.4 summarizes the dosing rationale derived from pharmacometric analyses.

Table 3.4 Approved adult doses not directly evaluated in phase 3 trials

Drug ^a	Dose recommendation based on pharmacometric analysis
Zometa [®] Injection (zoledronic acid), for hypercalcemia and osteolytic metastases	Risk of further renal deterioration due to increased drug exposure in renal impairment formed basis for dose-adjustment in patients with reduced renal function. Recommended Zometa doses for patients with mild-moderate renal impairment were calculated to achieve the same AUC as that achieved in patients with creatinine clearance of 75 mL/min (Bhattaram <i>et al.</i> 2005)
Zemplar [®] Capsules (paricalcitol); for hyperparathyroid hormone excess in chronic kidney disease	In stage 5 chronic kidney disease, the Zemplar dose in the phase 3 study was based on baseline iPTH/60. Subsequent dose adjustments were based on iPTH/60 and serum chemistries. Trial simulations showed the incidence of hypercalcemia with Zemplar is reduced with a lower dose based on the iPTH/80 formula. Simulations showed increased efficacy in patients with baseline serum calcium ≤ 9.5 mg/dL (Drug Approval Package 2005)
Xenazine [®] Tablets (tetraabenazine) for Huntington's chorea	Dose-reductions for patients who are CYP2D6 poor metabolizers or patients taking strong CYP2D6 inhibitors were based on pharmacokinetic simulations. (Drug Approval Package 2008c)
Chantix [®] (varenicline tartrate) for smoking cessation	Exposure–response analyses for both efficacy and safety were basis for dose selection. Lower dose for patients who cannot tolerate adverse effects was included in label. (Bhattaram <i>et al.</i> 2007)
Clevisprex [®] (clevidipine) for hypertensive emergencies	Clevisprex dosing regimen used in clinical trials resulted in overshooting and oscillations around the target blood pressure. Simulations of the exposure–response relationship were used to optimize the dosing regimen to quickly achieve and maintain target blood pressure. (Drug Approval Package 2008b)
Sotalol HCl Injection for arrhythmias	Bioavailability of oral sotalol is 90–100%. PK modeling was used to select an IV dosing regimen that gave comparable C_{max} values to oral 80-mg dose. Conversion from 80-mg oral sotalol to 75-mg intravenous sotalol over 5 h gave comparable C_{max} values. (Sotalol Label 2009)
Cimzia [®] (certolizumab pegol) for rheumatoid arthritis	The Cimzia dosing regimen used in the monotherapy clinical trial (RA-IV) did not include loading dose. Based on exposure–response relationship for ACR-20, a 400-mg loading dose initially, and at

(continued)

Table 3.4 (continued)

Drug ^a	Dose recommendation based on pharmacometric analysis
Humira [®] (adalimumab) for Crohn's disease	<p>weeks 2 and 4 increased ACR-20 response rates at 12 weeks. Furthermore, the probability of developing antibodies to the drug was found to decrease with increasing Cimzia concentrations. (Drug Approval Package 2008a)</p> <p>Recommended Humira dose for adults is 160 mg initially, followed by 80 mg at 2 weeks. Induction dose may be given as 40 mg SC q6 h for 1 day, or 40 mg SC BID for 2 days. Predicted exposure at week 1 when splitting the induction dose over 2 days is superimposable to the exposure when the full dose is given on the first day. (Humira[®] Label 2007)</p>

^aRefer to drug approval package (Drugs@FDA) and product label for specific details

3.3.2.4 Pharmacometric Analysis Used as Evidence of Effectiveness

Provide Confirmatory Evidence

The FDA generally, but not always, requires two trials to replicate evidence of effectiveness in the drug approval process. A single registration trial can provide substantial evidence of effectiveness for additional indications, new populations, different dosing regimens, or changes in formulation. Pharmacometric analyses have been instrumental in providing confirmatory evidence typically when two positive registration trials are required but by themselves did not provide convincing data. Such analyses help investigate internal consistency of the results which forms a component of supportive evidence. Nine submissions of 198 (4.5%) used pharmacometric analyses of exposure–response data as confirmatory evidence for product registration (Table 3.5).

Model-Based Primary Endpoint for Phase 3 Trials

The primary clinical trial endpoint plays an important role in drug development. There is an increasing trend to use model-based primary endpoints in pivotal trials such as the slope in a dose–response model. There were five NDAs out of 198 submissions reviewed by pharmacometrics that used model-based endpoints. Interestingly, all were for pediatric submissions. Three drugs (candesartan, valsartan, and metoprolol succinate) were to treat pediatric hypertension, and the slope of the dose–response for reduction in systolic blood pressure was used as the primary endpoint. The other two submissions (oxcarbazepine and a confidential drug) were

Table 3.5 Examples of drugs where pharmacometric analyses were used as confirmatory evidence of effectiveness

Drug ^a	Indication	Confirmatory evidence
Toprol-XL [®] (metoprolol succinate)	Hypertension	Significant dose–response and exposure–response in blood pressure reduction in pediatrics Internal consistency across different blood pressure parameters (<i>e.g.</i> , systolic, diastolic)
Heparin sodium	Acute myocardial infarction	On- and off-heparin treatment significantly delays the time to secondary myocardial infarction Heparin’s mechanism of action and prior experience
Seroquel [®] XR (quetiapine fumarate)	Schizophrenia and bipolar affective disorder	Significant dose–response (PANSS score change from baseline) relationship in schizophrenia patients Similar treatment pattern observed following the treatment of Seroquel XR and immediate-release formulation
Trileptal [®] (oxcarbazepine)	Epilepsy	Significant exposure–response relationship in pediatrics from adjunct therapy trials Consistency with that in adults
Xenazine [®] Tablets (tetraabenazine)	Huntington’s chorea	Significant dose–response (chorea score) relationship Internal consistency of results across one positive, one negative trial and their extensions (Bhattaram <i>et al.</i> 2005; Drug Approval Package 2008c)
Revatio [®] (sildenafil) tablets	Pulmonary arterial hypertension	20 mg TID and higher doses do not provide additional benefit with respect to delay in clinical worsening, exercise capacity and vascular hemodynamics Internal consistency between two trials for exercise capacity and vascular hemodynamics
Lamictal [®] XR (lamotrigine) Extended-Release Tablets	Epilepsy	Significant dose–response alleviated concern for lack of effectiveness in the US population (center-effect) along with prior data from immediate-release formulation
Ranexa [®] (ranolazine) extended-release tablets	Angina	Significant exposure–response relationship in exercise tolerance testing
Atacand [®] (candesartan cilexetil) tablets	Hypertension	Significant dose- and exposure–response relationship for blood pressure in younger and older pediatric patients, in spite of negative result for the older pediatrics

^aRefer to drug approval package (Drugs@FDA) and product label for specific details

for pediatric epilepsy (monotherapy or adjunctive therapy). The primary endpoints in these two submissions were slopes of dose–response and exposure–response in reduction of seizure frequency.

3.4 Future Perspectives

The focus of Pharmacometrics as a scientific discipline has evolved over the decades. The development of pharmacometric concepts and tools, largely in academia occurred during the period from 1970 to 1990. This phase can be called the “scientific discovery period” of pharmacometrics. Initially, clinical pharmacologists quantified the relationship between dose or exposure and response at fixed times due to insufficiency of methods to analyze the time-course of drug action. An important advancement was the introduction of the effect compartment model (Sheiner *et al.* 1979), and later, indirect response models (Jusko and Ko 1994; Krzyzanski and Jusko 1997). These allow for quantitative descriptions of time delays between drug concentrations and observed responses. Many tools using regression and maximum-likelihood algorithms were introduced during this period. In terms of application, modeling was rarely employed in drug development, and then mainly early in drug development. The introduction of tools that model sparse data created opportunities for scientists to engage with the late phase trials.

Over the past two decades, pharmacometrics has evolved most notably as an important decision-making tool during drug development (Peck 1992a, b, 1997; Reigner *et al.* 1997; Olson *et al.* 2000; Miller *et al.* 2005; Zhang *et al.* 2006; Lalonde *et al.* 2007) and regulatory review, as illustrated by the many examples provided above. The concept of clinical trial simulations started to evolve during 1990s (Taylor and Bosch 1990; Gieschke *et al.* 1997; Hale *et al.* 1998; Krall *et al.* 1998). Gradually, pharmacometricians have been sought after to aid in higher-level go/no-go decisions, dose selection, trial design, endpoint selection, safety evaluation, evidence of effectiveness, approval, and labeling. The past 2 decades can be referred to as the “entrepreneurial period” of pharmacometrics.

What follows should be the “industrialization period.” Pharmacometrics managed prudently is already emerging as a major player in key drug development and regulatory decisions. In some areas, it has essentially revolutionized inadequate paradigms of dose optimization. An example would be in pediatric drug development, in which the ineffective practice of body-size scale-down from adult dosages has been replaced by the exposure-response guided approach. Currently, the two most important areas for investment are the development of standards for different diseases and training future pharmacometricians. The pharmacometric approaches during the “entrepreneurial period” have been, by and large, customized for each problem. In order for the discipline to expand its influence on the quality of drug development decisions, unifying standards for each disease need to be developed. Their purpose is to streamline data collection, analysis, reporting, and archiving, and to provide a common framework for interpretation of pharmacometric

analyses. Such a step fosters consistency, speed, quality, not only within, but also across organizations. Standardization will also enhance our ability to interact with other disciplines (e.g., statistics, medical). Among the 2020 goals for the Division of Pharmacometrics are the development of such standards (www.fda.gov/AboutFDA/CentersOffices/CDER/ucm167032.htm#FDAPharmacometrics2020-StrategicGoals).

References

- Advisory Committee Meeting (2006) Celebrex[®] (celecoxib) Application No. 020998. www.fda.gov/ohrms/dockets/ac/06/briefing/2006-4252b1-00-index.htm. Accessed 29 Nov 2006
- Benjamin DK Jr, Smith PB, Jadhav P, Gobburu JV, Murphy MD, Hasselblad V, Baker-Smith C, Califf RM, Li JS (2008) Pediatric antihypertensive trial failures: analysis of end points and dose range. *Hypertension* 51:834–840
- Bhattaram VA, Booth BP, Ramchandani RP, Beasley BN, Wang Y, Tandon V, Duan JZ, Baweja RK, Marroum PJ, Uppoor RS, Rahman NA, Sahajwalla CG, Powell JR, Mehta MU, Gobburu JV (2005) Impact of pharmacometrics on drug approval and labeling decisions: a survey of 42 new drug applications. *AAPS J* 7:E503–E512
- Bhattaram VA, Bonapace C, Chilukuri DM, Duan JZ, Garnett C, Gobburu JV, Jang SH, Kenna L, Lesko LJ, Madabushi R, Men Y, Powell JR, Qiu W, Ramchandani RP, Tornoe CW, Wang Y, Zheng JJ (2007) Impact of pharmacometric reviews on new drug approval and labeling decisions—a survey of 31 new drug applications submitted between 2005 and 2006. *Clin Pharmacol Ther* 81:213–221
- Bhattaram VA, Siddiqui O, Kapcala LP, Gobburu JV (2009) Endpoints and analyses to discern disease-modifying drug effects in early Parkinson’s disease. *AAPS J* 11:456–464
- Booth BP, Rahman A, Dagher R, Griebel D, Lennon S, Fuller D, Sahajwalla C, Mehta M, Gobburu JV (2007) Population pharmacokinetic-based dosing of intravenous busulfan in pediatric patients. *J Clin Pharmacol* 47:101–111
- Drug Approval Package (2005) Zemplar[®] Capsules (paricalcitol) Application No. 021606. www.accessdata.fda.gov/drugsatfda_docs/nda/2005/021606s000TOC.cfm. Accessed 25 May 2005
- Drug Approval Package (2008a) Cimzia[®] (certolizumab pegol) Application No. 125160. www.accessdata.fda.gov/drugsatfda_docs/nda/2008/125160s000TOC2.cfm. Accessed 28 Apr 2008
- Drug Approval Package (2008b) Cleviprex[®] (clevidipine butyrate) Application No. 022156. www.accessdata.fda.gov/drugsatfda_docs/nda/2008/022156_cleviprex_toc.cfm. Accessed 1 Aug 2008
- Drug Approval Package (2008c) Xenazine[®] Tablets (tetrabenazine) Application No. 021894. www.accessdata.fda.gov/drugsatfda_docs/nda/2008/021894s000TOC.cfm. Accessed 18 Aug 2008
- Florian FA, Tornoe CW, Brundage R, Parekh A, Garnett CE (2010) Population PK and concentration-QTc models for moxifloxacin: pooled analysis of 20 thorough QT studies. *J Clin Pharmacol* In press.
- Food and Drug Administration (1998) Guidance for industry: providing clinical evidence of effectiveness for human drug and biological products. www.fda.gov/downloads/Drugs/GuidanceComplianceRegulatoryInformation/Guidances/UCM078749.pdf
- Food and Drug Administration (1999) Guidance for industry: population pharmacokinetics. www.fda.gov/downloads/Drugs/GuidanceComplianceRegulatoryInformation/Guidances/ucm072137.pdf

- Food and Drug Administration (2003) Guidance for industry: exposure-response relationships – study design, data analysis, and regulatory applications. U.S. Department of Health and Human Services, Food and Drug Administration. www.fda.gov/downloads/Drugs/GuidanceComplianceRegulatoryInformation/Guidances/ucm072109.pdf
- Food and Drug Administration (2004) FDA critical path initiatives white paper: innovation or stagnation? Challenge and opportunity on the critical path to new medical products
- Garnett CE, Beasley N, Bhattaram VA, Jadhav PR, Madabushi R, Stockbridge N, Tornoe CW, Wang Y, Zhu H, Gobburu JV (2008) Concentration-QT relationships play a key role in the evaluation of proarrhythmic risk during regulatory review. *J Clin Pharmacol* 48:13–18
- Gieschke R, Reigner BG, Steimer JL (1997) Exploring clinical study design by computer simulation based on pharmacokinetic/pharmacodynamic modelling. *Int J Clin Pharmacol Ther* 35:469–474
- Gobburu JV, Lesko LJ (2009) Quantitative disease, drug, and trial models. *Annu Rev Pharmacol Toxicol* 49:291–301
- Hale MD, Nicholls AJ, Bullingham RE, Hene R, Hoitsma A, Squifflet JP, Weimar W, Vanrenterghem Y, Van de Woude FJ, Verpooten GA (1998) The pharmacokinetic-pharmacodynamic relationship for mycophenolate mofetil in renal transplantation. *Clin Pharmacol Ther* 64:672–683
- Humira® Label (2007) Humira® (adalimumab) Injection Application No. 125057. www.accessdata.fda.gov/scripts/cder/drugsatfda/index.cfm?fuseaction=SearchDrugDetails. Accessed 27 Feb 2007
- International Conference Harmonization (1994) E4: Dose-Response Information to Support Drug Registration. www.ich.org/LOB/media/MEDIA480.pdf
- International Conference Harmonization (2005) E14: The clinical evaluation of QT/QTc interval prolongation and proarrhythmic potential for non-antiarrhythmic drugs. www.ich.org/LOB/media/MEDIA1476.pdf
- Jadhav PR, Zhang J, Gobburu JV (2009) Leveraging prior quantitative knowledge in guiding pediatric drug development: a case study. *Pharm Stat* 8:216–224
- Jadhav PR, Burckart GJ, Choe S, Estes K, Huang SM, Lu S, Lesko LJ, Liu Q, Mulugenta L, Mummaneni P, Tandon V, Gobburu JV, Wang Y (2010a) Defining the quality of pediatric pharmacokinetic studies. *Clin Pharmacol Ther* In press.
- Jadhav PR, Burckart G.J., Lesko LJ, Gobburu JV (2010b) Paediatric Drug Development and Clinical Pharmacology. *Drug Development* In press.
- Jusko WJ, Ko HC (1994) Physiologic indirect response models characterize diverse types of pharmacodynamic effects. *Clin Pharmacol Ther* 56:406–419
- Kola I, Landis J (2004) Can the pharmaceutical industry reduce attrition rates? *Nat Rev Drug Discov* 3:711–715
- Krall RL, Engleman KH, Ko HC, Peck CC (1998) Clinical trial modeling and simulation – Work in progress. *Drug Information J* 32:971–976
- Krzyzanski W, Jusko WJ (1997) Mathematical formalism for the properties of four basic models of indirect pharmacodynamic responses. *J Pharmacokinet Biopharm* 25:107–123
- Lalonde RL, Kowalski KG, Hutmacher MM, Ewy W, Nichols DJ, Milligan PA, Corrigan BW, Lockwood PA, Marshall SA, Benincosa LJ, Tensfeldt TG, Parivar K, Amantea M, Glue P, Koide H, Miller R (2007) Model-based drug development. *Clin Pharmacol Ther* 82:21–32
- Li F, Nandy P, Chien S, Noel GJ, Tornoe CW (2010) Pharmacometrics-based dose selection of levofloxacin as a treatment for post-exposure inhalational anthrax in children. *Antimicrob Agents Chemother* 54:375–379
- Madabushi R, Cox DS, Hossain M, Boyle DA, Patel BR, Young G, Choi YM, Gobburu JV (2010) Pharmacokinetic and pharmacodynamic basis for effective argatroban dosing in pediatrics. *J Clin Pharmacol*
- Miller R, Ewy W, Corrigan BW, Ouellet D, Hermann D, Kowalski KG, Lockwood P, Koup JR, Donevan S, El-Kattan A, Li CS, Werth JL, Feltner DE, Lalonde RL (2005) How modeling and simulation have enhanced decision making in new drug development. *J Pharmacokinet Pharmacodyn* 32:185–197

- Olson SC, Bockbrader H, Boyd RA, Cook J, Koup JR, Lalonde RL, Siedlik PH, Powell JR (2000) Impact of population pharmacokinetic-pharmacodynamic analyses on the drug development process: experience at Parke-Davis. *Clin Pharmacokinet* 38:449–459
- Peck CC (1992a) Population approach in pharmacokinetics and pharmacodynamics: FDA view. Conference on new strategies in drug development and clinical evaluation: the population approach, Manchester, England, September 1991. Published by the Commission of the European Communities: European cooperation in the field of scientific and technical research, 157–168
- Peck CC (1992b) Streamlining clinical testing: presented at first Princeton conference on drug development, October 1991. Lasagna L (ed) Published by Excerpta Medica, Inc., Princeton, NJ, 33–35
- Peck CC (1997) Drug development: improving the process. *Food Drug Law J* 52(2):163–167
- Peck CC, Barr WH, Benet LZ, Collins J, Desjardins RE, Furst DE, Harter JG, Levy G, Ludden T, Rodman JH (1992) Opportunities for integration of pharmacokinetics, pharmacodynamics, and toxicokinetics in rational drug development. *Clin Pharmacol Ther* 51:465–473
- Reigner BG, Williams PE, Patel IH, Steimer JL, Peck C, van Brummelen P (1997) An evaluation of the integration of pharmacokinetic and pharmacodynamic principles in clinical drug development. Experience within Hoffmann La Roche. *Clin Pharmacokinet* 33:142–152
- Rock EP, Finkle J, Fingert HJ, Booth BP, Garnett CE, Grant S, Justice RL, Kovacs RJ, Kowey PR, Rodriguez I, Sanhai WR, Strnadova C, Targum SL, Tsong Y, Uhl K, Stockbridge N (2009) Assessing proarrhythmic potential of drugs when optimal studies are infeasible. *Am Heart J* 157(827–36):836
- Sheiner LB, Stanski DR, Vozeh S, Miller RD, Ham J (1979) Simultaneous modeling of pharmacokinetics and pharmacodynamics: application to d-tubocurarine. *Clin Pharmacol Ther* 25:358–371
- Sotalol Label (2009) Sotalol HCl Application No. 022306. http://www.accessdata.fda.gov/drugsatfda_docs/label/2009/022306s000lbl.pdf. Accessed 2 Jul 2009
- Taylor DW, Bosch EG (1990) CTS: a clinical trials simulator. *Stat Med* 9:787–801
- Tornøe CW, Tworzyński JJ, Imoisili MA, Alexander JJ, Korth-Bradley JM, Gobburu JV (2007) Optimising piperacillin/tazobactam dosing in paediatrics. *Int J Antimicrob Agents* 30:320–324
- Tornøe CW, Garnett CE, Wang Y, Florian JA, Li M, Gobburu JV (2010) Creation of knowledge management system for QT analyses. *J Clin Pharmacol* In press
- Wang Y, Bhattaram AV, Jadhav PR, Lesko LJ, Madabushi R, Powell JR, Qiu W, Sun H, Yim DS, Zheng JJ, Gobburu JV (2008) Leveraging prior quantitative knowledge to guide drug development decisions and regulatory science recommendations: impact of FDA pharmacometrics during 2004–2006. *J Clin Pharmacol* 48:146–156
- Wang Y, Garnett CE (2010) Letter to the editor: statistical issues of QT prolongation assessment based on linear concentration modeling by Yi Tsong et al. *J Biopharm Stat* 20:689–692
- Wang Y, Sung C, Dartois C, Ramchandani R, Booth BP, Rock E, Gobburu J (2009) Elucidation of relationship between tumor size and survival in non-small-cell lung cancer patients can aid early decision making in clinical drug development. *Clin Pharmacol Ther* 86:167–174
- Yan LK, Zhang J, Ng MJ, Dang Q (2010) Statistical characteristics of moxifloxacin-induced QTc effect. *J Biopharm Stat* 20:497–507
- Zhang L, Sinha V, Fargue ST, Callies S, Ni L, Peck R, Allerheiligen SR (2006) Model-based drug development: the road to quantitative pharmacology. *J Pharmacokinet Pharmacodyn* 33:369–393
- Zhu H, Wang Y, Gobburu JV, Garnett CE (2010) Considerations for clinical trial design and data analysis of thorough QT studies using drug–drug interactions. *J Clin Pharmacol*. doi:10.1177/0091270009358710

Part II
Strategic Applications of M&S
in Drug Development

Chapter 4

Decision-Making in Drug Development: Application of a Model Based Framework for Assessing Trial Performance

Mike K. Smith, Jonathan L. French, Kenneth G. Kowalski,
Matthew M. Hutmacher, and Wayne Ewy

Abstract This chapter proposes a general framework for the formal integration of model-based predictions and their uncertainty in the planning of prospective trials and in quantitative decision-making. Standard operating characteristics such as statistical power, which are conditional on a chosen effect size, quantify the performance of the design. Optimising trials based solely on power does not fully address the needs of drug development teams interested in understanding the performance of the compound as well as the performance of the proposed study design. Many Phase 3 trials fail due to lack of significant efficacy despite being adequately powered. Power does not take into consideration the *likelihood* of achieving the assumed treatment effect. Metrics such as probability of a correct decision, probability of a Go decision, and probability of reaching a target value are proposed to evaluate the performance of the compound and trial. A conceptual clinical trial simulation (CTS) approach is outlined for calculating these trial performance metrics and to evaluate the ‘false positive’ and ‘false negative’ error rates for the proposed metrics. An example is presented to illustrate the CTS procedure and show how different choices of trial design, analytic technique and trial metric influence the probability of making correct decisions.

4.1 Introduction

Drug development proceeds via a series of many interlocking cycles of questions, answers and decisions. We ask questions about what the drug candidate does and how best to use it, guided by medical needs, commercial reality and regulatory requirements. We get answers from clinical trials, literature and laboratory experiments. We make decisions based on these answers, often using formal decision criteria to generate decision recommendations, which are evaluated within the

M.K. Smith (✉)
Pharmacometrics, Pfizer Ltd., Sandwich, Kent CT, USA
e-mail: mike.k.smith@pfizer.Com

wider development context (*i.e.*, considering all the answers to many relevant questions) to make the actual decisions.

In his landmark paper, Sheiner (1997) discussed how the alternating steps of induction and deduction of Box (1966) could apply to drug development and remarked how the emphasis on regulatory approval drove the intellectual focus on demonstrating (confirming) efficacy. There is a commonly held view that “learning” and “confirming” apply to individual trials or even phases of drug development, however we maintain that it is possible to learn and confirm within the same trial – a single trial can address some confirmatory *questions* while providing valuable information to help formulate *new* questions or learn about the action of the drug in other areas. The primary goal in addressing confirmatory questions is to demonstrate statistically *whether* the drug has the desired effect. In these cases the hypothesis being tested, the study design, test statistic and operating characteristics can be well defined and in general these attributes have been well discussed and are well understood across the statistical literature. However, the corresponding designs, statistics, operating characteristics and decision criteria to address “learning” questions are less well understood and may be driven to some extent by context of the disease area, drug characteristics, precedent, prior information, and decision making processes within the individual drug company. It should be pointed out that a design optimised for “confirmatory” questions is often less than optimal for addressing “learning” questions. As drug development proceeds, various studies carry different emphases for learning and confirming – some are purely “learning” studies while some are purely “confirming” studies.

In this chapter, we discuss some of the issues for addressing “learning” questions – decision making in clinical trials where the principle aim is to evaluate whether the drug works well *enough*, in selecting doses that give sufficient efficacy for further development, or in evaluating whether a study designed to estimate dose-response will provide sufficient information for a decision to progress to the next stage of development. The methods discussed can also be extended to addressing “confirming” questions where the decision is based not just on statistical significance, but where the magnitude of treatment effect is a key metric in the decision making process – especially when comparing a novel treatment to a reference treatment or competitor.

Decision criteria can be viewed in the same way as diagnostic tests – we are interested in the sensitivity and specificity of the criteria (Chuang-Stein *et al.* 2010). In diagnostic tests, the criteria are driven by choosing values such that false positive and false negative results are reduced, but the predictive value of the criteria are also influenced by the underlying prevalence of the disease, or the underlying rates of positive or negative outcomes. In the same way, the probability of making the correct decision in a clinical trial is a function of the chosen decision criteria, but also the underlying probability of a positive outcome for the drug itself. This probability is in part intrinsic to the drug and is influenced by the disease and its stage and choice of clinical endpoint, but also includes uncertainty in the effectiveness of the treatment expressed through models of disease and drug action. For example, a given drug may have a low probability of success in a given indication so we may wish to ensure that we employ a decision criteria to stop the next trial as

soon as possible if the drug indeed fails to show sufficient efficacy. Note that we do not limit ourselves to thinking in terms of statistically significant efficacy; if we have a low probability of achieving the clinical and commercial profile for the drug, we may (and probably should) stop development early regardless of statistical significance.

Lalonde *et al.* (2007) described the framework for model-based drug development and identified six key components: PK-PD and disease models; competitor information and meta-analysis; design and trial execution models; data analytic models; quantitative decision criteria; and trial performance metrics. In this chapter we describe how these components integrate together to provide quantitative assessment of drug and trial performance metrics. In Sect. 4.2 we introduce terminology and notation to describe the quantities of interest, define decision criteria and calculate the trial performance metrics. Section 4.3 illustrates how decision criteria choice can influence trial performance metrics, through probabilistic results from a very simple bivariate normal distribution. We then describe in Sect. 4.4 a real-world example where information from meta-analysis and information about trial design, execution and imputation were used to simulate trial performance metrics. In Sect. 4.5 we discuss some practicalities of performing model-based drug development and simulation within this context. Finally, Sect. 4.6 provides a discussion of how this new paradigm of drug development requires close collaboration within drug development teams, especially between the quantitative disciplines – clinical pharmacologists, statisticians and pharmacometricians.

4.2 Notation and Terminology

In order to formally describe the quantitative decision criteria and operating characteristics we first introduce some notation. Let Δ be the true, unknown and unobservable value of some measure of treatment effect. For example, this could be the difference relative to a comparator compound for a specific treatment, a model-based estimate of the effect at a given dose of the investigational drug or, as in the example of Sect. 4.4, the relative potency of two compounds from the same drug class. In the context of trial design for “confirming” questions, Δ is usually assumed to have a fixed value, usually the minimally important clinical difference and is reflected in the choice of alternative hypothesis. Alternatively, we can view Δ as having a distribution describing our prior belief about the likelihood of given values for Δ . At a given stage of drug development, we should account for the fact that our knowledge of Δ is incomplete. What is known about Δ may be based on analysis of prior information through PK-PD exposure-response models, disease progression models, meta-analysis of prior data, etc. If Δ is defined in this way we can express our current knowledge about Δ through model parameters θ for fixed effect relationships, Ω for between subject variability parameters and Σ for within subject

or residual error. Thus, for a given set of model assumptions and this prior information we will have an estimate of Δ :

$$\hat{\Delta} = f(\theta, \Omega, \Sigma) \quad (4.1)$$

When we estimate values for θ , Ω and Σ we generally also calculate the uncertainty around these values. As a consequence we can view θ , Ω and Σ as having probability distributions and so $\hat{\Delta}$ will also have a probability distribution through a combination of these parameters using the functional forms in $f(\dots)$. Note that if the model includes random effects in the non-linear parts of the model or a non-additive residual error model, then the expected difference from placebo would also be functions of the between-subject variances and/or the residual variance. Note that the estimate $\hat{\Delta}$ is dependent on all *currently available* information and, as new information emerges, we should update our models and parameter estimates to reflect this. Thus, the distribution for $\hat{\Delta}$ becomes a “snapshot” of our knowledge about Δ at a given moment.

We also need to define a target value TV, which is a reference value for the effect Δ such that if we knew that $\Delta > \text{TV}$ then we would make a decision to continue drug development with the investigational drug. The target value TV is usually based on a synthesis of clinical and commercial opinion of what constitutes a meaningful difference relative to a reference treatment. It may also take into consideration trade-offs between efficacy and safety and, increasingly recently, differentiation over current therapies for the disease under study. We may impose a further stricture on Δ such that we would recommend further development only if we have sufficient confidence that $\hat{\Delta} > \text{TV}$. Note that we do not *know* the “true” Δ , and we only have our “best guess” at it through $\hat{\Delta}$. As a consequence, when we make strategic and operational decisions based on this we will want to have reasonable confidence that $\hat{\Delta} > \text{TV}$ so that in turn Δ is also likely to be $> \text{TV}$. Note that Δ and $\hat{\Delta}$ do not depend on any particular sample size or trial design. They may however depend on *when* the treatment effect is measured if the endpoint of interest is measured longitudinally. In such cases, we would include time as a covariate in the function (4.1) above. Similarly, other covariate influences on Δ can be incorporated. From here on, we will treat Δ and $\hat{\Delta}$ as synonymous in the context of making decisions at a given stage in drug development. $\hat{\Delta}$ changes as new data becomes available. This data can be specific to the drug in question or influenced by externally available information on disease, dropout models, relationships between early and late outcomes, data on comparator compounds, etc.

We define the trial level *estimate* of the treatment effect, T . That is, T is our estimate of Δ for given trial data and is the result of an applied analytical technique to the trial data. T may be a point estimate or an interval estimate based metric such as the lower or upper confidence limit. For the trial results, we construct a decision criteria that compares the trial test statistic T to the target value TV. If we have sufficient confidence that $T \geq \text{TV}$ then we make the decision to continue development with the investigational drug based on the data from the current trial.

If there is sufficient evidence to show that $T < TV$ or alternatively, or if our confidence that $T \geq TV$ is low, then we stop development. In most cases we will compare Δ and T against the same value of TV , particularly in the case where both Δ and T are based on point estimates of treatment effect. If T is based on a confidence limit then since Δ does not have an analogous equivalent (recall that Δ does not depend on sample size or design) then we may need to select different values of TV for T and Δ . An example of this is given in Sect. 4.4.

The traditional approach to trial design and decision criteria for answering “confirming” questions is to assume $\Delta = \delta \neq 0$ is fixed and known, where δ is assumed effect size. However, in this case there is typically little formal evaluation of the probability of achieving the assumed effect size δ . In addressing learning questions we wish to be confident that our inference about T agrees closely with inference about Δ . For example, if we see $T \geq TV$ in a given trial, then we want to be sure that the true state is that Δ is also greater than TV . If our design, analysis and application of decision criteria to the results lead to high probability of inference about T and Δ agreeing, then we can be more confident that we are able to make correct and consistent decisions. In the case where Δ is a nonlinear function of model parameters as described in (4.1) we must turn to clinical trial simulation (CTS) to calculate T and assess these probabilities since analytical solutions for these types of trials are seldom available.

For a given trial simulation replicate, we draw values of θ, Ω, Σ and covariate values, calculate Δ and then for the same set of model inputs calculate T for a given design. It is a key step here to compare decisions for identical inputs (*i.e.*, for the same set of θ, Ω, Σ) so that we can compare the “truth” vs. “trial” outcomes within each simulation replicate. Based on simulating Δ and T for the “truth” and “trial” outcomes respectively, we can construct a 2×2 contingency table by counting the number of replicate outcomes that fall into each of the 4 cells (Table 4.1).

We define $P(\text{Correct})$ as the sum of the diagonal elements $P(T \geq TV \ \& \ \Delta \geq TV) + P(T < TV \ \& \ \Delta < TV)$, and $P(\text{Incorrect})$ as the sum of off-diagonal elements. Which incorrect decision is most critical depends on the stage of development – in early phase development we may consider a “continue” decision on a drug with $\Delta < TV$ less critical than a decision to halt development on a compound where $\Delta \geq TV$. However, later in development the converse will certainly hold. Through the CTS procedure then, we can calculate and quantify the probability of achieving the target value ($PTV) = P(\Delta \geq TV)$, $P(\text{Correct decision})$, and $P(\text{Incorrect decision})$.

It is the sponsor’s decision which limits for PTV and $P(\text{Correct})$ are acceptable at each stage of drug development and for each disease area. A therapy with high

Table 4.1 Contingency table of “truth” vs. “trial”

Truth vs. trial	$T < TV$	$T \geq TV$	Total
$\Delta < TV$	$P(T < TV \ \& \ \Delta < TV)$	$P(T \geq TV \ \& \ \Delta < TV)$	$P(\Delta < TV)$
$\Delta \geq TV$	$P(T < TV \ \& \ \Delta \geq TV)$	$P(T \geq TV \ \& \ \Delta \geq TV)$	$P(\Delta \geq TV)$
Total	$P(T < TV)$	$P(T \geq TV)$	1.0

unmet medical need may be progressed in early development even when PTV is low if, and only if, we can be assured that $P(\text{Correct})$ is high. In other indications where the investigational drug needs to be strongly differentiated over competitor compounds, we may decide to halt development if PTV is low without even conducting a trial. We also need to acknowledge that the choice of acceptable PTV is a portfolio decision since resources are finite and that resources are generally only assigned to compounds that have a reasonable probability of success. Although we are concentrating within this chapter on making decisions about design, analytic methods and decision criteria at the trial level, we must bear in mind that good decisions at the portfolio level are also vital. For this reason, quantification of PTV is important *throughout* a compound's development and should be assessed and updated whenever new information becomes available.

In the absence of prior information for Δ , for example if this is an unprecedented disease area or a novel endpoint, we may choose to use discrete values for Δ , examining trial outcomes for a variety of values for Δ and comparing $T \geq \text{TV}$ at the trial level when we know whether $\Delta \geq \text{TV}$. We may also wish to incorporate a discrete probability distribution for the chosen values for Δ – this will allow us to establish the likelihood of achieving $\Delta \geq \text{TV}$ as well as $T \geq \text{TV}$. In this latter case we move close to what could be considered Bayesian subjective prior concerning $P(\Delta \geq \text{TV})$.

4.3 Illustrative Example Using Bivariate Normal Distributions

4.3.1 Introduction to the Example

We illustrate the concepts above using a simple example where the operating characteristics of the “trials” can be calculated theoretically using bivariate normal distributions. The results of these theoretical calculations can be compared to those obtained using CTS of individual trials. First, let us imagine that analysis of prior data has estimated a treatment effect, Δ to have mean = 3.27 with associated standard error (σ_{Δ}) = 0.6 and standard deviation of the endpoint of interest measured for an individual is ($\sigma_{Y|\Delta}$) = 7. For simplicity here we will not take into consideration uncertainty on this standard deviation. Theoretically, we should take into account uncertainty in all quantities in our simulations – the example in Sect. 4.4 illustrates this. In some cases, though, we have good information about the variability in the measurement of interest, usually from prior data or experience, even when the effect of the novel treatment on the endpoint (*i.e.*, Δ) is not well known.

To simulate N replicated trials with n subjects per treatment group within each trial we use the following method:

1. The uncertainty in Δ is assumed to be follow a normal distribution having a mean Δ of 3.27 and standard deviation, σ_{Δ} of 0.6, the prior estimate of the

standard error of Δ . Let Δ_i denote the realisation of Δ for the i th trial. The measurement model, where Y_{ij} denotes the observation for the j th subject in the i th trial, also has a normal distribution with mean set to Δ_i and standard deviation $\sigma_{Y|\Delta}$ set to 7, the prior estimate of the measurement standard deviation. This simple mean model can be used to simulate clinical trial data with one observation per subject for n subjects for each of N simulated trials. Using the notation introduced above for the simple quantitative decision, the data-analytic model is simply, $T = \bar{Y}$, the arithmetic mean.

- Now consider the simple quantitative decision rule where a ‘‘True’’ Go decision is made if the value of Δ is greater than or equal to a target value (TV) of 3 and conversely, a true No Go decision is made if Δ is less than 3. Similarly, data-analytic Go and No Go decisions are made if the observed arithmetic mean is greater than or equal to 3 or less than 3, respectively. Using with the model assumptions above, it can be shown that the joint distribution of Δ_i and \bar{Y} is bivariate normal. Thus:

$$\begin{pmatrix} \Delta_i \\ \bar{Y}_i \end{pmatrix} \sim \text{MVN} \left[\begin{pmatrix} \Delta \\ \Delta \end{pmatrix}, \begin{pmatrix} \sigma_\Delta^2 & \sigma_\Delta^2 \\ \sigma_\Delta^2 & \sigma_\Delta^2 + \frac{1}{n}\sigma_{Y|\Delta}^2 \end{pmatrix} \right] \tag{4.2}$$

So, for this example

$$\begin{pmatrix} \Delta_i \\ \bar{Y}_i \end{pmatrix} \sim \text{MVN} \left[\begin{pmatrix} 3.27 \\ 3.27 \end{pmatrix}, \begin{pmatrix} 0.6^2 & 0.6^2 \\ 0.6^2 & 0.6^2 + \frac{1}{n}7^2 \end{pmatrix} \right]$$

Moreover, the joint probability that both \bar{Y} and Δ_i are less than or equal to the target value of 3 can be calculated using readily available functions such as the SAS/BASE software PROBBNRM function, pmnorm and rmnorm in the R package ‘‘mnormt’’ (Azzalini and Genz 2009) and pmvnorm in Tibco Spotfire S+. These joint probabilities essentially populate the 2×2 table from which the decision criteria operating characteristics can be calculated.

This example is sufficiently simple such that the operating characteristics can be calculated theoretically. Simulation in this case consists of drawing values of Δ_i for each trial and then drawing a \bar{Y}_i conditional on the Δ_i with variability depending on the size of the trial (through n). Thus, we have a very simple method for simulating both ‘‘truth’’ and ‘‘trial’’ results under this simplified framework. In Sect. 4.5 we discuss simulation practicalities for more complex situations.

4.3.2 Operating Characteristics for Decision Criteria Based on Point Estimates

We introduce below a mathematical notation for frequency-based calculations of the probability of a data-analytic Go decision or $P(\text{Go})$, probability of a correct

decision or $P(\text{Correct})$, and the conditional probabilities for false Go and false No Go decisions. In the notation, the function I denotes an indicator variable which is assigned the value of 1 when the argument in parentheses is true and is assigned the value of 0 when the argument in parentheses is false.

$$P(\text{Go}) = \frac{1}{N} \sum_{i=1}^N I(\bar{Y}_i \geq 3)$$

$$P(\text{Correct}) = \frac{1}{N} \sum_{i=1}^N I(\bar{Y}_i \geq 3, \Delta_i \geq 3) + I(\bar{Y}_i < 3, \Delta_i < 3)$$

$$P(\text{FalseGo}) = P(\text{Go}|\Delta_i < 3) = \frac{P(\text{Go}, \Delta_i < 3)}{P(\Delta_i < 3)} = \frac{\frac{1}{N} \sum_{i=1}^N I(\bar{Y}_i \geq 3, \Delta_i < 3)}{\frac{1}{N} \sum_{i=1}^N I(\Delta_i < 3)}$$

$$P(\text{FalseNoGo}) = P(\text{NoGo}|\Delta_i \geq 3) = \frac{P(\text{NoGo}, \Delta_i \geq 3)}{P(\Delta_i \geq 3)} = \frac{\frac{1}{N} \sum_{i=1}^N I(\bar{Y}_i < 3, \Delta_i \geq 3)}{\frac{1}{N} \sum_{i=1}^N I(\Delta_i \geq 3)}$$

Specifically, $P(\text{Go})$ is obtained by summing the number of simulated trials where \bar{Y}_i is greater than or equal to 3 and dividing this sum by N , the total number of simulated trials. Similarly, $P(\text{Correct})$ is obtained by summing the number of simulated trials where \bar{Y}_i and Δ_i are both greater than or equal to 3 or both are less than 3 and dividing this sum by N . The probability of a false Go decision or $P(\text{False Go})$ is obtained by summing the number of simulated trials where jointly \bar{Y}_i is greater than or equal to 3 and Δ_i is less than 3 and dividing this sum by the total number of trials where Δ_i is less than 3. Similarly, the probability of a false No Go decision or $P(\text{False No Go})$ is obtained by summing the number of simulated trials where jointly \bar{Y}_i is less than 3 and Δ_i is greater than or equal to 3, and dividing this sum by the total number of trials where Δ_i is greater than or equal to 3.

Frequency-based calculations such as these were used to generate the complete 2×2 table of operating characteristics. For example, Table 4.2 shows the operating characteristics of a trial of size $n = 225$, based on 10,000 simulated trials. The numbers in parentheses are the theoretical probabilities based on the R function `pmnorm`

Note that the PTV for this scenario is approximately 67%. Again, this intrinsic property of the drug is based on predictions from our current models of drug action,

Table 4.2 Operating characteristics for $n = 225$ using point decision criteria

	No Go $\bar{Y}_i < 3$	Go $\bar{Y}_i \geq 3$	Total
$\Delta_i < 3$	23.71% (24.61%)	7.69% (8.02%)	31.4% (32.63%)
$\Delta_i \geq 3$	11.49% (11.51%)	57.11% (55.86%)	68.6% (67.37%)
Total	38.75% (36.12%)	61.25% (63.88%)	10,000 Simulations 100%

disease mechanisms and competitor information and is not related to the design or sample size of the study. In Table 4.2, PTV is calculated simply through drawing values of Δ_i and comparing these values against our target value and so for the 10,000 simulations above is subject to a small amount of sampling error – as the number of simulations increases we will approach our theoretical result that $PTV = 67.37\%$. In this example we know the distribution of Δ and so could state the probability of achieving the target value of 3 explicitly. In more realistic situations, we will not know this probability distribution – it may result from a nonlinear combination of many model parameters. A more detailed discussion of the practicalities of quantifying this value is discussed in more detail in Sect. 4.5.

The probability of a correct decision or $P(\text{correct})$ is obtained by summing up the probabilities of the diagonal cells in the 2×2 table corresponding to 23.71 and 57.11% for a total of 80.3%. The corresponding exact calculation for $P(\text{Correct})$ is reported as 80.5%. Whether this is high enough is a decision for the sponsor but in this case we consider it very reasonable. One additional question is whether the proportions of false Go and false No Go decisions are acceptable. While, overall, the design is achieving reasonable $P(\text{Correct})$, we may decide to investigate other designs if in the sponsor's view the probability of false No Go is unacceptably high.

In this example, our probability of making a correct decision is deemed reasonable. This suggests that for a sample size of $n = 225$, we can make good decisions based on this rule. The next question of interest may be whether we can continue to make reasonable decisions with smaller sample sizes and how $P(\text{Correct})$ varies with sample size. In a general sense, it is worth pointing out that there are several factors that influence the probabilities shown in this table: the underlying effectiveness of the drug characterised through the model describing treatment effects and the associated uncertainty in model parameters, the trial design, and the decision criteria. When investigating how the probabilities vary it is important to ensure that the practitioner is comparing like with like – comparing decision criteria within designs or comparing designs for fixed decision criteria.

If we vary the sample size, we can plot out how $P(\text{Correct})$, $P(\text{Go})$ and $P(\text{Go}|\Delta)$ change with sample size. Similar simulations were performed for sample sizes ranging from 10 to 1,000 subjects per trial. Figure 4.1 below shows selected operating characteristics as a function of sample size with probability of a Go decision, or $P(\text{Go})$ shown as the grey dashed line in Fig. 4.1 probability of a correct decision, or $P(\text{Correct})$, shown as the solid black line and probability of a Go decision given Δ , or $P(\text{Go}|\Delta)$, shown as the solid grey line. $P(\text{Go}|\Delta)$ was computed in the CTSs where Δ is fixed to the mean estimate of 3.27 for all trials, that is, the uncertainty in the estimate of Δ is not taken into account. Thus, $P(\text{Go}|\Delta)$ is somewhat analogous to a power calculation except that in this example the data-analytic decision rule is not a formal test of statistical significance.

Note that for this example $P(\text{correct}) > P(\text{Go}|\Delta)$ for sample sizes less than or equal to 1,000. Moreover, as the sample size increases, both $P(\text{correct})$ and $P(\text{Go}|\Delta)$ converge to 100% while $P(\text{Go})$ converges to the probability of a true Go decision corresponding to the probability that $\Delta_i \geq 3$ which equals 67.36% for this example. The reason that $P(\text{Go})$ does not converge to 100% is because the marginal variance

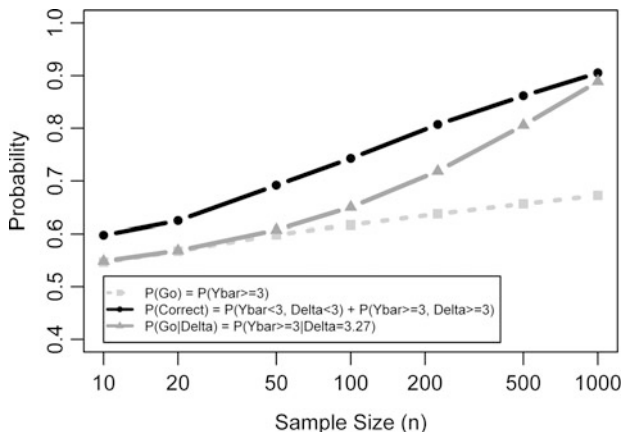


Fig. 4.1 Operating characteristics for point estimate criteria as a function of sample size

of \bar{Y} depends on both the variability or uncertainty in Δ denoted as σ_{Δ}^2 as well as the measurement variability denoted as $\sigma_{Y|\Delta}^2$ and only the latter term goes to zero as the sample size goes to infinity. In other words, the uncertainty in our prediction of \bar{Y} will always have a contribution due to our uncertainty in the prediction of Δ , which can only be reduced after the trial is conducted and an updated model prediction of Δ is obtained based on the data from the new trial.

4.3.3 Operating Characteristics for Decision Criteria Based on Interval Estimates

Now let us extend the discussion to the operating characteristics for the same “Truth” decision criteria (*i.e.*, Go if $\Delta_i \geq 3$), but with trial level decision criteria that are based on confidence limits. In choosing doses or treatments for further development we may decide to accelerate development of treatments or doses with good evidence of efficacy and some confidence that they might ultimately meet our target value efficacy, while dropping or stopping development of doses or treatments that show low probability of ever meeting our target value. If neither of these criteria is met, or if there is too much uncertainty in the current estimates, we may decide to pause and gather more information before making a “Go” or “No Go” decision. This latter decision may be seen as a “Pause” or “Grey” outcome. Figure 4.2 below shows how we might construct interval estimates based on trial data and compare these against two values: a null, zero effect (no difference between treatments) and our target value = 3.

If the treatment shows statistical significance (testing against 0) and the upper confidence limit of T is ≥ 3 then we would choose to develop that treatment further.

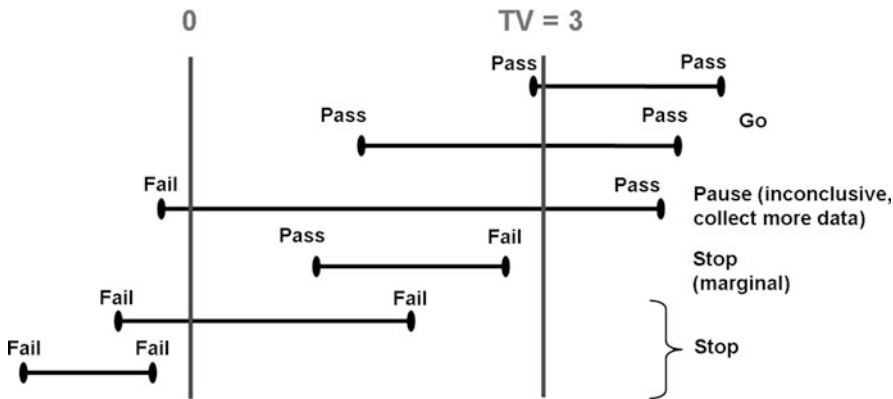


Fig. 4.2 Quantitative decision criteria based on interval estimates

If the lower confidence limit is <0 and the upper confidence limit is <3 then we stop further development. Where the interval estimate is wide and spans both 0 and $TV = 3$, the result is clearly inconclusive and we may decide to refine the study design with a view to reducing variability in the data analytic estimate. In the other case, where the lower limit is above zero but the upper limit does not reach our $TV = 3$ (vs. say $TV = 2.5$) and/or consider carefully whether the effect shown is sufficient to warrant further development given the costs, benefit risk of the treatment relative to any safety issues, etc. These cases are likely to involve a lot of cross-disciplinary discussion and, through our evaluations of the operating characteristics, we can facilitate discussion of these cases in advance of the trial itself, allowing refinement of the decision criteria or target value if required without biasing the actual trial outcome.

The mechanics of simulation for trials using interval estimate decision criteria are very similar to those described above in Sect. 4.3.1 for the point estimate decision criteria, and we use the same frequency-based calculations. Suppose, for example, we choose to make a Go decision if the data analysis shows $LCL_{80} > 0$ and $UCL_{80} > 3$, where LCL_{80} and UCL_{80} are the lower and upper limits of an 80% confidence interval (CI). Then, the probability of a Go decision, a correct decision and a Pause decision are given below.

$$P(\text{Go}) = \frac{1}{N} \sum_{i=1}^N I(LCL_{80} > 0, UCL_{80} \geq 3)$$

$$P(\text{Correct}) = \frac{1}{N} \sum_{i=1}^N I(LCL_{80} > 0, UCL_{80} \geq 3, \Delta_i \geq 3) + I(UCL_{80} < 3, \Delta_i < 3)$$

$$P(\text{Pause}) = \frac{1}{N} \sum_{i=1}^N I(LCL_{80} \leq 0, UCL_{80} \geq 3)$$

Table 4.3 Operating characteristics for a design with $n = 20$ using confidence limit criteria

	No Go $UCL_{80} < 3$ (%)	Go $LCL_{80} > 0$ and $UCL_{80} \geq 3$ (%)	Pause $LCL_{80} \leq 0$ and $UCL_{80} \geq 3$ (%)	Total
$\Delta_i < 3$	5.28	19.98	6.9	32.16%
$\Delta_i \geq 3$	3.70	56.35	7.79	67.84%
Total	8.98	76.33	14.69	10,000
				Simulations 100%

Table 4.4 Operating characteristics for a design with $n = 225$ using confidence limit criteria

	No Go $UCL_{80} < 3$ (%)	Go $LCL_{80} > 0$ and $UCL_{80} \geq 3$ (%)	Total
$\Delta_i < 3$	10.95	20.45	31.4%
$\Delta_i \geq 3$	1.3	67.3	68.6%
Total	12.25	87.75	10,000
			Simulations 100%

Note that the Pause decision does not depend on the “truth” and so we have a 2×3 table (Table 4.3) showing the results of 10,000 simulations when $n = 20$.

In this case, $P(\text{Go}) = 76.33\%$ while $P(\text{Correct}) = 61.63\%$. Again, $P(\text{Go})$ includes cases where the true effect is less than our target value. With this small sample size we have some “Pause” decisions made.

If we increase the sample size to $n = 225$, we get the results as shown in Table 4.4. Note that having increased the sample size we now have no “Pause” or Inconclusive results. $P(\text{Go})$ for this decision criteria and design is 87.75% while $P(\text{Correct}) = 78.25\%$. Using the confidence limit based approach we increase our $P(\text{Go})$ but slightly decrease our $P(\text{Correct})$ from the mean value criteria for the same design. We have an increased $P(\text{False Go})$ and decreased $P(\text{False No Go})$ using this criteria since the confidence limit approach is less stringent than the mean $> TV$ criteria. We only need to have 10% of the probability distribution above TV rather than 50%. Figure 4.3 below shows the influence of sample size on the operating characteristics for these decision criteria:

Interestingly, $P(\text{Go})$ is non-monotonic for increasing n , while $P(\text{Correct})$ and $P(\text{Go}|\Delta)$ tend to 100%. The non-monotonicity of $P(\text{Go})$ is due to the boundary condition when Δ approaches the target value of 3. For small sample sizes to reach a “Go” decision the lower confidence limit must be >0 but the interval estimate will be wide regardless of the true value of Δ . For larger values of n , the confidence limit shrinks so that even though the lower confidence limit is >0 the upper limit may be less than 3 resulting in a “No Go” decision. This non-monotonic property of $P(\text{Go})$ across sample sizes suggests that it is not a robust metric for trial performance.

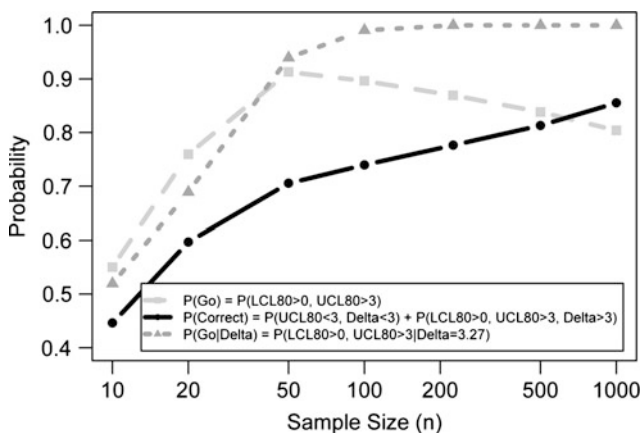


Fig. 4.3 Operating characteristics for interval estimate criteria as a function of sample size

Note also that for the confidence limit criteria, $P(\text{Correct}) < P(\text{Go}|\Delta)$, while for the point estimate (*e.g.*, mean) criteria $P(\text{Correct}) > P(\text{Go}|\Delta)$. Requiring the point estimate from the data analysis to be greater than a target value may be a high hurdle in early studies with small sample sizes, whereas in later studies, where achieving a threshold of efficacy is essential for labelling and marketing claims, it may be particularly relevant. In contrast, interval estimate approaches allow us to say something about the plausibility of achieving a target level of efficacy without ruling out effects that are close but less than this value.

4.4 Applying Decision Criteria in a Dose-Response Example

In the previous section we have shown the simulation process and how frequency-based calculations (counting different outcomes) are used to quantify the operating characteristics. We have shown how operating characteristics are affected by the choice of metric (mean value or confidence limit), target value, design (through sample size). In this section we look at how these methods are extended from a simple case to a more complex case study – where we derive quantitative decision criteria for dose selection and assess the operating characteristics of candidate trial designs.

4.4.1 Introduction to the Dose-Response Example

Smith and Marshall (2006) describe how informative prior information, based on the analysis of prior data, can be used in the context of evaluating the dose-response of a new compound and comparing it to that of a compound in the same drug class. They show how an E_{\max} model was used to describe the dose-response relationship in a meta-analysis of an existing compound across five studies, fitting a random

between-study effect to allow for study to study variability, and how the parameter estimates from this analysis were used to form an informative prior for the Bayesian analysis of a proof of concept design for the new compound by estimating the relative potency (RP) of the new compound relative to the previous compound. A key feature of the design was that the randomisation could be biased towards the new compound, using the informative prior to reduce the number of patients on placebo and the positive control treatment (the existing compound) within the trial.

To compare efficacy of a new treatment against placebo benchmarked against an existing compound the trial design would ideally consist of placebo, two active doses of the new compound and the existing drug – as positive control. We would normally power this type of trial for comparisons vs. placebo based on the performance of the existing compound. However, due to the sample size necessary for this comparison and the overall cost of the trial, this type of design was not considered feasible. As a result, instead of formal comparisons against placebo, the primary goal was to show improved selectivity of efficacy over safety in the novel compound and estimate relative potency between compounds on the primary efficacy endpoint.

The data generation model for the response Y for subject i with a given baseline covariate value Base_i is shown below:

$$Y_i = E_0 \left(\frac{\text{Base}_i}{\text{mean Base}} \right)^\lambda \left(1 + \frac{E_{\max} \cdot \text{Dose}_i}{(1 - \text{flag})\text{ED50} + \text{flag}(\text{ED50}/\text{RP}) + \text{Dose}_i} \right) + \varepsilon_i$$

E_0 , E_{\max} , ED50 and λ are parameters estimated using the historical data on the existing compound. $\varepsilon_i \sim N(0, \sigma^2)$ for subject i . flag is set to 1 for the dose of the new compound, and 0 if the prior compound. This allows us to simulate data for two different compounds sharing the same E_0 and E_{\max} effects.

The main criteria of interest reported in Smith and Marshall was the magnitude of the relative potency estimate RP. The study was to be considered a success if there was sufficient posterior probability of RP exceeding 1, *i.e.*, evidence that the ED50 for the new compound was statistically distinguishable from the ED50 of the prior compound *and* that the point estimate for the relative potency estimate was greater than 3, which was considered the minimal acceptable difference. A relative potency or increased selectivity for efficacy of 3 or greater was considered useful in terms of separation between efficacy and safety *i.e.*, equivalent efficacy at $3 \times$ lower dose than the prior compound without the associated safety issues. The paper provides operating characteristics for the analysis of various trial designs and investigates sensitivity to prior choice and input conditions, specifically different values of RP.

4.4.2 Operating Characteristics for Decisions Based on Relative Potency Alone

Here we consider the operating characteristics for different choices of decision criteria and use the ‘‘Truth vs. Trial’’ 2×2 table described in Sect. 4.2 above.

Table 4.5 Operating characteristics for decision criteria based on relative potency alone

	No Go (%)	Go $P(\text{RP} > 1) > 0.9$ and median $\text{RP} > 3$ (%)	Total
True $\text{RP} < 3$	45.5	5.2	50.7%
True $\text{RP} \geq 3$	7.6	41.7	49.3%
Total	53.1	46.9	1,000 Simulations 100%

Our chosen design is a 4 treatment study with placebo and the prior compound at its clinical dose, and two doses of our new compound. Randomisation is weighted towards the new drug; $n = 25/\text{group}$ in placebo and the prior compound arms and $n = 50/\text{group}$ in each of the new drug arms giving a total sample size of $N = 150$. In our simulations we use a distribution for RP so that we can examine the trial level operating characteristics across a range of plausible values for RP – Smith and Marshall used discrete values for RP in simulations to assess sensitivity. Here we generate values for RP from a log-normal distribution $\log(\text{RP}) \sim N(\log(3), 0.5625)$ which gives a distribution for RP centred around 3 with a 95% of potential values falling in (0.67, 13.45). This distribution for RP was considered a prior to be a realistic range for the relative potency of the new drug based on information from two different preclinical tests, one of which suggested an RP close to 3, while another suggested a larger RP. We weighted the distribution towards the former since large increases in RP or selectivity based on preclinical tests usually result in lower values when examining clinical efficacy.

For the “Go” criteria specified in Smith and Marshall (and described above: $P(\text{RP} > 1) > 0.9$ and posterior median $\text{RP} > 3$), we get the following 2×2 table for Truth versus Trial (Table 4.5).

Note that since the “No Go” criteria here is simply the complement of the “Go” criteria. The “true” RP in this case is generated from a log-normal distribution centred around 3 we expect to see at approximately 50% probability of simulated candidate drugs meeting the target value. $P(\text{Correct})$ for this criteria is 87.2%, so the combination of design, analysis and criteria together could successfully distinguish those cases where the true $\text{RP} < 3$ and those where true $\text{RP} \geq 3$, with little mis-classification.

4.4.3 *Operating Characteristics for Decisions Based on Relative Potency and Efficacy at the Top Dose*

The above study question and associated criteria only focus on the estimate of relative potency from the study, *i.e.*, whether the new compound has a higher relative potency or better selectivity than the prior compound. But, what if the study also had to determine whether the highest dose was sufficiently efficacious to

Table 4.6 Operating characteristics for decision criteria based on relative potency and effect at top dose

	No Go (%)	Go median RP > 3 and UCL of difference at 150 mg < -1 (%)	Total
True RP < 3 or difference at 150 mg \geq -1.5	47.9	6.3	54.2%
True RP \geq 3 and difference at 150 mg < -1.5	6.0	39.8	46.1%
Total	53.9	46.1	1,000 Simulations 100%

warrant further development? That is, we would want any dose taken forward for further development to have at least a certain magnitude of effect. To examine the impact of choosing different decision criteria using the same simulated data, we would now want to show that the estimated $RP > 3$ and that the difference between the top dose (150 mg) and placebo achieves a minimum clinically meaningful difference of < -1 . Thus, we take a trial criteria that point estimate $RP > 3$ and that the $UCL_{0.5} < -1$ for the difference between the maximum dose and placebo. This gives the following table (Table 4.6).

For these criteria $P(\text{Correct}) = 87.7\%$ although the PTV has decreased slightly – due in part to the additional criterion of requiring at least 1.5 points decrease in mean score at 150 mg vs. placebo.

One problem in the comparison between “truth” and “trial” here is that the trial criteria is a composite of a point estimate based criteria ($RP > 3$) and a confidence based criteria (UCL of difference at 150 mg < -1). Remember that the “truth” criteria is not tied to any particular design or analytical technique (assumes “perfect” knowledge) and so there is no equivalent to the confidence limit based criteria because the interval width would be infinitely small. We could say that the point estimate of the difference at 150 mg for the “truth” should be < -1 , but this is not exactly comparing like with like for “trial” vs. “truth”, since for the trial the point estimate is always < -1 . Therefore, we have constructed an argument that if the “true” difference at 150 mg is < -1.5 then we would expect the UCL of the difference at 150 mg < -1 in the trial

We now have two criteria, with which to evaluate the same design and the same analytic technique. With both of these criteria the $P(\text{Correct})$ is similar, but at this stage we would normally wish to discuss the operating characteristics of these criteria with the project team to discuss the fact that we achieve slightly lower $P(\text{False No Go})$ with the additional product requirement of an adequate effect size at 150 mg and the fact that this is a trade-off against a slightly higher $P(\text{False Go})$. Which criteria is more favourable depends on the particular research question of interest and what the plan is for future development of this compound. If 150 mg is the maximum dose that may be studied in a future trial, then we may wish to have

some assurance that this dose could achieve a clinically meaningful difference *as well as* the new compound having improved relative potency or selectivity over the existing compound. However, if higher doses are available, we may wish to simply show improved relative potency from this trial and then use model predictions to select the optimal dose for future trials.

4.4.4 Operating Characteristics for Decisions Based on the Estimated Effect at Each Dose

A third criteria worthy of investigation captures the ability of the design to pick the correct dose for future development. Ideally, we would like to take forward the lowest dose that provides the clinically meaningful effect, *i.e.*, the dose for which the effect is < -1 difference from placebo. Our design uses two dose levels of the new compound (75 and 150 mg) and we examine the design performance at each dose. It may also be possible that neither of these doses can achieve the requisite difference over placebo. To apply this criterion for a single simulated trial, we simply compare the estimated effect at each dose, based on the E_{\max} fit to the observed data for each simulation replicate, and count when each dose is the lowest dose with an estimated value < -1 . For the “truth” we must use the model parameters generated from corresponding data and evaluate the function at each dose level and count when this value is < -1 . If neither dose is < -1 then we count this for the column where no doses show the requisite effect. Using this criteria, we need to expand our 2×2 table to look at the truth and trial level results for each outcome (Table 4.7).

Table 4.7 Operating characteristics for decisions based on the estimated effect at each dose

	Estimated difference at 75 mg < -1 (%)	Estimated difference at 150 mg < -1 (%)	No doses show difference < -1 (%)	Total
True difference at 75 mg < -1	37.7	6.6	0.3	44.6%
True difference at 150 mg < -1	6.9	20.6	6.3	33.8%
No doses show difference < -1	0	4.4	17.2	21.6%
Total	44.6	31.6	23.8	1,000 Simulations 100%

$P(\text{Correct})$ here is the sum of the diagonal elements – where the criteria for the trial level estimated difference over placebo matches the truth based on showing a difference of at least -1 vs. placebo. Here, $P(\text{Correct}) = 75.5\%$. Note that there are some cases where the trial level “lowest dose” to achieve the criteria is higher than the truth (6.6%) and similarly some cases where the trial predicts a lower dose than the truth (6.9%). The impact of these incorrect decisions could potentially have serious implications for dose selection. If we take too low a dose into Phase 3 then we may find that our Phase 3 trial is underpowered, since we are overestimating the true effect at that dose, and fail to achieve significance. Conversely, if we take too high a dose into Phase 3 then although we will likely show a good effect, we may leave ourselves open to debate about whether a lower dose would indeed have still been effective. There should be further examination and consideration of simulation results for cases where we conclude that neither of the doses have sufficient effect, yet the truth is that one of the doses would indeed have delivered sufficient efficacy. Fortunately, the proportion of simulations where 75 mg is effective (in truth) but we conclude no effect is only 0.3%. The reasons for the other incorrect conclusions needs careful examination but in this instance we surmise that it is because the simulated E_{\max} and relative potency (RP) work together to make the efficacy at the top dose borderline, *i.e.*, just above -1 so the trial and truth outcomes are marginal. In a real trial the decisions for such borderline cases would doubtless be a trade off between safety, efficacy and other considerations. However, in simulations we can only apply a hard and fast decision rule.

4.5 Practicalities of Simulation in Model-Based Drug Development

Running simulations, collating results and conducting discussions of operating characteristics within project teams is a labour intensive and time consuming business. Smith and Marshall (2010) describe the need for proper planning of CTS and caution that poor planning of simulations can lead to poor inference in simulations just as in clinical trials themselves. Poorly defined objectives and poorly chosen metrics can lead to inconclusive results and no clear decision. Agreeing on clear objectives for the simulation exercise, and getting buy-in to a simulation plan or “protocol” will make it easier to define the necessary simulations and also make quality control of simulation outputs much easier. It is good practice to fully describe the simulation inputs – data generation models, parameter inputs, covariate distributions, design choices, assumptions – as well as analytical techniques and, of course, decision criteria. Due to the multi-disciplinary nature of CTS, it is also good practice to get buy-in from key stakeholders that the design space for simulations has been well described and that key scenarios are being addressed. There is an obvious tension between the desire to “optimise” a clinical trial design and the practicality of implementing that design. Successful clinical trial design

relies on good communication between the group conducting the simulations and operational colleagues.

There are two main methods for simulating the “truth” for each set of model parameters. In cases where random effects enter the model in nonlinear parameters, the mean of the individual response profiles is not the same as the typical individual (*i.e.*, with random effects set equal to zero). Usually we will wish to compare the mean of the simulated data against observed means from prior studies or literature in order to compare like with like. In these cases we must simulate for an arbitrarily large number of individuals, to integrate over the random effects, and then calculate the mean from the simulated data. If we are interested only in the central tendency or mean effect, then relatively small numbers of patients will yield accurate results. However, if we are using this data to categorise the proportion of responders or proportion of patients in a given category then much larger numbers of patients (*e.g.*, thousands) may be needed. If we remember that we are trying to simulate “truth” and trial for the same set of parameters then we can simulate for the “truth” and then subsample trial level results from this database of subjects.

It is important when interpreting simulation results to bear in mind that the operating characteristics also depend on the assumptions in the data generation model and analytic technique. If we only examine scenarios where the assumptions behind the data generation and data analysis match, our operating characteristics will be overly optimistic. If the assumptions do not match, our operating characteristics are likely to become worse. We should examine robustness of our decision making process to changes in our assumptions, examining operating characteristics to systematic changes (bias) in the data generation model parameters and population covariate distributions. Although these cases may not be very likely, it will allow us to look at “worst case” scenarios and check the performance of our decision criteria in these outlying cases. Despite the attempt of controlling inclusion and exclusion criteria in our trials to make them in some way “similar” to prior trials or investigations, invariably there are some changes in population that we cannot control for or anticipate. It is good practice to examine the sensitivity of our decision making process for these cases, since we wish to ensure that we make reasonable decisions even when the unexpected happens.

One useful benefit of performing CTS and evaluating operating characteristics in the early stages of trial design is that it provides an opportunity to evaluate the statistical methods outlined in the proposed statistical analysis plan (SAP) before the protocol is finalised. This means that early feedback into the SAP and statistical methods section of the protocol is possible much earlier than usual. Close collaboration between the statisticians responsible for the protocol statistics section and the SAP and the individuals responsible for running the CTS is vital to make best use of all information available in planning the analysis of the study.

Note that in the example above we generated new parameter values for the data generation model for each trial replicate. In this way we have a distribution of “true” outcomes across the trial replicates. CTSs are sometimes performed by fixing model parameters at a single value and then generating many replicates where the only difference between replicates is the draw of subjects from the residual error

distribution. This conforms to testing null and alternative hypotheses using simulation as long as the true treatment difference is fixed. While this may be of interest for hypothesis testing questions, we have found in practice that running a large number of simulations, drawing the data generation model parameters from a probability distribution addresses questions of false positive and false negative decision making for the “learning” type of questions. We may also wish to additionally evaluate simulations for particular “null” data generation models with no treatment effect in order to specifically and formally address Type I error questions for a particular design and analytic method.

How many simulations is “sufficient” is a subjective matter, but there may be considerations around generating sufficient parameter sets to adequately explore the parameter space, in order to ensure that the design, analytic technique and decision criteria are robust to extreme values of the parameter space. If there are many competing designs or decision criteria then it may be worth doing “pilot” simulations of a few hundred simulations in order to find any gross differences and perhaps eliminate certain designs before commencing simulations of thousands of replicates. Note that with smaller numbers of simulations the possibility of simulation error – differences purely due to the stochastic nature of simulation – may contribute more to differences between simulation runs.

If the operating characteristics of the decision criteria are not acceptable, we have a number of possible factors that could be changed to improve the situation. We may change the design, taking more doses or more subjects per dose. We may change the analytical method, perhaps employing a different form of analysis or allowing a flexible class of models to allow for different observed data or we may employ Bayesian methods with informative priors on certain parameters to quantitatively borrow strength from prior information or subjective opinion, as we have done in the example in Sect. 4.4. Finally we may change the decision criteria themselves – although we caution against changing the target value since this has presumably been agreed at a project wide, or perhaps indication level – or we can investigate whether criteria based on point estimates or interval estimates increase $P(\text{Correct})$.

4.6 Discussion

CTS is predicated on having predictive models for the data generation step. Generating these models is not a trivial task since it often involves the synthesis of a large amount of previous data into pharmacokinetic, pharmacodynamic, longitudinal disease models, dropout models, meta-analysis and many other possible sources of information. Kowalski *et al.* (2008) describe how these various models came together to predict trial outcomes and assess operating characteristics for a pain compound. By combining these models these authors were able to simulate realistic trial data and predict to a change in formulation and account for different data imputation methods in the event of missing data. When making predictions

from one formulation to another and across different drugs it is often required to combine these models in order to get the most predictive data generation model.

A model which is predictive of future data and describes the outcomes necessary for analysis and evaluation of the decision criteria is all that is required for this process. One should add complexity to the models only if it improves the ability to generate realistic trial data or to address specific questions of interest in the simulation and evaluation of the operating characteristics. Note that a modelling effort to describe the structural, covariate and stochastic models (population analysis) for a single trial usually attempts to describe and quantify all sources of variability between and within individuals. For example, if a given covariate is not a design feature of the future study, *i.e.*, if we are not stratifying by a covariate value or changing inclusion/exclusion criteria within the new study, then it may be possible to subsume this covariate effect into the more general between-subject variability and simplify the model. Again, the only strict criteria is that the resulting model should still be predictive of a future trial.

However, the general maxim “garbage in – garbage out” certainly applies. Ensuring that both individual model components (disease model, drug efficacy model, drug safety model, dropout model, etc.) accurately describe data on which they are built, as well as the *joint* model being predictive of clinical trial results is critical in the success of this whole procedure. This joint model drives the quantification of PTV and portfolio decision making, as well as the trial level evaluations. The model should be built early in the drug development lifecycle and then refined and updated regularly to ensure that the best available information informs our decisions. Of course, each time we have clinical trial data from the compound itself we should update these models to reflect the new information. The scope of impact of these models is wide: mechanistic models of biologic process informing preclinical work; clinical pharmacology informing dosage regimen; clinical trial results informing clinical trial programmes and individual trial design; meta-analysis of comparator data informing trial programmes and also post-licencing reimbursement discussions.

In the example described in Sect. 4.4, we did not use the full complexity of these models since we were predicting from one compound to another within the same class and with identical study conduct and inclusion/exclusion criteria to the previously studied compound. Also, in this case we were primarily interested in the operating characteristics of the design and analytic technique rather than making accurate predictions about the likely trial outcomes. As a consequence, our simple model was sufficient for this stage of simulations.

What values of $P(\text{Correct})$, PTV, $P(\text{False GO})$, $P(\text{False NO GO})$ are acceptable? This is entirely up to the sponsor. We advocate that, analogous to the concept of “power”, $P(\text{Correct})$ can be set at an organisational level – perhaps the organisation would not consider decision criteria with $P(\text{Correct})$ less than 0.8. This seems a reasonable approach since this metric incorporates both correct NO GO and correct GO decisions and so in a sense is independent of the ability of the drug to achieve the target value and is influenced chiefly by the design, analytic method and decision criteria themselves.

Acceptable levels of PTV are more problematic to define, and as mentioned previously, these will change throughout the drug development life cycle as we gain more information about the drug and competitive landscape. The decision will also be influenced by whether this is a drug in an area of high unmet medical need perhaps with unprecedented mechanism. In these cases an organisation may be prepared to carry a much higher risk since the benefits of a successful drug are much higher. As a consequence, acceptable PTV is essentially a portfolio decision. Acceptable levels of $P(\text{False GO})$ and $P(\text{False NO GO})$ are again difficult to define, since they are context specific to an individual drug, disease area and stage of drug development. If we fix an acceptable $P(\text{Correct})$ and we know PTV then all that we can do is to trade off $P(\text{False GO})$ and $P(\text{False NO GO})$. Which of these incorrect decisions is more critical than the other is again context specific and may be influenced by the stage of drug development. Having false GO decisions in late development is to be avoided purely due to the cost of running large clinical trials and the fact that carrying forward a drug which ultimately does not meet our predefined criteria will lead to a lack of confidence from stakeholders, internal and external.

Model-based drug development and quantitative decision making in particular involves input from many different sources gathering the right data at the right time to increase our understanding of drug and disease effects, quantified through our models; building predictive models to allow us to make inferences and predictions about the likely range of effect of our new drug; defining decision criteria relevant to clinical practice; performing simulations to quantify the probability of achieving a successful drug, then comparing our decisions at the high level to the trial level analytic results (as described in detail in this chapter); and then using those metrics to underwrite decisions made about our drug in the light of the newly accumulated data. This cycle of data collection, modelling, prediction and inference underpins much of the learn and confirm cycling of drug development. Our experience is that this process has highest impact when it is truly multi-disciplinary. When all parties bring their particular knowledge and skills to the table, there is great potential to make better decisions, reduce the number of cycles in the drug development process and ultimately to get useful medicines to patients more quickly.

References

- Azzalini A, Genz A (2009) mnormt: R package for multivariate normal and t distributions. <http://cran.r-project.org/web/packages/mnormt/index.html>. R Package version 1.3-3
- Box GEP (1966) Use and abuse of regression. *Technometrics* 8:625–628
- Chuang-Stein C, Kirby S, French J, Marshall S. Choose right metrics to enable sound decisions. Presented at the FDA/Industry workshop, Washington DC, 23 September 2009. (<http://www.amstat.org/meetings/fdaworkshop/index.cfm?fuseaction=AbstractDetails&AbstractID=300608>)
- Kowalski KK, Olson S, Remmers AE, Hutmacher MM (2008) Modeling and simulation to support dose selection and clinical development of SC-75416, a selective COX-2 inhibitor for the treatment of acute and chronic pain. *Clin Pharm Ther* 83:857–866

- Lalonde RL, Kowalski KG, Hutmacher MM, Ewy W, Nichols DJ, Milligan PA, Corrigan BW, Lockwood PA, Marshall S, Benincosa LJ, Tensfeldt TG, Parivar K, Amantea M, Glue P, Koide H, Miller R (2007) Model-based drug development. *Clin Pharm Ther* 82:21–32
- Sheiner LB (1997) Learning and confirming in clinical drug development. *Clin Pharmacol Ther* 61:275–291
- Smith MK, Marshall S (2006) A Bayesian design and analysis for dose-response using informative prior information. *J Biopharm Stat* 16:695–709
- Smith MK, Marshall A (2010) Importance of protocols for simulation studies in clinical drug development. *Stat Methods Med Res* (Available online. doi: 10.1177/0962280210378949; <http://smm.sagepub.com/content/early/2010/08/03/0962280210378949>)

Chapter 5

Decision-Making in Drug Development: Application of a Clinical Utility IndexSM

Timothy J. Carrothers, F. Lee Hodge, Robert J. Korsan, William B. Poland,
and Kevin H. Dykstra

Abstract The Clinical Utility IndexSM (CUISM) is a practical and useful approach for informing drug development decisions where multiple aspects of a drug's clinical profile must be optimally balanced. In its most common application, a CUI is a model of population-level preferences across and within the various efficacy, safety, and tolerability attributes of a product profile for a given indication. By combining the multiple dimensions of a product profile into a single unit of utility, the CUI can easily be linked to pharmacometric simulations of clinical endpoints, thus extending the reach of clinical trial modeling and simulations further into the decision-making process. Although the use of CUI (and related multiattribute methods) is relatively new to the field of drug development, its application is steadily growing as project teams discover the benefits of integrating “utility” models into the overall pharmacometric toolbox.

5.1 Introduction

It is well understood that any drug has both beneficial and adverse effects, and that the balance of these, the benefit-risk tradeoff, depends on dosage and regimen. Other aspects of a particular drug may also make it more or less attractive as a treatment choice, whether to the patient, prescriber, payer, or drug developer, including, for example, convenience of the regimen, increased cost of goods for a higher dose, and perceived benefit of a new mechanism of action. Together, the safety and efficacy attributes, along with the other drug characteristics, comprise the product profile for a potential new drug.

Drug development teams face many challenges in understanding how their compounds perform across these various dimensions (*e.g.*, safety, efficacy,

T.J. Carrothers (✉)

Pharsight Consulting Services, Pharsight – A Certara Company,
100 Mathilda Place, Suite 160, Sunnyvale, CA 94086, CA, USA
e-mail: timothy.carrothers@certara.com

tolerability, convenience of regimen, etc.), including both the high degree of uncertainty in actual performance as well as the ambiguity surrounding the relative importance of the tradeoffs among them. As an example, the expected drop in mean arterial pressure due to a candidate antihypertensive can be estimated from clinical data (or perhaps extrapolated from a relevant preclinical model). However, the importance of that effect relative to an increased incidence of orthostatic hypotension is a subjective judgment. In this example, and throughout drug-development decision-making, there is a need to systematically and transparently weigh these tradeoffs and to clearly communicate the basis for the tradeoffs to stakeholders external to the project team.

Within each dimension, there is substantial uncertainty regarding key compound attributes that will be used to compare the candidate to current and future potential competing products. This uncertainty arises from the lack of sufficient evidence, given the stage of development, for efficacy compared to placebo or the standard of care, the incidence of key adverse effects, etc. For instance, questions such as “What is the expected placebo-adjusted change from baseline in mean arterial pressure and its associated uncertainty in the specified patient population for Drug X under a given dose regimen?” can only be answered based on the scientific understanding available at that time. The information relevant to assessment of the effect sizes is often found across a variety of sources (*e.g.*, *in vitro*, animal, human healthy subjects, and human patients) that must be integrated to predict how the candidate compound will perform on specific endpoints (such as mean arterial pressure) that prescribing physicians and patients can understand.

Other chapters of this book show examples of how the proper application of pharmacometric modeling and simulation can help project teams answer such questions by improving the knowledge gathering and assimilation process. In a broad sense, the practice of modeling and simulation enables decision-makers to better characterize what they know, what they do not know, and to what extent additional information-gathering activities can improve their understanding regarding specific drug attributes. At a tactical level, simulations of the developed models can give a prediction of the likelihood of achieving a specified goal for an attribute (*e.g.*, a 2-mmHg decrease in mean arterial pressure) in the projected patient population.

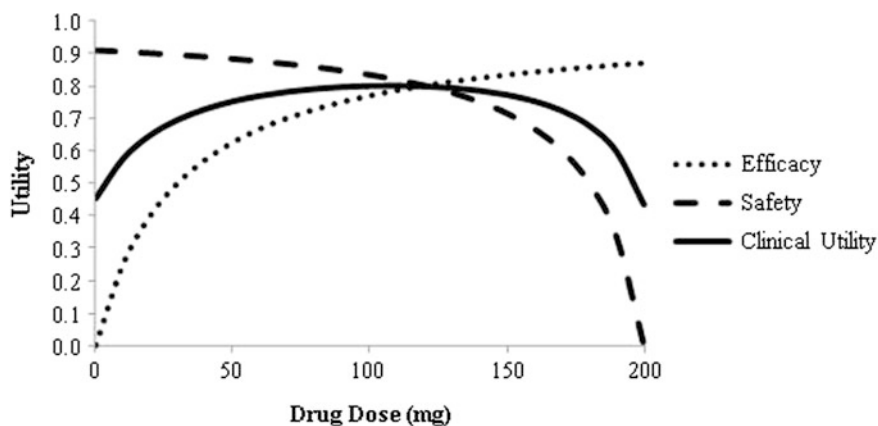
If the decision at hand depends on only one key attribute, then these approaches can be sufficient. In general, however, project teams face decisions that require them to confront tradeoffs between the competing attributes of the drug relative to its potential competitors. In other words, while the typical scope of pharmacometric modeling and simulation allows the project team to assess their *scientific* understanding of each attribute, this alone will leave decisions ambiguous when attributes compete with one another (*e.g.*, more efficacy but more adverse effects at higher doses). Another set of tools is needed to assess the team’s *preferences* among the different possible product profiles. For instance, would patients prefer the higher dose of antihypertensive Drug X that is expected to provide additional efficacy at the expense of slightly more risk of postural hypotension? If an optimal balance of efficacy and safety can be found at twice-daily dosing, to what extent would

patients be willing to trade some efficacy and/or safety for the additional convenience of once-daily dosing? Moving beyond the realm of determining the optimal dose and regimen, how does Drug X compare in value to patients and market share to competing established therapies, as well as other potential competitors in development, and how can different levels of uncertainty (*e.g.*, between compounds in development vs. those on market for several years) be incorporated into the decision?

Project teams in drug development thus face what can be called multiattribute decisions under uncertainty. For these situations, varieties of approaches have been used by project teams, not all of which are optimal. In an extreme but not uncommon example, a dominant team member may impose his/her beliefs regarding the “right” or “acceptable” level of safety. In spite of the fact that the pharmacometrics team member may have done an excellent job in modeling and simulating safety and efficacy attributes, a suboptimal decision may be made that is not formally informed by the pharmacometrics contribution. Another potentially suboptimal mode is for team members to focus just on a few best-studied characteristics such as immediate efficacy and tolerability; while net benefits may be calculated, the true complexity, along with possible key drivers at the margin (*e.g.*, “long-term” safety), of the patient prescribing decision are neglected. In many cases, the project team may feel it is making a good decision when in fact it may not be. In any case, where the decision involves multiple objectives, attributes not explicitly considered by the team during the decision process are implicitly treated as irrelevant to the decision, which may or may not ultimately be the case.

To meet this challenge, over roughly the last 10 years some project teams have been introduced to a multiattribute utility modeling approach (Keeney and Raiffa 1976; Keeney 1992) known in the drug development field as the “Clinical Utility IndexSM,” or CUISM (Korsan *et al.* 2005). Using this approach, preferences regarding the various relevant product attributes (which typically have different units) are modeled, allowing one to translate each attribute’s predicted performance to a common metric – “utility.” Once this is done, the attributes can be combined (*i.e.*, added together), generating a description of the compound’s net utility. Thus, this utility reduces the multiple attributes to a single number. This concept is illustrated in Fig. 5.1, which shows two attributes, efficacy and safety, being combined into a single metric of clinical utility to identify an optimal dose. Note that the quantities (*i.e.*, efficacy, safety, and clinical utility) being plotted share the common unit of utility. Also, note how each attribute changes at different doses. The CUI process incorporates formal techniques for creating this “preference” model in which the conversion from the original attributes’ units takes place. (Details of the process, such as the methods by which within-attribute utility functions and cross-attribute weights are determined, will be shown in detail later in the chapter.) When the questions being addressed imply that a single metric exists, *e.g.*, “What is our *optimal* dose?,” “Are we *better* than the competition?” these features of the CUI and its process are well suited to the problem.

CUI is a specific application of principles from the theory of multiattribute utility. Although somewhat new to the field of drug development, multiattribute



Note: Here, 'Safety' refers to relative lack of drug-related side effects. "Negative" attributes will decrease in utility with greater incidence (or value); thus, higher levels of utility correspond to lower levels of the adverse event.

Fig. 5.1 A basic illustration of the utility concept

utility modeling has been successfully applied in a variety of fields since its development in the field of decision theory many decades ago. Specific examples of other applications include design of public museums and libraries, siting of an electric power plant, natural gas exploration, and blood bank operation (Keeney 1992).

The outputs of the certain pharmacometric procedures, in which the likelihoods of the possible multiattribute product profiles can be assessed, provide the estimates of how the drug will perform and how uncertain the estimates are, given the available information. Beyond the estimation of the index, use of the CUI allows modelers and the broader project team to become decision-focused and to align the quality of their scientific understandings with a comprehensive and systematic decision-making process (Hammond *et al.* 1999; Matheson and Matheson 1998). The process of creating the index provides a framework for communicating the assumptions, trade-offs and state of knowledge, allowing increased information sharing. Often, participants of the process report that the process itself enables them to become better aligned with respect to their overall goals, which contributes to an efficient organization. In addition, having calculated the index, one can then investigate it to discover key sensitivities. This allows one not only to understand the value of the decision alternatives at hand, but also to assess how to *improve* those options.

In this chapter, we provide a case study-based introduction to the CUI process in practice. The first section following the introduction provides an overview of the CUI process. The next section gives a more detailed example of an anonymized, real-life case study. We then review the recent literature with respect to other applications of the CUI and related approaches. Finally, we assess the state of the current application of CUI in drug development, offering practical tips for its successful implementation as well as warnings regarding potential pitfalls.

5.2 A CUI Overview

5.2.1 *Setting the Decision Context Before CUI Creation*

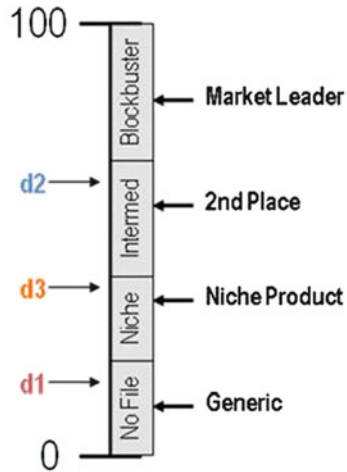
A multi-step process is used in the application of a CUI. While the creation of the CUI (*i.e.*, the multiattribute preference function) is central to the process, it should be thought of as just a means to the end of making a high-quality decision – one that meets the needs of relevant stakeholders. As such, the first step should be to carefully define the decision to be made, the point(s) of view of the decision-maker(s), and the scope boundaries. This step should also include a discussion of the overall goals for the compound's development (Keeney 1992). Although some of these steps may not be later explicitly incorporated into the CUI function itself, they each contribute to the overall quality of the process.

Defining the overall questions that the project team needs to answer is essential, as a variety of questions can be addressed by CUI, and the project team needs to be “on the same page” amongst themselves for the process to be effective. There is often a nesting of the questions to be addressed, and a high-quality discussion will allow the team to drill down to the specific preference “decision” that they wish to model. For instance, one stream of questions could look like this:

- Should we make a no-go decision before advancing this compound into late-phase clinical trials? Note: the CUI is better suited for a no-go than a go decision at this stage, because it may not incorporate development cost, market value, and risk factors that could make a go decision a poor choice (Poland *et al.* 2009), but such factors can certainly be included, if data is available.
- How can this compound be differentiated from its competitors in a crowded market?
- Will the regulatory agencies approve the compound given the expected product profile and associated evidentiary database?

In addition to the obvious application to dose optimization, a popular application is to support go/no-go decisions. In these cases, a CUI can be constructed to model the prescribing decision as a proxy for overall sales, and thus, commercial viability of the product. Because utility is a relative metric, scaled from 0 to 100, or, equivalently, 0 to 1, (*i.e.*, the overall units do not have meaning in isolation), the end goal may be to compare the compound relative to competitors. In the example shown in Fig. 5.2, utility is displayed on a vertical axis, and the 0–100 interval has been discretized into categories based on the relative utility of four currently marketed products, denoted as “Market Leader,” “2nd Place,” “Niche Product,” and “Generic.” These categories are labeled as “Blockbuster,” “Intermediate,” “Niche,” and “No File” (*i.e.*, “no-go”), corresponding to the overall outcome expected for each interval. Possible profiles of the candidate drug, denoted “d1,” “d2,” “d3,” “d4,” etc., are placed on the scale based on their utility and can then be mapped to commercial viability based on their place relative to marketed therapies.

Fig. 5.2 Using utility to link to commercial viability



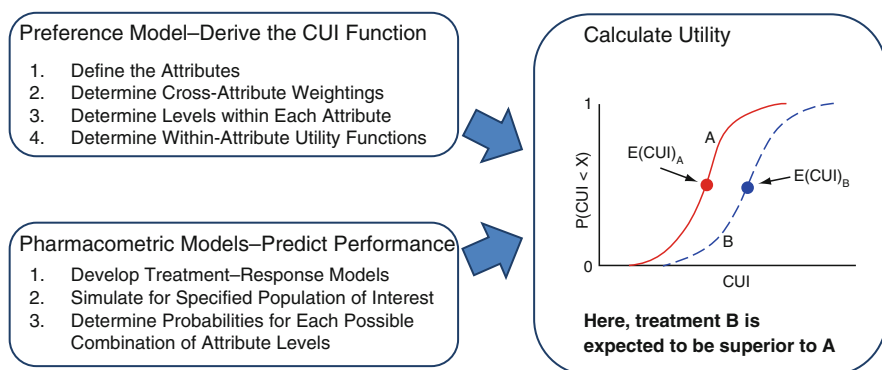
Note: d1, d2, and d3 are possible product profiles. “No File” (i.e., “no-go”), “Niche”, “Intermed.”, and “Blockbuster” represent discretization of the 0-100 utility range into market-meaningful categories. These categories are defined based on the translation of the known profiles of currently marketed products (“Market Leader”, “2nd Place”, “Niche Product”, and “Generic”) with specific levels of known commercial success (or lack thereof).

The second step is to clarify the perspective of the decision-maker(s), the person or group whose preferences are being modeled. In the case of the prescribing decision, this is defined as a typical physician, incorporating his/her perceptions of the patient’s preferences as well. In the case of a regulatory decision, it is the regulatory agency. In the case of a sponsor’s overall “Go/No-Go,” it can be the preferences of senior management acting in the best interests of the company shareholders. Once the decision and decision-maker are clarified, it is easier to define the scope of the decision.

Finally, it is necessary to define whose preferences will be elicited for the CUI construction, as a proxy for the ultimate decision-maker. Typically, this is the project team or a group of key opinion leaders.

5.2.2 The Clinical Utility Index: “Nuts and Bolts”

Figure 5.3 shows the integration of construction of the preference model (i.e., “Derive the CUI Function”) with standard pharmacometric modeling (i.e., “Predict Performance”) in order to calculate utility for two competing treatments. The steps



Note: The x-axis is utility. $E(CUI)_A$ is the expected CUI for treatment A. The y-axis is in units of probability, where $P(CUI < X)$ is the probability that the CUI of a treatment is less than the value X .

Fig. 5.3 The Integrated Clinical Utility Index (CUI)-pharmacometric process

in the derivation of the CUI function are explained in greater detail later in this section; they can be summarized in broad terms as the interconnected processes of defining “how to measure the dimensions of performance” (*i.e.*, attributes and their levels) and defining stakeholders’ strengths of preference among possible outcomes (*i.e.*, cross-attribute weightings and within-attribute utility functions). The steps in the pharmacometric process are likely familiar to the reader, with the exception of the third step, which arranges pharmacometric simulation output into a form suitable for linking to the product profile-focused CUI function. Since each possible product profile will have both an overall utility (represented by the CUI “score”) as well as an associated probability of realization, the net result of integrating the pharmacometric output with the CUI function is a probabilistic description of the treatment’s clinical utility. This process can be used to compare competing treatments, as shown in Fig. 5.3, or to identify optimal doses, as shown in Fig. 5.1, or to benchmark against established therapies, as depicted in Fig. 5.2.

Once pharmacometric simulations are complete, the calculation of CUI typically requires just simple algebra within a Monte Carlo simulation procedure. Simple algebra is used to translate drug performance on each attribute (*e.g.*, measured in its own unit at a particular dose and regimen) into its contribution to CUI (converted into the unit of utility). Monte Carlo simulation is used to integrate the uncertainty in this performance, producing predicted CUI and its uncertainty. (The example calculation in Sect. 5.2.3 is divided into two parts, corresponding to each of these elements.)

For each treatment (*e.g.*, drug and dose) and for a particular drug performance outcome (*e.g.*, level of efficacy AND safety AND other attributes’ levels), the following formula is the basic linear CUI model (5.1). The CUI for a given treatment is a weighted sum of the individual attributes’ utilities. This is described in decision

analysis texts (Clemen 1991; Keeney 1992) as linearly additive; there are neither interactions between the preference models of individual attributes nor inclusion of decision-maker risk aversion in the utility calculation. (This assumption is important for providing tractability to the process used to define the CUI function.)

$$\text{CUI}(x_1, x_2, \dots, x_n | \text{treatment}) = \sum_{i=1}^n w_i U_i(x_i | \text{treatment}) \quad (5.1)$$

where x_i is the performance level of the i th attribute of the treatment, w_i is the weight of the i th attribute (characterizing the relative importance between attributes), and $U_i(\cdot)$ = the utility function providing the utility (typically with range of 0–1, or 0–100) of the i th attribute given its performance level. The attribute levels and their associated weights establish the association between the different performance level outcomes and utilities.

The relative strength of preferences is captured by the CUI function’s weights that pre-multiply the preferences in the utility function. This is known as the “elicitation” of the CUI function. It consists of two interconnected parts: weighting of attributes and definition of utility functions within each attribute. The steps need not be rigidly ordered; in fact, some iteration is often necessary to provide a “reality check” as to the acceptability of the preference function being created (for related reading, see the online supplemental material for Poland *et al.* 2009).

We will now describe one implementation for the elicitation process that we have utilized in over a dozen applications. The process is implemented in two sequential procedures: (1) Identify critical attributes, their ranges of relevance, and their overall preference weights relative to one another, and (2) Identify metrics and relevant response levels for each attribute, then assign preference values for each level within an attribute.

In procedure (1), a method known as “swing-weighting” is used (von Winterfeldt 1986; Clemen 1991). Here, a critical first step is to define the relevant ranges of each attribute (units used in defining the ranges are determined by the attribute). The least acceptable level of each attribute (*i.e.*, “bottom” of range in a utility sense, as “more” or “less” of an attribute can be preferred in different situations, depending on the attribute) should be preferred to any level at which the drug would automatically be discontinued – this is a critically important part of the elicitation process; otherwise, the assumption of a strict zero to one range behind the utility function is violated. Similarly, the most desirable level (*i.e.*, “top” of range in a utility sense) of each attribute should be defined by the best value for attribute that can be achieved by any of the competing therapies under discussion. As a second step, inter-attribute weights are elicited via a process in which the attributes are all each first set to their respective lowest levels. Next, it is determined which attribute would provide the greatest utility if moved to its highest level, keeping all others at their lowest. This attribute then receives a preliminary weight of 100. Subsequently, each other attribute’s weight is elicited as a comparison to the utility of moving it from “Lowest to Highest” relative to doing the same for the reference attribute. For example, the next attribute may receive a weight of 50, reflecting a feeling that moving it from its

“Lowest” to its “Highest” is about half as impactful compared to the first attribute. The process continues (*e.g.*, for five attributes, it could result in preliminary weights of 100, 50, 30, 30, and 10) until all attributes have received a preliminary weight. Once this is complete, the preliminary weights are normalized so that they sum to one (*e.g.*, as $100 + 50 + 30 + 30 + 10 = 220$, the final inter-attribute weights would be 0.454 [100/220], 0.227 [50/220], 0.136 [30/220], 0.136 [30/220], and 0.045 [10/220]).

In procedure (2), utility functions are elicited for each attribute independent of the other attributes. This measures preferences within each attribute, in contrast to procedure (1), which measured preferences across attributes. Standard methods (see “standard gamble” as defined in Keeney and Raiffa 1976) for additive utility functions are typically used, but simpler methods are also possible (Poland 2009, online supplemental material). Again, it is critical that this is done only within the ranges of relevance; otherwise, the preference weights will be inaccurate. Typically, as part of this procedure, the ranges for continuous attributes can be discretized into several meaningful levels. The top level for each attribute is given a utility of one, and the bottom level is given a utility of zero. Intermediate levels are assigned utilities between these based on relative preference between levels within that attribute, while considering only that attribute.

5.2.3 *Calculating Utility: A Quick Example*

Once the utility function for CUI is fully defined, it is used in conjunction with predicted likelihoods of different attribute levels to calculate an expected CUI. In the following fictitious and simplified example (Fig. 5.4), a single dose of a new drug and of a comparator are being compared. Given the performance of each of these treatments (which for now is assumed to be known with certainty), their attributes provide the following utilities which, when summed, provide an overall assessment of the tradeoffs via total CUI. Note that “negative” attributes, such as adverse event #1 (AE 1), will decrease in utility with greater incidence (or value); thus, higher levels of utility in AE 1’s row of the table correspond to lower levels of the adverse event.

In this example, despite having a large advantage on the first attribute (an efficacy measure we will call “Effect 1”) compared to the comparator, the new chemical entity (NCE) performs far worse in terms of adverse events (AE 1). Given this tradeoff, its CUI is lower than the comparator’s.

An attribute, whether having discrete or continuous outcomes, can be translated into one with discrete probabilities for calculations. For example, Effect 1 in the above example may be expressed as a continuous metric. Either via statistical analysis, subjective assessment by clinical subject matter experts, or modeling and simulation, the effect and its degree of uncertainty can be characterized. The uncertainty can be computed so that it correctly includes the impact of between-patient and/or – trial variability as well as underlying parameter uncertainty. As an example, assume the

Fig. 5.4 Example of CUI calculation

NCE			
Attribute	U_i	w_i	Contribution
Effect 1	0.4	0.4	0.16
AE 1	0.32	0.3	0.096
Effect 2	0.25	0.3	0.075
Total CUI			0.331

Comparator			
Attribute	U_i	w_i	Contribution
Effect 1	0.3	0.4	0.12
AE 1	0.61	0.3	0.183
Effect 2	0.25	0.3	0.075
Total CUI			0.378

true population mean value of Effect 1 for the drug is uncertain. Also, assume this uncertainty can be characterized by a probability distribution from patient level data across multiple clinical trials using mixed effects regression and simulation. For example, when the effect is estimated to be 100, the uncertainty in this value can be summarized by a standard error of 20 (curve in Fig. 5.5).

Assume the team has provided cutoffs between Effect 1 levels and their associated values as follows:

- <60: Effect 1 contributes zero to utility of Effect 1
- 60–90: contributes 0.3
- 90–120: contributes 0.4
- >120: contributes 1.0

The continuous distribution can be used to assess the discrete probabilities that the Effect 1 value falls into each of these categories (Fig. 5.5).

In a real case, one would use Monte Carlo simulation to incorporate the uncertainty in the performance of the drug and thus generate predictions that include uncertainty. The CUI calculation process is as above; however, it is repeated many times with performance levels randomly sampled each time, and the overall CUI is captured for each of these samples. The result is a distribution of CUIs for each treatment. This distribution can be summarized using a mean or median, along with an uncertainty interval.

The generic process for performing this Monte Carlo simulation is as follows:

- Randomly draw a utility outcome for each attribute, given the possible levels, their values, and their probabilities
- Multiply the utility for each attribute by that attribute’s weight to derive its contribution to total CUI

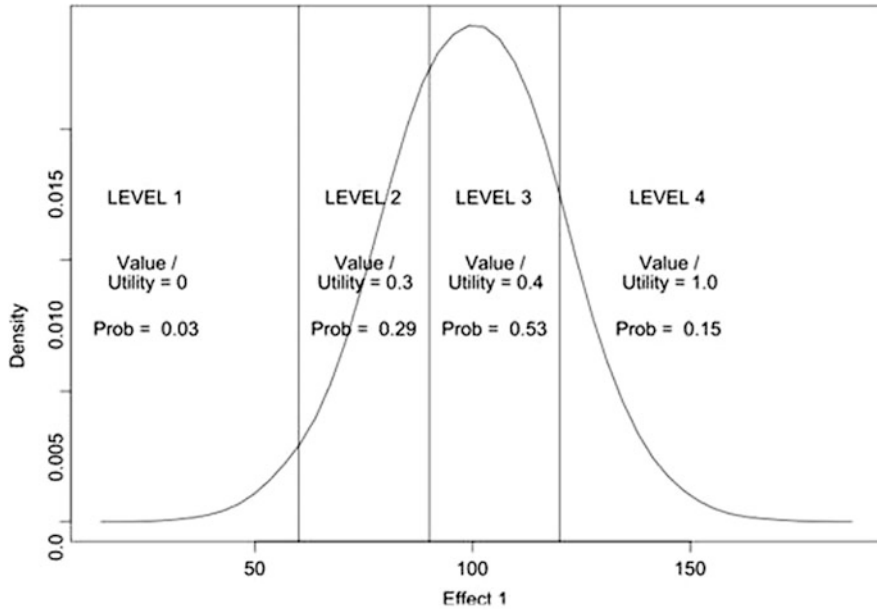


Fig. 5.5 Discrete levels for drug efficacy

Iteration	Randomly drawn U_i			Weights W_i			Contribution			Total CUI
	Effect 1	AE 1	Effect 2	Effect 1	AE 1	Effect 2	Effect 1	AE 1	Effect 2	
1	1.00	0.50	0.10	0.40	0.30	0.30	0.400	0.150	0.030	0.580
2	0.30	0.32	0.25	0.40	0.30	0.30	0.120	0.096	0.075	0.291
3	0.30	0.32	0.25	0.40	0.30	0.30	0.120	0.096	0.075	0.291
...
998	0.40	0.50	0.10	0.40	0.30	0.30	0.160	0.150	0.030	0.340
999	1.00	0.32	0.25	0.40	0.30	0.30	0.400	0.096	0.075	0.571
1000	0.40	0.32	0.10	0.40	0.30	0.30	0.160	0.096	0.030	0.286
mean	0.179	0.106	0.092							0.377
median	0.160	0.096	0.075							0.331
95th percentile	0.400	0.150	0.300							0.610
05th percentile	0.120	0.000	0.030							0.195

Fig. 5.6 Integrating CUI predictions using Monte Carlo simulation

- Sum the contributions across all attributes to derive total CUI
- Record the total CUI (and each attribute’s individual contribution)
- Repeat this process for n iterations

The resulting distribution of recorded CUIs will characterize the uncertainty in CUI, as well as metrics that represent its expected value and central tendency. The uncertainty in CUI reflects the uncertainty in the current understanding of how the product would perform in an infinitely large population.

Continuing the example above (but now assuming there is uncertainty in how the drug will perform), the results of a Monte Carlo simulation process like that just described may be as shown above (Fig. 5.6).

Thus, for this particular treatment (a particular dose of the drug) the mean total CUI would be 0.377 with a 90% prediction interval of 0.195–0.610.

Here, the “treatment” that was assessed was a specific dose of a specific drug given under a specific regimen. Note that the CUI for additional treatments (as represented by different combinations of drug, dose, regimen, etc.) can also be calculated by repeating the above process for each unique treatment.

5.3 A Detailed Example of CUI

Following is a disguised case study in which the CUI process was applied to help inform formulation decisions for a drug. Dopahexadine was a mature drug already on the market, indicated for a chronic neuromuscular condition. A drug company RePharmaCo was interested in whether a reformulation of this drug could provide any improved patient benefit, how to tap the available information to inform the decision, and how to reformulate it to provide the best “blend” of benefit. Implicitly, this would also inform the decision as whether to pursue a reformulation at all.

Historical data existed to describe both the efficacy and tolerability of the drug. Efficacy was closely related to plasma concentrations in humans and was measured on a standard efficacy scale (SES). Adverse events were also related to drug levels. Dopahexadine was eliminated from the body quickly, and thus to achieve an acceptable duration of efficacy, relatively large doses had to be given multiple times daily. This caused brief exposure to high drug plasma levels, and consequently increased incidence of adverse events. Published studies were available with data to characterize the efficacy and tolerability, although most examined the pharmacokinetics *or* dynamics, but not both.

As the CUI includes a process as well as mathematics, a group of stakeholders was formed in order to gather inputs to the analysis as well as help ensure decision quality (*i.e.*, senior management participation and buy-in to the eventual analysis results). This was important given the strategic, portfolio-level importance of the decision. The analysis team included representatives from many functions, including the vice president of Clinical Development, a representative from Project Management, Commercial Development, Biostatistics, and Drug Metabolism and Pharmacokinetics. A consulting pharmacometrician trained in CUI led the overall process and facilitated the team discussions that established the CUI model.

Eliciting the inputs to translate drug attributes into a preference model consisted of several steps: determining attributes, defining response levels for each attribute, quantifying the relative preference levels for levels of responses within each attribute, and finally assigning weights to attributes, signifying their relative importance. The products of these discussions included the following (Table 5.1).

Initially, attributes were elicited from the team, and these choices were later assessed in a small survey of prescribing physicians. Note the rankings changed somewhat, but overall the attribute weights were similar. The analysis was later repeated using both alternative sets of weights, illustrating the ability to do

Table 5.1 Dopahexadine CUI attributes

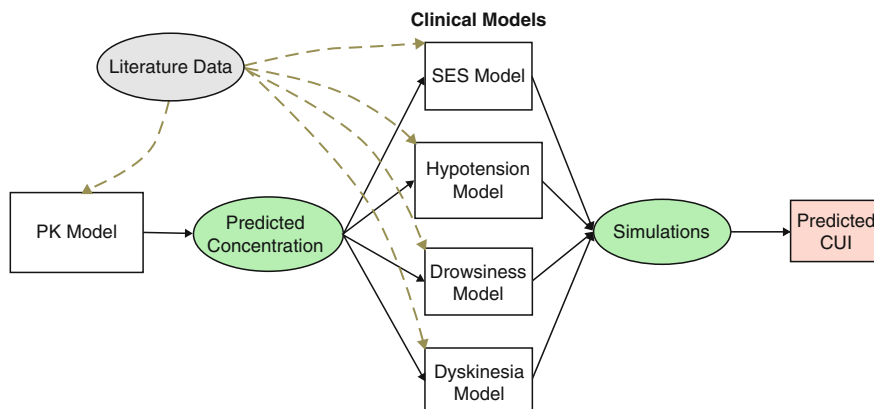
Treatment attribute	Physician survey		Team	
	Rank	Weight	Rank	Weight
Efficacy (maximal change in standard efficacy scale (SES))	1	0.228	1	0.207
Compliance (%)	2	0.169	5	0.120
Hypotension (change in mmHg, systolic BP)	3	0.139	4	0.140
Drowsiness/somnolence (% incidence)	4	0.135	3	0.154
Duration of effect (h)	5	0.112	7	0.098
Elevated LFTs (incidence over 3× ULN transaminase)	6	0.109	2	0.182
Dyskinesia (% incidence)	6	0.109	6	0.101

Endpoint	Range Name	Range		Utility "Value"
		Low	High	
Efficacy (maximal change in SES)	Not clinically meaningful	-0.3	0	0.00
	Moderately effective	-0.6	-0.3	0.60
	Excellent (super drug)	-1.2	-0.6	1.00
Hypotension (maximal change in SBP, mmHg)	Worse than competitor X	-30	-15	0.20
	Effectively the same	-15	-5	0.70
	Clearly better	-5	0	1.00
Drowsiness/Somnolence (% incidence)	Severe impact	52	78	0.20
	Moderate impact	26	52	0.60
	Mild impact	0	26	1.00
Duration of effect (h)	Worse than competitor X	0	2	0.00
	Effectively the same	2	5	0.50
	Clearly better	5	12	1.00
Dyskinesia (% incidence)	Worse than competitor X	35	40	0.15
	Effectively the same	15	35	0.70
	Clearly better	0	15	1.00

Fig. 5.7 Dopahexadine outcomes translated to utility

sensitivity analysis with CUI. Finally, since there were insufficient data to assess the incidence of liver function test (LFT) value elevation and compliance, the treatment alternatives were considered to show identical levels of attainment on each of these attributes.

The meaningful response range for each attribute was assessed, and inputs were gathered to translate these outcomes into utility "values" (Fig. 5.7). In this case, the response ranges were discretized, allowing for easier elicitation and communication. For example, the range of possible efficacy outcomes was divided into three levels: "Not clinically meaningful," "Moderately effective," and "Excellent." For each attribute, the best outcome was assigned a utility "value" of one, and the worst assigned zero. The middle outcome was assigned a value to signify how its value fell relative to the extremes.



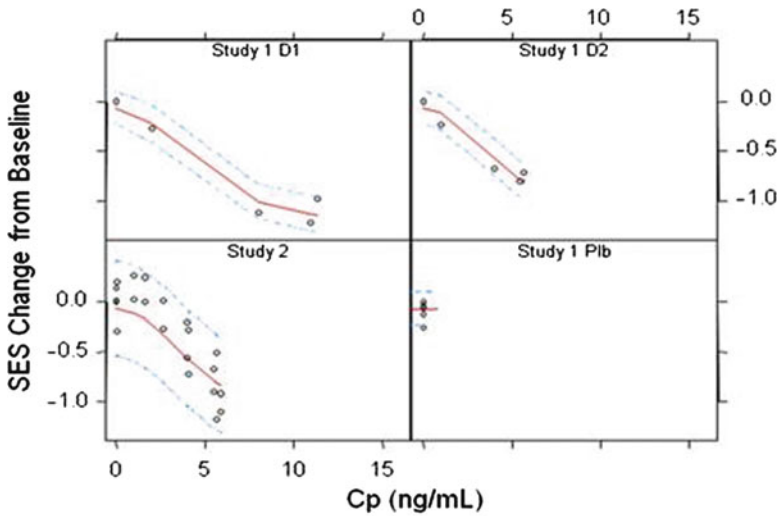
Note: Figure depicts the steps in an integrated CUI-pharmacometric modeling project, with detail on the pharmacometric steps. Literature data is used to guide the construction of the PK and exposure-response models, which are based on subject-level data where possible. “Simulations” incorporates the integration of the CUI model with the PM output, as previously depicted in Figure 5.3. Predicted CUI is the variable of final interest.

Fig. 5.8 Translating literature data into predictions

With the inputs to translate attribute performance into utilities available, the focus was next placed on deriving predictions and uncertainty for how the drug and its possible reformulation would fare on these attributes. Literature data were used to create a pharmacokinetic model and clinical models of efficacy and tolerability were linked to predicted concentration (Fig. 5.8).

Predictive regression models thus characterized the studies’ findings and were used to project the responses from the drug and potential reformulations. For example, the SES efficacy and incidence of drowsiness/somnolence side effects were characterized with a sigmoidal E_{\max} model to relate SES change from baseline data to concentration. This is shown in Fig. 5.9, where decreases in SES are improvements. Incidences of drowsiness/somnolence were characterized using a simple linear model vs. maximum concentration, based on the team’s input that spikes in concentration drove the incident. Reflecting the binary nature of the endpoint (a patient either has the incident or not), a logistic model was appropriate (Fig. 5.10).

Having both gathered inputs to translate outcomes to utility and created models to predict various formulations’ performance, the team took the next step to integrate these to form predictions for alternative formulations. For example, the company examined the question “what if we slowed the absorption of dopahexadine; could we give a higher dose and still have the same level of effect without the peak in concentration?” The chart on the left illustrates the time course of effect with the existing formulation of 8 mg of dopahexadine. The solid curved line is the expected (mean) efficacy, and the shaded bands denote its 95% confidence interval.



Note: Predictions with 95% CI (lines) and observations (circles).

Fig. 5.9 Predictions and observations for dopahexadine efficacy

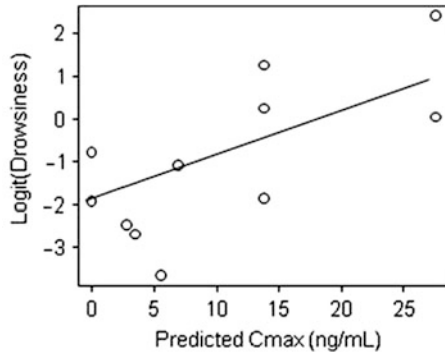
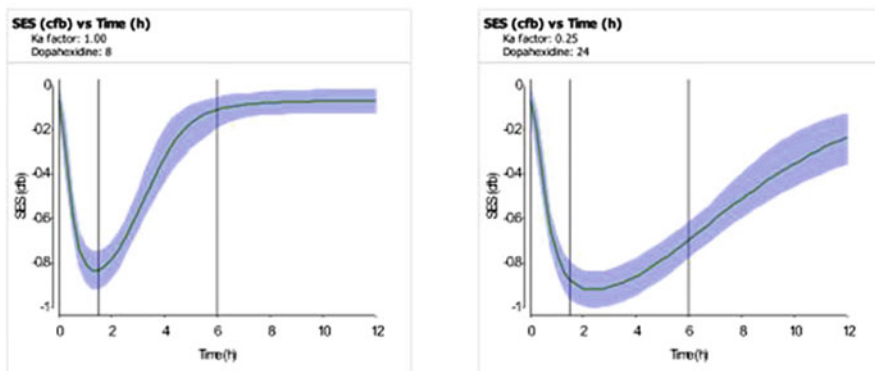


Fig. 5.10 Predictions and observations for dopahexadine drowsiness

Note: Predictions (line) and observations (circles).

The company found by slowing the absorption by 75% (by adjusting the absorption rate to 0.25 of its former value), it could administer 24 mg and have about the same effect (Fig. 5.11).

Finally, integrating these findings with the other attributes, RePharmaCo explored which dose and absorption rate would yield net benefit to patients. For example, the following illustrate how much better a 24-mg dose with absorption 20% as fast as the current formulation vs. the *best* dose of the that formulation. The y-axis illustrates the difference in this alternative’s CUI; thus, values above zero are improvements (Fig. 5.12).



Note: Predictions with 95% CI (curved lines) and reference times (vertical lines).

Fig. 5.11 Predicted efficacy for dopahexadine reformulation

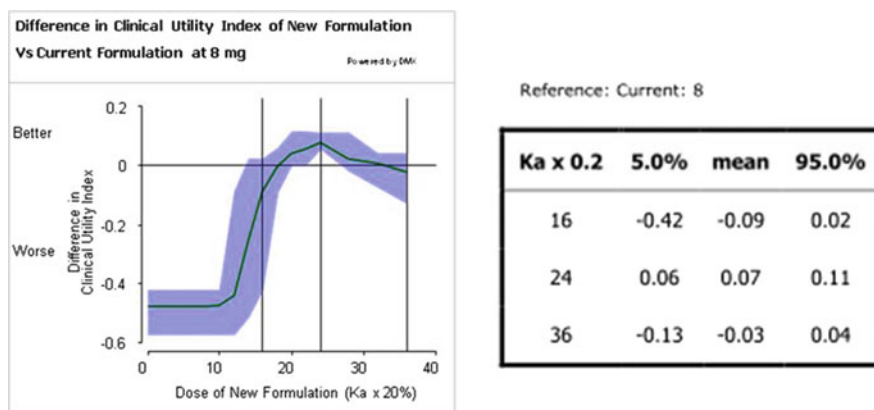


Fig. 5.12 Predicted CUI of reformulated dopahexadine

Therefore, the team was able to reformulate their drug to provide more benefit. With the analysis informing them of the inherent tradeoffs, they identified specific and actionable recommendations. Supported by these insights, the project continued into development.

5.4 Related Publications on CUI

In what was likely the first journal article describing a multiattribute approach to joint assessment of the risks and benefits of a pharmaceutical, Eriksen and Keller (1993) described the development of a proposed multiattribute utility function

through a case study of an anti-glaucoma drug. The authors posed the problem as a business decision, as opposed to the well-published decision-making scenario of choosing the optimal course of treatment for an individual (Weinstein *et al.* 1980; Sox *et al.* 1988; Hunink *et al.* 2001), because the decision was from the point of view of a company intending to compare the overall relative merit of different doses for a given drug as well as the different drugs for a given medical need. The authors described the details of combining information on human efficacy, human toxicity, and animal toxicity via a multiplicative-form multiattribute utility index. For efficacy, the authors focused only on the primary attribute of intraocular pressure, but noted that in other cases multiple efficacy attributes could be modeled if market knowledge indicated as such. For human toxicity, pulse rate and ocular irritation were used as attributes. Individual utility functions for human efficacy and toxicity were each elicited using the standard methods described for multiplicative functions as in Keeney and Raiffa (1976). For animal toxicity, an expert judgment process was also employed in order to translate the two animal toxicity attributes (LD50 and SGOT effects) to risk in humans. Further elicitations were performed to define the scaling factors. Three decision-makers were elicited separately; no group elicitation was performed. With limited data, the authors concluded that the utility curve was flat up to doses of 1% L-bunolol, at which point the utility lost due to increased toxicity outpaced any marginal utility gains on efficacy. The authors' conclusion was later confirmed with approval of the drug in the dose range identified by the utility analysis.

This original publication by Eriksen and Keller followed a similar purpose and overall form to later work in the application of clinical utility functions. In their discussion, they addressed one of the differences, which was their use of three separate decision-makers in elicitation, noting that there would be significant merit to a firm having a single set of utility functions and associated weights. Since they found that their three subjects differed in their assessments, the authors point to structured group discussions (Spetzler 1968) as a possible solution. In contrast to their example, in our implementation of CUI elicitations over the past 10 years, we have typically used structured group discussions.

Another difference between Eriksen and Keller and more recent work is their use of the multiplicative form instead of an additive form for the utility function. Use of the additive form allows for a simpler and more straightforward elicitation process, especially in a group setting. The swing-weight process described in the prior section is an example of an additive form. However, use of the additive form assumes that the decision-maker's preferences within one attribute are independent of the levels of another attribute. This distinction should be well understood by practitioners in the area of CUI. While most CUI's may utilize the additive form, preferences are generally not purely additive. Typically, the benefits of an easier assessment process will outweigh the marginal increases in theoretical accuracy, but CUI practitioners should not be ignorant as to the underlying assumptions from decision theory.

The paper by Korsan *et al.* (2005) may have been the first publication to explicitly use the term "Clinical Utility Index." In this publication, the concept of

the CUI was introduced to the field via two case studies (dose selection and identifying “no go’s”) and a discussion of how use of CUI can accelerate the realization of benefits from pharmacometric modeling and simulation.

In Ouellet *et al.* (2009), a CUI was used to compare two calcium channel $\alpha 2\delta$ ligands in development for treatment of insomnia. This example is notable for its link with a form of quantitative market research (*i.e.*, hybrid conjoint analysis) performed regularly by marketing/commercial groups in drug development. Here, the list of attributes as well as the levels and weightings among them were all taken from the results of the conjoint analysis. When possible, this approach to the derivation of the utility function should be thought of as the “gold standard” for the construction of an index. Although a CUI derived with the interdisciplinary project team can be robust and valuable, a CUI derived from a structured conjoint analysis of several hundred prescribing physicians is likely to better model the true preferences in the marketplace. Obviously, many more resources are required to implement this level of preference modeling, but as conjoint analyses are ubiquitous within the industry, pharmacometricians can use the CUI-conjoint interface as a means to better link with the commercial side of their company.

Recently, two additional overviews of the CUI process and its use in early clinical development were published (Poland *et al.* 2009; Khan *et al.* 2009). Both of these publications cover the theoretical background and the place of CUI in the overall move to model-based drug development. The reader is strongly encouraged to consult both of these publications for additional reading.

5.5 Conclusion: Putting the CUI into Practice

This chapter has presented the reader an introduction to the CUI process. In the move to model-based drug development, other authors have noted the need for models that allow for decision rules in the multiattribute setting of a drug’s product profile (Zhang *et al.* 2008) and metamodels to incorporate all components of the decision that are important to stakeholders (Grasela *et al.* 2005). Like so many other aspects of the transition to model-based drug development, putting the CUI into practice is often a joint effort of pharmacometrics staff and other interested groups within the organization. Although CUI is particularly useful in early clinical development, it can also be integrated into adaptive trials regardless of phase. With its strong theoretical grounding in the field of decision theory, the CUI has the potential to address many needs for the transition to model-based drug development. Because multiattribute utility theory is typically the realm of decision analysis but not pharmacology nor statistics, many pharmacometricians will be new to its underpinnings as well as its use. With education and application, however, CUI can become an important and standard part of the overall “pharmacometric” toolkit.

Appendix: History and Theory

Decision theory traces its roots back to the classic text by John Von Neumann and Oskar Morgenstern, *Games and Economic Behavior* (Von Neumann and Morgenstern 1944). Although the concept of utility can be traced back to the even earlier philosophers, this text gave the first axiomatic foundation for the concept of utility. Many authors elaborated on the work of Von Neumann and Morgenstern, but the classic text of Keeney and Raiffa (1976) provided one of the most detailed explorations of this area. Edwards (1961) was an early proponent of Bayesian methods in psychological research. He and his colleagues investigated additive utility functions in great detail. In general, they found that this approximation works extremely well in practice, even though it may be criticized on theoretical grounds for lack of preferential independence.

Francis Anscombe was one of the first to point out the problems with traditional Neyman–Pearson statistics in the performance of clinical trials and advocated the Bayesian sequential approach (Anscombe 1963, 1990). Although he did not specifically identify utility functions, he advocated a “decision function” approach or a “net profitability” as a result of “economic valuation.” This approach is very similar to the “west coast school of decision analysis,” which uses a utility function to reflect the risk aversion of the decision-maker.

This approach lay dormant and essentially ignored by the pharmaceutical industry until recently. A series of papers by Berry and various colleagues has proposed the use of sequential trials and the use of financial evaluations (Rosner and Berry 1995; Berry 2006).

Notes on Multiplicative Functions

Multiattribute additive utility has been widely used and demonstrated to be robust. An attribute is “preferentially independent” from all other attributes when changes in the rank ordering of preferences of other attributes does not change the preference order of the attribute. Since the change in utility with respect to any individual attribute (indicated as a derivative) does not depend upon any other attribute, multiattribute additive utility is “preferentially independent.” Additive independence is slightly stronger than preferential independence. As an example (Fig. 5.13), consider two attributes: (1) vehicle color and (2) vehicle type. Further, let us restrict ourselves to two colors: red and black. The vehicle types are: (1) sports car and (2) SUV. If the decision-maker (DM) is shown the following two lotteries (note that “lottery” here refers to simple “coin-flip” games of chance), and if the DM is indifferent between the two lotteries, then color is additively independent of car type and the multiattribute additive utility form is appropriate.

If these conditions do not hold, multiplicative forms of the utility function may be appropriate. There is one last condition, called “utility independence,” which

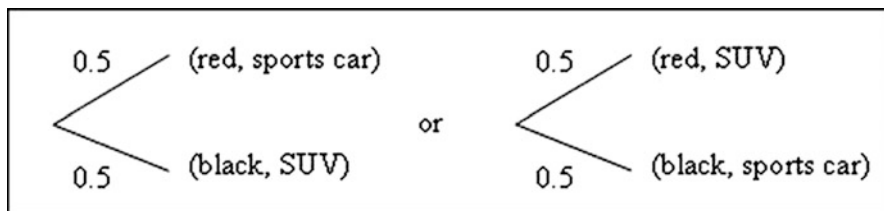


Fig. 5.13 Illustration of preferential independence

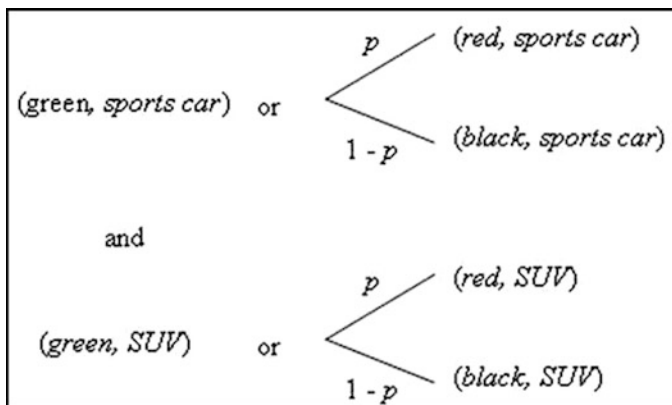


Fig. 5.14 Illustration of utility independence

$$u(x_1, x_2, \dots, x_n) = \sum_{i=1}^n k_i u_i(x_i) + k \sum_{\substack{i=1 \\ j>i}}^n k_i k_j u_i(x_i) u_j(x_j) + k^2 \sum_{\substack{i=1 \\ j>i \\ \ell>j}}^n k_i k_j k_\ell u_i(x_i) u_j(x_j) u_\ell(x_\ell) + \dots + k^{n-1} k_1 k_2 \dots k_n u_1(x_1) u_2(x_2) \dots u_n(x_n)$$

Fig. 5.15 Mathematical form of a multiplicative utility function

implies a specific multiplicative form. Suppose we have two characteristics: (1) vehicle type (sports car and SUV once again) and (2) vehicle color (red, green and black in rank order), and suppose a probability p can be found such that the following two indifference conditions (Fig. 5.14) hold: the DM is indifferent to a green sports car and a 50–50 lottery for a red or black sports car *and* the DM is also indifferent between the same color choices of red or black with SUV replacing sports car (with the same probability). In this case, the DM is said to be “utility independent” and the form of the utility function is appropriate (Fig. 5.15).

Once again, it is important to note that simpler forms of the utility function are often pretty reliable, in terms of choosing the right decision, even though the precise conditions needed to employ a particular form of the utility function are not fully met.

Basic Elicitation Steps

There are generally five parts to an elicitation of a univariate utility function (Keeney and Raiffa 1976):

1. *Structure and scope relevant outcomes*: Frame the decision problem which includes understanding the most important outcomes and attributes, developing the appropriate scales for measuring each attribute, exploring and explaining the assessment process and tools.
2. *Identify relevant characteristics*: Are certain attributes bounded, continuous, binary, categorical, monotonic, and preferentially independent? These attributes provide important information about the form of the utility index to be assessed.
3. *Quantify specific values along the decision-makers utility index*: Usually a series of comparisons among gambles is used to provide this insight.
4. *Select the functional form of the CUI*: The elicitor must make a judgment about the specific family of mathematical functions that will be used to encode the information obtained previously. The multiple attributes can be combined in an additive or multiplicative fashion.
5. *Check for consistency*: During this phase, certain lotteries not previously assessed are performed and compared to the preferences implied by the functional form fitted to previous assessments.

These parts are not necessarily performed in sequence. During the course of the assessment, it may be necessary to revisit previous parts. This serves to refine the judgments of the decision-maker or decision-making body. Assessments made in a group tend to be more difficult to perform but more robust in their application and acceptance. Committees should, if possible, be allowed to share information with each other and come to a joint belief. If a common view cannot be assessed, individual assessments can be made. There are mathematical procedures for combining several assessments, although sensitivity analysis is more useful to focus upon. Basically, if the decisions are identical regardless of the CUI chosen, we do not care about the differences. If the clinical recommendations would be different based on differing CUIs, then we may need to revisit this with the relevant decision makers.

Link to Conjoint Analysis

In a pharmaceutical company, it is typical that there is someone with fiduciary responsibility for the decision making. However, the decisions need to be made with two major groups in mind: (1) regulatory agencies and (2) prescribing physicians. This means that the CUI should reflect the judgments of these groups. There are group assessment methods that can be applied to a sample from either or both populations. These techniques are generally known as conjoint analysis (Elrod *et al.*

1992). Preference measurement comprises three interrelated components: (1) the problem that the study is ultimately intended to address; (2) the design of the preference measurement task and the data collection approach; (3) the specification and estimation of a preference model. Most of the group CUIs made by techniques such as conjoint analysis are limited in structure and less flexible than those assessed in the manner described earlier. However, they have one great advantage; they are direct measurements from a large sample of the population such as prescribing physicians who are ultimately the means by which prescription pharmaceuticals reach the target population. Hence, pharmaceutical development decisions can be focused to maximize the match between the preferences of the prescribing physicians and the target product profile.

Conjoint analysis requires research participants to make a series of tradeoffs. Analysis of these tradeoffs will reveal the relative importance of component attributes. The data is collected from survey respondents in a number of different ways. Traditionally it is administered as a ranking exercise and sometimes as a rating exercise (where the respondent awards each tradeoff scenario a score indicating appeal). In recent years it has become common practice to present the tradeoffs as a choice exercise (where the respondent simply chooses the most preferred alternative from a selection of competing alternatives – common when simulating consumer choices) or as a constant sum allocation exercise (common in pharmaceutical market research, where physicians indicate likely shares of prescribing, and each alternative in the tradeoff is the description of a real or hypothetical therapy). Analysis is traditionally carried out with some form of multiple regressions, but recently, the use of hierarchical Bayesian analysis has become widespread, enabling robust statistical models of individual respondent decision behavior to be developed.

References

- Anscombe FJ (1963) Sequential medical trials. *JASA* 58:365–383
- Anscombe FJ (1990) The summarizing of clinical experiments by significance levels. *Stat Med* 9:703–708
- Berry DA (2006) Bayesian clinical trials. *Nat Rev Drug Discov* 5:27–36
- Clemen RT (1991) Making hard decisions: an introduction to decision analysis. Duxbury, Belmont, CA
- Edwards W (1961) Behavioral decision theory. *Annu Rev Psychol* 12:473–492
- Elrod T, Louviere JJ, Davey KS (1992) An empirical comparison of ratings-based and choice-based conjoint models. *J Mark Res* 29:368–377
- Eriksen S, Keller LR (1993) A multiattribute-utility-function approach to weighting the risks and benefits of pharmaceutical agents. *Med Decis Making* 13:125–188
- Grasela TH, Fielder-Kelly J, Walawander CA, Owen JS, Cirincione BB, Reitz KE, Ludwig EA, Passarell JA, Dement CW (2005) Challenges in the transition to model-based development. *AAPS J* 7:E488–E495
- Hammond JS, Keeney RL, Raiffa H (1999) Smart choices: a practical guide to making better decisions. Harvard Business School Press, Boston, MA

- Hunink MG, Glasziou PP, Siegel JE, Weeks J, Pliskin J, Elstein AS, Weinstein MC (2001) Decision making in health and medicine. University Press, Cambridge, UK
- Keeney RL (1992) Value-focused thinking. Harvard University Press, Cambridge, MA
- Keeney RL, Raiffa H (1976) Decisions with multiple objectives. Wiley, New York
- Khan AA, Perlstein I, Kristna R (2009) The use of clinical utility assessments in early clinical development. *AAPS J* 11:33–38
- Korsan B, Dykstra K, Pullman W (2005) Transparent tradeoffs: a clinical utility index openly evaluates a product's attributes and chance of success. *Pharmaceutical Executive*, March 2005
- Matheson D, Matheson J (1998) The smart organization: creating value through strategic R&D. Harvard Business School Press, Boston, MA
- Ouellet D, Werth J, Parekh N, Feltner D, McCarthy B, Lalonde RL (2009) The use of a clinical utility index to compare insomnia compounds: a quantitative basis for benefit-risk assessment. *Clin Pharmacol Ther* 85:277–282
- Poland B, Hodge FL, Khan A, Clemen RT, Wagner JA, Dykstra K, Krishna R (2009) The clinical utility index as a practical multiattribute approach to drug development decisions. *Clin Pharmacol Ther* 86:105–108
- Rosner GL, Berry DA (1995) A Bayesian group sequential design for a multiple arm randomized clinical trial. *Stat Med* 14:381–394
- Sox HC, Blatt MA, Higgins MC, Marton KI (1988) Medical decision making. Butterworth-Heinemann, Boston, MA
- Spetzler CS (1968) The development of a corporate risk policy for capital investment decisions. *IEEE Trans Syst Cybern* 4:279–300
- Von Neumann J, Morgenstern O (1944) Theory of games and economic behavior. Princeton University Press, Princeton, NJ
- Von Winterfeldt D, Edwards W (1986) Decision analysis and behavioral research. Cambridge University Press, Cambridge, UK
- Weinstein MC, Fineberg HV, Elstein AS, Frazier HS, Neuhauser D, Neutra RR, McNeil BJ (1980) Clinical decision analysis. WB Saunders, Philadelphia, PA
- Zhang L, Pfister M, Meibohm B (2008) Concepts and challenges in quantitative pharmacology and model-based drug development. *AAPS J* 10:552–559

Chapter 6

Adaptive Trial Designs

José C. Pinheiro, Frank Bretz, and Chyi-Hung Hsu

Abstract Adaptive designs (AD) have received a great deal of attention in recent years because of the potential they offer to improve the efficiency of clinical drug development. In an increasingly challenging environment, characterized by escalating costs and decreasing likelihood of regulatory approval, sponsors and regulators alike have a keen interest in strategies to modernize drug development – the use of AD is a key one among them.

This chapter presents an overview of AD and their use in clinical drug development. It starts with some background and definitions, followed by sections on AD in the Learn and Confirm phases of clinical development. In later sections, the importance of trial simulations in the context of AD is discussed, followed by thoughts on the future of AD.

6.1 Background: What are Adaptive Designs and Why Can They Be Useful?

We start with a general definition of AD, provided by the PhRMA Adaptive Designs working group (Gallo *et al.* 2006): “a clinical study that uses accumulating data to decide how to modify aspects of the study as it continues, without undermining the validity and integrity of the trial.” The appeal of being able to make midcourse changes in design, analysis strategy, and other aspects of a trial is certainly clear. Indeed, most studies already incorporate various changes during their conduct, often implemented via protocol amendments – these are usually done in an unplanned way, intended to address unforeseen problems that only reveal themselves after the start of the study.

J.C. Pinheiro (✉)

Adaptive Designs, Johnson & Johnson Pharmaceutical Research & Development,
Raritan, NJ, USA
e-mail: jpinhei1@its.jnj.com

AD, on the other hand, allow midcourse modifications that are preplanned, often times discussed in advance with Health Authorities (HA), and prespecified in the study protocol. This is key to ensure that possible adaptations will not jeopardize the integrity of the trial and the validity of its results and conclusions, as highlighted in (Gallo *et al.* 2006). AD should not be used to salvage a poorly planned trial – in fact, the higher standards against which this type of designs are held will often require more careful planning and more detailed protocol specification than traditionally done in drug development.

The use of preplanned adaptations in clinical trials is certainly not new. In the area of dose escalation, for example, most designs that have been proposed for use have an adaptive component. Examples include the traditional 3 + 3 design (Chevret 2006) and the continual reassessment method (CRM) (Garret-Mayer 2006) used in oncology Phase I trials. Group sequential designs (Jennison and Turnbull 2000) provide another example of adaptive designs with a well-established history in clinical development. However, the focus of this chapter is on more novel adaptive designs approaches, which, to varying degrees, are still being developed, tested in practice, and discussed with HA.

A key appeal of adaptive trials is the intention to revisit, and possibly modify, the original design of the study, based on (partial) information accumulated during the actual trial. This includes revisiting design assumptions (*e.g.*, variability in primary endpoint, dose-response profile) or making design decisions (*e.g.*, treatment and/or population selection) for which there was limited or insufficient information at the planning stage.

These appealing features of AD also come with an intrinsic risk: because adaptations are decided based on partial, often variable information, they may lead to incorrect decisions that may cause efficiency losses, instead of gains. This results in a conflict about the ideal timing of adaptations: reliable decision-making requires sufficient information, but to have any meaningful impact on the ongoing trial, the adaptation(s) cannot come too late. Indeed, depending on the patient accrual and “information accumulation” rates, an adaptive design may not be advantageous, or even feasible, in a particular trial.

Therefore, it is critical to evaluate, and quantify, beforehand the potential gains associated with any AD approach under consideration, taking into account the characteristics of the particular trial (*e.g.*, recruitment rate, primary endpoint availability), available resources, and project timelines. Such an evaluation should also include an assessment of operating characteristics (OC) of the AD, such as Type I error rate and statistical power of hypothesis tests, distribution of trial duration and sample size, etc. The decision of whether or not to use an AD in a particular context will, or at least should, depend on the outcome of such evaluations.

The higher complexity of AD (compared to more conventional fixed designs) will usually require that the evaluation of its OC be done via computer simulations. Because of the probabilistic nature of the decision making process underlying AD, as well as the uncertainty surrounding the assumptions made in their planning, sensitivity analyzes, including multiple alternative scenarios, are necessary in such simulation studies. For the most part, simulation programs are developed

on a customized, application-specific basis, often requiring considerable time and resources. The availability of more general purpose, reliable simulation software for planning AD is one of the limiting factors for their widespread use and acceptance.

6.2 Adaptive Designs in the Learn Phase of Development

Exploratory investigation is the rule during the learn phase of development. Several key questions about dose range and dose selection, based on both efficacy and safety, need to be answered during this stage of clinical development, starting with the determination of the maximum tolerated dose and ADME in normal volunteers, followed by the investigation of proof-of-concept (PoC) in its various forms and the estimation of the dose-response (DR) relationships (safety and efficacy), culminating with the decision to progress, or not, to Phase III and the selection of dose(s) to use in the confirmatory trials. AD have a key role to play in these learning trials, as scientific learning is iterative by nature and can be made most efficient by informed adaptation. This section discusses the use of AD in learning trials, focusing on adaptive dose-ranging (ADR) approaches.

The U.S. FDA has recently released a draft guidance on adaptive designs (FDA 2010) in which it indicates its support to adequately planned, conducted, and analyzed AD. The guidance sheds important light on the regulatory requirements and expectations with regard to AD, and it is certain to have a significant impact in the field. The EMEA has issued a reflection paper focusing on the use of AD in confirmatory trials (EMEA/CHMP 2007) which is in broad agreement with the FDA guidance.

6.2.1 Objectives: Finding an Adequate Dose and Learning About Dose-Response

Selection of a dose (or doses) to carry into confirmatory trials is among the most difficult decisions required during drug development. Although the exact numbers are unknown, it is believed that the high attrition rate plaguing the pharmaceutical industry in Phase III studies are due, at least in part, to inadequate dose selection for confirming safety and efficacy in the intended patient population – doses that are too low to achieve adequate benefit, as well as doses that are too high and lead to dose-related safety events. There is also evidence that, even after registration, dose-adjustments in the label continue to be required with some frequency (Cross *et al.* 2002; Heerdink *et al.* 2002).

The basic problem is illustrated in the dose-response relationships depicted in Fig. 6.1 below. The initially specified study doses (in gray) would provide reasonable information about the DR profile under the gray curve scenario, but would be basically useless for that purpose under the other two alternative DR scenarios.

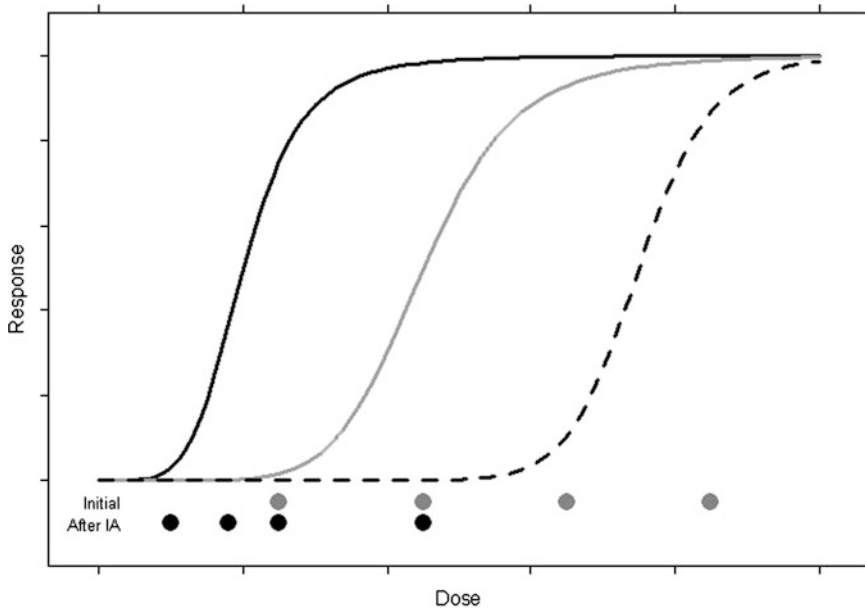


Fig. 6.1 Hypothetical dose-response profiles for given specifications of study doses. *Gray dots* represent the initial doses and *black dots* the doses chosen after the interim analysis (IA) in the adaptive design

Of course, in practice there is not much knowledge about the true underlying DR relationship at the time the study is being designed, so the initial dose specification is tentative at best. The appeal of ADR methods is to allow the allocation of patients to the study doses, and the choice of study doses themselves, to adaptively change over the course of the trial, taking into account the state of knowledge about the underlying DR profile.

For example, suppose one starts the dose-finding trial with equal allocation to the four initial doses (gray dots) depicted in Fig. 6.1 and, after 25% of patients have their responses observed, an interim analysis (IA) is performed and is interpreted to show a plateau in response for the three highest doses consistent with the solid black DR profile. At that point, it would make sense to explore the lower end of the dose range, possibly dropping the two highest doses and randomizing patients to two new doses, along with the two lower doses from the original set, indicated by the black dots in Fig. 6.1.

The process can be repeated in another early learn trial, with the dose allocation being adaptively modified as more knowledge about the underlying DR profile became available. Some of the key methodological questions involved in this approach are:

- What doses to choose for the initial design (*e.g.*, few vs. many doses)?
- How many adaptations, and when (*i.e.*, how much information is needed to reliably adapt the dose allocation)?

- What adaptation rule should be used to modify dose allocation (e.g., focus on target dose, or on entire DR profile)?
- Early stopping rules (e.g., futility, sufficient information about DR)?

Essentially any ADR method is determined by the set of questions above.

6.2.2 Adaptive Dose-Ranging Approaches

The ADR methods discussed here have all been investigated by the PhRMA Adaptive Dose-Ranging Studies working group (WG) in two extensive simulation studies aimed at quantifying the benefits of ADR methods over traditional, fixed design approaches. A brief overview of these studies and their key results are included in Sect. 6.4 – further details can be found in the white papers from the WG (Bornkamp *et al.* 2007; Pinheiro *et al.* 2010). The ADR methods differ primarily in the objective function employed in the adaptive allocation algorithm, and whether or not a parametric model is assumed. Some of the ADR approaches focus on the estimation of target doses, such as the minimum effective dose (MED) or the dose corresponding to 95% of the maximum possible effect (ED95). Others consider the estimation of the full DR profile. Combination approaches are also featured below.

6.2.2.1 General Adaptive Dose Allocation (GADA)

Bayesian non-parametric dose-response modeling is used to determine the most informative dose to administer to each new subject (Berry *et al.* 2002), generalizing the approach used in the ASTIN trial (Krams *et al.* 2003). The key elements of general adaptive dose allocation (GADA) are depicted in Fig. 6.2, which also serves as an illustration for the general flow of other ADR approaches – with the difference

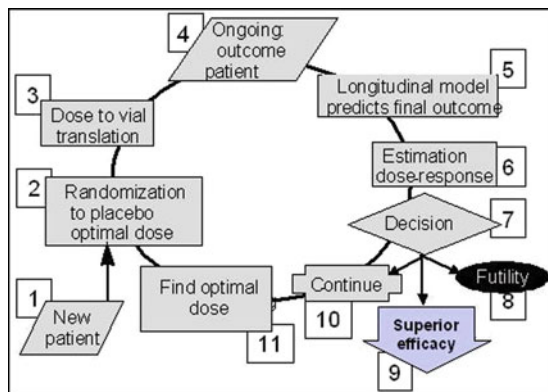


Fig. 6.2 General adaptive dose allocation (GADA) approach

that, typically, data and randomization of cohorts of patients are utilized, instead of individual patients.

In the GADA algorithm, each new patient (1) is allocated to either placebo or an active dose based on the optimal allocation rule (2 – minimum response variance at target dose). As the trial proceeds, interim and final results from patients are gathered and sent to the central data management system, (4), being used to update the estimated DR model (6), using Bayesian methods. Based on the posterior distribution of the response at the target dose (*e.g.*, ED95 or MED), a decision (7) is made on whether to stop the trial for futility (8) or sufficient evidence of efficacy (9), or to continue with the dose finding algorithm (10). The optimal dose for the next patient is chosen to minimize the response variance at the target dose (optimal allocation rule).

6.2.2.2 Adaptive Multiple Comparison Procedure-Modeling (aMCP-Mod)

This approach consists of a response-adaptive extension of the MCP-Mod methodology introduced in (Bretz *et al.* 2006a), preserving the original key motivation of DR testing and estimation under model uncertainty. Like the original MCP-Mod, adaptive multiple comparison procedure-modeling (aMCP-Mod) utilizes a set of predefined candidate models to represent the uncertainty about the true underlying DR relationship. The adaptations aim to maximize the precision of the estimated MED (extensions to other objective functions are available, too, but not discussed here). At each IA, the optimal allocation for MED estimation proposed by Dette *et al.* (2008) is determined based on the updated information on the candidate models – their probabilities of being the true model (in a Bayesian framework) and corresponding parameter estimates. As the knowledge about the candidate models is updated, so do the optimal allocation ratios. At the end of the study, the observed data is analyzed using the original MCP-Mod approach.

6.2.2.3 Combined D- and C-Optimality (DcoD)

Two optimal design methods are applied in two successive stages to adaptively determine dose-allocation ratios. In the first stage, the adaptive dose-allocation is determined using the D-optimality criterion based on a sigmoid- E_{\max} model, with parameter estimates updated as data accrues. From a predetermined IA onward, the adaptation function is switched to C-optimality, focusing on maximizing the precision of the MED estimate under the assumed sigmoid- E_{\max} DR model. As in the first stage, adaptation is a result of successively updating the model parameter estimates, as information accumulates. The time point for switching the criteria is a design parameter that should be investigated via simulations. The main appeal of this approach is that it combines a more global criterion focused on the overall estimation of the DR relationship (D-optimality), with a local criterion targeted at the estimation of the MED (C-optimality).

6.2.2.4 Focus on Interesting Region of DR Profile (IntR)

The objective function driving the adaptive updates of the dose allocation ratios for this method is the (mean) precision of the estimated DR relationship over an “interesting region” of the dose range. For example, this region can be defined as the dose range for which the corresponding DR is at least 80% of the clinically relevant effect – the key idea being that one is usually only interested in regions where reasonably good efficacy has been observed. Similarly, to the DcoD approach, the underlying DR relationship is assumed to be properly represented by a sigmoid- E_{\max} model. The underlying optimal design criterion, called I_L -criterion, was introduced in Miller *et al.* (2007). Similarly, to aMCP-Mod, it utilizes a Bayesian framework to account for model uncertainty (in this case, uncertainty about the parameters in the sigmoid- E_{\max} model). The method uses a set of (six or so) pre-determined sigmoid- E_{\max} models, which were assumed a-priori equally likely, with model probabilities updated using Bayesian methods, as information accumulates.

6.2.2.5 Multiple Objectives (MULTOB)

A weighted product of multiple objective functions is used to determine optimal dose allocations in the adaptive algorithm for this method. Similarly, to DcoD and IntR, a single flexible functional form is assumed to represent the underlying DR relationship – in this case, an inverse quadratic model with an intercept. The choice of objective functions and weights is application-dependent, and can be tailored to focus on different quantities (*e.g.*, detection of DR signal, estimation of MED, estimation of ED95, etc). Adaptive allocation is implemented via a Bayesian approach, with a set of plausible, predetermined DR models, like in aMCP-Mod. Prior model probabilities are assigned at the start of the trial and updated within a Bayesian framework. The overall objective function is the weighted product of objective functions for the individual models (themselves a weighted product of individual component functions), with weights given by the posterior model probabilities at the time of adaptation.

6.2.2.6 *t*-Test Adaptation

This approach focuses on the estimation of the target dose, defined as the dose producing a predetermined, clinically relevant target effect. This approach places less importance in the estimation of the DR relationship. Unlike most previous ADR methods described, it does not assume any parametric model(s) for the DR relationship, only that it is monotone. The data accumulates in cohorts of patients adaptively assigned to doses according to the adaptation rule, which is reevaluated after each cohort has completed the study. Within each cohort, a fixed percentage of patients are assigned to placebo and the remaining patients are assigned to a single dose determined by the adaptation rule (this can be either a new dose, or a dose used in a previous cohort). The adaptation objective function is the *t*-statistic for testing

equality to the target effect, based on the difference between the mean responses of all subjects assigned to the dose selected in the last observed cohort and placebo. An up-and-down algorithm, based on a threshold for the t-statistic, is then used to determine the next cohort dose, or whether the trial should stop. When, and if, the criterion for finding the target dose is met, the DR profile is estimated via isotonic regression.

6.2.3 Remarks on ADR Methods

Although ADR approaches certainly have an important role to play in improving dose finding and dose-response understanding in clinical drug development, they will not, by themselves, be able to address the lack of proper dose selection problem facing the pharmaceutical industry. Given the current level of resources (*e.g.*, sample sizes, drug availability) allocated to Phase II trials, there is a limit on how much can be improved via better design and analysis methods alone. In particular, under the current resource constraints, there can be no silver-bullet approach capable, by itself, of producing the knowledge level needed to adequately address the dose selection problem. This has been clearly illustrated by the simulations conducted by the PhRMA ADRS WG (Bornkamp *et al.* 2007; Pinheiro *et al.* 2010), which demonstrated that high quality dose selection can only be achieved with a combination of increased investment in dose-response learning and an optimized selection of design/analysis strategies.

An important point when choosing among alternative ADR methods are the learning goals of the associated trial. For example, if dose selection is the key goal, methods focused on optimizing target dose (*e.g.*, MED and ED95) estimation, such as aMCP-Mod and GADA, may be more appropriate. If the focus is on DR estimation, however, methods like IntR, which optimize quantities based on the full DR profile, are generally preferable. Methods combining multiple objectives (MULTOB), such as DcoD and MULTOB, provide more uniform performance with respect to target dose and dose-response profile estimation. As no method can be simultaneously optimal with respect to multiple criteria, one should carefully take the relative importance of the individual objectives into account when selecting methods for a specific trial. As discussed in Sect. 6.4, trial simulations are of key importance for this type of evaluation.

The ADR methods described in this section are entirely empirical, focusing on the DR relationship. An alternative class of designs for estimating exposure-response relationships and determining target exposures, which involves adaptation, is that of Randomized Concentration-Controlled Trials (RCCT) described in Kraiczl *et al.* (2003). In these designs, patients are randomized to target concentration ranges, with the individual patient dose regimens being adaptively adjusted to meet the corresponding target concentration range. Additional flexibility is possible by allowing the target concentration ranges allocations to vary as information accrues, similarly to what is done in the context of ADR studies.

6.3 Adaptive Designs for Confirmatory Studies

The objectives of adequate and well-controlled confirmatory studies, so-called pivotal trials, need to be accompanied by statistical hypotheses and prespecified in the study protocol. Regulatory practice requires that the false positive rate (*i.e.*, the Type I error rate) for the associated hypothesis tests be strictly controlled at a prespecified significance level α . This requirement distinguishes confirmatory trials from earlier, exploratory studies, where a strict Type I error rate control is not mandatory. If more than one hypothesis is tested, and simultaneous inference across the several hypotheses is foreseen, multiplicity becomes an issue. For example, repeatedly looking at accumulating data with the possibility of early stopping for efficacy or other design modifications may inflate the overall Type I error rate. Similarly, if multiple treatments or dose levels are compared with a control, the significance level for the individual comparisons has to be adjusted. Therefore, special analysis methods are required to maintain the inferential validity of confirmatory adaptive clinical trials (Bretz *et al.* 2009).

This section identifies some of the methods for the design and analysis of confirmatory adaptive trials. Section 6.3.1 describes group sequential designs, a class of designs involving adaptive components that has been in use for several decades. Newer AD, which provides more flexibility to overcome some of the inherent limitations of group sequential designs, is the topic of Sect. 6.3.2. The following two sections cover some of the more common types of AD in confirmatory trials, including blinded and unblinded sample size reassessment, treatment selection and enrichment designs. The section concludes with some practical considerations on the use of AD.

6.3.1 Group Sequential Designs

Traditionally, the sample size in a clinical trial is fixed before the study is carried out and the data are analyzed. There are clear advantages in using a more flexible approach, where it is possible to stop a study earlier if the available information is deemed sufficient for sound decision making. For example, it would be natural, and ethical, to stop a two-arm clinical trial if interim data clearly indicated that one treatment was superior to (or dangerously less safe than) the other. One might also want to stop the same trial, if the goal was to establish superiority, when there were clear signs that the two treatments were equivalent, or non-inferior to each other. Potential interim stopping of a trial should be preplanned and, as mentioned, the Type I error rate could be seriously inflated unless the analysis method accounts for the sequential nature of the decision making.

Group sequential designs have been in use for clinical trials since the 1970s, becoming the gold standard for major long-term confirmatory trials nowadays. Some of the early seminal work in the field can be found in several articles (Armitage 1975; Pocock 1977; O'Brien and Fleming 1979). In a group sequential

design, the null hypothesis of no treatment effect is rejected if the associated p -value is below a predetermined critical value c , chosen such that the overall probability of a false positive result does not exceed the significance level α . Clearly, c depends on α and on the number of planned stages. Pocock's design (Pocock 1977) uses a constant c for all sequential tests in the trial, while O'Brien and Fleming (1979) require more conservative bounds for early tests followed by larger critical values.

Approaches that are more flexible are available, most prominently α -spending function approaches (Lan and DeMets 1983) in which one only needs to specify the amount of significance level spent up to an interim analysis, rather than the full shape of the adjusted critical levels. With this approach, not even the number of interim analyzes needs to be fixed in advance (although the timing of the interim looks must be independent from data in the ongoing study). Instead, a maximum amount of information must be specified which in the simplest case is the maximum sample size of the trial. The α -spending approach is particularly attractive if the interim analyzes are planned at specific time points, rather than after a specific number of observations. Reliable software implementations of group sequential methods, including different α -spending function approaches, are available in several commercial packages, such as ADDPLAN and East, as well as in freely available software, such as the gsDesign package in R (Wassmer and Vandemeulebroecke 2006). Further details on the theory of group sequential designs can be found in Jennison and Turnbull (2000).

6.3.2 Adaptive Designs

Even though group sequential methods lead to more efficient trials designs than traditional ones, they still do not provide the desired level of flexibility needed in clinical drug development. As discussed in Sect. 6.3.1, group sequential designs are characterized by a prespecified adaptivity, and trial design modifications based on the information collected up to an interim analysis are not possible. Standard design aspects, such as the number of interim analyzes, the group sample sizes and the decision boundaries, have to be specified in the planning phase and cannot be changed during the ongoing trial.

Confirmatory AD has been developed with the goal of extending the flexibility provided by group sequential methods. In particular, they allow for design modifications of an ongoing clinical trial while maintaining control over the overall Type I error rate (Bauer and Koehne 1994). This new class of trial designs is characterized by the potential for unscheduled adaptivity, such as modifying design parameters without the need to completely prespecify the adaptation rules. Adaptive designs allow one to learn from the data observed in an ongoing trial, as well as information external to the trial (*e.g.*, historical data, parallel study results) to modify, at interim, design aspects of subsequent stages, and thereby to react quickly to emerging, possibly unexpected results. In particular, Bayesian interim decision tools can be applied to guide the

interim decision process without undermining the overall Type I error rate (Bretz *et al.* 2009). Important examples include unblinded sample size reestimation (SSR) (Sect. 6.3.3) and dropping of treatment arms in combined Phase II/III trials (Sect. 6.3.4).

A common hypothesis testing approach in AD is based on the combination test principle that combines stage wise p -values using a prespecified combination function (Bauer and Koehne 1994). The key idea is to calculate separate test statistics from the samples at the different stages (*e.g.*, before and after an interim analysis) and to combine them in a prespecified way for the final test decisions. It can then be shown that any design modification which preserves the distributional properties of the separate stagewise test statistics under a given null hypothesis of interest does not lead to an inflation of the overall Type I error rate.

Examples of combination function approaches include Fisher's product combination test (Bauer and Koehne 1994) and the inverse normal combination method (Lehmacher and Wassmer 1999; Cui *et al.* 1999). In fact, the use of the latter method allows establishing a connection between the adaptive designs considered here and the group sequential designs from Sect. 6.3.1.

An approach closely related to the combination function principle is based on the conditional error rate, that is, the Type I error rate for the final analysis (calculated under the null hypothesis), conditional on the observed interim data (Proschan and Hunsberger 1995; Mueller and Schaefer 2004). It can be shown that, if the interim analyzes occur at the preplanned information fractions and the design is not adapted during the conduct of the trial, the resulting stopping boundaries are the same as in classical group sequential methods, but not the resulting test statistics. Procedures based on the conditional error rate are often the most flexible adaptive methods that still guarantee a tight Type I error rate control. However, in practice, the use of these methods is often restricted by the need of a tailored application. For example, if nuisance parameters are present, the conditional error can only be approximated, and the computation of the conditional error rate in the presence of covariates remains an open research problem.

6.3.3 *Sample Size Re-Estimation*

When designing a clinical study, one often has to rely on uncertain assumptions about the values of key underlying parameters, which typically can only be assessed at the conclusion of the trial. One may realize at that point that the trial could have been designed, undertaken or analyzed in a different manner that would have been more efficient, or would have increased its likelihood of success. A straightforward illustration of this is provided by the sample size determination using an estimate of the response variability, often obtained from early-phase trials or historical data. There is always potential for imprecision, or even bias, in this estimate, as it may not directly relate to the trial being designed. Some factors affecting the pre-trial estimated variability may be obvious, but most are quite difficult to quantify, or

realize, in advance. The potential implications are that a trial that would be successful may have its outcome jeopardized because of insufficient statistical power, or substantial resources may have been wasted because the trial was needlessly large. This motivates the idea of updating the sample size, as interim observed data seems to contradict pre-trial assumptions.

For example, consider a trial with a normally distributed response that was designed to have 90% power to detect a treatment difference, and where the standard deviation was assumed to be one. Under these conditions, a small increase of 25% in the standard deviation would reduce the power from 90 to 73%, a nearly threefold increase in the risk of failure.

The mid-trial assessment for possible sample size adjustment is commonly referred to as SSR. Such methods fall into two general categories: (1) blinded, when the SSR uses revised estimates of nuisance parameters, without requiring treatment assignment identification and (2) unblinded, based on revised estimates of treatment.

Statistical methods, such as the combination function approach, can be used to control the Type I error rate under unblinded SSR. Alternatively, group sequential designs can also be used for a similar purpose, by initially sizing the trial to detect a smaller treatment effect than anticipated. If the true effect size is larger than the postulated one, a stopping boundary would likely be crossed during interim monitoring and the trial would terminate early. This could be characterized as a “plan big and then cut” approach, while the SSR approach would favor “plan small and then increase.” Budget constraints and logistical considerations may lead sponsors to prefer the SSR approach over the group sequential alternative.

Wittes and Brittain (1990), who referred to them as internal pilots, first introduced the concept of blinded SSR. They reported that these methods could be used in large randomized clinical trials with little, if any, impact on the Type I error rate. When data remains blinded, concerns related to maintaining the intended significance level for the trial are greatly reduced. Methods using blinded data also tend to be more acceptable to regulatory agencies (EMEA/CHMP 2007; CHMP 1995; ICH 1999).

An additional appeal of blinded SSR is that no Data Monitoring Committee (DMC) is required for implementation and no independent interim analysis team needs to be assembled; both would be needed under the unblinded SSR case. For these reasons, using blinded data is the preferred method for SSR. Unblinding may be considered, if other design features besides sample size are to be adapted. It can then be implemented as part of an AD. Care must be taken to avoid “backward calculations” (adjusted sample size may give hint on treatment effect). SSR is an active area of research in adaptive designs, with many methods having been proposed for a variety of trial situations (Proschan 2005; Friede and Kieser 2006).

6.3.4 Applications: Treatment Selection and Enrichment Designs

A particularly appealing application of AD is in the context of combined Phase II/III studies with treatment selection at interim. Such studies start with several

treatments and a control, with a subset of treatments being selected in the middle of the trial based on the available information at interim, including observed data from the ongoing trial, external information and expert knowledge. Recruitment would continue, but only for the selected treatment(s) and the control, with possibly reassessed sample sizes. The final analysis of the selected treatment(s) includes the patients in both stages and is performed such that the overall Type I error rate is controlled at a prespecified level, regardless of the adaptation rule used at interim (Bretz *et al.* 2006b, 2009; Posch *et al.* 2005).

To illustrate the use of AD with dose selection at interim, we consider the case study from Barnes *et al.* (2010). This trial was one of two pivotal trials to support registration and label claims in a chronic disease. An AD was chosen to (1) perform dose selection at interim and (2) confirm the selected doses in the final analysis. The aim of this two-stage trial was therefore to provide pivotal confirmation of efficacy, safety, and tolerability of the selected doses, where the dose selection was done within the ongoing trial, at a prespecified interim analysis time. At Stage 1, patients were randomized to one of seven treatments arms (four distinct dose levels, placebo and two active control groups). Based on the observed interim data, two dose levels were continued into Stage 2, together with placebo and one of the active control arms. The final analysis consisted of comparing the two selected dose groups with the two active controls for a prespecified sequence of primary and secondary endpoints, while combining the evidence from both stages in a rigid statistical hypothesis framework. A Bonferroni adjustment at level $\alpha/4$ was used, since the study started with four dose levels and any two doses could have been included in the final analysis. More powerful approaches along the lines described in Sect. 6.3.2 could have been applied, but were not pursued because of the complexity of the trial design. Note that the interim decision rules for dose selection did not need to be prespecified in the study protocol, as proper statistical methods are used. Dose selection guidelines for a variety of possible interim scenarios were compiled and included in the DMC charter. The use of proper statistical methods, however, allowed the independent DMC, if necessary, to deviate appropriately from these guidelines, and to select the doses on its own, possibly after consultation with senior representatives from the sponsor (further details of such practical considerations are given in Sect. 6.3.5).

A second application area of growing interest for AD comprises sub-group selection (Brannath *et al.* 2009), or enrichment designs (Wang *et al.* 2009). The increasingly important area of target or personalized medicine is founded upon a premise that heterogeneity in differential benefit to a therapeutic intervention can be explained, and thus predicted, by a (possibly composite) measurable difference between individuals, or groups of individuals. In this context, it is critical to be able to clearly identify the subpopulation of patients (*e.g.*, using diagnostic tests) anticipated to benefit from the targeted treatment. The motivation is clear: if the therapy only benefits patients in a subgroup, the treatment effect assessed in the overall population will be diluted. Therefore, depending on the prevalence of the subgroup in the population, the benefit that this targeted therapy can provide might be inadvertently missed. Under those circumstances, a conventional

clinical trial evaluating the (target) therapy in the overall population would be inefficient (Wang *et al.* 2007).

If there is a sufficient biological understanding, and a corresponding plausible body of evidence supporting the hypothesis that the targeted therapy will only benefit an a priori identifiable subgroup of patients, restricting recruitment to those patients (referred to as an enrichment design in Wang *et al.* (2007, 2009)) will generally suffice. However, the most frequent setting is one in which there is not enough confidence on the targeted benefit of the drug (or the identification of the target subgroup) to restrict the patient population upfront. Instead, one would need to assess the cumulative information and restrict recruitment only after sufficient confidence could be established (Wang *et al.* 2007). This type of design has composite objectives: to assess the benefit in the overall population and in the target subgroup. AD provide a particularly efficient approach for composite objective trials, as they allow for learning and confirmation within a unified, inferentially valid framework.

6.3.5 Practical Considerations

An important aspect to be considered when planning a confirmatory AD is to expand input on trial design to the project planning level. Before embarking on a confirmatory AD, one needs to ensure that the totality of information that will be available at its conclusion is expected to be sufficient to support a submission at the end of Phase III. For example, a second pivotal trial is typically needed to replicate the findings of an independent first pivotal trial, so a single AD cannot replace the full Phase III program. Additionally, adequate information on safety, regimen, mode of application, endpoint, etc., which is needed for a successful filing, should be available prior to the start of a combined Phase II/III study. For example, an AD in a combined Phase II/III study with treatment selection at interim does not replace a proper dose ranging study.

Most basic considerations for planning and conducting a clinical trial with a confirmatory AD are the same as in other, more conventional monitoring settings, such as group sequential trials. This is in particular true for the need to set up independent DMCs, to restrict access to the (unblinded) interim analysis results in order to protect the integrity of the trial, and to facilitate quick access and analyzes of validated data at interim. Other aspects of designing and executing an AD, however, may be different, both at the trial level, as well as at the level of the drug development program. This includes implications on manufacturing and drug supply management, which are often underestimated.

Regulatory considerations play a major role when planning an AD. Their impact, however, depends to some extent on the type of adaptive design and at which point in the overall drug development program it is being used. Health Authorities are typically less concerned about the use of AD in early development, but, in Phase III trials to confirm the treatment effect, adaptations should be kept to a minimum.

Health Authorities are generally open to accept AD in late development stages, if properly conducted and adhering to scientific and statistical rigor, as discussed in the recent FDA draft guidance (FDA 2010) and the EMEA reflection paper (EMEA/CHMP 2007) on the topic. AD are also mentioned explicitly in the Critical Path Opportunities List published by the FDA as an example for creating innovative and efficient clinical trials (FDA 2004).

6.4 Adaptive Designs and Trial Simulations

As discussed in the previous sections, AD approaches typically involve more complex designs, conduct and analysis methods than more conventional, fixed designs. As a result, the evaluation of their operating characteristics (OC), such as Type I error rate, trial duration, etc., can usually only be determined using trial simulations. Because the derivation of such OC is key to adequate protocol design, as well as to determine the potential benefit of alternative AD and fixed approaches, trial simulations for planning is necessary in this context.

In addition, a number of AD also incorporate simulation-based approaches during the trial (*e.g.*, determining a change in dose allocation at an interim analysis) and for the final analysis (*e.g.*, exploring probability of success and net present value calculations for the program, at the end of Phase II). These types of simulations tend to be more focused and embedded in the particular method being implemented. This section focuses on the use of trial simulations for planning a study and deciding among alternative trial design approaches.

6.4.1 Operating Characteristics

The OC of a given design/analysis method are critical to determine the statistical adequacy of the approach, as well as to allow its comparison to alternative approaches. Listed below are some of the most common OC used in practice – not to be taken as an exhaustive list, though. To be most meaningful, trial simulations should include a variety of scenarios, which are feasible to be observed in practice – in the case of dose-ranging trials, this should include different DR profiles.

- *Type I error rate*: the probability of a false positive result, *e.g.*, declaring a treatment better than a control, when in fact it is not. This OC presupposes the existence of one, or more, hypotheses being tested in the trial. When multiple hypotheses are present, a family wise error rate (FWER), that is, the probability of observing at least one false positive result in the set of hypothesis tests, should also be reported. An important point to be made is that AD relying on simulation-based approaches to determine critical value(s) may not control a Type I error rate control at a prespecified significance level α (Posch *et al.* 2010). Their use in confirmatory

studies is therefore limited. Analytical results, such as multiplicity adjusted critical values, are often needed in the latter case to guarantee a strict FWER control.

- *Statistical power*: the probability of a true positive result – related to the OC above, but calculated under scenarios in which an effect of some kind (e.g., a DR signal) is present. When multiple hypothesis tests are included, should be calculated for subsets of hypotheses (e.g., true positive in all tests, in at least one test, etc).
- *Stopping rules probabilities*: often times AD include early termination rules, such as futility rules. Their stoppage probabilities under varying scenarios (e.g., no effect, clinically irrelevant effect, etc.) should be characterized.
- *Trial duration and sample size*: in AD with early termination rules and/or information-driven termination (e.g., stop when adequate precision of MED estimate has been reached, or maximum sample size is attained); the distribution of trial duration and total sample size should be investigated as part of the simulations. Summaries, such as average and standard deviation, and plots, such as histograms and box plots, are useful for that purpose.
- *Distribution of allocated patients/doses*: in AD involving adaptation in dose allocation, the average and standard deviation of the number of patients per dose provide useful characterizations.
- *Precision and bias of point estimates*: there will typically be a variety of point estimates used in any given trial, including differences between treatment arms, target doses, predicted values for dose response, etc. Measures of precision (e.g., median absolute deviation between estimated and true values) as well as of potential bias (e.g., difference between estimated and true values, divided by the latter) are of critical importance to evaluate the information value of the trial, and compare alternative approaches.
- *Coverage and length of confidence intervals*: to be evaluated when confidence intervals are to be derived for the quantities investigated by the point estimates references above.

Whenever feasible, the OC should be displayed using graphical methods to allow side-by-side comparison of alternative design/analysis methods, under the different scenarios considered. When evaluating OC in a given trial, one should not only have in mind the comparison of alternative approaches, but also the adequacy of any approach to properly address the relevant scientific questions, under the resource restrictions. It may be that the best method is not good enough for the intended purposes of the study.

6.4.2 An Illustration: Comparing ADR Approaches

We use a subset of the simulations produced by the PhRMA ADRS WG (Bornkamp *et al.* 2007) to illustrate the value of trial simulations to derive OC and compare alternative approaches. This particular simulation study included the last five ADR

methods described in Sect. 6.2.2 plus a non-adaptive ANOVA approach based on Dunnett comparisons (Dunnett 1955).

The underlying indication considered was neuropathic pain, with a primary endpoint of change from baseline in a visual analog pain score. The target clinical effect was a pain reduction from baseline of 1.3 units over placebo. The total sample size was fixed at 250 patients, for all methods. Simulation scenarios were defined by three factors:

- Seven DR models: flat plus six active DR profiles, displayed in Fig. 6.3
- Number of doses: five (0, 2, 4, 6, and 8) or nine (0, 1, 2, . . . , 8)
- Number of equally spaced interim analyses: 0 (no adaptation), 1, 2, 4, and 9

The purposes of the simulation study were to: (1) evaluate and quantify possible performance gains of ADR approaches over ANOVA and (2) compare the performances of various ADR approaches. The following key study goals were considered.

- *Detecting dose-response*: evidence of a DR signal, *i.e.*, PoC
- *Identifying clinical relevance*: if PoC is established, determine if a clinically relevant response can be obtained within the maximal allowed dose range

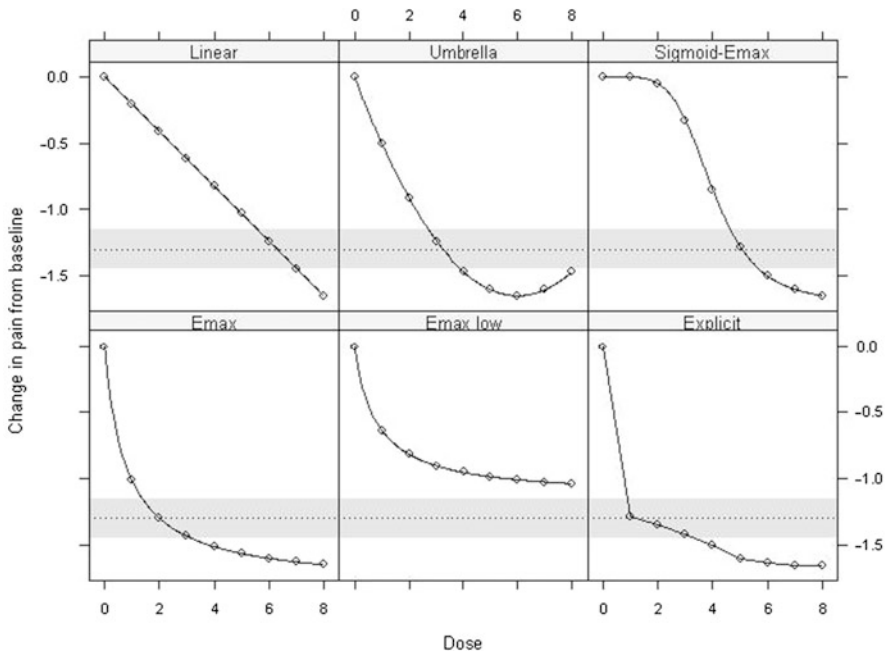


Fig. 6.3 DR profiles used in simulations. *Dotted horizontal line* indicates clinically relevant pain reduction from baseline of 1.3 units and *shaded region* gives the target response interval of $\pm 10\%$ of the clinically relevant effect. *Dots* indicate doses 0, 1, 2, . . . , 8

- *Selecting a target dose*: when the previous goal is met, select the dose to be brought into the confirmatory phase, the so-called target dose
- *Estimating the dose-response*: DR profile within the observed dose range

We focus here just on the last two items, for illustration purposes. The full set of results and associated discussions are given in Pinheiro *et al.* (2010).

The dose selection accuracy was evaluated by the probability that the selected dose was within the target dose interval, *i.e.*, within $\pm 10\%$ of the target clinical response. The corresponding target dose range depends on the shape of the DR profile as highlighted in Fig. 6.3. Figure 6.4 summarizes the simulation results for this OC.

The probability of target dose interval selection improves with adaptation for most of ADR methods (especially aMCP-Mod and IntR), under the majority of simulation scenarios. No method is a clear winner, with relative performances depending on the shape of the underlying DR profile and the number of doses. Note that increasing the number of IA beyond 2 does not lead to further improvement for most ADR methods.

The adequacy of DR estimation was measured by the relative average prediction error obtained as the average absolute difference between estimated and true DR values at each of the available doses 0, 1, . . . , 8, divided by the average by the

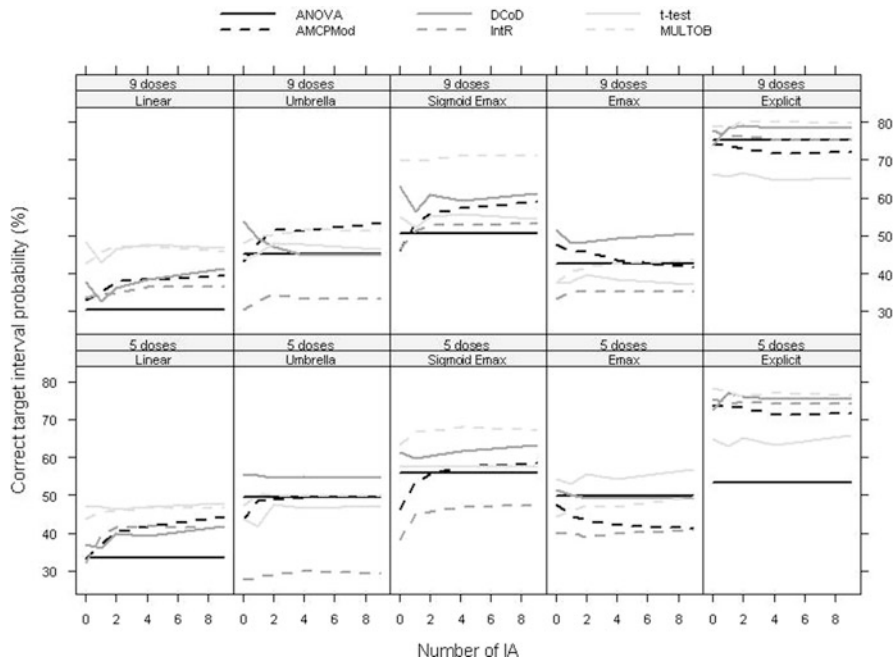


Fig. 6.4 Probability of selecting dose in correct target interval vs. number of IA corresponding to the adaptive dose-ranging (ADR) methods under the different DR models and number of doses

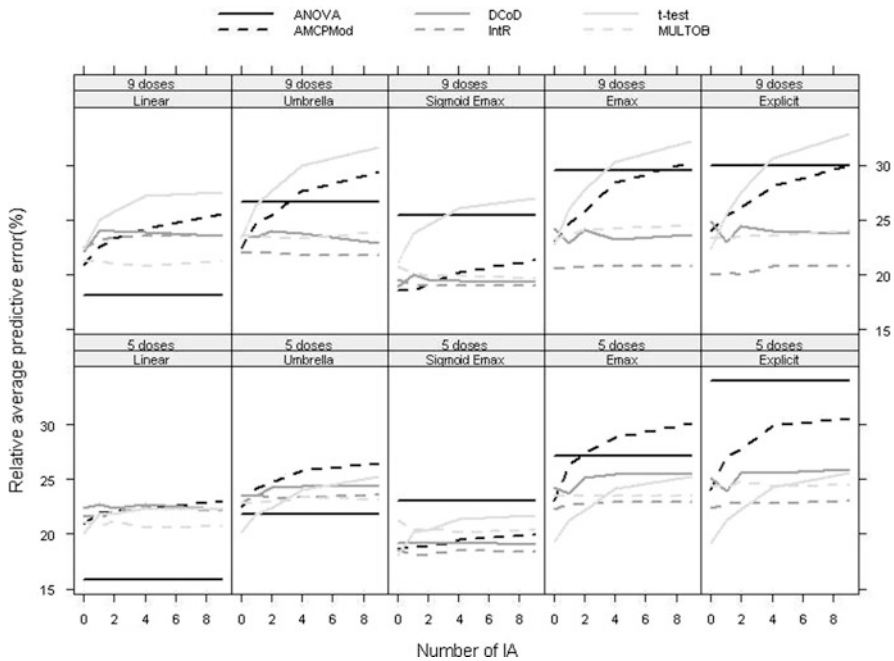


Fig. 6.5 Relative average prediction error vs. number of IA for ADR methods under the different DR models and number of doses

absolute target clinical effect. Figure 6.5 displays the values of this OC for the various methods under the different scenarios.

For t-test and aMCP-Mod, the prediction error increases with the number of IA under most of the scenarios. This is likely a consequence of these methods focusing on maximizing the precision of the target dose estimate. Consequently, the resulting adaptive allocation algorithms place more patients around the estimated dose, possibly to the detriment of learning about the full DR. The remaining ADR methods, which incorporate overall DR estimation criteria in their adaptation rules, have more stable performance with regard to the number of adaptations. Furthermore, the DR estimation performance of these methods does not change much with the number of adaptations, suggesting that the performance is driven more by the use of optimal design methods than the adaptations themselves. As before, no method is clearly superior, or inferior, under all scenarios, including ANOVA.

6.5 Concluding Remarks and Further Thoughts on Adaptive Designs

Because of their flexibility, adaptive designs can provide substantial gains over more traditional fixed designs. To maintain the scientific validity and integrity of

AD, it is critical that adaptations be prespecified and stated in the study protocol, and that guidelines and protections are put in place to ensure that information is not leaked beyond the strictly necessary people involved in the adaptation process (*e.g.*, DMC members), see FDA (2006) and Gallo *et al.* (2010) for further guidance on the topic for exploratory and confirmatory trials.

The added flexibility and higher standards of planning and conduct of AD come at a price. Typically more upfront planning is needed, and more costly logistics and operational processes are required (*e.g.*, drug supply management, centralized randomization). When considering an AD, one should carefully take into consideration the pros and cons involved. In some situations, the potential benefits associated with an AD may not justify its higher costs. To that end, clinical trial simulations play a key role in evaluating and deciding among alternative approaches, including AD. These should be conducted under varied and realistic scenarios, taking into account the multitude of aspects involved.

An important point to keep in mind is that no single best approach exists for all cases of practical interest. For some indications in which accrual occurs relatively slowly with regard to the availability of the response, AD may be a more natural and appealing choice, while in cases that accrual has terminated by the time the endpoint is available, AD would be of little, or no benefit. The choice of design and analysis method will also heavily depend on the goals of the study and the availability of resources.

Therefore, a toolbox strategy may provide the best approach. The toolbox should encompass a reasonably comprehensive set of design and analysis methods with demonstrated usefulness for a given type of studies, *e.g.*, dose ranging. These should include response-adaptive designs, optimal designs, model-based estimation, Bayesian methods, futility rules, etc.

As mentioned earlier, methodological improvements in design and analysis alone cannot ensure improved success rates and better labeling in drug development. Adequate allocation of resources across the different phases of development is also necessary. Program-level evaluations of alternative strategies, including resource allocation, should become the norm in drug development. The use of forward-looking metrics such as probability of program success and distribution of net present value would help placing the program-level evaluations into a better quantitative decision-making context.

References

- Armitage P (1975) Sequential medical trials. Wiley, New York
- Bauer P, Koehne K (1994) Evaluation of experiments with adaptive interim analyses. *Biometrics* 50:1029–1041
- Berry DA, Mueller P, Grieve AP, Smith MK, Parke T, Krams M (2002) Bayesian designs for dose-ranging drug trials. In: Gatsonis C, Kass RE, Carlin B, Carriquiry A, Gelman A, Verdine I, West M (eds) Case studies in Bayesian statistics, vol 5. Springer, New York, pp 99–181

- Bornkamp B, Bretz F, Dmitrienko A, Enas G, Gaydos B, Hsu CH, Koenig F, Krams M, Liu Q, Neuenschwander B, Parke T, Pinheiro J, Roy A, Sax R, Shen F (2007) Innovative approaches for designing and analyzing adaptive dose-ranging trials (with discussion). *J Biopharm Stat* 17:965–995
- Brannath W, Zuber E, Branson M, Bretz F, Gallo P, Posch M, Racine-Poon A (2009) Confirmatory adaptive designs with Bayesian decision tools for a targeted therapy in oncology. *Stat Med* 28(10):1445–1463
- Barnes PJ, Pocock SJ, Magnussen H, Iqbal A, Kramer B, Higgins M, Lawrence D (2010) Integrating Indacaterol dose selection in a clinical study in COPD using an adaptive seamless design. *Pulmonary & Therapeutics* 23:165–171
- Bretz F, Pinheiro J, Branson M (2006a) Combining multiple comparisons and modeling techniques in dose-response studies. *Biometrics* 61(3):738–748
- Bretz F, Schmidli H, König F, Racine A, Maurer W (2006b) Confirmatory seamless phase II/III clinical trials with hypotheses selection at interim: general concepts (with discussion). *Biom J* 48(4):623–634
- Bretz F, König F, Brannath W, Glimm E, Posch M (2009) Adaptive designs for confirmatory clinical trials. *Stat Med* 28(8):1181–1217
- Chevret S (2006) *Statistical methods for dose-finding experiments*. Wiley, Chichester, England
- CHMP Working party on Efficacy of Medicinal Products (1995) *Biostatistical methodology in clinical trials in applications for marketing authorizations for medicinal products*. *Stat Med* 14:1659–1682
- Cross J, Lee H, Westelinck A, Nelson J, Grudzinkas C, Peck C (2002) Postmarketing drug dosage changes of 499 FDA-approved new molecular entities, 1980–1999. *Pharmacoepidemiol Drug Saf* 11(6):439–446
- Cui L, Hung HMJ, Wang S-J (1999) Modification of sample size in group sequential clinical trials. *Biometrics* 55:853–857
- Dette H, Bretz F, Pepelyshev A, Pinheiro J (2008) Optimal designs for dose finding studies. *J Am Stat Assoc* 103:1225–1237
- Dmitrienko A, Tamhane AC, Bretz F (eds) (2009) *Multiple testing problems in pharmaceutical statistics*. Taylor & Francis, New York
- Dunnnett CW (1955) A multiple comparison procedure for comparing several treatments with a control. *J Am Stat Assoc* 50:1096–1121
- EMA/CHMP (2007) Reflection paper on methodological issues in confirmatory clinical trials with flexible design and analysis plan (draft CHMP/EWP/2459/02, 23-Mar-2006). www.ema.europa.eu/pdfs/human/ewp/245902en.pdf
- FDA (2004) Innovation/stagnation: critical path opportunities report. www.fda.gov/downloads/ScienceResearch/SpecialTopics/CriticalPathInitiative/CriticalPathOpportunitiesReports/UCM077258.pdf
- FDA (2006) Guidance for clinical trial sponsors on the establishment and operation of clinical trial data monitoring committees. www.fda.gov/downloads/RegulatoryInformation/Guidances/UCM127073.pdf
- FDA (2010) Adaptive design clinical trials for drug and biologics draft guidance. www.fda.gov/downloads/Drugs/GuidanceComplianceRegulatoryInformation/Guidances/UCM201790.pdf
- Friede T, Kieser M (2006) Sample size recalculation in internal pilot study designs: a review. *Biom J* 48(4):537–555
- Gallo P, Chuang-Stein C, Dragalin V, Gaydos B, Krams M, Pinheiro J (2006) Adaptive designs in clinical drug development – an executive summary of the PhRMA Working Group. *J Biopharm Stat* 16:275–283
- Gallo P, Fardipour P, Dragalin V, Krams M, Litman GS, Bretz F (2010) Data monitoring in adaptive dose ranging trials. *Stat Biopharm Res* (in press)
- Garret-Mayer E (2006) The continual reassessment method for dose-finding studies: a tutorial. *Clin Trials* 3(1):57–71

- Heerdink ER, Urquhart J, Leufkens HG (2002) Changes in prescribed dose after market introduction. *Pharmacoepidemiol Drug Saf* 11(6):447–453
- ICH E-9 Expert Working Group (1999) Statistical principles for clinical trials (ICH Harmonized Tripartite Guideline E-9). *Stat Med* 18:1905–1942
- Jennison C, Turnbull BW (2000) Group sequential methods with applications to clinical trials. Chapman & Hall/CRC, Florida
- Kraiczi H, Jang T, Ludden T, Peck CC (2003) Randomized concentration-controlled trials: motivations, use, and limitations. *Clin Pharmacol Theory* 74:203–214
- Krams M, Lees KR, Hacke W, Grieve AP, Orgogozo JM, Ford GA for the ASTIN Study investigators (2003) ASTIN: an adaptive dose-response study of UK-279, 276 in acute ischemic stroke. *Stroke* 34:2543–2548
- Lan K, DeMets DL (1983) Discrete sequential boundaries for clinical trials. *Biometrika* 70:659–663
- Lehmacher W, Wassmer G (1999) Adaptive sample size calculations in group sequential trials. *Biometrics* 55:1286–1290
- Miller F, Guilbaud O, Dette H (2007) Optimal designs for estimating the interesting part of a dose-effect curve. *J Biopharm Stat* 17:1097–1115
- Mueller HH, Schaefer H (2004) A general statistical principle for changing a design any time during the course of a trial. *Stat Med* 23:2497–2508
- O'Brien PC, Fleming TR (1979) A multiple testing procedure for clinical trials. *Biometrics* 35:549–556
- Pinheiro J, Sax R, Antonijevic Z, Bornkamp B, Bretz F, Chuang-Stein C, Dragalin V, Fardipour P, Gallo P, Gillespie W, Hsu CH, Miller F, Padmanabhan SK, Patel N, Perevozskaya I, Roy A, Sanil A, Smith JR (2010) Adaptive and model-based dose ranging trials: quantitative evaluation and recommendations (with discussion). *Stat Biopharm Res* (in press)
- Pocock SJ (1977) Group sequential methods in the design and analysis of clinical trials. *Biometrika* 64:191–199
- Posch M, Koenig F, Branson M, Brannath W, Dunger-Baldauf C, Bauer P (2005) Testing and estimation in flexible group sequential designs with adaptive treatment selection. *Stat Med* 24:3697–3714
- Posch M, Maurer W, Bretz F (2010) Type I error rate control in adaptive designs for confirmatory clinical trials with treatment selection at interim. *Pharm Stat* (in press) 10.1002/pst.413
- Proschan M (2005) Two-stage sample size reestimation based on a nuisance parameter: a review. *J Biopharm Stat* 15:559–574
- Proschan MA, Hunsberger SA (1995) Designed extension of studies based on conditional power. *Biometrics* 51:1315–1324
- Wang SJ, O'Neill RT, Hung JHM (2007) Approaches to evaluation of treatment effect in randomized clinical trials with genomic subset. *Pharm Stat* 6:227–244
- Wang SJ, Hung HMJ, O'Neill R (2009) Adaptive patient enrichment designs in therapeutic trials. *Biom J* 51:358–374
- Wassmer G, Vandemeulebroecke M (2006) A brief review of software developments for group sequential and adaptive designs. *Biom J* 48(4):732–737
- Wittes J, Brittain E (1990) The role of internal pilot studies in increasing the efficiency of clinical trials. *Stat Med* 9:65–72

Chapter 7

Keys of Collaboration to Enhance Efficiency and Impact of Modeling and Simulation

**Anthe S. Zandvliet, Rik de Greef, Anton F.J. de Haan,
Pieta C. IJzerman-Boon, Maya Z. Marintcheva-Petrova,
Bernadette M.J.L. Mannaerts, and Thomas Kerbusch**

Abstract Modeling and Simulation (M&S) can be a key factor in efficient drug development. It is well recognized that collaboration of multiple disciplines is critical to the success of M&S in supporting drug development decisions. This chapter provides guidance on how the main collaborators (biostatistics, clinical research and clinical PK-PD) can achieve co-ownership of M&S efforts to make better informed decisions on trial designs. The clinical development program of corifollitropin alfa is presented as an example of successful model-based drug development. Throughout a long-lasting collaborative effort, biostatistics and clinical PK-PD scientists have learned to appreciate each other's methods, all collaborators have shared their expertise to integrate physiological and pharmacological concepts with clinical data and clinical research has started to pro-actively conduct model-informed trials. Cultural barriers and logistical difficulties were overcome, resulting in an organizational structure that ensures better informed decisions on trial designs and more efficient drug development.

7.1 Introduction

Modeling and Simulation (M&S) is a valuable tool to integrate knowledge throughout the various stages of drug development. Models informed by data from preclinical pharmacology experiments may be used to guide dose selection for the first-in-human trial. Models of clinical pharmacokinetic-pharmacodynamic relationships based on early clinical trials may be used to optimize the design and informativeness of later trials, contributing to efficiency of late stage development.

R. de Greef (✉)

Pharmacokinetics, Pharmacodynamics and Pharmacometrics (P3),
Global Drug Metabolism and Pharmacokinetics, Merck Research Labs,
Merck Sharp and Dohme, AP1110, 5340 BH, Oss, The Netherlands
e-mail: rik.degreef@merck.com

For an optimal interplay between modeling activities and clinical studies, close collaborations between various scientific disciplines are necessary.

Modeling in the drug development context comprises more than the development of a model that adequately describes the data. Models are most useful if current and/or basic knowledge of physiology and pharmacology is incorporated into the models. Hence, modeling allows integration and quantification of established scientific principles and new experimental data. Input from multiple areas of expertise is essential to collect and amalgamate all available knowledge in a model framework that is both scientifically valid and appropriate for the goals of the project.

During the model building process, multiple pharmacostatistical techniques may be applied, especially when complex model frameworks are involved. Different types of data (*e.g.*, continuous vs. ordinal; longitudinal vs. end-point) require different analytical methods, different software tools and different modeling expertise. Interdisciplinary collaboration between the various quantitative sciences, such as statistics, applied mathematics, systems biology and preclinical/clinical pharmacokinetics and pharmacodynamics (PK-PD) can greatly enhance the variety of modeling components and may broaden the scope of modeling impact.

In our organization, knowledge integration using modeling and simulation has been initiated through the KD₃ paradigm. KD₃ is an acronym for Knowledge Driven Drug Development. The KD₃ paradigm provides an organizational structure for large modeling initiatives in clinical development and fosters close collaboration between the principle disciplinary scientist teams: clinical PK-PD, biostatistics and global clinical research. Figure 7.1 presents a graphical representation of the KD₃ concept.

Within KD₃ teams, the clinical PK-PD group focuses on modeling of longitudinal PK-PD data using software such as NONMEM (nonlinear mixed effects modeling software, Icon Development Solutions, Elliott City, MD, USA), the biostatistics group focuses on statistical models using programs like SAS (Statistical Analysis Software,

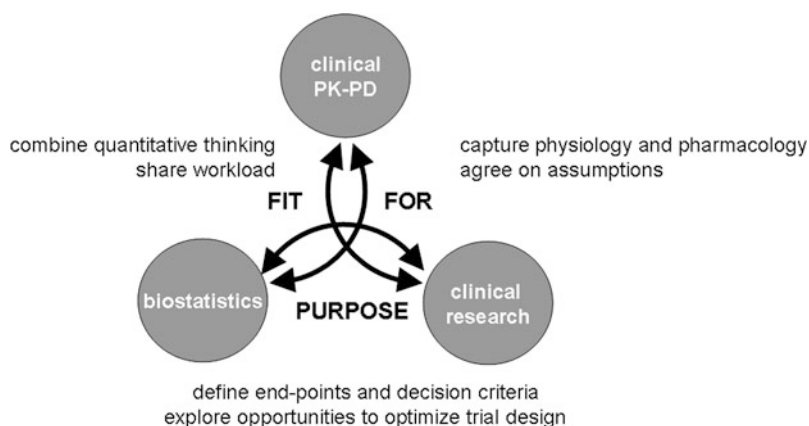


Fig. 7.1 KD₃: important elements in the collaboration between clinical PK-PD, biostatistics and global clinical research to enhance the efficiency and impact of modeling and simulation

SAS Institute Inc., Cary, NC, USA) and the global clinical research group fosters applications of modeling and simulation (M&S) by conducting model-informed clinical studies to obtain valuable data for M&S and by prospective confirmation of M&S results. The objectives of KD₃ are to make optimal use of all available information and knowledge (1) to optimize trial design, (2) to optimize development projects and (3) to assist decision making at critical program milestones.

In this chapter, we will highlight the keys of collaboration between clinical PK-PD, biostatistics and global clinical research to ensure successful quantitative drug development. We will also evaluate the difficulties and challenges encountered. This chapter provides guidance regarding effective behavior of the major players to overcome cultural barriers and logistical hurdles. Our lessons learned on the way to a successful collaborative organizational structure will be illustrated, using the clinical development of corifollitropin alfa as an example of a successful M&S project.

The indication of corifollitropin alfa is controlled ovarian stimulation (COS) for *in vitro* fertilization (IVF) or intracytoplasmic sperm injection (ICSI). COS requires treatment with an FSH (follicle-stimulating hormone) agonist for the duration of approximately 9 days, in order to stimulate the growth of multiple follicles in the ovaries. Corifollitropin alfa is a new long-acting recombinant gonadotropin with similar pharmacodynamic properties as conventional recombinant follicle-stimulating hormone (recFSH), but with differing pharmacokinetic characteristics.

Figure 7.2 is a graphical representation of the recommended COS treatment regimen with the FSH agonist corifollitropin alfa. In this new treatment regimen,

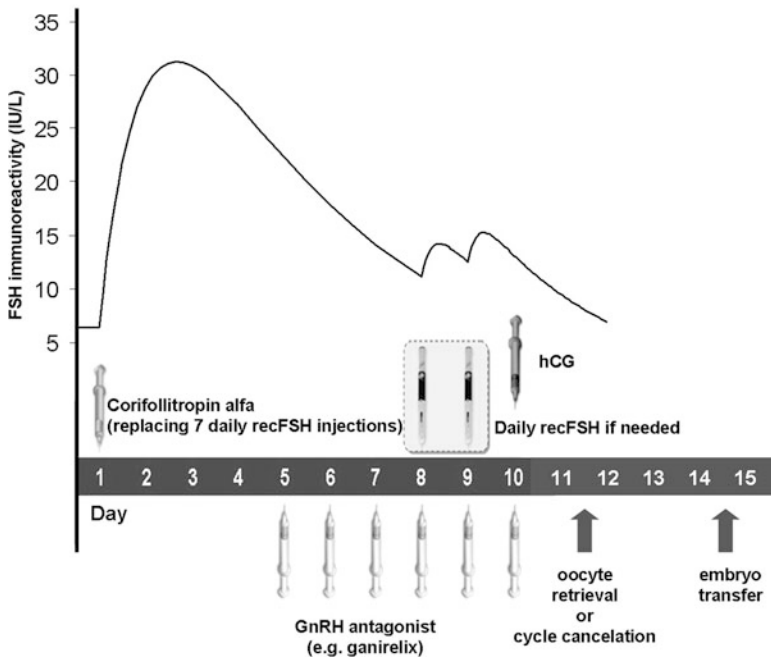


Fig. 7.2 Schematic representation of the therapeutic interventions in the corifollitropin alfa treatment regimen

a single injection of corifollitropin alfa on stimulation day 1 is sufficient to initiate and sustain an ovarian response for 1 week, because of the extended half-life of corifollitropin alfa as compared to recFSH. In a traditional regimen for COS, daily injections of recFSH were required for follicular stimulation. From stimulation day 8 onward, if needed, treatment must be continued with daily injections of recFSH, until the criteria for triggering final oocyte maturation (3 follicles ≥ 17 mm) have been reached. A gonadotropin-releasing hormone (GnRH) antagonist (*e.g.*, ganirelix) is administered daily from stimulation day 5 onward, preventing an endogenous luteinizing hormone (LH) surge and untimely, uncontrolled ovulation. As soon as three or more follicles have a diameter of at least 17 mm, a single injection of hCG (human chorion gonadotropin) is administered to trigger final oocyte maturation. Approximately 34–36 h following hCG administration, a transvaginal ultrasound-guided oocyte retrieval is performed followed by standard IVF or ICSI to achieve pregnancy. If treatment is discontinued prior to oocytes retrieval, this is defined as a “cycle cancellation” and the proportion of subjects with no oocyte retrieval is called the “cancellation rate” ($P_{\text{cancellation}}$). Embryo transfer is performed 2–5 days after oocyte retrieval.

7.2 Corifollitropin Alfa Development Program

The development program of corifollitropin alfa consisted of several well-designed clinical trials, in concert with M&S efforts. The interplay between clinical trials and M&S efforts is illustrated in Fig. 7.3. The KD₃ initiative for this program was launched immediately after Phase I development and continued throughout dose-response trials and pivotal development. The M&S efforts for corifollitropin alfa were initiated as a pilot project to assess the feasibility of KD₃. Apart from clinical PK-PD and biostatistics, clinical research provided a strong drive to the project, especially through the therapy area head, who articulated the potential benefits of making use of the extensive internal database for COS. However, there were also doubts whether a model for COS could be developed, because treatment outcome was considered to be influenced by subjective decisions of the fertility specialist (*e.g.*, adjustments to treatment during ovarian stimulation based on the follicular response).

The model framework included longitudinal PK-PD models as well as non-longitudinal statistical models. Hence, model development was conducted in close collaboration between clinical PK-PD and biostatistics colleagues and was executed using NONMEM and SAS. For simulation purposes, all longitudinal models were converted to statistical models and the final simulations were conducted by biostatistics.

The design of a Phase II dose-response trial was informed and optimized using M&S (de Greef *et al.* 2008; The corifollitropin alfa dose-finding study group 2008). Prior to the conduct of the Phase II dose-response trial, it was agreed by all KD₃ collaborators that the recommended dose for Phase III development would also be

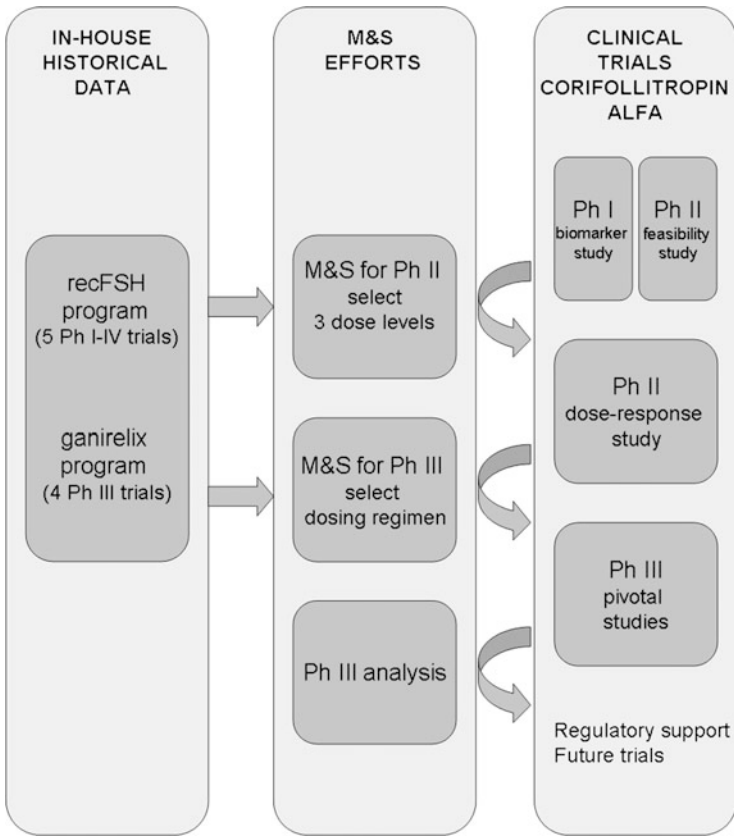


Fig. 7.3 Clinical development program of corifollitropin alfa: interplay between M&S efforts and clinical trials

based on M&S. Therefore, the recommended dose for Phase III development would possibly be different from the doses tested during Phase II development. The design of the Phase II dose-response trial was selected based on a maximal probability to demonstrate a dose-response relationship, wherein the number of oocytes (NOoc) retrieved (the anticipated registration endpoint) was correlated with the corifollitropin alfa dose. This study was designed to allow optimal selection of doses for Phase III development, based on the assumption that an optimal dose could be best established using M&S if the Phase II data supported the characterization of a well-defined dose-response relationship.

Prior to Phase III development, M&S was used to select the optimal dose of corifollitropin alfa. In these evaluations, the time profile of the hormone inhibin-B was identified to play a crucial role as a biomarker of follicular growth (de Greef *et al.* 2010). Inhibin-B is an FSH induced hormone, originating from follicles, and has been shown to be a sensitive marker of follicular development. The recommended dosing regimen based on M&S using inhibin-B as a biomarker was

subsequently evaluated in two large Phase III pivotal trials ENGAGE and ENSURE, where the primary clinical outcomes were pregnancy rate and the NOoc (Devroey *et al.* 2009; The corifollitropin alfa ENSURE study group 2010). The model framework continues to be used in responses to regulatory questions and to support the design of future clinical studies. Corifollitropin alfa drug development resulted in successful regulatory approval.

7.3 Phase II Development: Design of a Dose-Response Study

The major Phase I trial was a study in healthy female volunteers to evaluate the pharmacokinetics, pharmacodynamics and safety of a single injection of corifollitropin alfa of 15–120 μg (Duijkers *et al.* 2002). The first Phase II clinical trial was a feasibility study, with three corifollitropin alfa dose groups (120, 180 and 240 μg) and a daily recFSH reference group, and 25 subjects per treatment arm (Devroey *et al.* 2004). This study design was not based on M&S, even though that would have been feasible on the basis of the Phase I study data. At that time, there were doubts whether the available Phase I data would be predictive for the outcome in Phase II trials. The feasibility study demonstrated that a single dose of corifollitropin could initiate and sustain follicular growth for 7 days and that doses up to 240 μg were well tolerated. However, the data did not demonstrate a dose-response relationship.

The second Phase II clinical trial was a dose-response trial (The corifollitropin alfa dose-finding study group 2008). The aims of the study were (1) to determine the optimal dose (*i.e.*, resulting in a similar NOoc as daily injections with recFSH) and minimal effective dose of corifollitropin alfa and (2) to generate data for model-based Phase III dose selection. Dose selection for three corifollitropin alfa dose groups was based on M&S (de Greef *et al.* 2010). Extensive internal databases were available from three previous development programs in COS. Data from five clinical trials of recFSH (1,142 patients) and four clinical trials from ganirelix (1,525 patients) were used in addition to Phase I and II data from the corifollitropin alfa program (de Greef *et al.* 2010) (Fig. 7.3). All three compounds (*i.e.*, recFSH, ganirelix and corifollitropin alfa) are used for COS. In all three development programs, women were treated with a follicle stimulant (recFSH or corifollitropin alfa) and a GnRH analog to prevent an endogenous LH surge (pretreatment with a GnRH agonist or coadministration with a GnRH antagonist (*e.g.*, ganirelix)), resulting in data to populate the COS model framework (*e.g.*, follicular volume, cancellation rate, NOoc).

The model framework is depicted in Fig. 7.4. Panel A shows that data from the corifollitropin alfa development program (Phase I trial in healthy volunteers) were used for PK model building (Model 1, M1) and to model the initial follicular response (M2). The clinical PK-PD group had the modeling responsibility (see Panel B) and used nonlinear mixed effects modeling to develop a population PK model of corifollitropin alfa. Using Bayesian estimates of the area under the concentration-vs.-time curve (AUC) for the subjects included in the trial, the

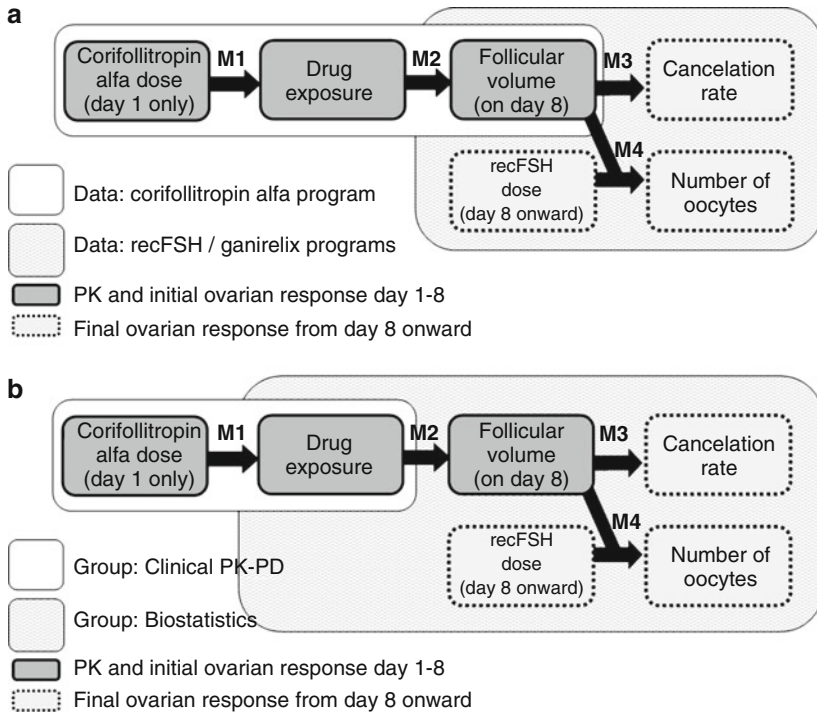


Fig. 7.4 Model framework to support design of phase II dose-response trial (a) data used for the various model components (b): disciplines in the lead for the various model components

biostatistics group developed a regression model for the relationship between drug exposure and the total follicular volume (FV) on stimulation day 8 (FV8) (M2).

FV8 was an important determinant for the risk of cycle cancellation (M3) and for the NOoc in subjects without cycle cancellation (M4). Cycle cancellation was defined as the retrieval of one or more oocytes. The NOoc was not only dependent on the follicular growth during stimulation from days 1 to 8, but also on the dose of recFSH from day 8 onward (FSHdose). Other covariates in models M1–M4 were age and the type of GnRH analog (GnRH agonist or GnRH antagonist).

Both clinical PK-PD and biostatistics were involved in model building (see Fig. 7.4b) using NONMEM (M1) as well as SAS (M2–4). However, all simulations were performed by the biostatistics group to prevent back-and-forth transfer of simulated data between the two groups and their respective preferred software tools. In order to consolidate all trial simulations in SAS, the population PK model M1 (using all serum concentrations at all time points) was replaced by a regression model describing the relationship between the corifollitropin alfa dose and drug exposure expressed as the AUC (which is a parameter without a time component and which was derived from the population PK analysis).

The regression models for M1–4 are listed in Table 7.1. These models were used to simulate the trial outcome for different Phase II designs. The probability of

Table 7.1 Regression models for trial simulations of the phase II dose-response trial

Model	Relationship	Equation
M1	Dose ~ AUC	$\ln(\text{AUC}) = \alpha_1 + \beta_1 \cdot \ln(\text{dose}) + \eta_1$
M2	AUC ~ FV8	$\ln(\text{FV8}) = E_0 + E_{\max} \cdot \text{AUC}^n / (\text{AUC}_{50}^n + \text{AUC}^n) + \eta_2$
M3	FV8 ~ $P_{\text{cancellation}}$	$\text{logit}^1(P_{\text{cancellation}}) = \beta_{3a} \cdot \ln(\text{FV8}) + \beta_{3b} \cdot \text{GnRH analog} + \beta_{3c}(\text{age}-33) + \beta_{3d}$
M4	FV8 ~ NOoc	$\ln(\text{NOoc}) = E_{\max} \cdot \text{FSHdose}^h / (\text{FSHdose}^h + \text{ED}_{50}^h) + \eta_3$

α and β are fixed effects; η represents random variability between patients

$^1\text{logit}(P_{\text{cancellation}}) = \ln(P_{\text{cancellation}}/(1-P_{\text{cancellation}}))$

success was defined as the probability of a significant dose-response relationship for the NOoc. In statistical terms, the slope of $\text{NOoc} \sim \log(\text{Dose})$ should be significantly larger than zero at $p < 0.05$.

The first design to be simulated was the design of the Phase II feasibility trial, *i.e.*, three corifollitropin alfa dose groups (120, 180, and 240 μg) with 25 women per group. For each patient, values for AUC, FV8 and $P_{\text{cancellation}}$ were simulated as described by De Greef *et al.* 2010. Next, it was determined if the patient's cycle was canceled or not, based on the probability of cycle cancellation and a random sampling process. If the cycle was canceled, the NOoc was zero by default. If the cycle was not canceled, the NOoc was simulated.

Simulations showed that the dose-response relationship was relatively flat at doses of $\geq 120 \mu\text{g}$ (see Fig. 7.5). In hindsight, the probability to find a significant dose-response relationship in the Phase II feasibility study was about 10% with three active treatment arms of 120, 180 and 240 μg with 25 subjects per cohort (see Fig. 7.6). Simulated and observed results for the Phase II feasibility study were in good agreement, although model uncertainty was large in this stage of development, which resulted in wide prediction intervals for the feasibility study (Fig. 7.5).

The results presented in Fig. 7.5 demonstrated that the developed model framework provided post-hoc predictions that were in line with the feasibility trial outcomes. This was an important impetus for the clinical research scientists to embrace the M&S project that thus far mainly was driven from clinical PK-PD and biostatistics. It also constituted a motivation to use M&S to select a model-informed design for a subsequent Phase II dose-response trial.

Trial simulations were conducted to evaluate various study designs. In addition to a design using the same dose groups as the Phase II feasibility trial (*i.e.*, 120, 180 and 240 μg), three new designs were evaluated ((1) 50, 100, 200 μg ; (2) 60, 120, 180 μg ; (3) 90, 135, 180 μg) for various group sizes (10–200 subjects per dose group). Dose scenarios (1) and (2) were expected to result in the highest probability of success (see Fig. 7.6). The dose range for design (2) was narrower and was therefore expected to result in a better safety profile as compared to design (1), with limited impact on study power. The probability of success for

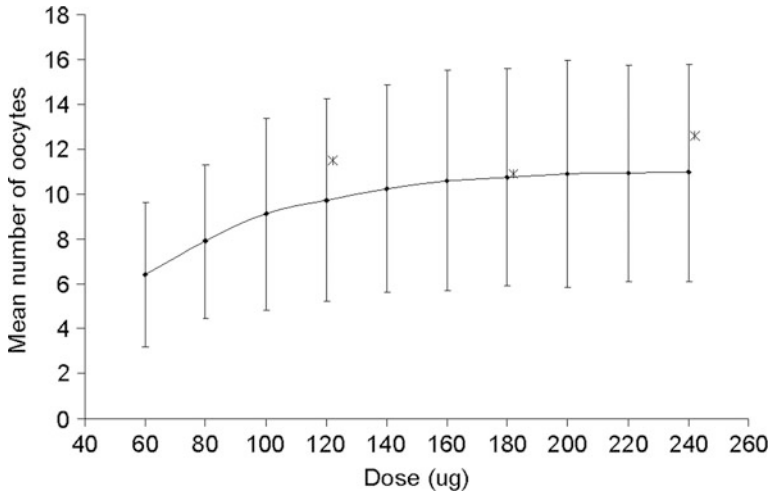


Fig. 7.5 Simulated mean number of oocytes (NOoc) for 25 subjects per dose level and 1,000 cohorts for each dose level. *Observed mean NOoc in the phase II feasibility study. Vertical lines represent ± 2 SD of $n = 1,000$ simulations

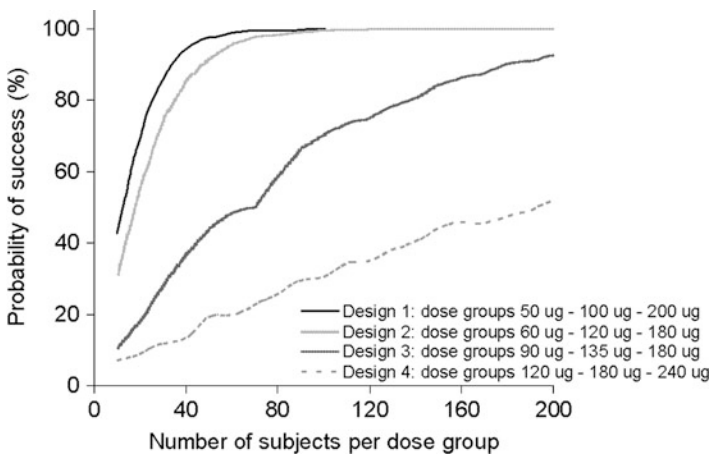
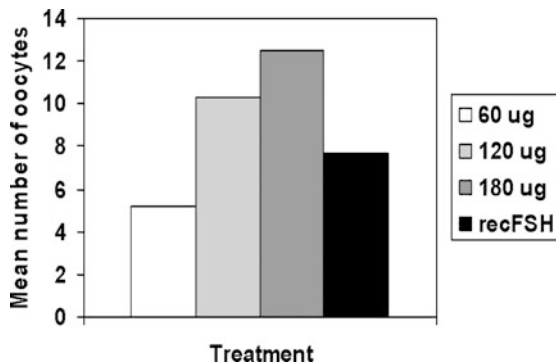


Fig. 7.6 Probability of success for four dose scenarios and various group sizes

design (2) increased with group size and reached a sufficiently high level at the selected group size of $n = 80$.

In the Phase II dose-response trial, four cohorts of 80 patients were included, each treated with 60, 120 or 180 μg corifollitropin alfa (treatment groups), or with daily recFSH injections (reference group). Based on the simulation results, this trial was adequately powered to provide a significant dose-response in terms of the NOoc retrieved as shown in Fig. 7.6 (approximately 95% probability of success). Figure 7.7 shows the observed mean numbers of oocytes for all dose groups. The

Fig. 7.7 Results of phase II dose-response trial



mean NOoc retrieved increased significantly ($p < 0.0001$) with the corifollitropin alfa dose. For the 120 and 180 μg corifollitropin alfa groups, the ovarian response in terms of the NOoc was statistically significantly higher than in the daily recFSH reference group. The cancellation rate was highest for the 60 μg corifollitropin alfa group (43.6%) whereas 120 and 180 μg corifollitropin alfa resulted in cancellation rates of 9.1 and 11.4%, respectively. The cancellation rate was 18.5% for the recFSH group. The main reason for cancellation in the 60 μg corifollitropin alfa group was a too short duration of follicular stimulation, which was reflected by a premature decline in inhibin-B levels from day 6 onward, well before daily recFSH was to be initiated on day 8 (see Fig. 7.1). This was the reason to include inhibin-B in the models (see below).

7.4 Phase III Development: Dose Selection

Based on the results of the Phase II dose-response trial, which showed a clear dose-response relationship, it was concluded that the recommended dose of corifollitropin alfa for Phase III development was predicted at 120–180 μg . Subsequently, a sophisticated data analysis was conducted to precisely determine the recommended dose of corifollitropin alfa for Phase III development. M&S was deployed to further investigate the impact on treatment outcome of various doses of corifollitropin alfa and patient characteristics.

The model framework that was used for the Phase II dose-response trial design, served as a basis for this continued M&S effort. The framework was expanded to include both corifollitropin alfa PK and inhibin-B, a causal path biomarker of follicular growth (see Fig. 7.8).

An exploratory analysis demonstrated the clinical relevance of a decrease in inhibin-B levels. After treatment with 60 μg corifollitropin alfa in the Phase II dose-response trial, several subjects showed an early inhibin-B decrease, whereas follicles continued to grow for some time. A typical example of insufficient stimulation, reflected by an inhibin-B gap and a delayed arrest of follicular growth, ultimately resulting in cycle cancellation, is illustrated in Fig. 7.9. This observation motivated a

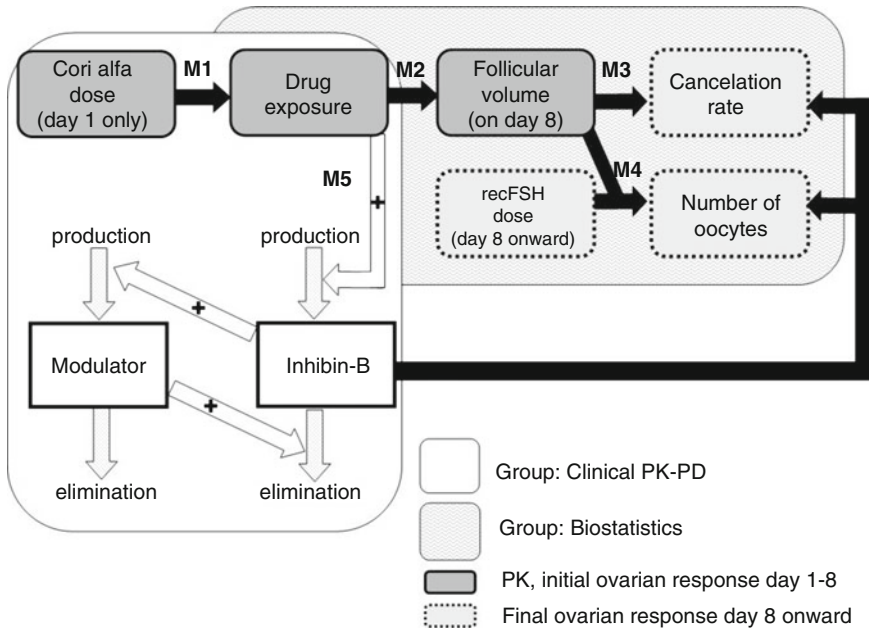


Fig. 7.8 Model framework to support dose selection for phase III pivotal development

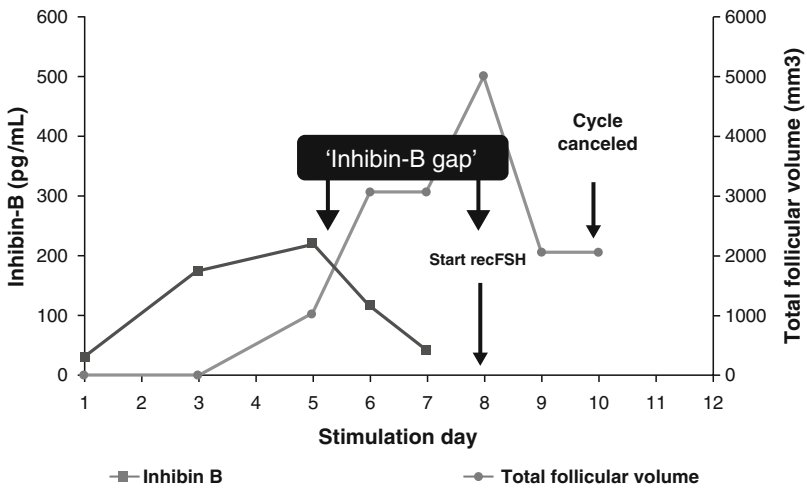


Fig. 7.9 Inhibin-B gap as an early marker of insufficient follicular stimulation and cycle cancellation

more thorough analysis of the time profile of inhibin-B levels in relation to cycle cancellation. In the 60- μ g treatment group, 64 of 77 patients had an inhibin-B gap, defined as a time interval ≥ 1.5 days of decreasing inhibin-B levels (on days 6 and 7, or even earlier) prior to the first injection of daily recFSH treatment (on day 8). The

cancelation rate in patients with an inhibin-B gap was 42 vs. 8% for patients without an inhibin-B gap. Inhibin-B was shown to be a relevant biomarker for good follicular stimulation because it is sensitive and because a decline in inhibin-B precedes the arrest of follicular growth in time. Inhibin-B profiles are predictive of an unsustained ovarian response and ultimately treatment failure.

The recommended dose of corifollitropin alfa would need to result in steadily increasing serum inhibin-B levels, reflecting a sustained ovarian response for 7 days with a minimal risk of cycle cancelation. A population PK-PD model was developed by the clinical PK-PD group to describe the time profiles of corifollitropin alfa concentrations and inhibin-B levels (Fig. 7.8). An indirect effect model was used to link drug exposure to an increased production of inhibin-B (Krzyzanski and Jusko 1998). A modulator-compartment was included to describe a negative feedback mechanism (Wakelkamp *et al.* 1996). More details on the PK-PD model of inhibin-B are available in De Greef *et al.* 2010 (Supplementary data section) (de Greef *et al.* 2010). This population PK-PD model (describing the inhibin-B profile over time) was transformed into a non-longitudinal regression model (describing the relationship between the day of the inhibin-B decrease and AUC) to allow simulations in SAS, run by biostatistics (Table 7.2, M5).

The population PK model was updated using new PK data from the Phase II dose-response trial. A covariate analysis demonstrated that body weight was an important determinant of the PK profile of corifollitropin alfa. For simulation purposes, this model (describing the serum concentration of corifollitropin alfa over time) was also implemented as a regression model, describing the relationship between AUC, body weight and dose, without a time component (Table 7.2, M1). All regression models for the model framework (M1–5) are listed in Table 7.2. De Greef *et al.* 2010 have previously published the parameter estimates of the final models.

Figure 7.10 represents the impact of body weight on drug exposure and on the time profile of serum inhibin-B levels. After equal doses, the AUC of corifollitropin alfa was approximately two-fold higher in a subject with body weight 45 kg compared with a subject with body weight 90 kg (Fig. 7.10a). The day when the inhibin-B decrease occurred was also strongly related to body weight (Fig. 7.10b). Because an inhibin-B gap of ≥ 1.5 days was related to an increased cancelation rate, an inhibin-B decrease should not occur before day 6.5 in order to support follicular

Table 7.2 Regression models for phase III trial simulations

Model	Relationship	Equation
M1	Dose \sim AUC	$\ln(\text{AUC}) = \alpha_1 + \beta_1 \cdot \ln(\text{dose}) - \gamma_1 \text{ body weight} + \eta_1$
M2	AUC \sim FV8	$\ln(\text{FV8}) = E_0 + E_{\max} \cdot \text{AUC}^n / (\text{AUC}_{50}^n + \text{AUC}^n) + \eta_2$
M3	FV8 $\sim P_{\text{cancelation}}$	$\text{logit}^1(P_{\text{cancelation}}) = \beta_{3a} \cdot \ln(\text{FV}) + \beta_{3b} \cdot (8\text{-day USS}) + \beta_{3c} \cdot \text{inhibin-B gap} + \beta_{3d} \cdot \text{GnRH analog} + \beta_{3e} \cdot \text{body weight} + \beta_{3f} \cdot (\text{age}-33) + \beta_{3gi}$
M4	FV8 \sim NOoc	$\ln(\text{NOoc}) = E_{\max} \cdot \text{FSHdose}^h / (\text{FSHdose}^h + \text{ED}_{50}^h) + \eta_4$
M5	AUC \sim InhB	$\ln(\text{day of inhibin-B decrease}) = \alpha_5 + \beta_5 \cdot \ln(\text{AUC}) + \eta_5$

α and β are fixed effects; η represents random variability between patients; β_{3gi} represents differences between trials ($i = 1, 2, \dots, 11$)

¹ $\text{logit}(P_{\text{cancelation}}) = \ln(P_{\text{cancelation}} / (1 - P_{\text{cancelation}}))$

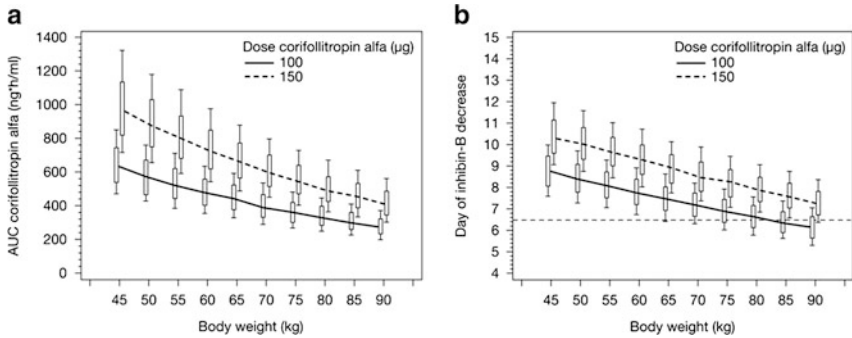


Fig. 7.10 (a) Relationship between exposure to corifollitropin alfa, expressed as the AUC, and body weight. (b) Relationship between the day of inhibin-B decrease and body weight. The horizontal line indicates an inhibin-B decrease on day 6.5, corresponding to a clinically relevant inhibin-B gap of 1.5 days. Data were simulated for 1,000 subjects per dose and body weight group. Box-whisker plots represent P10, P25, P75, P90. This figure is adapted from *Clinical Pharmacology and Therapeutics* (de Greef *et al.* 2010)

stimulation during 7 days (in a regimen with daily recFSH injections from day 8 onward), which is indicated by the horizontal line in Fig. 7.10b. After a single dose of 100 µg corifollitropin alfa, the day of inhibin-B decrease was predicted to be after day 6.5 for more than 90% of the subjects with body weight ≤60 kg, whereas subjects with body weight >60 kg required a higher dose of 150 µg to maintain sufficient follicular stimulation during 7 days.

The optimal dose should be sufficiently high to support COS during 7 days, but should also be as low as possible to prevent ovarian hyperstimulation. Hence, a balance was required to select an optimal dose of corifollitropin alfa, taking into account patient-related characteristics that may affect exposure and/or response. The lowest dose of corifollitropin alfa resulting in a minimal cancellation rate was to be selected as the optimal dose for Phase III clinical development.

Figure 7.11a shows the predicted cancellation rate in future trials for various doses of corifollitropin alfa. For subjects weighing ≤60 kg, the cancellation rate decreased up to a dose of 100 µg, but did not show a clinically relevant decrease between 100 and 200 µg. For subjects weighing >60 kg, the minimal cancellation rate was reached at a dose of 150 µg. For these subjects, the cancellation rate was predicted to be approximately two-fold higher after treatment with a single dose of 100 µg compared with 150 µg.

The predicted mean NOoc increased with dose (Fig. 7.11b). For a dose of 100 µg for women weighing ≤60 kg and a dose of 150 µg for women weighing >60 kg, the mean NOoc per started cycle was anticipated to be 12.1 (P5–P95: 9.7–14.8) and 13.2 (P5–P95: 10.5–16.0), respectively.

The selected dosages of 100 and 150 µg were prospectively evaluated in Phase III clinical trials. As expected, the recommended dose based on two body weight categories resulted in similar drug exposure for women with body weight ≤60 kg and women with body weight >60 kg (Fig. 7.12a). The observed mean numbers of

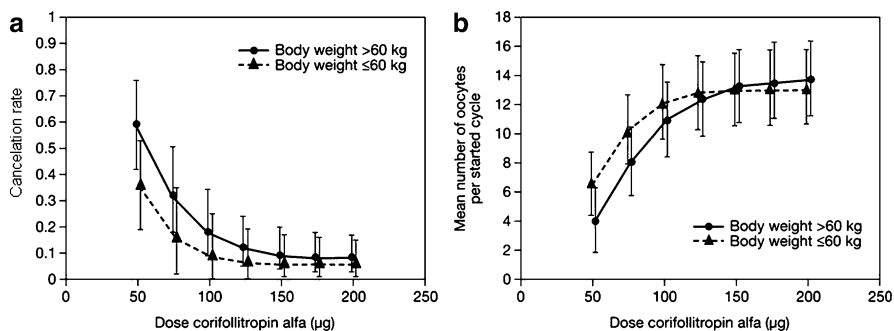


Fig. 7.11 (a) Relationship between the cancellation rate and the dose of corifollitropin alfa. (b) Relationship between the mean NOoc and the dose of corifollitropin alfa. Data were simulated for 1,000 clinical trials of subjects weighing ≤ 60 kg (220 subjects per trial) and for 1,000 clinical trials of subjects weighing >60 kg (700 subjects per trial). Plotted values are the median values (P50) of the simulated clinical trial results. Whiskers represent P5-P95. This figure is adapted from Clinical Pharmacology and Therapeutics (de Greef *et al.* 2010)

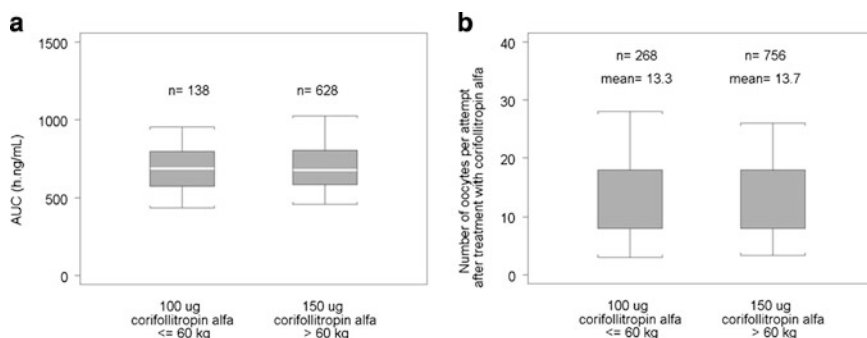


Fig. 7.12 (a) Drug exposure; (b) NOoc. Horizontal white marks represent median values, boxes represent interquartile ranges, whiskers represent P5-P95. Drug exposure data are from Caucasian subjects from two phase III trials

oocytes were also similar in women weighing ≤ 60 and >60 kg (*i.e.*, 13.3 and 13.7, respectively, Fig. 7.12b) and were consistent with the model-based predictions (*i.e.*, 12.1(P5–P95: 9.7–14.8) and 13.2(P5–P95: 10.5–16.0), respectively).

7.5 Discussion

Collaboration of multiple disciplines is well recognized to be critical to the success of M&S in supporting drug development decisions (Grasela *et al.* 2007; Zhang *et al.* 2008). In many M&S initiatives in pharmaceutical industry, focus has been on

bringing together the two quantitative disciplines PK-PD and biostatistics and liaising them with the experimentalists in clinical research or clinical pharmacology. This is a logical focus, as an understanding of exposure response relationships through PK-PD should enable statisticians to better inform clinical trial designs (De Ridder 2005).

Clearly, a considerable effort is required to achieve the level of connectivity and understanding that enables a successful partnership between scientists from different backgrounds. Effective, timely and trustful collaboration between all parties is essential to guide decision making in the drug development process based on M&S. Frequent, intensive interactions are required to have a common understanding of each other's contributions to the overall M&S deliverables and to find the opportunities where the synergy between multiple disciplines can bring most added value. It also requires an open culture, where constructive criticism and questions from colleague scientists are appreciated. Lastly, sufficient prioritization across all involved disciplines of M&S activities vs. other activities performed in support of the setup, conduct and reporting of clinical trials is essential to allow a timely delivery of required M&S output.

For optimal synergy between the main collaborators in such M&S organization (*i.e.*, clinical PK-PD, biostatistics and clinical research), all groups need to beware of their own specific challenges and opportunities as listed in Table 7.3. Explicit identification of the challenges and the cultural barriers between the groups will enhance interdisciplinary collaboration. Moreover, the intrinsic motivation and enthusiasm of all collaborators will be increased when the opportunities and goals are clearly defined.

The impact of M&S is maximal when data are analyzed retrospectively (learn) and when modeling results are evaluated prospectively (confirm) (Sheiner 1997). Data are analyzed retrospectively from one trial to predict prospectively the next trial, whereas the outcome of the new trial will confirm the model and its assumptions. This results in optimal knowledge propagation, throughout the development program (Lalonde *et al.* 2007).

In this chapter, corifollitropin alfa was discussed as an example of a successful model-based drug development program. This project demonstrates how multiple learn-and-confirm cycles can result in a synergy between M&S and clinical trial design. This interplay did not exist immediately from the start of the program, but when the outcome of the Phase II feasibility study proved to be in line with model-based predictions, M&S was embraced by global clinical research and was utilized to design a subsequent Phase II dose-response trial. The data from this Phase II trial were used to refine and expand the model framework, to apply it for Phase III dose selection (de Greef *et al.* 2010). The outcome of those pivotal trials matched the model-based predictions very well, thus closing the loop on the learn-and-confirm cycle. Overall, these two learn-and-confirm cycles have resulted in efficient trials and in a minimal risk of selecting a suboptimal dose for pivotal development, and have therefore maximized the utility of the Phase II dose-response trial and the two Phase III trials (Burman *et al.* 2005). In addition, the models provided supportive evidence in the registration of corifollitropin alfa.

Table 7.3 Challenges and opportunities for optimal synergy between the key players in M&S projects

	Challenges	Opportunities
Clinical PK-PD	<p>Be explicit and transparent about assumptions and limitations of PK-PD and disease models</p> <p>Provide adequate model validation <i>e.g.</i>, by comparing data-derived statistics to model predictions</p> <p>Appreciate the limitations to the application of PK-PD models: confirmatory trials are required at some point</p>	<p>Share quantitative insights</p> <p>Peer review; <i>e.g.</i>, more easily detect underlying assumptions</p>
Biostatistics	<p>Embrace assumption-rich models (<i>e.g.</i>, nonlinear mixed models, longitudinal data analyses)</p> <p>Discriminate between learning (internal decision-making in early clinical development) and confirming (registration)</p> <p>Appreciate the value of integrating physiological and pharmacological concepts with clinical data</p>	<p>Access to a broader range of methods and resources</p>
Clinical research	<p>Appropriately value model based predictions vs. trial outcomes</p> <p>Allow sufficient time for analysis, interpretation and trial simulations</p> <p>Provide quantitative objectives and decision criteria</p>	<p>Increase effectiveness of personal knowledge through integration with data from all relevant sources</p> <p>Make better informed decisions on trial designs</p> <p>Increase likelihood of success of clinical trials</p>

Over the course of this process, the clinical research team has become highly involved in the M&S efforts. The clinical research scientists had co-ownership of the model framework, were actively participating in discussions about the methodology and were pro-actively requesting additional analyses and/or simulations. This involvement ensured that the models were in line with clinical practice, reflected relevant elements of physiology, and allowed for prospective planning of M&S in complete alignment with the clinical trial program. The intensive collaboration between the M&S scientists (biostatistics, clinical PK-PD) and their customer (clinical research) also ensured a shared ownership of the model assumptions, approaches and ultimately results.

In the interactions between biostatistics and clinical PK-PD scientists, an early decision on the model framework was crucial. Longitudinal modeling was only performed where needed (PK, inhibin-B) and statistical modeling was applied for the clinical outcome parameters (cancellation rate, NOoc). Prespecified modeling strategies allowed for a clear and close interaction between biostatistics and clinical PK-PD. The efficiency of simulations based on this extensive model framework was greatly enhanced by the decision to replace the (longitudinal) PK and PK-PD models with (non-longitudinal) regression models, thus allowing simulations to be performed within a single software platform. It should be noted that these regression models would not have been possible without the prior longitudinal modeling, as derived parameters from the PK and PK-PD models (AUC and Day of inhibin B decrease, respectively) were used as the dependent variable. For the corifollitropin alfa M&S project, all clinical trial simulations were conducted by the biostatistics group, which was planned in advance, resulting in the selection of SAS as the platform to conduct clinical trial simulations. Generally, trial simulations based on regression models may also be conducted by the clinical PK-PD group and/or using alternate software.

Clear communication regarding the assumptions and restrictions of the model components enabled biostatisticians to accept nonlinear mixed effects models, and enabled clinical PK-PD scientists to have confidence in statistical regression models (Lalonde *et al.* 2007). This dual acceptance by both technical experts subsequently resulted in greater confidence by the clinicians on the development team in the appropriateness of the modeling and increased the willingness to make model-based drug development decisions.

The long-lasting collaboration between clinical PK-PD, biostatistics and clinical research in this project has resulted in an increased understanding of the benefit of combining forces. Equal involvement of all parties has ensured an optimal balance between scientific validity and fit-for-purpose approaches in support of decision-making and has enabled effective model-based responses to regulatory questions. The collaboration has evolved over time across various drug development programs and will continue to be valuable for future projects.

The corifollitropin alfa project was originally selected as pilot project for KD₃. It seemed challenging to capture all subtle aspects of fertility treatment in a mathematical model. Throughout 8 years (2002–2010), the KD₃ team has proven that complex physiological processes can indeed be successfully described by PK-PD and statistical models in a fit-for-purpose manner. The results of the corifollitropin alfa project have made it a key example of model-based drug development and have helped to convince our R&D management of the benefit of M&S to optimally inform decision-making.

Acknowledgments George Borm, Martin Struijs, Huub Jan Kleijn, Michiel van den Heuvel, Norbert Koper, Klaas Prins.

References

- Burman CF, Hamrén B, Olsson P (2005) Modeling and simulation to improve decision-making in clinical development. *Pharmaceut Statist* 4:47–58
- de Greef R, de Haan AFJ, Marintcheva-Petrova M, Mannaerts BMJL. (2008) Integrating PK-PD and statistics to support decision making in clinical drug development of corifollitropin alfa: a case study in controlled ovarian stimulation. American Conference on Pharmacometrics, Tucson, AZ, USA. Abstract has been published on website: http://tucson2008.go-acop.org/pdfs/Abstract_de_Greef.pdf
- de Greef R, Zandvliet AS, de Haan AFJ, IJzerman-Boon PC, Marintcheva-Petrova M, Mannaerts BMJL (2010) Dose selection of corifollitropin alfa in controlled ovarian stimulation using modeling and simulation. *Clin Pharmacol Ther* 88(1):79–87
- De Ridder F (2005) Predicting the outcome of phase III trials using phase II data: a case study of clinical trial simulation in late stage drug development. *Basic Clin Pharmacol Toxicol* 96:235–241
- Devroey P, Boostanfar R, Koper NP, Mannaerts BM, IJzerman-Boon PC, Fauser BC (2009) A double-blind, noninferiority RCT comparing corifollitropin alfa and recombinant FSH during the first seven days of ovarian stimulation using a GnRH antagonist protocol. *Hum Reprod* 24:3063–3072
- Devroey P, Fauser BC, Platteau P, Beckers NG, Dhont M, Mannaerts BM (2004) Induction of multiple follicular development by a single dose of long-acting recombinant follicle-stimulating hormone (FSH-CTP, corifollitropin alfa) for controlled ovarian stimulation before in vitro fertilization. *J Clin Endocrinol Metab* 89:2062–2070
- Duijkers IJ, Klipping C, Boerrigter PJ, Machielsen CS, De Bie JJ, Voortman G (2002) Single dose pharmacokinetics and effects on follicular growth and serum hormones of a long-acting recombinant FSH preparation (FSH-CTP) in healthy pituitary-suppressed females. *Hum Reprod* 17:1987–1993
- Grasela TH, Dement CW, Kolterman OG, Fineman MS, Grasela DM, Honig P, Antal EJ, Bjornsson TD, Loh E (2007) Pharmacometrics and the transition to model-based development. *Clin Pharmacol Ther* 82:137–142
- Krzyzanski W, Jusko WJ (1998) Integrated functions for four basic models of indirect pharmacodynamic response. *J Pharm Sci* 87:67–72
- Lalonde RL, Kowalski KG, Hutmacher MM, Ewy W, Nichols DJ, Milligan PA, Corrigan BW, Lockwood PA, Marshall SA, Benincosa LJ, Tensfeldt TG, Parivar K, Amantea M, Glue P, Koide H, Miller R (2007) Model-based drug development. *Clin Pharmacol Ther* 82:21–32
- Sheiner LB (1997) Learning versus confirming in clinical drug development. *Clin Pharmacol Ther* 61:275–291
- The corifollitropin alfa dose-finding study group (2008) A randomized dose-response trial of a single injection of corifollitropin alfa to sustain multifollicular growth during controlled ovarian stimulation. *Hum Reprod* 23:2484–2492
- The corifollitropin alfa ENSURE study group (2010) Corifollitropin alfa for ovarian stimulation in IVF: a randomized trial in lower body-weight women. *Reproductive BioMedicine Online* 21(1):66–76
- Wakelkamp M, Alvan G, Gabriellson J, Paintaud G (1996) Pharmacodynamic modeling of furosemide tolerance after multiple intravenous administration. *Clin Pharmacol Ther* 60:75–88
- Zhang L, Pfister M, Meibohm B (2008) Concepts and challenges in quantitative pharmacology and model-based drug development. *AAPS J* 10:552–559

Chapter 8

Leveraging Pharmacometrics in Early Phase Anti-inflammatory Drug Development

Ene I. Ette and Christopher J. Godfrey

Abstract The application of pharmacometrics to knowledge acquisition adds value to the drug development process because it enables the translation of information about drug action and interaction with the disease process into knowledge by enabling quantitative descriptions of drug actions, and the leveraging of this knowledge across different stages of drug development. This chapter describes a pharmacometrics based strategy of evolving a drug candidate from the nonclinical phase of drug development to the early phase of clinical drug development using an anti-inflammatory drug candidate as an example. Modeling was used to extract knowledge from nonclinical data and used to simulate a first time-in-human study. The results of the simulation study formed the basis for recommending a range of doses for a single dose escalation study, which were later compared with the results of the simulation study to determine the usefulness of the approach.

8.1 Introduction

The ultimate goal of drug development is to bring the much desired safe and efficacious pharmaceutical/biopharmaceutical drug products to the market. It was estimated in 1999 that there were 5,000 compounds in preclinical (or nonclinical) development and approximately 2,100 in clinical development (Clemento 1999). With progress in high throughput screening capabilities the number of compounds available for entry into preclinical development can only be larger. However, the advancement in discovery technology has not been coupled with faster clinical development time. In fact, it has been estimated that the clinical development time has increased by 33% (DiMasi 2001). Traditionally, the drug development process has been a lengthy and expensive series of nonclinical and clinical studies followed by regulatory reviews. Traditional drug development approaches are unlikely to

E.I. Ette (✉)
Anoixis Corporation, Natick, MA, USA
e-mail: ene_ette@anoixiscorp.com

achieve high rates of success in the near future, given the rapidly evolving changes in health care economics and consumer expectations. The quest for a new approach to drug development is further motivated by the escalating cost of introducing a new drug into the market. Estimates of the cost of developing a new drug vary widely, from a low of \$802 million in 2003 to nearly \$1 billion per drug in 2010 (Dimasi *et al.* 2003; Adams and Brantner 2010). In addition, it can take 7–12 years to bring a drug through development to final Food and Drug Administration (FDA) approval (Peck 1997). Moreover, the complexity of drug development and clinical testing procedures has increased significantly (Kleinberg and Wanke 1995).

In addition to the complexities of drug development, sophisticated new technologies and approaches in the discovery and design of new drugs are replacing the traditional methods of discovery. Availability of supercomputers and advances in the understanding of molecular interactions that underlie diseases have spurred the growth of structure-based, or rational drug design, whereby drugs can be designed by analyzing the structure of the molecular target and its active site. Integration of X-ray crystallography, computational chemistry, and nuclear magnetic resonance spectroscopy –all structure-based techniques– and genomics are slowly replacing more traditional methods such as random screening and structural modification of existing compounds (Bugg *et al.* 1993). Drugs can be designed with highly specific receptor or enzyme interactions (Zial and Beer 1990).

Despite the revolution in the discovery technology, the success rate of new chemical entities (NCEs) in development has not changed over the years. At the end of 1999, 20.9% of the NCEs filed as investigational new drug applications (INDs), from 1981 to 1992, have been approved for marketing in the U.S. (DiMasi 2001). Further, during that period, 80% of all NCEs failed to reach market, of which 37.6% were due to lack of efficacy (activity too weak) and 33.8% were due to commercial/financial decisions (commercial market too limited, or insufficient return on investment), 19.6% because of safety concerns (human or animal toxicity), and 9% for non-specific reasons (DiMasi 2001). An approximate 21% success rate for INDs is an indication of the fact that there is room for improvement in the drug discovery and development process. The fact is that innovation in drug development has not kept pace with innovation in drug research. In 2004, the FDA released a report titled “Innovation or Stagnation: Challenge and Opportunity on the Critical Path to New Medical Products” (hereafter referred to as “The Critical Path Report”) (FDA 2004). The report with its sobering statistics regarding the huge gap between the substantial investment in basic biomedical research and the disappointing number of submissions of new drugs and biological products to the FDA and regulatory agencies worldwide served as a wake-up call to all stakeholders in drug research, development, evaluation and regulation. The Critical Path Initiative, action taken by the FDA as a sequel to The Critical Path Report, is the “FDA’s national strategy for transforming the way FDA-regulated products are developed, evaluated, manufactured, and used.” (FDA 2010) As stated in The Critical Path Report the aim is, “To get medical advances to patients, product developers must successfully progress along a multidimensional critical path that leads from discovery or design concept to commercial marketing.” (FDA 2004) The “Critical

Path” as identified in the FDA’s Critical Path Report Paper is a process beginning with the identification of a drug candidate and culminating in marketing approval.

The Critical Path Report recognized the fact that traditional drug development has been empirical and sequential; from Phase 0 (preclinical (or nonclinical) development) to Phase 3. In the report, the FDA advocated a shift from empiricism to a more model based approach based on the Sheiner’s learn – confirm paradigm (Sheiner 1997). Sheiner proposed a major paradigm shift in drug development away from an empirical approach to the learn-confirm approach based on Box’s inductive versus deductive cycles (Box 1979). This process has been re-named the learn-confirm-learn approach because of their emphasis on the fact that learning continues throughout the entire drug development process (Williams *et al.* 2003). The learn-confirm-learn process contends that drug development ought to consist of alternate cycles of learning from experience and then confirming what has been learned, but that one never proposes a protocol where learning ceases.

8.2 The Learn-Confirm-Learn Process

Learning and confirming are actually parts of each drug trial (whether in animals or humans) although the relative emphasis changes as the drug progresses towards approval. For instance, a proof of concept study is not only conducted to learn about the efficacy of the drug in a patient population, but it is also to confirm if the pharmacokinetics and safety of the drug in patients are similar to that observed in healthy volunteers. Although learning and confirming can be performed to varying degrees on the same data set, their goals are quite different. Clinical trial designs that optimize confirming often inhibit learning, though never completely. Learning is not completely inhibited because data from confirmatory trials can be subjected to exposure – response analysis which increases the chances of learning from such studies. The focus of commercial drug development on confirmation is understandable as this immediately precedes and justifies regulatory approval. However, the focus on confirming has led to a low level of learning which has in turn resulted in drug development that is most often inefficient and inadequate.

Learning has as its objective answering many questions such as the relationships between dose, prognostic variables, and outcome. Learning is often model based and focuses on creating a quantitative model linking pharmacodynamic outcome, *i.e.*, biomarkers and clinical endpoints, and many variables such as dosing strategy, exposure, patient type and prognostic variables. The model that is built based on these variables defines a response surface. This complex multidimensional response surface can be conceptually collapsed to one occupying a three-dimensional Cartesian coordinate system where on one independent variable axis is an input variable (controllable factor) such as dosage regimen, exposure or concurrent therapies; and another axis incorporates subject characteristics which summarizes all the important ways subjects can differ that affect the benefit to toxicity ratio. The final axis (dependent variable) represents the benefit to toxicity ratio. The response surface,

therefore, characterizes the outcome of drug activity in those who were administered the drug taking into account the factors discussed above. That is, the response surface deals with a complex of relationships to answer the question of “what is the relationship between input profile and dose magnitude to beneficial and harmful pharmacological effects and how does this relationship vary with individual subject characteristics and time to explain tolerance or sensitivity?” For rational drug development and the optimization of individual therapy, this response surface must be mapped for the target population using pharmacometric (*i.e.*, model-based) approaches. These models then allow extrapolation beyond the immediate study subjects to predict the effect of competing dosing strategies, patient type selection, competing study structures, endpoints; and therefore aid in the design of future studies. One important feature of model-based learning is that models increase the signal: noise ratio because they can separate less apparent signals from the noise. This is important because the information content of a data set is proportional to the signal: noise ratio. For the learning study, attempt is made to define the dose-concentration-effect model. Pharmacokinetics (PK) delineates the dose-concentration component and pharmacodynamics (PD) defines the concentration-effect component of the model. PD is used here in the broadest sense in that it includes all of pharmacological action, pathophysiological effects, and therapeutic responses, both beneficial and adverse, of an active ingredient, therapeutic moiety, and/or its metabolite(s) on various systems of the body from subcellular effects to clinical outcomes (Derendorf *et al.* 2000). PD describes the intensity of a drug effect in relation to its concentration in the body fluid (Derendorf *et al.* 2000).

In contrast, the goal of “confirming” is to reject the hypothesis that efficacy is absent and the only question that it aims to answer is “is the null hypothesis true or false?” Therefore, factors that increase learning such as administering various dose levels and enrolling subjects who differ with regard to demographics and disease state are often eliminated from confirming studies as these actions tend to increase variability and reduce statistical power. Confirming studies proceed by contrasting the average outcomes between two study groups.

It is important to note that the whole drug development process from nonclinical to clinical development is an exercise in the learn-confirm-learn paradigm. In preclinical development the safety information about an NCE obtained during late discovery and lead optimization phase is confirmed in good laboratory practice (GLP) safety pharmacology and toxicology studies, and more is learned about the toxicity of the compound. The PK characteristics of the NCE are further defined in rodents and non-rodents and used for extrapolation of the dose-exposure relationship to man, and PK/PD models are developed that can provide a platform for understanding the exposure-response relationship of the compound in man. In clinical development the drug activity that was observed during discovery and nonclinical (preclinical) development is confirmed, while learning about compound safety and efficacy is done to define the response surface.

To facilitate the steps along the critical path to innovation, better scientific tools and processes are being developed to improve the efficiency of preclinical and clinical research, including new approaches to safety testing, trial design, end-point

development, and analyses. The intent is for these tools (*e.g.*, biomarkers, patient-reported outcome measures, modeling and simulation) to bring efficiencies to the drug development process and thereby increase pharmaceutical industry productivity. The application of the model-based approach to drug development is a key component of the critical path.

8.3 The Model-Based Approach to Drug Development and Pharmacometrics

Model-based drug development is an approach to and a philosophy of drug development that seeks to employ quantitative, mathematical/statistical methods in the understanding of relationships between administered doses, systemic and/or local exposure, target and off-target pharmacologic effect and (un-)favorable clinically relevant outcomes. In quantifying and characterizing these relationships, the impact of intrinsic and extrinsic factors is examined and assumptions are tested. MBDD is a core feature of the pharmacometrically-guided drug development program (PGDD). PGDD builds on the use of models by considering both the deterministic and stochastic nature of the biologic system and its response to pharmacologic intervention. It also considers how this nature impacts upon the (un-)certainty associated with system responses and the decisions that are made about how to successfully optimize and develop the drug. The use of models, simulation, and novel analytical methods are hallmarks of the PGDD program. PGDD approach also incorporates linking and integrating the expanding database of information obtained from studies conducted during the development process.

Given the rising costs of drug development and the attendant societal implications of rapidly rising medication costs, MBDD, or more broadly, PGDD has been advocated to stem this tide. Since drug development costs continue to increase and the price of computation continues to decrease rapidly, it is imperative that an increasing fraction of post-discovery drug development resources be allocated to pharmacometric approaches to enhance knowledge extraction/generation from drug development studies about a drug candidate's response surface.

The appeal of PGDD as will be illustrated in the rest of the chapter is the integration of knowledge across studies and different stages of drug development based on the learn-confirm-learn paradigm, and pharmacometrics enables the integration of such knowledge.

8.3.1 Pharmacometric Knowledge Integration

Pharmacometric knowledge integration is the combination and assimilation of quantitative knowledge (see Sect. 8.4 below) gained from different experiments performed at any given stage of the development of a drug to inform the next step

in the drug development process. For instance, knowledge gained from the modeling of *in vitro* data, animal disease models, animal PK, can be used as input models into the simulation of a first time-in-human study.

For further insight into pharmacometric knowledge integration it is important to examine the information, knowledge, understanding, and wisdom paradigm in drug development.

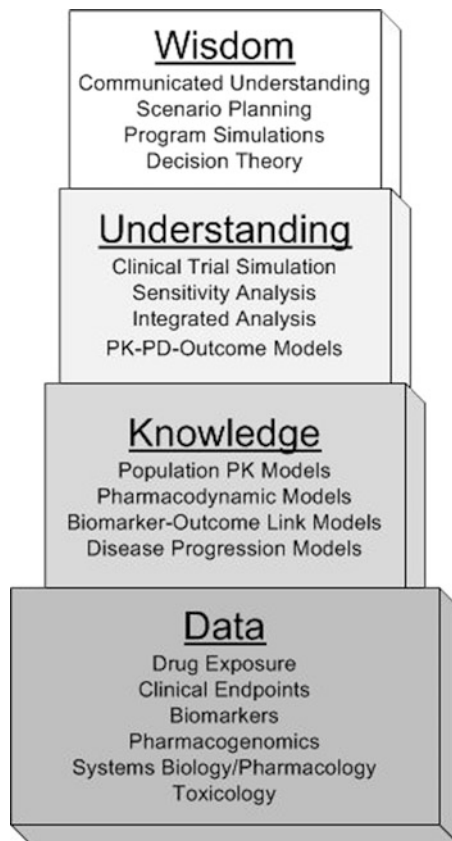
8.4 Information, Knowledge, Understanding, and Wisdom Paradigm

From the time that the drug candidate is selected to marketing approval large amounts of data (*i.e.*, data from biomarkers, pharmacogenomics, animal disease models, nonclinical PK, toxicology, and clinical trials data) are generated. These data we term information because information by itself is insufficient to support marketing authorization and optimal use of the drug (see Fig. 8.1). For information to be useful to stakeholders it must be turned into knowledge. Pharmacometrics offers one approach to accomplish this through the use of quantitative models. Models are a type of data reduction that allow one to characterize the relationship between variables of interest. However, knowledge of a system's behavior does not necessarily equate with understanding the system. Understanding comes to full fruition when the model is now used to examine the future response of the system by testing assumptions, perturbing the system virtually, performing sensitivity analyses, and successfully predicting outcomes. Simulation methods are particularly well suited to gain this level of understanding. In short, use of modeling and simulation to answer "what if?" questions provides a framework for our understanding. The ultimate value in a PGDD philosophy is the extent that drug development and regulatory decisions are made and actions taken that are consistent with the knowledge and understanding gained through this approach. Thus, implementing the PGDD philosophy in drug development makes wisdom for improved efficient and rational drug development possible.

8.5 Leveraging Pharmacometrics in Early Phase Drug Development

Acquisition of drug development knowledge must begin with a thorough understanding of the pathophysiology and biochemical pathways of the disease. The pharmacology of a drug must be understood in terms of where the drug intervenes in the disease process. The application of pharmacometrics to knowledge acquisition adds value to the drug development process because it enables the translation of information about drug action and interaction with the disease process into

Fig. 8.1 The information, knowledge, understanding, and wisdom paradigm



knowledge by enabling quantitative descriptions of drug actions, and the leveraging of this knowledge across different stages of drug development. The process of the development of a drug can be no better than the knowledge on which it is based. Without adequate knowledge it is impossible to have a thorough understanding of one's drug. The consequence of lack of knowledge impedes derivation of an optimal development strategy for a drug candidate. Leveraging pharmacometrics in drug development through the application of the processes of pharmacometric knowledge discovery and creation (Ette *et al.* 2001, 2004) results in understanding the process that generated the clinical trial data, for instance, and permits acquisition of knowledge beyond the trial data set. This provides the drug developer the necessary wisdom to make the right decisions about future trials and the strategic path for the development of a drug candidate.

Recently, some FDA reviewers in their survey of new drug application (NDA) reviews commented on the lack of leveraging pharmacometrics in the analysis of exposure – response data (Bhattaram *et al.* 2007). The authors stated as follows: “Usually in our experience, exposure – response data from each study are analyzed separately and are not well integrated to make more informed decisions during drug

development. During NDA reviews, we often perform exposure–response analysis across late-phase clinical trials (so-called phase 2 and 3 trials) looking for consistency across trials in a larger population. Sponsors could routinely provide these analyses in their NDA submissions. It is traditional to underutilize information from registration trials to “confirm” pre-specified hypothesis and not attempt to “learn” how to better utilize the drug. This prescriptive behavior assumes that either one should know about the drug characteristics fully well before embarking on the trial or conduct endless prospective trials.” This speaks to the leveraging of pharmacometrics not only in early drug development which is the focus of this chapter but also across all phases or stages of drug development.

The importance of PGDD in early-phase drug development is illustrated below with an application example. The intent is to show how pharmacometrics can be used to integrate knowledge across different stages of drug.

8.5.1 Example of Model-Based Early Development

Early-phase drug development decision making tends to be empirical and deterministic, and does not fully integrate all of the available nonclinical and clinical data or knowledge, and fails to consider the impact of uncertainty. Employing pharmacometrics methods based on modeling and simulation to integrate the available knowledge and gain further insight about a drug candidate at the early stage of development enables informed decision making. A consequence of this approach is the optimization of early phase development.

A key component in the design of a first-time-in-human (FTIH) study for an investigational drug is the selection of a starting dose and dose escalation scheme to demonstrate the safety and tolerability of the drug at doses expected to produce a therapeutic effect with minimal toxicity. This selection involves balancing the need to ensure that the subjects in the study are not exposed to unreasonable risks against the need to achieve exposures that are sufficiently high with respect to efficacy. Some of the risks associated with specifying a starting dose and dose escalation scheme arise from the uncertainty inherent in predicting pharmacokinetic and pharmacodynamic responses in humans based upon nonclinical data.

The objective of the example described hereafter is to provide a model for pharmacometrically-guided early clinical development with exposure-response serving as the unifying basis. The example illustrates how the evaluation of exposure-response using pharmacometric approaches was applied to drive early-phase clinical development of an anti-inflammatory drug candidate. The key objectives of the investigation were: (a) to establish a paradigm for rational dose selection (and escalation scheme) for FTIH study that maximizes safety for human subjects, (b) to capture uncertainty associated with extrapolation of animal PK data to humans, and (c) to study a therapeutically relevant range of doses.

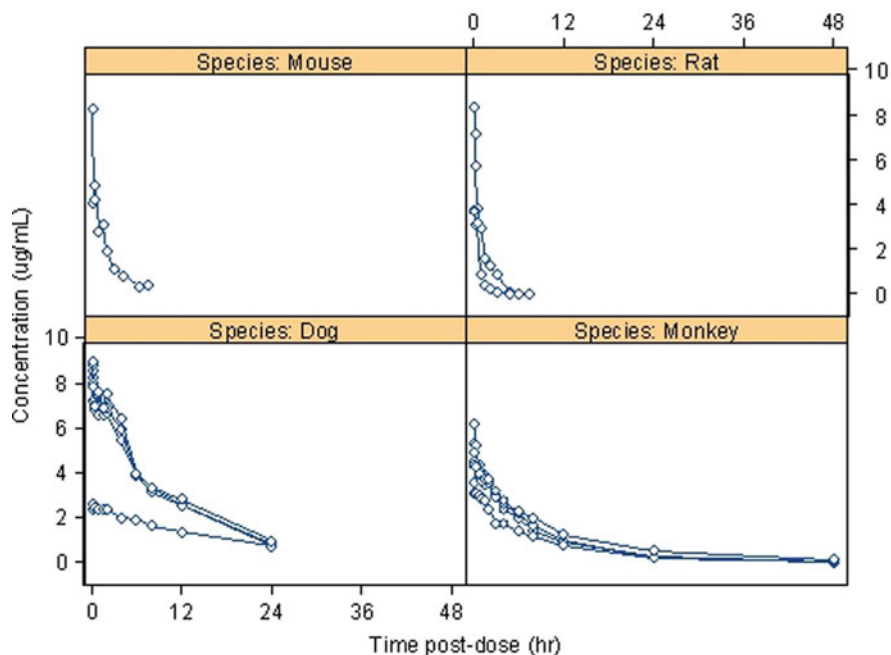


Fig. 8.2 Drug concentration vs. time by species

To address these objectives data were available from a number of nonclinical sources. Concentration-time data obtained after intravenous bolus administration of the compound to mice, rats, dogs, and monkeys (see Fig. 8.2), was available as well as exposures obtained in a GLP toxicology study. Because the compound was intended to treat a disease involving inflammation, data were available from control animals and treated animals in the adjuvant-induced arthritis (AIA) disease model in rats and also from *in vitro* lipopolysaccharide (LPS) stimulated human whole blood experiments. LPS was used to cause an inflammatory reaction, which involves the production of the inflammatory cytokines, tumor necrosis factor alpha ($\text{TNF-}\alpha$), interleukin 6 (IL-6), and IL-1 β , that can be assayed in circulating whole blood. However, the only inflammatory biomarker that will be discussed in this example is $\text{TNF-}\alpha$. As a first step to achieving the objectives, nonclinical information had to be transformed into knowledge.

8.5.1.1 Translation of Nonclinical Information into Knowledge

To transform the available information into knowledge, a nonlinear mixed effects modeling approach to allometry-based interspecies scaling (Cosson and Fuseau 1997; Martin-Jimenez and Riviere 2002) was used to scale the PK of the compound from animals to man while an inhibitory E_{max} model was used to characterize the

in vitro TNF- α data. Of the different variables (paw weight, ankle joint swelling, inflammation score, and bone resorption score) measured in the adjuvant induced arthritis (AIA) rat, paw weight and ankle joint data are the only ones that will be discussed in this example. Paw weight and ankle joint data were analyzed using the E_{\max} model.

Figure 8.2 shows the concentration – time profiles of the compound in the four species that contributed data for the analysis. A one compartment PK model was used to characterize the pooled PK data across the species. Figure 8.3 shows the prediction of clearance from the population model developed. The typical values of clearance (TVCL) and volume of distribution (TVV) were characterized by the following equations, parameter estimates and associated standard errors:

$$\begin{aligned} \text{TVCL} &= 0.239(0.0359) \times \text{WT}^{0.603(0.0419)} \\ \text{TVV} &= 1.17(0.125) \times \text{WT}^{0.961(0.0609)} \end{aligned} \quad (8.1)$$

The typical value for EC_{50} estimates from the paw weight exposure – response model and the E_{\max} model characterizing the *in vitro* inhibition of TNF- α production from LPS stimulation were 180 and 99 ng/mL, respectively. Thus an integrated knowledge was gained about the PK of the compound in animals, and its anti-inflammatory effect *in vivo* (in an animal model of inflammation) and *in vitro* (in the LPS stimulated whole blood assay). The emphasis here is on EC_{50} since this is the parameter of a high value in the translation of knowledge from the nonclinical domain to the human domain.

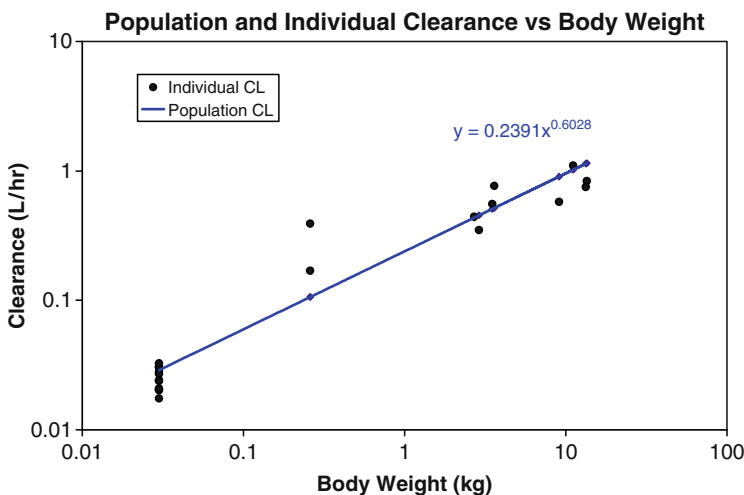


Fig. 8.3 Nonlinear mixed effects allometric model estimated clearance values

8.5.1.2 Pharmacometric Leveraging of Nonclinical Knowledge to Gain Insight into a Proposed FTIH Study

To be able to leverage the knowledge extracted from the nonclinical data for the design of a FTIH study, a simulation of the proposed clinical trial was undertaken. The objectives were to: (1) implement a simulation model leveraging nonclinical knowledge to project the outcome a proposed FTIH, including impact of absorption-related assumptions and uncertainty in PK projections on PK and PD outcomes; and (2) compare simulated exposure distributions with pharmacodynamic and toxicology endpoints to select optimal starting dose and dose range for the proposed FTIH study.

The allometric model, the *in vivo* and *in vitro* exposure – response models were used inputs in the simulation of the proposed trial based on a proposed study design shown in Fig. 8.4. The design has certain features that are advantageous for a single dose escalation FTIH study (see also Chu *et al.* 2007, 2008). It has leading dose to ensure that all subjects at any given dosing occasion are not exposed to the same dose, except on the very first dosing occasion. This is to ensure patient safety. Another important feature is the repetition of the highest dose studied in the first panel in the second panel to confirm safety of the highest dose from the previous panel while few subjects are exposed to the next higher dose. Because each subject is exposed to three doses of the drug, detection of nonlinearity in the PK of the drug is possible. This is a definite advantage over a parallel dose escalation design.

Because the compound was to be administered orally while the animal PK data were obtained via intravenous administration, assumptions had to be made about the absolute bioavailability (F) and absorption rate constant (KA) for the compound. The simulation input model from Eq. (1) was developed using intravenous PK data from animals. Different values of F (low (0.25), medium (0.5), and high (1.0)) were tested in the simulation. A range of KA values were also tested.

Panel #	Subject #	Occasion							
		1	2	3	4	5	6	7	8
1	1	P	1X	2X	4X				
	2	1X	P	2X	4X				
	3	1X	2X	P	4X				
	4	1X	2X	4X	P				
2	5					P	8X	16X	32X
	6					4X	P	16X	32X
	7					4X	8X	P	16X
	8					8X	16X	32X	P
	9					P	8X	16X	32X
	10					4X	P	16X	32X
	11					4X	8X	P	16X
	12					8X	16X	32X	P

Fig. 8.4 Proposed first time-in-human single ascending study design P placebo; $1X$ starting dose, remainder indicate multiple of starting dose

Also, since the level of intersubject variability in disposition was unknown, levels of intersubject variability ranging from 30 to 45% were evaluated. The range takes into account the fact that variability in healthy subjects often does not exceed 45%. Residual variability in the PK model was assumed to be twenty percent, while a value of twenty five percent was assumed for PD (TNF- α) response component of the simulation model. Uncertainty associated with the estimation of PK and exposure-response models were accounted for in the simulation model. This was done, in part, to account for the uncertainty in the parameter estimates in moving from animals to humans. Five hundred replicates of datasets were simulated for each combination of KA value and intersubject variability level. The simulations were performed using the Pharsight Trial Simulator (Pharsight Corporation, Mountain View, California).

Taking into consideration the no adverse effect level (NOAEL) AUC from the repeat dose toxicology study with the compound in the most sensitive toxicology species, a distribution of safety factors by dose following the dose escalation scheme in the proposed study design was determined. In doing this the starting doses were varied so that an appropriate starting dose could be determined, given the NOAEL and the dose escalation scheme.

The variables of interest from the simulation study were empirical distribution of exposure metrics: $AUC_{0-\infty}$, average concentration (C_{average}), and concentration at 24 h after dosing ($C_{24\text{ h}}$). The empirical distribution here represents both variability and uncertainty. For the PD response, the probability of median 24-h post-dose concentration exceeding EC_{50} for the inhibition of TNF- α production was of interest. Also of interest was the distribution of the simulated average concentration by dose relative to EC_{50} s for the reduction of paw weight and ankle joint swelling, respectively, from the AIA model.

The boxplots in Fig. 8.5 show the distribution of AUC values from simulated concentration – time curves by dose level for various starting doses and absorption assumptions. It can be observed from bottom panel in Fig. 8.5 that a starting dose of 1 mg (*i.e.*, 1X) irrespective of the absorption assumptions would result in low exposures even at the highest dose 32 mg (*i.e.*, 32X). This can be contrasted with the exposures obtained with a starting dose of 2.5 mg (*i.e.* 1X, the middle panel) and ending at a dose of 80 mg (*i.e.*, 32X). A starting dose of 5 mg (*i.e.*, 1X, the top panel) and ending with a dose of 160 mg (*i.e.*, 32X) would result in much higher exposures, given the assumptions.

Figure 8.6 shows the predicted probability of the median $C_{24\text{ h}}$ values exceeding the EC_{50} for TNF- α inhibition at the different doses investigated in the simulation study. Selection of the ideal starting dose and scheme would show minimal to negligible pharmacologic effect at the starting dose and high probability of pharmacologic effect at the top end of the escalation. With a starting dose of 1 mg, the predicted probability of $C_{24\text{ h}}$ exceeding the EC_{50} for TNF- α inhibition is only 25% at 8 mg (*i.e.*, 8X, Fig. 8.6 (bottom panel)). At this dose only two dose escalations would have been left to achieve a reasonable probability of biomarker inhibition. Better coverage was predicted with starting doses of 2.5 and 5 mg (see Fig. 8.6 middle and top panels, respectively). The simulation results indicated that a starting

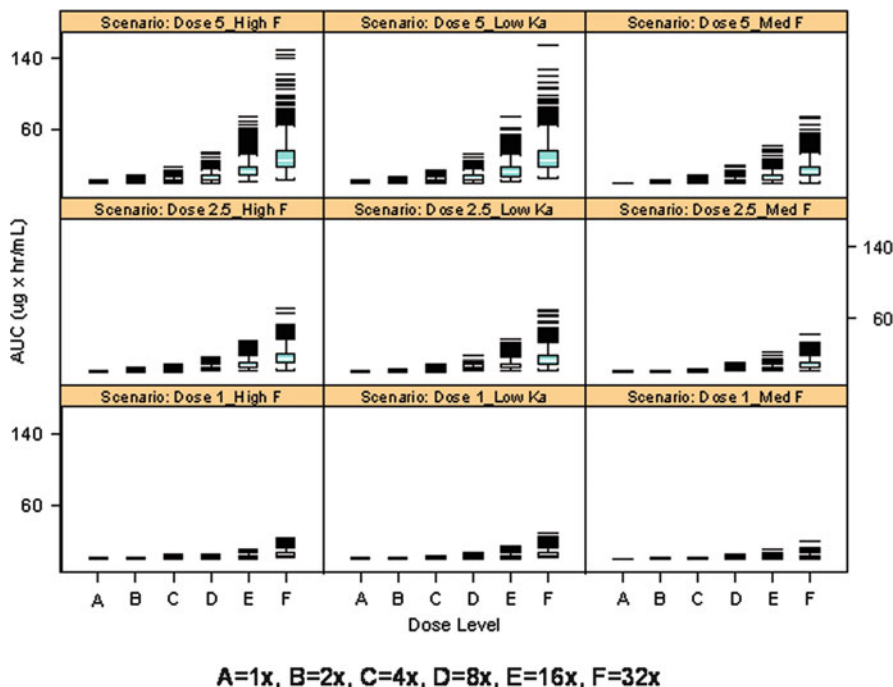


Fig. 8.5 Simulated distribution of AUC by dose level for various starting doses and absorption assumptions A 1X; B 2X; C 4X; D 8X; E 16X; F 32X. Each scenario show a combination of starting dose (1X), and assumptions about absorption rate and bioavailability

dose of 1 mg would likely result in a FTIH study that would have a higher probability of being extended as more dose escalations might be required beyond 32X – highest dose multiple from the starting dose stipulated in the study design. The insight gained from Fig. 8.6 is important because one of the purposes of the simulation project was to ensure that therapeutically relevant doses (*i.e.*, a dose range that would result in low to maximal TNF- α inhibition) would be studied in the FTIH study.

In addition, the relationship between the C_{average} and the EC_{50} s from the AIA model was also examined. Figure 8.7 shows that the predicted C_{average} for the 2.5 and 5 mg dose levels were below the EC_{50} s (180 and 300 $\mu\text{g/mL}$ for paw weight and ankle joint, respectively) of the AIA model.

The insight gained from the predicted drug exposures, the probability of TNF- α inhibition over 24 h, and the relationship between C_{average} and AIA model EC_{50} s was coupled with the NOAEL from repeated dose toxicology study to determine safety factors across the doses investigated in the simulation study with the different starting doses of 1, 2.5, and 5 mg. Figure 8.8 shows the safety factors across doses 2.5–80 mg. The 1 mg dose is omitted in this figure because of the insight gained from Figs. 8.5 and 8.6.

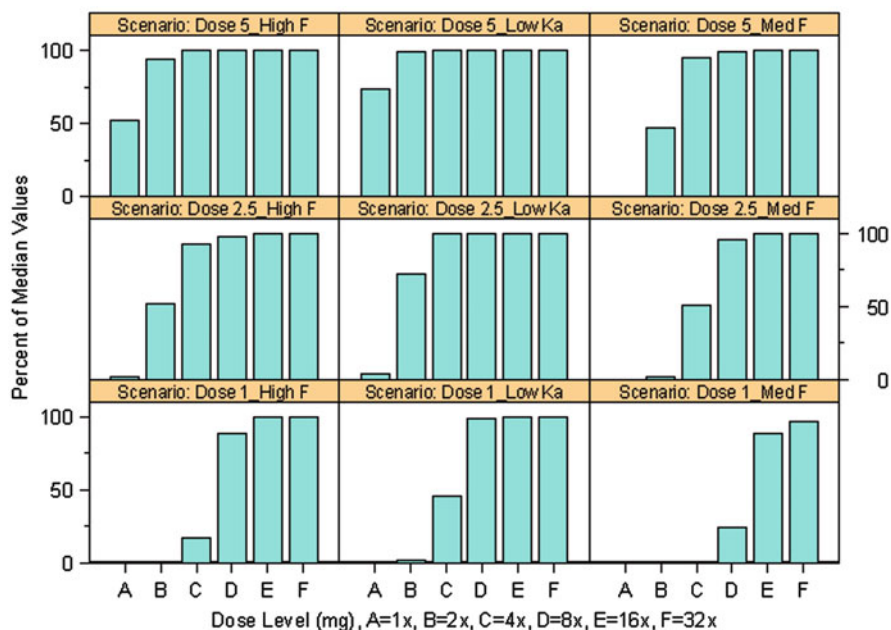


Fig. 8.6 Probability of median 24-h post-dose concentration exceeding IC_{50} for $TNF\alpha$ A 1X; B 2X, C 4X; D 8X; E 16X; F 32X

8.5.1.3 Wisdom for the Performance of FTIH Study

Given the knowledge gained from the output of the simulation study discussed above, the starting dose was chosen to be 2.5 mg. With a predicted safety factor of 200 at this dose and 10 at the last dose (80 mg) of the escalation subject safety was given high priority. Also, the proposed escalation dose range would cover therapeutically relevant exposures (*i.e.*, exposure ranges for target inhibition) to enable a go/no go decision to be made with the outcome of the FTIH trial. Also, the choice of 2.5 mg starting would enable the FTIH to last for only 8 weeks.

The FTIH study was conducted with this recommendation. The PK and PD data collected were analyzed, and the results compared with the outcome from the clinical trial simulation study.

8.5.1.4 The First-Time in Human Study

Data

The FTIH was conducted based on the study design (Fig. 8.4). PK and PD (inhibition of cytokines from *ex vivo* whole blood LPS stimulation) data were obtained at

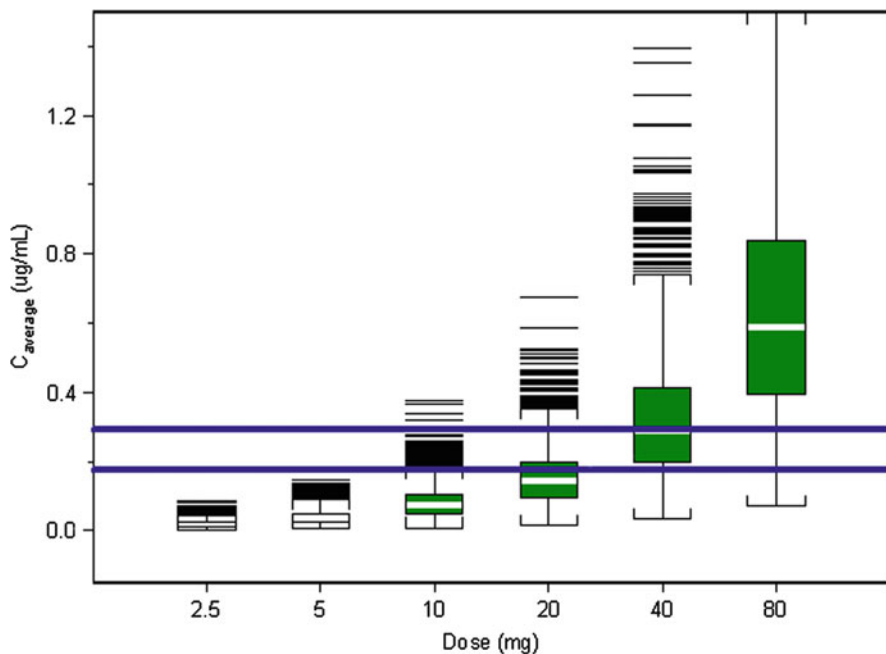


Fig. 8.7 Simulated distribution of average concentration by dose relative to EC_{50} s from nonclinical adjuvant-induced arthritis model. *Solid horizontal lines* show EC_{50} s for paw weight and ankle diameter endpoints

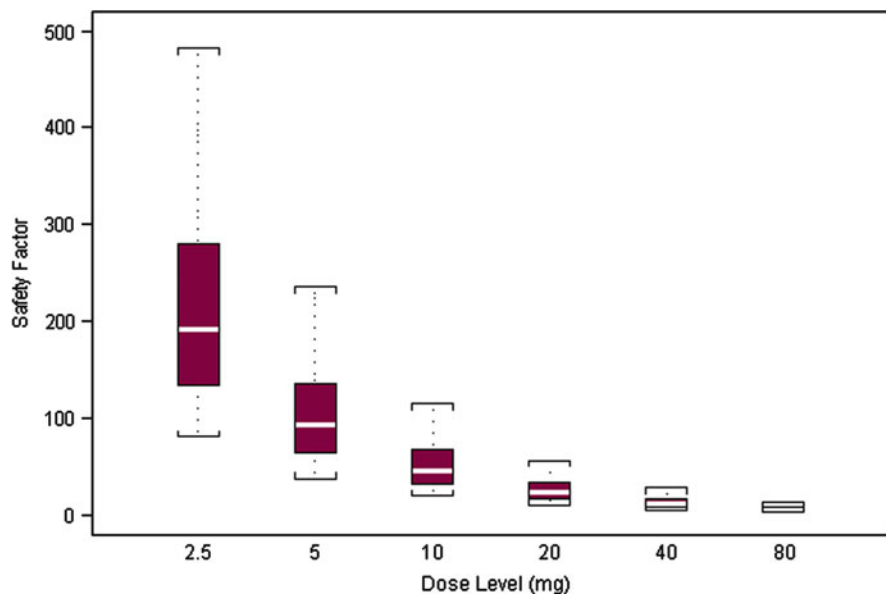


Fig. 8.8 Simulated distribution of a NOAEL-based safety factor

specified time points over 72 h, and were intensively sampled. Time matched PK and PD data were collected. The biomarker data that is of interest here is TNF- α . Thus, data were available from 20 subjects for analysis.

Population Pharmacokinetic Analysis

A nonlinear mixed effects modeling approach was used to analyze the PK data. The NONMEM software (ICON Development, Ellicott City, MD) was used for the analysis. The one compartment PK model for oral dosing was the best structural model to describe the data. The rate of absorption was parameterized as a Michaelis–Menten-type function as follows:

$$\frac{dA1}{dt} = -\left(\frac{A_{\max}}{K_m + A1}\right) \times A1$$

where $A1$ is the amount of drug in the gut, $dA1/dt$ is the rate of change of the amount of drug in the gut, A_{\max} is the maximum absorption rate, and K_m is the amount of drug in the gut associated with 50% of the maximum absorption rate. The one compartment model with nonlinear absorption was statistically highly favored over the first order absorption model. This was also confirmed with diagnostics plots.

The preference for the “nonlinear” model should not be construed as suggesting that absorption was a nonlinear process or that absorption depended on active transport. The model is simply an empirical representation of an absorption process that is more complex than simple first order absorption. For example, if a limiting solubility was reached at high doses, absorption may appear as a nonlinear process. Despite the connotation of the nonlinear model, the drug concentrations and exposures were very predictable and showed modest variability (see Fig. 8.9). Inter-occasion variability (IOV) was important model additions on oral clearance, volume of distribution, K_m , and lag time (LAG). Fasted state was included as an important covariate on LAG ($p < 0.001$) and apparent volume of distribution was modeled as a linear function of body weight ($p < 0.001$). Body weight values were centered on the median body weight of 75.2 kg. A combination of residual and proportional error model was preferred over proportional or residual error models. Figure 8.10 shows that the model adequately described the data. The irreducible final population pharmacokinetic model, given the data, is detailed below:

$$\frac{dA1_{i,j,k}}{dt} = -\left(\frac{A_{\max_i}}{K_{m_{i,j}} + A1_{i,j,k}}\right) \times A1_{i,j,k}$$

$$\frac{dA2_{i,j,k}}{dt} = -\left(\frac{A_{\max_i}}{K_{m_{i,j}} + A1_{i,j,k}}\right) \times A1_{i,j,k} - \left(\frac{CL_{i,j}}{V_{i,j}}\right) \times A2_{i,j,k}$$

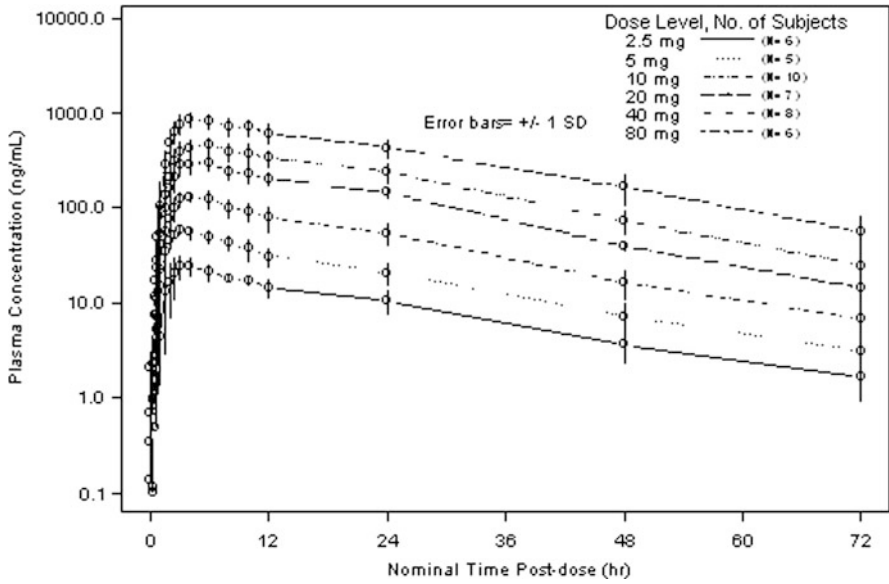


Fig. 8.9 Observed drug concentration versus time by dose level

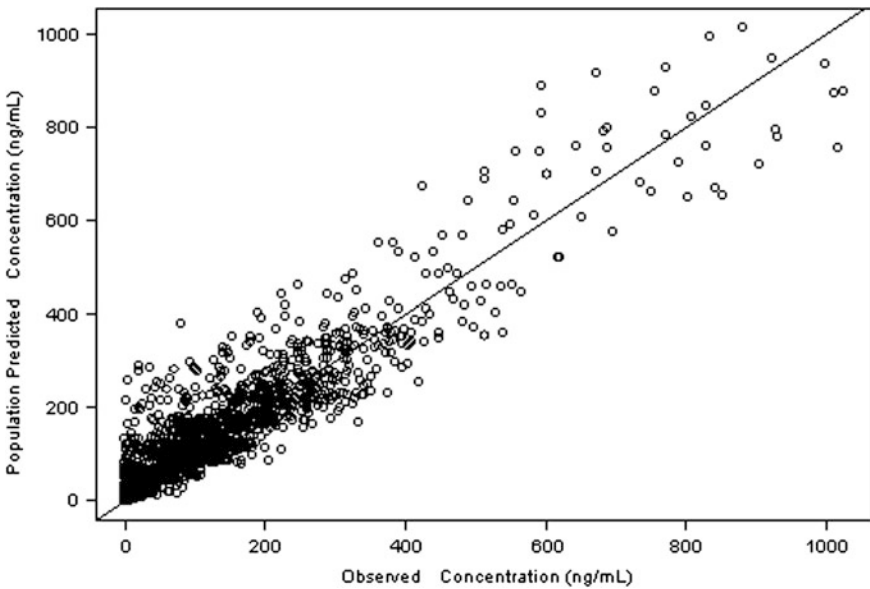


Fig. 8.10 Population predicted versus observed drug concentration. *Solid line* is the line of unity

$$C_{i,j,k} = \frac{A2_{i,j,k}}{V_{i,j}}$$

$$C_{i,j,k} = \hat{C}_{i,j,k} + \hat{C}_{i,j,k} \times \varepsilon1_{i,j,k} + \varepsilon2_{i,j,k}$$

$$CL_{i,j} = \theta1 \times \exp(\eta1_i + \kappa1_{i,j})$$

$$V_{i,j} = (\theta2 + \theta7 \times (WT_i - 75.2)) \times \exp(\eta2_i + \kappa2_{i,j})$$

$$A_{max_i} = \theta3 \times \exp(\eta3_i)$$

$$K_{m,i,j} = \theta4 \times \exp(\eta4_i + \kappa3_{i,j})$$

$$Lag_{i,j} = (\theta5 \times (1 + \theta6 \times FAST_{i,j})) \times \exp(\eta5_i + \kappa4_{i,j})$$

$$\eta_x \sim N(0, \omega_x^2), \quad \kappa_w \sim N(0, \omega_w^2), \quad \varepsilon_u \sim N(0, \sigma_u^2)$$

where variable definitions are: subscript $i = i$ th subject, subscript $j = j$ th occasion, subscript $k = k$ th timepoint, $A1$ is the amount in compartment 1 (gut compartment), $A2$ is the amount in compartment 2 (central compartment), t is time, A_{max} is the maximum absorption rate, K_m is the amount of drug in the gut resulting in 50% of the maximum absorption rate, CL is the apparent systemic clearance, V is the apparent volume of distribution, C is the observed concentration, \hat{C} is the predicted concentration, $\varepsilon1$ and $\varepsilon2$ are random effects that characterize the deviation of the prediction from the observation, σ^2 is the variance of the residual error random effects, θ_{1-7} are the fixed effects (population) estimates, η_{1-5} are interindividual random effects with corresponding variances ω^2 , and κ_{1-4} are interoccasion random effects with corresponding variances, ω^2 . The parameter estimates from this model are summarized in Table 8.1.

Table 8.1 Population pharmacokinetic parameter estimates from the first time-in-human study

PK parameter	Description	Estimate	Units	IVV ^a (%)	IOV ^b (%)
CL	Clearance	3.75	L/h	25.1	9.0%
V	Volume at median body weight	72.8	L	15.5	11.4%
	Change in volume w.r.t body weight	0.825	L/kg	–	–
Amax	Max absorption rate	38	mg/h	81.7%	–
K_m	Amount of drug in gut resulting in 50% of max rate	24.9	mg	75.4	75.2%
Lag	Oral absorption lag time in fed state	0.454	h	6.2	4.2%
	Change in lag time in fasted state	–46.9	%	–	–

^a IVV: intersubject variability expressed as approximate coefficient of variation of the pharmacokinetic parameter

^b IOV: intersubject variability expressed as approximate coefficient of variation

Exposure: Response Analysis

The exposure – *ex vivo* LPS-stimulated TNF α production data were modeled using nonlinear mixed effects modeling as implemented in the nlme 3.3 library in S-PLUS. The data were hierarchically structured into groups according to subject and occasion nested within subject. Figure 8.11 is a line plot of the TNF α – time data by dose level. The data was baseline normalized for ease of presentation. The untransformed cytokine concentration was modeled as a function of observed drug concentration according to an inhibitory E_{max} model, parameterized as follows:

$$\hat{E}_{i,j,k} = E0_{i,j,k} \times \left(1 - \frac{E_{max_i} \times Conc_{i,j,k}}{IC50_i + Conc_{i,j,k}} \right) \tag{8.2}$$

where $\hat{E}_{i,j,k}$ is the predicted cytokine concentration in the i th subject, on the j th occasion at the k th time point. $E0_{i,j,k}$ is the baseline LPS-stimulated TNF α concentration, E_{max_i} is the maximum inhibition expressed as a fraction of the baseline value, $IC50_i$ is the plasma drug concentration resulting in 50% of the maximum inhibition and $Conc_{i,j,k}$ is the observed plasma drug concentration. The data obtained during periods of placebo administration were modeled together with data obtained during periods of drug administration. Therefore, $E0$ is subscripted with time to permit a time-varying baseline.

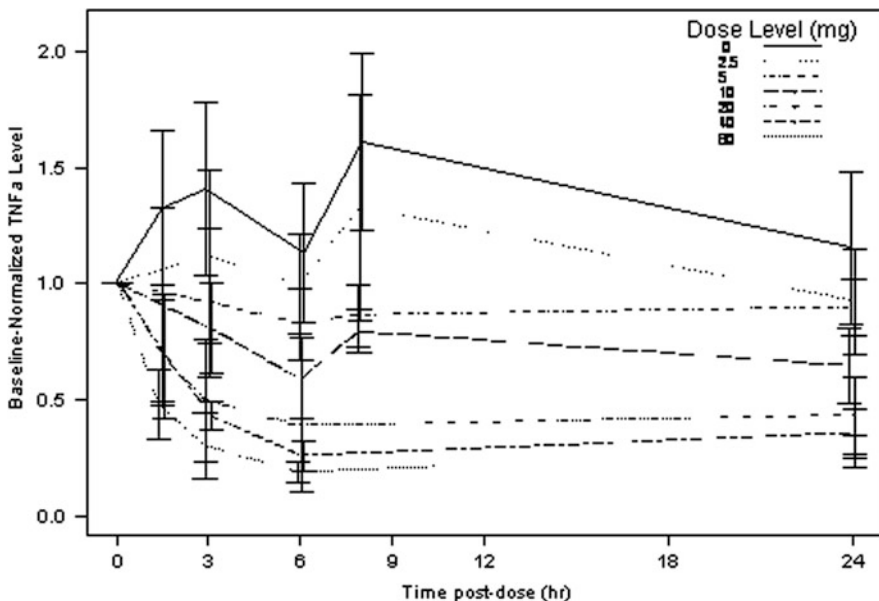


Fig. 8.11 *Ex vivo* inhibition of LPS-stimulated cytokine production data – mean baseline-normalized TNF α concentration vs. time LPS lipopolysaccharide; error bars represent ± 1 standard deviation

A structured approach (Ette *et al.* 2001) was used for the development of the exposure – response model. The initial base model included $E0$ as a mixed effect, *i.e.* a fixed and a random effect component, and E_{\max} and IC_{50} as fixed effects. The initial model for $E0$ was expressed as follows:

$$\begin{aligned} E0_i &= \beta_0 + b_{0,i} \\ b_0 &\sim N(0, \omega_{b_0}^2) \end{aligned}$$

where $E0_i$ is the subject-specific estimate of $E0$, β_0 is the population estimate, and $b_{0,i}$ is the i th subject-specific deviation of $E0_i$ from the population estimate. The variable $b_{0,i}$ is a random variable with mean zero and variance $\omega_{b_0}^2$. The variance-covariance matrix of random interindividual effects was to be optimized, *i.e.*, evaluated for appropriateness of inclusion of random effects for E_{\max} and IC_{50} and off-diagonal covariance terms. Residual variability was assumed to be homoscedastic and was to be modeled as:

$$E_{i,j,k} = \hat{E}_{i,j,k} + \varepsilon_{i,j,k}$$

where $E_{i,j,k}$ is the observed cytokine concentration in the i th subject, on the j th occasion at the k th time point, $\hat{E}_{i,j,k}$ is the corresponding predicted cytokine concentration and $\varepsilon_{i,j,k}$ is the deviation of the predicted from the observed concentration. A heteroscedastic error model was also tested.

Monocyte count associated with each blood sample was evaluated as a covariate. The monocyte count at each time point was centered on the median value calculated from all observations. Thus, $E0$ was modeled as a linear function of centered monocyte count:

$$E0 = \beta_0 + \beta_1 \times (\text{monocyte count} - \text{median}(\text{monocyte count}))$$

Inclusion and retention of an additional variance term or covariate was to be determined by the likelihood ratio test in the case of nested models or the Akaike Information Criterion (AIC) for non-nested models. The a priori significance level was set at $\alpha = 0.05$. Graphical diagnostics played a major role in model development, as expected. Figure 8.12 shows that the population exposure – response model developed adequately described the data. The final irreducible population model, given the data, is detailed below:

$$\begin{aligned} E_{i,j,k} &= \hat{E}_{i,j,k} + \varepsilon_{i,j,k} \\ \hat{E}_{i,j,k} &= E0_{i,j,k} \times \left(1 - \frac{E_{\max_i} \times \text{Conc}_{i,j,k}}{IC50_i + \text{Conc}_{i,j,k}} \right) \end{aligned}$$

$$\text{CMC}_{i,j,k} = (\text{monocyte count} - \text{median}(\text{monocyte count}))$$

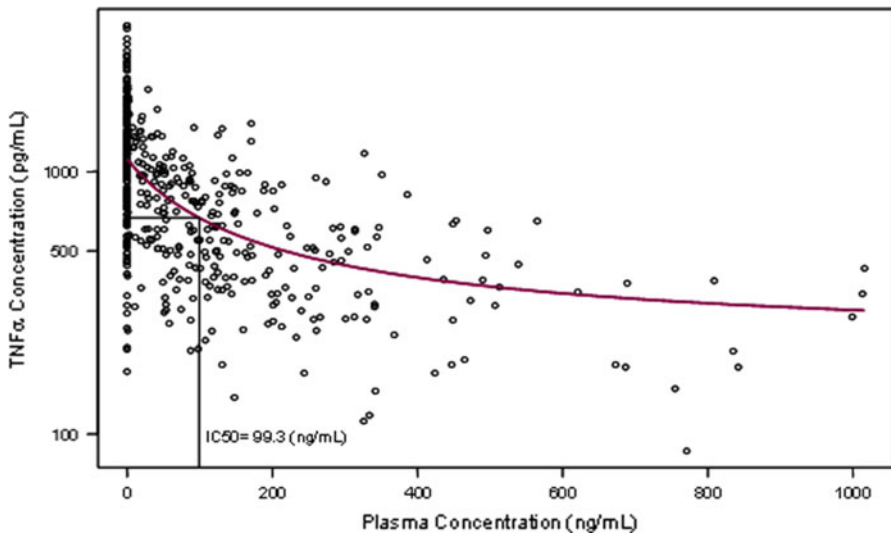


Fig. 8.12 Population predicted and observed TNFα concentration versus drug concentration

$$E_{0_{i,j,k}} = (\beta_0 + b_{0,i} + b_{0(1),i,j}) + (\beta_1 + b_{1,i}) \times CMC_{i,j,k}$$

$$E_{max_i} = \beta_2 + b_{2,i}$$

$$IC50_i = \beta_3 + b_{3,i}$$

$$b_x \sim N(0, \omega_{bx}^2), \quad b_{0(1)} \sim N(0, \omega_{b0(1)}^2), \quad \varepsilon_{i,j,k} \sim N(0, \sigma^2 |\hat{E}_{i,j,k}|^{2\delta})$$

where variable definitions are: subscript $i =$ i th subject, subscript $j =$ j th occasion, subscript $k =$ k th time point, E is the observed effect, \hat{E} is the predicted effect, ε is the deviation of the prediction from the observation which is proportional to the absolute value of the prediction, σ^2 is the unscaled variance of the error, δ is a parameter of the variance function estimating the magnitude of the proportionality between the variance and the magnitude of the prediction, $\beta_0, \beta_1, \beta_2,$ and β_3 are the fixed effects (population) estimates, b_0, b_1, b_2, b_3 are interindividual random effects with corresponding variances ω^2 , and $b_{0(1)}$ is an interoccasion random effect with corresponding variance ω^2 . The fixed effects parameter estimates for the final irreducible model, given the data, are summarized in Table 8.2.

Comparison of Performance of the FTIH Study Outcome with FTIH Clinical Trial Simulation Outcome

To investigate the performance of the clinical trial simulation of the FTIH relative to the clinical study outcome, a graphical approach was used. The similarity of AUC from the simulated study and the clinical trial is shown in Fig. 8.13. The results

Table 8.2 Population pharmacodynamic parameters from the first time-in-human study

Parameter	Units	TNF α		
		Estimate	IIV	IOV
IC50	ng/mL	99.3	45.9	–
Emax		0.807	0.047	–
EO intercept	pg/mL	1120	283	148
EO w.r.t	pg/mL/10 ⁻³			
Monocyte Count	cells	2310	919	–

¹IIV – intersubject variability expressed as approximate coefficient of variation of the pharmacodynamics parameter
²IOV – intersubject variability expressed as approximate coefficient of variation

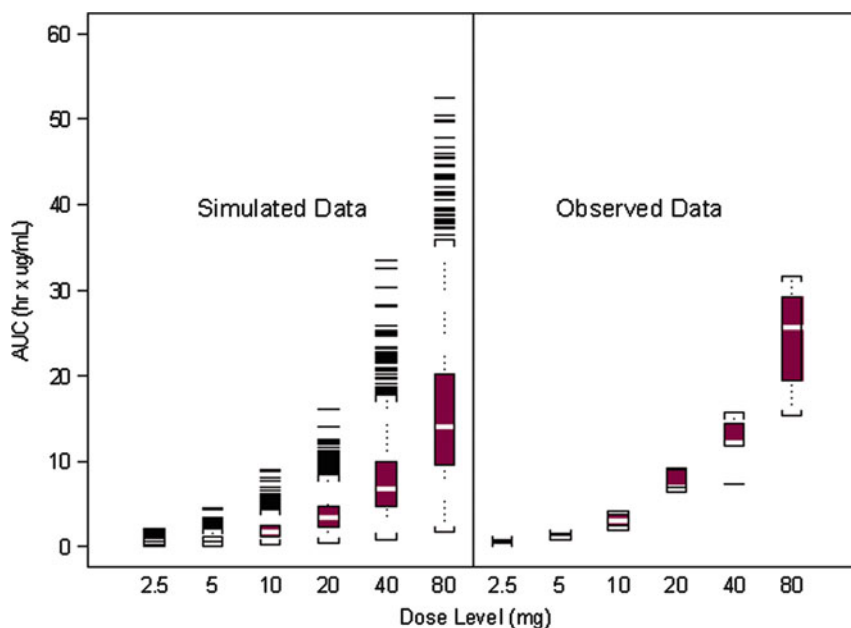


Fig. 8.13 Comparison of simulated AUC to observed AUC in first-time in human study

indicate the usefulness of incorporating uncertainty into the clinical trial simulation was important. In this case it provided the necessary predictive “cushion” for going from the nonclinical domain to the clinical domain.

Similarly, the maximal response obtained in the clinical trial was similar to that predicted from the simulation study (Fig. 8.14). It is important to note that one of the objectives of the FTIH study simulation was the recommendation doses to be studied that would cover therapeutically relevant doses in terms of biomarker inhibition. Figure 8.13 shows that this objective was achieved with the responses at doses for 20–80 mg from the clinical trial similar to those from the simulation study.

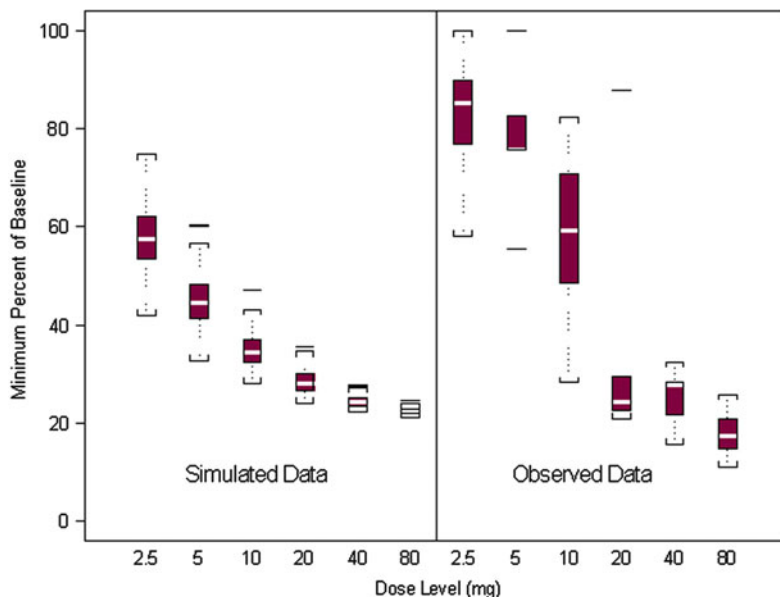


Fig. 8.14 Comparison of simulated TNF α inhibition to observed TNF α inhibition in first-time in human study

8.5.1.5 Wisdom for the Design of Proof of Concept Study

The knowledge gained from the results of the FTIH clinical trial provided the basis for the design of a proof of concept study for the future development of the drug candidate. The discussion of that study is beyond the scope of this chapter. However, it is important to note that doses from 5 to 40 mg were tested in that study. The recommendation, based on leveraging pharmacometric knowledge and understanding, was that drug activity would reach a maximum at 20 mg, and this is what was observed.

8.6 Summary

Implementing pharmacometrically guided drug development strategies founded on informative, powerful, and robust clinical trials would greatly improve the drug development process. Leveraging (pharmacometric) knowledge gained from every stage of drug development (or drug trial) to gain a better understanding of drug candidate's response surface provides for better decision making for the next step in the process. The result is the application of appropriate wisdom in deploying resources for each stage of the drug development process. Pharmacometrics enables the deployment of appropriate methodologies that permit the utmost extraction of hidden knowledge from study data and the leveraging of same in drug development. An application example has been used to illustrate how PGDD can be applied in early phase drug development.

References

- Adams CP, Brantner VV (2010) Spending on new drug development. *Health Econ* 19:130–141
- Box GEP (1979) Robustness in the strategy of scientific model building. In: Laurer RL, Wilkinson GN (eds). Academic Press, New York, pp 275–291
- Chu H-M, Zha J, Roy A, Ette EL (2007) Designs for first time-in-human studies in non-oncology indications. In: Ette EI, Williams PJ (eds) *Pharmacometrics: the science of quantitative pharmacology*. Wiley, Hoboken, NJ, pp 761–780
- Chu H-M, Zha J, Roy A, Ette EI (2008) Determination of the efficiency of first time-in-man studies in healthy volunteers. *Clin Res Regul Affairs* 25:157–172
- Bhattaram VA, Bonapace C, Chilukuri DM, Duan JZ, Garnett C, Gobburu JVS, Jang SH, Kenna L, Lesko LJ, Madabushi R, Men Y, Powell JR, Qiu W, Ramchandani RP, Tornoe CW, Wang Y, Zheng JJ (2007) Impact of pharmacometrics review on new drug approval and labeling decisions—a survey of 31 new drug applications submitted between 2005 and 2006. *Clin Pharmacol Ther* 81:213–221
- Box GEP (1979) Robustness in the strategy of scientific model building. In: Laurer RL, Wilkinson GN (eds) Academic press, Newyork, pp 275–291
- Bugg CE, Carson WM, Montgomery JA (1993) Drugs by design. *Sci Am* 269:92–98
- Clemento A (1999) New and integrated approaches to successful accelerated drug development. *Drug Info J* 33:699–710
- Cosson VF, Fuseau E (1997) Mixed effect modeling of sumatriptan pharmacokinetics during drug development. I: Interspecies allometric scaling. *J Pharmacokinet Biopharm* 25:149–167
- Department of Health and Human Services (2004) Challenge and opportunity on the critical path to new products. US Food and Drug Administration, Rockville, MD
- Derendorf H, Lesko LJ, Chaikin P, Colburn WA, Lee P, Miller R, Powell R, Rhodes G, Stanski D, Venitz J (2000) Pharmacokinetic/pharmacodynamic modeling in drug research and development. *J Clin Pharmacol* 40:1399–1418
- DiMasi JA (2001) Risks in new drug development: approval success rates for investigational drugs. *Clin Pharmacol Ther* 69:297–307
- DiMasi JA, Hansen RW, Grabowski HG (2003) The price of innovation: new estimates of drug development costs. *J Health Econ* 22:151–185
- Ette EI, Williams PJ, Sun H, Fadiran EO, Ajayi FO, Onyiah LC (2001) The process of knowledge discovery from large pharmacokinetic data sets. *J Clin Pharmacol* 41:25–34
- Ette EI, Chu H-M, Godfrey CJ (2004) Data supplementation: a pharmacokinetic/pharmacodynamic knowledge creation approach for characterizing an unexplored region of the response surface. *Pharm Res* 22:523–531
- Kleinberg MI, Wanke LA (1995) New approaches and technologies in drug design and discovery. *Am J Health Syst Pharm* 52(1323–1336):1341–1343
- Martin-Jimenez T, Riviere JE (2002) Mixed-effects modeling of the interspecies pharmacokinetic scaling of oxytetracycline. *J Pharm Sci* 91:331–341
- Peck CC (1997) Drug development: improving the process. *Food Drug Law J* 52:163–167
- Sheiner LB (1997) The intellectual health of clinical drug evaluation. *Clin Pharmacol Ther* 50:4–9
- US Food and Drug Administration (2010) Critical path initiative. <http://www.fda.gov/Science-Research/SpecialTopics/CriticalPathInitiative/default.htm>. Accessed 26 May 2010
- Williams PJ, Desai A, Ette EI (2003) The role of pharmacometrics in Cardiovascular drug development. In: Pugsley MK (ed) *Cardiac Drug Development Guide*. Humana, Totowa, NJ, pp 365–387
- Zial MR, Beer B (1990) Making business sense of science with rational drug design. *Pharm Exec* 10: 40, 42, 44, 46

Part III
Application of M&S in
Selected Therapeutic Areas

Chapter 9

The Application of Drug-Disease Models in the Development of Anti-Hyperglycemic Agents

Jenny Y. Chien and Vikram P. Sinha

Abstract Diabetes is a chronic disease characterized by hyperglycemia resulting from defects in the regulation of glucose and insulin homeostasis. Hyperglycemia, if not well controlled, will progress to more serious complications. Therefore, all available treatments aim to lower blood glucose by various mechanisms of action. Glucose and glycosylated hemoglobin (HbA1c) are well established and readily measurable biomarkers of the disease. The application of model-based approaches to optimize patient therapy and to gain understanding of the physiology of glucose-insulin regulation is widely accepted in the area of diabetes research and development. In this chapter, we attempt to give a brief overview of the disease and the types of drug-disease models that may be applied in various stages of drug development, including references to key publications of drug-disease models. Through simulations, these models are the essential tools to aid the optimization of clinical trials and to learn about the safety and efficacy of new drugs relative to the standards of care and to face the increasing challenges of drug development for the treatment of diabetes.

9.1 Diabetes Mellitus

Diabetes mellitus (hereafter, diabetes) is a condition in which a person has higher than normal blood sugar (glucose) levels either because the body does not produce enough insulin in response to meal intake (impaired β cell functions), or because the body does not properly respond to the insulin that is produced (insulin resistance). Insulin is a hormone produced by the β cells in the Islets of Langerhans located in the pancreas that promotes the uptake of glucose by tissues such as muscles and adipose thereby mediating the clearance of glucose. Therefore, diabetes is a disease that has been

J.Y. Chien (✉)

Lilly Research Laboratories, Eli Lilly and Co., Lilly Corporate Center,
Indianapolis, IN 46285, USA
e-mail: jchien@lilly.com

defined as “a group of metabolic disorders characterized by hyperglycemia resulting from defects in insulin secretion, insulin action, or both” (American Diabetes Association 2007). If there is diminished uptake of glucose by tissues due to resistance to insulin, then the β cell will compensate by secreting enough insulin to normalize glucose level (euglycemia). Over time, the acute insulin secretory response to glucose (first phase insulin secretion) may diminish and glucose may accumulate in the blood, leading to hyperglycemia and ultimately diabetes mellitus. A persistent state of hyperglycemia is associated with increased susceptibility to infections, ketoacidosis, microvascular diseases, such as nephropathy or retinopathy and may lead to early macrovascular complications, such as heart attack and stroke (Morghissi *et al.* 2007).

Nearly 6.4% of the global population, including 8% of the population in the U.S., suffer from diabetes (Center for Disease Control Factsheets 2010). The number of newly diagnosed cases world-wide continues to grow every year. By 2030 the number is expected to rise to approximately 400 million (Wild *et al.* 2004). Diabetes is estimated to be the fifth leading cause of death globally and is associated with a high risk of cardiovascular disease.

The most common types of diabetes which result from a combination of genetic and environmental factors that cause β -cell failure are:

- Type 1 diabetes which results from the body’s failure to produce insulin, and thus requires an exogenous source of insulin. In type 1 diabetes, a T-cell mediated autoimmune response appears to be the main disease mechanism. This type of diabetes is highly prevalent in children and adolescents.
- Type 2 diabetes which results from insulin resistance, a condition in which cells fail to use insulin properly and often is associated with insulin deficiency. Historically, type 2 diabetes has been a disease exclusively seen in adults. However, in recent years, there has been a significant emergence of type 2 diabetes in children. Similar to adults, the disease in youth is primarily driven by lifestyle factors leading to increased body weight and obesity. Type 2 diabetes is by far the most common type of diabetes, affecting 90–95% of the U.S. diabetes population.
- Gestational diabetes is when pregnant women, who have never had diabetes before, develop a high blood glucose level during pregnancy. These women may proceed to develop full-blown type 2 diabetes.

Other forms of diabetes mellitus include congenital diabetes, which is due to genetic defects of insulin secretion, cystic fibrosis-related diabetes, steroid diabetes induced by high doses of glucocorticoids, and several forms of monogenic diabetes.

Treatment for all forms of diabetes became available since the discovery of insulin as a medicine in 1923 (Bliss 2007; American Diabetes Association Guidelines 2010). Type 2 diabetes can be controlled with various treatment modalities; however, diabetes is a chronic and progressive condition that currently has no medicinal cure. Inadequate treatment of diabetes can lead to complications: acute (*e.g.*, susceptibility to infections, hypoglycemia, diabetic ketoacidosis, or nonketotic hyperosmolar coma) and serious long-term complications (*e.g.*, cardiovascular

disease, chronic renal failure and retinal damage). Regimented treatment of diabetes is thus important and, generally, a holistic approach that includes blood glucose and blood pressure control, and lifestyle changes such as smoking cessation and maintaining a healthy body weight is recommended (American Diabetes Association 2010). Diabetes is also a progressive disease, thus the choice of treatments depends on the disease status and often includes more than one medication.

9.1.1 Treatment Option and Drug Class

The treatment of Type 1 diabetes is limited to insulin, which currently must be injected. Patients with Type 2 diabetes may be able to manage their diabetes on diet and exercise alone for a few years. However, the disease usually progresses over time requiring additional medicines to be given in combinations. Numerous drugs of different mechanisms of action that are effective in the treatment of Type 2 diabetes are available for oral administration. The therapeutic combination for the treatment of Type 2 diabetes may include insulin, but not necessarily due to failure of the oral agents, to provide better glycemic control in combination with the more convenient oral agents. The anti-hyperglycemic medicines that are available in the market by pharmacologic class include:

- Insulins (meal-time insulins, intermediate mixes of meal-time and long-acting insulins and long-acting basal insulins)
- Insulin secretagogues (sulfonylureas, glinides)
- Insulin sensitizers (glitazones)
- Biguanides for inhibition of hepatic gluconeogenesis (metformin)
- α -Glucosidase inhibitors for glucose or starch absorption (acarbose)
- Incretin mimetics for glucose-dependent insulin secretion (glucagon-like peptide, or GLP-1, analogs and agonists)
- Dipeptidyl peptidase-4 (DPP-4) inhibitors for sustained endogenous GLP-1 (gliptins)

There are many investigational agents in various stages of drug discovery and development such as (Levien and Baker 2009):

- GKA (glucokinase activator)
- SGLT2 (sodium-dependent glucose co-transporter)
- 11 β HSD (11- β hydroxysteroid dehydrogenase inhibitor)
- GIP (gastric inhibitory polypeptide) analogs
- G-protein coupled receptor agonists
- Anti-CD3 targeted monoclonal antibody

Many newer agents are designed to have pleiotropic effects and have beneficial attributes beyond glucose lowering reflecting the need to manage multiple facets of this complex metabolic disorder.

9.1.2 Biomarkers

There are numerous biomarkers and pharmacodynamic measurements available to assess glycemic status and pancreatic β cell health as well as evaluate the effects of pharmacologic interventions. The pancreas releases insulin which is produced in the pancreatic β cells and glucagon, produced in the α cells. Other substances, including hormones (somatostatin, growth hormone, cortisol, gastrointestinal hormones, etc), amino and fatty acids influence this complex system. Glucagon is an antagonist to insulin causing hepatic glucose to rise either by gluconeogenesis or glycogen breakdown – its effect visible in cases of prolonged hypoglycaemia.

The choice of a pharmacodynamic biomarker is dependent on the new medicinal entity's (NME) mechanism of action, the duration of the trial and the objective of the assessment. In addition, during the translational phase of development, the choice of animal models of disease is often dependent on the mechanism of action of the pharmacologic agent and known inter-species differences in the target expression and biomarker response (Shafirir 2007).

Acute biomarkers are measured in preclinical and early clinical phases of drug development in trials of short duration (*e.g.*, days to weeks). The standard biomarker panel often consists of fasting plasma glucose (FPG) and postprandial glucose (PPG) or insulin, in addition to representative biomarkers of the drug target (*e.g.*, glucagon, DPP-4 enzyme activity, GLP-1, GIP). The most common biomarker in early trials is FPG which is frequently used to monitor day-to-day variation in glycemia. In addition, prandial glucose measurements are used to assess effects in response to meals or glucose administration. Glycosylated hemoglobin (HbA1c), formed through a non-enzymatic and irreversible reaction between glucose and hemoglobin, is the well-accepted surrogate of drug effect and used as an efficacy endpoint in long-term trials (*e.g.*, months to years). Other exploratory markers may include fructosamine and adiponectin.

Fasting insulin and C-peptide levels are measures of endogenous insulin production and are used to assess insulin resistance and β cell function as well as markers of disease progression.

The increasing awareness in the treatment of diabetes to consider the comorbidities of diabetes, namely, obesity and cardiovascular diseases, has led to expansion of biomarker panels to include measures of weight (*e.g.*, body mass index, waist circumference, body fat composition) and safety biomarkers reflecting hemodynamics (*e.g.*, blood pressure, pulse rate) and risk of arrhythmias (QT prolongation).

9.1.3 Experimental Techniques

Throughout the drug discovery and development cycle there are many standard experiments or tests in which biomarkers are assessed in the evaluation of a pharmacologic agent. In this section, two types of experimental techniques

designed to study glucose homeostasis are briefly discussed. Many of these techniques can be used in preclinical animal models as well as in clinical testing. Their application is to gain insight into mechanisms of action and often establish proof of mechanism or concept (glucose lowering). These tests are typically conducted after an overnight fast and in many cases employ the use of radiolabeled glucose to distinguish between endogenously produced glucose and exogenously administered glucose.

9.1.3.1 Glucose Tolerance Tests

In these tests, a high glucose load is administered and counter-regulatory responses are assessed over 2–5 h. There are three categories of these tests. Intravenous glucose tolerance test (IVGTT), oral glucose tolerance test (OGTT) and standardized mixed meal tolerance tests (MMTT). Of these, OGTT and MMTT are more common in drug development. The description of the techniques, application and recommended model-based approach to data analysis are summarized in Table 9.1.

9.1.3.2 Clamp Studies

The fundamental principle with a clamp study is to achieve a steady-state condition by keeping one of the two, either glucose or insulin, constant. There are three types of clamp experiments: euglycemic-hyperinsulinemic, hyperglycemic and hyperinsulinemic-hypoglycemic clamp experiments. The description, application and recommended model-based approach to data analysis are summarized in Table 9.2. These studies are technically complex, labor intensive and require serial collection of blood samples at frequent intervals. Typically conducted early in

Table 9.1 Types of glucose tolerance tests

Type	Experiment	Application
Intravenous glucose tolerance test (IVGTT)	Short glucose infusion (~300 mg/kg BW) with intensive blood sample collection; may include glucose tracer or insulin infusion	Assessment of β cell impairment and glucose vs. insulin mediated glucose disposal. Not appropriate for incretin (gut hormone) mediated responses; may not be feasible for large trials
Oral glucose tolerance test (OGTT)	Administration of 50–100 g of glucose as tablet or liquid form. Periodic sample collection at 30–60 min intervals over 2 (short OGTT) to 4 or 5 (long OGTT) hours	Simple diagnostic of diabetes; commonly used in clinical trials and feasible for large trials
Mixed meal tolerance tests (MMTT)	Standardized meal of caloric, carbohydrate, fat and protein content	Most representative of real-world response to dietary intake; feasible for large trials

Table 9.2 Types of clamp studies

Type	Experiment	Application
Euglycemic-hyperinsulinemic	Assess the amount of glucose required to maintain normal glycemia (~90 mg/dL) under elevated insulin levels (to suppress hepatic glucose output)	Partial or total amount of glucose infused is the pharmacodynamic measurement of response; commonly used for PK/PD evaluations of insulin formulations
Hyperglycemic	Infusion of glucose to sustain hyperglycemia	Gold standard for assessment of β cell sensitivity and function; peripheral tissue sensitivity
Hyperinsulinemic-hypoglycemic	Elevated insulin levels not corrected with variable glucose infusion	Assessment of hypoglycemia and counterregulatory response

drug development with the aim of elucidating mechanisms of action, these experiments have been widely used in the evolution of insulin preparations (DeFronzo *et al.* 1979).

9.2 Drug-Disease Models of Diabetes

Diabetes is a disease in which mechanism-based modeling is appropriate since feedback regulation and control mechanisms play a crucial role in glucose homeostasis. In this section, selected drug-disease models are described. These models offer the opportunity of measuring clinically relevant parameters that can be used for gaining information about the disease state of diabetic patients, for understanding and quantifying the sources of variability and can be ultimately used as tools for simulation of clinical trials of a novel antihyperglycemic agent as monotherapy or in combination with other therapies. As such, the application of these models should be specific to each phase of drug development for the investigational agent. Depending on the stage-specific drug development questions (Chien *et al.* 2005), models can be adapted to predict both acute and long term events (Fig. 9.1).

9.2.1 Mechanistic Models of Glucose-Insulin Regulation

Historically, the best known model of the glucose-insulin system is Bergman's "minimal model" for glucose (Bergman *et al.* 1979; Bergman 2007; Caumo *et al.* 2000). The model has two main parameters – insulin sensitivity and glucose effectiveness. Subsequent improvements included the incorporation of a peripheral compartment for glucose distribution and models that simultaneously analyze both glucose and insulin data (Cobelli *et al.* 2007). These models do not take into account dynamic control mechanisms and were not ideal for predictive purposes. A more recent model of glucose-insulin regulation was developed using data from

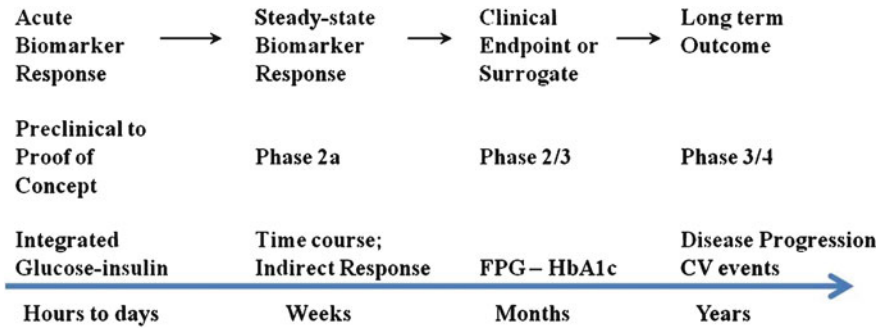


Fig. 9.1 Biomarker and model progression. The diagram illustrates in chronological order of drug development the types of models and biomarker responses that are modeled

both healthy and Type 2 diabetic subjects in glucose provocation experiments (Silber *et al.* 2007; Jauslin *et al.* 2007) (Fig. 9.2).

Briefly, the glucose model is described using a two-compartment model with a glucose absorption component. The glucose model also includes two effect compartments accounting for effects on glucose production and insulin secretion. The model for insulin incorporates both secretion and distribution. Baseline glucose and insulin values are represented as population values with inter-subject variability terms. One application of this model is for evaluation of combination of treatments with different mechanisms of action. An example of this application is for predicting the glucose response to investigational insulins or incretin mimetics, when added to metformin, a drug that affects hepatic glucose production, combined with sulfonyl-urea, a drug that increases insulin secretion. The pharmacokinetic component of drug treatment can be introduced into the model by linking to the “site” of action represented by the arrows in Fig. 9.2. The application of this model to predicting long-term steady-state biomarker response is limited. For such an application, the placebo response with respect to inter-occasion glycemic variability and links to HbA1c response will need to be considered.

9.2.2 Time-Course Models

A typical profile of fasting plasma or blood glucose as a function of time is presented in Fig. 9.3.

In trials of add-on therapy during which patients continue taking their antihyperglycemic medications, without washout, fasting blood glucose levels are stabilized at baseline. In contrast, trials to evaluate a new agent for a monotherapy indication may include a lead-in phase, during which patients discontinue and washout their previous antihyperglycemic agents. In these trials, during the lead-in phase, glucose levels will rise as shown by the placebo response curve in Fig. 9.3. Upon treatment, fasting blood glucose decreases from baseline to reach a maximum

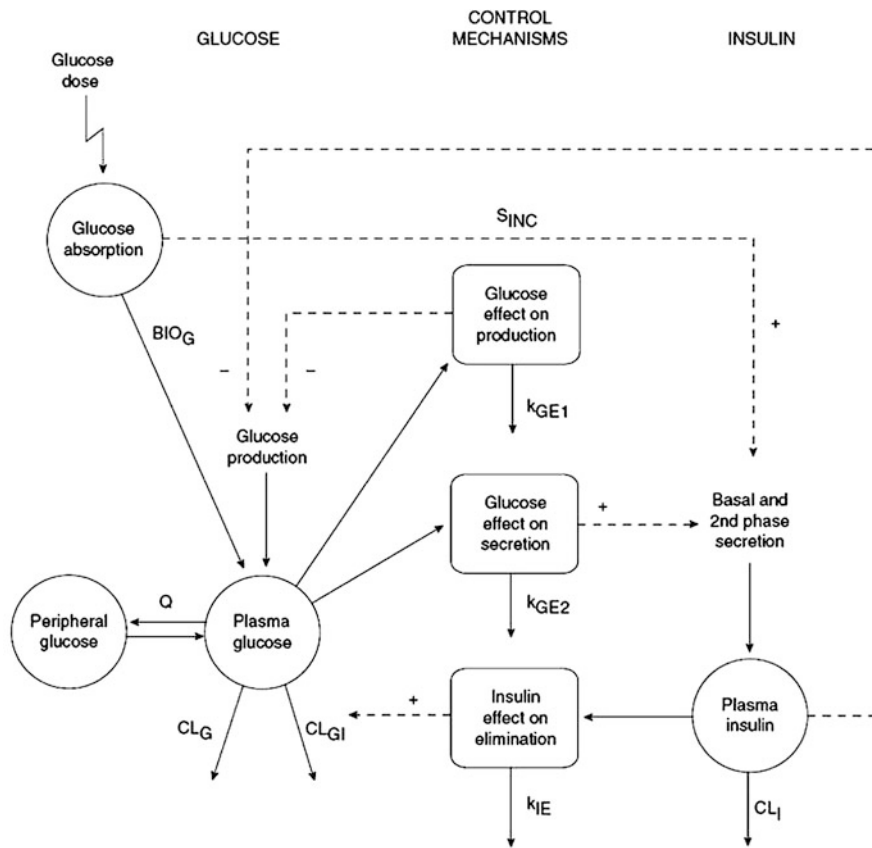


Fig. 9.2 Integrated physiologic model of glucose-insulin regulation. *Broken arrows* indicate control mechanisms with + and - symbols indicate stimulatory or inhibitory effect; Q , CL_G and CL_{GI} are glucose clearance parameters; BIO_G is bioavailability of glucose; S_{INC} is incretin effect; CL_I is insulin clearance parameter; k_{GE1} , k_{GE2} and k_{IE} are rate constants for the effect compartments. Figure reproduced with permission

possible effect (E_{max}), or change from placebo. The following model can be used to describe the rise in glucose in the placebo group and the fall in glucose levels with drug treatment.

$$\text{Change in FPG} = \text{Placebo effect} + \text{Drug effect} \tag{9.1}$$

$$\text{Change in FPG} (t) = P_{max} + OAD + (E_{max} \times \exp(\text{BaseFPG} - \text{median}) \times C^{\gamma}) / (EC_{50}^{\gamma} + C^{\gamma}) \times (1 - \exp(-k_{eff} \times t)) + \eta + \varepsilon \tag{9.2}$$

where, P_{max} is the maximum change in FPG for placebo; E_{max} is the maximal drug effect, EC_{50} is the drug concentration that produces half maximal effect.

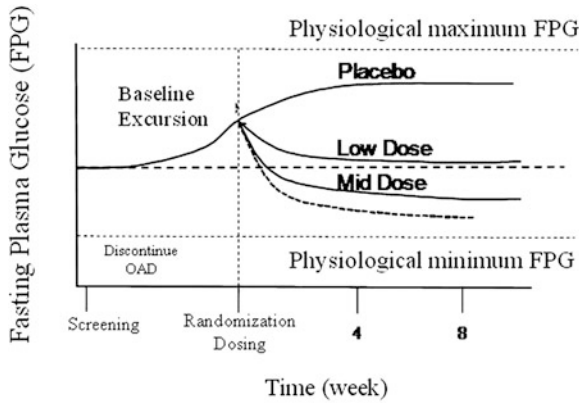


Fig. 9.3 Time course of fasting plasma glucose (FPG) model with washout of antihyperglycemic agents. The *solid curves* indicate glucose response on placebo and treatment and baseline excursion following washout of oral antihyperglycemic medications OAD is defined as oral antidiabetic drug

C is the drug concentration (which may be the area-under-curve (AUC)) or average concentration during a dosing interval, or Dose/Day/Clearance; BaseFPG is the mean baseline FPG; k_{eff} is a rate constant of glucose turnover in determining the time required to achieve the maximum treatment or placebo effect; γ is a concentration–response steepness parameter (Hill coefficient); OAD stands for oral antihyperglycemic drug which is the excursion between initiation of washout of antihyperglycemic medications to baseline FPG; η and ε are inter-subject and residual variability.

In some cases, when the time-course of biomarker response may not be critical (*i.e.*, when the dose–response relationship to be evaluated is at steady-state), a model describing the changes at a pre-defined endpoint (*e.g.*, at 12 weeks) may be sufficient. The equation above may be modified as:

$$FPG = BaseFPG \times \exp(\eta) + (ChgPCB + OAD - E_{max} \times C^\gamma) / (EC_{50}^\gamma + C^\gamma) + \varepsilon \quad (9.3)$$

where, BaseFPG is the baseline FPG for the population; ChgPCB is the change in FBG for placebo; E_{max} the maximal drug effect; C is the concentration of the drug; EC_{50} is the concentration of drug that produces half-maximal effect; η and ε are inter-subject and residual (intra-trial) variability.

9.2.3 Indirect Response Models

For trials with dose titration, dose escalation or de-escalation or crossover designs, alternatively, an indirect response (IDR) model can be used (de Winter *et al.* 2006).

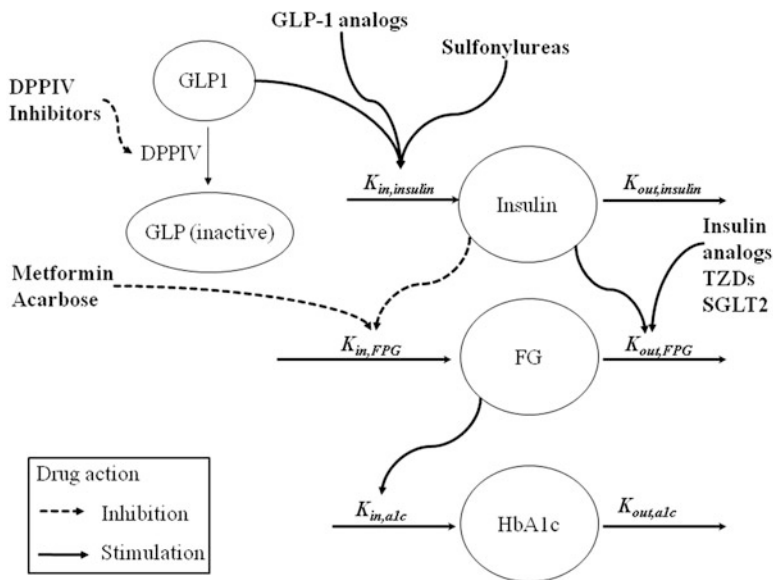


Fig. 9.4 Schematic of a pharmacodynamic model linking insulin, glucose and HbA1c. Circles represent endogenous biomarkers or surrogate of response; solid and dashed arrows indicate placement of drug effects either on stimulation of formation or inhibition of turnover; C drug concentration

The added advantage of using an IDR model is the linkage of glucose changes to those of HbA1c, by simultaneously fitting to both glucose and HbA1c data. The IDR model is a mechanistic approach to the incorporation of the effects of drugs with different mechanisms of actions for evaluation of combination therapy. Therefore, in the IDR model, depending on the putative mechanism of action, a drug can be assumed to inhibit the input or stimulate the output of glucose response (Fig. 9.4). The FPG-HbA1c linked model can be expressed as:

$$dFPG/dt = K_{in,fpg} - K_{out,fpg} \times (1 + (E_{max} \times C^\gamma)/(EC_{50}^\gamma + C^\gamma)) \times FPG \quad (9.4)$$

$$dHbA1c/dt = K_{in,alc} \times FPG - K_{out,alc} \times HbA1c \quad (9.5)$$

where, K_{in} and K_{out} represent stimulation of FPG or A1c formation and turnover, respectively.

9.2.4 Mechanistic Linked Model of FPG-HbA1c

A variation of the IDR model linking fasting glucose and HbA1c is the transit compartment model (Hamren *et al.* 2008). In this model, a series of (four) transit

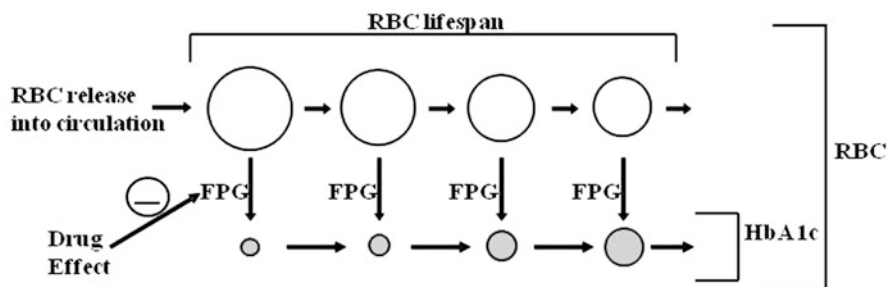


Fig. 9.5 FPG-HbA1c transit model. The model incorporates the turnover of HbA1c pools. Figure reproduced with permission

compartments describe red blood cell (RBC) aging with a zero-order release of RBC's into the circulation. A first-order rate constant defines the transition of RBC's from one stage to the next until the cell dies (Fig. 9.5).

9.2.5 Models Incorporating Disease Progression

Other models that incorporate long-term antihyperglycemic effects based on the time courses of FPG, fasting plasma insulin (FPI) and HbA1c have been developed (de Winter *et al.* 2006; DeGaetano *et al.* 2008). These models are tools for the evaluation of disease modifying properties by distinguishing between short-term symptomatic offset and long-term disease modifying effects. With precedented drug targets (known mechanisms of action), or novel agents in the later stages of drug development, the application of such a model in combination with literature data can be of great value in aiding the design of trials intended to demonstrate effect on prevention of disease progression or slowing of deterioration of β cell function (Ploeger and Holford 2009).

9.2.6 Literature Data for Developing Drug-Disease Models

A wealth of information is available in the literature for developing a diabetes literature database. Developing a model based on literature data has two main purposes (1) project a product profile (Mandema *et al.* 2005a; Samtani 2010) and (2) conduct population simulations that can be used in simulating clinical trials. An extensive review of published clinical trial data for time-course and dose-response information for the marketed comparator(s) should be initiated very early in the development process. Data used in developing these models can be obtained from various publicly accessible sources and from literature in the

Table 9.3 Resources of Literature Data

Data	Source location
Pubmed	http://www.ncbi.nlm.nih.gov/pubmed
FDA Drug Database	http://www.accessdata.fda.gov/scripts/cder/drugsatfda/index.cfm
Clinical trial	http://clinicaltrials.gov/
NIH clinical alerts	http://www.nlm.nih.gov/databases/alerts/clinical_alerts.html
NHANES	http://www.cdc.gov/nchs/about/major/nhanes/datalink.htm
European Diabetes Association conference posters and presentation archive	http://www.easd.org/
American Diabetes Association conference posters and presentation archive	http://professional.diabetes.org/
National Diabetes Information Clearinghouse (NDIC)	http://diabetes.niddk.nih.gov/statistics/index.htm

public domain such as Food and Drug Administration's (FDA) Approval Package (formerly Summary Basis of Approval or SBA) or the European Medicines Agency's Summary of Product Characteristics (SPC). Table 9.3 lists the common sources of information for literature data curation to support subsequent diabetes model building. Information about the stage of development and the type of trials are available from the centralized clinical trial database accessible at www.ClinicalTrials.gov.

The literature data on marketed antihyperglycemic agents can provide information for evaluation of dose–response relationships of comparator drugs, trial design (*e.g.*, monotherapy with washout vs. add-on to standard of care (SOC)) and baseline characteristics of patient population on fasting glucose, insulin, HbA1c and β cell function. For example, models can be developed based on literature data alone to demonstrate the difference in potency and the onset of action of all available treatments to reduce glucose and HbA1c levels. Trials with meal-time agents such as insulin or sulfonylureas demonstrated more rapid glucose response than metformin or pioglitazone, thus allowing the design of trials with shorter dosing duration.

An integrated database of monotherapy, combination and add-on therapy trials can be used to address questions related to optimization of combination strategy. Dose–response relationships for FPG and HbA1c are often available from Phase 2 trials. Dose–response relationships developed for FPG in short term trials can be assumed for prediction of HbA1c for most antihyperglycemic agents (de Winter *et al.* 2006; Hamren *et al.* 2008).

Models developed using data from the literature (Mandema *et al.* 2005b; Samtani 2010) are similar to models developed using patient data, with the exception that the estimates of variability represent trial to trial variability (Normand 1999; Berry *et al.* 2003; Mandeman *et al.* 2005). The mean results from each study need to be adjusted for differences in study design and patient population, such as the duration of lead-in and treatment, drug class, drug potency and baseline glucose or HbA1c. The model can be used to simulate the expected dose-response relationships and associated uncertainty for the change in glucose or HbA1c relative

to placebo after the administration of the drug, alone or in combination, for different patient populations. The distribution of the dose–response relationships is simulated by sampling the full set of model parameters from the variance matrix of the parameter estimates. For each set of the parameters, the dose–response relationship of the drugs can be simulated for a particular trial scenario. The 5th and 95th percentile of the predictive distribution represent the 90% uncertainty interval of the response.

Published literature data from long-term (>1 year) trials of metformin, sulfonylureas or pioglitazone in Type 2 diabetic patients or outcome trials of usually greater than 3 years in duration, such as the United Kingdom Prospective Diabetes Study (UKPDS), can be used to develop disease progression models. Disease progression models developed based on literature data and clinical knowledge have been published (de Winter *et al.* 2006; DeGaetano *et al.* 2008; Ploeger and Holford 2009).

9.2.7 *Biologically Based Mathematical Models*

Systems biology-based models have gained increasing use in diabetes aiming to increase confidence in working with biological targets prior to advancing molecules for testing in humans. This bottom–up modeling (Fitzgerald *et al.* 2006) in the translational attempts to simulate the disease features and interaction of various pathways using algebraic and differential equations are being used to prioritize hypothesis, evaluate combination therapies and differentiate drug classes based on outcomes (Waters *et al.* 2009).

9.3 Applications in Drug Development

The application of drug disease models in development of a new molecular entity can be categorized under three critical and related areas: (1) identify the optimal dose regimen; (2) assess drug attributes relative to SOC; (3) optimize clinical trial design and development plans using clinical trial simulations and associated statistical analysis models. The current trend in the development of anti-hyperglycemic agents involves not only glucose reduction but also beneficial effects on the cardiovascular system (such as lowering triglycerides, low density lipoprotein or blood pressure) and weight loss benefit, alone or in combination with other interventions, with the intent of optimizing treatment regimen for a patient population. Thus, in addition to models that describe glucose lowering, additional drug disease models will be needed to fully maximize the value of a model-based approach, as integrated in the learn and confirm cycle (Sheiner 1997). An advantage of working in this disease state is the availability of readily measurable pharmacodynamic endpoints such as FPG and HbA1c; both are “causal” path biomarkers of diabetes that are well accepted by clinicians and regulators world-wide (Lathia *et al.* 2009). Both biomarkers are used as pharmacodynamic measures of efficacy. Another

consideration in the application of drug disease models is whether the NME aims at an unprecedented target (hence large uncertainty in model-based prediction) vs. a drug in a class that has some prior information (reduce uncertainty by borrowing from a literature-based model).

It is extremely challenging within this chapter to cover every possible application. Therefore key applications are cited with the aim of illustrating how drug-disease models can be used in different phases of drug development. Critical drug development questions have been previously identified for the various phases of drug development (Chien *et al.* 2005; Zhang *et al.* 2006). Table 9.4 summarizes a

Table 9.4 Stage-dependent application of drug-disease models

Phase	Objective	Question	Task
0	Demonstrate pharmacologic activity and safety in preclinical models	What are the attributes of a successful candidate?	Guide developmental strategy with an integrated decision criteria based on predicted PK, PD, exposure–response and margin of safety in animal models
1	Assess tolerability, safety, PK and PD	What are the biomarker responses?	Develop physiologic models of PK–glucose–insulin
2a	Demonstrate response in representative patient population	What are the dose- or concentration–response relationships? How long should be the duration of the study to demonstrate proof of concept?	Estimate dose–concentration–response in typical patient population and predict long-term response from short-term proof of concept study
2b	Establish dose–response for Phase 3 decision	What are the efficacy and safety attributes? What trial design will unequivocally demonstrate noninferiority or superiority relative to comparators or standard of care (SOC)? What is the probability of trial success?	Develop drug attribute models and clinical utility for multiple endpoints Perform simulations to optimize trial design
3	Demonstrate safety and efficacy at target doses	Do the intended doses demonstrate the desired safety and efficacy in the population? What are the optimal combination therapy and effect on disease progression? Are there subpopulations of responders?	Predict disease progression and cardiovascular outcome with intervention in patient populations Assess the impact of relevant covariates on dose recommendation

stage-dependent approach in utilizing drug disease models in discovery and development. Based on this summary, these models can be applied in the following areas.

9.3.1 Discovery and Candidate Selection

In the discovery phase, the focus is on understanding target engagement, pharmacologic effects of target engagement and druggability. A physiological-based approach can be of great value in answering questions regarding target engagement and gaining insight into designing a molecule with desired pharmacokinetic properties.

Prior to candidate selection, *in vitro* activity and *in vivo* pharmacokinetic and pharmacodynamic (*e.g.*, glucose lowering or insulin secretion) studies are conducted to understand the mechanism of action and preliminary toxicology profile of the new drug in preparation for human testing. Simulations can be effectively used to evaluate whether a drug candidate possesses the necessary balance of efficacy (*e.g.*, potency) and safety characteristics, to allow determination of margin of safety and of the appropriate dose range to be explored in early clinical trials.

Prediction of human exposure: Using pharmacokinetic data obtained following intravenous and oral administration of the NME in animals, the human clearance and volume of distribution can be projected using allometry or a battery of available scaling methods (Hu and Hayton 2001). For many of these scaling approaches, the uncertainty in the parameters of the models can be incorporated in the prediction of clearance. An estimate of oral bioavailability can be assumed or estimated from preclinical data.

Estimating human potency: An estimate of the expected human potency (EC_{50}) can be obtained from preclinical PK/PD studies. Typically, the change in fasting glucose at the end of a 2-week, repeat-dose, dose-ranging study in an animal model of pharmacology, such as Zucker diabetic fatty (ZDF) rats or ob/ob mice (Shafir 2007) allows the prediction of potency (EC_{50}). For a first-in-class agent, this EC_{50} estimate is assumed scalable to clinical potency. For a precedented target with clinical data, the inclusion of a comparator in the same drug class with known clinical potency in the preclinical PK/PD experiment allows assessment of potency with greater precision. The prediction of potency based on the comparator's potency, or relative potency, is expressed as:

$$EC_{50,DrugX}^{human} = \frac{EC_{50,comparator}^{human} \cdot EC_{50,DrugX}^{ZDF}}{EC_{50,comparator}^{ZDF}} \quad (9.6)$$

A desired target exposure leveraging the comparator information from literature can be estimated. This target concentration is used to calculate an initial margin of safety to the nonclinical toxicology exposure, which is critical component of candidate selection criteria.

Projecting human doses: Clinical doses of the NME can be projected based on the projected human clearance and target efficacious exposures:

$$\text{Target dose (mg)} = \text{Target exposure (EC}_{\text{target}}) \times \text{CL/F}$$

where, $\text{EC}_{\text{target}}$ is the exposure required to achieved a desired percentage (*e.g.*, 90%) of E_{max} estimated in the preclinical PK/PD model; CL is the predicted human clearance following intravenous administration; F is the expected bioavailability in human based on nonclinical PK data in rat or dog. Dose is a single integrated metric that allows the team to select candidate with optimal druggable or margin of safety profile, plan pharmaceutical formulation development and develop an appropriate dose–escalation scheme in early safety and tolerability study. A consideration for the candidate selection stage of development is whether the predicted efficacious dose range is commercially viable, *i.e.*, dose amount is feasible for manufacturing scale-up. This is of particular importance in the development of biologics.

9.3.2 Proof of Concept and Time-Course of Response

An important milestone for all clinical development programs is to establish proof of concept early and efficiently. In diabetes, this includes assessing glucose response (fasting and/or prandial) and related biomarkers. Depending on the duration of the study some information of changes to HbA1c may be obtained. Drug-disease models can be used to define the dose range; select the most efficient or shortest duration of treatment (typically 2–4 weeks); optimize the size of the study and, if applicable; define critical success criteria against the appropriate comparator(s). For precedent targets, it may be more informative to confirm efficacy in a longer study. Clinical trial simulation in this case is a useful tool to assess the value of a small POC study. The first step is to identify plausible target doses. The application of a population simulation that incorporates estimates of inter- and intra-subject variability and important covariates such as baseline glucose in generating a distribution of possible outcomes is necessary. In addition, the glucose dose–response relationship should account for the uncertainty in parameter estimates, including alternate estimates of EC_{50} . Simulations including alternate EC_{50} parameter values are used to address “what-if” questions. A time course model can be used to simulate the dose–concentration–glucose relationship; this model should take into account uncertainty in the placebo response, E_{max} , EC_{50} and k_{eff} (rate constant governing the time course of glucose change) should be incorporated. Figure 9.6 illustrates dose–response curves, where each curve represents the median response from 1,000 virtual patients over the time-course of treatment. These simulations reveal that the 1 mg dose will achieve a desired effect (*e.g.*, 50 mg/dL decrease in glucose) but requires 12 weeks of treatment while a shorter study (4 weeks) will have a smaller change from baseline effect at the same dose. The aim of the simulations would be to

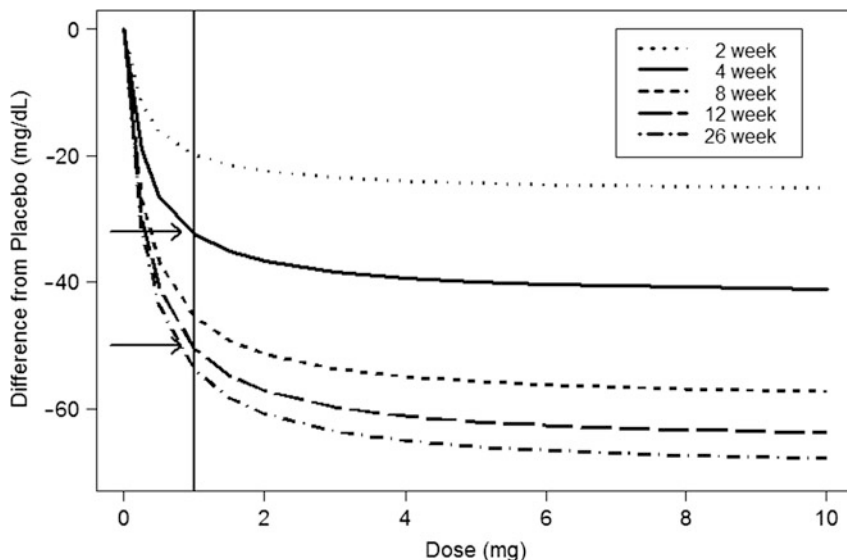


Fig. 9.6 Model predicted dose–response of change from baseline fasting glucose relative to placebo under various study duration scenarios. *Vertical line* indicates the 1 mg dose predicted to achieve target response at 12 weeks; *arrows* indicate the predicted responses at 4 and 12 weeks for the target dose

Table 9.5 Probability of selecting the right dose that meets the target response (within 50%) from a 4-week proof of concept study of various dose placement and sample size trial simulation scenarios

Design	Dose groups (mg)	Number of patients per trial			
		24	48	72	96
1	0, 1, 5, 15	0.066	0.095	0.098	0.14
2	0, 0.3, 1, 5, 15	0.13	0.16	0.2	0.17
3	0, 1, 5, 10, 15	0.047	0.073	0.13	0.13
4	0, 0.1, 1, 3, 10	0.32	0.46	0.51	0.52
5	0, 0.3, 1, 5, 10, 15	0.12	0.13	0.18	0.17
6	0, 0.1, 1, 5, 10, 15	0.33	0.42	0.53	0.56
7	0, 0.2, 0.6, 2, 6, 15	0.2	0.26	0.27	0.3

assess whether a small POC study can reliably predict longer term response. In this example, at 12 weeks, the model predicts a near steady-state of glucose response, whereas, at 4 weeks, the median glucose response attained is approximately 60% of the steady-state response.

Based on this time-course model, simulations can be conducted to evaluate the ability of a 4-week trial to predict the change in glucose at 12 weeks. A successful trial is one in which the “true” target dose at 12 weeks could be predicted within an acceptable interval (*e.g.*, 50–200%) of the target dose. Thus,

under a plausible EC_{50} scenario, the target dose to achieve 50 mg/dL response at 12 weeks was predicted to be 1 mg. A 4-week trial design would be deemed successful if it predicts the dose to achieve 50 mg/dL effect between 0.5 and 2 mg at 12 weeks using the time-course model. Different designs (varying dose placement and sample size per arm) can be simulated and the probability of a study with only 4 weeks of data to accurately estimate the target dose can be estimated as shown in Table 9.5.

Design number 4 and 7 showed the highest probability of estimating the target dose; whether these probabilities are acceptable can be weighed in the decision to proceed with such a study or modify the design. If the fasting blood glucose is the primary endpoint, then the time-course models, including the IDR models, are useful in predicting long-term or steady-state glucose response from short-term trial data.

9.3.3 Dose Response of Efficacy and Safety Attributes

A Phase 2 trial (typically 12 weeks in duration) aims to confirm efficacy in the target population and to establish dose–response to aid selection of doses in future trials. A drug disease model can be used to simulate a Phase 2 study. The objectives for simulation may be to ensure that (1) all active dose arms demonstrate a significant glycemic reduction vs. placebo; (2) one of the dose arms will result in a reduction that will be at least non-inferior to the comparator and finally; (3) and the trial will identify a statistically significant dose response relationship (*i.e.*, at least two of the active treatment arms differentiate from each other and from placebo in the change from baseline HbA1c responses). Thus, the aim is to ensure that an appropriate dose range is being tested, that dose placement is optimized and all sources of variability are taken into account.

Time-course and IDR models linking glucose to HbA1c can be used to analyze data from Phase 2 trials. Either model can be used to simulate longer-term steady-state effects (at 6 months to 1 year) from short-term (*e.g.*, 12 weeks) trials. Typically, the uncertainty in drug potency is taken into consideration as well as the drop-out rates. The variability in compliance rate may also be included in the simulations. Pharmacokinetic sampling design in Phase 2, which are typically sparse, should be optimized using tools such as the Population Fisher Information Matrix (PFIM) using the PFIM/PFIM_OPT program and simulations using the mixed-effects models (Kowalski and Hutmacher 2001; Duffull *et al.* 2001; Retout and Mentre 2003).

An important task of the Phase 2 analysis is comparison with existing SOC. Typically, most Phase 2 studies include a comparator or SOC. However, virtual comparison using literature data allows comparison to multiple comparators. In this case, the effect size is quite dependent on the baseline characteristics of the population. Therefore, simulations that include the effect of baseline glucose and HbA1c as a predictor of response are important.

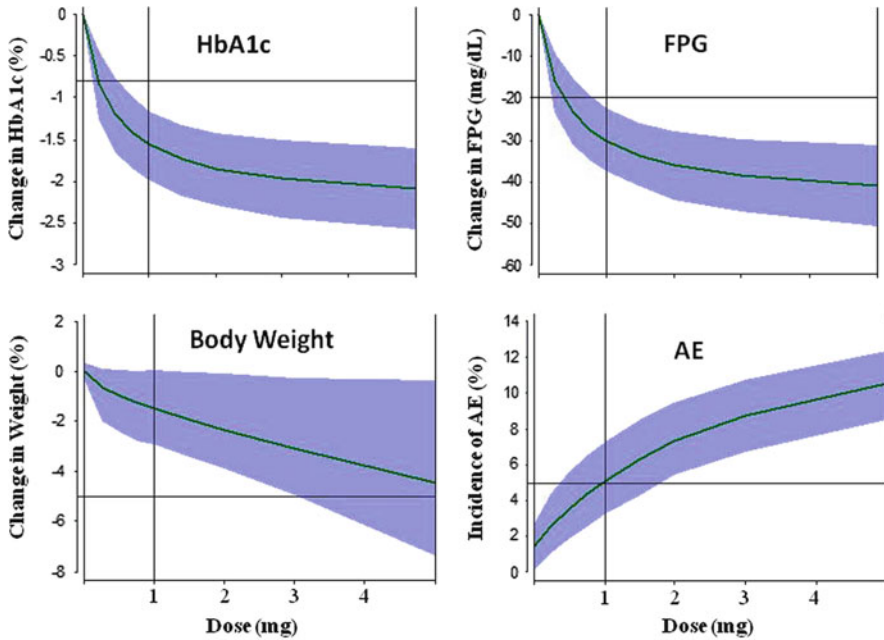


Fig. 9.7 Model predicted dose–response relationships for multiple safety and efficacy attributes. *Solid lines* are the median and shaded regions are 5th and 95th percentiles of the mean responses from 250 replicate trials; *horizontal lines* represent the individual target responses desired for Phase 3 dose

9.3.4 Dose Selection

The doses selected for the Phase 3 trials are, by intent, the same doses targeted for final approval. Therefore, justification of these doses is necessary. If the NME has additional attributes, such as lowering of body weight or lipids, these should be included in the justification. The meta-analyses that include both literature data (comparators or SOC) and patient level information are very valuable.

Clinical utility functions can be developed as joint metrics of multiple safety and efficacy endpoints. A clinical utility index captures the clinical interpretation or trade-off between benefit and risk in a single metric that can be used as a framework for decision making (Chap. 5). An example of utilizing model predicted dose–response for long-term safety and efficacy in conjunction with clinical utility functions is illustrated in Figs. 9.7 and 9.8. The dose that has the highest total clinical utility is selected as the Phase 3 dose expected to maximize glycemic control (HbA1c reduction with weight benefit) while minimize safety risks (*e.g.*, QTc prolongation or drug–drug interactions).

Dosing recommendations in sub-populations: Identifying sub-populations that are at a greater risk for adverse effects or poor responders for efficacy is an integral

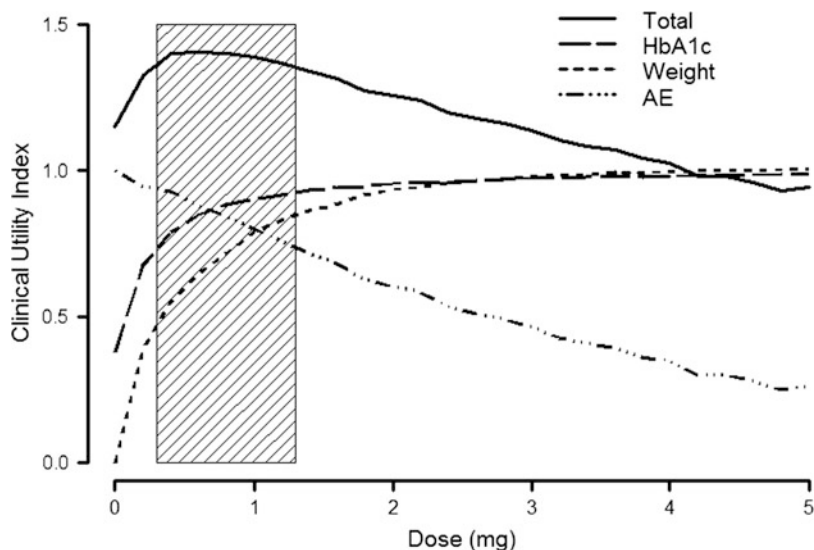


Fig. 9.8 The total and individual clinical utility curves for multiple safety and efficacy endpoints. The shaded region indicates the plausible dose range of maximum clinical utility

part of the development program. Drug-disease models that describe beneficial effects on glycemia should be integrated as needed with exposure-response analysis (Holford *et al.* 1981) or relevant safety endpoints.

For example, patients over the age of 65 with compromised renal or hepatic function may require a dose reduction to minimize cardiovascular risk while maintaining acceptable glycemic benefit. As ethical and practical recruitment issues limited the amount of data available from confirmatory Phase 3 trials, use of population analyses that integrates pharmacokinetics (*e.g.*, age, body size, renal function) can be used to form the basis for dose adjustments in these special populations.

9.4 Regulatory Considerations

The cost of developing drugs has been steadily rising while the number of new drugs being approved has been falling despite advances in the identification of new drug targets through proteomics and genomics. This critical situation has resulted in a white paper published in 2004 (Food and Drug Administration 2004) by the FDA encouraging the use of novel approaches. The initiative encourages the use of quantitative approaches using model-based drug development in all phases of drug development. Since then, model-based approaches in drug development have been embraced by many scientists in the pharmaceutical industry as well as regulatory agencies. As discussed in Chaps. 1 and 3, the FDA has initiated an “End

of Phase 2a” meeting opportunity to encourage early communication between drug development scientists and regulators (Food and Drug Administration 2009). Early agreement on the proposed model-based approaches to define the Phase 2/3 program, trial design and dose selection strategy can facilitate subsequent discussion at the end of Phase 2 meeting and at the time of New Drug Application (NDA) submission.

Recently published regulatory guidances for evaluation of investigation drugs for treatment of diabetes (Food and Drug Administration 2008; European Medicines Agency 2010) have revealed the potential for greater regulatory challenges ahead. The FDA requirement to include cardiovascular outcome events in the clinical trials of new investigational agents has created a higher hurdle for anti-diabetic drug approval. Therefore, understanding the effects of drug on both glycemic benefit and cardiovascular risk is important in early phase of drug development.

9.5 Future Directions

As the need for new medicines to treat diabetes and associated complications increases, pharmaceutical companies are faced with three key challenges: (1) identifying targets and developing medicines that differentiate from existing standards of care in an efficient manner; (2) convincing regulators of the added benefit of such treatments and (3) providing useful guidance to prescribers and payers (including patients) on using these medicines effectively.

The traditional pharmacokinetic/pharmacodynamic models are evolving to include integrated predictive models that can be utilized in quantitative decision making. These predictive models can be applied in the following areas:

1. *Target prioritization*: using physiological models to assess effects of target modulations and test possible combinations. These *in silico* models in combination with preclinical testing offer an effective platform to explore mechanisms of action, tailoring opportunities and design treatments.
2. *Clinical trial simulations*: using models to simulate the exposure–response relationships of investigational drugs that form the basis of exploring aspects of variability using clinical trial simulations.
3. *Benefit-risk assessments*: using clinical utility functions and codifying the trade-off between benefit and risk allow more quantitative comparison with standards of care, between patient subpopulations and between treatment regimens.
4. *Assessing clinical outcomes*: using outcome models to project from randomized controlled trial data to long-term clinical outcomes, costs or commercial viability of a new investigational drug.
5. *Dosing calculators and guidance tools*: using models that form the basis for interactive computer program that, based on a patients’ characteristics and glucose-insulin metabolism information, predicts the individual patient’s response and identifies the optimal therapeutic regimen for the patient.

6. *Disease progression*: using model to predict long-term improvements to glycemic control and β -cell function and potential to delay or modify progression of the disease.

Acknowledgments The authors wish to thank the Editors for the invitation and the opportunity to share our perspectives on the application of model-based approaches to diabetes research and development. We dedicate this manuscript in memory of Dr. Tom Forgue who has been a mentor, friend and colleague. We also wish to acknowledge the contributions of Dr. Bill Ebling for his insights over the years with special thanks to Dr. Tom Hardy for providing medical expertise and critical review of this chapter. The authors are thankful for the many thought-provoking comments and suggestions from colleagues in academia and industry and coworkers at Eli Lilly and Company who are dedicated to finding treatments for diabetes.

References

- American Diabetes Association (2007) Diagnosis and classification of diabetes mellitus. *Diabetes Care* 30(suppl 1):S42–S47
- American Diabetes Association (2010) Standards of medical care in diabetes. *Diabetes Care* 33 (suppl 1):S11–S61
- Bergman RN (2007) Orchestration of glucose homeostasis – from a small acorn to the California oak. *Diabetes* 56:1–13
- Bergman RN, Ider YZ, Bowden CR, Cobelli C (1979) Quantitative estimation of insulin sensitivity. *Am J Physiol* 236:E667–E677
- Berry DA, Berry SM, McKellar J, Pearson TA (2003) Comparison of the dose-response relationships of 2 lipid-lowering agents: a Bayesian meta-analysis. *Am Heart J* 145:1036–1045
- Bliss M (2007) The discovery of insulin. The University of Chicago Press, Chicago
- Caumo A, Bergman RN, Cobelli C (2000) Insulin sensitivity from meal tolerance tests in normal subjects: a minimal model index. *J Clin Endocrinol Metab* 85:4396–4402
- Center for Disease Control Factsheets International Diabetes Federation (2010) Diabetes atlas, 4th edn. <http://apps.nccd.cdc.gov/DDTSTRS/FactSheet.aspx> Oct. 18th, 2010
- Chien JY, Friedrich S, Heathman MA, deAlwis DP, Sinha V (2005) Pharmacokinetics/pharmacodynamics and the stages of drug development: role of modeling and simulation. *AAPS J* 7(3): E544–E559
- Cobelli C, Toffolo GM, Dalla Man C (2007) Assessment of betacell function in humans, simultaneously with insulin sensitivity and hepatic extraction, from intravenous and oral glucose tests. *Am J Physiol Endocrinol Metab* 293:E1–E15
- de Winter W, DeJongh J, Post T, Ploeger B, Urquhart R, Moules I, Eckland D, Danhof M (2006) A mechanism-based disease progression model for comparison of long-term effects of pioglitazone, metformin and gliclazide on disease processes underlying type 2 diabetes mellitus. *J Pharmacokinet Pharmacodyn* 33(3):313–343
- DeFronzo RA, Tobin JD, Andres R (1979) Glucose clamp technique: a method for quantifying insulin secretion and resistance. *Am J Physiol* 237(3):E214–E223
- DeGaetano A, Hardy T, Benoit B, Abu-Raddad E, Pasquale P, Bue-Valleskey J, Pørksen N (2008) Mathematical models of diabetes progression. *Am J Physiol Endocrinol Metab* 295(6): E1462–E1479
- Food and Drug Administration (2004) Challenge and opportunity on the critical path to new medical products. <http://www.fda.gov/oc/initiatives/criticalpath/whitepaper.html> Oct. 18th, 2010
- Food and Drug Administration (2008) Guidance for the industry: evaluating cardiovascular risk in new antihyperglycemic therapies to treat type 2 diabetes. <http://www.fda.gov/downloads/Drugs/GuidanceComplianceRegulatoryInformation/Guidances/ucm071627.pdf> Oct. 18th, 2010

- Food and Drug Administration (2009) End of Phase 2a meeting. <http://www.fda.gov/oc/initiatives/criticalpath/whitepaper.html> Oct. 18th, 2010
- Duffull SB, Mentré F, Aarons L (2001) Optimal design of a population pharmacodynamic experiment for ivabradine. *Pharm Res* 18:83–89
- European Medicines Agency (2010) Guideline on clinical investigation of medicinal products in the treatment of diabetes mellitus. <http://www.ema.europa.eu/pdfs/human/ewp/108000enrev1.pdf> Oct. 18th, 2010
- Fitzgerald JB, Schoeberl B, Nielsen UB, Sorger PK (2006) Systems biology and combination therapy in the quest for clinical efficacy. *Nat Chem Biol* 2(9):458–466
- Hamren B, Björk E, Karlsson MO (2008) Models for plasma glucose, HbA1c, and hemoglobin interrelationships in patients with type 2 diabetes following tesaglitazar treatment. *Clin Pharmacol Ther* 84(2):228–235
- Holford NHG, Coates PE, Guentert TW, Riegelman S, Sheiner LB (1981) The effect of quinidine and its metabolites on the electrocardiogram and systolic time intervals: concentration-effect relationships. *Br J Clin Pharmacol* 11:187–195
- Hu TM, Hayton WL (2001) Allometric scaling of xenobiotic clearance: uncertainty versus universality. *AAPS PharmSci* 3(4):1–14
- Jauslin PM, Silber HE, Frey N (2007) An integrated glucose-insulin model to describe oral glucose tolerance test data in type 2 diabetics. *J Clin Pharmacol* 47:1244–1255
- Kowalski KG, Hutmacher MM (2001) Design evaluation for a population pharmacokinetic study using clinical trial simulations: a case study. *Stat Med* 20:75–91
- Lathia CD, Amakye D, Dai W, Girman C, Madani S, Mayne J, MacCarthy P, Pertel P, Seman L, Stoch A, Tarantino P, Webster C, Williams S, Wagner JA (2009) The value, qualification, and regulatory use of surrogate end points in drug development. *Clin Pharmacol Ther* 86(1):32–43
- Levien LT, Baker DE (2009) New drugs in development for the treatment of diabetes. *Diabetes Spectr* 22(2):92–106
- Mandema JW, Cox E, Alderman J (2005a) Therapeutic benefit of Eletriptan compared to Sumatriptan for the acute relief of migraine pain – results of a model-based meta-analysis that accounts for encapsulation. *Cephalalgia* 25:715–725
- Mandema JW, Hermann D, Wang W, Sheiner T, Milad M, Bakker-Arkema R, Hartman D (2005b) Model-based development of gemcabene, a new lipid-altering agent. *AAPS J* 7(3):E513–E522
- Morghissi ES, Korytkowski MT, DiNardo M, Einhorn D, Hellman R, Hirsch IB, Inzucchi SE, Ismail-Beigi F, Kirkman MS, Umpierrez GE (2007) American Association of Clinical Endocrinologists and American Diabetes Association consensus statement on inpatient glycemic control. *Diabetes Care* 30(suppl 1):S42–S47
- Normand SL (1999) Meta-analysis: formulating, evaluating, combining, and reporting. *Stat Med* 18:321–359
- Ploeger BA, Holford NH (2009) Washout and delayed start designs for identifying disease modifying effects in slowly progressive diseases using disease progression analysis. *Pharm Stat* 8(3):225–238
- Retout S, Mentré F (2003) Optimisation of individual and population designs using Splus. *J Pharmacokinet Pharmacodyn* 30(6):427–443
- Samtani M (2010) Simple pharmacometric tools for oral anti-diabetic drug development: competitive landscape for oral non-insulin therapies in type 2 diabetes. *Biopharm Drug Dispos* 31:162–177
- Shafir E (2007) Animal models of diabetes: frontiers in research, 2nd edn. CRC, Boca Raton
- Sheiner LB (1997) Learning versus confirming in clinical drug development. *Clin Pharmacol Ther* 61:275–291
- Silber HE, Jauslin PM, Frey N, Gieschke R, Simonsson USH, Karlsson MO (2007) An integrated model for glucose and insulin regulation in healthy volunteers and type 2 diabetic patients following intravenous glucose provocations. *J Clin Pharmacol* 47:1159–1171
- Waters SB, Topp BG, Siler SQ, Alexander CM (2009) Treatment with sitagliptin or metformin does not increase body weight despite predicted reductions in urinary glucose excretion. *J Diabetes Sci Technol* 3(1):68–82

- Wild S, Roglic G, Green A, Sicree R, King H (2004) Global prevalence of diabetes. *Diabetes Care* 27:1047–1053
- Zhang L, Sinha VP, Forgue ST, Callies S, Ni L, Peck R, Allerheiligen SRB (2006) Model-based drug development: the road to quantitative pharmacology. *J Pharmacokinet Pharmacodyn* 33(3):369–393

Chapter 10

Modeling and Simulation in the Development of Cardiovascular Agents

Diane R. Mould, Bill Frame, and Timothy Taylor

Abstract Cardiovascular pharmacology encompasses a wide range of diseases. With most agents in this therapeutic area, there are specific therapeutic targets for biomarkers such as systolic blood pressure or LDL cholesterol levels that need to be met to ensure adequate clinical response in patients. Overdoses of these agents may be associated with toxicity. Modeling and simulation have proven to be valuable tools to target and adjust doses in patients. Because most cardiovascular agents are adaptively dosed based on individual response, the dose adjustment strategy must be implemented for model evaluation and simulation. This chapter reviews the cardiovascular pharmacology areas of treatment of hypercholesterolemia, stroke and hypertension, and applications of modeling and simulation in these disease states.

10.1 Hypercholesterolemia

10.1.1 Overview of Hypercholesterolemia

Atherosclerosis is a diffuse, chronic, progressive disease that is characterized by endothelial dysfunction, atherogenesis and atheromatous plaque progression. Atherosclerosis often presents as clinical cardiovascular disease (CVD) events (*e.g.*, heart attack and stroke). Elevated cholesterol is strongly associated with the development of atherosclerotic diseases. The risk of progression from atherosclerosis to CVD increases with increasing levels of total serum cholesterol or low-density lipoprotein (LDL) cholesterol. Currently, one of the primary therapeutic treatments to reduce LDL cholesterol is administration of statins. A schematic of the progression of atherosclerotic disease and the interactions of statins in this process is provided in Fig. 10.1.

D.R. Mould (✉)

Projections Research Inc., 535 Springview Lane, Phoenixville, PA 19460, USA
e-mail: drmould@pri-home.net

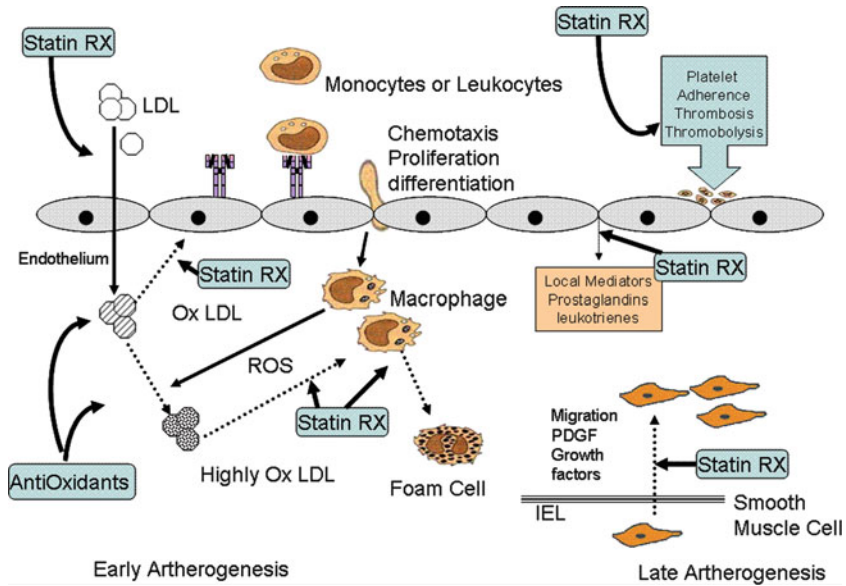


Fig. 10.1 Schematic of atherosclerosis

Elevated cholesterol levels promote entry and accumulation of LDL into subendothelial space at lesion-prone arterial sites. Monocyte chemoattractant protein-1 (MCP-1) and oxidized-LDL (Ox-LDL) act as chemoattractants to direct accumulation of monocytes and their migration to the sub-endothelial space, where monocytes transform into macrophages. Concurrently, oxygen free radicals modify LDL that is taken up by non-down-regulating macrophage receptors to form lipid-rich foam cells. Foam cells develop into fatty streaks, a precursor of atherosclerotic plaques. Statins are thought to act at numerous sites through the entire process, slowing the development of plaques and reducing the probability of development of CVD.

10.1.2 Overview of Pharmacology of Statins

Clinically, the beneficial effects of statins are attributable to their ability to reduce cholesterol synthesis by reversibly inhibiting HMG-CoA reductase, which converts HMG-CoA to mevalonate (Hunninghake 1992). Mevalonate is not only a precursor for cholesterol, but is also important for the synthesis of other nonsteroidal isoprenoidic compounds, which suggests that the statins may exert pleiotropic effects (Stancu and Sima 2001). These effects are broadly divided into two categories: the first involving the effect of statins on lipids including inhibition of cholesterol synthesis and reduction of LDLs; the second category involves a mixture of effects

including reduction of the accumulation of esterified cholesterol into macrophages, increase of endothelial NO synthetase, reduction of inflammatory processes, increased stability of the atherosclerotic plaques, restoration of platelet activity, and normal coagulation (Bellosta *et al.* 2000).

In the first category of activity, the liver is the primary therapeutic target of the statins because it is the major site of cholesterol synthesis, lipoprotein production, and LDL catabolism (Stancu and Sima 2001; Blum 1994). However, cholesterol synthesis in other tissues is necessary for normal cell function. The adverse effects associated with statins may depend in part upon the degree to which they act in extrahepatic tissues (Lennernäs and Fager 1997). Consequently, pharmacokinetic factors such as hepatic extraction and systemic exposure may be important when comparing the clinical utility of various statins.

Statins are generally metabolized by cytochrome P450 (CYP) enzymes depending in part on their lipophilicity making them susceptible to drug interactions (Williams and Feely 2002). Statins are metabolized to different degrees, and for some statins (*e.g.*, atorvastatin (Mason *et al.* (2006)), active metabolites are formed. The CYP3A enzymes metabolize lovastatin, simvastatin, and atorvastatin; CYP2C9 is involved in the metabolism of fluvastatin. Pravastatin and rosuvastatin are not significantly metabolized by CYP enzymes (Williams and Feely 2002; Schachter 2004). Lovastatin, pravastatin and simvastatin have elimination half-lives of approximately 1–3 h. Atorvastatin, fluvastatin, pitavastatin, and rosuvastatin have longer elimination half-lives ranging from 1 h for fluvastatin to 19 h for rosuvastatin. In addition, statins are substrates for P-glycoprotein (PgP) with various affinities affecting bioavailability.

10.1.3 Model Based Evaluations of Cholesterol Lowering Agents

Because of their pleiotropic activity and pharmacokinetic complexities, investigation of the relationship between statin concentrations, inhibition of HMG-CoA reductase, and cholesterol levels is not usually characterized using a direct effect type (E_{\max}) model. For most clinical trials, the primary endpoint is reduction of plasma LDL-cholesterol, which takes approximately 4–5 weeks to show a reduction after treatment initiation. Consequently, a dose-effect relationship instead of a concentration-effect relationship is commonly employed to describe the pharmacodynamics of the statins. Several authors have suggested methods for analyzing dose-response time data in certain defined situations, where it may be convenient or necessary to simplify pharmacokinetic behavior (Gabrielsson *et al.* 2000; Jacqmin *et al.* 2001; Pillai *et al.* 2004). In cases where computational evaluation of the complete system of equations is time consuming or the system of equations is “stiff” this simplification is often helpful. For example, Pillai *et al.* used simplified using a “kinetics of drug action” or a K-PD model (*i.e.*, a dose-response model as opposed to a dose-concentration-response model) to describe the effect of ibandronate on

osteoporosis (Pillai *et al.* 2004). Model performance for this simplified system was found to be acceptable.

Faltaos *et al.* (2006) used an indirect effect type model with a precursor pool to describe the time course of the LDL following administration of statins. A one compartment forcing function was used to relate statin dose to the measured response. In their model, the first compartment is a precursor pool describing LDL synthesis (rate K_{in}), and the second compartment is circulating LDL (site of measurement of the response). The LDL time course was affected by statins that can alter either the production or the elimination of LDL. The differential equations describing this K-PD model are provided below:

$$\frac{d\text{Precursor}}{dt} = K_{in} \cdot (1 - \text{INH}) - K_{out} \cdot \text{Precursor}$$

$$\frac{d\text{LDL}}{dt} = K_{out} \cdot \text{Precursor} - (\text{STIM}) \cdot K_{out} \cdot \text{LDL}$$

$$\text{STIM} = 1 + \frac{\text{Dose}}{(\text{Dose} + D_{50})}$$

In these equations, K_{in} is the LDL production rate constant; K_{out} is the exit rate from the precursor pool as well as the LDL elimination rate constant; INH and STIM denote the drug inhibition and stimulation effects of the statins, respectively; D_{50} denotes the dose that produced a 50% increase in LDL elimination. The parameters for this model for several statins are proved in Table 10.1.

The results obtained from the model developed by Faltaos *et al.* are in good agreement with results reported by Lennernäs and Fager (1997), who found that fluvastatin, lovastatin, pravastatin, and simvastatin have similar pharmacodynamic properties, with the ability to reduce LDL-cholesterol by 20–35%, which was shown to achieve decreases of 30–35% in major cardiovascular outcomes. Simvastatin has this effect at doses of about half those of the other three statins.

Another model-based approach that is commonly implemented to evaluate and compare the activity of statins is a “meta-model,” which combines the results of several studies addressing a set of related research hypotheses and evaluates

Table 10.1 Parameters from statin KPD model

Parameter (unit)	Final model (CV%)	Bootstrap median	Bootstrap 2.5th–97.5th
Kin (g/L/day)	0.14 (11%)	0.15	0.10–0.24
INH	0.21 (8.5%)	0.22	0.19–0.28
D50 Atorvastatin (mg)	26 (30%)	27	19–66
D50 Simvastatin (mg)	1.3 (37%)	1.3	1–3.7
D50 Fluvastatin (mg)	15 (35%)	14	9–34
IIV Kin (%)	0.72 (30%)	0.73	0.36–1.21
IIV D50 (%)	1.6 (33%)	1.62	1.0–2.9
Residual variability (%)	0.11 (14%)	0.12	0.10–0.16

Taken from Faltaos *et al.* (2006)

a common measure of effect size. The resulting overall average, when appropriately controlled for study characteristics, can be considered as a meta-effect size, which is generally a more powerful estimate of the true effect size than that derived from a single study. Meta analyses are often used in drug development to compare new agents with marketed agents to define critical Go/No-Go decision points. Simulations based on meta-models provide a range of expected outcomes or dose/response relationships for published results of other therapeutic intervention, which can be used to guide both dose selection of new agents in development and to provide insight on the relative efficacy for new agents (Lalonde *et al.* 2007).

Implementation of a meta-analysis is generally a straightforward process with the following steps:

1. Conduct literature search
2. Select reported studies to be included in the meta-database (*e.g.*, based on prespecified “incorporation criteria”)
 - (a) Study design quality, *e.g.*, the requirement of randomization and blinding in a clinical trial or the use of a placebo or active control arm
 - (b) Well-specified patient type or indication
 - (c) Decide whether unpublished studies should be included (if feasible, this is a good way to avoid publication bias which tends to provide only positive results)
 - (d) Decide which dependent variables or summary measures are to be evaluated, such as mean response data
3. Model development

With Nonmem[®], a random effects meta-regression is generally conducted on such data.

$$\hat{Y}_i(t) = f(\theta, D_i, t) + \eta_i + \varepsilon_i$$

where \hat{Y}_i is the mean effect size in study i ; $f(\theta, D_i, t)$ is the function describing the relationship between dose and time and the mean effect size; ε_i is the variance of the effect size in the i th study; and η_i is the between study variability.

LaRosa *et al.* (1999) conducted a meta-analysis of five large randomized controlled trials following long term treatment (average 5.4 years) with statins. Both proportional and absolute risk reduction were used to measure the effect of statin drug treatment on clinical outcomes. The model database was augmented with data from 12 small studies that were not designed to evaluate clinical outcome (*e.g.*, prevention of major coronary events) for sensitivity analysis. The authors reported that statin treatment was associated with a 20% reduction in total cholesterol, 28% reduction in LDL-C, 13% reduction in triglycerides, and 5% increase in high-density lipoprotein cholesterol. In addition, treatment with statins was found to provide a 31 and 21% reduced risk of major coronary events and all-cause mortality, respectively. The authors reported that risk reduction in major coronary events was similar for both men and women and was not age dependent.

Generally, for random-effects meta-analysis, study is used as the grouping factor for data (rather than ID, which is the usual grouping factor for population, based modeling). This is appropriate for data with a single observation per subject such as LaRosa *et al.* described previously. However, meta-analysis is often conducted using longitudinal data such as mean LDL per week. For such data, it may be appropriate to use both study and treatment arm as grouping factors. As suggested by Ahn and French (2009), there is correlation between observations over time within a treatment arm because the same subjects are contributing to the means at each time point. This correlation depends on the ratio of the between-subject variance to the sum of the between subject and residual variance. When this additional level of correlation is included in the meta-model, the equation then becomes:

$$\hat{Y}_{ij}(t) = f(\theta, D_{ij}, t) + \eta_i^{\text{Study}} + \frac{1}{\sqrt{n_{ij}}} \eta_{ij}^{\text{arm}} + \frac{1}{\sqrt{n_{ij}}} \varepsilon_{ij}$$

where \hat{Y}_{ij} is the mean effect size in study i for arm j ; $f(\theta, D_{ij}, t)$ is the function describing the relationship between dose and time and the mean effect size; ε_i is the variance of the effect size in the i th study; η_i is the between study variability; and η_{ij} is the between arm variability.

“Interarm” variability can be implemented using either the usual approach used for interoccasion variability (Karlsson and Sheiner 1993), or using the L2 (level-two) data item of NONMEM[®] to group together the data records of the same realization of the second level of random effects (Beal *et al.* 2006). The authors reported that when the hierarchy of random effects was misspecified, random effect parameter estimates were biased. The standard errors of the parameter estimates were also affected by the parameterization of random effects, showing the importance of correctly specifying study and treatment arm level variability for meta-analysis.

10.2 Antithrombus Therapy

10.2.1 Overview of Pathophysiology of Thrombus Formation

Excessive platelet activation and aggregation are common components in many vascular diseases, which results in atherothrombosis. For example, unstable angina and acute myocardial infarction are characterized by persistent platelet hyper-reactivity and thrombin generation (Merlini *et al.* 1994). Hypercholesterolemia and hyper-reactive platelets are synergistic in their pathology. Hypercholesterolemia has been shown to prime platelets for recruitment to lesion-prone sites before lesions can be detected (Theilmeier *et al.* 2002).

The growth of a thrombus follows a complex pathway, requiring multiple adhesive receptor-ligand interactions (Jackson *et al.* 2003). Platelet-vessel wall interactions at lesion-prone sites contribute to the initiation and maintenance of the inflammatory process of atherosclerosis. The rupture of an atherosclerotic lesion exposes the thrombogenic lipid core and subendothelial matrix proteins to circulating platelets, initiating platelet recruitment to the injured vessel wall similar to primary hemostasis (Steinhubl and Moliterno 2005). The efficiency with which platelets adhere and aggregate at sites of vessel wall injury depends on the action of various adhesive and soluble agonist receptors, with the relative contribution of each of the individual receptors being dependent on the prevailing blood flow conditions at the injury site. Adherence and activation of platelets at the site of ruptured endothelium initiates a cascade of events that ultimately results in thrombotic occlusion.

In addition to reducing the risk of thrombotic events in patients with atherosclerotic disease, anticoagulants are also used to reduce the risk of venous and arterial thromboembolism during and following surgery, particularly for patients with specific risk factors (Kearon and Hirsh 1997). Administration of agents such as unfractionated heparin or low molecular weight heparin is common, and the use of such agents is dependent on the risk of causing a bleeding event versus the benefit of preventing embolism.

10.2.2 Pharmacology of Anticoagulant Agents

The platelet-vessel wall interaction and local generation of agonists at the site of vascular injury provide the stimulus for platelet activation. The main inducers of platelet activation are collagen, thrombin, adenosine diphosphate (ADP), epinephrine, platelet activating factor, and thromboxane A₂ (TXA₂). An overview of the factors involved in platelet aggregation and the sites of common antithrombotic agents is provided in Fig. 10.2.

Aspirin and the thienopyridines have well established clinical efficacy, which supports platelet cyclo-oxygenase-1 (COX) and ADP receptors as appropriate clinical targets for antiplatelet drugs. Aspirin is an irreversible inhibitor of cyclo-oxygenase (COX), which leads to a substantially (98%) decreased production of platelet thromboxane A₂. Thromboxane A₂ induces platelet aggregation by binding to its receptor on platelets. This receptor also binds prostanoids, which can promote platelet aggregation through vasoconstriction. Thienopyridines such as ticlopidine (Clopidogrel) are converted into active metabolites, which in turn irreversibly inhibit P2Y₁₂ (a major ADP receptor) on the platelet surface. However, the need for metabolic activation results in a delay to the onset of effect. A new agent, cangrelor, is a direct competitive inhibitor of P2Y₁₂ that does not require conversion to an active metabolite. Therefore, cangrelor produces an almost immediate dose-proportional inhibition of ADP-induced platelet aggregation after IV administration with recovery of platelet function within an hour after the drug has been cleared.

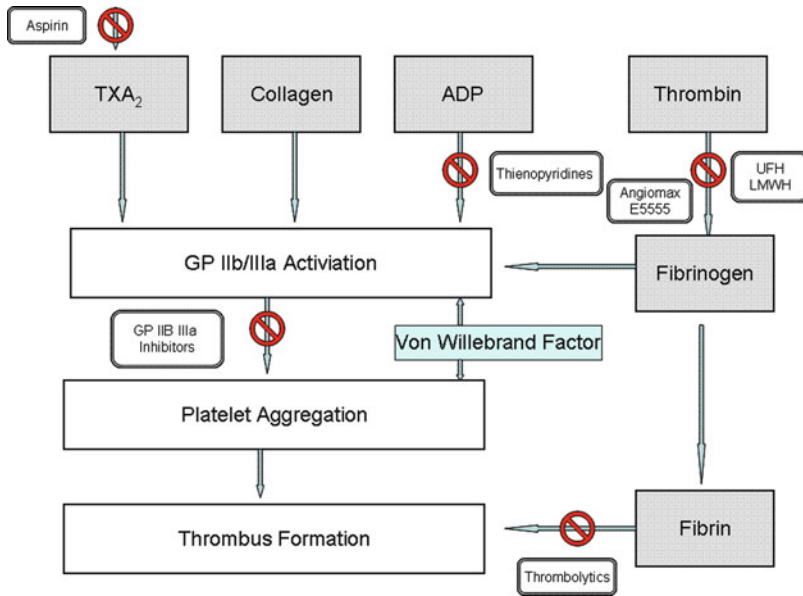


Fig. 10.2 Schematic of factors involved in platelet aggregation

GPIIb/IIIa inhibitors prevent fibrinogen binding, which is a prerequisite for platelet-platelet binding and aggregation. GPIIb/IIIa inhibitors are either monoclonal antibodies (*e.g.*, Abciximab) or low molecular weight peptides such as Eptifibatid and Tirofiban. Angiomax, a low molecular weight peptide, is a reversible inhibitor of thrombin. Thrombin-mediated activation of PAR-1 on endothelial and smooth muscle cells, fibroblasts, and cardiac myocytes may contribute to the proliferative and proinflammatory effects of thrombin (Seiler and Bernatowicz 2003). E5555 is an orally administered PAR-1 inhibitor that is in clinical development. The anticoagulant effect of low molecular weight heparins (LMWH) such as enoxaparin can be directly correlated to the ability to inhibit factor Xa in the clotting cascade, which catalyzes the conversion of prothrombin to thrombin. The inhibition of this process results in decreased thrombin and ultimately the prevention of fibrin clot formation.

From the platelet coagulation cascade, numerous additional sites can be identified to inhibit coagulation. Again, many agents that act on the coagulation cascade are already available for clinical use, while others are in development. Warfarin and related coumarins decrease blood coagulation by inhibiting vitamin K epoxide reductase, an enzyme that recycles oxidized vitamin K to its reduced form after it has participated in the carboxylation of several blood coagulation proteins, mainly prothrombin and factor VII. Thrombin, which converts fibrinogen to fibrin, can be inhibited either directly or indirectly. Direct inhibitors bind to thrombin and block its interaction with substrates. Indirect inhibitors act by catalyzing heparin cofactor II.

10.2.3 Modeling and Simulation for Dosing of Anticoagulants

Anticoagulants have associated risks of bleeding and bruising events, so dosing for these agents is usually individualized and doses are adaptively adjusted to a particular response. Identifying a starting dose that gives reasonable clinical response while reducing the likelihood that a patient will experience adverse events is important; therefore modeling and simulation have been particularly important to help develop dose regimens. For example, dose regimens for enoxaparin in obese patients were developed by Green and Duffull (2003) using modeling and simulation. The simulated results suggested that patients over 50 years of age with a total body weight >90 kg, or under 50 years of age with a total body weight $i > 120$ kg should experience less bruising if a dose of 100 IU/kg (1-mg/kg) based on lean body weight rather than total body weight is administered every 8 h.

Depending on both the mechanism of action and the pharmacokinetic behavior of individual agents, the pharmacodynamic activities of antiplatelet and anticoagulants are commonly described using direct effect (*e.g.*, E_{\max} model), indirect effect (Dayneka *et al.* 1993) or transit (Friberg and Karlsson 2003) models. For example, warfarin indirectly inhibits the synthesis of several vitamin K-dependent coagulation factors (*e.g.*, factors II, VII, IX, X, proteins C, and S). The precursors of these factors require carboxylation to allow them to bind to phospholipid surfaces. This step is linked to the oxidation of vitamin K to form vitamin K epoxide, which is then recycled back to its reduced form by vitamin K epoxide reductase complex (VKORC). As mentioned previously, warfarin inhibits this enzyme, effectively reducing available vitamin K stores. Consequently, when the pharmacodynamics of warfarin is being modeled, there is a need to provide a mechanism allowing for a delay to onset of effect as well as a prolonged recovery time.

Therapy with warfarin is characterized by pronounced variability in individual dose requirements (Sconce *et al.* 2005) and a narrow therapeutic index. Recently, three single nucleotide polymorphisms (SNPs), two in the CYP2C9 gene (which is the primary enzyme for warfarin metabolism) and one in the VKORC1 gene, have been found to play key roles in determining individual exposure and response to warfarin. On average, patients expressing the CYP2C9*2 and CYP2C9*3 alleles require a 19% and 33% reduction in dose, respectively, as compared to patients who have the *1 allele. Carriers of the VKORC1 A allele require, on average, a 28% reduction per allele in their warfarin dose compared to those who do not carry this allele (Schwarz *et al.* 2008). Consequently, patients expressing *2 or *3 alleles of CYP2C9 experience an approximately two- to threefold increased risk of serious bleeding events. Similarly, carriers of the VKORC1 A allele are also at a two- to threefold higher risk of an international normalized ratio (INR) >4.0 during initiation of therapy when standard dosing algorithms are used.

Because of the possibility of undesirable bleeding events together with the need to ensure adequate anticoagulation, warfarin is generally dosed adaptively depending on assessment of INR, which is a measure of the functionality of the extrinsic pathway of coagulation. Because of the well-known need to individualize dose and the

complexities inherent in the pharmacokinetic and pharmacodynamic behavior of warfarin, this agent has been frequently investigated through model-based approaches. Furthermore, the additional dose adjustments required for individuals carrying these alleles often substantially increases the time required to achieve the target INR.

In 2005, Holford presented several models for the pharmacodynamics of warfarin (Holford 2005), showing that the indirect effect (turnover) type model was best to account for the delay between measured warfarin concentration and anticoagulation response. A somewhat more elegant pharmacodynamic model for warfarin was developed by Hamberg *et al.* (2007). In this model, the anticoagulant response to warfarin was best described by an inhibitory E_{\max} model where the delay between exposure and response was accounted for by a transit compartment model with two parallel transit compartment chains (Fig. 10.3).

The equations for this model are shown below.

$$\frac{dA(1)}{dt} = k_{tr1,i} \cdot \left(1 - \frac{E_{\max} \cdot \hat{C}_{s,ij}^{\gamma}}{EC50_i^{\gamma} + \hat{C}_{s,ij}^{\gamma}} \right) - k_{tr1,i} \cdot A(1)$$

$$\frac{dA(2)}{dt} = k_{tr1,i} \cdot A(1) - k_{tr1,i} \cdot A(2)$$

$$\frac{dA(3)}{dt} = k_{tr1,i} \cdot A(2) - k_{tr1,i} \cdot A(3)$$

$$\frac{dA(4)}{dt} = k_{tr1,i} \cdot A(3) - k_{tr1,i} \cdot A(4)$$

$$\frac{dA(5)}{dt} = k_{tr1,i} \cdot A(4) - k_{tr1,i} \cdot A(5)$$

$$\frac{dA(6)}{dt} = k_{tr1,i} \cdot A(5) - k_{tr1,i} \cdot A(6)$$

$$\frac{dA(7)}{dt} = k_{tr2,i} \cdot \left(1 - \frac{E_{\max} \cdot \hat{C}_{s,ij}^{\gamma}}{EC50_i^{\gamma} + \hat{C}_{s,ij}^{\gamma}} \right) - k_{tr2,i} \cdot A(7)$$

$$k_{tr1,i} = \frac{1}{MTT_{1,i}}$$

$$k_{tr2,i} = \frac{1}{MTT_{2,i}}$$

$$\text{LN}(\text{INR}_{ij}) = \text{LN}(\text{BASE}_i + \text{INR}_{\text{MAX}} \cdot (1 - A(6) \cdot A(7))^{\lambda}) + \varepsilon_{\text{INR}_{ij}}$$

In these equations, $A(n)$ is the amount in the designated compartment with A(1)–A(6) being the long transit chain and A(7) is the amount in the short transit chain, $k_{trn,i}$ the transit rate constant for the i th individual, which is inversely related to the individual mean transit time ($MTT_{n,i}$), E_{\max} is the maximal inhibition of coagulation, and was fixed to one, $EC50_i$ is the concentration of s-warfarin producing half-maximal inhibition and was modeled as a function of VKORC1 genotype, γ is the sigmoidicity factor. For the INR function, BASE_i is the individual

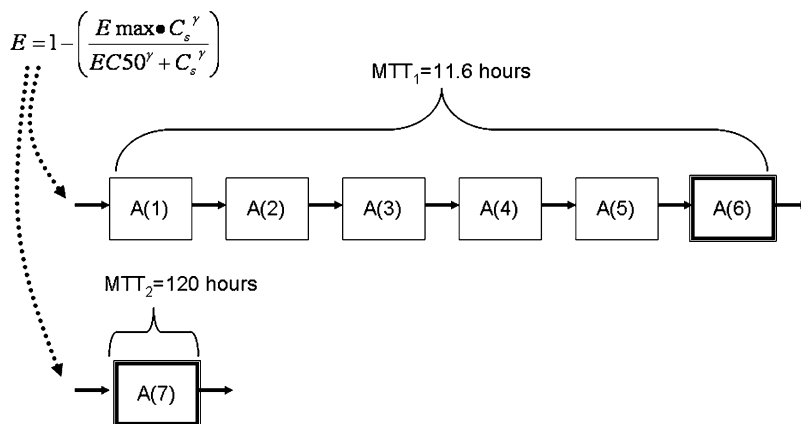


Fig. 10.3 Schematic of warfarin pharmacodynamic model

baseline INR, INR_{MAX} is the maximal increase in INR (fixed to 20), λ is a scaling factor and ϵ_{ij} is the residual error for the j th observation for the i th individual.

Using this model, the authors reported that CYP2C9 genotype and age were predictors for S-warfarin clearance, and that the VKORC1 genotype was identified to be predictor of warfarin sensitivity, which was consistent with earlier evaluations (Sconce *et al.* 2005). This model was later employed to investigate various warfarin dosing strategies (Salinger *et al.* 2009) using clinical trial simulation. The authors reported that a pharmacogenomic-guided warfarin dosing may be more useful than the standard of care in clinical settings with less intensive patient follow-up, and when adjustments are made for slower therapeutic response in patients with a CYP2C9 variant. These findings are consistent with the updated labeling for warfarin proposed by the FDA that people with variations in CYP2C9 and VKORC1 may require a lower initial dose of the drug (FDA 2007a, b).

10.3 Stroke

10.3.1 Overview of Stroke and Clinical Endpoints

Numeric rating scales such as the National Institutes of Health Stroke Scale (NIHSS), Canadian Neurological Scale (CNS), and the Scandinavian Stroke Scale (SSS) have been devised to quantify the neurologic examination after stroke and are routinely used in clinical trials (Brott *et al.* 1989; Cote *et al.* 1986; Scandinavian Stroke Study Group 1985; Lindenstrom *et al.* 1991). Severity of deficits as quantified by the NIHSS and the CNS can predict long-term functional outcome after stroke (Fiorelli *et al.* 1995; Muir *et al.* 1996). Rating scales are usually implemented at patient admission (baseline) and periodically after admission. The typical regulatory approach to the

analysis of stroke scores is to compare the baseline score to interim or end-of-study scores (change from baseline) and then comparing treatment of the investigation drug to placebo or other treatment (FDA 1998). However, a longitudinal multivariate analysis of the time course of disease progression makes it possible to assess the rapidity of the response to drug treatment.

The disease progression approach using the raw stroke scale data or change from baseline data using linear or asymptotic models based on exponential, E_{\max} , nonzero asymptotic, and inverse Bateman functions can be applied (Mould 2007), although more complex approaches can be used, such as the two-part model developed by Jonsson *et al.* (2005). This was done using Markovian probabilistic models to describe the transition from disease to full health (*i.e.*, the improvement or decline in the total health status relative to the previous disease state) and occurrences of dropout.

10.3.2 Example Stroke Disease Progression Models

CP-101,606 is a substituted 4-phenylpiperidine that is a glutamatergic NR2B subunit specific *N*-methyl-d-aspartate (NMDA) receptor antagonist and has been evaluated for use in stroke. NMDA receptor antagonists may reduce probability of death and functional impairment caused by stroke by inhibiting neuron death caused by glutamate-mediated excitotoxicity (Choi 1988). Large increases in synaptic glutamate concentrations following a stroke activate glutamate receptors and have been shown to result in neuronal death (Bullock *et al.* 1995a, b). Blocking of the NMDA receptors has shown to prevent neuron death caused by glutamate *in vitro* (Rosenberg and Aizenman 1989).

The NMDA receptor is differentially distributed with different subunit combinations throughout the brain and spinal cord. Receptors with the NR2B subunit are distributed in specific forebrain regions that are vulnerable to cortical strokes (Monyer *et al.* 1992). Therefore, the specificity of CP-101,606 for the NR2B subunit of the NMDA receptor is thought to increase the specificity to vulnerable portions of the brain to stroke.

CP-101,606 is a known substrate of the polymorphic cytochrome P450 2D6. Some 5–10% of the Caucasian population possess inactivating alleles for the gene (Johnson *et al.* 2003). Individuals who possess normal activity of the CYP2D6 gene are referred to as extensive metabolizers (EM) and are known to exhibit broad ranges of metabolism of CYP2D6 substrates. Individuals, who possess no CYP2D6 activity because of the inactivating alleles, are referred to as poor metabolizers (PM). These individuals are readily identified by genotypic analysis of patient DNA samples. Other individuals possess reduced activity caused by combinations of inactive and reduced activity alleles. These individuals are more difficult to determine their genotypes because they exhibit broad phenotypic ranges of drug metabolism and are referred to as intermediate metabolizers (IM).

CP-101,606 demonstrates two distinct clearance mechanisms in CYP2D6 EMs and PMs. In EM subjects, the plasma clearance is high at ~16-ml/min/kg resulting in a short half-life (~4 h). The clearance in these subjects is mediated by primary hydroxylation followed by conjugation (Johnson *et al.* 2003). In PM subjects the plasma clearance is low (~4 ml/min/kg) resulting in a moderate half-life (~16 h). The clearance in these subjects is mediated by primary hydroxylation (approximately 27%), primary sulfation (approximately 12%), and renal clearance of unchanged CP-101,606 (approximately 50%).

The primary objective of this pharmacokinetic–pharmacodynamic (PK/PD) analysis was to evaluate the exposure-response relationship of CP-101,606 to the National Institute of Health Stroke Scale (NIHSS). The study was designed as a placebo controlled, double-blind study, with intrasubject and intergroup comparisons made to baseline. Patients were randomized in a 1:1 ratio to receive CP-101,606 or placebo after diffusion magnetic resonance imaging evidence of an acute cortical ischemic stroke. Either CP-101,606 or placebo was delivered by intravenous infusion started within 8 h of the onset of neurological symptoms. For subjects receiving CP-101,606, a loading infusion of 0.75-mg/kg/h for 2 h followed by a maintenance infusion of 0.37-mg/kg/h for 70 h, for a total of 72 h was administered. The target plasma concentration was 200 ng/ml. Pharmacokinetic samples were collected at the end of the loading infusion, and at times throughout and after the end of the maintenance infusion.

The NIHSS is a 15-item neurologic examination stroke scale used to evaluate the effect of acute cerebral infarction on the levels of consciousness, language, neglect, visual-field loss, extra ocular movement, motor strength, ataxia, dysarthria, and sensory loss (Brott *et al.* 1989). The minimum score is zero, which signifies a normal subject and the maximum score is 42, with scores greater than 15–20 considered severe. NIHSS assessments were performed at screening and daily until discharge, and then at 30 and 90 days after treatment. If the patients' neurological status deteriorated, NIHSS was to be performed more frequently.

Whole blood samples were collected to prepare genomic DNA for the purpose of cytochrome P450 2D6 genotyping. A panel of CYP2D6 alleles was screened for the determination of CYP2D6 metabolizer status using polymerase chain reaction (PCR). The alleles included *1, *2, *3, *4, *5 (gene deletion) and *6, *8, *9, *10, *11, *12, *14, *15, *16 (gene duplication). Subjects that carried two PM alleles (*3, *4, *5, *6, *8, *11, *12, *14, *15 and *16) were classified as poor metabolizers. Individuals who possessed the *4/*10, *9/*4, and *9/*10 genotype have been shown to exhibit reduced substrate activity. For the purpose of this study, these individuals were considered to be IM.

The final database that was used for model building and evaluation included 53 subjects treated with CP-101,606 and 61 subjects treated with placebo. In general, the demographic characteristics such as age, sex, weight, and race of the subjects were similar for each treatment group. There were 399 pharmacokinetic observations from the 53 subjects administered CP-101,606 and 1,030 NIHSS observations from the 114 subjects in the study.

Table 10.2 Population pharmacokinetic parameters for CP-101,606

Parameter	Formula	Metabolizer type	Typical value	Interindividual variability (%)
Clearance (ml/min/kg)	$CL = CL*(WT/70)^{0.75}$	Extensive	5.42	33.3
		Poor	16.0	33.3
Volume (L)	$V = V*(WT/70)$	NA	5.04	25.1

Most patients were EM, three were genotyped as IM and two patients genotyped as PM accounting for ~13% of the patients administered CP-101,606 in this study. Nine patients were not genotyped, but based on their CP-101,606 plasma concentration profiles, these patients were not expected to be PM. For all the subjects, the steady state average concentration was greater than or equal to the target of 200 ng/ml. The EM subjects had concentrations that were approximately threefold lower than the PM subjects.

The best model for CP-101,606 pharmacokinetics was a one compartment linear model with first order elimination. The parameter estimates are shown in Table 10.2. A mixture model for metabolizer type (slow or fast) was used to mimic CYP2D6 genotype effect and resulted in a proportion of approximately 27.1% of the subjects being slow metabolizers. Age, weight, BSA, sex, and race were evaluated as predictors of pharmacokinetic variability. Covariate inclusion selection was based on a forward addition/backward deletion method using the likelihood ratio test with a significance of level of $p < 0.001$ and decreases interindividual variability. An allometric model of weight was the only predictor for clearance and volume.

The pharmacodynamic model was modeled as two groups; depending on if they were improving or worsening, using a mixture model. An asymptotic inhibitory E_{max} model was used for subjects that improved after the baseline evaluation in which a decrease in their NIHSS scores was observed. For subjects that worsened, as measured by an increase in their NIHSS score, a linear model was used. Sex, race, age, weight, BSA, infarct volume, baseline NIHSS, and prior statin and ACE inhibitor treatment were evaluated as predictors of disease progression using the same method and criteria described previously.

Once the final model was selected the effect of drug treatment as a covariate on the model parameters was added. Several measures were tested including active or placebo treatment as a categorical covariate and total CP-101,606 dose or the CP-101,606 exposure parameters AUC and $C_{ss, avg}$ as continuous covariates estimated from the population pharmacokinetic model. $C_{ss, avg}$ was found to be the most significant predictor of response and was included as a covariate on the IMAX parameter.

The final parameter estimates are provided in Table 10.3. The model results showed that the probability a patient would worsen during the study was 0.146. Higher baseline NIHSS values were associated with poorer recovery (lower inhibitory E_{max}). Older age and larger lesion volume lengthened recovery time. Higher

Table 10.3 Population pharmacodynamic parameters for stroke model

Patient outcome	Formula	Parameter	Typical value	Inter-individual variability (%)
Worsening	$\text{NIHSS}(t) = \text{NIHSS}_{\text{day0}} + \text{Slope} * \text{Day}$	Slope	1.86/day	94.0
Improving	$\text{NIHSS}(t) = \text{NIHSS}_{\text{day0}} + \text{IEmax} * \text{Day} / (\text{INHC} + \text{Day})$ $\text{INHC} = \text{IC50} * (1 + \text{LV} * \text{LVE}) * (60 / \text{Age})^{\text{AgeE}}$	Intercept	12	21.0
		IMAX	-10.1	
		Css, avg	0.0002	
		Baseline	0.612	196
		NIHSS		
		IC50	2.16	
		AgeE	-2.52	
		LVE	0.0185	

LV lesion volume; AgeE age effect on IC50; LVE lesion volume effect on IC50

CP-101,606 C_{ss, avg} was associated with greater recovery. While the addition of drug effect significantly decreased the variability of the parameters, based on the likelihood ratio test, the statistical significance of the drug effect was $p < 0.05$.

Overall, the dosing regimen administered in this study resulted in stroke patients achieving or exceeding the targeted minimum C_{ss, avg} of 200 ng/ml. The non-compartmental pharmacokinetic analysis showed that EM patients had 66% lower exposure than PM patients did. Population pharmacokinetic modeling with the use of a mixture model for assignment of EM/PM status resulted in a larger proportion (~27%) of slow metabolizers than observed in the general population (~15%), and by genotyping (~10%), possibly caused by the large variability of CYP2D6 expression in the population.

Plots of individual concentration versus time since the start of the infusion from three subjects are presented in Fig. 10.4a. Subject 15 is a 67-year-old patient that was a CYP2D6 PM (*4/*4 genotype) and had a baseline NIHSS value of 18. Subject 18 is a 52-year-old patient that was a CYP2D6 EM (*2/*4 genotype) with a baseline NIHSS value of seven. Lastly subject 53 is an 80-year-old patient that was a CYP2D6 EM (*2/*16 genotype) and had a baseline NIHSS value of seven. These plots show that CYP2D6 genotype had a great influence in the exposure of CP-101,606. The EM subjects 18 and 53 had an approximately twofold difference in concentrations, which demonstrates the large variability in exposure within CYP2D6 genotypes. The PM subject 15 had much higher concentrations than the other two subjects showing the impact of PM status on exposure. The individual predicted concentrations (thick line Y) were close to the observed data (triangles). The thin line (PRED) is the population predicted values.

Similar plots of the NIHSS values over time for these same subjects are in Fig. 10.4b. This plot shows that for subjects 15 and 18, who both showed improving signs and symptoms based on the decrease in NIHSS values over time, have an asymptotic profile versus time. Subject 53 who showed worsening signs and symptoms over time had a linear increase although there was a spike in the values between days 2 and 4.

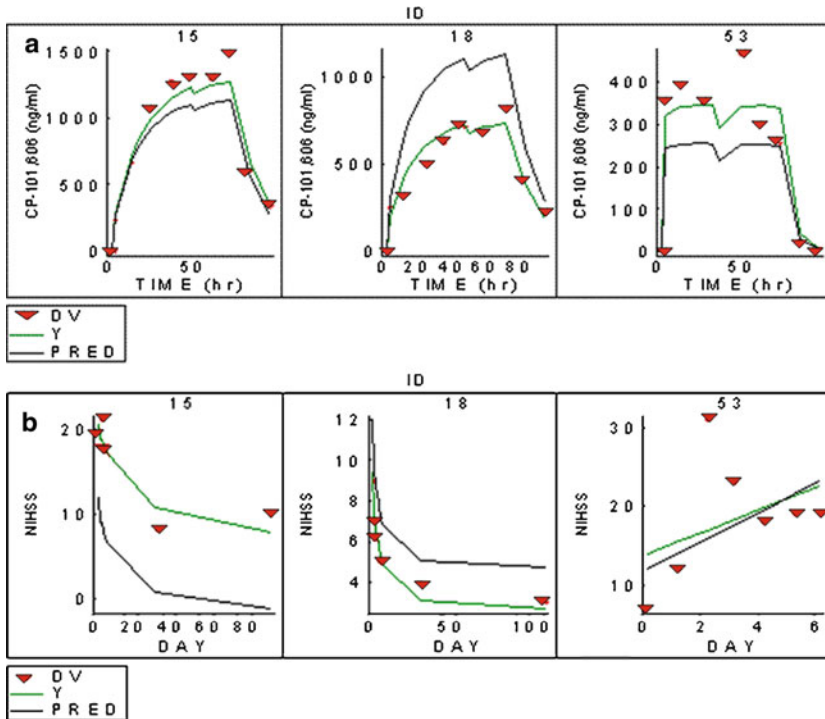


Fig. 10.4 Plots of individual observed, population predicted and individual predicted observations versus time since the start of the infusion from representative subjects (a) CP-101,606 Concentration; (b) NIHSS scores

The pharmacodynamic modeling results show that administration of CP-101,606 to acute stroke patients results in greater recovery and less variability in time and extent of maximum recovery. The modeling results were consistent with the statistical analysis for this study, which used a dichotomized NIHSS with adjustments for age and baseline NIHSS imbalances (Grotta 1997), and indicated a benefit for CP-101,606-treated stroke patients. Simulation of NIHSS values over time using this model for three levels of CP-101,606 C_{ss}, avg suggests greater exposure to CP-101,606 results in more complete recovery (Fig. 10.5).

An example control stream and data for NIHSS disease progression model is provided on the associated FTP site.

10.3.3 Longitudinal Model for Nonmonotonic Stroke Scale Data

Another stroke model was reported by Jonsson *et al.* (2005). In this two-part analysis, in addition to the modeling of the disease progress over time, an additional part was

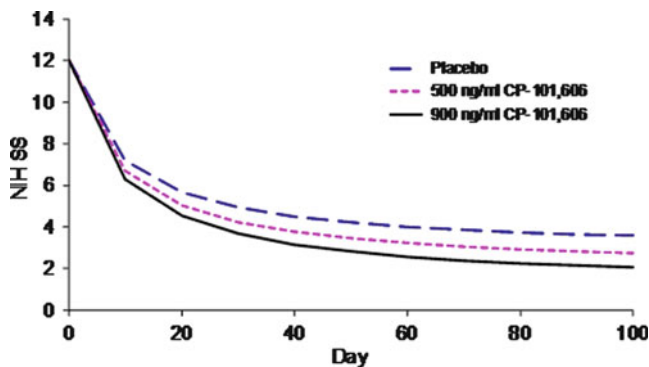


Fig. 10.5 Simulated NIHSS values for selected steady state plasma concentrations of CP-101,606

added that would potentially decrease the random variability in the model. In the previous example a mixture model was used to assign a subject to either a monotonic worsening of disease with a linear function or a monotonic improvement in the disease state as an inhibitory E_{\max} function. Here a nonmonotonic disease progression is modeled where a subject may have a worsening score after an improving score or vice versa. The rationale being that with the previous example, once the subject was assigned to either worsening or improving via the mixture model; all changes in the score that are different from the overall trend were included in random variability in the NIHSS values. The Jonnson *et al.* model allowed for nonmonotonic score changes as well as patients dropping out from the study.

The authors implemented five submodels that were either continuous or probabilistic. The probabilistic submodels were set up to determine the probability that a subject fully recovered, dropped out or had an improvement in disease state from one occasion where the stroke score was assessed to the next. The continuous submodels were implemented as linear models that described the relative magnitude of score change given and observed improvement or worsening of the disease state.

The advantage of this more complex method is that it allows for accurate simulation of clinical trial data including subject dropout and the use of sparse sample collection. From these simulations, traditional statistical analyses can be performed a priori on the simulated data where placebo groups and “last observation carried forward” imputation schemes can be included.

Whelan *et al.* (2008) developed a tradeoff model evaluating the efficacy and toxicity of tPA. The tradeoff function was constructed from several pairs of efficacy/toxicity probabilities specified by the investigators. The authors used the model for clinical trial simulation to develop an adaptive dose ranging trial for pediatric stroke patients. The simulation assigned doses to successive cohorts of patients on the basis of each dose’s desirability, based on the tradeoff between efficacy and toxicity. Each cohort dose was selected adaptively based on dose-outcome data from the patients treated previously to optimize the efficacy–toxicity tradeoff. The authors concluded that this approach avoids the more time-consuming and expensive conventional

approach of conducting a phase I trial based on toxicity alone followed by a phase II trial based on efficacy alone. This is especially useful in settings with low accrual rates, such as trials of tPA for pediatric acute ischemic stroke.

10.4 Hypertension

10.4.1 Overview of Hypertension

Essential hypertension has a complex underlying pathology. There are many risk factors such as sedentary lifestyle and obesity. Insulin resistance, a component of metabolic syndrome and is also associated with obesity, is also thought to be a causative factor in the development of hypertension. Other factors include stress leading to increased sympathetic nervous system activity; dietary factors such as protracted high sodium intake, inadequate potassium and calcium intake; increased renin secretion with resulting elevations in angiotensin II and aldosterone; deficiencies of vasodilators; alterations in expression of the kallikrein–kinin system; and abnormalities of resistance vessels. Hypertension is also related to aging. Family history, including some inherited genetic mutations, has also been shown to increase the risk of developing hypertension.

Guyton (1991) suggested that renal mechanisms might play a primary role in the development of essential hypertension. More recently, Johnson *et al.* (2002) suggested that renal microvascular disease be a causative component. They suggest that the kidney undergoes subclinical injury over time, resulting in selective afferent arteriopathy and tubulointerstitial disease. This theory has only been tested in animal models.

10.4.2 Pharmacology of Antihypertensive Agents

There are several classes of antihypertensive agents. Commonly used antihypertensive agents fall into one of the four groups listed below:

1. Angiotensin converting enzyme (ACE) inhibitors such as captopril, enalapril, fosinopril, and lisinopril
2. Angiotensin II receptor antagonists such as telmisartan, irbesartan, losartan, and valsartan
3. Diuretics such as bendroflumethiazide, chlortalidone, and hydrochlorothiazide
4. Calcium channel blockers such as nifedipine, amlodipine, diltiazem, and verapamil
5. Beta blockers such as propranolol, atenolol, labetalol, carvedilol, and metoprolol

A schematic diagram of the renin-angiotensin-aldosterone system and sites of drug action for several classes of antihypertensives is shown in Fig. 10.6. Angiotensin II increases blood pressure by various mechanisms. In addition, angiotensin II promotes cardiac and vascular cell hypertrophy and hyperplasia by activating

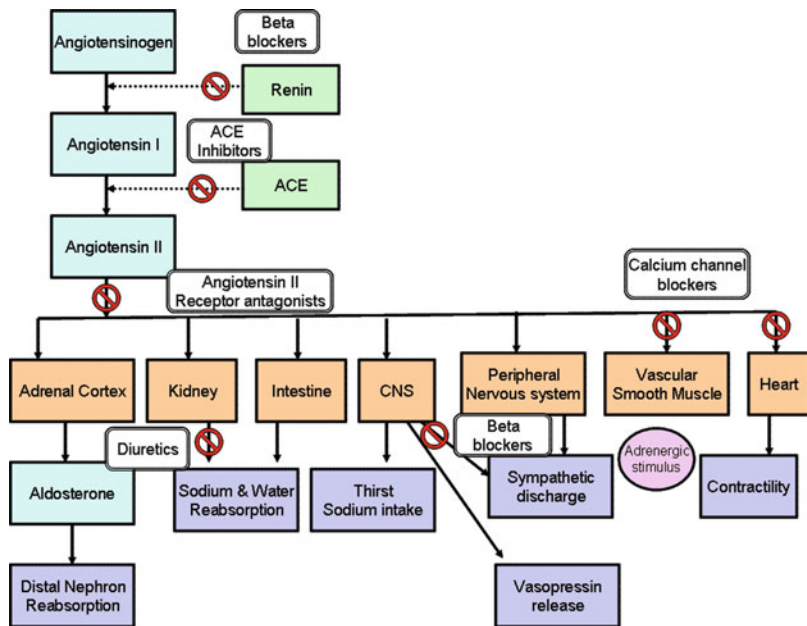


Fig. 10.6 Schematic of the renin-angiotensin-aldosterone system

the angiotensin II type 1 receptor and acts indirectly by stimulating release of several growth factors and cytokines (McConnaughey *et al.* 1999). The angiotensin II type 2 receptor has the opposite effects. Following administration of an angiotensin II receptor antagonist, renin is released from the kidney because of removal of feedback inhibition by angiotensin II. The release of renin then increases angiotensin II levels, which in turn binds to the AT2 receptor, providing blood pressure reduction and other consequent cardiovascular benefits.

In addition to reducing circulating angiotensin II by blocking its formation, ACE inhibitors act to decrease the stiffness of peripheral arteries as well as reducing pulse pressure and pulse wave velocity, independent of a corresponding reduction in systolic blood pressure in the periphery (Stergiou 2004).

Calcium-channel blockers and diuretics exert a similar action on arterial stiffness (Laurent *et al.* 2002). These agents work by blocking voltage-gated calcium channels in cardiac muscle and blood vessels, decreasing intracellular calcium, which results in reduced in muscle contraction. Decreased calcium causes decreased cardiac contractility in the heart and less contraction of the vascular smooth muscle in blood vessels with a resulting increase in arterial diameter. Vasodilation decreases total peripheral resistance, while a decrease in cardiac contractility decreases cardiac output ultimately reducing blood pressure.

There are three types of β receptors, with β_1 receptors being primarily in the heart and kidneys. Consequently, stimulation of β_1 receptors by epinephrine induces a positive chronotropic and inotropic effect on the heart and increases

cardiac conduction velocity and automaticity. In the kidney, stimulation of β_1 receptors enhances the release of renin. Beta-blockers inhibit normal epinephrine-mediated sympathetic actions, reducing the effect of physical exertion on heart rate and contractile force, and dilating of blood vessels with minimal effect on resting subjects. The antihypertensive mechanism of β -blockers is attributable to reduction in cardiac output (because of their negative chronotropic and inotropic effects), reduction in renin release from the kidneys, and in some cases, effects on the central nervous system to reduce sympathetic activity.

10.4.3 Modeling and Simulation for Antihypertensive Agents

As was seen with anticoagulants, structural models for blood pressure are frequently described using direct or indirect effect type models. However, with antihypertensive agents, there is a tendency with some agents for rebound hypertension to occur on abrupt cessation of treatment. For example, clonidine is well known to exhibit rebound hypertension and increase in heart rate when dosing is abruptly stopped (Geyskes *et al.* 1979). Clonidine is an α_2 agonist that suppresses the sympathetic nervous system, decreasing cardiac output and peripheral vascular resistance. Clonidine also has some inhibitory activity against plasma

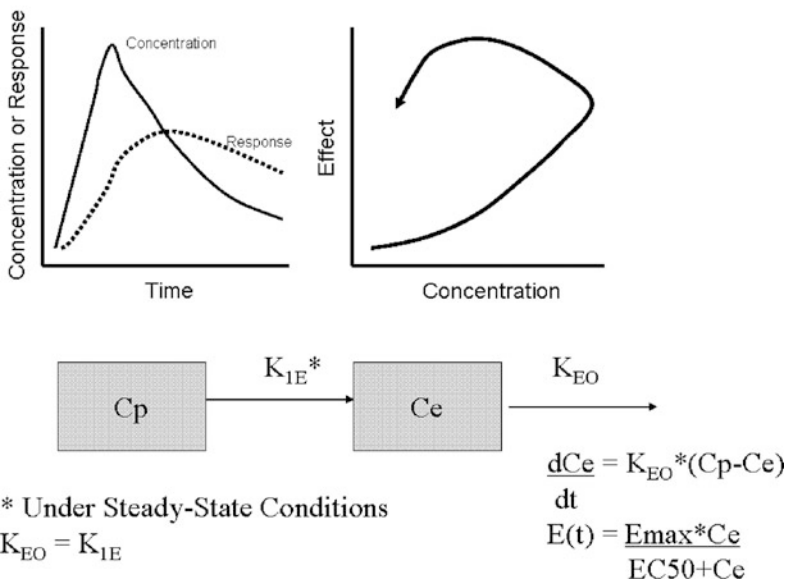


Fig. 10.7 Plot of concentration and response showing hysteresis. C_p is the plasma concentration of a drug, C_e is the effect site concentration, $E(t)$ is the effect at time “t”, E_{max} is the maximum response elicited by a drug, and EC_{50} is the concentration in the effect compartment that can elicit 50% of the maximal response

renin activity, further reducing blood pressure. The rebound phenomenon is attributed to its α_2 agonist activity and necessitates careful withdrawal of this drug.

Porchet *et al.* (1992) developed a pharmacodynamic model that used an effect compartment (Verotta *et al.* 1989; Unadkat *et al.* 1986) as proposed by Sheiner to describe the delay between concentration and response that leads to hysteresis when concentration is plotted versus effect as shown in Fig. 10.7.

However, the effect compartment type model does not describe a rebound response well. A precursor pool model as described by Sharma *et al.* (1998) allows both for the lag time to onset of effect and characterizes the rebound component of response as well. A schematic of this model is shown in Fig. 10.8 along with a plot of response versus time showing a modest rebound.

The equations describing this model are shown below:

$$\frac{d\text{Precursor_Pool}}{dt} = K_0 - K_{in} \cdot \text{Precursor_Pool} - K_s \cdot \text{Precursor_Pool}$$

$$\frac{d\text{Response}}{dt} = K_{in} \cdot \text{Precursor_Pool} - K_{out} \cdot \text{Response}$$

In these equations, K_0 is the zero order formation rate of the precursor, K_s is the rebound rate constant, K_{in} is the first order transfer rate constant between the precursor pool and the response and K_{out} is the first order rate constant of loss of

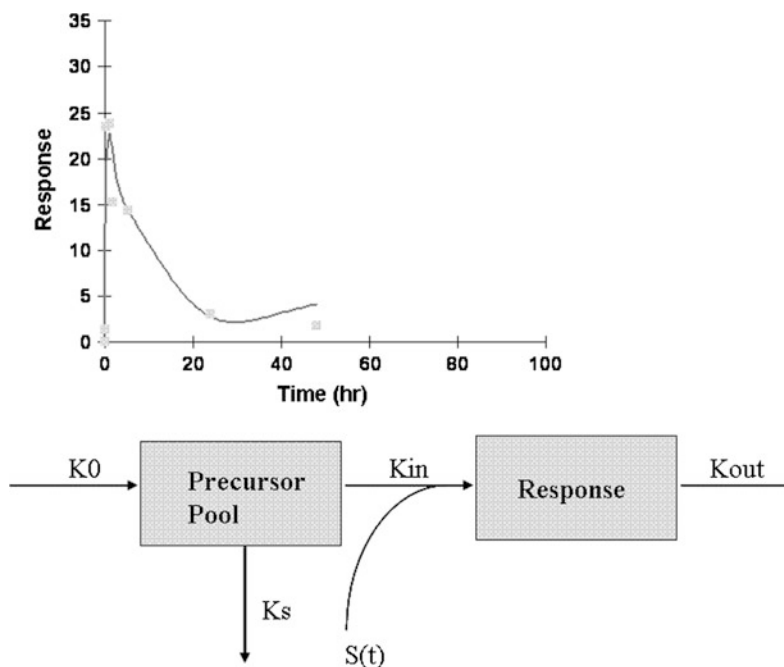


Fig. 10.8 Schematic for a precursor pool model. In this figure, $S(t)$ is the drug effect model and K_s is a rebound rate constant

response. The magnitude of K_s describes the magnitude of the rebound response. Such a model is a valuable tool for investigating whether or not cessation of treatment with a hypertensive agent shows rebound.

Not all antihypertensive agents exhibit rebound, however. Fenoldopam is a rapid-acting vasodilator used to manage hypertension in adults. It is a selective dopamine₁-receptor agonist that increases renal blood flow, creatinine clearance, urinary flow, and sodium excretion, thus lowering blood pressure. Hammer *et al.* (2008) investigated the pharmacodynamics of fenoldopam in pediatric patients and was able to use a simple direct effect E_{\max} model to describe the change in mean arterial pressure following administration. Similarly, the pharmacodynamics of clevidipine were investigated by Bailey *et al.* (2002) and were found to be well described using a direct effect E_{\max} type model.

Chabaud *et al.* (2002) developed a semimechanistic pharmacokinetic–pharmacodynamic model for ivabradine. The clinical outcome, chest pain, was described using a physiologic model in which the coronary reserve was derived from the heart rate. Safety was defined as being heart rate dependent. This model was used to evaluate the drug regimen (2.5, 5, 10, 20, and 40 mg administered once or twice daily), and number of patients for a pediatric trial using Monte Carlo simulation.

The authors found that 25% of the simulated trials showed a significant clinical effect with doses up to 10 mg once daily; 48 and 55% of the trials with doses of 10 mg twice daily and 20 mg once daily, respectively, and more than 80% of the trials with a 40-mg daily dose. Approximately 4% of untreated patients had at least one adverse event and 5–13% patients in the treated groups for the lowest to the highest dose, respectively. The authors estimated that the number of subjects needed to obtain a 15% decrease in chest pain under the assumption of a 68% base risk was 239 subjects per treatment arm with 10 mg twice daily or 196 with 20 mg given once daily. Given the practical difficulty in conducting pediatric trials, the use of modeling and simulation to identify potentially useful doses and to develop a study design that will provide robust determination of efficacy was an important component in the clinical development of this agent in pediatric patients.

10.5 Adaptive Dosing Simulation Techniques: Focus on Cardiovascular Medicines

For drugs in the cardiovascular therapeutic area, many late phase clinical trials use dose titration algorithms to ensure patient safety and allow the treating physician adjust individual patient doses based on measured responses to achieve a response that is within a recommended or target range. For example, in late phase clinical trials of an antihypertensive agent, a basic starting dose will be recommended but doses will be adjusted until a patient's blood pressure is near 130/80 mmHg. Consequently, during the conduct of the study, individual patient doses may stay the same, increase, or decrease over time; or a patient may be put on hold until the

response of interest returns to some satisfactory range. Dose adjustments may be based on recent measurements; time averaged measurements or may take into account multiple types of responses.

Developing a pharmacokinetic/pharmacodynamic model with such data is usually straightforward involving the techniques described previously. However, simulation, particularly of pharmacodynamic data, when adaptive dosing is used can be challenging. In this case, the doses become random because they are determined by the subject’s response(s). Simulations using the original data (index database) are usually inappropriate in this setting because the simulation scenarios often contain much higher and lower responses than those observed with the index data. This is because the simulated subject’s response to the drug usually does not reflect the original (index) patient’s sensitivity so the dose adjustment for the index patient is not appropriate for the simulated subject.

For example, consider a subject in the index data who was unresponsive to the drug, and therefore was dose escalated several times. Random effects (between subject variability) drawn during simulation could result in a simulated subject who is very sensitive to drug effect. Unless care is taken, the simulated subject will use the dose records associated with the index subject who was insensitive to the drug.

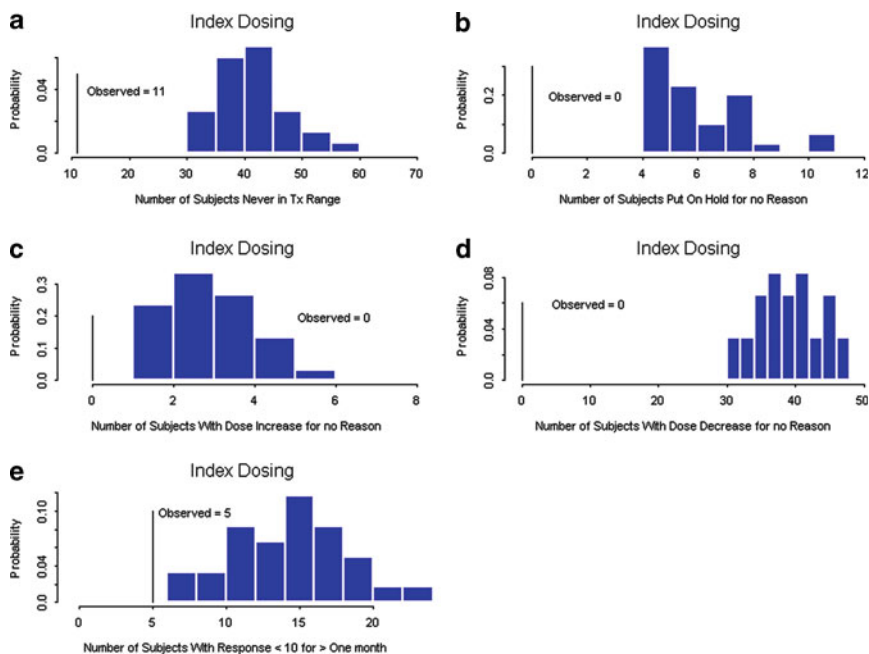


Fig. 10.9 Diagnostic plots for dose adjustments for simulations conducted using index dosing. Panel a – Number of subjects never in the therapeutic range; Panel b – Number of subjects put on hold for no reason; Panel c – Number of subjects with dose increase for no reason; Panel d – Number of subjects with dose decrease for no reason; Panel e – Number of subjects with response below 10 for more than one month

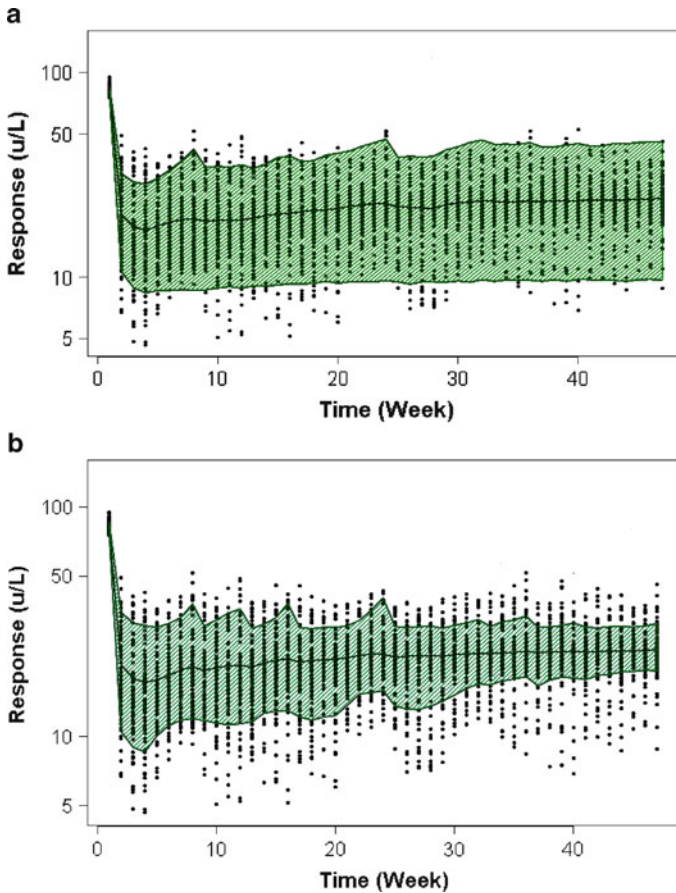


Fig. 10.10 Comparison of visual predictive check using index data dosing and adaptive dosing. (a) Visual predictive check conducted using index dosing; (b) Visual predictive check conducted using adaptive dosing implemented in the simulation

For the simulated subject then, very high responses would be simulated using the index dosing records. The resulting simulated data are not realistic because in a clinical setting, the clinician would never increase the dose. To illustrate what can go wrong when simulations are done with the index data, four check statistics should be considered when simulating data arising from a study that implements adaptive dosing:

1. Number of subjects never in the therapeutic range.
2. Number of subjects that were put on hold for no reason.
3. Number of subjects that ever received an inappropriate dose increase.
4. Number of subjects that ever received an inappropriate dose decrease.

Because of between subject variability in the pharmacokinetic and pharmacodynamic parameters, simulations done with the dose records in the index dataset as well as from a simulation that incorporates the adaptive dosing design will generate some subjects that are never observed to be in the therapeutic range. On the other hand, for the last three check statistics listed above, when the simulation incorporates the same adaptive dosing used in the clinical trial, such subjects cannot be simulated. Using the index data as a basis for simulation can easily generate subjects that receive dosing errors. Figure 10.9a–e depict this situation.

Figure 10.9a–e demonstrates the limitation of using dosing information from an index dataset when, in reality, a clinical investigator would try to adapt dosing to achieve a target. It would be inappropriate to make versions of Fig. 10.9b–d for adaptive dosing as the events in question cannot happen.

In addition, when doses were adjusted during a clinical study, using the index dataset for model evaluation such as a visual predictive check (VPC) can result in inflated prediction intervals or can result in biased prediction intervals. Implementation of adaptive dosing during simulation provides a more realistic assessment of model performance. Figure 10.10a,b show VPCs conducted when the index data dosing information were used during the simulation (a) and when the doses were adaptively adjusted during the simulation following the dose adjustment rules in the clinical trial (b). The 80% prediction intervals in Fig. 10.10a are clearly inflated, with the majority of observations being inside the prediction intervals, and the prediction intervals also appear to have some bias, with more observed data being outside the intervals at the lowest response values, whereas the 80% intervals in Fig. 10.10b are much narrower (*e.g.*, they are not inflated), and cover approximately 80% of the observed data with equal numbers of observations being higher and lower than the intervals.

Adaptive dosing during simulations can be implemented in a variety of software packages. Additional text on the implementation of this approach in Nonmem 6, as well as example data and control streams are provided on the FTP site.

Acknowledgments The authors would like to acknowledge Professor Stuart Beal for his suggestion of the “incredible” mixture model, and Ms. Tracey Thomas for help in formatting and preparing this chapter.

References

- Ahn JE, French J (2009) Longitudinal model-based meta-analysis with NONMEM. ACoP Meeting Mystic CT USA. http://www.go-acop.org/sites/all/assets/webform/ahn_1.doc
- Bailey JM, Lu W, Levy JH, Ramsay JG, Shore-Lesserson L, Prielipp RC, Brister NW, Roach GW, Jolin-Mellgard A, Nordlander M (2002) Clevidipine in adult cardiac surgical patients: a dose-finding study. *Anesthesiology* 96(5):1086–1094
- Beal SL, Sheiner LB, Boeckmann AJ (1989–2006) NONMEM Users Guides, ICON Development Solutions, Ellicott City, MD
- Bellosta S, Ferri N, Bernini F, Paoletti R, Corsini A (2000) Non-lipid-related effects of statins. *Ann Med* 32:164–176

- Blum CB (1994) Comparison of properties of four inhibitors of 3-hydroxy-3-methylglutaryl-coenzyme A reductase. *Am J Cardiol* 73:3D–11D
- Brott T, Adams HP, Olinger CP, Marler JR, Barsan WG, Biller J, Spilker J, Holleran R, Eberle R, Hertzberg V (1989) Measurements of acute cerebral infarction: a clinical examination scale. *Stroke* 20:864–870
- Bullock R, Zauner A, Myseros JS, Marmarou A, Woodward JJ, Young HF (1995a) Evidence for prolonged release of excitatory amino acids in severe human head trauma relationship to clinical events. *Ann NY Acad Sci* 765:290–297
- Bullock R, Zauner A, Woodward J, Young HF (1995b) Massive persistent release of excitatory amino acids following human occlusive stroke. *Stroke* 26:2187–2189
- Chabaud S, Girard P, Nony P, Boissel JP (2002) Clinical trial simulation using therapeutic effect modeling: application to ivabradine efficacy in patients with angina pectoris. *J Pharmacokinetic Pharmacodyn* 29(4):339–363
- Choi DW (1988) Glutamate neurotoxicity and diseases of the nervous system. *Neuron* 1(8):623–634
- Cote R, Hachinski V, Shurvell B, Norris JW, Wolfson C (1986) The Canadian Neurological Scale: a preliminary study in acute stroke. *Stroke* 17:731–736
- Dayneka NL, Garg V, Jusko WJ (1993) Comparison of four basic models of indirect pharmacodynamic responses. *J Pharmacokinetic Biopharm* 21(4):457–478
- Faltaos DW, Urien S, Carreau V, Chauvenet M, Hulot JS, Giral P, Bruckert E, Lechat P (2006) Use of an indirect effect model to describe the LDL cholesterol-lowering effect by statins in hypercholesterolaemic patients. *Fundam Clin Pharmacol* 20(3):321–330
- FDA (1998) Guidance for industry: E9 statistical principles for clinical trials
- FDA (2007) New labeling information for warfarin (marketed as Coumadin). <http://www.fda.gov/cder/drug/infopage/warfarin/default.htm>. Accessed 16 Aug 2007
- FDA (2007) FDA approves updated warfarin (Coumadin) prescribing information [press release]. <http://www.fda.gov/bbs/topics/NEWS/2007/NEW01684.html>. Accessed 16 Aug 2007
- Fiorelli M, Alperovitch A, Argentino C, Sacchetti ML, Toni D, Sette G, Cavalletti C, Gori MC, Fieschi C (1995) Prediction of long-term outcome in the early hours following acute ischemic stroke. *Arch Neurol* 52:250–255
- Friberg LE, Karlsson MO (2003) Mechanistic models for myelosuppression. *Invest New Drugs* 21(2):183–194
- Gabrielsson J, Jusko WJ, Alari L (2000) Modelling of dose-response-time data: four examples of estimating the turnover parameters and generating kinetic functions from response profiles. *Biopharm Drug Dispos* 2:41–52
- Geyskes GG, Boer P, Dorhout Mees EJ (1979) Clonidine withdrawal. Mechanism and frequency of rebound hypertension. *Br J Clin Pharmacol* 7(1):55–62
- Green B, Duffull SB (2003) Development of a dosing strategy for enoxaparin in obese patients. *Br J Clin Pharmacol* 56(1):96–103
- Grotta J (1997) Lubeluzole treatment of Acute Ischemic Stroke. *Stroke* 28:2338–2346
- Guyton AC (1991) Blood pressure control—special role of the kidneys and body fluids. *Science* 252:1813–1816
- Hamberg AK, Dahl ML, Barban M, Scordo MG, Wadelius M, Pengo V, Padriani R, Jonsson EN (2007) A PK-PD model for predicting the impact of age, CYP2C9, and VKORC1 genotype on individualization of warfarin therapy. *Clin Pharmacol Ther* 81(4):529–538
- Hammer GB, Verghese ST, Drover DR, Yaster M, Tobin JR (2008) Pharmacokinetics and pharmacodynamics of fenoldopam mesylate for blood pressure control in pediatric patients. *BMC Anesthesiol* 8:6
- Holford NH (2005) The visual predictive check – superiority to standard diagnostic (Rorschach) plots PAGE. <http://www.page-meeting.org/page/page2005/PAGE2005P105.pdf>
- Hunninghake DB (1992) HMG-CoA reductase inhibitors. *Curr Opin Lipidol* 3:22–28
- Jackson SP, Nesbitt WS, Kulkarni S (2003) Signaling events underlying thrombus formation. *J Thromb Haemost* Jul 1(7):1602–1612

- Jacqmin P, Gieschke R, Jordan P, Steimer JL, Goggin T, Pillai G (2001) Modeling drug induced changes in biomarkers without using drug concentrations: introducing the K-PD model. 10th Population Approach Group Conference, Basel, Switzerland. <http://www.page-meeting.org>
- Johnson RJ, Herrera-Acosta J, Schreiner GF, Rodriguez-Iturbe B (2002) Subtle acquired renal injury as a mechanism of salt-sensitive hypertension. *N Engl J Med* 346:913–923
- Johnson K, Shah A, Jaw J, Baxter J, Prakash C (2003) Metabolism, pharmacokinetics, and excretion of a highly selective NMDA receptor antagonist, traxoprodil, in human cytochrome P450 2D6 extensive and poor metabolizers. *Drug Metab Dispos* 31:76–87
- Jonsson F, Marshall S, Krams M, Jonsson E (2005) A longitudinal model for non-monotonic clinical assessment scale data. *J Pharmacokinet Pharmacodyn* 32(5–6):795–815 (21)
- Karlsson MO, Sheiner LB (1993) The importance of modeling interoccasion variability in population pharmacokinetic analyses. *J Pharmacokinet Biopharm* 21:735–750
- Kearon C, Hirsh J (1997) Management of anticoagulation before and after elective surgery. *N Engl J Med* 336(21):1506–1511
- Lalonde RL, Kowalski KG, Hutmacher MM, Ewy W, Nichols DJ, Milligan PA, Corrigan BW, Lockwood PA, Marshall SA, Benincosa LJ, Tensfeldt TG, Parivar K, Amantea M, Glue P, Koide H, Miller R (2007) (2007) Model-based drug development. *Clin Pharmacol Ther* 82(1):21–32
- LaRosa JC, He J, Vupputuri S (1999) Effect of statins on risk of coronary disease: a meta-analysis of randomized controlled trials. *JAMA, J Am Med Assoc* 282(24):2340–2346
- Laurent S, Kingwell B, Bank A, Weber M, Struijker-Boudier H (2002) Clinical applications of arterial stiffness: therapeutics and pharmacology. *Am J Hypertens* 15(5):453–458
- Lennernäs H, Fager G (1997) Pharmacodynamics and pharmacokinetics of the HMG-CoA reductase inhibitors. Similarities and differences. *Clin Pharmacokinet* 32(5):403–425
- Lindenstrom E, Boysen G, Christiansen LW, Hansen BR, Nielsen PW (1991) Reliability of Scandinavian Stroke Scale. *Cerebrovasc Dis* 1:103–107
- Mason RP, Walter MF, Day C, Jacob RF (2006) Active metabolite of atorvastatin inhibits membrane cholesterol domain formation by an antioxidant mechanism. *J Biol Chem* 281:9337–9345
- McConnaughey MM, McConnaughey JS, Ingenito AJ (1999) Practical considerations of the pharmacology of angiotensin receptor blockers. *J Clin Pharmacol* 39:547–559
- Merlini PA, Bauer KA, Oltrona L, Ardissino D, Cattaneo M, Belli C, Mannucci PM, Rosenberg RD (1994) Persistent activation of coagulation mechanism in unstable angina and myocardial infarction. *Circulation* 90(1):61–68
- Monyer H, Sprengel R, Schoepfer R, Herb A, Higuchi M, Lomeli H, Burnashev N, Sakmann B, Seeburg PH (1992) Heteromeric NMDA receptors: molecular and functional distinction of subtypes. *Science* 256:1217–1221
- Mould D (2007) Developing models of disease progression. In: Ette EI, Williams PJ (eds) *Pharmacometrics: the science of quantitative pharmacology*. Wiley, Hoboken, NJ, pp 547–581
- Muir KW, Weir CJ, Murray GD, Povey C, Lees KR (1996) Comparison of neurological scales and scoring systems for acute stroke prognosis. *Stroke* 27:1817–1820
- Pillai G, Gieschke R, Goggin T, Jacqmin P, Schimmer RC, Steimer JL (2004) A semimechanistic and mechanistic population PK-PD model for biomarker response to ibandronate, a new bisphosphonate for the treatment of osteoporosis. *Br J Clin Pharmacol* 58(6):618–631
- Porchet HC, Piletta P, Dayer P (1992) Pharmacokinetic-pharmacodynamic modeling of the effects of clonidine on pain threshold, blood pressure, and salivary flow. *Eur J Clin Pharmacol* 42(6):655–661
- Rosenberg PA, Aizenman E (1989) Hundred-fold increase in neuronal vulnerability to glutamate toxicity in astrocyte-poor cultures of rat cerebral cortex. *Neurosci Lett* 103:162–168
- Salinger DH, Shen DD, Thummel K, Wittkowsky AK, Vicini P, Veenstra DL (2009) Pharmacogenomic trial design: use of a PK/PD model to explore warfarin dosing interventions through clinical trial simulation. *Pharmacogenet Genomics* 19(12):965–971
- Scandinavian Stroke Study Group (1985) Multicenter trial of hemodilution in ischemic stroke: background and study protocol. *Stroke* 16:885–890

- Schachter M (2004) Chemical, pharmacokinetic and pharmacodynamic properties of statins: an update. *Fundam Clin Pharmacol* 19(1):117–125
- Schwarz UI, Ritchie MD, Bradford Y, Li C, Dudek SM, Frye-Anderson A, Kim RB, Roden DM, Stein CM (2008) Genetic determinants of response to warfarin during initial anticoagulation. *N Engl J Med* 358(10):999–1008
- Sconce EA, Khan TI, Wynne HA, Avery P, Monkhouse L, King BP, Wood P, Kesteven P, Daly AK, Kamali F (2005) The impact of CYP2C9 and VKORC1 genetic polymorphism and patient characteristics upon warfarin dose requirements: proposal for a new dosing regimen. *Blood* 106:2329–2333
- Seiler SM, Bernatowicz MS (2003) Peptide-derived protease-activated receptor-1 (PAR-1) antagonists. *Curr Med Chem* 1:1–11
- Sharma A, Ebling WF, Jusko WJ (1998) Precursor-dependent indirect pharmacodynamic response model for tolerance and rebound phenomena. *J Pharm Sci* 87(12):1577–1584
- Stancu C, Sima A (2001) Statins: mechanism of action and effects. *J Cell Mol Med* 5(4):378–387
- Steinhuibl SR, Moliterno DJ (2005) The role of the platelet in the pathogenesis of atherothrombosis. *Am J Cardiovasc Drugs* 5(6):399–408
- Stergiou GS (2004) Angiotensin receptor blockade in the challenging era of systolic hypertension. *J Human Hypertens* 18:837–847
- Theilmeyer G, Michiels C, Spaepen E, Vreys I, Collen D, Vermylen J, Hoylaerts MF (2002) Endothelial von Willebrand factor recruits platelets to atherosclerosis-prone sites in response to hypercholesterolemia. *Blood* 99(12):4486–4493
- Unadkat JD, Sheiner LB, Hennis PJ, Cronnelly R, Miller RD, Sharma M (1986) An integrated model for the interaction of muscle relaxants with their antagonists. *J Appl Physiol* 61(4):1593–1598
- Verotta D, Beal SL, Sheiner LB (1989) Semi parametric approach to pharmacokinetic-pharmacodynamic data. *Am J Physiol* 256(4 Pt 2):R1005–R1010
- Whelan HT, Cook JD, Amlie-Lefond CM, Hovinga CA, Chan AK, Ichord RN, Deveber GA, Thall PF (2008) Practical model-based dose finding in early-phase clinical trials: optimizing tissue plasminogen activator dose for treatment of ischemic stroke in children. *Stroke* 39(9):2627–2636
- Williams D, Feely J (2002) Pharmacokinetic-pharmacodynamic drug interactions with HMG-CoA reductase inhibitors. *Clin Pharmacokinet* 41(5):343–370

Chapter 11

Viral Dynamic Modeling and Simulations in HIV and Hepatitis C

Philippe Jacqmin and Eric Snoeck

Abstract Viral dynamic modeling and simulations have dramatically improved our understanding of the life cycle of chronic viral infections such as HIV and hepatitis C virus (HCV). These viral dynamic models account for the interaction between virus and host, and how antiviral agents interfere with this system thereby reducing the measured viral load and clearing the virus. In this chapter, the basic viral dynamic modeling concepts such as the predator–prey interaction introduced by Lotka–Volterra, the basic reproductive ratio (R_0), the reproductive minimal inhibitory concentration (RMIC) and the physiologically based viral eradication boundary are explained and illustrated by viral dynamic models developed for HIV and HCV. Examples are presented showing how simulations based on these models can be used to better understand the virus–host system and the mechanism of action of antiviral drugs, and to optimize treatment.

11.1 Introduction

During the past 15 years, mathematical principles have been used to understand the life cycle of the three prevalent chronic viral infections; *i.e.*, HIV, hepatitis C virus (HCV) and hepatitis B virus (HBV). The use of mathematical models has provided nonintuitive insights into the dynamics of viral diseases and how antiviral agents act to reduce viral levels and clear virus. Evaluation of a patient with a chronic viral illness includes the determination of serum viral load, as reflected in measurement of serum RNA copies. The viral load in HIV or HCV is frequently observed to reach a constant or set point level and then remains approximately at that level for years (Layden *et al.* 2003). To maintain this constant level, the virus must be produced and cleared at the same rate. If this was not the case and more virus was produced than was cleared, then the viral load would slowly increase. Once this steady-state level is

P. Jacqmin (✉)
Exprimo NV, Mechelen, Belgium
e-mail: philippe.jacqmin@exprimo.com

established, measuring viral load thus does not provide any information regarding the production and elimination rate of the virus and the turnover rate of the infected cells. To gain this information, one thus has to perturb the system, *e.g.*, with antiviral therapy. For example, if virion production is blocked, viral load falls and the rate at which it falls provides important information about the aforementioned rates. Fitting mathematical models to viral decay data can therefore elucidate the kinetic parameters governing viral infection, infected cell death and the efficacy of antiviral therapy.

Mathematical modeling of viral dynamics was first applied in HIV. Modeling of HIV infection has allowed estimation of (1) the number of virus particles that are produced and eliminated daily, (2) the lifespan of productively infected CD4+ T cells and (3) the expected time to elimination of various virus-producing cell populations, assuming a 100% effective antiviral therapy (Ho *et al.* 1995; Perelson *et al.* 1996, 1997). As the multidimensional interactions between HCV virus, host and drug are nonlinear and equilibrium outcomes quickly become counter-intuitive (Bernardin *et al.* 2008), HCV RNA viral load data have also been modeled. The methods that were used to analyze HIV dynamics *in vivo* can also be modified to give insights into HCV dynamics and the effects of antiviral therapy in chronic hepatitis C (CHC) patients. In this chapter, we will be primarily focusing on the viral dynamic modeling of chronic HIV and HCV. However, the general viral dynamic modeling principles that are described may also be applied to other viral infections such as HBV (Nowak *et al.* 2000).

11.2 Basic Viral Dynamic Model

The basic viral dynamic model consists of three quantitative elements, *i.e.* the population sizes of uninfected cells or target cells (T), infected cells (I), and free virions (V). A system of three differential equations can describe how these three elements are changing as a function of time. These quantities can denote either the total abundance in a host or the abundance in a given volume of blood, plasma, or tissue. The three differential equations of the basic viral dynamic model are based on the Lotka–Volterra predator–prey models that were first developed in the field of epidemiology to describe the dynamics of biological systems in which two species interact, *i.e.* one as a predator and one as its prey (Nowak and May 2000). This traditional epidemiology approach describes the spread of an infection within populations of individuals. However, similar mathematical models can be used to describe what happens within the body of a virus-infected individual.

The basic Lotka–Volterra equations are a pair of first-order, nonlinear differential equations. It is interesting to note that Vito Volterra was an Italian mathematician whose son-in-law, Huberto D’Ancona, was a biologist who completed a statistical study of fish populations in the Adriatic Sea in 1926. D’Ancona asked Volterra whether he could devise a mathematical description for the increase in predator fish and decrease in prey fish that he observed during the World War I period. Within a couple of months, Volterra produced a series of models for the interaction of

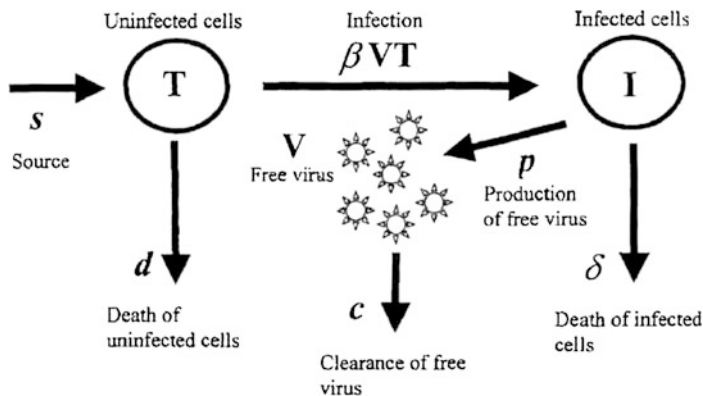


Fig. 11.1 Basic model used to study the viral dynamics of HIV, HCV and hepatitis B virus (HBV). Reprinted from Layden *et al.* (2003)

two or more species. Alfred J. Lotka was an American biologist and actuary who independently developed similar models (Fig. 11.1).

The basic viral dynamic model is depicted in Fig. 11.1 and can be described mathematically by (11.1–11.3) (Nowak *et al.* 1996; Nowak and May 2000). Uninfected cells (T) are assumed to be produced at a rate constant s , and die at a rate, dT . The average life span of a healthy target cell is therefore $1/d$. In the absence of an infection, the change of the abundance of target cells is in a steady state and equals zero so that the number of target cells (*i.e.* abundance) is equal to s/d .

$$\frac{dT}{dt} = s - d \cdot T - \beta \cdot V \cdot T \tag{11.1}$$

$$\frac{dI}{dt} = \beta \cdot V \cdot T - \delta \cdot I \tag{11.2}$$

$$\frac{dV}{dt} = p \cdot I - c \cdot V \tag{11.3}$$

Free virions (V) are assumed to infect uninfected cells at a rate proportional to the product of the abundance of the free virus particles and the uninfected cells (βVT). The second order rate constant β describes the efficiency of this infection process that includes the rate at which the virions “find” uninfected cells, the rate of virus entry into cells and the rate and probability of a successful infection. Infected cells are thus produced at a rate βVT and die at a rate δI . Infected cells produce new free virions at a rate proportional to their abundance (pI), and free virions are removed from the body at a rate cV . The average life span of an infected cell is thus $1/\delta$, whereas the average life span of a free virion is $1/c$.

Initially, the system is at an uninfected state and uninfected cells are at an equilibrium value of s/d . After a number of virions have managed to enter the

system, they will infect a number of cells, which will produce new virions, which will infect new cells. A chain reaction has thus started. This chain reaction can go two ways: either it dies out or it leads to a massive explosion of free virions and infected cells. Whether or not the chain reaction will take off and establish an infection depends on a condition very similar to the epidemiological spread of an infectious disease in a population of individuals. The crucial quantity here is the basic reproductive ratio R_0 of an infection. R_0 is defined as the average number of newly infected cells that arise from one infected cell when almost all infected cells are uninfected (*i.e.* in the beginning of the infection). The theoretical concept of the R_0 was first described in epidemiology (Anderson and May 1997a, b; Heffernan *et al.* 2005). The rate at which one infected cell gives rise to new infected cells is given by $\beta pT/c$ (Fig. 11.1). If all cells are uninfected, then $T = s/d$. Because the life span of an infected cell is $1/\delta$, the basic reproductive ratio is equal to (Nowak *et al.* 1996):

$$R_0 = \frac{\beta \cdot s \cdot p}{\delta \cdot d \cdot c} \quad (11.4)$$

If every infected cell produces on average less than one newly infected cell ($R_0 < 1$), the virus population will die out. If on the other hand $R_0 > 1$, the infection will enlarge. Finally, if $R_0 = 1$ the virus population will not spread but will also not die out. An antiviral drug therapy will thus be successful in case every infected cell produces on average less than one newly infected cell because of drug therapy, or in other words, the reproductive ratio during drug therapy (R_{0INH}) is less than 1 (Callaway and Perelson 2002; Huang *et al.* 2003; Jacqmin *et al.* 2010).

11.3 Viral Dynamic Modeling and Simulations in HIV

The basic model defined above has been further developed over the past 15 years to describe the HIV infection (Nowak and May 2000; Perelson 2002).

Generally, HIV viral dynamic models include five different types of cells (Fig. 11.2) (Nowak *et al.* 1997; Bonhoeffer *et al.* 1997; Bonhoeffer 1998; Funk *et al.* 2001): (1) HIV-targeted CD4 cells (T), (2) actively or productively infected cells (A), (3) latently infected cells (L) which eventually can be reactivated to actively infected cells, (4) persistently infected cells (P) with a very long half-life ($\geq 1,000$ -days), and (5) defectively infected cells (D), as well as the free infectious virus particles (V_1). However, in most modeling work, in which the viral load (and the CD4+ count) time profiles are analyzed, the persistently and defectively infected cells have been removed from the model because they do not significantly contribute to the viral load at equilibrium or at initiation of antiviral treatment. However, these entities may be a basis for postulating why cure may not be achieved in HIV infected patients.

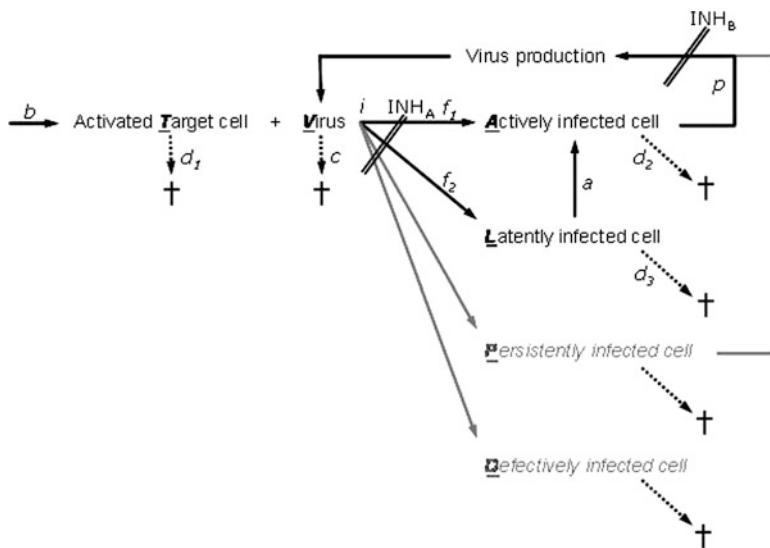


Fig. 11.2 The viral dynamic model for HIV adapted from Funk *et al.* (2001). INH indicates the site of drug action. Parameter definitions can be found in the text

As above, the interaction between the target cells and the virus can be described by differential equations (11.5–11.9). In these equations, anti-HIV drug effects are usually expressed by inhibitory E_{\max} models (11.10), decreasing the infection rate constant (i) for drugs that act before DNA replication (*e.g.*, cell entry inhibitors, reverse transcriptase inhibitors), or decreasing the production rate constant (p) of infectious viruses (V_I) for drug acting after replication (*e.g.*, protease inhibitors). In the case of a protease inhibitor, an additional cell type is needed to describe the formation of noninfectious viruses (V_{NI}), and the measured total viral load, expressed as RNA copies mL^{-1} , being representative of the sum of infectious and noninfectious viruses.

Target cell (activated cells):

$$\frac{dT}{dt} = b - d_1 \cdot T - (1 - INH_A) \cdot i \cdot V_I \cdot T \tag{11.5}$$

Actively infected cells (short-lived):

$$\frac{dA}{dt} = f_1 \cdot (1 - INH_A) \cdot i \cdot V_I \cdot T - d_2 \cdot A + a \cdot L \tag{11.6}$$

Latently infected resting cells (long-lived):

$$\frac{dL}{dt} = f_2 \cdot (1 - INH_A) \cdot i \cdot V_I \cdot T - d_3 \cdot L - a \cdot L \tag{11.7}$$

Infectious virus (copies HIV-1 RNA):

$$\frac{dV_I}{dt} = (1 - INH_B) \cdot p \cdot A - c \cdot V_I \quad (11.8)$$

Noninfectious virus (copies HIV-1 RNA):

$$\frac{dV_{NI}}{dt} = INH_B \cdot p \cdot A - c \cdot V_{NI} \quad (11.9)$$

where:

b is the activation rate constant of healthy target cells (T).

d_1 is the death rate constant of T cells.

i is the infection rate constant of T cells.

V_I is the number of infectious free viruses.

V_{NI} is the number of noninfectious free viruses.

f_1 is the fraction of healthy T cells that become actively infected T cells (A).

d_2 is the death rate constant of actively infected T cells.

$f_2 (=1-f_1)$ is the fraction of healthy T cells becoming latently infected T cells (L).

d_3 is the death rate constant of latently infected resting cells.

a is the reactivation rate constant of latently infected resting cells.

p is the viral production rate constant of actively infected T cells.

c is the death rate constant of virus.

INH is the inhibition of the infection rate constant (i) for drugs acting before DNA replication (INH_A) or of the viral production rate constant (p) for drugs acting after DNA replication (INH_B).

$$INH = \frac{IC}{(IC_{50} + IC)} \quad (11.10)$$

where INH is the inhibition ranging from 0 to 1, IC is the plasma concentration of the inhibitor and IC_{50} is the plasma concentration of inhibitor that results in 50% inhibition.

This more complex system is also characterized by a R_0 (11.11) (Rosario *et al.* 2006). Here the R_0 can be defined as the average number of secondary viruses generated by viruses introduced into an uninfected environment.

$$R_0 = \frac{b}{d_1} \cdot i \cdot \frac{p}{c} \cdot \left(\frac{f_1}{d_2} + \frac{f_2 \cdot a}{d_2 \cdot (d_3 + a)} \right) \quad (11.11)$$

where b/d_1 is the number of activated target cells in the absence of virus, i is the infection rate, p/c is the amount of circulating virus per infected cell at steady state, and $f_1/d_2 + (f_2 \cdot a/d_2 \cdot (d_3 + a))$ is the factor for living, actively infected cells.

As mentioned for the basic model and illustrated in Fig. 11.3 for the HIV model, if R_0 is less than one the virus is unable to maintain the infection and will become

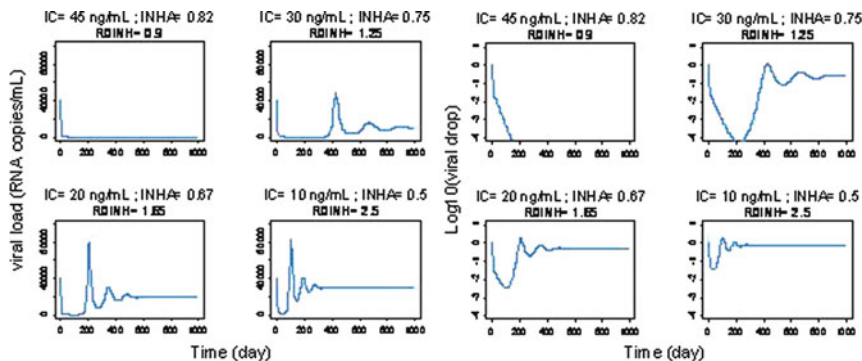


Fig. 11.3 Simulated viral load-time profiles for different levels of constant inhibition based on (11.5–11.10) and parameters values from Jacqmin *et al.* (2010) (e.g., $R_0 = 5$, $IC_{50} = 10 \text{ ng mL}^{-1}$ and $RMIC = 40 \text{ ng mL}^{-1}$). IC is the constant concentration of inhibitor to which the system is exposed continuously. INH_A is calculated with (11.10) and R_{0INH} is calculated using (11.12). The four graphs on the left hand side are linear plots of the viral load. The four graphs on the right hand side are logarithmic plots of the same viral load. Note that viral load rebounds during treatment when R_{0INH} is higher than 1 or IC is lower than RMIC. The rebound occurs sooner when the IC/RMIC ratio is lower. Adapted from Jacqmin *et al.* (2010)

extinct; if $R_0 > 1$ the virus can establish an infection that will lead to an equilibrium between infected and uninfected cells.

The role of anti-HIV inhibitors is to bring the reproductive ratio during treatment to a value less than 1 (and optimally as low as possible). In the model described above it can be shown that the reproductive ratio in the presence of inhibitor (R_{0INH}) is given by (11.12):

$$R_{0INH} = \frac{b}{d_1} \cdot (1 - INH) \cdot i \cdot \frac{p}{c} \cdot \left(\frac{f_1}{d_2} + \frac{f_2 \cdot a}{d_2 \cdot (d_3 + a)} \right) = (1 - INH) \cdot R_0 \quad (11.12)$$

The concentration of inhibitor that brings R_{0INH} to 1 is called the reproductive minimal inhibitory concentration (RMIC) (Jacqmin *et al.* 2010). It has been demonstrated that in the system developed above, the critical concentration at which the system switches from growth to extinction depends on two model parameters:

$$RMIC = (R_0 - 1) \cdot IC_{50} \quad (11.13)$$

where the basic reproductive ratio (R_0) represents the capacity of the system to replicate and the IC_{50} represents the potency of the drug to inhibit the replication of the system (Jacqmin *et al.* 2010). The RMIC is constant for a given system and a given drug and represents the concentration that needs to be achieved for stopping the system to grow. As illustrated in Fig. 11.3, when the inhibitor concentration (IC) is higher than the RMIC (40 ng mL^{-1}), success (*i.e.*, sustained viral load below the detection limit) can be expected in the long term.

11.3.1 Basic PK-PD Principles of R_0 and RMIC

Understanding the attributes of R_0 and RMIC is essential in predicting the binary outcomes of therapeutic success or failure. These attributes have been recently reviewed in detail (Jacqmin *et al.* 2010). Briefly:

11.3.1.1 For R_0 and RMIC

1. When the inhibitory concentration equals the RMIC, the system is in dynamic equilibrium; the infecting species neither increase nor decrease in number.
2. Depending on the value of R_0 , system survival (*i.e.*, $R_{0INH} = 1$) can occur at different levels of inhibition:

For $R_0 = 2$, $RMIC = IC_{50}$

For $R_0 = 10$, $RMIC = 9 \cdot IC_{50} = IC_{90}$

3. In case *in vitro* and *in vivo* R_0 are different, which can be expected, *in vitro* and *in vivo* RMIC will also be different.
4. From (11.13), it can be seen that the RMIC is a joint distribution of R_0 and IC_{50} in the population.

11.3.1.2 For Binary Outcomes Analysis

In HIV, the treatment is regarded as a success if viral load is decreased and maintained below the limit of quantification. Consequently,

1. Inhibition of the system leads to the binary outcomes listed below, and logistic analysis used to analyze the outcomes can be interpreted from a modeling perspective as follows:
 - IC greater than RMIC leads to success (*i.e.*, viral load is decreased and maintained below the limit of quantification) (Fig. 11.3).
 - IC less than RMIC leads to failure (*i.e.*, viral load is not decreased or maintained below the limit of quantification) (Fig. 11.3).
2. The time of failure is a function of the IC/RMIC ratio; for failure (when the ratio is below 1), the smaller the ratio, the sooner the failure will occur (Fig. 11.3).
3. Mechanistically, logistic regression of binary outcomes such as failure/success rates in function of inhibitor exposure (IC) allows estimation of the RMIC distribution across the population.

11.3.2 Dose and Dosing Schedule

One of the goals of modeling and simulations is to help defining the dose and dosing schedule of the drug. As shown above, viral dynamic models are complex.

The interaction with PK adds more complexity to the system. The choice of a successful dose and dosing schedule is therefore not easy. Indeed, the time course of inhibition of virus proliferation depends on the time course of drug concentrations, and with the complex viral dynamic system, it becomes challenging to predict the clinical outcome for a given drug treatment. In this context, it is always a discussion point to know whether the clinical outcome depends on C_{\max} , AUC_{τ} or C_{trough} . The combination of viral dynamic systems with PK/PD has been discussed by several authors in the context of effective dose, treatment adherence/compliance and resistance/mutation (Wahl and Nowak 2000; Huang *et al.* 2006; Ferguson *et al.* 2005; Wu *et al.* 2006). It has been mathematically demonstrated that it is the average R_{OINH} that drives the success of the therapy, if resistance/mutation does not happen (Wahl and Nowak 2000; Jacqmin *et al.* 2010).

Knowing the R_0 of the system, the IC_{50} and the PK of the inhibitory drug and using (equation 11.12), it is possible to predict the R_{OINH} -time profile after drug administration and to calculate the corresponding AUC and average R_{OINH} for a dose interval (Fig. 11.4). It can be demonstrated that if the *average* R_{OINH} is higher than one the system will survive, whereas if it is lower than one the system will go to extinction (Fig. 11.5) (Heffernan *et al.* 2005; Jacqmin *et al.* 2010).

In addition to the concept of R_{OINH} , it has also been demonstrated that time varying inhibition of viral dynamic systems can be predicted by calculating the equivalent effective constant concentration (ECC) (Rosario *et al.* 2006) – the constant plasma concentration that would give rise to the average inhibition at steady state:

$$\text{Time varying inhibition } INH_{ss} = \frac{C_{ss}(TAD)}{IC_{50} + C_{ss}(TAD)} \quad (11.14)$$

$$INH_{avg^{ss}} = \frac{AUC_{0-x} \text{ under } INH \text{ curve}}{\tau} \quad (11.15)$$

$$INH_{avg^{ss}} = \frac{ECC}{IC_{50} + ECC} \quad (11.16)$$

$$ECC_{ss} = \frac{IC_{50} \cdot INH_{avg^{ss}}}{1 - INH_{avg^{ss}}} \quad (11.17)$$

where C_{ss} (TAD) is the concentration at time after dose (TAD) administration at steady state. The ECC_{ss} is the calculated concentration that gives rise to $INH_{avg^{ss}}$ across the dosing interval.

When ECC_{ss} is higher than the RMIC, eradication of the system can be expected (Fig. 11.5). In addition, it is shown that scenarios with the same ECC_{ss} regardless of the dose, dosing schedule or PK parameters also have the same average R_{OINH} and therefore lead to the same outcome. For example, as illustrated in Fig. 11.5, when the ECC_{ss} is just lower than the RMIC for both QD and BID dosage regimens, the viral load rebounds after an initial drop, whereas when it is just higher than the

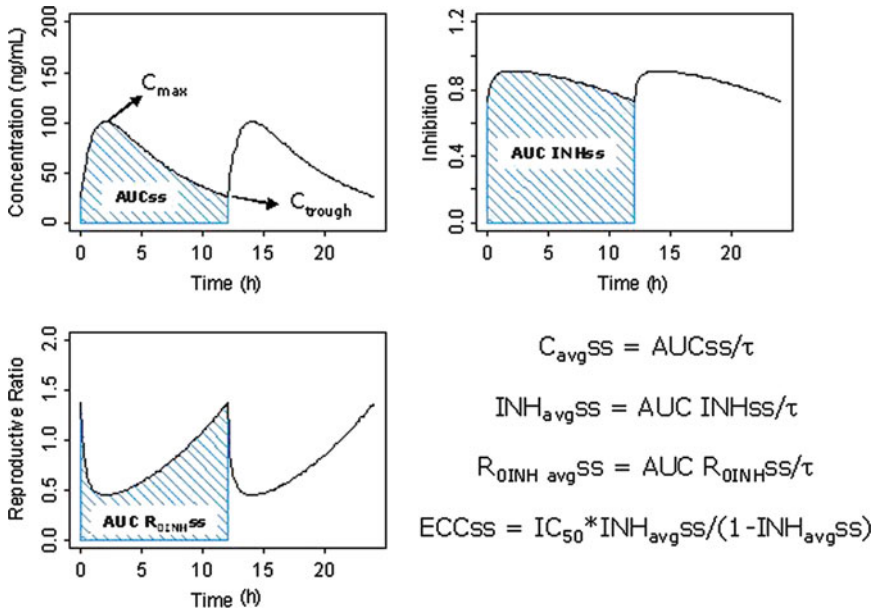


Fig. 11.4 Simulated time profiles of inhibitor concentration (*top left*), inhibition (INH, *top right*) and R_{OINH} (*bottom left*) at steady state. Simulations are based on a one-compartment PK model. The drug is given twice daily at 8-mg. Absorption rate constant (K_a) = $1\ h^{-1}$, Elimination rate constant (K_e) = $0.15\ h^{-1}$, $V = 70\ L$, $R_0 = 5$ and $IC_{50} = 10\ ng\ mL^{-1}$. Inhibition is calculated with (11.14) and R_{OINH} is calculated using (11.12). AUCs are calculated by the trapezoidal rule assuming rich sampling. Formulas for derived parameters such as average R_{OINH} and effective constant concentration (ECC) at steady state are given at the *bottom right hand side* of the figure

RMIC, the viral load continuously decreases. Interestingly, the total daily doses (and consequently AUC_{τ} , C_{max} and C_{trough}) that are necessary to reach the same ECC_{ss} can be significantly different between QD and BID dosage regimens (Fig. 11.5) and are driven by the half life of the drug in question (Jacqmin *et al.* 2010). Accordingly, how the patient adheres to the dosing schedule – missing a single dose at several days or missing the same number of doses consecutively – will have a direct but different impact on treatment outcome, depending on the frequency of daily dosing (Wahl and Nowak 2000; Paterson *et al.* 2000; Ferguson *et al.* 2005; Wu *et al.* 2006). The ECC_{ss} concept allows predicting equivalent active doses and dosing schedules in viral dynamic systems when the IC_{50} and pharmacokinetic characteristics of the drugs are known. Therefore, for a given system (defined by its RMIC), it can be shown that in HIV treatments, success depends mainly on the pharmacokinetic characteristics of the drug, the dosing schedule and the adherence pattern to the treatment. This approach does not take into account the resistance/mutation aspects. These aspects have been widely discussed by several authors using “simplified” two-strain models (Wahl and Nowak 2000; Phillips *et al.* 2001; Ferguson *et al.* 2005; Wu *et al.* 2006; Huang *et al.* 2006; Rong *et al.* 2007).

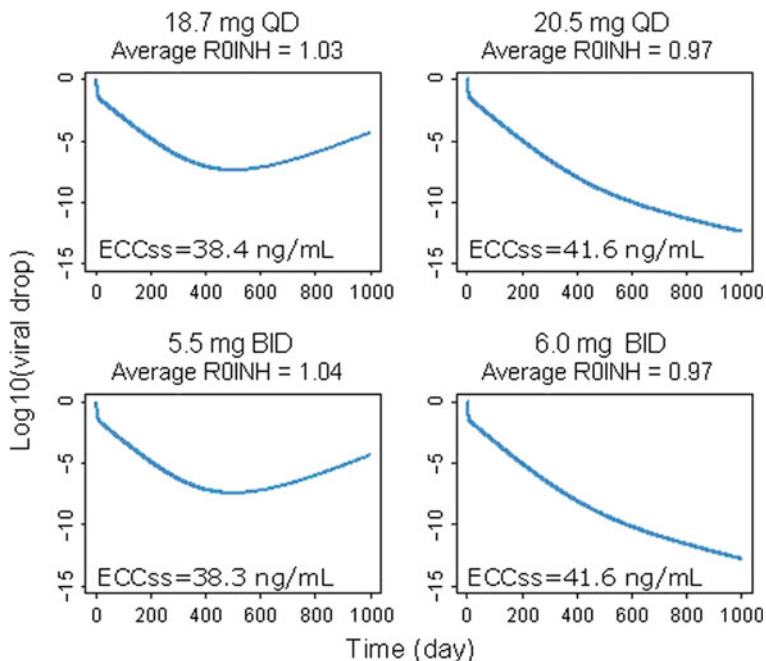


Fig. 11.5 Simulated viral load-time profiles based on (11.5–11.14) and parameters values from Jacqmin *et al.* (2010) (*e.g.*, $R_0 = 5$, $IC_{50} = 10 \text{ ng mL}^{-1}$ and $RMIC = 40 \text{ ng mL}^{-1}$) and Fig. 11.4. Equivalent once (*top plots*) and twice (*bottom plots*) daily doses leading to average R_{0INH} just above 1 or ECC_{ss} just below the $RMIC$ (*left plots*) and to average R_{0INH} just below 1 or ECC_{ss} just above the $RMIC$ (*right plots*) have been selected. Average R_{0INH} and ECC_{ss} are calculated as indicated in Fig. 11.4. Note that viral load rebound occurs during treatment when average R_{0INH} is higher than 1 and ECC_{ss} is lower than $RMIC$. Adapted from Jacqmin *et al.* (2010)

11.3.3 Estimation of Model Parameters

In clinical drug development, the potency of an antiretroviral agent is usually evaluated in short-term monotherapy studies by assessing the early viral response such as viral decay rate or change in viral load (number of copies of HIV RNA) in the plasma.

As shown in Fig. 11.6, just after initiation of a mono-therapy (*e.g.*, 10 days), the drop in viral load is expected to be driven by the exposure to the drug (IC or ECC). However, it is difficult from short-term viral load-time profiles to empirically derive the minimal dose that will lead to long-term success (*i.e.*, at equilibrium). Modeling of the data can provide an answer to this question. Linear, parametric nonlinear and semi parametric nonlinear mixed-effects models have been used to estimate viral decay rates in viral dynamic models. Wu *et al.* (2004) have applied these models to data from an AIDS clinical trial of potent antiviral treatments and found significant incongruity in the estimated rates of reduction in viral load. Simulation studies

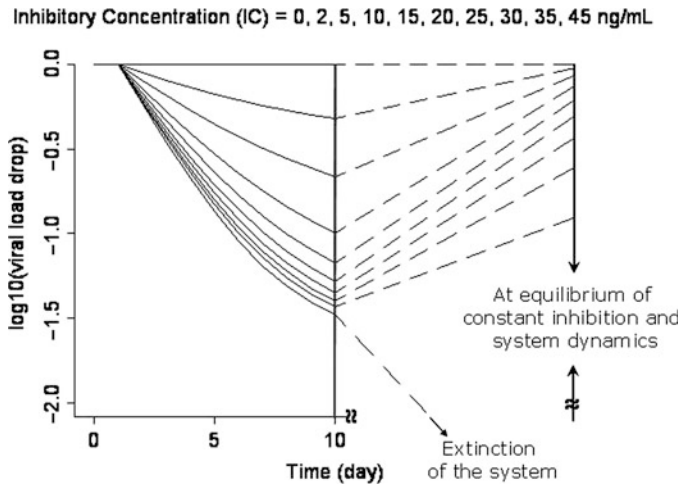


Fig. 11.6 Simulated viral load-time profiles in a typical subject for the first 10 days and at equilibrium of constant exposure to various inhibitory concentrations (IC or ECC). Simulations are performed using (11.5–11.14) and parameters values from Jacqmin *et al.* (2010) (e.g., $R_0 = 5$, $IC_{50} = 10 \text{ ng mL}^{-1}$, $RMIC = 40 \text{ ng mL}^{-1}$). Note that, despite a significant drop in viral load during the first 10 days at all simulated IC or ECC concentrations, only the viral load profile with IC or ECC higher than RMIC leads to a success in the long term (i.e., at equilibrium of system dynamics). Reprinted from Jacqmin *et al.* (2010)

indicated that reliable estimates of viral decay rate were obtained by using the parametric and semiparametric nonlinear mixed-effects models. Their analysis also indicated that the decay rates estimated by using linear mixed-effects models should be interpreted differently from those estimated by using nonlinear mixed-effects models. The semiparametric nonlinear mixed-effects model was preferred to other models because arbitrary data truncation was not needed.

From the RMIC concept presented above, it can be deduced that, for dosing recommendation, the main parameters to be estimated are the R_0 and the IC_{50} . Indeed knowing these two parameters, the RMIC can be calculated and the minimum target ECC_{ss} can be derived. Accurate estimation of both R_0 and IC_{50} parameters can be achieved only if the study design contains information on the onset and offset of drug effect. The onset (i.e., drop in viral load) observed at different doses provides information on the IC_{50} of the drug and the offset (i.e., increase in viral load after treatment discontinuation) mainly provides information on the capacity of the virus to (re-)grow in the given system (i.e., R_0). This has been illustrated by Chan *et al.* (2009, 2010), who have analyzed 10-day monotherapy studies of maraviroc, a CCR5 inhibitor (Wood and Armour 2005). The data consisted of individual maraviroc concentration- and viral load-time profiles during (10 days) and after (30 days) maraviroc QD or BID treatments at different doses in asymptomatic CCR5-tropic HIV-1 infected subjects (Fätkenheuer *et al.* 2005). The analysis was performed using similar equations than those described above but

reparameterized to estimate R_0 and IC_{50} as primary parameters. The NONMEM software system, version VI level 1.2 (Beal and Sheiner 1998) and the SAEM algorithm implemented in MONOLIX (<http://www.monolix.org>; Kuhn and Lavielle 2005) were used. Population PK-PD analysis with MONOLIX allowed the estimation of R_0 and IC_{50} , which were equal to 4.96- and 8.57-ng mL⁻¹, respectively, leading to a RMIC of 33.9-ng mL⁻¹. From this information and based on the theory described above, it is predicted that an ECC_{ss} higher than 34-ng mL⁻¹ would lead to a long-term success in a typical (median) subject. With regard to the technical aspects, the authors indicated that SAEM algorithm in MONOLIX was a useful tool for fitting complex mechanistic models requiring multiple differential equations. The implemented SAEM algorithm allowed simultaneous estimation of PK/PD and viral dynamics parameters, as well as investigation of different model subcomponents during the model building process which was not possible with NONMEM (version VI or below).

11.4 Viral Dynamic Modeling and Simulations in Hepatitis C

An estimated 170 million people or 2.1% of the world population are currently infected with HCV, which is more than four times the number of people living with HIV (<http://www.who.int/mediacentre/factsheets/fs164/en/>). The current standard of care for CHC patients is the combination of pegylated interferon- α with ribavirin (NIH 2002; Strader *et al.* 2004). Successful HCV treatment outcome (*i.e.*, sustained virologic response (SVR)) is when a patient's viral load is below the HCV RNA detection limit at a follow-up evaluation that is 24 weeks after treatment completion. Patients infected with the HCV genotype 1 (G1), which represent about 70% of CHC patients in the United States (Zein *et al.* 1996), are less likely to achieve an SVR than genotype non-1 (Gn1) infected patients. Approximately 50% of HCV G1 infected patients achieved an SVR when treated with peginterferon α -2a plus ribavirin, whereas approximately 80% of HCV Gn1-infected patients achieved an SVR (Fried *et al.* 2002; Hadziyannis *et al.* 2004). Thus, HCV patients represent a population with continued unmet medical need, having the potential to achieve a higher SVR rate through optimized treatment approaches.

Typical therapy outcome begins with a rapid viral decline followed by a second slower decline until HCV RNA becomes undetectable (Zeuzem 2001; Colombatto *et al.* 2003). However, after long-term treatment with the current standard of care, the virus is not eradicated in all CHC patients (Fried *et al.* 2002; Hadziyannis *et al.* 2004). In the patients who do not achieve an SVR (*i.e.*, the virus is not eradicated), viral load either rebounds to pretreatment levels during therapy (*i.e.*, breakthrough), or returns to pretreatment levels on cessation of therapy (*i.e.*, relapse) (Zeuzem 2001; Zeuzem and Herrmann 2002). The possible different viral load profiles after long-term therapy are depicted in Fig. 11.7.

A model of HCV infection was originally proposed by Neumann *et al.* (1998) who adapted a model of HIV infection (Wei *et al.* 1995; Perelson *et al.* 1996).

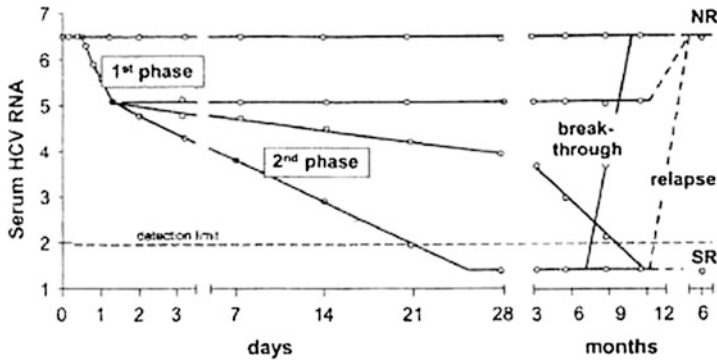


Fig. 11.7 Possible viral load profiles after long-term antiviral therapy. HCV RNA may or may not decline during the first 1–2 days (first phase responder/nonresponder) which can be followed by a slower second phase decline (second phase responder/nonresponder). The HCV RNA decay during the second phase is highly variable. Some patients with an initial virological response may experience a breakthrough during therapy and some virological end-of-treatment responders may have a relapse after discontinuation of therapy. *NR* nonresponse; *SR* sustained virological response. Reprinted from Zeuzem (2001) and Zeuzem and Herrmann (2002)

This model adequately describes the typical short-term therapy outcome. However, this model is unable to explain all of the observed HCV RNA profiles during and after long-term treatment; observed phenomena such as a null response, a partial response exhibiting a flat second phase, a triphasic viral decay, a breakthrough during therapy, a relapse after therapy, and crucially, an SVR cannot be described by this model (Zeuzem 2001). In addition, the original HCV model including three ordinary differential equations (ODEs) representing the population of target cells, infected hepatocytes and virus was simplified by assuming a constant population of hepatocytes, which is known to be only valid for a short duration (Neumann *et al.* 1998). Despite these shortcomings, this original model has been frequently used to describe the initial decreases of HCV RNA after treatment (Layden and Layden 2002; Layden-Almer *et al.* 2006), and to compare different treatment regimens and outcomes in different patient populations (Perelson *et al.* 2005). Most of these analyses have used a naïve method of handling the HCV RNA measurements below the lower limit of quantification (LLOQ) by simply omitting all these measurements even though these values contain critical information regarding long-term treatment outcome (*i.e.*, SVR).

A first important contribution to improving the initial HCV viral dynamic model was made by Colombatto *et al.* (2003). Known information of the physiology of the liver was used, allowing to introduce some constant variables into their model. The total number of hepatocytes present in a healthy individual liver was assumed to be 2.50×10^{11} hepatocytes (Sherlock and Dooley 1998). Because HCV RNA is known to be distributed in plasma and extracellular fluids (Liou *et al.* 1992), the computed values of both target cells (T) and infected cells (I) were referred to this volume of approximately 13.5×10^3 mL. Assuming a hepatocyte turnover in a healthy liver of 300 days (Mc Sween *et al.* 1987), the death rate of target cells

(*d*) was set to $1/300 \text{ day}^{-1}$, wherefrom the production of new hepatocytes in the absence of liver disease (*s*) could be assumed to be $61.7 \times 10^3 \text{ cells mL}^{-1} \text{ days}^{-1}$ (Colombatto *et al.* 2003).

A second major contribution was made by Dixit *et al.* (2004). In addition to the effect of pegylated interferon, Dixit *et al.* also incorporated an effect of ribavirin into the HCV viral dynamic model so that observed patterns of HCV RNA decline after short-term standard of care treatment could be described. Interferon inhibits the production of new virions and therefore it has been assumed that interferon is lowering the virion production *p* by a factor $(1-\epsilon)$, where ϵ is the effectiveness of pegylated interferon (Neumann *et al.* 1998; Layden-Almer *et al.* 2003). However, the mechanism(s) of ribavirin action against HCV are poorly understood (Lau *et al.* 1996). Ribavirin alone causes either a limited and transient decrease in viral load or no effect at all (Zoulim *et al.* 1998; Pawlotsky *et al.* 2004), but in combination with pegylated interferon, it significantly improves SVR rates (Fried *et al.* 2002; Hadziyannis *et al.* 2004; Manns *et al.* 2001). Ribavirin is phosphorylated within cells and incorporated into the RNA of replicating virions, thereby increasing the mutation frequency and reducing the specific infectivity of new virions (Crotty *et al.* 2001). It was therefore assumed by Dixit *et al.* (2004) that ribavirin renders a fraction ρ of newly produced virions noninfectious. Simulated viral load decay profiles based on their model nicely reconciled the seemingly conflicting observations that the addition of ribavirin enhances viral load decline in some cases but not in others (Fig. 11.8).

A third important contribution was made by Dahari *et al.* (2007), who incorporated a density-dependent liver proliferation term into the model describing the liver regeneration. The liver is a unique organ as it self-heals by regeneration as

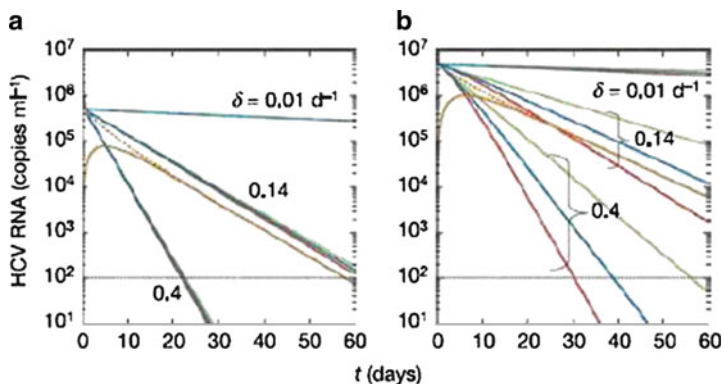


Fig. 11.8 Theoretical viral load decay profiles for an interferon effectiveness $\epsilon = 0.95$ (a) and $\epsilon = 0.50$ (b), and ribavirin effectiveness $\rho = 1$ (red lines), 0.5 (blue lines) and 0 (green lines), a virion clearance rate $c = 6.2\text{-day}^{-1}$, an initial viral load of $10^7 \text{ copies mL}^{-1}$ and different values of the infected cell death rate δ . The number of target cells was assumed to remain constant at the pretreatment value $\delta \cdot c / p \cdot \beta$ (Neumann *et al.* 1998). Interestingly, when the interferon effectiveness ϵ is high, ribavirin has negligible influence on viral load decay (a). However, when ϵ is low, ribavirin has a noticeable effect on viral load decay (b). Reprinted from Dixit *et al.* (2004)

opposed to repair. However, the exact cellular and molecular mechanisms of liver regeneration are not yet fully understood (Michalopoulos and DeFrances 1997; Khan and Mudan 2007). In addition, Dahari *et al.* (2007) also defined and characterized a critical drug efficacy value, above which the virus should ultimately be cleared. This matches with the concept of $R_{0INH} < 1$ described earlier.

Recently, a novel approach of modeling the viral dynamics in hepatitis C was proposed (Snoeck *et al.* 2010). Firstly, a nonlinear mixed effects model was developed using the *MONOLIX* software (Delyon *et al.* 1999; Kuhn and Lavielle 2005; <http://www.monolix.org/>), allowing simultaneous description of the individual long-term HCV RNA viral load profiles of 2,100 CHC patients treated with peginterferon α -2a alone or in combination with ribavirin. Secondly, all available 21,284 HCV RNA measurements, of which 59% were below the LLOQ, were modeled by accounting for the left-censoring (Samson *et al.* 2007). Thirdly, cure or complete virion eradication was included in the model by the implementation of a physiologically based viral eradication boundary, representing a milestone contribution in enabling linking the complexity and diversity of clinically observed Hepatitis C viral dynamics to SVR. The cure boundary was based on the assumption that virion production (p) should cease when all infected cells are cleared, *i.e.*, when there is less than one infected cell present.

The model structure of the recent HCV viral dynamic model (Fig. 11.9), including a density dependent proliferation of hepatocytes (Dahari *et al.* 2007), is described by the following mass balance equations:

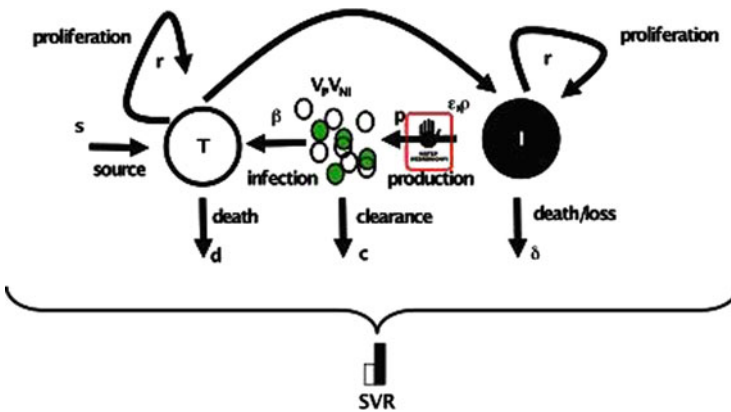


Fig. 11.9 Representation of the extended hepatitis C virus (HCV) viral dynamic model. Infectious HCV virions (V_I) infect target cells (T), creating productively infected hepatocytes (I). Uninfected hepatocytes (T) are produced at rate s and die at rate d . Infected hepatocytes die at rate δ . A density dependent proliferation of hepatocytes (r) is assumed. Infectious (V_I) and noninfectious (V_{NI}) virions are produced at rate p and cleared at rate c . Peginterferon α -2a dose-dependently inhibits the production of new virions (ϵ), and ribavirin dose-dependently renders a fraction of newly produced virions noninfectious (ρ). SVR is the primary clinical endpoint desired to be predicted in the treatment of hepatitis C. Reprinted from Snoeck *et al.* (2010)

$$\frac{dT}{dt} = s + r \cdot T \left(1 - \frac{T+I}{T_{max}}\right) - d \cdot T - \beta \cdot V_I \cdot T \quad (11.18)$$

$$\frac{dI}{dt} = \beta \cdot V_I \cdot T + r \cdot T \cdot \left(1 - \frac{T+I}{T_{max}}\right) - \delta \cdot I \quad (11.19)$$

$$\frac{dV_I}{dt} = (1 - \rho) \cdot (1 - \varepsilon) \cdot p \cdot I - c \cdot V_I \quad (11.20)$$

$$\frac{dV_{NI}}{dt} = \rho \cdot (1 - \varepsilon) \cdot p \cdot I - c \cdot V_{NI} \quad (11.21)$$

Infectious HCV virions (V_I) infect target cells (T), creating productively infected cells (I) at a rate $\beta \cdot V_I \cdot T$. Uninfected hepatocytes are produced at rate constant s and die at rate d . Infected hepatocytes die at rate δ . Similar to Dixit *et al.* (2004), it is assumed that infectious and noninfectious (V_{NI}) virions are produced at rate p and cleared at rate c . The measured viral load (V) represents the sum of infectious and noninfectious virions ($V_I + V_{NI}$). Finally, E_{max} dose–response relationships were assumed describing the effects of peginterferon α -2a and ribavirin:

$$\varepsilon = \frac{Dose_{PEG}}{ED_{50PEG} + Dose_{PEG}} \quad (11.22)$$

$$\rho = \frac{Dose_{RBV}}{ED_{50RBV} + Dose_{RBV}} \quad (11.23)$$

The daily dose of ribavirin and ED_{50RBV} was expressed as mg kg^{-1} , as ribavirin in mg kg^{-1} has been previously found to be one of the prognostic factors for SVR (Snoeck *et al.* 2006). The maximum number of hepatocytes present in an individual liver (T_{max}), the death rate of target cells (d), and the daily production of new hepatocytes in the absence of liver disease (s) were fixed to the biologically justifiable values as proposed by Colombatto *et al.* (2003). As the basic reproductive ratio (R_0) is an important predictor for a successful drug therapy (Jacqmin *et al.* 2010), the model was parameterized in terms of R_0 , using (11.4).

Individual viral load profiles showed that the HCV viral dynamic model was able to describe the typical phenomena observed after long-term therapy such as null response, partial virologic response, breakthrough during therapy, relapse after therapy, as well as SVR (Fig. 11.10). Simulated liver regeneration based on the estimated maximum hepatocyte proliferation rate r matched well with the measured increase in liver volume of donors having provided right-lobe liver grafts (Pomfret *et al.* 2003). The infected cell death rate (δ) appeared to be dependent on HCV genotype, and was in line with previously reported values of δ (Neumann *et al.* 2000). R_0 and ED_{50PEG} were found to be generally lower in patients with an SVR. A relatively low R_0 before treatment combined with a relatively high peginterferon

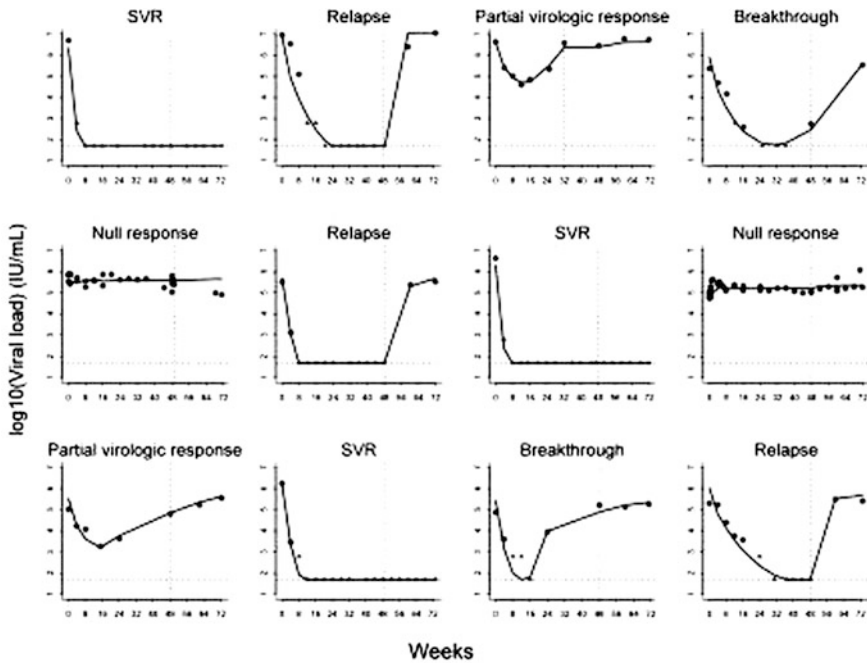


Fig. 11.10 Observed and model-predicted long-term viral load profiles in 12 representative chronic hepatitis C (CHC) patients. *Solid lines* are the fits of the model to the individual viral load data that either are detectable (*closed circles*) or below the lower limit of quantification (LLOQ) (*closed triangles*). *Dotted horizontal lines* show the LLOQ of the assay. *Dotted vertical lines* indicate the end of treatment. Reprinted from Snoeck *et al.* (2010)

effectiveness ε was expected to increase the likelihood of $R_{0INH} < 1$, hence increase in the likelihood of SVR.

In patients experiencing a breakthrough during therapy, it was confirmed that drug therapy failed to decrease the reproduction number (R_{0INH}) below 1 (Callaway and Perelson 2002; Dahari *et al.* 2007). A treatment with either higher doses or an alternative drug treatment could be an option in these patients in order to achieve $R_{0INH} < 1$. Relapsing patients could have had a $R_{0INH} < 1$ during treatment, but were not treated long enough so that the viral load quickly returned to baseline at the end of therapy. Alternatively, drug therapy could have failed to decrease the R_{0INH} below 1 in relapsing patients. Similar but prolonged treatment in relapsing patients could therefore be an option in the former situation but not in the latter. Based on these hypotheses, treatment may thus be optimized in individual CHC patients in case the R_0 and antiviral effectiveness would be known.

The model was successfully qualified for simulations based on an external model evaluation procedure using the data of a large clinical trial not included in the model building dataset (Snoeck *et al.* 2010).

Subsequently, mechanistic simulations were undertaken with the aim to better understand current treatment success and failure and to predict and evaluate

the outcome of alternative treatment options (*e.g.*, alternative doses, treatment durations and new drug combinations). An example of such a mechanistic simulation is depicted in Fig. 11.11 (Snoeck *et al.* 2008). The viral load profile of an individual patient receiving a 48-week monotherapy of weekly 180- μg peginterferon α -2a was fitted to the observed data of that patient using the HCV viral dynamic model. On the basis of the estimated viral dynamic parameters of that specific patient, the time profile of the infected cells was simulated. Although this patient showed a relapse after cessation of treatment, the simulated time profile of the infected cells revealed that the number of infected cells was already increasing again from approximately treatment week 32 onward (Fig. 11.11). It is thus predicted that this specific patient would not benefit from a longer than 48-week treatment with weekly 180- μg peginterferon α -2a, and an alternative treatment

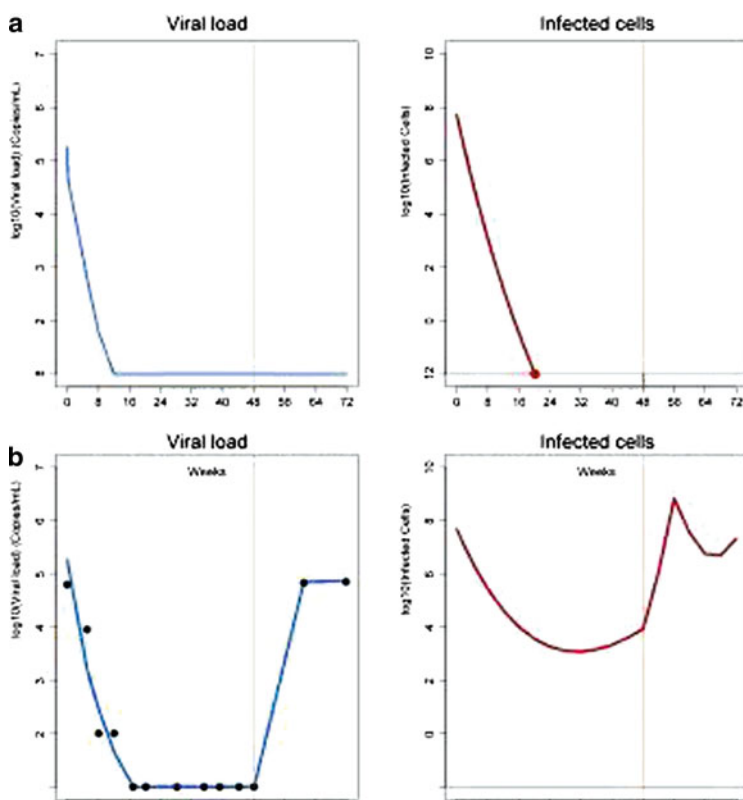


Fig. 11.11 Observed and predicted viral load profile of a CHC patient receiving weekly 180 μg peginterferon α -2a for 48 weeks (**b: left panel**). Based on the estimated $R_0 = 5$, $c = 4.1 \text{ day}^{-1}$, $\delta = 0.156 \text{ day}^{-1}$ and $\text{ED}_{50\text{PEG}} = 71 \mu\text{g}/\text{week}$, the time-profile of the infected cells was simulated for the same treatment (**b: right panel**). Based on the estimated parameters, the viral load profile (**a: left panel**) and the time-profile of the infected cells (**a: right panel**) was also predicted in case this patient would have received weekly 180 μg peginterferon α -2a for 48 weeks combined with daily 1200 mg ribavirin. Reprinted from Snoeck *et al.* (2008)

would be appropriate. However, in the case that the number of infected cells would still be decreasing at week 48, longer treatment duration with the same treatment might have been an option. Only a clinical evaluation based on the viral load profile of this specific patient would not have been able to distinguish between both treatment options as the time course of the infected cells would be unknown. This example thus illustrates the power of a HCV viral dynamic model-based analysis. If this specific CHC patient received a 48-week combination treatment of weekly 180- μg peginterferon α -2a combined with daily 1,200-mg ribavirin, it is predicted that this specific patient would have been cured as the HCV virus would have been eradicated as no infected cells were left after treatment (Fig. 11.11). This example nicely shows the importance of knowing the viral dynamic parameters of an individual patient, allowing evaluation of alternative CHC treatment options to ultimately develop and test hypotheses for personalizing treatments in this disease.

11.5 Conclusions

In clinical drug development, modeling is used to explain and quantify in an integrated way observations made in clinical studies. The increasing use of modeling has allowed a better understanding of the kinetic and dynamic mechanisms underlying these observations. Based on parameter estimates, simulations are performed to interpolate or extrapolate to situations that have not yet been tested (*e.g.* new doses, dosage schedules, or new drug combinations).

In the past 15 years, viral dynamic modeling has dramatically altered our understanding of the life cycles of three prevalent chronic viral infections. It has provided us with information on how antiviral agents act to reduce viral load and clear virus. In addition, viral dynamic modeling has provided predictive information whether a patient is likely to clear the virus. The basic reproductive ratio R_0 represents the corner stone of the viral dynamic models and is a derived model parameter that summarizes the host and virus interaction. The RMIC is also a derived model parameter that integrates the interaction with a third player, the antiviral agent. These parameters can be used to define doses and dosing schedules that can be successful in the long-term. Semimechanistic models also allow getting insight in nonobservable parts of a system. This is particularly true in HIV and HCV for which the left censoring of the observations, because of the LLOQ of the virus in plasma, limits the empirical interpretation of the data. The viral dynamic models presented in this chapter have been widely used to derive nondirectly observable or nonobservable parts of the systems. For example, in HCV, a viral dynamic model can provide information on infected cell (*i.e.*, hepatocytes) dynamics during treatment. This information is not easily assessable but is essential for therapeutic decisions regarding the dose, dosing schedule, and treatment duration.

Substantial progresses have been made in clinical virology, thanks to modeling of the viral dynamics and its interaction with antiviral drugs. However, from a PK-PD modeling perspective, some major challenges still need to be resolved such

as the optimal combination of drugs with different mechanisms of action and the individualization of therapeutic decisions based on short-term (or long-term) observations.

Acknowledgments Our viral dynamic modeling projects in HIV and Hepatitis C have been performed in collaboration with respectively Pfizer Global Research and Development, Sandwich, UK and F. Hoffmann-La Roche, Basel, Switzerland. We therefore thank Lynn McFadyen, Phylinda Chan, Barry Weatherley, Scott Marshall and Peter Milligan from Pfizer and Pascal Chanu, Karin Jorga, Timothy Goggin, Joe Grippo, Nelson L. Jumbe and Nicolas Frey from Hoffmann-La Roche for their contributions and scientific support. We thank Niclas Jonsson and Janet Wade, our Colleagues at Exprimio, for their contribution. We also thank Marc Lavielle from INRIA, Paris, France for his help with the implementation of our viral dynamic models into the *MONOLIX* software.

References

- Anderson RM, May RM (1997a) Population biology of infectious diseases: part 1. *Nature* 280:361–367
- Anderson RM, May RM (1997b) Population biology on infectious diseases: part 2. *Nature* 280:455
- Beal SL, Sheiner LB (1998) NONMEM users guides. NONMEM Project Group. University of California, San Francisco
- Bernardin F, Tobler L, Walsh I, Williams JD, Busch M, Delwart E (2008) Clearance of hepatitis C virus RNA from the peripheral blood mononuclear cells of blood donors who spontaneously or therapeutically control their plasma viremia. *Hepatology* 47:1446–1452
- Bonhoeffer S (1998) Models of viral kinetics and drug resistance in HIV-1 infection. *AIDS Patient Care STDS* 12:769–774
- Bonhoeffer S, May RM, Shaw GM, Nowak MA (1997) Virus dynamics and drug therapy. *Proc Natl Acad Sci USA* 94:6971–6976
- Callaway DS, Perelson AS (2002) HIV-1 infection and low steady state viral loads. *Bull Math Biol* 64:29–64
- Chan P, Jacqmin P, Lavielle M, McFadyen L, Weatherley B (2009) Population pharmacokinetic-pharmacodynamic-viral dynamics modeling of maraviroc monotherapy data using MONOLIX, PAGE 18, Abstract 1517. <http://www.page-meeting.org/?abstract=1517> october 2010
- Chan P, Jacqmin P, Lavielle M, McFadyen L, Weatherley B (2010) The use of the SAEM algorithm in MONOLIX software for estimation of population pharmacokinetic-pharmacodynamic-viral dynamics parameters of maraviroc in asymptomatic HIV subjects. *J Pharmacokin Pharmacodyn* (submitted for publication)
- Colombatto P, Civitano L, Oliveri F, Coco B, Ciccorossi P, Flichman D, Campa M, Bonino F, Brunetto MR (2003) Sustained response to interferon-ribavirin combination therapy predicted by a model of hepatitis C virus dynamics using both HCV RNA and alanine aminotransferase. *Antivir Ther* 8:519–530
- Crotty S, Cameron CE, Andino R (2001) RNA virus error catastrophe: direct molecular test by using ribavirin. *Proc Natl Acad Sci USA* 98:6895–6900
- Dahari H, Lo A, Ribeiro RM, Perelson AS (2007) Modeling hepatitis C virus dynamics: liver regeneration and critical drug efficacy. *J Theor Biol* 247:371–381
- Delyon B, Lavielle M, Moulines E (1999) Convergence of a stochastic approximation version of the EM algorithm. *Ann Stat* 27:94–128
- Dixit NM, Layden-Almer JE, Layden TJ, Perelson AS (2004) Modelling how ribavirin improves interferon response rates in hepatitis C virus infection. *Nature* 432:922–924

- Fätkenheuer G, Pozniak AL, Johnson MA, Plettenberg A, Staszewski S, Hoepelman AIM, Saag MS, Goebel FD, Rockstroh JK, Dezube BJ, Jenkins TM, Medhurst C, Sullivan JF, Ridgway C, Abel S, James IT, Youle M, van der Ryst E (2005) Efficacy of short-term monotherapy with maraviroc, a new CCR5 antagonist, in patients infected with HIV-1. *Nat Med* 11:1170–1172
- Ferguson NM, Donnelly CA, Hooper J, Ghani AC, Fraser C, Bartley LM, Rode RA, Vernazza P, Lapins D, Mayer SL (2005) Adherence to antiretroviral therapy and its impact on clinical outcome in HIV-infected patients. *J R Soc Interface* 2:349–363
- Fried MW, Shiffman ML, Reddy KR, Smith C, Marinos G, Gonçalves FL Jr, Häussinger D, Diago M, Carosi G, Dhumeaux D, Craxi A, Lin A, Hoffman J, Yu J (2002) Peginterferon alfa-2a plus ribavirin for chronic hepatitis C virus infection. *N Engl J Med* 347:975–982
- Funk GA, Fischer M, Joos B, Opravil M, Günthard H, Ledergerber B, Bonhoeffer S (2001) Quantification of *in vivo* replicative capacity of HIV-1 in different compartments of infected cells. *J Acquir Immune Defic Syndr* 26:397–404
- Hadziyannis SJ, Sette H Jr, Morgan TR, Balan V, Diago M, Marcellin P, Ramadori G, Bodenheimer H Jr, Bernstein D, Rizzetto M, Zeuzem S, Pockros PJ, Lin A, Ackrill AM; Pegasis International Study Group (2004) Peginterferon-alpha2a and ribavirin combination therapy in chronic hepatitis C: a randomized study of treatment duration and ribavirin dose. *Ann Intern Med* 140:346–355
- Heffernan JM, Smith RJ, Wahl LM (2005) Perspectives on the basic reproductive ratio. *J R Soc Interface* 2:281–293
- Ho DD, Neumann AU, Perelson AS et al (1995) Rapid turnover of plasma virions and CD4 lymphocytes in HIV-1 infection. *Nature* 373:123–126
- Huang Y, Rosenkranz SL, Wu H (2003) Modeling HIV dynamics and antiviral response with consideration of time-varying drug exposures, adherence and phenotypic sensitivity. *Math Biosci* 184:165–186
- Huang Y, Liu D, Wu H (2006) Hierarchical Bayesian methods for estimation of parameters in a longitudinal HIV dynamic system. *Biometrics* 62:413–423
- Jacqmin P, McFadyen L, Wade JR (2010) Basic PK/PD principles of drug effects in circular/proliferative systems for disease modelling. *J. Pharmacokinetic Pharmacodyn.* 2010 Apr; 37(2):157–77. Epub 2010 Mar 4
- Khan AZ, Mudan SS (2007) Liver regeneration: mechanisms, mysteries and more. *ANZ J Surg* 77:9–14
- Kuhn E, Lavielle M (2005) Maximum likelihood estimation in nonlinear mixed effects models. *Comput Stat Data Anal* 49:1020–1038
- Lau JYN, Tam RC, Liang TJ, Hong Z (1996) Mechanism of action of ribavirin in the combination treatment of chronic HCV infection. *Hepatology* 35:1002–1009
- Layden JE, Layden TJ (2002) Viral kinetics of hepatitis C: new insights and remaining limitations. *Hepatology* 35:967–970
- Layden TJ, Layden JE, Ribeiro RM, Perelson AS (2003) Mathematical modeling of viral kinetics: a tool to understand and optimize therapy. *Clin Liver Dis* 7:163–178
- Layden-Almer JE, Ribeiro RM, Wiley T, Perelson AS, Layden TJ (2003) Viral dynamics and response differences in HCV-infected African American and white patients treated with IFN and ribavirin. *Hepatology* 37:1343–1350
- Layden-Almer JE, Cotler SJ, Layden TJ (2006) Viral kinetics in the treatment of chronic hepatitis C. *J Viral Hepat* 13:499–504
- Liou TC, Chang TT, Young KC, Lin XZ, Lin CY, Wu HL (1992) Detection of HCV RNA in saliva, urine, seminal fluid and ascites. *J Med Virol* 37:203–209
- Manns MP et al (2001) Peginterferon α -2b plus ribavirin compared with interferon α -2b plus ribavirin for the initial treatment of chronic hepatitis C: a randomized trial. *Lancet* 358:958–965
- Mc Sween RNM, Anthony PP, Scheuer PJ (1987) *Pathology of the liver*, 2nd edn. Churchill Livingstone, Edinburgh

- Michalopoulos GK, DeFrances MC (1997) Liver regeneration. *Science* 276:60–66
- MONOLIX software supported by the MONOLIX Group. <http://www.monolix.org/> october 2010
- National Institutes of Health Consensus Development Conference Statement: Management of hepatitis C: 2002–June 10–12, 2002
- Neumann AU, Lam NP, Dahari H, Gretch DR, Wiley TE, Layden TJ, Perelson AS (1998) Hepatitis C viral dynamics *in vivo* and the antiviral efficacy of interferon-alpha therapy. *Science* 282:103–107
- Neumann AU, Lam NP, Dahari H, Davidian M, Wiley TE, Mika BP, Perelson AS, Layden TJ (2000) Differences in viral dynamics between genotypes 1 and 2 of hepatitis C virus. *J Infect Dis* 182:28–35
- Nowak MA, Anderson RM, Boerlijst MC, Bonhoeffer S, May RM, McMichael AJ (1996) HIV-1 evolution and disease progression. *Science* 274:1008–1011
- Nowak MA, Bonhoeffer S, Shaw GM, May RM (1997) Antiviral drug treatment: dynamics of resistance in free virus and infected cell population. *J Theor Biol* 184:203–217
- Nowak MA, May RM (2000) *Virus dynamics: mathematical principles of immunology and virology*. Oxford University Press, New York
- Paterson DL, Swindells S, Mohr J, Brester M, Vergis EN, Squier C, Wagener MM, Singh N (2000) Adherence to protease inhibitor therapy and outcomes in patients with HIV infection. *Ann Intern Med* 133:21–30
- Pawlowsky JM et al (2004) Antiviral action of ribavirin in chronic hepatitis C. *Gastroenterology* 126:703–714
- Perelson AS (2002) Modeling viral and immune system dynamics. *Nat Rev Immunol* 2:28–36
- Perelson AS, Neumann AU, Markowitz M, Leonard JM, Ho DD (1996) HIV-1 dynamics *in vivo*: virion clearance rate, infected cell life span, and viral generation time. *Science* 271:1582–1586
- Perelson AS, Essunger P, Cao Y et al (1997) Decay characteristics of HIV-1 infected compartments during combination therapy. *Nature* 387:188–191
- Perelson AS, Herrmann E, Micol F, Zeuzem S (2005) New kinetic models for the hepatitis C virus. *Hepatology* 42:749–754
- Phillips A, Youle M, Johnson M, Loveday C (2001) Use of a stochastic model to develop understanding of the impact of different patterns of antiretroviral drug use on resistance development. *AIDS* 15:2211–2220
- Pomfret EA, Pomposelli JJ, Gordon FD, Erbay N, Lyn Price L, Lewis WD, Jenkins RL (2003) Liver regeneration and surgical outcome in donors of right-lobe liver grafts. *Transplantation* 76:5–10
- Rong L, Zhilan Feng Z, Perelson A (2007) Emergence of HIV-1 drug resistance during antiretroviral treatment. *Bull Math Biol* 69:2027–2060
- Rosario MC, Poland B, Sullivan J, Westby M, van der Ryst E (2006) A pharmacokinetic-pharmacodynamic model to optimize the phase IIa development program of maraviroc. *J Acquir Immune Defic Syndr* 42:183–191
- Samson A, Lavielle M, Mentré F (2007) The SAEM algorithm for group comparison tests in longitudinal data analysis based on non-linear mixed-effects model. *Stat Med* 26:4860–4875
- Sherlock S, Dooley J (1998) *Disease of the liver and biliary system*. Blackwell Science, Oxford
- Snoeck E, Wade JR, Duff F, Lamb M, Jorga K (2006) Predicting sustained virological response and anaemia in chronic hepatitis C patients treated with peginterferon alfa-2a (40KD) plus ribavirin. *Br J Clin Pharmacol* 62:699–709
- Snoeck E, Laveille M, Chanu P, Jorga K, Frey N (2008) The challenge of modelling hepatitis C virus dynamics after long term treatment: application of Monolix. Presented at PAGE 17, Abstract 1348. <http://www.page-meeting.org/?abstract=1348> october 2010
- Snoeck E, Chanu P, Lavielle M, Jacqmin P, Jonsson EN, Jorga K, Goggin T, Grippo J, Jumbe NL, Frey N (2010) A comprehensive hepatitis C viral kinetic model explaining cure. *Clin Pharmacol Ther* (accepted for publication). *Clinical Pharmacology & Therapeutics* 87:706–713 (June 2010) | doi:10.1038/clpt.2010.35

- Strader DB, Wright T, Thomas DL, Seeff LB; American Association for the Study of Liver Diseases (2004) Diagnosis, management, and treatment of hepatitis C. *Hepatology* 39:1147–1171
- Wahl LM, Nowak MA (2000) Adherence and drug resistance: predictions for therapy outcome. *Proc Biol Sci* 267:835–843
- Wei X, Ghosh SK, Taylor ME, Johnson VA, Emini EA, Deutsch P, Lifson JD, Bonhoeffer S, Nowak MA, Hahn BH et al (1995) Viral dynamics in human immunodeficiency virus type 1 infection. *Nature* 373:117–122
- Wood A, Armour D (2005) The discovery of the CCR5 receptor antagonist, UK-427, 857, a new agent for the treatment of HIV infection and AIDS. *Prog Med Chem* 43:239–271
- World Health Organization (2008) Hepatitis C. <http://www.who.int/mediacentre/factsheets/fs164/en/>. Accessed 15 Sept 2008
- Wu H, Zhao C, Liang H (2004) Comparison of linear, nonlinear and semi parametric models for estimating HIV dynamic parameters. *Biom J* 46:233–245
- Wu H, Huang Y, Acosta EP, Park JG, Yu S, Rosenkranz SL, Kuritzkes DR, Eron JJ, Perelson AS, Gerber JG (2006) Pharmacodynamics of antiretroviral agents in HIV-1 infected patients: using viral dynamic models that incorporate drug susceptibility and adherence. *J Pharmacokinet Pharmacodyn* 33:399–419
- Zein NN, Rakela J, Krawitt EL, Reddy KR, Tominaga T, Persing DH (1996) Hepatitis C virus genotypes in the United States: epidemiology, pathogenicity, and response to interferon therapy. Collaborative Study Group. *Ann Intern Med* 125:634–639
- Zeuzem S (2001) The kinetics of hepatitis C virus infection. *Clin Liver Dis* 5:917–930
- Zeuzem S, Herrmann E (2002) Dynamics of hepatitis C virus infection. *Ann Hepatol* 1:56–63
- Zoulim F et al (1998) Ribavirin monotherapy in patients with chronic hepatitis C: a retrospective study of 95 patients. *J Viral Hepat* 5:193–198

Chapter 12

A Model-Based PK/PD Antimicrobial Chemotherapy Drug Development Platform to Simultaneously Combat Infectious Diseases and Drug Resistance

N. L'ntshotsholé “Shasha” Jumbe and George L. Drusano

Abstract The impact of antibiotics on health care likely exceeds that of any other class of drugs by greatly reducing the likelihood of debilitating disease and/or death prevalent in the preantibiotic era. However, the coincidence of (1) medicinal chemists' continuing struggle to produce druggable antibiotics with novel targets that overcome emergence of drug resistance altogether, (2) the general decline of active development of new antimicrobial agents, (3) the prevalence (and growth because of increased use) of antimicrobial resistance to legacy molecules, and (4) the ever-present threat of bioterrorism, mean that antibiotic drug development must necessarily focus on resistance counter-measures throughout the discovery and development process. Thus, in essence, antiinfective discovery and development programs are (or should be) intrinsically charged with the combined responsibility of minimization of resistance selection and targeting drug resistant infections from the outset.

12.1 Introduction

The central thesis of this chapter is that drug resistance counter-measures are indivisible from traditional antimicrobial chemotherapy pharmacokinetics/pharmacodynamics (PK/PD) to clinical trial simulation (CTS). This *defensive* approach necessarily provides the only direct *offensive* toward control of antibiotic resistance and facilitates overall effective and responsible antimicrobial drug development.

This chapter on modeling and simulation strategies in “defensive” antimicrobial chemotherapy drug-development is organized as follows: the threat of drug resistance is elaborated with immediate extension to a logical value proposition of PD principles that determine the proposed quantitative platform from a

N. L'ntshotsholé “Shasha” Jumbe (✉)
Roche, Palo Alto, CA, USA
e-mail: drshasha@gmail.com

resistance prevention/avoidance standpoint. Self-contained monographs are presented to enable the reader to conceptualize and apply ideas presented.

12.2 Why Develop a Platform to Simultaneously Combat Infectious Diseases and Drug Resistance?

The rapid development antimicrobial resistance, first observed by Davis and Maas (1952) and subsequently explained and characterized by the venerated Eagle (1954, 1955) (who will be mentioned several times during this chapter) has become an increasingly serious public health problem in a wide range of infectious diseases (Alonso *et al.* 1999; Barclay and Begg 2001; Boshoff *et al.* 2003; Bull *et al.* 2002; Centers for Disease Control and Prevention 2006; Cirz *et al.* 2005; Coates *et al.* 2002; Drusano 1998a; Drusano *et al.* 2006; Jacobs 2004; Lipsitch and Samore 2002; Neu 1992). Conventionally, it was thought that mutations were the inevitable consequence of imperfect DNA replication and repair. However, mounting evidence suggests that bacteria may play a more active role in the mutation of their own genomes by inducing proteins that actually promote error-prone replication (Cirz *et al.* 2005; Cirz and Romesberg 2006; Drlica and Zhao 1997; McKenzie *et al.* 2000; Miller *et al.* 2004; Srivastava *et al.* 2010). The deluge of antibiotics that have varying effectiveness in inhibiting processes that are essential for bacterial growth have introduced extreme selection pressure for resistant bacteria since the use of penicillin in 1942 (Davis and Maas 1952; Eagle 1954, 1955; Eagle *et al.* 1953b). This has resulted in an unprecedented acceleration of bacterial evolution that has culminated in the emergence of resistance to every approved antibiotic, and in some cases, multidrug-resistant bacteria that are increasingly difficult to treat (Alonso *et al.* 1999; Boshoff *et al.* 2003; Centers for Disease Control and Prevention 2006; Chen *et al.* 2004; Gumbo *et al.* 2005; Mwangi *et al.* 2007).

As a design strategy to prevent or delay the emergence of antimicrobial-resistant pathogens, we consider four major axes of interaction that have impact on microbiological and/or clinical outcome – the infective organism, microbiota (local environment), host, and antiinfective agent.

(a) Infective organism

Difficulties in targeting essential proteins support the importance of pre-existing microorganism diversity in the form of subpopulations or quasi-species variants that are spontaneously resistant to inhibition even in the absence of selection pressure (LeClerc *et al.* 1996; Weigel *et al.* 2003). The clinical failure in targeting MetRS (Drlica and Zhao 1997; Miller *et al.* 2004), determined to be essential in laboratory reference strains of *Streptococcus pneumoniae*, because of the presence of a resistant variant of MetRS, highlights the impact of pre-existing drug-resistant mutants and rapidly evolving diversity on microbiological outcome.

(b) Microbiota

The infective organism usually competes with normal host microflora to produce an infection. Therefore, a temporal displacement of commensal bacteria may be essential for successful infection (Srivastava *et al.* 2010). Antibiotic treatment also displaces normal host microflora, thereby permitting recolonization by exogenous antibiotic-resistant (often slower growing) bacteria as well as by antibiotic-resistant mutants belonging to commensal microflora. Thus, the microbiota axis is influenced and influences the infective organism, host, and exposure to antibiotics.

(c) Host

It is postulated that the ability of bacteria to infect mammalian tissues has most probably had an effect on human evolution (Chen *et al.* 2004). The necessary evolution of an extremely complex immunological response system and a body temperature (37°C, which is higher than the mean environmental temperature) are provided as evidence of mammalian evolutionary traits driven by virulent microorganisms, as postulated by Haldane more than 50 years ago (Gumbo *et al.* 2005). Furthermore, the coincident prevalence of sickle cell anemia in regions with a high rate of malaria infections, because sickle-shaped hemoglobin is protective against malaria, is given as evidence of specific infectious microorganisms in different geographic allocations as a driving force in human evolution (LeClerc *et al.* 1996; Mwangi *et al.* 2007).

(d) Antiinfective therapies

One of the most important factors contributing to the evolution of resistance is the acquisition of mutations during therapy (Gniadkowski 2008). For many antibiotics, including the fluoroquinolones (Chung *et al.* 2006; Drusano *et al.* 2009; Fish *et al.* 1995; Hooper 2000), cephalosporins (Drusano 1998b; Palmer *et al.* 1995), and rifamycins (Cirz *et al.* 2005; Gumbo *et al.* 2007), resistance typically results from the acquisition of point mutations in genes that encode the drug's molecular targets or proteins involved in drug inactivation (Davies 1994) or drug efflux (Dean *et al.* 2003; Hirata *et al.* 2004; Jumbe *et al.* 2006; Williams 1996). Mutation and inducible efflux pumps appear to be the primary mechanisms to acquire resistance in *Mycobacterium tuberculosis* (Boshoff *et al.* 2003; Zhang and Young 1994) and some *Pseudomonas aeruginosa* infections (Alonso *et al.* 1999; Jumbe *et al.* 2003; Livermore 2002). Although mutation and horizontal gene transfer have long been appreciated as important forces in evolution, it has recently become apparent that in some cases they may be accelerated by the use of antibiotics to the point where they could contribute to therapy failure on the timescale of an infection. In addition to "true" resistance, under certain conditions, bacteria (mostly slow growing) have a remarkable ability to tolerate antibiotic therapy; some manage to survive apparently lethal conditions until therapy ceases or "true" resistance is acquired by mutation and/or horizontal transfer (Beaber *et al.* 2004; Krylov 2003; Lipsitch and Samore 2002). These organisms have been referred to as "non-replicating persisters."

12.2.1 Classical Empirical Antibiotics vs. Synthetic Antibacterials

Two platforms have been leveraged, either separately or in combination, for the discovery of novel antibiotics. The classical empirical age of early antibiotics and synthetic antibacterials (1940–1960s) predominantly involved search for novel inhibitors of lethal bacterial targets either by using natural sources or by screening of synthetic compounds, without preselection of targets (Bull *et al.* 2002; Chopra and Roberts 2001; Hopwood 1985; Kucers and Bennett 1989). The more recent novel-target-first paradigm strategies also include the search for inhibitors of resistance systems, with the aim of recovering a susceptible phenotype in a previously resistant population (Coates *et al.* 2002; Gross *et al.* 2003; Hawser 2006). However, the discovery and/or development of antibiotics targeting either historically validated or newly proposed essential bacterial targets continue to be disproportionately difficult to identify as no antibacterial agent derived from the novel-target-first paradigm has yet to reach the market. Therefore, an important element in meeting the challenge of antibiotic resistance requires the abandonment of traditional back-loaded (Phase II and Phase III weighted) antiinfective agents development paradigm, and requires efficient (and early) integration of knowledge and data gained from historical data, competitive/comparative intelligence, *in vitro* and *in vivo* nonclinical data and volunteer studies (Phase I) to rapidly arrive at efficacious/drug-resistance suppressing dosing regimens.

The remainder of this chapter will discuss information integration strategies leveraging early nonclinical data for impactful CTS strategies early in antiinfective program lifecycles. To inform and increase the likelihood of success of Phase II/III studies, it is crucial that these studies be designed properly so that the resulting data are robust, are interpretable for dose and schedule recommendations, and reliably predict the success or failure of the proposed treatment regimens in target patients.

12.3 PK/PD-Driven Clinical Trial Design for Chemotherapeutic Antimicrobial Dose-Regimen Rationalization

Failure to determine a safe and effective dosage regimen for use in pivotal clinical trials is acknowledged as a frequently encountered flaw during the development of many drugs (Andes and Craig 1999; Craig 1998b; Dagan 2003; Drusano *et al.* 1996, 2000; Peck and Cross 2007). PK/PD models integrate the relationship between dose and concentration-vs.-time (PK), and the relationship between concentration and effect-vs.-time (PD). Paramount antibiotic drug development questions “Have we selected the RIGHT drug?,” “Have we established the RIGHT dosage regimen?” and “Have we established the RIGHT exposure variable necessary to suppress emergence of resistance?” are best addressed directly using an integrated PK/PD approach. When a PK/PD model is employed as the platform to guide learning and integrate

knowledge, both the time course and variability in the effect-vs.-time relationship can be ascertained and subsequently used to interpolate (and extrapolate, if valid) to different dosage-regimen scenarios to inform confirmatory clinical testing.


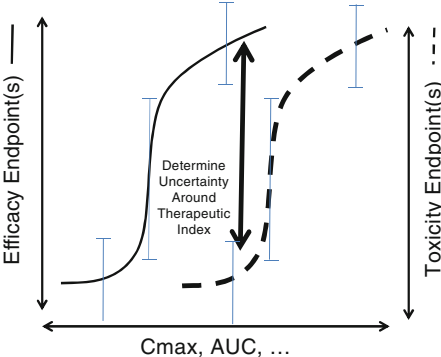
The realm of antimicrobial PK/PD is special because of the particular advantage of access to direct measurement of the active-concentration of drug against the intended target pathogen at or near the site of drug action. Therefore, most chemotherapeutic antimicrobials can leverage nonclinical (*in vitro* and *in vivo*) PK/PD data extensively. With this advantage in hand, fundamental PK/PD knowledge generation for antiinfectives from nonclinical and early clinical studies can be efficiently employed according to four primary *pharmaco-microbiological* principles (see Monograph 1): (1) the microbiological effect concentration (the *in vitro* or *in vivo*

Monograph 1 Primary pharmicrobiological PK/PD principles

<p><i>Microbiological effect concentration</i> A primary advantage of antimicrobial therapy PK/PD is primarily driven by the ability to directly measure requisite concentrations of the anti-infective agent required in order to illicit the effects for which it was designed. Taking into account inherent PK variability, there is almost always a better relationship between the action of a given drug and its concentration in the blood or at its site(s) of effect than between the dose of the drug given and the effect. Antimicrobial potency towards pathogens is indicated by the minimal inhibitory concentration (MIC) and the minimal bactericidal concentration (MBC).</p>	
<p><i>Drug-input forcing function (shape of the concentration-vs.-time curve)</i> Over the last years, the impact of the shape of the concentration-vs.-time curve on antibacterial efficacy has been validated both in experimental animals and in man (), based on the correlation between dynamic PK/PD variables and microbiological outcome. It has been clearly shown that antibiotic serum concentration (and, as a result, infected tissue antibiotic concentration) influences intensity and duration of the antimicrobial effect. Antibiotics are frequently divided across the essential continuum spanning from those that exhibit concentration-dependent killing (time-independent with prolonged persistent effects) through to those exhibiting time-dependent (concentration-independent with minimally persistent effects) killing, see Monograph 2.</p>	

(continued)

Monograph 1 (continued)

<p><i>Microbiological efficacy window</i> Drug development success is driven by attainment of maximum clinical efficacy while minimizing the risk of toxicity, which provides a miniscule target for success surrounded by a large opportunity of potential failure. Therefore, it is important to understand that the higher the drug concentrations required for a drug to elicit desired effect (for example, a higher MIC or EC90), the smaller the opportunity window for successful development for a potential drug candidate. Furthermore, with the insistence of consideration of resistance endpoints at the outset as the thesis of this chapter, higher microbiological concentration targets directly correlate with narrow margins of expected microbiological effect.</p>	
<p><i>Pharmacokinetic/pharmacodynamic (exposure/effect) integration and variability</i> Population PK/PD models are a vital aid to the drug development process by providing reliable predictions of the individualized dose±exposure-vs.-effect (efficacy and toxicity) relationship, which is key to therapy individualization. The purpose of population modeling is to describe the statistical distribution of exposure/effect parameter estimates and identify potential sources (demographic and/or pathophysiological) of intra- and inter-individual variability among patients. Informed dosing-regimen selection integrates the knowledge structure and associated characterization of all sources of variability.</p>	

microbiologically active concentration), (2) the shape of the drug-input microbiological-effect forcing function (shape of the concentration-vs.-time curve), (3) the microbiological efficacy window, describing the “window-of-opportunity” of the molecule, engendered by the therapeutic index of the drug, and (4) integration of between- (and within-) patient PK and PD (exposure AND effect) variability (Bradley *et al.* 2003; Drusano 2004; Drusano *et al.* 2000, 2002, 2006; Preston *et al.* 1998).

12.3.1 Knowledge Generation for Design and Simulation of Antiinfective Clinical Trials

12.3.1.1 Microbiological Effect Concentration

The minimum inhibitory concentration (MIC) is a well-established laboratory parameter routinely determined in microbiology. The standard definition of MIC is the minimum concentration that inhibits visible growth of the organism as detected by the unaided eye following 18- to 24-h incubation. In this context, the importance of the MIC in antimicrobial chemotherapy cannot be underestimated. Frequently the MIC is regarded as the primary PD biomarker parameter of interest, even though antibiotics with the same MIC may exhibit very distinct PK/PD relationships. It is currently by far the most commonly used PD parameter for the evaluation of efficacy of antiinfective agents. Drug trough concentrations in the target population are also often compared to the MIC to make dosing decisions. Two important factors are often overlooked with respect to the importance of the MIC. From a PK point of view protein binding and tissue distribution must be taken into consideration. Protein binding is relevant because only unbound drug is available to exert a pharmacological effect. Tissue distribution also needs to be taken into account, given that most of infections do not occur in plasma, but in tissue interstitial space.

From a PD point of view, the MIC is a static measurement, which does not provide information on the kinetics of the drug action. Furthermore, the MIC determination depends on the inoculum-density and outcome is determined at a single time point following incubation. Therefore, different combinations of growth and kill rates can result in the same MIC. Semidynamic information can be derived from standard MIC determinations as shown in Fig. 12.1. Following MIC determination, using the standard twofold dilution method, subsequent experiment(s) with log dilutions above and below the established MIC are performed to generate a log-log plot of change in bacterial density-vs.-MIC dilution. In this way, the MIC can be extended beyond the all-or-nothing threshold concentration-effect relationship, permitting quantitative distinction of concentrations around the MIC via curve fitting of observed data, *i.e.*, the change in bacterial density with antibiotic concentration is determined from

$$\Delta[a] = \Delta_{\max} - \gamma_{[a]} \quad (12.1)$$

where $[a]$, the antibiotic concentration, is some multiple of the “qualitative” MIC; Δ_{\max} is the maximum observed bacterial density change from MIC, and $\gamma_{[a]}$, nonsaturable concentration dependent bacterial growth suppression over the incubation period. In the instance where antibiotic concentration effect is saturable and assuming symmetry around the MIC, the Hill function can be imposed on (12.1) to yield (Zhi *et al.* 1986):

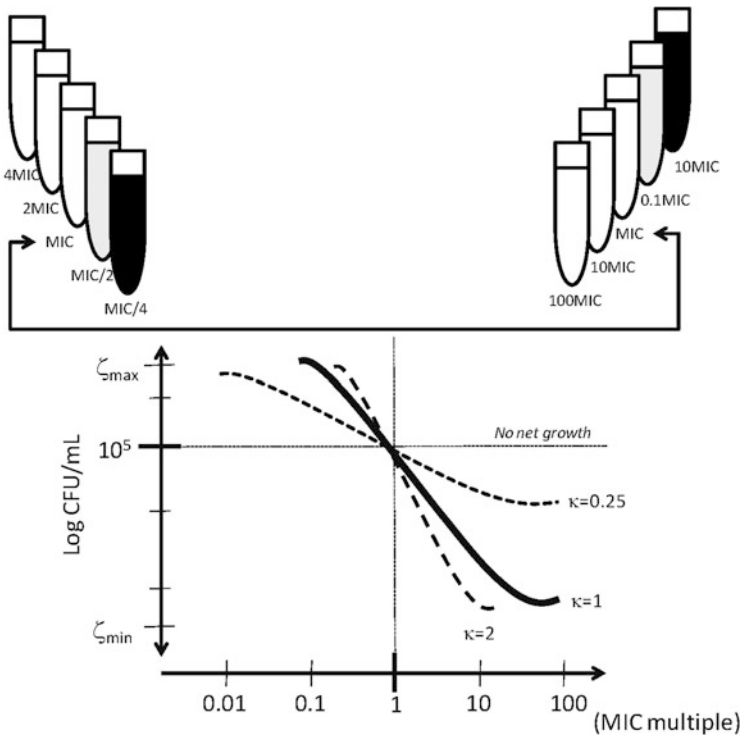


Fig. 12.1 Semi-dynamic determination of MIC. Following classical twofold dilution a qualitative MIC is determined, with subsequent experiment(s) with log dilutions above and below the established MIC performed in order to generate a log–log plot of change in bacterial density- vs.-MIC dilution

$$\gamma_{[a]} = \gamma_{\max} \frac{([a]/\gamma_{50})}{1 + ([a]/\gamma_{50})} \tag{12.2}$$

where γ_{\max} designates maximum growth inhibition, $[a]/\gamma_{50}$ is the antibiotic quantitative MIC.

Of note, classical MIC determination is performed at microorganism-inocula usually 100- to 1,000-fold below the inverse of the mutational frequency to resistance for most pathogens, leading to absurdities like an *E. cloacae* that appears ampicillin susceptible. The quantitative MIC method described above possibly provides a means to quantify and get around the issues with regard to higher inocula for resistance suppression/minimization.

12.3.1.2 Time-Kill Study Evaluation

Because the static MIC does not reflect the *in vivo* scenario, where bacteria are exposed to constantly changing antibiotic concentrations, various alternative types

of *in vitro* models with variable antibiotic concentrations (known generally as time-kill studies) have been devised (Blaser *et al.* 1985; Craig and Ebert 1990; Firsov *et al.* 1998, 1999; Frimodt-Moller 2002; Guerillot *et al.* 1993; Tam *et al.* 2005). Primary classes include those with constant antibiotic concentrations, which study the effects of a constant concentration of drug against bacteria as a function of time; and those, in which the antibiotic concentrations fluctuate by dilution or diffusion (Craig and Ebert 1990; Frimodt-Moller 2002; Keil and Wiedemann 1995; MacGowan *et al.* 1996). Time-kill curves generated from these studies can follow microbial killing and growth as a function of both time and antibiotic concentration, Fig. 12.2. The resulting kill curves are subsequently analyzed with appropriate PK/PD models to design nonclinical *in vivo* studies and/or confirmatory clinical studies to optimize dosage regimens based on a rational and quantitative platform.

Similar to the dynamic MIC approach described above, PK/PD analysis of time-kill data considers changes in bacterial density relative to antibiotic concentration. Importantly, the rate of change in bacterial density, B , is accessible in these studies and is determined as:

$$\frac{d}{dt}B(t) = \zeta_G \cdot B(t) - \Psi_K \cdot B(t) \tag{12.3}$$

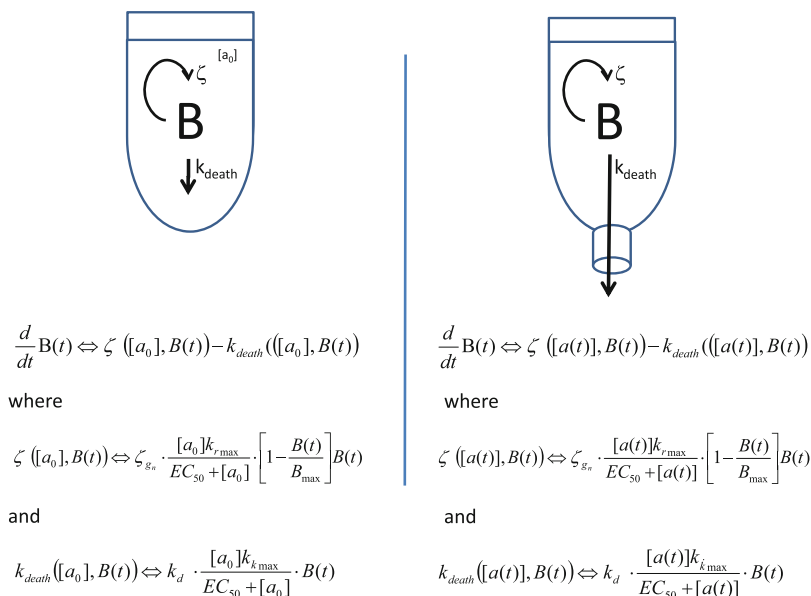


Fig. 12.2 Constant and variable antibiotic concentration experimental platforms. Constant concentration studies follow change of microorganism density as a function of time when exposed to fixed-drug concentration. Latter studies, consider both fluctuating antibiotic concentrations and microorganism density via dilution or diffusion

where ζ_G and Ψ_K are first-order rate constants describing natural growth/replication and death of microorganisms in the absence of drug. Letting $\zeta_N = \zeta_G - \Psi_K$ and including the drug effect (using Hill equation), (12.3) becomes

$$\frac{d}{dt}B(t) = \left(\zeta_N - \frac{K_{\max} \cdot [a]}{K_{50} + [a]} \right) \cdot B(t) \quad (12.4)$$

where $B(t)$ (CFU/mL) is the bacterial density at any time t , ζ_N , the net bacterial growth rate in the absence of drug, K_{\max} , K_{50} , maximal bacterial kill rate (time^{-1}) and concentration that provides half of the maximal kill rate (mg/L), respectively. This relationship has a closed form solution for B and is pharmacodynamically similar to the dissipation rate constant stimulation indirect response model (Mager *et al.* 2003). Capacity-limited growth of the microorganism is introduced linearly using the logistic function $\zeta_N = \zeta_0 \cdot (1 - (B(t)/B_{\max}))$ or nonlinearly as $\zeta_N = B_{\max}/B_{50} + B(t)$ where B_{\max} is the maximal velocity of bacterial replication, and B_{50} the number of microorganisms at which the replication rate is half maximal. From a mechanistic point of view, capacity-limited expansion of the microorganism should be on the replication rate (ζ_G) rather than the growth of the microorganism (ζ_N), which implicitly suggests a decrease in the natural death rate of the microorganism, which may or may not always be true.

An additional implicit, therefore often overlooked, assumption in the description of (12.2)–(12.5) is the employment of the Hill equation. Application of the Hill equation assumes that the antibiotic antibacterial effect (E)-vs.-concentration $[a]$ curve is symmetrical and that the point of inflection occurs at the antibiotic concentration that produces 50% of the maximum response. This assumption, however, is rarely tested, and full evaluation of $E/[a]$ curve symmetry is not performed routinely (Black *et al.* 1985; Van Der Graaf and Danhof 1997; Van der Graaf and Schoemaker 1999).

12.3.1.3 Evaluating Effect (E)-vs.-Concentration $[a]$ Curve Symmetry/Asymmetry

The four parameter Richards model attempts (12.5) to quantify symmetry/asymmetry of concentration-vs.-effect curves including an asymmetry factor, δ (Van Der Graaf and Danhof 1997; Van der Graaf and Schoemaker 1999), as shown in Fig. 12.3

$$E = \frac{\alpha}{(1 + \delta \cdot \varepsilon^{-\ln \cdot (10)^p \cdot [\log[a] - \log K_i]})^{1/\delta}} \quad (12.5)$$

The Hill (Goutelle *et al.* 2008) and Gompertz (Dalla Costa *et al.* 1997) models are nested, *i.e.*, are special cases of the four-parameter Richards model and can be formulated by setting one or more of the parameters to fixed values, *e.g.*,

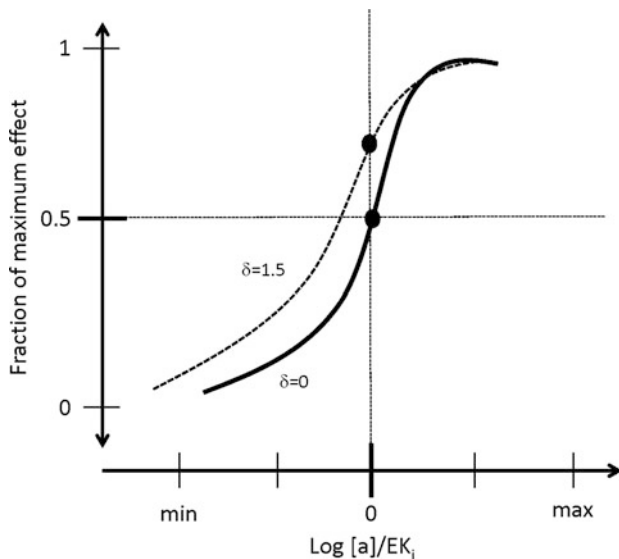


Fig. 12.3 The commonly used Hill effect equation assumes that the antibiotic antibacterial effect (E)-vs.-concentration [a] curve is symmetrical and that the point of inflection occurs at the antibiotic concentration that produces 50% of the maximum response. The four parameter Richards model attempts to quantify symmetry/asymmetry of concentration-vs.-effect curves including an asymmetry factor, δ

$$E = \frac{\alpha}{1 + \varepsilon^{-\ln(10)p[\log[a] - \log K_i]}} \quad \text{where } \delta \rightarrow 1 \tag{12.6}$$

is the logistic model equivalent to the Hill equation, and the Gompertz model can be derived where $\delta \rightarrow 0$

$$E = \frac{\alpha}{\varepsilon^{\varepsilon - \ln(10) \cdot p \cdot [\log[a] - \log K_i]}} \tag{12.7}$$

where α is the upper asymptote, $pa_i(-\log_{10} Ea_i)$ is the inflection point, and p the slope parameter.

Simultaneous analysis of all available data, implementing the full $E/[a]$ curve without the symmetry assumption, is best performed using nonlinear mixed effects methods to allow for correct selection of the appropriate model and adequate estimation of ill-defined parameters.

12.3.1.4 Relating the Hill Model to MICs

Coming back full circle, time-kill curve PK/PD relationship determinations can be related to stationary MICs via model-based identification of the antibiotic

concentration that results in instantaneous equilibration of microorganism growth and kill rates, *i.e.*, where net change in bacterial density is zero. Falling back to the $E/[a]$ symmetry assumption, and setting net change in bacterial density to zero

$$\frac{d}{dt}B(t) = \left(\zeta_N - \frac{K_{\max} \cdot [a]}{K_{50} + [a]} \right) \cdot B(t) \quad (12.8)$$

is rearranged to

$$\frac{d}{db}B(t) = \left(\zeta_N - \frac{K_{\max} \cdot [a]}{K_{50} + [a]} \right) \cdot dt \quad (12.9)$$

which can be integrated on both sides

$$\int_{B_0}^{B_t} \frac{1}{B} \cdot dB = \int_0^t \left(\zeta_N - \frac{K_{\max} \cdot [a]}{K_{50} + [a]} \right) \cdot dt \quad (12.10)$$

When drug concentrations result in no net change in bacterial density this simplifies to

$$0 = \left(\zeta_N - \frac{K_{\max} \cdot [a]_{SC}}{K_{50} + [a]_{SC}} \right) \quad (12.11)$$

$$\zeta_N = \frac{K_{\max} \cdot [a]_{SC}}{K_{50} + [a]_{SC}} \quad (12.12)$$

$$[a]_{SC} = \frac{\zeta_N \cdot K_{50}}{K_{\max} - \zeta_N} \approx [IBS] \approx MIC_{in\ vivo} \quad (12.13)$$

where $[a]_{SC}$ is the antibiotic concentration (stasis concentration [SC]) that results in instantaneous bacterial stasis (IBS) which is equivocal to the *in vivo* MIC.

12.3.1.5 Antimicrobial Drug Combinations

Before leaving *in vitro* studies entirely it is important to consider antibiotic drug combinations. In some cases, it might be desirable to combine a potent pair of drugs, with each drug targeting a different (serial or parallel) molecular target in the same pathogen, to increase patient compliance by improving dose-administration schedule, sparing toxicity/side-effects, and/or reducing pill burden (Chen *et al.* 2004; Dalla Costa *et al.* 1997; Drusano 1990; Drusano *et al.* 1996, 2000; Giamarellou 1986). Most importantly, it is possible that combination chemotherapy can suppress the emergence of resistance of the microorganism to either or both of the

drugs in the combination (Cappelletty and Rybak 1996; Drusano 1990; Jacobs 2004; King *et al.* 1981; Wainberg and Friedland 1998).

Determination of drug interaction using statistical criteria has been illustrated to be a challenging problem by Greco *et al.* (1990). However, it appears that there is passive agreement that evaluation of differentiating drug interactions should be based on formal declaration of additivity. There from, the definitions of synergy and antagonism are based on statistical comparison of observed effect to the defined “additive null reference,” whereby the nature of drug combination interaction can be deduced based on anti-bacterial effectiveness, where $1+1 \gg 2$ or $1+1 \ll 1$ is synergy and antagonism, respectively. Bliss Independence and Loewe Additivity (discussed below) constitute the primary additivity null reference models currently used for the evaluation of antimicrobial combination therapies (Boik *et al.* 2008; Boucher and Tam 2006; Fidler and Kern 2006; Lee and Kong 2009; Lee *et al.* 2007; Whitehead *et al.* 2008).

Bliss Independence assumes a multiplicative interaction of drugs, *i.e.*,

$$E = \gamma_{\max} \frac{E_0 \cdot ([a_1]/IC_{50,1})^{s_1} \cdot ([a_2]/IC_{50,2})^{s_2}}{[1 + ([a_1]/IC_{50,1})^{s_1}] \cdot [1 + ([a_2]/IC_{50,2})^{s_2}]} \quad (12.14)$$

where $[a_1]$, $[a_2]$ and $IC_{50,1}$, $IC_{50,2}$ are drug concentrations and drug concentrations resulting in 50% inhibition for antibiotic 1 and antibiotic 2, respectively, E_0 is the control inhibitory effect measured output in the absence of either drug, E is the observed (measured) effect, and s_1 and s_2 are the antibiotic-effect slope parameters for antibiotic 1 and 2, respectively.

The MacSynergy II program of Prichard *et al.* (1993) is currently the mainstay “plug-and-play” utility tool for Bliss Independence additivity analysis. In this analysis, standard deviations of the observed effect are used to determine statistical difference from the Bliss Independence null reference model.

Loewe additivity is simply defined as the effect seen on addition of the second, third, etc., as compared to simple addition of the first antibiotic when it is added to itself. Greco *et al.* have proposed the following sigmoid E_{\max} interaction model to describe Loewe additivity.

$$1 = \frac{[a_1]}{IC_{50,1} \cdot [E/E_0 - E]^{1/m_1}} + \frac{[a_2]}{IC_{50,2} \cdot [E/E_0 - E]^{1/m_2}} + \frac{\omega [a_1] [a_2]}{IC_{50,1} \cdot IC_{50,2} \cdot [E/E_0 - E]^{(1/2m_1 + 1/2m_2)}} \quad (12.15)$$

The sum of the first two terms defines the additive effect whereas the third term is the drug interaction term, where ω is the synergism-antagonism interaction parameter. When ω is exactly zero, then (12.15) collapses to the simple Loewe Additivity model. If the 95% confidence interval of ω overlaps zero, the combination is additive, $\omega \gg 0$ the interaction is synergistic, and $\omega \ll 0$ the interaction is antagonistic.

In summary, use of drugs in combination may be advantageous, particularly as a means to suppress the emergence of antibiotic resistance, however, the determination and design of optimal regimens to achieve this major advantage poses inherent experimental and operational difficulties. Part of the difficulty in selecting a regimen involves the potential high dimensionality resulting from the combinatorial nature of the problem. For instance, a modest three dose-by-three dose evaluation, often necessary to learn about the drug interaction, requires at least nine different combination regimens (without individual-agent concurrent controls). Alternatively, learning and generating knowledge on drug combination interaction in nonclinical (*in vitro* and *in vivo*) studies prior to modest confirmatory clinical studies reduces costs and operational complexity inherent in Phase I/II studies.

12.3.1.6 *In Vivo* Thigh Model

The mouse-thigh infection model (and derivatives thereof) pioneered by Eagle and coworkers (Eagle 1948, 1949, 1952; Eagle *et al.* 1953a, b) and rediscovered and expanded on by Craig (1998a, b) and Craig *et al.* (1991) provides a very useful and validated experimental disease system for expanding, testing and corroborating nonclinical *in vitro* PK/PD knowledge. Furthermore, impact of drug pressure on the amplification of the drug-resistant subpopulation can be quantitatively enumerated, effects of the host defense (cytotoxic and humoral immunity) on microorganisms can be ascertained, and correlations between the shape of the concentration-vs.-time curve and microbiological and clinical outcomes can be delineated.

Antimicrobial chemotherapy decreases the natural rate of bacterial replication (ζ_G) or increases the natural rate of bacterial death (Ψ_K), for some agents, this is NOT either/or but both, and is described mathematically as,

$$\frac{d}{dt}B = \zeta_G \cdot E_R[a(t)] \cdot B(t) - \Psi_K \cdot E_D[a(t)] \cdot B(t) \quad (12.16)$$

where drug effect ($E_R[a(t)]$ and $E_D[a(t)]$) relate to the microorganism replication and death antimicrobial concentration-dependent effect. The decrease of microorganism replication and/or increase of microorganism death because of drug effect is related to antibiotic concentration preferably using the Richards full model from (12.5) instead of making the *à priori* assumption that the concentration-vs.-effect relationship is symmetrical (without any additional burden in number of parameters to be fit). Furthermore, simultaneously fitting all available data using nonlinear mixed effects enables combining information of each individual animal in individual experiments to allow adequate estimation of the mean parameters and associated interindividual variabilities of the three or four estimates that may be ill-defined when considered on an individual animal or individual experiment basis.

12.3.1.7 Emergence of Resistance Submodel

The probability that a resistant subpopulation exists within a predominantly drug-susceptible wild-type population is dependent on the number of organisms at the infection site (total population burden) and the mutational frequency to resistance to the antibiotic prescribed. In addition, amplification of a resistant subpopulation is also dependent on the fitness of the selected mutants, and the selection pressure exerted by the drug concentrations experienced by the microorganisms, thus transforming (12.16) to

$$\begin{aligned} \frac{d}{dt}B_s &= \zeta_{G,s} \cdot E_{R,s}[a(t)] \cdot (1 - P)B_s(t) + \zeta_{G,r} \cdot E_{R,r}[a(t)] \cdot P \cdot \Gamma \cdot B_r(t) \\ &\quad - \Psi_{K,s} \cdot E_{D,s}[a(t)] \cdot B_s(t) \end{aligned} \quad (12.17)$$

$$\begin{aligned} \frac{d}{dt}B_r &= \zeta_{G,r} \cdot E_{R,r}[a(t)] \cdot (1 - P) \cdot \Gamma \cdot B_r(t) + \zeta_{G,s} \cdot E_{R,s}[a(t)] \cdot P \cdot B_s(t) \\ &\quad - \Psi_{K,r} \cdot E_{D,r}[a(t)] \cdot B_r(t) \end{aligned} \quad (12.18)$$

$$\frac{d}{dt}B = B_s(t) + B_r(t) \quad (12.19)$$

where (12.17) and (12.18) describe the rates of change of the sensitive (*s*) and resistant (*r*) subpopulation densities, respectively, over time. P is the probability of mutation and Γ the relative fitness of the sensitive/drug resistant microorganism. Although these models are complex they still do not fully characterize the system under study. Even when fully stochastic, they do not appreciate the role played by rapid up-regulation of resistance mechanisms, *e.g.*, efflux-pumps and inducible beta-lactamases.

12.3.1.8 Host Defense Submodel

The importance of immune (innate and adaptive) response to infection can vary widely depending on the infective microorganism and can be quantified in the nonneutropenic infection model as compared to the neutropenic model (Andes *et al.* 2001; Ariano *et al.* 2005; Drusano *et al.* 1993; Ernst *et al.* 2002; Louie *et al.* 2001; Zinner and Blaser 1986). Innate and adaptive responses are dynamic and also interact. Recruitment of immune responses to the site of infection is microorganism density-dependent and when the combined effects of these mechanisms exceed the microorganism natural growth rate, $\Psi_K \gg \zeta_G$, the host defense alone can eliminate the infection in the absence of drug. The general form of an antiinfective model incorporating host defenses is

$$\frac{d}{dt}B(t) = \zeta_G \cdot E_R[a(t)] \cdot B(t) - \Psi_K \cdot (E_D[a(t)] + E_{\Pi} + E_{\Pi} \circ E_1 + E_1) \cdot B(t) \quad (12.20)$$

where E_{Π} and E_I relates antimicrobial effects of humoral and cellular immunity recruitment at the site of infection, respectively, and $E_{\Pi} \circ E_I$ is the innate-adaptive immunity interaction. The cellular response limits bacterial density by cell-mediated lysis. Similarly, the humoral response reduces bacterial density by antibody mediated neutralization (Bermejo Martin *et al.* 2003; Khangarot *et al.* 1999; Liehl *et al.* 2007). Both the cellular and humoral responses are generated by clonal expansion proportional to the bacterial density with determinable responsiveness (r)/persistence (p) and natural dissipation (d) of immune response, $E_{\Pi,I}$:

$$\frac{d}{dt}E_{\Pi,I} = rpE_{\Pi,I} - dE_{\Pi,I} \quad (12.21)$$

12.4 Antimicrobial Chemotherapy Knowledge Integration, from Bench-to-Bedside

A primary advantage in antimicrobial therapy drug development is the ability to quantitatively determine requisite concentrations of the antiinfective agent required to illicit the effects for which it was designed. Nonclinical (*in vitro* and *in vivo*) data plays a fundamental in the delineation of PK/PD characteristics, including antimicrobial activity spectrum, type of bactericidal activity, and antibacterial potency for rational dose regimen selection.

The bench-to-bedside piece-wise knowledge integration PK/PD platform outlined in Fig. 12.4 replaces the outdated and debatable maximum tolerated dose and empirical paradigms for optimizing efficacy and minimizing toxicity. Furthermore, the PK/PD platform offers a powerful general framework for extrapolation of data across single- or multistep cycles. The generated data from *in vitro* assessment of the MICs for the wild-type strain, clinical isolates and laboratory drug-resistant mutants are subsequently used to design *in vitro* time-kill studies and tested in nonclinical *in vivo* infection experiments.

Extrapolation from *in vitro* to *in vivo* is another fruitful application of the PK/PD paradigm. If an efficacious concentration (EC for stimulation, IC for inhibition) is obtained on the basis of an *in vitro* or ex vivo assay, then a dose can be proposed by incorporating the *in vitro* EC directly into (12.5). The design of *in vivo* nonclinical studies can be optimized by using time-kill data to determine the dose range using the relationship:

$$ED_{50} = \frac{CL_t \cdot EC_{50}}{F} \quad (12.22)$$

where ED_{50} is a hybrid PK/PD variable denoting the drug-dose resulting in 50% maximal efficacy, CL_t is the total plasma clearance, F is bioavailability, and EC_{50} is the concentration need to reach 50% of some maximum effect (a true PD parameter not influenced by PK parameters) in the nonclinical disease model of choice.

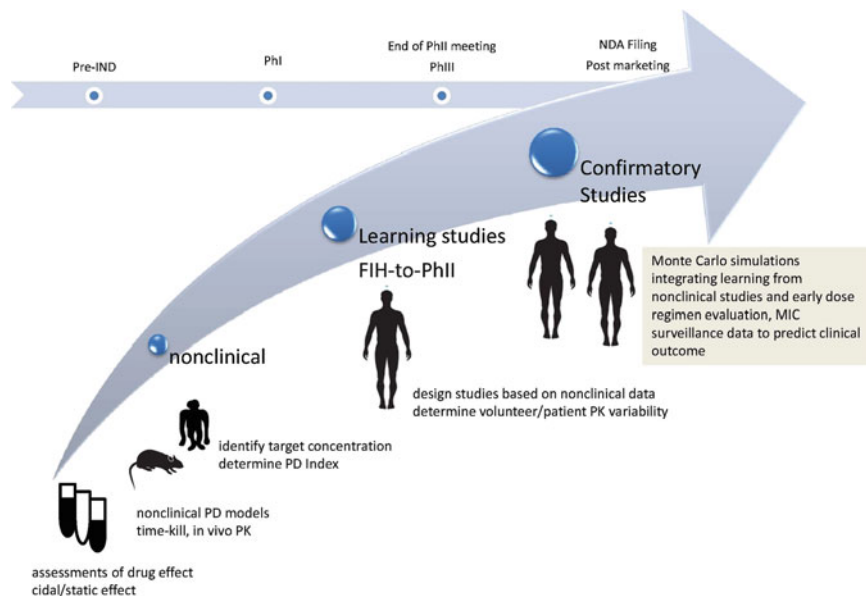


Fig. 12.4 The bench-to-bedside piece-wise knowledge integration PK/PD platform offers a powerful general framework for extrapolation of data across single- or multi-step cycles to support decision-making over the entire life-cycle of an antimicrobial agent

In turn, once a dose-vs.-response relationship has been established in one species, that knowledge can be extrapolated from one species to the next (including humans) by assuming that drug potency is species independent – that is, the same overall body exposure (AUC for plasma concentration) will produce the same effect in both species. This assumption, however, does not always hold up, especially where the rate and extent of drug distribution and/or penetration differs considerably across species. An alternative approach suggested by Rodvold *et al.* (2009) proposes setting exposure targets at the primary infection site from nonclinical studies and subsequently obtaining penetration estimates in man in order to support development decisions with greater certainty.

Of note, within a given nonclinical species, the intraindividual and interindividual PK variability is commonly low (because of this, median group weights are often used to determine mg/kg doses). However, the variability of PD parameters is often higher than that associated with the PK parameter estimates. On the other hand, the primary source of between-species variability is often attributable to PK variability. More precisely, whereas the (free) drug plasma concentration required to elicit a given response is similar between species, the corresponding dose for eliciting the same effect can differ widely (Allen *et al.* 1998; Chambers and Kennedy 1990; Hollenstein *et al.* 2000; Lister *et al.* 1997; Peterson *et al.* 1989). In this regard, the PK/PD approach offers a powerful general framework for interspecies extrapolation, based on AUC-exposure for example:

$$\frac{\text{Dose}_{\text{species 1}}}{\text{CL}_{t \text{ species 1}}} = \text{AUC}_{\text{species 1}} = \frac{\text{Dose}_{\text{species 2}}}{\text{CL}_{t \text{ species 2}}} = \text{AUC}_{\text{species 2}} \quad (12.23)$$

Because it is only the free concentration that is responsible for the ultimate effect, (12.23) is refined to include bioavailability, F , for extravascular administration, and correction for plasma protein binding, for free fraction, f_u :

$$\text{Dose}_{\text{species 2}} = \frac{F_{\text{species 1}} \text{Dose}_{\text{species 1}} \cdot f_{u1} \cdot \text{CL}_{t \text{ species 2}}}{f_{u2} \cdot \text{CL}_{t \text{ species 1}}} \quad (12.24)$$

Thus the PK/PD approach of dose selection avoids disproportionately high doses in laboratory animals based on the surface law (*i.e.*, dosage regimen adjustments on the basis of a power function to the measured body weight, which is taken to represent skin surface area).

12.5 Clinical Application

What is not apparent from Fig. 12.4 is that broad and successful application of the proposed PK/PD platform relies on quantitative establishment of target drug-effect and/or outcome measurement in each drug development minicycle. Thus far, this chapter has focused on microbiological drug-effects (*i.e.*, change in bacterial load over time), however it is also possible to model (and there may be justifiable preference for) dichotomous clinical outcomes (duration of febrile infection or time to fever reduction) and/or other endpoints including safety, etc. Therefore, the effect of ultimate interest in a PK/PD trial may be replaced by a surrogate endpoint. This could be a biomarker (physical, chemical or physiological measurement, etc.) that is objectively measured and validated as an indicator pharmacological response to intervention. In such a case, the surrogate endpoint could plausibly substitute for a clinical endpoint (Biomarkers Definitions Working Group 2001; Colburn 2000; Fridodt-Moller 2002). The clinical validity (relevance) of a surrogate is determined by its statistical association and mechanistic links with a clinical outcome. In addition, the surrogate should have desirable metrological properties, *i.e.*, reproducibility of measurement, objectivity, and high specificity and sensitivity (Biomarkers Definitions Working Group 2001; Hyatt *et al.* 1995). Proposed outcome surrogates that are clearly becoming widely accepted and commonly used in antimicrobial chemotherapy include PK/PD indices such as exposure variable/MIC ratios (*e.g.*, AUC/MIC, C_{max} /MIC, and time above MIC ($T > \text{MIC}$)). These PK/PD indices have been demonstrated in prospective and retrospective trials to predict clinical success, bacteriological cure and/or prevention of resistance (Fridodt-Moller 2002). See Monograph 2, which discusses the basis of PK drivers of response and their implications on dose regimen selection. Probably the most successful surrogate markers of all time have been plasma viral load for HIV and Hepatitis C.

Monograph 2 PK/PD drivers of microbiological response

<p style="text-align: center;">Time > MIC</p>	<p>$R_0 \approx R_1 > R_2$</p> <p>Kill rate is largely independent of drug concentration where drug concentrations exceed MIC. Kill/inhibition rates of concentration-independent agents become saturated at low multiples of the drug concentrations leading to minimum drug activity [typically >4 times the instantaneous bacterial stasis concentration (BSC- concentration of a molecule at which there is no net microorganism-growth or microorganism -kill)] with higher concentrations not providing faster or more extensive antibacterial activity (time driven anti-infective activity).</p> <p>The goal of the dosing regimen of agents in this group is to optimize the duration of exposure by frequent dosing</p>
<p style="text-align: center;">AUC</p>	<p>$R_0 > R_1 > R_2$</p> <p>Kill rate is engendered by drug concentration and time. Time- and concentration-dependent agents have greater kill rates in proportion with the duration and extent that drug concentrations exceed the MIC. Since the integral of the concentration-vs.-time curve itself is the area under the plasma concentration-vs.-time curve (AUC), the AUC/MIC is the most closely PK/PD Index linked to measured microbiological outcome for these agents- AUC driven anti-infective activity).</p> <p>Agents in this group can be dosed frequently or infrequently without substantive differences in microbiological outcome.</p>
<p style="text-align: center;">Peak</p>	<p>$R_0 \approx R_1 \approx R_2 = \dots R_x = 0$</p> <p>Kill rate is engendered by drug concentration. Concentration-dependent agents elicit antibacterial activity when their concentrations are well above the MIC- (concentration driven anti-tumor activity). The maximum serum concentration (Cmax) of the anti-microbial agent is the pharmacodynamic predictor of microbiological outcome for concentration-dependent killing agents. The extent of killing is determined primarily by the maximum achieved serum drug concentration, and subsequent lower levels of drug do not contribute substantially to total kill rate. This phenomenon is associated with persistent effects following drug exposure and is strongly linked to the mechanism of action of the molecule.</p> <p>The goal of the dosing regimen of agents in this group is to provide the maximum tolerable dose.</p>

(continued)

Monograph 2 (continued)

Current state of the art exploration of antimicrobial PK/PD relates treatment (microbiological) outcome to a PK/PD index such as the time above MIC ($T > MIC$, for time-dependent, concentration independent antibiotics), or area under the concentration curve divided by MIC (AUC/MIC), or the maximum concentration divided by MIC (C_{max}/MIC , for concentration dependent, time independent antibiotics). Because of high colinearity between $T > MIC$, AUC, and C_{max} at increasing doses, full factorial experimental design schemes must be explored in order to empirically distinguish the dynamic index that is most correlated with microbiological outcome

When categorical (cured or not cured, febrile or nonfebrile, toxic or nontoxic) endpoints are considered as the selected endpoint of interest, the exposure-vs.-effect curve relates a proportion (cumulative frequency distribution of individuals achieving the target effect) to a continuous variable (PK and/or bacterial density). Logistic regression relates the proportions, p of a dependent variable (observed outcome) to an independent measure of drug input variable X according to the following model:

$$\hat{p} = \frac{e^{a+bX}}{1 + e^{a+bX}} \quad (12.25)$$

where \hat{p} is the probability outcome of an event for a given X (concentration, AUC, dose, etc.), where a is a location parameter, and b is a scale (slope) parameter. To see what this function will look like for the logit transform of \hat{p} , we first evaluate the probability of no event:

$$1 - \hat{p} = \frac{1 + e^{a+bX} - e^{a+bX}}{1 + e^{a+bX}} = \frac{1}{1 + e^{a+bX}} \quad (12.26)$$

in order to determine the odds (likelihood) ratio describing the relative risk of response:

$$\frac{\hat{p}}{1 - \hat{p}} = \frac{e^{a+bX}/(1 + e^{a+bX})}{1/(1 + e^{a+bX})} = e^{a+bX} \quad (12.27)$$

Consequently the natural logarithm of the odds ratio gives the logit(L) of \hat{p} :

$$\ln\left(\frac{\hat{p}}{1 - \hat{p}}\right) = a + bX \quad (12.28)$$

where the logit(\hat{p}) = $\ln[\hat{p}/(1 - \hat{p})]$ is related to X by simple linear regression. Thus the logit is linear in its parameters (and may be continuous), and it ranges from $-\infty$ to $+\infty$, rather than from 0 to 1. Moreover, the error around the line is distributed binomially rather than normally. Therefore, the maximum-likelihood method is

used to fit a regression line to the logit-transform data rather than the least-squares method. A typical logistic regression analysis is complex and in practice can be carried out iteratively only by computer to yield estimates for a and b , as well as their standard errors that make the observed values most probable. Furthermore, the logit can be written as a more general linear function, allowing expansion of the model into a more advanced logistic model that includes several continuous or categorical independent variables (*e.g.*, sex- b_1 , age- b_2 , metabolic status- b_n) and their interactions:

$$\ln\left(\frac{\hat{p}}{1-\hat{p}}\right) = a + b_1X_1 + b_2X_2 + \cdots + b_nX_n \quad (12.29)$$

Significance of the results is determined from the ratio of the estimated coefficients over the standard errors of the estimates, or alternatively the ratios are evaluated as normal deviates.

Once the treatment target response has been defined and a modeling framework established, simulation should be performed to support decision-making, challenge and explore explicit and implicit assumptions. The requisite level of complexity in the simulation activity is driven by the question(s) being addressed. Following nonlinear mixed effects modeling of available data, stochastic (Monte Carlo) simulation is almost always preferable over deterministic simulation for clinical team decision-support. Variability is introduced into the underlying model from random draws driven by the statistical (random and residual effects) model [$X \sim (\mu, \sigma^2)$], where X is a random parameter draw from a log-normal distribution with mean μ and variance σ^2 . An additional level of uncertainty around the estimated may be included into simulation in order to increase confidence in simulation output. In this case, simulations are performed by first drawing μ , from $\mu \sim \mu_\mu, \sigma_\mu^2$, *i.e.*, the fixed effect parameter hyperparameter is drawn from a normal distribution with mean μ_μ and variance σ_μ^2 according to central limit theory. Thus, a simulated trial population could be generated following a fixed dose regimen, in order to determine the proportion of simulated subjects that exceed an exposure/MIC ratio target (AUC/MIC ratio value, for example). If a small proportion of patients exceed the target PK/PD index then a dose-increase may be warranted (Fig. 12.5).

Monte Carlo simulation allows the incorporation of all sources of potential variability of drug exposure and drug effect encountered when an agent is administered to a large population. Monte Carlo simulation methods have been widely used to integrate knowledge in antimicrobial chemotherapy (Bradley *et al.* 2003; Deshpande *et al.* 2010; Drusano *et al.* 2000, 2006; Dudley and Ambrose 2002; Jumbe *et al.* 2003; Zelenitsky *et al.* 2005). Of note, Monte Carlo simulations are relatively easy to perform across a wide platform on integrated data sources and submodels across a platform, provided the underlying models are well defined. However, even when multiple knowledge-sources or submodels are correlated, covariances of off-diagonal coefficients are often ignored and carryover

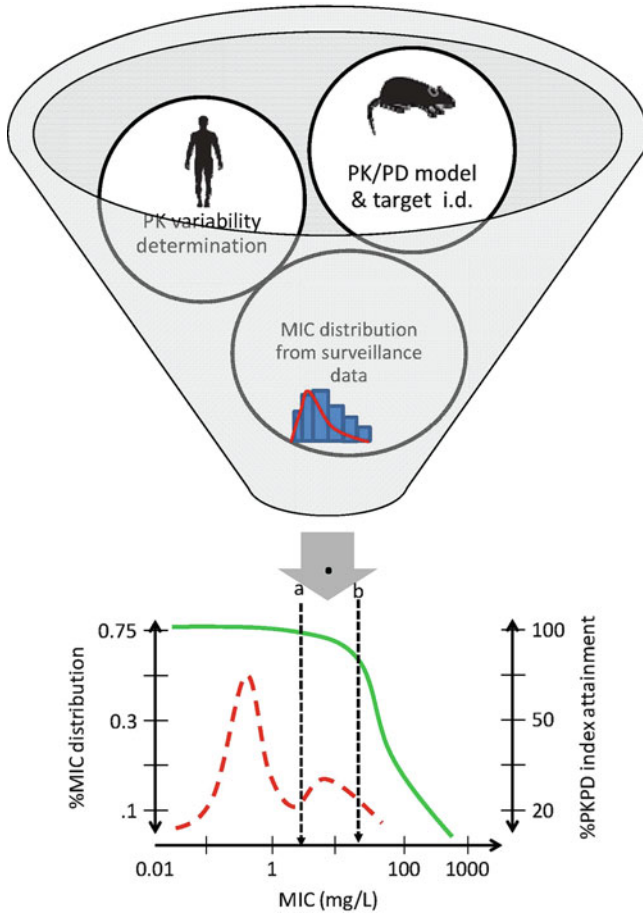


Fig. 12.5 Most chemotherapeutic antimicrobials can leverage nonclinical (*in vitro* and *in vivo*) data extensively. Information regarding the microbiological effect concentration, the shape of the drug-input microbiological-effect forcing function, the microbiological efficacy/toxicity window, and learned between- (and within-) patient PK and PD (exposure AND effect) variability is integrated to determine the proportion of patients that can be adequately treated by a drug to make informed dose-regimen recommendations. Dose recommendation decisions are supported by determination of the inflection points (a and b) integrating clinical surveillance data and the target drug exposure

assumptions are inadvertently made on the cumulative effect of known sources of variability. Therefore, a common assumption in Monte Carlo simulations, especially across a knowledge-integration platform such as presented here, is that all parameter estimates follow normal/log-normal distributions, with correlation/covariance coefficients of zero, neither of which are typical in any interaction. It is therefore important for data analysts and teams to realize that these underlying assumptions can lead to problems with analyses and interpretation.

Once the knowledge-base has been integrated through simulation, statistical tools such as Classification and regression tree (CART) analysis are powerful methods to examine how different factors interact and can influence outcome across entire simulated databases. In the area of anti-infective CTS, CART is particularly useful for determining factors that will lead to potential failure (breakpoint) of an anti-infective agent (Ambrose *et al.* 2007; Dalla Costa and Derendorf 1996; Drusano 2001; Drusano *et al.* 2004; Dudley and Ambrose 2002; Jacobs 2003; Meagher *et al.* 2007; Zelenitsky *et al.* 2005). It would be particularly interesting to see a retrospective study performed in which simultaneous PK/PD/clinical outcome analysis is performed in order to confirm simulation-based breakpoint determinations, performed prospectively by others, such as in studies of levofloxacin in both community-acquired infections and nosocomial pneumonia and fluoroquinolone therapy of pneumococcal respiratory tract infections (Ambrose *et al.* 2001; Drusano *et al.* 2004; Dudley and Ambrose 2002; Madaras-Kelly *et al.* 1996; Montgomery *et al.* 2001; Paterson and Bonomo 2005).

12.6 Summary

Antimicrobial *pharmactuarial science* is an evolving discipline that integrates pharmacometrics, microbiology and pharmacology, benefit-vs.-risk analysis, which is currently seeing tremendous growth. This domain benefits directly from the advantage of being able to directly measure the effective concentration and/or potency of the antimicrobial agent for the target pathogen. Following delineation of the effect-vs.-exposure relationship using data from nonclinical studies and measures of PK/PD variability from early clinical trials in normal volunteers and patients, it is possible to determine drug dosing regimens that have a high likelihood of achieving the desired goals of therapy, while also having an acceptably low probability of concentration-related toxicity and emergence of resistance. In this way the benefit-vs.-risk for the treated patient is maximized.

References

- Allen MC, Shah TS, Day WW (1998) Rapid determination of oral pharmacokinetics and plasma free fraction using cocktail approaches: methods and application. *Pharm Res* 15(1):93–97
- Alonso A, Campanario E, Martinez JL (1999) Emergence of multidrug-resistant mutants is increased under antibiotic selective pressure in *Pseudomonas aeruginosa*. *Microbiology* 145(Pt 10):2857–2862
- Ambrose PG, Bhavnani SM, Rubino CM, Louie A, Gumbo T, Forrest A, Drusano GL (2007) Pharmacokinetics-pharmacodynamics of antimicrobial therapy: it's not just for mice anymore. *Clin Infect Dis* 44(1):79–86

- Ambrose PG, Grasela DM, Grasela TH, Passarell J, Mayer HB, Pierce PF (2001) Pharmacodynamics of fluoroquinolones against *Streptococcus pneumoniae* in patients with community-acquired respiratory tract infections. *Antimicrob Agents Chemother* 45(10):2793–2797
- Andes DR, Craig WA (1999) Pharmacokinetics and pharmacodynamics of antibiotics in meningitis. *Infect Dis Clin North Am* 13(3):595–618
- Andes D, Stamsted T, Conklin R (2001) Pharmacodynamics of amphotericin B in a neutropenic-mouse disseminated-candidiasis model. *Antimicrob Agents Chemother* 45(3):922–926
- Ariano RE, Nyhlen A, Donnelly JP, Sitar DS, Harding GK, Zelenitsky SA (2005) Pharmacokinetics and pharmacodynamics of meropenem in febrile neutropenic patients with bacteremia. *Ann Pharmacother* 39(1):32–38
- Barclay ML, Begg EJ (2001) Aminoglycoside adaptive resistance: importance for effective dosage regimens. *Drugs* 61(6):713–721
- Beaber JW, Hochhut B, Waldor MK (2004) SOS response promotes horizontal dissemination of antibiotic resistance genes. *Nature* 427(6969):72–74
- Bermejo Martin JF, Jimenez JL, Munoz-Fernandez A (2003) Pentoxifylline and severe acute respiratory syndrome (SARS): a drug to be considered. *Med Sci Monit* 9(6):SR29–SR34
- Biomarkers Definitions Working Group (2001) Biomarkers and surrogate endpoints: preferred definitions and conceptual framework. *Clin Pharmacol Ther* 69(3):89–95
- Black JW, Leff P, Shankley NP (1985) An operational model of pharmacological agonism: the effect of E/[A] curve shape on agonist dissociation constant estimation. *Br J Pharmacol* 84(2):561–571
- Blaser J, Stone BB, Zinner SH (1985) Efficacy of intermittent versus continuous administration of netilmicin in a two-compartment *in vitro* model. *Antimicrob Agents Chemother* 27(3):343–349
- Boik JC, Newman RA, Boik RJ (2008) Quantifying synergism/antagonism using nonlinear mixed-effects modeling: a simulation study. *Stat Med* 27(7):1040–1061
- Boshoff HI, Reed MB, Barry CE III, Mizrahi V (2003) DnaE2 polymerase contributes to *in vivo* survival and the emergence of drug resistance in *Mycobacterium tuberculosis*. *Cell* 113(2):183–193
- Boucher AN, Tam VH (2006) Mathematical formulation of additivity for antimicrobial agents. *Diagn Microbiol Infect Dis* 55(4):319–325
- Bradley JS, Dudley MN, Drusano GL (2003) Predicting efficacy of anti-infectives with pharmacodynamics and Monte Carlo simulation. *Pediatr Infect Dis J* 22(11):982–992; quiz 993–985
- Bull JJ, Levin BR, DeRouin T, Walker N, Bloch CA (2002) Dynamics of success and failure in phage and antibiotic therapy in experimental infections. *BMC Microbiol* 2:35
- Cappelletty DM, Rybak MJ (1996) Comparison of methodologies for synergism testing of drug combinations against resistant strains of *Pseudomonas aeruginosa*. *Antimicrob Agents Chemother* 40(3):677–683
- Centers for Disease Control and Prevention (2006) Emergence of *Mycobacterium tuberculosis* with extensive resistance to second-line drugs – worldwide, 2000–2004. *MMWR Morb Mortal Wkly Rep* 55(11):301–305
- Chambers HF, Kennedy S (1990) Effects of dosage, peak and trough concentrations in serum, protein binding, and bactericidal rate on efficacy of teicoplanin in a rabbit model of endocarditis. *Antimicrob Agents Chemother* 34(4):510–514
- Chen YH, Peng CF, Lu PL, Tsai JJ, Chen TP (2004) *In vitro* activities of antibiotic combinations against clinical isolates of *Pseudomonas aeruginosa*. *Kaohsiung J Med Sci* 20(6):261–267
- Chopra I, Roberts M (2001) Tetracycline antibiotics: mode of action, applications, molecular biology, and epidemiology of bacterial resistance. *Microbiol Mol Biol Rev* 65:232–260
- Chung P, McNamara PJ, Campion JJ, Evans ME (2006) Mechanism-based pharmacodynamic models of fluoroquinolone resistance in *Staphylococcus aureus*. *Antimicrob Agents Chemother* 50(9):2957–2965
- Cirz RT, Chin JK, Andes DR, de Crecy-Lagard V, Craig WA, Romesberg FE (2005) Inhibition of mutation and combating the evolution of antibiotic resistance. *PLoS Biol* 3(6):e176

- Cirz RT, Romesberg FE (2006) Induction and inhibition of ciprofloxacin resistance-conferring mutations in hypermutator bacteria. *Antimicrob Agents Chemother* 50(1):220–225
- Coates A, Hu Y, Bax R, Page C (2002) The future challenges facing the development of new antimicrobial drugs. *Nat Rev Drug Discov* 1(11):895–910
- Colburn WA (2000) Optimizing the use of biomarkers, surrogate endpoints, and clinical endpoints for more efficient drug development. *J Clin Pharmacol* 40(12 Pt 2):1419–1427
- Craig WA (1998a) Choosing an antibiotic on the basis of pharmacodynamics. *Ear Nose Throat J* 77(6 Suppl):7–11; discussion 11–12
- Craig WA (1998b) Pharmacokinetic/pharmacodynamic parameters: rationale for antibacterial dosing of mice and men. *Clin Infect Dis* 26(1):1–10; quiz 11–12
- Craig WA, Ebert SC (1990) Killing and regrowth of bacteria *in vitro*: a review. *Scand J Infect Dis Suppl* 74:63–70
- Craig WA, Redington J, Ebert SC (1991) Pharmacodynamics of amikacin *in vitro* and in mouse thigh and lung infections. *J Antimicrob Chemother* 27(Suppl):S29–S40
- Dagan R (2003) Achieving bacterial eradication using pharmacokinetic/pharmacodynamic principles. *Int J Infect Dis* 7(Suppl 1):S21–S26
- Dalla Costa T, Derendorf H (1996) AUC – a general target for the optimization of dosing regimens of antibiotics? *Ann Pharmacother* 30(9):1024–1028
- Dalla Costa T, Nolting A, Rand K, Derendorf H (1997) Pharmacokinetic-pharmacodynamic modelling of the *in vitro* anti-infective effect of piperacillin-tazobactam combinations. *Int J Clin Pharmacol Ther* 35(10):426–433
- Davies J (1994) Inactivation of antibiotics and the dissemination of resistance genes. *Science* 264:375–382
- Davis BD, Maas WK (1952) Analysis of the biochemical mechanism of drug resistance in certain bacterial mutants. *Proc Natl Acad Sci USA* 38(9):775–785
- Dean CR, Visalli MA, Projan SJ, Sum PE, Bradford PA (2003) Efflux-mediated resistance to tigecycline (GAR-936) in *Pseudomonas aeruginosa* PAO1. *Antimicrob Agents Chemother* 47:972–978
- Deshpande D, Srivastava S, Meek C, Leff R, Hall GS, Gumbo T (2010) Moxifloxacin pharmacokinetics/pharmacodynamics and optimal dose and susceptibility breakpoint identification for the treatment of disseminated *Mycobacterium avium* infection. *Antimicrob Agents Chemother* 54:2534–2539
- Drlica K, Zhao X (1997) DNA gyrase, topoisomerase IV, and the 4-quinolones. *Microbiol Mol Biol Rev* 61(3):377–392
- Drusano GL (1990) Human pharmacodynamics of beta-lactams, aminoglycosides and their combination. *Scand J Infect Dis Suppl* 74:235–248
- Drusano GL (1998a) Factors influencing the emergence of resistance to indinavir: role of virologic, immunologic, and pharmacologic variables. *J Infect Dis* 178:360–367
- Drusano GL (1998b) Infection in the intensive care unit: beta-lactamase-mediated resistance among Enterobacteriaceae and optimal antimicrobial dosing. *Clin Infect Dis* 27(Suppl1): S111–S116
- Drusano GL (2001) Use of preclinical data for the choice of a Phase II/III dose for evernimicin with application to decision support for identification of a preclinical MIC breakpoint. *Antimicrob Agents Chemother* 45:13–22
- Drusano GL (2004) Antimicrobial pharmacodynamics: critical interactions of “bug and drug”. *Nat Rev Microbiol* 2(4):289–300
- Drusano GL, Johnson DE, Rosen M, Standiford HC (1993) Pharmacodynamics of a fluoroquinolone antimicrobial agent in a neutropenic rat model of *Pseudomonas sepsis*. *Antimicrob Agents Chemother* 37(3):483–490
- Drusano GL, Prichard M, Bilello PA, Bilello JA (1996) Modeling combinations of antiretroviral agents *in vitro* with integration of pharmacokinetics: guidance in regimen choice for clinical trial evaluation. *Antimicrob Agents Chemother* 40(5):1143–1147
- Drusano GL, D’Argenio DZ, Preston SL, Barone C, Symonds W, LaFon S, Rogers M, Prince W, Bye A, Bilello JA (2000) Use of drug effect interaction modeling with Monte Carlo simulation

- to examine the impact of dosing interval on the projected antiviral activity of the combination of abacavir and amprenavir. *Antimicrob Agents Chemother* 44(6):1655–1659
- Drusano GL, Moore KHP, Kleim JP, Prince W, Bye A (2002) Rational dose selection for a non-nucleoside reverse transcriptase inhibitor through the use of population pharmacokinetic modeling and Monte Carlo simulation. *Antimicrob Agents Chemother* 46:913–916
- Drusano GL, Preston SL, Fowler C, Corrado M, Weisinger B, Kahn J (2004) Relationship between fluoroquinolone area under the curve: minimum inhibitory concentration ratio and the probability of eradication of the infecting pathogen, in patients with nosocomial pneumonia. *J Infect Dis* 189(9):1590–1597
- Drusano GL, Louie A, Deziel M, Gumbo T (2006) The crisis of resistance: identifying drug exposures to suppress amplification of resistant mutant subpopulations. *Clin Infect Dis* 42(4):525–532
- Drusano GL, Liu W, Brown DL, Rice LB, Louie A (2009) Impact of short-course quinolone therapy on susceptible and resistant populations of *Staphylococcus aureus*. *J Infect Dis* 199(2):219–226
- Dudley MN, Ambrose PG. Monte Carlo PK-PD Simulation and New Cefotaxime (CTX), Ceftriaxone (CRO), and Cefepime (FEP) Susceptibility Breakpoints for *S. pneumoniae*, including Strains with Reduced Susceptibility to Penicillin. *Abstr Intersci Conf Antimicrob Agents Chemother Intersci Conf Antimicrob Agents Chemother*. 2002 Sep 27–30; 42: abstract no. A-635. Interscience Conference on Antimicrobial Agents and Chemotherapy (42nd: 2002: San Diego, Calif.)
- Eagle H (1948) The paradoxically retarded bactericidal activity of penicillin at high concentrations *in vitro* and *in vivo*. *J Clin Invest* 27(4):531
- Eagle H (1949) The effect of the size of the inoculum and the age of the infection on the curative dose of penicillin in experimental infections with streptococci, pneumococci, and *Treponema pallidum*. *J Exp Med* 90(6):595–607
- Eagle H (1952) Experimental approach to the problem of treatment failure with penicillin. I. Group A streptococcal infection in mice. *Am J Med* 13(4):389–399
- Eagle H (1954) The multiple mechanisms of penicillin resistance. *J Bacteriol* 68(5):610–616
- Eagle H (1955) The mechanism of action of penicillin. *J Lancet* 75(1):1–6
- Eagle H, Fleischman R, Levy M (1953a) Continuous vs. discontinuous therapy with penicillin; the effect of the interval between injections on therapeutic efficacy. *N Engl J Med* 248(12):481–488
- Eagle H, Fleischman R, Levy M (1953b) On the duration of penicillin action in relation to its concentration in the serum. *J Lab Clin Med* 41(1):122–132
- Ernst EJ, Klepser ME, Petzold CR, Doern GV (2002) Evaluation of survival and pharmacodynamic relationships for five fluoroquinolones in a neutropenic murine model of pneumococcal lung infection. *Pharmacotherapy* 22(4):463–470
- Fidler M, Kern SE (2006) Flexible interaction model for complex interactions of multiple anesthetics. *Anesthesiology* 105(2):286–296
- Firsov AA, Shevchenko AA, Vostrov SN, Zinner SH (1998) Inter- and intraquinolone predictors of antimicrobial effect in an *in vitro* dynamic model: new insight into a widely used concept. *Antimicrob Agents Chemother* 42(3):659–665
- Firsov AA, Vasilov RG, Vostrov SN, Kononenko OV, Lubenko IY, Zinner SH (1999) Prediction of the antimicrobial effects of trovafloxacin and ciprofloxacin on staphylococci using an *in vitro* dynamic model. *J Antimicrob Chemother* 43(4):483–490
- Fish DN, Piscitelli SC, Danziger LH (1995) Development of resistance during antimicrobial therapy: a review of antibiotic classes and patient characteristics in 173 studies. *Pharmacotherapy* 15(3):279–291
- Frimodt-Moller N (2002) How predictive is PK/PD for antibacterial agents? *Int J Antimicrob Agents* 19(4):333–339
- Giamarellou H (1986) Aminoglycosides plus beta-lactams against gram-negative organisms. Evaluation of *in vitro* synergy and chemical interactions. *Am J Med* 80(6B):126–137
- Gniadkowski M (2008) Evolution of extended-spectrum beta-lactamases by mutation. *Clin Microbiol Infect* 14(Suppl 1):11–32

- Goutelle S, Maurin M, Rougier F, Barbaut X, Bourguignon L, Ducher M, Maire P (2008) The Hill equation: a review of its capabilities in pharmacological modelling. *Fundam Clin Pharmacol* 22(6):633–648
- Greco WR, Park HS, Rustum YM (1990) Application of a new approach for the quantitation of drug synergism to the combination of cis-diamminedichloroplatinum and 1-beta-D-arabinofuranosylcytosine. *Cancer Res* 50(17):5318–5327
- Gross M, Burli R, Jones P, Garcia M, Batiste B, Kaizerman J, Moser H, Jiang V, Hoch U, Duan JX, Tanaka R, Johnson KW (2003) Pharmacology of novel heteroaromatic polycycle antibacterials. *Antimicrob Agents Chemother* 47(11):3448–3457
- Guerillot F, Carret G, Flandrois JP (1993) Mathematical model for comparison of time-killing curves. *Antimicrob Agents Chemother* 37(8):1685–1689
- Gumbo T, Louie A, Deziel MR, Drusano GL (2005) Pharmacodynamic evidence that ciprofloxacin failure against tuberculosis is not due to poor microbial kill but to rapid emergence of resistance. *Antimicrob Agents Chemother* 49(8):3178–3181
- Gumbo T, Louie A, Deziel MR, Liu W, Parsons LM, Salfinger M, Drusano GL (2007) Concentration-dependent Mycobacterium tuberculosis killing and prevention of resistance by rifampin. *Antimicrob Agents Chemother* 51(11):3781–3788
- Hawser SP (2006) Antibacterial drug discovery and development [mdash] SRI's 11th annual summit. *IDrugs* 9:390–393
- Hirata T, Saito A, Nishino K, Tamura N, Yamaguchi A (2004) Effects of efflux transporter genes on susceptibility of Escherichia coli to tigecycline (GAR-936). *Antimicrob Agents Chemother* 48:2179–2184
- Hollenstein U, Brunner M, Mayer BX, Delacher S, Erovic B, Eichler HG, Muller M (2000) Target site concentrations after continuous infusion and bolus injection of cefpirome to healthy volunteers. *Clin Pharmacol Ther* 67(3):229–236
- Hooper DC (2000) Mechanisms of action and resistance of older and newer fluoroquinolones. *Clin Infect Dis* 31(Suppl 2):S24–S28
- Hopwood DA (1985) Production of “hybrid” antibiotics by genetic engineering. *Nature* 314:642–644
- Hyatt JM, McKinnon PS, Zimmer GS, Schentag JJ (1995) The importance of pharmacokinetic/pharmacodynamic surrogate markers to outcome. Focus on antibacterial agents. *Clin Pharmacokinet* 28(2):143–160
- Jacobs MR (2003) How can we predict bacterial eradication? *Int J Infect Dis* 7(Suppl 1):S13–S20
- Jacobs MR (2004) Building in efficacy: developing solutions to combat drug-resistant *S. pneumoniae*. *Clin Microbiol Infect* 10(Suppl 2):18–27
- Jumbe N, Louie A, Leary R, Liu W, Deziel MR, Tam VH, Bachhawat R, Freeman C, Kahn JB, Bush K, Dudley MN, Miller MH, Drusano GL (2003) Application of a mathematical model to prevent *in vivo* amplification of antibiotic-resistant bacterial populations during therapy. *J Clin Invest* 112(2):275–285
- Jumbe NL, Louie A, Miller MH, Liu W, Deziel MR, Tam VH, Bachhawat R, Drusano GL (2006) Quinolone efflux pumps play a central role in emergence of fluoroquinolone resistance in Streptococcus pneumoniae. *Antimicrob Agents Chemother* 50(1):310–317
- Keil S, Wiedemann B (1995) Mathematical corrections for bacterial loss in pharmacodynamic *in vitro* dilution models. *Antimicrob Agents Chemother* 39(5):1054–1058
- Khangarot BS, Rathore RS, Tripathi DM (1999) Effects of chromium on humoral and cell-mediated immune responses and host resistance to disease in a freshwater catfish, *Sacchariscus fossilis* (Bloch). *Ecotoxicol Environ Saf* 43(1):11–20
- King TC, Schlessinger D, Krogstad DJ (1981) The assessment of antimicrobial combinations. *Rev Infect Dis* 3(3):627–633
- Krylov VN (2003) Role of horizontal gene transfer by bacteriophages in the origin of pathogenic bacteria. *Genetika* 39(5):595–620
- Kucers A, Bennett NM (1987) Vancomycin. In: Kucers A, Bennett NM, eds. *The Use of Antibiotics: A Comprehensive Review with Clinical Emphasis*. 4th ed. Philadelphia, JB Lippincott Co, pp 1045–1068

- LeClerc JE, Li B, Payne WL, Cebula TA (1996) High mutation frequencies among *Escherichia coli* and *Salmonella* pathogens. *Science* 274(5290):1208–1211
- Lee JJ, Kong M (2009) Confidence intervals of interaction index for assessing multiple drug interaction. *Stat Biopharm Res* 1(1):4–17
- Lee JJ, Kong M, Ayers GD, Lotan R (2007) Interaction index and different methods for determining drug interaction in combination therapy. *J Biopharm Stat* 17(3):461–480
- Liehl B, Hlavaty J, Moldzio R, Tonar Z, Unger H, Salmons B, Gunzburg WH, Renner M (2007) Simian immunodeficiency virus vector pseudotypes differ in transduction efficiency and target cell specificity in brain. *Gene Ther* 14(18):1330–1343
- Lipsitch M, Samore MH (2002) Antimicrobial use and antimicrobial resistance: a population perspective. *Emerg Infect Dis* 8(4):347–354
- Lister PD, Pong A, Chartrand SA, Sanders CC (1997) Rationale behind high-dose amoxicillin therapy for acute otitis media due to penicillin-nonsusceptible pneumococci: support from *in vitro* pharmacodynamic studies. *Antimicrob Agents Chemother* 41(9):1926–1932
- Livermore DM (2002) Multiple mechanisms of antimicrobial resistance in *Pseudomonas aeruginosa*: our worst nightmare? *Clin Infect Dis* 34(5):634–640
- Louie A, Kaw P, Liu W, Jembe N, Miller MH, Drusano GL (2001) Pharmacodynamics of daptomycin in a murine thigh model of *Staphylococcus aureus* infection. *Antimicrob Agents Chemother* 45(3):845–851
- MacGowan AP, Wootton M, Hedges AJ, Bowker KE, Holt HA, Reeves DS (1996) A new time-kill method of assessing the relative efficacy of antimicrobial agents alone and in combination developed using a representative beta-lactam, aminoglycoside and fluoroquinolone. *J Antimicrob Chemother* 38(2):193–203
- Madaras-Kelly KJ, Ostergaard BE, Hovde LB, Rotschafer JC (1996) Twenty-four-hour area under the concentration-time curve/MIC ratio as a generic predictor of fluoroquinolone antimicrobial effect by using three strains of *Pseudomonas aeruginosa* and an *in vitro* pharmacodynamic model. *Antimicrob Agents Chemother* 40(3):627–632
- Mager DE, Wyska E, Jusko WJ (2003) Diversity of mechanism-based pharmacodynamic models. *Drug Metab Dispos* 31(5):510–518
- McKenzie GJ, Harris RS, Lee PL, Rosenberg SM (2000) The SOS response regulates adaptive mutation. *Proc Natl Acad Sci U S A* 97(12):6646–6651
- Meagher AK, Passarell JA, Cirincione BB, Van Wart SA, Liolios K, Babinchak T, Ellis-Grosse EJ, Ambrose PG (2007) Exposure-response analyses of tigecycline efficacy in patients with complicated skin and skin-structure infections. *Antimicrob Agents Chemother* 51(6):1939–1945
- Miller C, Thomsen LE, Gaggero C, Mosseri R, Ingmer H, Cohen SN (2004) SOS response induction by beta-lactams and bacterial defense against antibiotic lethality. *Science* 305(5690):1629–1631
- Montgomery MJ, Beringer PM, Aminimanizani A, Louie SG, Shapiro BJ, Jelliffe R, Gill MA (2001) Population pharmacokinetics and use of Monte Carlo simulation to evaluate currently recommended dosing regimens of ciprofloxacin in adult patients with cystic fibrosis. *Antimicrob Agents Chemother* 45(12):3468–3473
- Mwangi MM, Wu SW, Zhou Y, Sieradzki K, de Lencastre H, Richardson P, Bruce D, Rubin E, Myers E, Siggia ED, Tomasz A (2007) Tracking the *in vivo* evolution of multidrug resistance in *Staphylococcus aureus* by whole-genome sequencing. *Proc Natl Acad Sci USA* 104(22):9451–9456
- Neu HC (1992) The crisis in antibiotic resistance. *Science* 257(5073):1064–1073
- Palmer SM, Kang SL, Cappelletty DM, Rybak MJ (1995) Bactericidal killing activities of cefepime, ceftazidime, cefotaxime, and ceftriaxone against *Staphylococcus aureus* and beta-lactamase-producing strains of *Enterobacter aerogenes* and *Klebsiella pneumoniae* in an *in vitro* infection model. *Antimicrob Agents Chemother* 39(8):1764–1771
- Paterson DL, Bonomo RA (2005) Extended-spectrum beta-lactamases: a clinical update. *Clin Microbiol Rev* 18(4):657–686

- Peck CC, Cross JT (2007) Getting the dose right: facts, a blueprint, and encouragements. *Clin Pharmacol Ther* 82(1):12–14
- Peterson LR, Moody JA, Fasching CE, Gerding DN (1989) Influence of protein binding on therapeutic efficacy of cefoperazone. *Antimicrob Agents Chemother* 33(4):566–568
- Preston SL, Drusano GL, Berman AL, Fowler CL, Chow AT, Dornseif B, Reichl V, Natarajan J, Corrado M (1998) Pharmacodynamics of levofloxacin: a new paradigm for early clinical trials. *JAMA* 279(2):125–129
- Prichard MN, Prichard LE, Shipman C Jr (1993) Strategic design and three-dimensional analysis of antiviral drug combinations. *Antimicrob Agents Chemother* 37(3):540–545
- Rodvold KA, Nicolau DP, Lodise TP, Khashab M, Noel GJ, Kahn JB, Gotfried M, Murray SA, Nicholson S, Laohavaleeson S, Tessier PR, Drusano GL (2009) Identifying exposure targets for treatment of staphylococcal pneumonia with ceftobiprole. *Antimicrob Agents Chemother* 53(8):3294–3301
- Srivastava S, Musuka S, Sherman C, Meek C, Leff R, Gumbo T (2010) Efflux-pump-derived multiple drug resistance to ethambutol monotherapy in *Mycobacterium tuberculosis* and the pharmacokinetics and pharmacodynamics of ethambutol. *J Infect Dis* 201(8):1225–1231
- Tam VH, Schilling AN, Nikolaou M (2005) Modelling time-kill studies to discern the pharmacodynamics of meropenem. *J Antimicrob Chemother* 55(5):699–706
- Van Der Graaf PH, Danhof M (1997) On the reliability of affinity and efficacy estimates obtained by direct operational model fitting of agonist concentration-effect curves following irreversible receptor inactivation. *J Pharmacol Toxicol Methods* 38(2):81–85
- Van der Graaf PH, Schoemaker RC (1999) Analysis of asymmetry of agonist concentration-effect curves. *J Pharmacol Toxicol Methods* 41(2–3):107–115
- Wainberg MA, Friedland G (1998) Public health implications of antiretroviral therapy and HIV drug resistance. *JAMA* 279(24):1977–1983
- Weigel LM, Clewell DB, Gill SR, Clark NC, McDougal LK, Flannagan SE, Kolonay JF, Shetty J, Killgore GE, Tenover FC (2003) Genetic analysis of a high-level vancomycin-resistant isolate of *Staphylococcus aureus*. *Science* 302(5650):1569–1571
- Whitehead A, Whitehead J, Todd S, Zhou Y, Smith MK (2008) Fitting models for the joint action of two drugs using SAS. *Pharm Stat* 7(4):272–284
- Williams JB (1996) Drug efflux as a mechanism of resistance. *Br J Biomed Sci* 53:290–293
- Zelenitsky S, Ariano R, Harding G, Forrest A (2005) Evaluating ciprofloxacin dosing for *Pseudomonas aeruginosa* infection by using clinical outcome-based Monte Carlo simulations. *Antimicrob Agents Chemother* 49(10):4009–4014
- Zhang Y, Young D (1994) Molecular genetics of drug resistance in *Mycobacterium tuberculosis*. *J Antimicrob Chemother* 34(3):313–319
- Zhi J, Nightingale CH, Quintiliani R (1986) A pharmacodynamic model for the activity of antibiotics against microorganisms under nonsaturable conditions. *J Pharm Sci* 75(11):1063–1067
- Zinner SH, Blaser J (1986) *In vitro* models in the study of antibiotic therapy of infections in neutropenic patients. *Am J Med* 80(5C):40–44

Chapter 13

PKPD and Disease Modeling: Concepts and Applications to Oncology

Oscar E. Della Pasqua

Abstract Despite the transition from chemotherapy with cytotoxic and cytostatic drugs to targeted therapy with monoclonal antibodies, clinical decisions regarding the benefit of pharmacological interventions still rely on the concept of a maximum tolerated dose (MTD). In this chapter, it is shown that a model-based approach can be used in oncology to optimize dose selection and characterize drug effect on tumor growth, overall survival and safety. Furthermore, modeling and simulation also provides insight into the underlying mechanisms of action, enabling translation of the differences in pharmacology, safety and disease processes from preclinical experiments to clinical trials. A paradigm shift is proposed to bring the benefits of model-based drug development to cancer patients, in which biomarkers of safety and prognostic markers of overall survival are assessed to predict treatment outcome and disease progression.

13.1 General Concepts and History of Model-Based Research in Oncology

Models aim to represent and simplify complex systems. The accurate representation and simplification of the complexity and heterogeneity of biological systems have characterized oncology modeling efforts in clinical pharmacology and translational medicine research (Rew 2000a; Quaranta *et al.* 2005). Although clinical oncologists can appreciate the value and potential implications of experimental models, the justification for the use of mathematical models remains unclear to most of them. Mathematical modeling can be a powerful tool for analyzing

O.E. Della Pasqua (✉)

Division of Pharmacology, Leiden-Amsterdam Center for Drug Research,
Gorlaeus Laboratories, Einsteinweg 55, 2300 RA Leiden, The Netherlands
and

Clinical Pharmacology & Discovery Medicine, GlaxoSmithKline
R & D, 1-3 Ironbridge Road Stockley Park, UB11 1BT Uxbridge, United Kingdom
e-mail: odp72514@gsk.com

biological problems, allowing one to develop and test hypotheses which can lead to a better understanding of the biological process itself. Most importantly, it can provide quantitative measures of biological functions that can be used for the purposes of prediction and prognosis. It is essential to understand that the mathematics is dictated by the biology and not vice-versa.

Cancer research has been a fertile ground for mathematical modeling (Swanson *et al.* 2003). Models were initially used to conceptualize the simple exponential growth of solid tumors, which show cell accretion at a constant rate: 1 cell, 2 cells, 4 cells, 8 cells, etc. This concept was advanced by Collins *et al.* (1956) who used it to describe malignant tumors, specifically metastases studied by serial X-rays. The survival time following resection of breast cancers was then correlated with the exponential tumor growth rate (Kusama *et al.* 1972). Subsequently, the introduction of the logistic growth model allowed for the description of reduced growth in the later stages as the tumor cells outgrew their blood supply, producing central necrosis. Despite the inherent complexity of the processes associated with growth, the ultimate simplification of this concept is illustrated by a particular rat sarcoma, in which linear growth is observed with viable tumor cells surrounding the necrotic core growing essentially in only two dimensions (Mayneord 1932).

With the recognition that tumor cells can spread, invade local tissue and/or metastasize to distant organs, and that not all tumor cells are immortal, the mathematical concepts necessarily became more complicated than what had been developed to describe the dynamics of solid tumors (Deisboeck 2001). Experimental studies and theoretical analyses began to employ cellular kinetics, in which the growth fraction and cell cycle kinetics figured extensively. However, the pioneering work of Steel (Steel 1977) revealed that there was an order of magnitude difference between the times involved in cellular and gross tumor growth kinetics: hours to a few days for individual cells, many days and even months for gross tumors. Subsequently, most of these concepts were formulated in terms of equations involving potential and actual volume doubling times, cell cycle and DNA-synthesizing times, mitotic and labeling indices, and cell loss and growth fraction.

It is important to realize that all models have limitations and those in oncology in particular. Simple models may produce elegant insights and describe existing data, but they also risk oversimplification and the oversight of critical variables. The recognition of apoptosis illustrates this conundrum, wherein a process fundamental to tissue growth and modeling was completely overlooked until the latter part of the twentieth century (Rew 2000a). Furthermore, most of the aforementioned efforts in modeling have not explored the impact of treatment effects. The focus and use of these models was primarily to describe tumor growth and understand the underlying mechanisms so that therapeutic strategies could be developed and justified (Table 13.1). Model parameterization did not account therefore for drug-specific parameters, which could be used in drug development.

The objective of this chapter is to provide a comprehensive overview of the modeling concepts employed in the evaluation of antitumor drug response in oncology. First, an overview of types of models used to characterize cellular

Table 13.1 Anticancer therapeutic intervention strategy and treatment options, including areas for further research to improve adjuvant therapies. Initial mathematical modeling efforts in clinical oncology were aimed to characterizing growth processes rather than drug effects. In contrast to these initial views, modeling can also be used as basis for dose selection, study design optimization and for prognostic purposes (adapted from Rew 2000b)

General strategy	Options
Tumor eradication	Radical surgery: infrequently radiotherapy and chemotherapy
Tumor mass reduction and partial response	Palliative surgery: often radiotherapy, chemotherapy
Long-term tumor growth modulation without eradication (cf. use of tamoxifen/ analogues)	Increase cell loss factor Identify/substitute for gene defects and abnormal pathways Change microenvironment Inhibit growth of metastases Alter angiogenesis
<i>Chemotherapy strategy</i>	<i>Technical challenges</i>
Make better use of existing agents and combination therapies and reduce empiricism	Tumour specific drug targeting assays (now feasible <i>in vivo</i> , e.g. using intrinsic fluorescence) in some classes of cytotoxic drug
Improve effective dose scheduling	Better understanding of tumour growth/cell loss kinetics
Reduction in drug toxicity	Increase effective concentration in target tissue at lower doses
Increase therapeutic index	Regional perfusion strategies Inhibit drug resistance mechanisms
<i>Radiotherapy strategy</i>	<i>Technical challenges</i>
Optimize dosage, fields, modality of radiation	Technical design, computer modelling, clinical trials
Optimize scheduling Access new schedules	Better knowledge of kinetics and cell repopulation dynamics, e.g. hyperfractionation (CHART)
Maximize effectiveness on target tissue	Improve therapeutic ratio, e.g. radiosensitisers, combined drug and r/t schedules
<i>Novel therapies strategy</i>	<i>Technical challenges</i>
Identify tumour specific molecular defects	Develop effective delivery vectors

tumor growth will be presented, beginning with descriptive models. Second, the implications of biomarkers and surrogate endpoints for the evaluation of the predictive performance will be considered qualitatively as well as quantitatively for each approach and illustrated with clinically relevant examples. Finally, some of the challenges for the implementation of clinical trial simulations will be highlighted and approaches of how these challenges can be met will be presented.

13.2 Modeling Tumor Growth and Disease Progression

In contrast to therapeutic areas such as psychiatry, in which descriptive, empirical approaches predominate due to the lack of a direct link between etiology, pathophysiology and clinical outcome (Della Pasqua *et al.* 2010), modeling in oncology encompasses a wide spectrum of methodologies and approaches, which vary from highly mechanistic models of signal transduction (*e.g.*, target-receptor interaction models for biologicals) to empirical probabilistic or stochastic models which describe the probability of overall survival or relapse (Tan and Chen 1998; Gilbert *et al.* 2006; McDougall *et al.* 2006; You *et al.* 2008a). In fact, a diagram of biological dynamic systems domains can be used to better understand the different types of mechanism-based models and their application in oncology (Fig. 13.1). Although not meant to be exhaustive, Fig. 13.1 depicts the areas to which modeling approaches have been applied, in which signaling networks are central and which aspects of cell physiology are involved in the parameterization of these models.

The main difficulties one faces when applying a model-based approach to drug development are the lack of suitable parameterization that allows for extrapolation or inferences about long-term treatment effects and the poor performance of models when treatment comparison is required for drugs which act by very different mechanisms or pathways (*e.g.*, cytotoxic vs. target-mediated response) (Wang *et al.* 2009; Buyse *et al.* 2010). For the sake of completeness, different types of

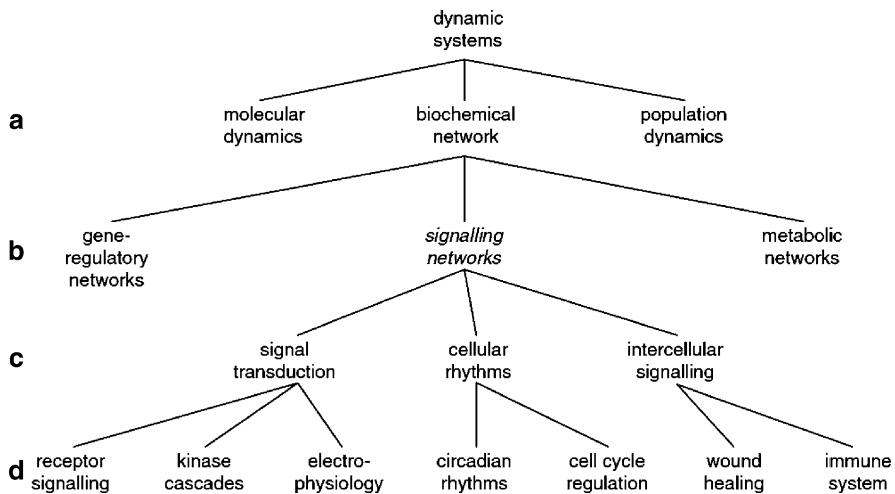


Fig. 13.1 A view of biological dynamic systems domains (a, b), to which modeling approaches have been applied. This diagram can be used to classify the different types of mechanism-based models, in which each of the three cellular functions (c) are parameterized. The lowest branch (d) illustrates concrete biological applications (d) (from Gilbert *et al.* 2006)

models developed in cancer research will be listed, most of which can be used for practical purposes such as prediction of tumor growth and progression of disease, pharmacokinetic-pharmacodynamic relationships or prognosis. To enable further discussions on the implementation of different approaches in drug development, the classification used in the original publications has been maintained in this chapter wherever possible (Rew 2000a; Rew and Wilson 2000a). It is important to realize, however, that the distinction between descriptive or empirical models vs. mechanism-based is not always simple. Truly empirical models or semi-mechanistic models are mostly used to characterize long term clinical outcome of symptoms associated with adverse events following chemotherapy or another type of intervention (Mukherjee and Majumder 2008; Fleischer *et al.* 2009).

- (a) *Static and graphical models.* One example is the cell cycle model, which reveals in a rather qualitative manner the proliferative behavior of cells. Similar concepts have also been used to describe organ and tumor architecture. These graphical representations have been useful because of its dimensionality, allowing understanding of mechanisms at molecular and physiological level, including the identification of targets (Fig. 13.2). This type of modeling has been the basis in computational biology research for analyzing interaction networks and simulating the behavior of each cellular component over time. (Bruggeman and Westerhoff 2006; Goel *et al.* 2006; Hornberg *et al.* 2006; Alfieri *et al.* 2007).
- (b) *Dynamic, stable and unstable system models.* Dynamic models describe the functional properties of a biological system. For instance, normal tissue functionality, such as bone marrow, is stable at steady-state conditions, despite being highly proliferative. This is due to a balance between cell synthesis and cell loss. In fact, thanks to such stationary conditions, mathematical models with high predictive performance have been developed in different areas of drug discovery and development. In contrast, tumors are unstable systems: more complex mathematical and statistical concepts are an essential tool to address these properties (Tan and Chen 1998; Goel *et al.* 2006; McDougall *et al.* 2006). It is the temporal instability (volume increase, invasion, diffusion or metastasis) rather than the existence of the tumor that characterizes its lethality. Tumor biology imposes therefore an additional dimension in predicting changes in (and modeling of) architecture, physiology and response. This type of modeling has been widely applied in the characterization of angiogenesis and tumor growth (Fig. 13.3). It has also supported the understanding of tissue invasion and metastatic processes (Swanson *et al.* 2003; Harpold *et al.* 2007; Chen *et al.* 2009).

Unfortunately, the approaches described above in (a) and (b) above do not address one of the primary interests in oncology and in clinical drug development, *i.e.*, modeling the future or prediction of treatment outcome and risk analysis, both of which are often handled by empirical methods as time to event analysis. Molecular or cellular function modeling has yielded valuable results in cell biology over the last decade, but such models have fallen short when extrapolating model

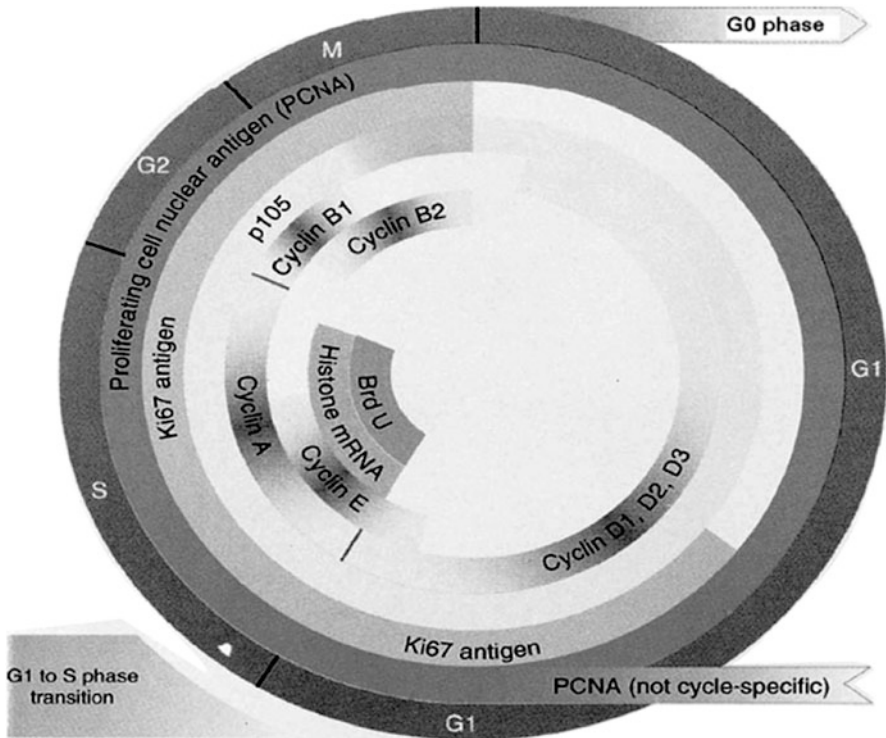


Fig. 13.2 The cell-cycle model describes the sequential phases of the cell-cycle from the diploid, G0/G1 resting phase, though DNA synthesis (the S phase) to the tetraploid, unstable G2 phase which precedes mitosis (from Howard and Pelc 1951). The model provides a simple framework for describing the expression of various cell-cycle regulatory proteins, such as the cyclin family; S phase specific markers, such as bromodeoxyuridine (BrdU); and the points of action of the various regulatory signals, such as the switch to S phase (Rew and Wilson 2000a)

findings to the whole population over wider time spans, when competing risks are involved and disease progression (*e.g.*, death) and treatment outcome (*e.g.*, disease-free survival) depend on other factors that cannot be represented in a mechanistic manner or are not even parameterized by the model, *e.g.*, unobserved covariates.

The first issue to be overcome in the development of models of disease progression in tumor biology is the parameterization of time. Modeling time in biological systems requires more than statistical concepts such as time to event, which is often used in clinical research to describe survival (Cameron *et al.* 1996; Fleischer *et al.* 2009). A single abnormal cell can grow into a lethal tumor. This phenomenon has been modeled as a staged progression of genetic and functional changes, which can be accelerated by intrinsic and extrinsic factors, such as hereditary genetic features or environment. On the other hand, time is also linked to the resulting imbalances between cell growth and decay. These models are also referred to as proliferative or circular models (Steel 1977; Jacquemin *et al.* 2010). In the “bathtub” analogy, water running in and out represents cell accretion and loss. The water level (or tumor volume) is determined by the ratio between inflow and outflow. However, these proposed

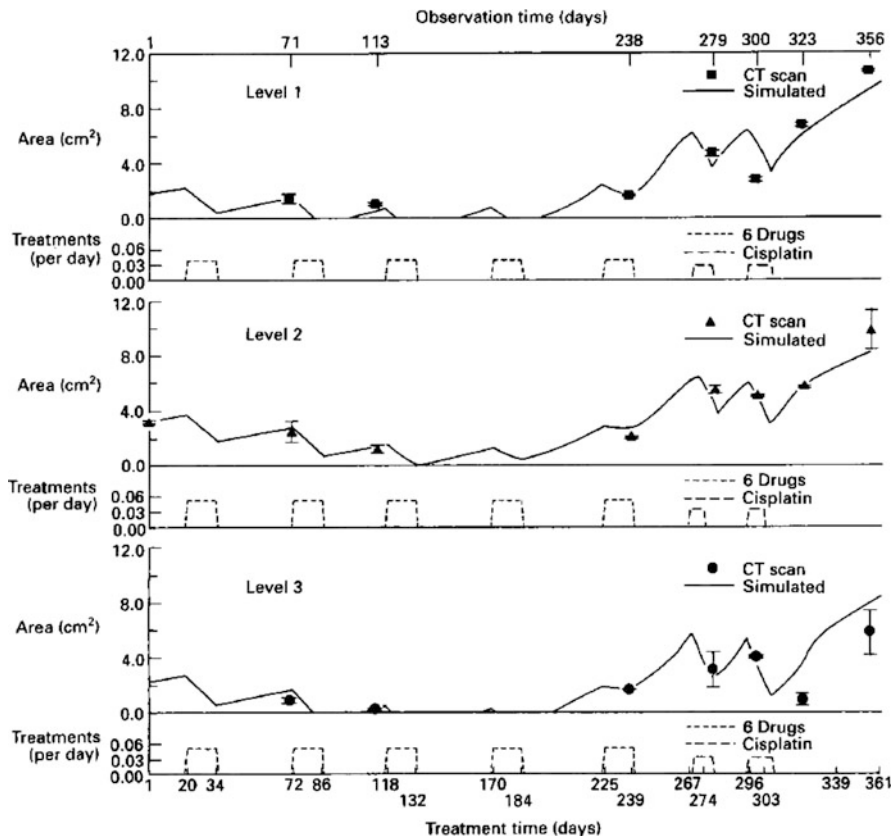


Fig. 13.3 Tumor area measured at anatomically different levels of the brain from eight CT scans taken during the 12 months before the patient’s death. The dashed bars represent chemotherapy cycles, as well as neutron beam irradiation during the last 3 weeks of the patient’s life. Simulation of the temporal evolution of the tumor area at each of the brain levels is considered. Conceptually, the rate of change over time in total cell population is described as a function of diffusion, motility, proliferation, and loss of tumor cells. The predicted effect of chemotherapy on each anatomical level calculated by the model is also shown (*solid line*). Despite the prediction of tumor growth, this model does not allow assessment of drug-specific properties (reprinted from Tracqui *et al.* 1995)

approaches neglect the spatial dimensionality of tumor growth, *i.e.*, the dynamic behavior of a tumor implies continuous changes in time and space. The existence of these two dimensionalities in disease progression means that over longer intervals of days to weeks, the physical and functional characteristics of a tumor can change significantly.

From a mechanistic point-of-view, these features require time to be defined in terms of biological processes (Tannock 1986). Not many models have attempted to describe the passage of time as a molecular clock, which represents the cell-cycle, including replication phases and passage of cell generations rather than the clock time. In fact, on much longer time scales, tumor mutation and resistance itself could also be modeled as a molecular clock, using gene mutation maps to define the rate of changes or speciation. Based on the aforementioned considerations, cell proliferation and

tumor cell population (viable and unviable) can be described by cell-cycle models, in which each cell phase is clearly represented with specific durations (Hartwell and Kastan 1994; Mathon and Lloyd 2001). Despite the characterization of apoptotic pathways and signal transduction rates *in vivo*, most pharmacological models have been based so far on hybrid rate constants reflecting overall tumor growth (Hornberg *et al.* 2006). This simplification of the tumor biology is partly due to the lack of distinction between the various processes underlying tumor cell accretion and loss (Fidler 2002; Coates *et al.* 2009).

Model complexity increases if one is interested in describing and predicting tumor behavior as opposed to tumor growth over time. Solid tumors are characterized by biological aggressiveness, with deregulated growth and angiogenesis, local tissue invasion and metastasis. Metastasis is what determines the aggressiveness of the tumor and the clinical outcome (Quaranta *et al.* 2005; Chen *et al.* 2009). It is thus an important subject for modeling. Metastasis encompasses a number of processes, including detachment of viable cells from the primary tumor, survival, migration and adhesion to a new metastatic site, with subsequent proliferation and angiogenesis. Most importantly, it is not necessarily a random process. Many tumors have an ordered pattern of metastasis. A mechanistic model to describe drug effect on metastasis has not been published to date, but examples exist of stochastic models for carcinogenesis: the one proposed by Tan and Chen (1998) can be used to predict tumor behavior and metastasis. The authors show how Markov processes have been used to model carcinogenesis, but highlight that this approach has some serious drawbacks. To get around these difficulties, they propose an alternative state-space model and multievent models (Fig. 13.4).

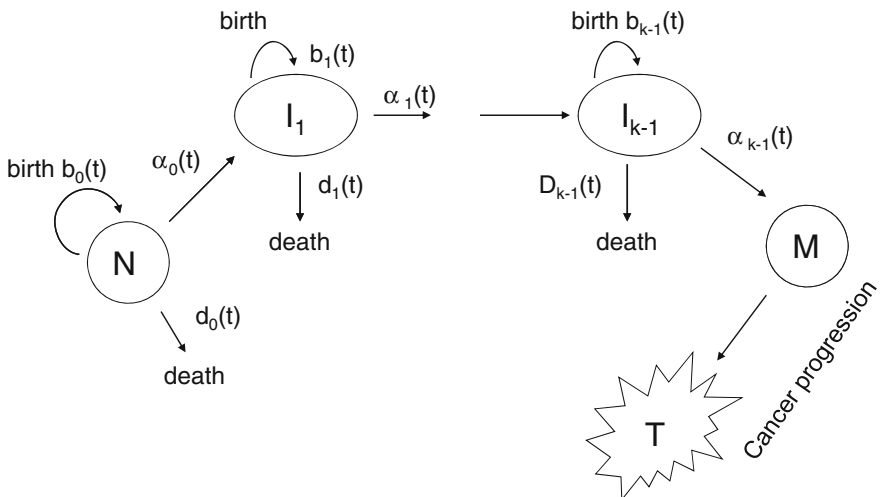


Fig. 13.4 Schematic representation of a k -stage multilevel Markov model of carcinogenesis. Despite the stochastic nature of the model, Markov processes allow for the characterization of complex tumor behavior, including dormancy and aggressiveness (metastasis). N = normal stem cell; I_i = the i th stage initiated cell; $i = 1, 2, \dots, k-1$; $I_k = M$ = proliferating cancer tumor cell; t = malignant tumor (from Tan and Chen 1998)

Recent advances in the understanding of angiogenesis and apoptosis have also revealed important aspects of tumor growth and decay, which demand a higher degree of complexity in terms of the mathematical representation of these biological phenomena, which cannot be described by the modeling concepts discussed so far, such as the use of hybrid turnover rates. In fact, there is discrepancy between cell production and tumor growth rates measured *in vivo*, which suggests that up to 95% of tumor cells may be lost at certain phases in tumor growth (Wilson 1991). In reality, a tumor consists of a complex mixture of proliferating, quiescent, noncycling and apoptotic cells, which defy simple models when all factors are present. For instance, the duration of apoptosis is known to be of approximately 3 h in many cell types. However, small modulations or a small percentage change in the rate or fraction of apoptosing cells can have profound consequences for the balance between cell gain and cell loss, or growth and shrinkage in a tumor. Cell proliferation measurements alone, thus, are insufficient to describe growth (Rew and Wilson 2000b). Unfortunately, there has been no methodology reported as yet to measure the apoptotic fraction of cells in human tumors. Mathematical models, however, can be used to explore a range of scenarios that show what percentage of cells must be induced into apoptosis to reverse tumor growth. For example, a small rapidly growing primary or metastatic tumor may have normal cell proliferation rate but minimal cell loss.

13.3 Modeling Tumor Growth and Decay Under Treatment

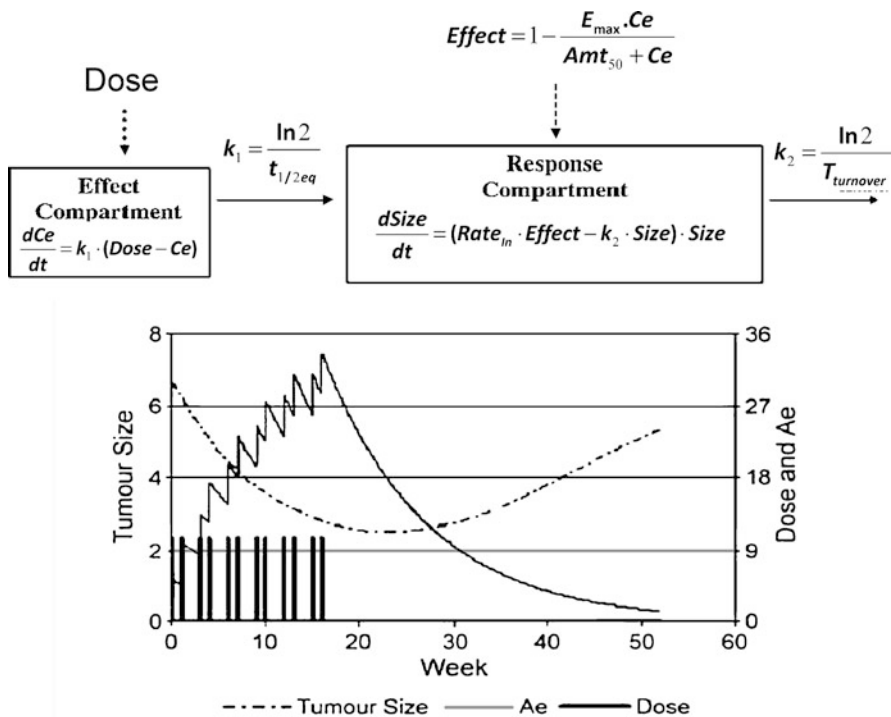
Over the last decade modeling efforts appeared to evolve toward differentiation of drug effects from the underlying disease processes associated with angiogenesis, tumor growth, tumor shrinkage, apoptosis and cell death (Steimer *et al.* 2010). Nevertheless, empirical mathematical models are still frequently used to describe the tumor growth curve (*e.g.*, sigmoid functions, such as logistic, Verhulst, Gompertz, and von Bertalanffy (Bajzer *et al.* 1996)), without an in-depth mechanistic description of the underlying physiological processes. In this context, the effect of a drug can be evaluated only in terms of changes of the parameter values describing the tumor growth. Such changes depend on the dose level and the administration schedule, so that these approaches can only be used retrospectively (Simeoni *et al.* 2004). Levasseur *et al.* (1998) illustrate this concept by applying an exponential kill (EK) model to predict the shape of dose-response curves based on the cell cycle phase specificity of a drug, the cell cycle time, the duration and concentration of drug exposure at the site of action, and a scaling factor for the level of drug resistance. Their work, albeit neither mechanistic nor predictive for understanding how drug and tumor cell characteristics affect the shape of the dose-response curve, highlights the importance of models that capture the time dependency of dose-response curves *in vivo*, as compared to the static measures obtained under stationary experimental conditions (Gardner 2000).

On the other hand, functional models rely on mechanistic, physiology-based hypotheses for the description of drug effects. In fact, the six essential alterations in cell physiology in malignancy may need to be considered: evasion of apoptosis; self-sufficiency in growth signals; insensitivity to antigrowth signals; sustained angiogenesis; limitless replicative potential and capacity for tissue invasion and metastasis. Such models require a set of assumptions about the tumor growth, involving cell-cycle kinetics (proliferating vs. quiescent cells) and biochemical processes, such as those related to antiangiogenic and/or immunological responses (Gasparini *et al.* 2001; Steimer *et al.* 2010). More complex models describe the cell population based on specific phases of the cell cycle. These models have a much larger number of parameters compared with the empirical ones. Their development is time consuming and a sufficient number of quantitative observations are required to avoid the identifiability problems due to the overparameterization (Simeoni *et al.* 2004). The situation becomes even more complex when the effect of the treatment with an anticancer drug is considered, because of the incomplete knowledge of the mode of action *in vivo*. In summary, despite the existence of several tumor growth models, a practical tool that supports oncology drug development in a prospective manner is still missing.

In addition to the lack of a mechanistic description of tumor growth under treatment conditions, historical choices in model parameterization have also created a gap between pathophysiology and clinical measures. More recently, it has become clear that clinical endpoints need to be taken into account from the very early stages of drug discovery. One of the first examples of translational modeling was the development of a pharmacodynamic model for gemcitabine that directly describes tumor shrinkage effects on the primary lesion(s) of patients with nonsmall cell lung cancer (Tham *et al.* 2008) (Fig. 13.5). This approach prevents some of shortcomings of the Response Evaluation Criteria in Solid Tumors Group (RECIST) and may have practical potential as a mid-term endpoint for decision making about effective doses and treatment duration (Ratain and Eckhardt 2004). In contrast to RECIST, which classifies the response of target and nontarget lesions into four categories (i.e., complete response, partial response, progressive disease, and stable disease), the authors apply a continuous scale to describe the time course of tumor response in relation to drug exposure. Despite the requirements for accurate measurements in deep-seated tumors, continuous measures offer many advantages as compared to the discrete categorization by RECIST. The evolution of this concept can be compared with the successful use of changes in hematological variables on a continuous scale that have been used as pharmacodynamic targets in early-phase clinical trials (Friberg *et al.* 2002; Friberg and Karlsson 2003).

13.4 Modeling Biomarkers vs. Surrogate Endpoints

From a drug development perspective, the ability to link antitumor activity in early phase studies to survival is critical for the progression of a compound. Even though advances in areas such as angiogenesis and apoptosis have enhanced our ability to



----- Tumour Size ——— Ae ——— Dose

Fig. 13.5 Upper panel shows a schematic representation of final turnover model on tumor size. This Gompertz-like tumor growth model depends on current tumor size and is expected to approach an asymptote. Because a delay exists between drug administration and tumor response, the time course of exposure to drug at the tumor effect site was described by a tumor effect compartment half-life ($t_{1/2,eq}$). k_1 is the first-order rate constant for effect equilibration; k_2 is the second-order rate constant for tumor loss; Amt_{50} represents the gemcitabine dose required to produce 50% of maximum inhibition in tumor growth; E_{max} , maximum gemcitabine effect on tumor is fixed to 1. Ae represents the effective exposure in the effect compartment. Lower panel shows a comparison of drug dose (thick solid vertical lines), effective exposure (thin solid line), and tumor size measurements (perforated line) on the same time scale measure in weeks (adapted from Tham *et al.* 2008)

identify novel targets and evaluate the potential of new therapies, the identification of sensitive, relevant measures of efficacy, other than survival itself remains a challenge. In fact, the topic of surrogate endpoints for efficacy in oncology is one of the most hotly debated issues in the cancer clinical trials arena (Sherrill *et al.* 2008; Wang *et al.* 2009; Saad *et al.* 2010). Yet, much of the focus of the discussion has been on the requirements for regulatory approval rather than on the understanding of the physiological mechanisms linking tumor activity to disease progression and clinical outcome.

Because of the high cost of therapeutic interventions, it has been argued that the only acceptable study endpoint is an equivocally documented improvement in overall survival (FDA 2007). Nevertheless, the role of alternative biomarkers as

early predictors of overall survival in oncology trials is subject of intensive research and the potential use of such predictors as independent indicators of patient-related clinical benefit remain highly desirable. Therefore, from a modeling standpoint, the first issue to be addressed is the definition of the term “surrogate endpoint” in cancer clinical trials. In much of the regulatory discussion regarding such trial endpoints, it has been questioned whether a positive result is an early indication that longer follow-up will detect a statistically significant improvement in overall survival (Johnson *et al.* 2003; EMA 2006). There are various examples that demonstrate the correlation between progression-free survival (PFS) with efficacy, defined as a documented improvement in overall survival. However, the strong correlation between PFS and overall survival is not universal across tumor types and will be likely less frequently observed in the future as more biologically and clinically active “second-line” treatment strategies are employed to augment initial disease progression (Burzykowski *et al.* 2008; Fleischer *et al.* 2009).

Regardless of the need to identify and validate surrogate endpoints in oncology, it is useful to consider the use of a mechanism-based classification of biomarkers (Danhof *et al.* 2005) for the purposes of modeling and simulation and subsequently distinguish them into either prognostic or predictive biomarkers. Prognostic biomarkers correlate with outcome independent of treatment or mechanism of action, whereas predictive biomarkers correlate with the impact of specific treatment on outcome. This concept has been recently illustrated by the Food and Drug Administration for the relationship between early tumor size reduction and patient survival in nonsmall-cell lung cancer (NSCLC) (Wang *et al.* 2009; Bruno and Claret 2009).

The importance of models combining biomarkers and overall survival is further illustrated by the longitudinal exposure-response tumor growth inhibition (TGI) model with a survival model based on tumor size together with other prognostic factors as the main predictors for survival (Claret *et al.* 2009) (Fig. 13.6). The use of drug specific and disease/patient-specific parameters allowed scaling of drug effect across patient populations and drug development phases. In contrast to previous publications, the authors conceptualize the progressive development of resistance in terms of a drug-constant cell kill rate that decreases exponentially with time. The approach is used to predict survival outcome of a phase III study of capecitabine vs. fluorouracil in metastatic colorectal cancer (mCRC). In this example, dose was used as a measure of exposure, instead of drug concentrations or pharmacokinetic parameters (Claret *et al.* 2009).

As illustrated by the example in Fig. 13.7, part of the problem in identifying a link between biomarkers and survival is the absence of evidence of the underlying PKPD relationship from oncology trials. The use of a nomogram for prediction of 2-year survival takes into account covariates such as World Health Organization performance status (WHO-PS), forced expiratory volume in 1 s (FEV1), positive lymph node station (PLNS) and gross tumor volume (GTV), but ignores drug-related factors, *i.e.*, pharmacokinetics and pharmacodynamics. This situation may be explained by the empiricism in the selection of the effective dose range during the development of oncology drugs. In addition, growth models have evolved without further consideration of the variable manifestations of disease in cancer

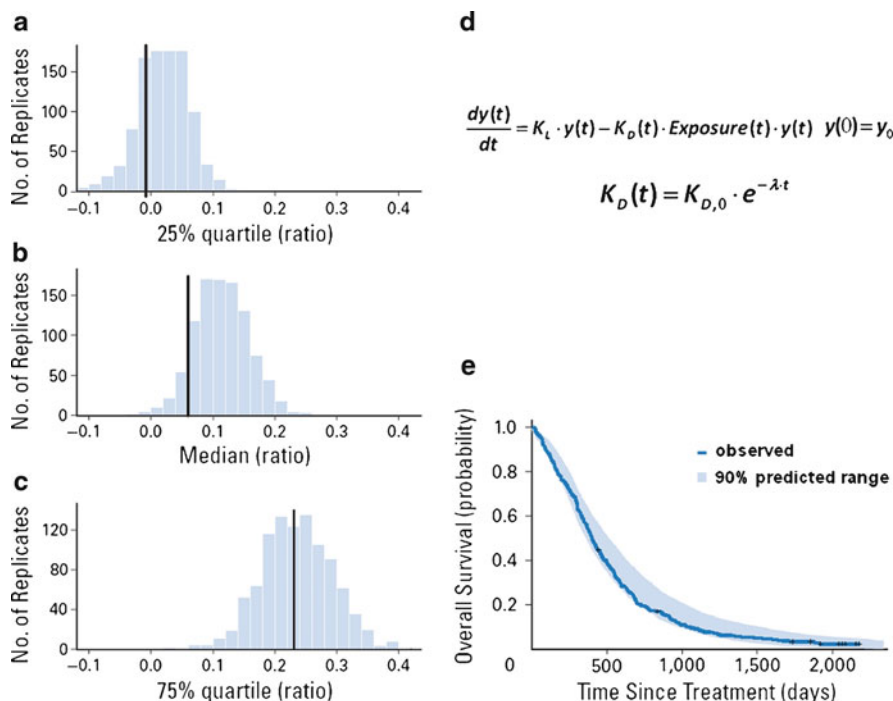


Fig. 13.6 *Left panel:* Distribution of predicted tumor size reduction (relative to baseline) compared with observations (*vertical lines*) for capecitabine in the phase III study. Simulations were performed by using the tumor-growth inhibition model, capecitabine-specific parameters, disease-specific growth rate, and baseline tumor sizes. The equation describes how drug exposure relates to tumor size. $y(t)$ is the tumor size at time t , y_0 is the baseline tumor size, K_L is the tumor growth rate, $K_D(t)$ is the drug-constant cell kill rate that decreases exponentially with time (according to λ) from an initial value of $K_{D,0}$ to account for the progressive development of resistance. Exposure (t) is the drug exposure at time t . *Right panel:* The 90% prediction interval (*shaded area*) and observed (*line*) survival curve for capecitabine in the phase III study. Simulations were performed by using the drug-independent survival model. The week 7 tumor size reduction was predicted by the tumor-growth inhibition model, and baseline tumor sizes (Claret *et al.* 2009)

patients. Thus, multivariate logistic models are often applied to describe survival, correlating it to patient/disease specific prognostic factors, without linking it to mechanism of action, drug exposure or other pathophysiological processes. The main implication of such a disconnection is the poor predictive or prognostic value of modeling and the potential bias due to confounders. Often mere statistical correlations are found without necessarily establishing a causal link among the variables or parameters under evaluation (Klein 2006). This is particularly relevant in oncology where the full effect of first-line therapy on overall survival may be confounded by the effects of subsequent treatments as well as by metastasis (Brekelmans *et al.* 2006; Brekelmans *et al.* 2007; Diva *et al.* 2007; Buyse 2009).

In contrast to the previous examples, You *et al.* have shown how pharmacokinetics can account for differences in response to treatment (You *et al.* 2008a, 2009).

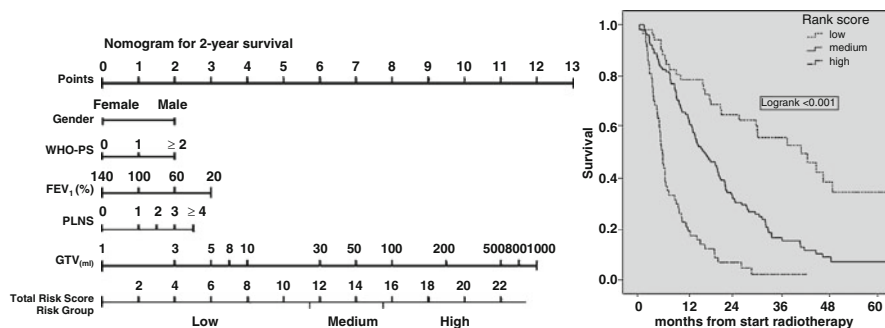


Fig. 13.7 (Left) Nomogram for prediction of 2-year survival. Patients in low-risk group have the greatest predicted probability of being alive at 2 years. Points, TNM staging score (T describes the size of the tumor and whether it has invaded nearby tissue; N describes regional lymph nodes that are involved; and M describes distant metastasis); *WHO-PS* World Health Organization performance status; *FEV₁* forced expiratory volume in 1 s; *PLNS* positive lymph node station; *GTV* gross tumor volume. (Right) Kaplan–Meier curves stratified by low- (top line), medium- (middle line), and high- (bottom line) risk score. No explicit pharmacokinetic-pharmacodynamic factors have been included in the nomogram. Disease progression is inferred from risk scores in a qualitative, rather than quantitative manner (modified from Dehing-Oberije *et al.* 2009)

The authors have demonstrated the strong influence of pharmacokinetic parameters on outcome following administration of etoposide to small cell lung cancer patients. Modeling findings suggest that etoposide dose should be individualized according to a target systemic exposure instead of being based on body surface area (You *et al.* 2008b). In another example, these authors use a kinetic population approach in which the decline in human chorionic gonadotropin (hCG) is incorporated as basis for the prediction of methotrexate resistance and consequently survival rates (You *et al.* 2010). Similar efforts for other types of tumors are urgently needed. Differences in drug exposure as well as in the underlying PKPD relationships must be accounted for accordingly when predicting treatment response and overall survival.

13.5 Translational Models

In addition to the lack of models combining biomarkers to clinical endpoints, another important gap in drug discovery and development is the shortage of tools to extrapolate and scale tumor activity, disease progression and treatment effects across species. The majority of mathematical models describing the effect of anticancer treatments on tumor growth in animals are of limited use within the drug industry (Bajzer *et al.* 1996; Gardner 2000; Sidorov *et al.* 2003; Luo *et al.* 2005). Unfortunately, these limitations highlight lack of collection of relevant quantitative information during preclinical development of oncology drugs. One of the first quantitative preclinical models of efficacy was proposed by Simeoni *et al.* (2004). Their model is based on a system of ordinary differential equations that link

the dosing regimen of a compound to the tumor growth in animals, with tumor growth in untreated animals being described by an exponential and linear growth phases. In treated animals, tumor growth rate decreases proportionally to both drug concentration and number of proliferating tumor cells. Furthermore, a transit compartmental system is used to model the process of cell death, which occurs at later times (Fig. 13.8). The authors elegantly distinguish parameters that are related to the growth characteristics of the tumor, to drug activity, and to the kinetics of the tumor cell death. Therefore, such parameters can be used for ranking compounds based on

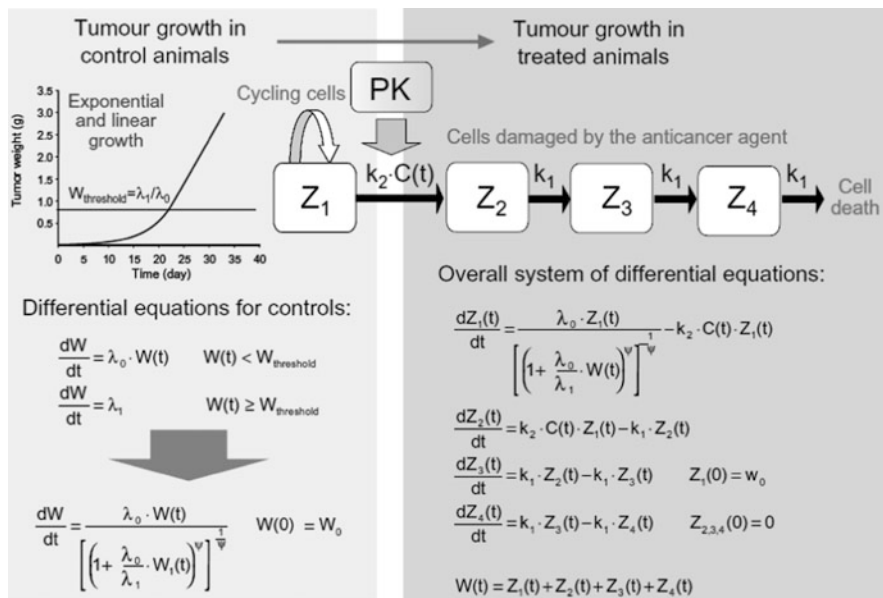


Fig. 13.8 Scheme and equations of the PKPD tumor growth inhibition model by Simeoni *et al.* (2004). The tumor growth in nontreated animals is described by an exponential phase followed by a linear growth phase. To facilitate the fitting procedure and reduce the complexity of the system, a single differential equation was used for modeling the derivative of the tumor weight ($w(t)$) (left panel). In this equation, w_0 represents the tumor weight at the inoculation time ($t = 0$), and λ_0 and k_1 are parameters characterizing the rate of exponential and linear growth, respectively. W is a constant modulating the transition from the exponential to the linear growth model. In the treated animals it is assumed that the anticancer treatment makes some cells nonproliferating eventually bringing them to death through a mortality chain (right panel). The system of differential equations is reported: for a given time t , $Z_1(t)$ indicates the portion of proliferating cells within the total tumor weight $w(t)$ and $c(t)$ indicates the plasma concentrations of the anticancer agent. In these equations, $w(t)$ is the total tumor weight, represented by the sum of the weights of the cells in the various states 1, 2, 3 and 4, and w_0 , λ_0 and k_1 are the parameters describing the growth of the proliferating cells in the control animals. The action of the drug on the tumor growth is determined uniquely by the two parameters k_1 (the micro-rate constant describing the kinetics of cell death) and k_2 (the proportionality factor linking the plasma concentration to the effect). In this context, k_2 is the parameter describing the antitumor potency of the compound. Based on the annihilation of the differential equations, a threshold concentration $C_T = \lambda_0 / k_2$ can be derived, such that, if animals are exposed to a steady state drug concentration $C_{ss} > C_T$, the model eventually predicts the tumor eradication (Rocchetti *et al.* 2007)

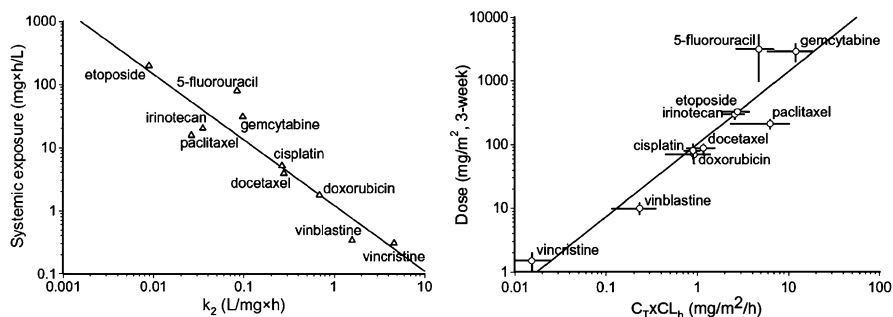


Fig. 13.9 (Right panel) Relationship between the systemic exposure obtained at the midpoint of the dose range used in the clinics (cumulative doses given in 3-week cycles) and k_2 (potency parameter) estimated in animals. Regression performed on log-log scale: *intercept* = 0.0835; *slope* = -1.03 ; $r = -0.927$. (Left panel) Relationship between clinical doses (cumulative doses given in 3-week cycles) and $C_7 \cdot CL_h$. Regression (based on the midpoint of the dose range) performed on log-log scale: *intercept* 2.01; *slope* = 1.14, $r = 0.939$. Vertical error bars represent the dose range reported in the literature. Horizontal error bars based on \pm standard deviation of CL_h (Rocchetti *et al.* 2007)

their potency and for evaluating potential differences in the tumor cell death process. The model was extensively tested on discovery candidates and known anticancer drugs (Fig. 13.9). On the basis of the parameters estimated in the first experiment, the model successfully predicted the response of tumors exposed to drugs given at different dose levels and/or schedules, which suggests its utility also for the optimization of the design of new experiments (Magni *et al.* 2006).

The parameterization proposed by Simeoni *et al.* represents an effective compromise between empirical and mechanism-based approaches. It relies on a few identifiable and biologically relevant parameters, the estimation of which requires only the data typically available in the preclinical setting: the pharmacokinetics of the anticancer agents and the tumor growth curves *in vivo*. Given that drug-related parameters are not specific to a given mechanism of action, but rather relate the degree of cell damage and cell death with the plasma concentrations of the drugs, it allows the assessment of treatment effect for compounds with novel mechanisms of action. Furthermore, it is possible to compute a time efficacy index (TEI: equal to the asymptotic delay between the growth curves in treated and control animals) which is used to estimate the effective threshold in prospective drug screening and can be linked to toxicity parameters to rank competing antitumor candidates (Magni *et al.* 2006).

Although the aforementioned approach offers various advantages with its generalizability and clear description of processes associated with tumor growth, its value for the evaluation of mechanism-specific and drug-specific biomarkers remains to be determined. Therefore, it is important to understand that the more mechanistic a model becomes, the less generalizable is its use across compounds or tumor type. This limitation is exemplified by the relationship between cMet phosphorylation and HGF receptor (autocrine loop) expression to antitumor activity (pharmacological response) in athymic mice implanted with human tumor

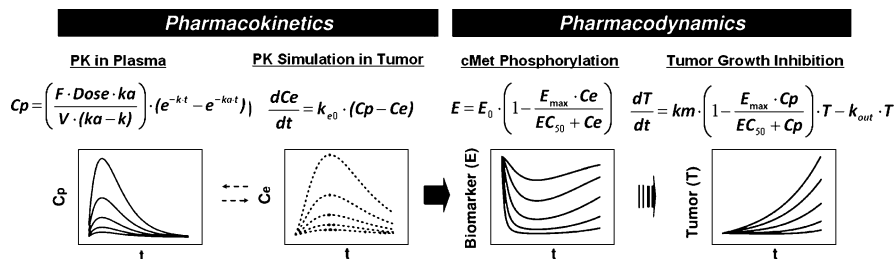


Fig. 13.10 The use of a link (effect) model to describe a time delay (hysteresis) between pharmacokinetics in plasma, cMet phosphorylation inhibition and antitumor efficacy by PF02341066 in a human tumor xenograft model is based on the theoretical hypothesis that there are circumstances in which the indirect response model could mimic a direct pharmacological response (Yamazaki *et al.* 2008)

xenografts (Yamazaki *et al.* 2008). Such a model may be specific for prospective evaluation of targets for cMet and HGF receptors, both of which have been implicated in the development and progression of multiple human cancers (Fig. 13.10). Using the proposed PKPD model together with *in vitro* and *in vivo* data, effective clinical doses could be projected for an investigational drug. In fact, their findings suggest that drug distribution from plasma to the effect site is the main reason for the observed hysteresis, whereas the factors controlling cMet phosphorylation might be of no importance to the phenomenon. However, in prospective evaluation of new compounds time-dependencies in response may occur for other reasons, particularly because of indirect mechanisms of action, such as stimulation or inhibition of formation (kin) or loss (kout) of the substrates underlying the antitumor activity (Mager and Jusko 2002; Ternant and Paintaud 2005; Peletier and Gabrielsson 2009; Mager *et al.* 2009; Mould and Green 2010). The parameterization used by Yamazaki would not allow for accurate prediction of the time course of response induced by the latter mechanisms.

Similarly, another mechanism-specific, but laborious approach has been proposed to assess the influence of biomarkers, tumor burden and survival on the dose-concentration-response relationships of rituximab in a murine lymphoma model. Rituximab concentrations were inversely correlated with tumor burden; mice with low tumor burden had high rituximab concentrations. Furthermore, rituximab exposure influenced response and survival. It is unfortunate that the authors did not consider the use of nonlinear mixed-effects modeling, despite the clear implications of between-subject variability (Dayd  *et al.* 2009) (Fig. 13.11).

Although the aforementioned preclinical efforts have contributed to the integration of biomarkers of pharmacological activity into the assessment tumor growth, an important challenge that needs to be overcome by translational models is their ability to incorporate *in vivo* processes which occur in parallel to tumor formation, invasion, and metastasis (Williamson *et al.* 2009). One of most clear examples of such an interaction is the assessment of treatment-related injury and consequently, the prediction and prevention of adverse events, in particular of hematological toxicity. Also the role of the immune system during tumor growth needs to be considered.

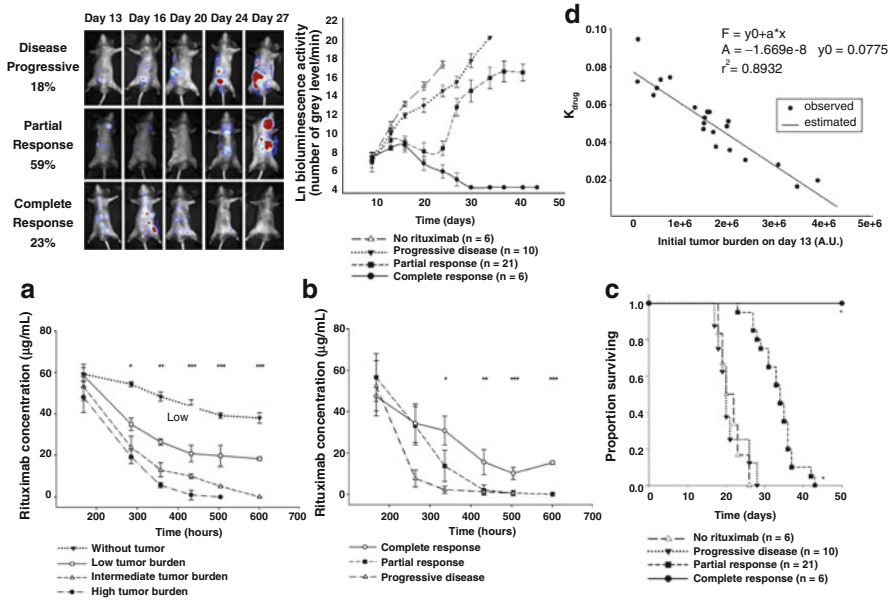


Fig. 13.11 (Upper panel) Variability of response to rituximab on pre-established lymphoma tumors. Bioluminescent imaging (BLI) pictures for a group of 37 mice was administered 20 mg/kg rituximab on day 13. 23% of complete response (CR) (filled circle), 59% of partial response (PR) (filled square), and 18% of progressive disease (PD) (filled inverted triangle) were observed. A relationship could be established between tumor burden and k_{drug} , a zero-order constant corresponding to maximal rituximab induced tumor lysis. (Lower panel) Rituximab exposure is influenced by tumor burden and influences response to treatment and survival. (a) Mice without tumor had significantly higher rituximab concentrations than mice with tumor (filled inverted triangle). Mice with low tumor burden ($<0.15 \times 10^6$ AU) (open square) had significantly higher rituximab concentrations than those with intermediate (from 0.15×10^6 to 3×10^6 AU) (open triangle) or high ($>3 \times 10^6$ AU) tumor burden (filled circle). (b) Mice in CR (open circle) had significantly higher rituximab concentrations compared with mice in PR (filled square) or in PD (open triangle). (c) Survival was significantly increased in mice in CR (filled circle) compared with those in PR (filled square), PD (filled inverted triangle), or control group receiving PBS (open triangle) on day 13. * $P < 0.05$, ** $P < 0.01$, *** $P < 0.001$ (adapted from Daydé *et al.* 2009)

Mechanisms of immune evasion of cancer may occur as result of its ability to down regulate the immune recognition. Those mechanisms are not taken into account by the majority of the models describing tumor growth and may be critical for the evaluation of biologicals and targeted therapy where immune cells may take part in the overall antitumor activity (Cappuccio *et al.* 2007).

13.6 Modeling and Prediction of Adverse Events

Although understanding of the relationship between tumor growth, biomarkers of drug activity and response remains at the core of modeling efforts in preclinical research, it is the prediction and prevention of safety and adverse events that has

dominated the clinical arena in this field. Disappointingly, these efforts reflect the historical evolution of decision-making in oncology, which still relies on maximum tolerated doses, irrespective of the introduction of targeted therapies. An extensive discussion of adverse-event modeling is beyond the scope of this chapter. However, several approaches have been proposed for the prediction hematological toxicity. Various models have been published for anemia, neutropenia, thrombocytopenia, and leucopenia, all of which attempt to characterize the onset, duration and severity of the events based on the underlying physiological processes. In many cases, modeling accounts for the effect of adjunctive therapy, which is aimed at rescue or recovery of baseline, physiological function.

A relevant example of this type of modeling effort is anemia, which is frequently observed in patients undergoing chemotherapy. Most erythropoiesis models are mechanism-based, taking into account hemoglobin dynamics (Fig. 13.12). Usually, turnover (indirect response) models are considered, wherein a zero-order production rate of hemoglobin is affected by adjunctive therapeutic intervention. Given that *in vivo* stimulation of hemoglobin production occurs through prevention of

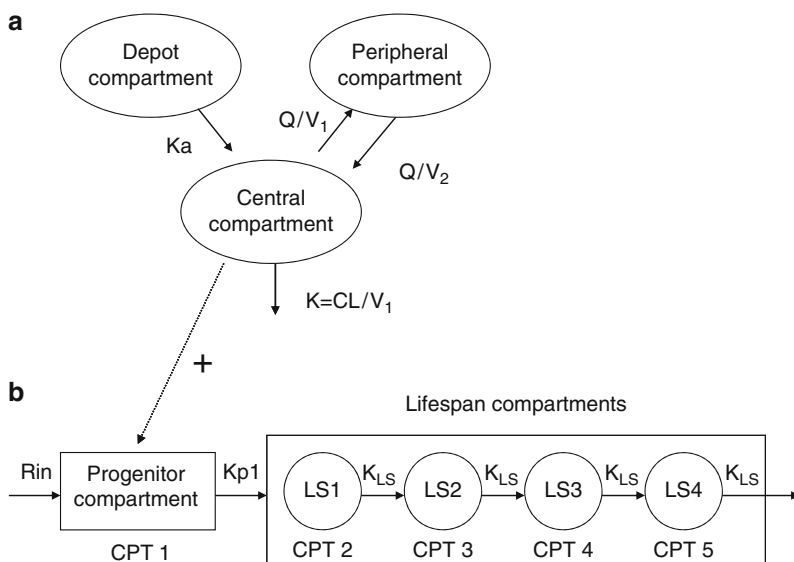


Fig. 13.12 Schematic diagram showing the link between the 2-compartment PK model and the indirect effect PD model of darbepoetin alpha in patients with nonmyeloid malignancies undergoing multicycle chemotherapy. Increases in mean hemoglobin concentration reduce risk of red blood cell transfusions and improves patient-reported outcomes. A modified indirect response model, wherein serum concentrations stimulated the production of hemoglobin through an E_{max} equation, described the hemoglobin levels after SC doses of 0.5 mg/kg every week to 15 mg/kg every 3 weeks in chemotherapy-induced anemia patients. In this model, the effect of endogenous EPO level fluctuation on the stimulation of hemoglobin production rate was ignored (adapted from Agoram *et al.* 2006)

apoptosis of erythroid progenitors in bone marrow, there is a delay before these progenitors mature into hemoglobin-carrying red blood cells (RBC) (Dormer *et al.* 1980; Agoram *et al.* 2006). In fact, transit compartments can be used as a general approach for the characterization of delays in response due to maturation processes. Furthermore, the assumption of physiological rates for maturation allows for parameterization of drug and system-specific terms, which facilitates the comparison of treatment effects across compounds (Dayneka *et al.* 1993; Friberg *et al.* 2000; Krzyzanski *et al.* 2008).

Similar modeling efforts to describe adverse events have become rather common in the published literature (Gieschke *et al.* 2003; Fetterly *et al.* 2008; Bulitta *et al.* 2009; Mould *et al.* 2009). However, none of them have attempted to integrate both efficacy and safety models as basis for the assessment of the risk-benefit ratio. The proposed optimization of the dose and dosing regimen of antitumor drugs in those investigations is driven by tolerability criteria only. To date, only a single publication is available, where multiple adverse events are evaluated in parallel, in an integrated manner. Joerger *et al.* have developed a population pharmacokinetics and pharmacodynamics for the prediction of neutropenia and thrombocytopenia induced by paclitaxel and carboplatin. They have shown that in this group of patients, paclitaxel concentrations greater than 0.05 $\mu\text{mol/L}$ is a good predictive marker for severe neutropenia and clinical outcome, whereas carboplatin exposure is a good predictive marker for thrombocytopenia (Joerger *et al.* 2007a).

One obvious flaw in the evaluation of antitumor activity in the absence of an integrated model for predicting adverse events may be explained by technical rather than scientific considerations. Barriers for the advancement of integrated models of efficacy and safety in oncology are the different types of variables used for the evaluation of adverse events. Although continuous variables are often applied for tumor growth and drug-induced activity, categorical variables are used in clinical safety, few of which can be converted into validated continuous measures. Hence, integrated modeling of disease progression and drug effect imposes computation and algorithm requirements, *i.e.*, the ability to handle both continuous and categorical variables at the same time. Moreover, past efforts have been heavily focused on parameter estimation, rather than on the predictive value of the models for clinical purposes. In fact, the use of simulations as a tool for the assessment of clinically relevant scenarios is often missing or disregarded in the aforementioned publications. Clinical trial simulations in which drop-out models are included are even less common.

A hint of the complexity in handling categorical variables and subsequent evaluation of safety by simulations can be found in the work by Hénin *et al.* (2006) who show how an empirical model can be used to predict hand and foot syndrome in colorectal cancer patients treated with capecitabine. In their work, drug exposure is linked to a transitional (logit) model to describe the changes in severity scores. Despite some difficulties, attempts have been made to describe such events using a mechanism-based approach. For instance, Hing *et al.* (2008) have applied pharmacokinetic-pharmacodynamic modeling to describe and predict grade 3 and grade 4 neutropenia trabectedin-induced neutropenia (Fig. 13.13). Depth and

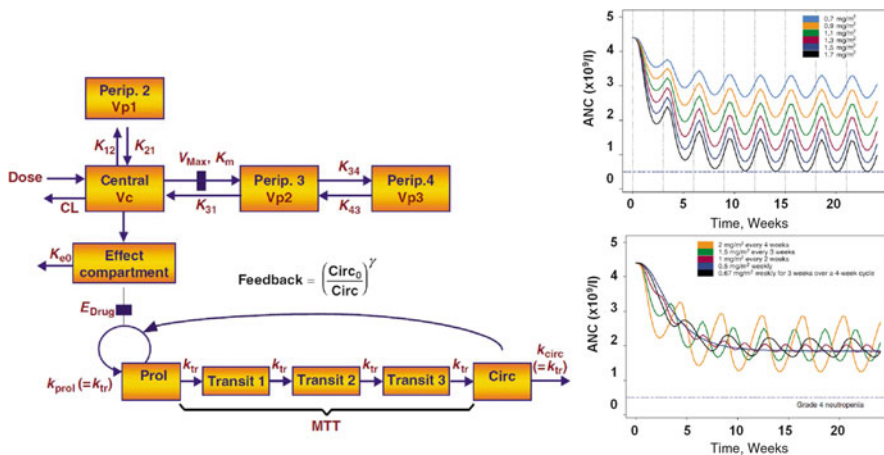


Fig. 13.13 Transit compartment model for the characterization of trabectedin-induced neutropenia. On the right, simulations depict the effect of different dose levels (*upper panel*) and frequency (*lower panel*) on the typical time course of ANC following a 24 h iv infusion of trabectedin (Hing *et al.* 2008)

duration of neutropenia were found to be dependent on trabectedin dose level and AUC, and infrequent dosing regimens with higher doses led to more severe neutropenia. In addition, model-based simulations demonstrated the absence of cumulative neutropenia toxicity with trabectedin in patients who received three or more cycles of therapy and revealed that patient’s covariates did not have any clinically relevant effects on model parameters.

The complexity in modeling categorical variables increases if one considers combination therapies, which may be used because of pharmacokinetic and/or pharmacodynamic drug–drug interactions. This is illustrated by the interaction model for hematological toxicity associated with indisulam and carboplatin (Zandvliet *et al.* 2008). Hematological toxicity (*i.e.*, the myelosuppressive effect of the combination) is described by a transit compartment approach. As in the previous examples, the main shortcoming of these analyses is that the selection of dosing regimens for prospective clinical trials or patient groups is made without considering an efficacy model or utility function to guide treatment optimization.

13.7 Clinical Trial Simulations

An assessment of the impact of a model-based approach in drug development and therapeutic interventions in oncology requires not only a comprehensive assessment of the predictive value of a drug-disease model, but also an evaluation of its performance in a clinical trial context, *i.e.*, including elements of optimization of the study design. Relying solely on PKPD model parameter estimates for decisions such as dose selection or population size may lead to wrong conclusions about

treatment efficacy and safety (Rabinowitz and Davidov 2008; Friberg *et al.* 2009; Santen *et al.* 2009). It is clear that to demonstrate clinically significant benefits over a control group demands more than just an empirical calculation of the statistical power of the trial, under the assumption of random variance and a predefined effect size. This is particularly important if one takes into account the adaptive nature of protocol designs for new investigational drugs. Variability depends on a variety of factors, including trial design features such as doses, in-/exclusion criteria, drop-ins and dropouts, trial duration etc. Effect-size will depend on disease status and progression as well as drug effect, all of which may also be influenced by trial duration, dose selection and in-/exclusion criteria. Clinical trial simulation (CTS) offers an opportunity to formally evaluate the implications for trial outcome of the role of each factor separately or in combination with each other.

In physics, the influence that the experimental setting may have on experimental results has since long been accepted. In oncology such acceptance has yet to come. The meticulous evaluation of design-related factors is critical in explaining failure and attrition rate in the development of antineoplastic agents. Before designing clinical trials, a few important questions need to be answered, in particular, whether the selected doses are indeed active in the targeted patient population and sufficiently safe. Given that disease progression ultimately leads to a fatal outcome in oncology, therapeutic choices have tolerated a somewhat reduced risk-benefit balance. Traditionally, decisions are based on a qualitative, overall interpretation of experimental results (*e.g.*, see Frame 2007), which do not always allow a straightforward answer to the aforementioned question. For accurate interpretation of study results, one should consider that differences may exist in dose range, patient baseline characteristics (*e.g.*, disease status and severity, medical history) and the definition of response. Simulations can potentially provide insight toward addressing these differences and enable extrapolation of findings to prospective patients or patient groups (Goggin *et al.* 2004; Bellmunt *et al.* 2009). Most importantly, one can assess the impact of uncertainty on model predictions and thus provide appropriate recommendations for trial design and/or label recommendations during drug therapy (Santen *et al.* 2009).

Even though the benefits and impact of clinical trial simulations in oncology have been highlighted in various publications (see Table 13.2) and recent regulatory guidance documents endorse its use for the design and optimization of Phase II and III trials, there are very few examples of clinical protocols defined according to a model-based analysis. Veyrat-Follet *et al.* (2000) simulated a Phase III oncology trial with an alternative dose intensification scheme that was used in a phase II study with patients with nonsmall-cell lung cancer receiving docetaxel. Taking into account modeling results, it was found that the cumulative docetaxel dose is a predictor of both time to progression and survival. Moreover, the analysis showed that baseline α 1-acid glycoprotein (AAG) was a significant prognostic factor: the higher the AAG, the less the clinical response both in terms of toxicity and efficacy. Patients with high AAG also had shorter survival. On the basis of these findings, the authors explored the benefit of dose increases in this subgroup of the population. In fact, this work is the only available publication in clinical oncology, in which the

Table 13.2 Implementation of a model-based approach to the development of drugs in oncology (adapted from van Kesteren *et al.* 2003)

Objectives	PKPD modeling in this phase	Benefits of PKPD modeling in previous phase	
Preclinical	Assessment of antitumor activity Determination of effective concentrations Mode of action Metabolism	Dose–effect relationships Schedule dependency for activity/toxicity	
Phase I	Determine most optimal dose and schedule Assess toxicity profile Study the PK and relations with toxicity and dose	PK model (linearity, schedule dependency) PKPD relationships (schedule dependency) Preliminary identification of patient characteristics influencing variability in PK and PD	Definition of a useful target for phase I study Selection of safe starting dose Selection of treatment schedules
Phase II	Establish activity in specific tumor types Study PK and PD in large patient population	Further assessment of PK and PKPD relationships and variability	Selection of dose or concentration/exposure measure Limited sampling schedule is available
Phase III	Confirmation of activity in large randomized trials and comparison with standard treatment	Learning about PK and PD (toxicity and efficacy) and PKPD relationships with variability in a large and diverse patient population	Target dose or measure of exposure is defined, taking into account efficacy and safety; limited sampling schedule is available; preliminary knowledge about sources of interpatient variability in PK and PD

authors contemplate toxicity (to drive dosage reduction), time to progression, overall survival and drop-out in an integrated manner (Fig. 13.14).

The few examples of CTS to oncology protocols reveal how far the field is from what should be considered a state of the art instrument. CTS is a powerful tool for the integration and quantification of the impact of multiple trial design factors. It is imperative that physicians realize that clear-cut assessment of such factors cannot be obtained by traditional meta-analysis, as confounding factors cannot be dissected independently. Consider the impact of differential diagnostic tools following the advancements in imaging and laboratory technologies in the past century; analogously, one must become aware that CTS is the instrument for differential diagnosis in clinical drug development. Differential diagnosis of clinical trials is the only alternative to trial and error in cancer research.

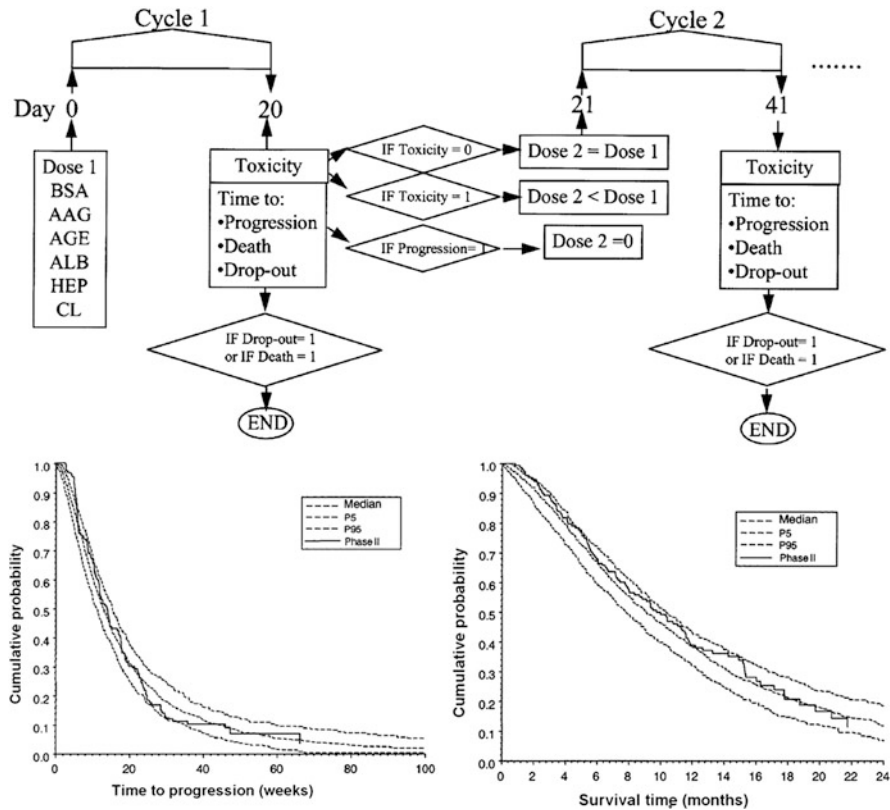


Fig. 13.14 (Upper panel) Schematic representation of the simulation procedure for the evaluation of clinical endpoints using hazard models. (Lower panel) Graphs indicate the ability of the simulations to predict time to progression and survival in phase II patients. *Solid line* represents the Kaplan–Meier estimate of the cumulative probability of survival in the phase II patients ($n = 151$). *Dotted lines* are the median, 5th (P5), and 95th (P95) percentiles of 100 Kaplan–Meier survival curves obtained from simulations of the phase II patients (adapted from Veyrat-Follet *et al.* 2000)

13.8 Concluding Remarks

Cancer research has undergone radical changes in the past few years. Exploring tumor dynamics and disease processes both at the basic and clinical levels is becoming routine. However, how to handle this information and integrate different dimensions of disease has become the major obstacle to further advancement of therapeutics in oncology. Intuitive, empirical approaches based on past experience or maximum tolerated dose are no longer acceptable. The use of mathematical modeling approaches is essential to integrate the enormous amount of data being produced and extract useful answers (i.e., a top-down approach to biology and medicine) and quantitatively assess the properties of novel molecules *in vivo*,

including impact on disease progression. Ultimately, models are required not only to translate pharmacological effects into treatment response, but also to establish the overall risk-benefit ratio for patients under clinically relevant situations.

Researchers and physicians have a unique opportunity to integrate knowledge to address clinical questions and improve decision making in areas such as candidate selection, dosing rationale and clinical trial design. Despite the potential implications of modeling and simulation concepts for drug development in oncology, considerable resistance still exists in terms of the changes they represent to preclinical protocols and to clinical research practice. The amount of evidence gathered so far has not been sufficient to trigger a permanent shift in the way stakeholders across industry, academia and regulators deal with the planning, design and execution of oncology protocols and subsequently analyze and interpret experimental results. This is further complicated by the lack of mathematical skills and often of clinical insight of researchers in this field. It is worth emphasizing that the debate about the suitability and predictive value of biomarkers and surrogate endpoints to replace survival and overall survival as measure of clinical benefit is unlikely to be conclusive unless concrete changes are introduced to experimental protocols. Actions are needed that ensure the assessment of pharmacokinetic–pharmacodynamic relationships for both efficacy and safety endpoint in an integrated manner. The limitations to the implementation of such an approach are not technical in nature; they are hampered by current beliefs.

References

- Agoram B, Heatherington AC, Gastonguay MR (2006) Development and evaluation of a population pharmacokinetic-pharmacodynamic model of darbepoetin alfa in patients with nonmyeloid malignancies undergoing multicycle chemotherapy. *AAPS J* 8(3):E552–E563
- Alfieri R, Merelli I, Mosca E, Milanese L (2007) A data integration approach for cell cycle analysis oriented to model simulation in systems biology. *BMC Syst Biol*. doi:[10.1186/1752-0509-1-35](https://doi.org/10.1186/1752-0509-1-35)
- Bajzer Z, Marusic M, Vuk-Pavlovic S (1996) Conceptual frameworks for mathematical modeling of tumor growth dynamics. *Math Comput Model* 23:31–46
- Bellmunt J, Carles J, Albanell J (2009) Predictive modelling in hormone-refractory prostate cancer (HRPC). *Clin Translat Oncol* 11:82–85
- Brekelmans CT, Seynaeve C, Menke-Pluymers M, Brüggewirth HT, Tilanus-Linthorst MM, Bartels CC, Kriege M, van Geel AN, Crepin CM, Blom JC, Meijers-Heijboer H, Klijn JG (2006) Survival and prognostic factors in BRCA1-associated breast cancer. *Ann Oncol* 17:391–400
- Brekelmans CT, Tilanus-Linthorst MM, Seynaeve C, vd Ouweland A, Menke-Pluymers MB, Bartels CC, Kriege M, van Geel AN, Burger CW, Eggermont AM, Meijers-Heijboer H, Klijn JG (2007) Tumor characteristics, survival and prognostic factors of hereditary breast cancer from BRCA2-, BRCA1- and non-BRCA1/2 families as compared to sporadic breast cancer cases. *Eur J Cancer* 43:867–876
- Bruggeman FJ, Westerhoff HV (2006) Approaches to biosimulation of cellular processes. *J Biol Phys* 32:273–288

- Bruno R, Claret L (2009) On the use of change in tumor size to predict survival in clinical oncology studies: toward a new paradigm to design and evaluate phase II studies. *Clin Pharmacol Ther* 86(2):136–138
- Bulitta JB, Zhao P, Arnold RD, Kessler DR, Daifuku R, Pratt J, Luciano G, Hanauske AR, Gelderblom H, Awada A, Jusko WJ (2009) Multiple-pool cell lifespan models for neutropenia to assess the population pharmacodynamics of unbound paclitaxel from two formulations in cancer patients. *Cancer Chemother Pharmacol* 63(6):1035–1048
- Burzykowski T, Buyse M, Piccart-Gebhart MJ, Sledge G, Carmichael J, Lück HJ, Mackey JR, Nabholz JM, Paridaens R, Biganzoli L, Jassem J, Bontenbal M, Bonnetterre J, Chan S, Basaran AG, Therasse P (2008) Evaluation of tumor response, disease control, progression-free survival, and time to progression as potential surrogate end points in metastatic breast cancer. *J Clin Oncol* 26:1987–1992
- Buyse M (2009) Use of meta-analysis for the validation of surrogate endpoints and biomarkers in cancer trials. *Cancer J* 15:421–425
- Buyse M, Sargent DJ, Grothey A, Matheson A, de Gramont A (2010) Biomarkers and surrogate end points—the challenge of statistical validation. *Nat Rev Clin Oncol* 7(6):309–317
- Cameron DA, Gregory WM, Bowman A, Leonard RC (1996) Mathematical modelling of tumor response in primary breast cancer. *Br J Cancer* 73(11):1409–1416
- Cappuccio A, Castiglione F, Piccoli B (2007) Determination of the optimal therapeutic protocols in cancer immunotherapy. *Mathl Biosci* 209:1–13
- Chen LL, Blumm N, Christakis NA, Barabási AL, Deisboeck TS (2009) Cancer metastasis networks and the prediction of progression patterns. *Br J Cancer* 101:749–758
- Claret L, Girard P, Hoff PM, Van Cutsem E, Zuideveld KP, Jorga K, Fagerberg J, Bruno R (2009) Model-based prediction of phase III overall survival in colorectal cancer on the basis of phase II tumor dynamics. *J Clin Oncol* 27(25):4103–4108
- Coates JM, Galante JM, Bold RJ (2009) Cancer therapy beyond apoptosis: Autophagy and anoikis as mechanisms of cell death. *J Surg Res*. doi:10.1016/j.jss.2009.07.011
- Collins VP, Loeffler RK, Tivey H (1956) Observations on growth rates of human tumors. *Am J Roentgenol Radium Ther Nucl Med* 76:988–1000
- Danhof M, Alvan G, Dahl SG, Kuhlmann J, Paintaud G (2005) Mechanism-based pharmacokinetic-pharmacodynamic modeling—a new classification of biomarkers. *Pharm Res* 22(9):1432–1437
- Daydé D, Ternant D, Ohresser M, Lerondel S, Pesnel S, Watier H, Le Pape A, Bardos P, Paintaud G, Cartron G (2009) Tumor burden influences exposure and response to rituximab: pharmacokinetic-pharmacodynamic modeling using a syngeneic bioluminescent murine model expressing human CD20. *Blood* 113(16):3765–3772
- Dayneka NL, Garg V, Jusko WJ (1993) Comparison of four basic models of indirect pharmacodynamic responses. *J Pharmacokinetic Biopharm* 21:457–478
- Dehing-Oberije C, Yu S, De Ruyscher D, Meersschout S, Van Beek K, Lievens Y, Van Meerbeek J, De Neve W, Rao B, van der Weide H, Lambin P (2009) Development and external validation of prognostic model for 2-year survival of non-small-cell lung cancer patients treated with chemoradiotherapy. *Int J Radiat Oncol Biol Phys* 74(2):355–362
- Deisboeck T (2001) Pattern of self-organization in tumor systems: complex growth dynamics in a novel brain tumor spheroid model. *Cell Prolif* 34:115–134
- Della Pasqua O, Santen GW, Danhof M (2010) The missing link between clinical endpoints and drug targets in depression. *Trends Pharmacol Sci* 31:144–152
- Diva U, Banerjee S, Dey DK (2007) Modelling spatially correlated survival data for individuals with multiple cancers. *Stat Modelling* 7:191–213
- Dormer P, Lau B, Wilmanns W (1980) Kinetics of bone marrow cell production in human acute and chronic myeloid leukemias. *Leuk Res* 4:231–237
- European Medicines Agency. Committee for Medicinal Products for Human Use (2006) Appendix I to the guideline on the evaluation of anticancer medicinal products in man (CHMP/ewp/205/95 rev.3). Methodological considerations for using progression-free survival (PFS) as

- primary endpoint in confirmatory trials for registration. <http://www.emea.europa.eu/pdfs/human/ewp/26757506en.pdf>
- Fetterly GJ, Grasela TH, Sherman JW, Dul JL, Grahn A, Lecomte D, Fiedler-Kelly J, Damjanov N, Fishman M, Kane MP, Rubin EH, Tan AR (2008) Pharmacokinetic/pharmacodynamic modeling and simulation of neutropenia during phase I development of liposome-entrapped paclitaxel. *Clin Cancer Res* 14(18):5856–5863
- Fidler IJ (2002) Critical determinants of metastasis. *Semin Cancer Biol* 12(2):89–96
- Fleischer F, Gaschler-Markefski B, Bluhmki E (2009) A statistical model for the dependence between progression-free survival and overall survival. *Stat Med* 28:2669–2686
- Frame D (2007) New strategies in controlling drug resistance in chronic myeloid leukemia. *Am J Health Syst Pharm* 64:S16–S21
- Friberg LE, Karlsson MO (2003) Mechanistic models for myelosuppression. *Invest New Drugs* 21:183–194
- Friberg LE, Brindley CJ, Karlsson MO, Devlin AJ (2000) Models of schedule dependent haematological toxicity of 2'-deoxy-2'-methylidene-cytidine (DMDC). *Eur J Clin Pharmacol* 56:567–574
- Friberg LE, Henningsson A, Maas H, Nguyen L, Karlsson MO (2002) Model of chemotherapy-induced myelosuppression with parameter consistency across drugs. *J Clin Oncol* 20:4713–4721
- Friberg LE, de Greef R, Kerbusch T, Karlsson MO (2009) Modeling and simulation of the time course of asenapine exposure response and dropout patterns in acute schizophrenia. *Clin Pharmacol Ther* 86(1):84–91
- Gardner SN (2000) A mechanistic, predictive model of dose-response curves for cell cycle phase-specific and -nonspecific drugs. *Cancer Res* 60:1417–1425
- Gasparini G, Biganzoli E, Bonoldi E, Morabito A, Fanelli A, Boracchi P (2001) Angiogenesis sustains tumor dormancy in patients with breast cancer treated with adjuvant chemotherapy. *Breast Cancer Res Treat* 65:71–75
- Gieschke R, Burger HU, Reigner B, Blesch KS, Steimer JL (2003) Population pharmacokinetics and concentration–effect relationships of capecitabine metabolites in colorectal cancer patients. *Br J Clin Pharmacol* 55:252–263
- Gilbert D, Fuss H, Gu X, Orton R, Robinson S, Vysheirsky V, Kurth MJ, Downes CS, Dubitzky W (2006) Computational methodologies for modelling, analysis and simulation of signalling networks. *Brief Bioinform* 7:339–353
- Goel G, Chou IC, Voit EO (2006) Biological systems modeling and analysis: a biomolecular technique of the twenty-first century. *J Biomol Tech* 17:252–269
- Goggin T, Nguyen QT, Munafo A (2004) Population pharmacokinetic modelling of Emfilermin (recombinant human leukaemia inhibitory factor, r-hLIF) in healthy postmenopausal women and in infertile patients undergoing in vitro fertilization and embryo transfer. *Br J Clin Pharmacol* 57(5):576–585
- Harpold HL, Alvord EC Jr, Swanson KR (2007) The evolution of mathematical modeling of glioma proliferation and invasion. *J Neuropathol Exp Neurol* 66:1–9
- Hartwell LH, Kastan MB (1994) Cell cycle control and cancer. *Science* 266:1821–1828
- Hénin E, Zuideveld KP, Dartois C, Tranchand B, Freyer G, Girard P (2006) A KPD model for ordered categorical data: application to toxicity score in colorectal cancer patients treated with capecitabine PAGE 15 (2006) Abstract 929. www.page-meeting.org/?abstract=929
- Hing J, Perez-Ruixo JJ, Stuyckens K, Soto-Matos A, Lopez-Lazaro L, Zannikos P (2008) Mechanism-based pharmacokinetic/pharmacodynamic meta-analysis of trabectedin (ET-743, Yondelis) induced neutropenia. *Clin Pharmacol Ther* 83:130–143
- Hornberg JJ, Bruggeman FJ, Westerhoff HV, Lankelma J (2006) Cancer: a Systems Biology disease. *Biosystems* 83:81–90
- Howard A, Pelc SR (1951) Nuclear incorporation of P-32 as demonstrated by autoradiographs. *Exp Cell Res* 2:178–187

- Jacqmin P, McFadyen L, Wade JR (2010) Basic PK/PD principles of drug effects in circular/proliferative systems for disease modelling. *J Pharmacokinet Pharmacodyn* 37(2):157–177
- Joerger M, Huitema AD, Richel DJ, Dittrich C, Pavlidis N, Briasoulis E, Vermorken JB, Strocchi E, Martoni A, Sorio R, Sleeboom HP, Izquierdo MA, Jodrell DI, Calvert H, Boddy AV, Hollema H, Fety R, van derVijgh WF, Hempel G, Chatelut E, Karlsson M, Wilkins J, Tranchand B, Schrijvers AHGL, Twelves C, Beijnen JH, Schellens JHM (2007a) Population pharmacokinetics and pharmacodynamics of paclitaxel and carboplatin in ovarian cancer patients: a study by the European organization for research and treatment of cancer-pharmacology and molecular mechanisms group and new drug development group. *Clin Cancer Res* 13:6410–6418
- Joerger M, Huitema AD, Richel DJ et al (2007b) Population pharmacokinetics and pharmacodynamics of doxorubicin and cyclophosphamide in breast cancer patients: a study by the EORTC-PAMM-NDDG. *Clin Pharmacokinet* 46:1051–1068
- Johnson JR, Williams G, Pazdur R (2003) Endpoints and United States Food and Drug Administration approval of oncology drugs. *J Clin Oncol* 21:1404–1411
- Klein JP (2006) Modelling competing risks in cancer studies. *Stat Med* 25:1015–1034
- Krzyzanski W, Perez-Ruixo JJ, Vermeulen A (2008) Basic pharmacodynamic models for agents that alter the lifespan distribution of natural cells. *J Pharmacokinet Pharmacodyn* 35(3):349–377
- Kusama S, Spratt JS Jr, Donegan WL, Watson FR, Cunningham C (1972) The gross rates of growth of human mammary cancer. *Cancer* 30:594–599
- Levasseur LM, Slocum HK, Rustum YM, Greco WR (1998) Modeling of the time-dependency of in vitro drug cytotoxicity and resistance. *Cancer Res* 58:5749–5761
- Luo FR, Yang Z, Dong H, Camuso A, McGlinchey K, Fager K, Flefleh C, Kan D, Inigo I, Castaneda S, Rose WC, Kramer RA, Wild R, Lee FY (2005) Correlation of pharmacokinetics with the antitumor activity of Cetuximab in nude mice bearing the GEO human colon carcinoma xenograft. *Cancer Chemother Pharmacol* 56:455–464
- Mager DE, Jusko WJ (2002) Receptor-mediated pharmacokinetic/pharmacodynamic model of interferon-beta 1a in humans. *Pharm Res* 19:1537–1543
- Mager DE, Woo S, Jusko WJ (2009) Scaling pharmacodynamics from in vitro and preclinical animal studies to humans. *Drug Metab Pharmacokinet* 24(1):16–24
- Magni P, Simeoni M, Poggesi I, Rocchetti M, de Nicolao G (2006) A mathematical model to study the effects of drugs administration on tumor growth dynamics. *Math Biosci* 200:127–151
- Mathon NF, Lloyd AC (2001) Milestones in cell division: Cell senescence and cancer. *Nature Rev Cancer* 1:203–213
- Mayneord WV (1932) On the law of growth in Jensen's rat sarcoma. *Am J Cancer* 16:841–846
- McDougall SR, Anderson AR, Chaplain MA (2006) Mathematical modelling of dynamic adaptive tumor-induced angiogenesis: clinical implications and therapeutic targeting strategies. *J Theor Biol* 241:564–589
- Mould DR, Green B (2010) Pharmacokinetics and pharmacodynamics of monoclonal antibodies: concepts and lessons for drug development. *Biodrugs* 24:23–39
- Mould DR, Sweeney K, Duffull SB, Neylon E, Hamlin P, Horwitz S, Sirotak F, Fleisher M, Saunders ME, O'Connor OA (2009) A population pharmacokinetic and pharmacodynamic evaluation of pralatrexate in patients with relapsed or refractory non-Hodgkin's or Hodgkin's lymphoma. *Clin Pharmacol Ther* 86(2):190–196
- Mukherjee A, Majumder D (2008) Mathematical modelling for the assessment of the effect of drug application delays in metronomic chemotherapy of cancer due to physiological constraints. *Biosystems* 91:108–116
- Peletier LA, Gabrielsson J (2009) Dynamics of target-mediated drug disposition. *Eur J Pharm Sci* 38(5):445–464
- Quaranta V, Weaver AM, Cummings PT, Anderson ARA (2005) Mathematical modeling of cancer: the future of prognosis and treatment. *Clin Chim Acta* 357:173–179
- Rabinowitz J, Davidov O (2008) The association of dropout and outcome in trials of antipsychotic medication and its implications for dealing with missing data. *Schizophr Bull* 34(2):286–291

- Ratain MJ, Eckhardt SG (2004) Phase II studies of modern drugs directed against new targets: if you are fazed, too, then resist RECIST. *J Clin Oncol* 22(22):4442–4445
- Rew DA (2000a) Modelling in tumor biology part I: modelling concepts and structures. *Eur J Surg Oncol* 26:87–94
- Rew DA (2000b) Modelling in tumor biology part II: modelling cancer therapy. *Eur J Surg Oncol* 26:181–188
- Rew DA, Wilson GD (2000a) Cell production rates in human tissues and tumors and their significance. Part I: an introduction to the techniques of measurement and their limitations. *Eur J Surg Oncol* 26:227–238
- Rew DA, Wilson GD (2000b) Cell production rates in human tissues and tumors and their significance. Part II: clinical data. *Eur J Surg Oncol* 26:405–417
- Rocchetti M, Simeoni M, Pesenti E, de Nicolao G, Poggesi I (2007) Predicting the active doses in humans from animal studies: a novel approach in oncology. *Eur J Cancer* 43:1862–1868
- Saad ED, Katz A, Hoff PM, Buyse M (2010) Progression-free survival as surrogate and as true endpoint: insights from the breast and colorectal cancer literature. *Ann Oncol* 21:7–12
- Santen G, Horrigan J, Danhof M, Della Pasqua O (2009) From trial and error to trial simulation. Part 2: an appraisal of current beliefs in the design and analysis of clinical trials for antidepressant drugs. *Clin Pharmacol Ther* 86(3):255–262
- Sherrill B, Amonkar M, Wu Y, Hirst C, Stein S, Walker M, Cuzick J (2008) Relationship between effects on time-to-disease progression and overall survival in studies of metastatic breast cancer. *Br J Cancer* 99:1572–1578
- Sidorov IA, Hirsch KS, Harley CB, Dimitrov DS (2003) Cancer treatment by telomerase inhibitors: predictions by a kinetic model. *Math Biosci* 181:209–221
- Simeoni M, Magni P, Cammia C, De Nicolao G, Croci V, Pesenti E, Germani M, Poggesi I, Rocchetti M (2004) Predictive pharmacokinetic-pharmacodynamic modeling of tumor growth kinetics in xenograft models after administration of anticancer agents. *Cancer Res* 64:1094–1101
- Steel GG (1977) Growth kinetics of tumors: cell population kinetics in relation to the growth and treatment of cancer. Clarendon, Oxford
- Steimer JL, Dahl SG, De Alwis DP, Gundert-Remy U, Karlsson MO, Martinkova J, Aarons L, Ahr HJ, Clairambault J, Freyer G, Friberg LE, Kern SE, Kopp-Schneider A, Ludwig WD, De Nicolao G, Rocchetti M, Troconiz IF (2010) Modelling the genesis and treatment of cancer: the potential role of physiologically based pharmacodynamics. *Eur J Cancer* 46:21–32
- Swanson KR, Bridge C, Murray JD, Alvord EC Jr (2003) Virtual and real brain tumors: using mathematical modeling to quantify glioma growth and invasion. *J Neurol Sci* 216(1):1–10
- Tan WY, Chen CW (1998) Stochastic modeling of carcinogenesis: some new insights. *Math Comput Modelling* 28(11):49–71
- Tannock I (1986) Experimental chemotherapy and concepts related to the cell cycle. *Int J Radiat Biol* 49:335–355
- Ternant D, Paintaud G (2005) Pharmacokinetics and concentration-effect relationships of therapeutic monoclonal antibodies and fusion proteins. *Expert Opin Biol Ther* 5(Suppl 1):S37–S47
- Tham LS, Wang L, Soo RA, Lee SC, Lee HS, Yong PW, Goh BC, Holford NHG (2008) A pharmacodynamic model for the time course of tumor shrinkage by gemcitabine + carboplatin in non-small cell lung cancer patients. *Clin Cancer Res* 14(13):4213–4218
- Tracqui P, Cruywagen GC, Woodward DE, Bartoo GT, Murray JD, Alvord EC Jr (1995) A mathematical model of glioma growth: the effect of chemotherapy on spatio-temporal growth. *Cell Prolif* 28:17–31
- U.S. Department of Health and Human Services, Food and Drug Administration, Center for Drug Evaluation and Research (2007) Guidance for industry: Clinical trial endpoints for the approval of cancer drugs and biologics.
- van Kesteren Ch, Mathôt RA, Beijnen JH, Schellens JH (2003) Pharmacokinetic-pharmacodynamic guided trial design in oncology. *Invest New Drugs* 21(2):225–241

- Veyrat-Follet C, Bruno R, Olivares R, Rhodes GR, Chaikin P (2000) Clinical trial simulation of docetaxel in patients with cancer as a tool for dosage optimization. *Clin Pharmacol Ther* 68 (6):677–687
- Wang Y, Sung C, Dartois C, Ramchandani R, Booth BP, Rock E, Gobburu J (2009) Elucidation of relationship between tumor size and survival in non-small-cell lung cancer patients can aid early decision making in clinical drug development. *Clin Pharmacol Ther* 86(2):167–174
- Williamson MJ, Silva MD, Terkelsen J, Robertson R, Yu L, Xia C, Hatsis P, Bannerman B, Babcock T, Cao Y, Kupperman E (2009) The relationship among tumor architecture, pharmacokinetics, pharmacodynamics, and efficacy of bortezomib in mouse xenograft models. *Mol Cancer Ther* 8:3234–3243
- Wilson GD (1991) Assessment of human tumor proliferation using bromodeoxyuridine – current status. *Acta Oncol* 30:903–910
- Yamazaki S, Skaptason J, Romero D, Lee JH, Zou HY, Christensen JG, Koup JR, Smith BJ, Koudriakova T (2008) Pharmacokinetic-pharmacodynamic modeling of biomarker response and tumor growth inhibition to an orally available cMet kinase inhibitor in human tumor xenograft mouse models. *Drug Metab Dispos* 36(7):1267–1274
- You B, Perrin P, Freyer G, Ruffion A, Tranchand B, Hémin E, Paparel P, Ribba B, Devonec M, Falandry C, Fournel C, Tod M, Girard P (2008a) Advantages of prostate-specific antigen (PSA) clearance model over simple PSA half-life computation to describe PSA decrease after prostate adenectomy. *Clin Biochem* 41:785–795
- You B, Tranchand B, Girard P, Falandry C, Ribba B, Chabaud S, Souquet PJ, Court-Fortune I, Trillet-Lenoir V, Fournel C, Tod M, Freyer G (2008b) Etoposide pharmacokinetics and survival in patients with small cell lung cancer: a multicentre study. *Lung Cancer* 62(2):261–272
- You B, Girard P, Paparel P, Freyer G, Ruffion A, Charrié A, Hémin E, Tod M, Perrin P (2009) Prognostic value of modeled PSA clearance on biochemical relapse free survival after radical prostatectomy. *Prostate* 69(12):1325–1333
- You B, Pollet-Villard M, Fronton L, Labrousse C, Schott AM, Hajri T, Girard P, Freyer G, Tod M, Tranchand B, Colomban O, Ribba B, Raudrant D, Massardier J, Chabaud S, Golfier F (2010) Predictive values of hCG clearance for risk of methotrexate resistance in low-risk gestational trophoblastic neoplasias. *Ann Oncol*. doi:[10.1093/annonc/mdq033](https://doi.org/10.1093/annonc/mdq033)
- Zandvliet AS, Schellens JHM, Dittich C, Wanders J, Beijnen JH, Huitema ADR (2008) Population pharmacokinetic and pharmacodynamic analysis to support treatment optimization of combination chemotherapy with indisulam and carboplatin. *Br J Clin Pharmacol* 66(4):485–497

Chapter 14

Application of Pharmacokinetic– Pharmacodynamic Modeling and Simulation for Erythropoietic Stimulating Agents

Juan José Pérez-Ruixo, Sameer Doshi, and Andrew Chow

Abstract Rigorous management of the knowledge generated with the modeling techniques requires the exploration of different scenarios of interest via simulations, which can be used to inform many key decisions during drug development. This process, termed model-based drug development, is illustrated in three examples at different stages of drug development of erythropoiesis stimulating agents (ESA). Each of these examples reflects an actual situation with key decisions made based on the knowledge obtained from these models. One of the beneficial outcomes of the modeling and simulation approach is to elicit discussion in the development team on the unverifiable assumptions at each stage and to guide risk calculations in decision making. This approach can facilitate the development of better dosing regimens of new medicines, which may lead to enhanced benefit of the drug therapy and improvements in the quality of life of the patients.

14.1 Introduction

The concept of model-based drug development has evolved as a way to improve drug development knowledge management and decision making processes through the use modeling and simulation techniques (Miller *et al.* 2005). This approach has been recognized by the pharmaceutical industry as one of the emerging technologies that can contribute to improve the business model for developing new therapeutically and commercially successful drugs, which ultimately will benefit the patients. In recent years, the field of pharmacokinetic and pharmacodynamic (PK/PD) modeling has advanced from using empirical functions to describe and summarize the data to the use of mechanism-based models. Mechanism-based PK/PD modeling is expected to provide meaningful model parameter estimates and improved predictions of the drug disposition and drug effects, as it incorporates

J.J. Pérez-Ruixo (✉)

Pharmacokinetics and Drug Metabolism, Amgen Inc., Thousand Oaks, CA, USA
e-mail: juanjose@amgen.com

underlying principles of pharmacology, physiology, and pathology (Sheiner and Wakefield 1999). We illustrate this approach here as applied to therapy with erythropoiesis stimulating agents (ESA), in which several mechanism-based PK/PD models have been developed to describe the dynamics of red blood cell turnover, and applied to enhance key decisions in the ESA development process.

In general, the quantity blood cells in the body is determined by two processes: cell production and cell loss. Under homeostatic conditions, constant proliferation, differentiation, and maturation of stem cells yield a steady-state level of functional cells, which remain in the circulation for a period of time, which is determined by tissue uptake, random destruction, or cell senescence. In addition, several diseases and pharmacological agents can inhibit or stimulate a biological mechanism that controls the production or elimination of selected blood cells. As the net balance of cell production and elimination processes is altered, the steady-state cell counts may increase or decrease and fall out of the normality range. However, the long time delays in drug responses observed in the erythropoietic system are mainly due to the long lifespan of red blood cells (RBC), which is an additional complexity to take into account in developing mechanism-based PKPD models to quantify the dynamics of RBC.

Semi-mechanistic PK/PD models, based on the lifespan concept, have been extensively used to characterize the erythropoiesis and the pharmacological response to ESA in different populations. Since these models have been applied during the drug development process, the main objective of this chapter is to provide real life examples in which modeling and simulation techniques have been efficiently used in different stages of ESA development. The three examples presented encompass the full course of clinical development from Phase I to Phase III, and include (1) the application of modeling and simulation techniques to integrate the information obtained from preclinical stages of drug development and to predict the outcome of first time in man (FTIM) studies, (2) the selection of an optimal dosing regimen for a clinical study intended to provide a confirmatory evidence for a drug label extension, and (3) use of adult PK/PD information to optimize the design and analysis of pediatric clinical studies.

14.2 Extrapolating PK/PD from Preclinical to Clinical

In this first case study, a simulation strategy based on a mechanistic PK/PD model was developed to predict the outcome of the FTIM and proof of concept (POC) study of a ESA. Description of the erythropoiesis model, along with the procedures to scale the pharmacokinetics and pharmacodynamics based on preclinical *in vivo* and *in vitro* information are presented. The Phase I study design is described, and the model-based predictions are also shown and discussed (Pérez-Ruixo 2006).

A mechanism-based PK/PD model for recombinant human erythropoietin rHu-EPO was used to describe the physiological basis of the biological system. An open, two-compartment disposition model with parallel linear and nonlinear clearance,

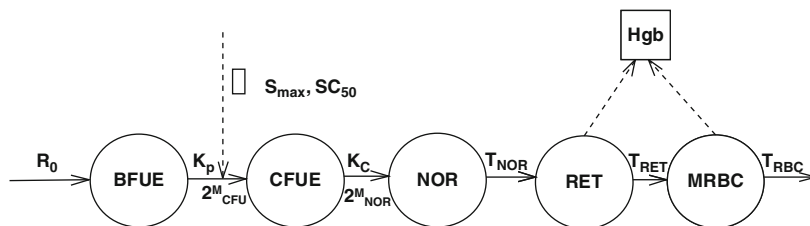


Fig. 14.1 Pharmacokinetic and pharmacodynamic model for rHu-EPO in healthy subjects

and endogenous EPO at baseline, was used to describe rHu-EPO disposition after intravenous administration (Olsson 2007). The pharmacodynamic effect of rHu-EPO on hemoglobin was characterized using a previously developed model, based on the precursor-dependent indirect pharmacodynamic response and cell life-span concepts (Kryzanski *et al.* 2005). This model has been also recently used to analyze the pharmacokinetics and pharmacodynamics of the erythropoietin mimetic-body™ construct, CNTO 528, in healthy subjects (Pérez-Ruixo *et al.* 2009).

Figure 14.1 displays the scheme of the PK/PD model. Briefly, it is assumed that the progenitor cells BFU-E are generated at a constant rate of R_0 and the differentiation of BFU-E cells into CFU-E is controlled by processes with a first order rate of k_p , which is stimulated by rHu-EPO serum concentration according to a sigmoid function, characterized by the maximum stimulation of BFU-E to differentiate to CFU-E (S_{\max}), and rHu-EPO serum concentration eliciting 50% of S_{\max} (SC_{50}). On average, the BFU-E cells proliferate M_{CFU} times and the factor $2^{M_{CFU}}$ is included to reflect that one BFU-E cell gives rise to $2^{M_{CFU}}$ CFU-E cells. Similarly, CFU-E cells proliferate, on average, M_{NOR} times and are transformed to NOR according to the first-order rate constant k_c . It is further assumed that normoblasts are transformed to reticulocytes (RET) after a maturation time T_{NOR} . The rate of NOR elimination to the RET pool becomes the NOR production rate delayed by the time T_{NOR} . An analogous mechanism controls the transformation of RET to mature RBC after their lifespan T_{RET} expires. The RBC production equals the RET transition rate and RBC are removed from the circulation because of senescence after their life span T_{RBC} . Hemoglobin concentration in blood (g/dL) is proportional to the absolute amount of RET and RBC (cells/L), and the proportionality constant is the mean corpuscular hemoglobin (MCH) (pg/cell). The PK/PD model described was developed in NON-MEM® software and the delay differential equations dealing with the lifespan of NOR, RETS, and RBC were implemented following the method as previously described (Pérez-Ruixo *et al.* 2005).

Population-based interspecies allometric scaling was used to predict the expected pharmacokinetic profile of an ESA candidate in normal healthy subjects according to the methodology previously described (Jolling *et al.* 2005). Data collected in rat, rabbit, dog, and monkey were used to extrapolate the model parameters of an open, two-compartment disposition model with linear elimination to humans, using body weight and maximum life time potential as scaling factors.

With this approach, the coefficients and exponents of the allometric scaling equations were estimated directly from the raw plasma concentration vs. time data, thus avoiding the inherent bias arising from the classical allometric scaling procedure that uses the mean pharmacokinetic parameters for each species and does not consider the different number of animals in each species and the within-species variability. Based on *in vitro* UT-7 cells proliferation assays (Erickson-Miller *et al.* 2000), the same intrinsic activity and a 45-fold lower potency of the ESA relative to rHu-EPO was assumed. This ratio was used to scale the potency of the ESA candidate in humans, given the rHu-EPO potency in healthy subjects obtained previously (Krzyzanski *et al.* 2005). In addition, a competitive agonist model was implemented via Gaddum's equation to quantify the pharmacodynamic interaction between the concentration of the ESA candidate and endogenous EPO (Lazareno and Birdsall 1993).

The Phase I study was designed as a randomized, double blind, placebo controlled, single ascending dose study to evaluate the pharmacokinetics and pharmacodynamics of an ESA candidate (Pérez-Ruixo *et al.* 2008). Cohorts of nine subjects with baseline hemoglobin levels less than 14.5 g/dL were randomized to receive ESA treatment ($N = 6$) at each dose level or matched placebo ($N = 3$). The various dose levels considered in this study were 1 \times , 3 \times , 10 \times , and 30 \times . The objective of the study was to identify the pharmacological effective dose (PED), defined as the dose level where four or more treated subjects achieve an increase in hemoglobin from baseline of more than 1 g/dL within 28 day.

Simulations were performed to evaluate the probability of identifying the PED with the current study design of an ESA candidate (Pérez-Ruixo *et al.* 2008a). One hundred cohorts of six subjects receiving ESA treatment were simulated per dose level according to the Phase I study design and the mechanistic PK/PD model described above. Body weight and endogenous EPO at baseline were obtained by resampling from a population of healthy subjects that were included in rHu-EPO Phase I studies (Olsson-Gislekog *et al.* 2007). Figure 14.2 displays the observed and the model-based predicted time course of the change in hemoglobin from baseline at various doses.

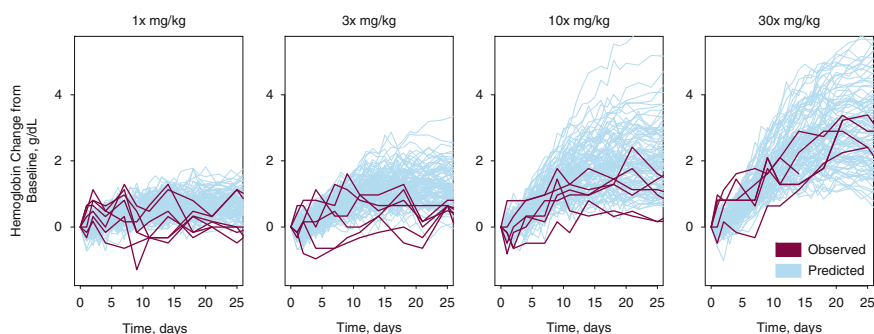


Fig. 14.2 Observed and model-based predicted hemoglobin change from baseline

Table 14.1 Probability (95%CI) of achieving the pharmacological effective dose (PED) as a function of dose

Dose level (mg/kg)	Probability of PED (95%CI)
1×	0.24 (0.08–0.73)
3×	0.75 (0.64–0.89)
10×	0.97 (0.95–0.99)
30×	0.99 (0.98–1.00)

From the simulated data, the number of subjects per cohort that achieved an increase in hemoglobin of greater than 1 g/dL within 28 days was calculated and the probability of achieving the PED was derived (Table 14.1). The dose range where more than 95% of the replicate cohorts will have four or more subjects with hemoglobin increases of more than 1 g/dL within 4 week was estimated to be between 20× and 70× mg/kg. Notably, the observed PED, 30× mg/kg, falls within the predicted dose range. A similar approach has been recently used to retrospectively analyze the preclinical data for rHu-EPO and has been proven to effective in predicting the human time course of hemoglobin using preclinical data (Mager 2009).

This example has shown that (1) the mechanistic PK/PD model of rHu-EPO previously published and preclinical information for an ESA candidate is suitable to provide a better quantification and prediction of the drug disposition and the time course of hemoglobin in adult healthy subjects and (2) this model was used to optimize the design of the Phase I studies of ESA candidates, with respect to key design features (*e.g.*, the number and selection of dose levels, the number of subjects per dose level, and the PK/PD sampling times). In this way, a quantitative risk-benefit assessment is obtained by determining the probability of success of a Phase I study with an ESA candidate, conditional on certain experimental design considerations, *in vitro* potency, and preclinical PKPD information.

14.3 Predicting the Outcome of an Extended Dosing Interval Regimen

In this second example, a simulation strategy based on a mechanistic PK/PD model (Doshi *et al.* 2010) was developed to retrospectively predict the outcome of a previously completed clinical study designed to evaluate monthly dosing of darbepoetin alfa (Aranesp[®]), a hyperglycosylated rHu-EPO analog. Darbepoetin alfa possesses five amino acid changes and two additional N-linked carbohydrate chains compared to rHu-EPO, but has the same mechanism of action. However, darbepoetin alfa has a threefold increased serum half-life, and increased *in vivo* potency, allowing for more convenient dosing regimens for the treatment of anemia associated with chronic renal failure (CRF), including extended dosing intervals such as biweekly dosing for patients who are either receiving or not receiving dialysis (Doshi *et al.* 2009). Description of the erythropoiesis model, along with the clinical

study design is presented and the model-based predictions are shown and discussed relative to the observed results of the clinical study. The dose adaptation algorithm based on the pharmacodynamic response is described in detail because it influences the clinical endpoint results, and is a key feature of this simulation exercise. Therefore, the clinical trial simulations should simultaneously consider both the dosing regimen conditioned by the pharmacodynamic response and the pharmacodynamic response given by a certain dosing regimen.

Darbepoetin alfa pharmacokinetics following s.c. administration was described by an open two-compartment disposition model with a linear elimination from the central compartment and a sequential zero-order input into the depot compartment, followed by a first-order absorption from the depot compartment into the central compartment.

Similar to rHu-EPO in the previous example, darbepoetin alfa is assumed to stimulate the production of progenitor cells in bone marrow, according to a precursor-dependent indirect pharmacodynamic response model (Sharma *et al.* 1998) as shown in the equation:

$$\frac{d\text{PRC}}{dt} = k_{\text{in}} \left[1 + \frac{E_{\text{max}} \cdot C^\gamma}{\text{EC}_{50}^\gamma + C^\gamma} \right] - k_{\text{PRC}} \cdot \text{PRC}$$

where C denotes the sum of endogenous erythropoietin and exogenous darbepoetin alfa, k_{in} represents the endogenous production rate of progenitor cells, E_{max} represents the maximal stimulatory effect of k_{in} , EC_{50} denotes the darbepoetin alfa serum concentration necessary to maintain progenitor cell production rate half maximum, γ represents the Hill coefficient of the sigmoid concentration-effect relationship, PRC represents the amount of precursor cells, and k_{PRC} is the first-order transition rate from precursor cell to mature RBC.

The dynamic model describing the time course of hemoglobin following administration of darbepoetin alfa in nondialysis CRF subjects was based on the concept of maturation-structured cytokinetic model introduced previously (Harker *et al.* 2000), and further applied later (Roskos *et al.* 2006; Agoram *et al.* 2006; Pérez-Ruixo *et al.* 2008b; Hamrén *et al.* 2008). The backbone structure of such a model is a series of compartments linked in a catenary fashion by first-order cell transfer rates. Each compartment represents a pool of RBC of the increased mean age by $1/k$, where k denotes the first-order rate constant between the aging compartments. A cascade of four aging compartments ($N_{\text{RBC}} = 4$) with the transfer rate constants equal to $N_{\text{RBC}}/T_{\text{RBC}}$ were selected to account for the hemoglobin level in the RBC, where T_{RBC} is the mean RBC lifespan. The number of compartments was arbitrarily selected based on previous literature and considered that four compartments would be sufficiently large to result in a smoothed gamma distribution of the RBC cell lifespan (Agoram *et al.* 2006).

The precursor cells in bone marrow are released to blood as the youngest circulating reticulocytes (RBC_1) with a first-order rate, k_{PRC} :

$$\frac{dRBC_1}{dt} = k_{PRC} \cdot PRC - \frac{N_{RBC}}{T_{RBC}} \cdot RBC_1$$

These reticulocytes then mature to RBC through a series of aging compartments as follows:

$$\frac{dRBC_j}{dt} = \frac{N_{RBC}}{T_{RBC}} \cdot (RBC_{j-1} - RBC_j), \quad j = 2, \dots, N_{RBC}$$

Therefore, the circulating RBC level is the sum of RBC at all ages,

$$RBC = RBC_1 + \dots + RBC_{N_{RBC}}$$

As hemoglobin is directly proportional to the product of RBC and MCH, assuming MCH remains constant within a subject;

$$Hb = Hb_1 + \dots + Hb_{N_{RBC}}$$

Therefore, the RBC lifespan is equivalent to hemoglobin lifespan and, the initial conditions for PRC and RBC_j (or Hb_j) can be determined from the baseline hemoglobin (Hb_0) assuming a steady-state condition holds before the drug is administered. The initial conditions were as follows:

$$PRC_0 = \frac{Hb_0 \cdot T_{PRC}}{T_{RBC}}, \quad i = 1, \dots, N_P$$

and

$$Hb_{j0} = \frac{Hb_0}{N_{RBC}}, \quad j = 1, \dots, N_{RBC}$$

In addition, the endogenous progenitor production rate constant at baseline was calculated as follows:

$$k_{in} = \frac{Hb_0}{T_{RBC} \cdot \left(1 + \frac{E_{max} \cdot eEPO^{\gamma}}{EC_{50}^{\gamma} + eEPO^{\gamma}} \right)}$$

This model structure has shown to adequately describe the hemoglobin time course following the administration of different dosing schemes of darbepoetin alfa in another target population (Agoram *et al.* 2006) and was used to determine the model ability to predict the outcome of a single arm clinical study (Agarwal *et al.* 2006) intended to demonstrate the efficacy of monthly darbepoetin alfa in nondialysis CRF subjects.

The objectives of the clinical study were to assess the efficacy and safety of the darbepoetin alfa monthly dosing for the maintenance treatment of anemia in subjects with CRF not receiving dialysis. A total of 152 subjects were enrolled in the study and treated with darbepoetin alfa once monthly (QM), administered subcutaneously for 32 weeks with 129 of 152 subjects completing the study. Subjects were eligible if (1) they were in maintenance treatment receiving stable biweekly darbepoetin alfa doses, with dose stability defined as less than 25% change in dose over the screening period (6 weeks immediately before enrollment) and no missed doses in this period, and (2) mean of two hemoglobin values drawn at least 3 days apart during the screening period was between 11 and 13 g/dL. The starting unit dose of subcutaneous darbepoetin alfa was determined by calculating a subject's total dose in the month preceding enrollment and rounding to the nearest unit dose (20, 30, 40, 50, 60, 80, 100, 150, 200, or 300 μg in each prefilled syringe). After starting the subcutaneous treatment with darbepoetin alfa treatment, doses were adjusted to maintain hemoglobin levels between 11 and 13 g/dL, while limiting the hemoglobin rate of rise to ≤ 1.0 g/dL in the 2-week period after each dose. Dose adjustments were made as increases or decreases to the next higher or lower dose level in the prefilled syringes according to the following:

1. Increased to the next prefilled syringe dose if the most recent hemoglobin measurement was < 11.0 g/dL
2. Maintained if the most recent hemoglobin concentration was ≥ 11.0 to ≤ 13.0 g/dL
3. Reduced to the next lower prefilled syringe dose if hemoglobin concentration was > 13.0 to ≤ 14.0 g/dL or the hemoglobin rate of rise was > 1.0 g/dL in the 2-week period following a dose
4. Withheld the dose if the most recent hemoglobin concentration was > 14.0 g/day, and then restarted darbepoetin alfa at the next lower prefilled syringe dose when the hemoglobin concentration was ≥ 13.0 g/dL

If a decrease to the next prefilled syringe dose level was required when receiving the lowest prefilled syringe (20 μg), placebo was administered until an increase to the next higher prefilled syringe (20 μg) was needed. Hemoglobin samples were collected prior to darbepoetin alfa administration, and then every 2 weeks for 32 weeks. Dose adjustments were made following the monthly hemoglobin observation and prior to the monthly dose. The study was conducted over a 32-week period, with the final 8 weeks defined as the evaluation phase for obtaining the trial endpoints. The primary endpoint of the study was the proportion of subjects who maintained a mean hemoglobin ≥ 11 g/dL during the evaluation period. Secondary endpoints included the time course of hemoglobin and darbepoetin alfa dose over the 32-week study duration.

The design of the clinical study and the dosing algorithm were implemented within the Trial Simulator version 2.2 (Pharsight Corporation, a Certara Company, Saint Louis, MO) software. Based on the PKPD parameters obtained from a bootstrap replicate and the design of the clinical study, the time course of hemoglobin and darbepoetin alfa dosing was simulated for 300 nondialysis CRF subjects receiving

darbepoetin alfa QM dosing. Individual subject parameters were sampled from the distribution provided by the fixed and random effects of the PKPD model. As body weight was related to PK model parameters, body weight was sampled from a distribution which described the population body weight of CRF subjects not on dialysis, who would be likely to enroll in the study. This process was repeated 250 times using the PKPD parameters obtained from different bootstrap replicates in order to account for the statistical uncertainty in model parameters at the clinical trial level.

As the clinical study was conducted in maintenance subjects with CRF not on dialysis receiving stable doses of darbepoetin alfa every 2 weeks, the clinical trial simulation required a pool of subjects receiving stable doses Q2W to enroll in the simulated clinical trial. To create the pool of subjects, nearly twice the number of subjects evaluated in the study were simulated and dosed with darbepoetin alfa Q2W with a run-in period of 92 weeks, assuming these subjects were darbepoetin alfa naïve subjects. The number of subjects simulated and the duration of the run-in period were chosen to ensure a sufficient number of eligible subjects, from which a sample of 129 subjects was randomly selected to match the 129 subjects evaluated in the clinical study. The duration of the run-in period was arbitrarily selected based on the RBC lifespan and considering that the duration of the study should be longer than five times the RBC lifespan in order to achieve steady-state hemoglobin levels. The primary and secondary endpoints for each virtual clinical trial were computed and then summary statistics across the 250 replicates were used to compare with the observed endpoints.

The primary endpoint of the clinical study was the proportion of subjects maintaining hemoglobin ≥ 11 g/dL and the model-based simulation suggested it should be 79.1% (95%CI: 70.5–86.8%), which was in line with the point estimate of 85% obtained in the clinical study. In addition, the mean change of hemoglobin from baseline over time and its standard deviation for the clinical study is presented in Fig. 14.3, together with the model-based prediction and 95% confidence interval (shaded areas). This figure provides clear evidence that the observed time course of mean change of hemoglobin from baseline and its variability in the clinical study falls within the 95% confidence interval of the model-based predictions for that particular trial. Actually, the mean hemoglobin concentrations remained between 11.2 and 12.35 g/dL throughout the study and the simulation subsequently confirmed that finding. The mean change in hemoglobin concentration between baseline and the evaluation period was -0.18 g/dL (95%CI: -0.34 to -0.01 g/dL) for the observed data, which matched the model based prediction -0.20 g/dL (95%CI: -0.34 to 0.06 g/dL). Furthermore, the mean darbepoetin dose observed during the evaluation period was 125 $\mu\text{g}/\text{month}$, which is similar to the model-based prediction of 104 $\mu\text{g}/\text{month}$, and clearly falls within the 95% confidence intervals (66–181 $\mu\text{g}/\text{month}$).

Taken together these results collectively have shown that (1) the mechanistic PK/PD model for darbepoetin alfa developed based on weekly and biweekly (Doshi *et al.* 2010) dosing is suitable to quantify the percentage of subjects within certain target, time course of hemoglobin and the darbepoetin dose following the monthly administration for the maintenance treatment in adult subjects with CRF not on dialysis and (2) this model was used to optimize the design of additional

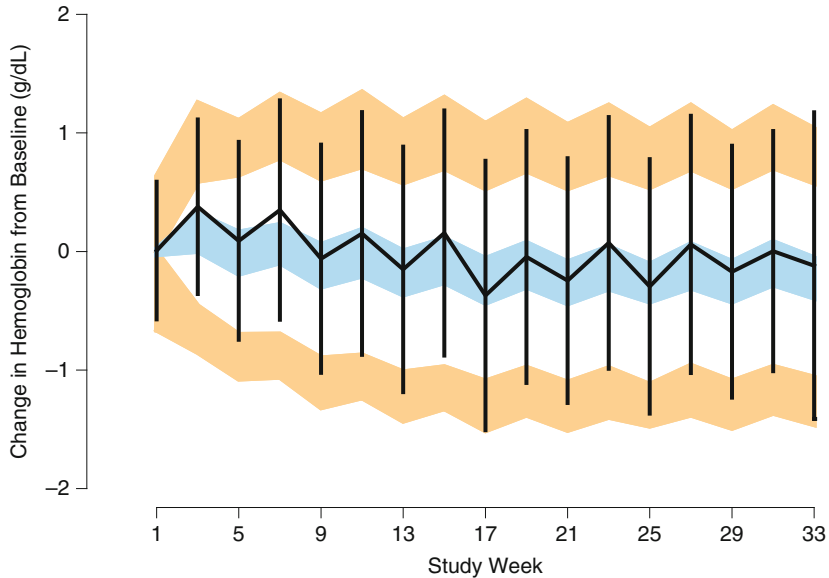


Fig. 14.3 Observed (*black lines*) and 95% confidence interval of model-based prediction (*shaded area*) of the mean and standard deviation of the change in hemoglobin from baseline over time following darbepoetin QM dosing

randomized studies intended to compare new darbepoetin alfa dosing regimens, with respect to key design features such as dose and schedule selection, dose adjustment algorithm, sample size and noninferiority margins. In this way, a quantitative risk-benefit assessment was obtained by determining the probability of success of a clinical study with new darbepoetin alfa dosing regimens, conditional on certain experimental design, the darbepoetin alfa initial dose and dose adjustment, and PKPD characteristics.

14.4 Pediatric Study Design

The rationale for dose selection for pediatric patients is often times based on empirical extrapolations from the recommended dose in adults. As specified in the International Conference on Harmonisation (ICH) E11 harmonized guideline, the extrapolation of drug efficacy is justified if the following requirements have been met: (1) the drug is to be used for the same indication in children and adults, (2) the disease process is similar in children and adults, and (3) the outcome of therapy is likely to be comparable in children and adults (US FDA 2000). These requirements are clearly met by ESA because the pathophysiological processes involved in chronic kidney failure in adults do not differ significantly from those observed in children, the end point for estimation of efficacy in clinical trials is the same in both populations, as indicated by the transfusion rate and/or the change

from baseline in hemoglobin, and given the mechanism of action of ESA, the exposure–effect relationship might be assumed to be independent of age. In this context, dose selection can be based on the evidence of pharmacokinetic differences in children relative to a reference adult population. The challenge is to determine the best use of prior information that is available from adults.

Traditional approaches have used size-related scaling because an implicit assumption is made that differences in drug exposure because of developmental growth can be accounted for by correcting for differences in body size (Anderson and Holford 2008). A logical step further is to determine whether combining pharmacokinetic prior information from adults and allometric relationships can be used to further improve pediatric dose prediction. To understand the basis of the differences in distributions of pharmacokinetic parameters after accounting for the differences in body size, important methodological aspects need to be considered. In this context, modeling and simulation techniques can be optimally used to apply the current guidelines for pharmacokinetic bridging.

Darbepoetin alfa was selected as a paradigm compound for the evaluation of different methodologies, after careful consideration of the regulatory guidelines for the use of pharmacokinetic bridging. Dosing recommendations exist for the use of darbepoetin alfa in children; however, in this example, the available pediatric data from a clinical study (Lerner *et al.* 2002) were treated as if this analysis was a prospective evaluation for a pediatric indication.

The objectives of the clinical study were to assess the pharmacokinetic profile of a single intravenous (i.v.) and subcutaneous (s.c.) dose of darbepoetin alfa in pediatric subjects with CRF receiving or not receiving dialysis, and to investigate the safety profile of darbepoetin alfa in this setting. Twelve pediatric subjects were treated with a single i.v. or s.c. injection of 0.5 $\mu\text{g}/\text{kg}$ darbepoetin alfa on day 1 followed by a second 0.5 $\mu\text{g}/\text{kg}$ injection via the alternate route 2 weeks later. Full pharmacokinetic profiles were obtained following the first dose (day 1) and after the second dose (day 15). Serum samples were drawn immediately prior to intravenous administration and at 5, 30, and 60 min, and 2, 5, 8, 24, 48, 72, 96, and 168 h postdose. Following subcutaneous administration, serum samples were drawn immediately prior to dosing and at 10, 24, 34, 48, 58, 72, 96, 120, and 168 h post dose.

Before analyzing the pediatric data, a previously developed population pharmacokinetic model (Doshi *et al.* 2010) for adults was evaluated by using visual predictive check (VPC) in order to confirm the ability of the model to describe adult (internal VPC) and pediatric (external VPC) data. A mixed-effect model based on a two compartment pharmacokinetic model with sequential zero-order input into depot compartment followed by first-order absorption from depot into central compartment was suitable to describe the darbepoetin alfa pharmacokinetics following intravenous and subcutaneous dosing (Fig. 14.4). Notably, both the clearance and volume of distribution parameters were allometrically scaled on the basis of body weight with exponents fixed to 0.75 and 1.00, respectively.

To analyze the pediatric data, three methods (A, B, and C) based on the population pharmacokinetic model developed for adults were evaluated using NONMEM software. Method A estimated the pediatric pharmacokinetic parameters

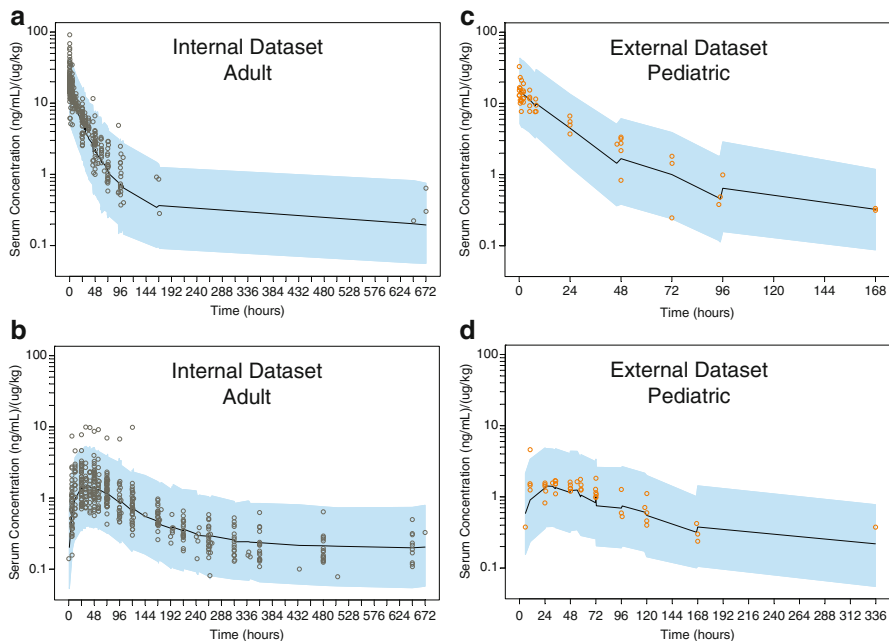


Fig. 14.4 Visual predictive check (VPC) for darbepoetin alfa concentrations in adult (*left*) and children (*right*) following intravenous (*upper*) and subcutaneous (*lower*) dosing

of the model developed for adults based on the data obtained from the pediatric trial. In method B, the estimates of the population pharmacokinetic model parameters obtained from adults were updated by fitting the model to a combined dataset of adult and pediatric data. Method C employed the population pharmacokinetic parameters derived from adults as prior information for a Bayesian estimation of the pharmacokinetic parameters in children using the data obtained from the pediatric trial (using the PRIOR subroutine in NONMEM VI) (Olsson-Gisleskog *et al.* 2002).

The parameter estimates from these three methods are shown in Table 14.2. Interestingly, the precision of parameter estimates using method A could not be obtained, probably because the data available were not sufficient to support the estimation of the parameters in the adult pharmacokinetic model. This reason can also explain the completely unrealistic estimates of some parameters using method A. The precision in the estimate of model parameters using method B is similar or lower than the precision obtained using method C, whereas the residual variability is higher for method B as compared to method C. Taken together, these results suggest that the method C provided the most accurate and precise parameter estimation in children, given the prior information available from adults.

To assess whether adults and children can be considered within the same parameter distributions, some authors have suggested dichotomizing the data by assuming that there exist two populations that do not share the same pharmacokinetic parameter distributions (Cella *et al.* 2010). After adjusting by relevant patient covariates, the

Table 14.2 Population pharmacokinetic parameters as a function of the analysis method

Pharmacokinetic parameter	Units	Method A ^a		Method B		Method C	
		Fixed effects	Random effects	Fixed effects (RSE)	Random effects (RSE)	Fixed effects (RSE)	Random effects (RSE)
Clearance (CL)	mL/day ^b	3,400	17.7	3,400 (4.50)	27.4 (25.1)	3,290 (5.29)	25.0 (31.9)
Central compartment volume (V_2)	mL ^b	1,470	65.1	3,460 (4.02)	22.6 (29.8)	3,290 (3.19)	26.6 (38.1)
Intercompartmental clearance (Q)	mL/day ^b	401,000	70.5	377 (47.7)	98.6 (47.3)	404 (26.7)	129 (44.1)
Peripheral volume (V_3)	mL ^b	2,930	21.9	2,460 (51.2)	39.7 (23.4)	2,220 (28.6)	57.7 (41.7)
Bioavailability (F)	%	0.497	63.2	0.422 (11.2)	65.7 (33.3)	0.402 (8.13)	80.7 (34.3)
First order absorption rate (K_a)	day ^{-1b}	0.770	46.9	0.469 (8.70)	48.6 (27.0)	0.421 (6.89)	57.6 (40.4)
Duration of zero order absorption (D1)	day	0.00691	358.0	0.146 (80.1)	94.0 (91.7)	0.153 (65.3)	79.7 (42.5)
Endogenous EPO (eEPO)	ng/mL	0.160	60.2	0.189 (6.88)	54.3 (54.9)	0.193 (5.39)	45.9 (37.7)
σ_{PK} (proportional)	%	–	26.0	–	37.9 (9.26)	–	31.8 (6.48)

%RSE: relative standard error, defined as the standard error of estimation/estimated value $\times 100\%$

^aCovariance step in NONMEM failed and standard errors were not provided

^bThese units are for a 70 kg subject

Table 14.3 Population pharmacokinetic parameters of darbepoetin alfa in pediatrics using Bayesian estimation compared with the nonparametric bootstrap distribution of darbepoetin alfa pharmacokinetic parameter from adult

Parameter	Units	Fixed effects			Random effects (%)		
		Method C	Bootstrap	Bootstrap	Model	Bootstrap	Bootstrap
		estimate (RSE)	mean (RSE)	95%CI	estimate (RSE)	mean (RSE)	95%CI
Clearance (CL)	mL/day ^a	3,290 (5.29)	3,420 (3.04)	3,210–3,610	25.0 (31.9)	29.3 (19.7)	24.9–36.1
Central compartment volume (V_2)	mL ^a	3,290 (3.19)	3,290 (1.51)	3,200–3,380	26.6 (38.1)	18.9 (18.9)	16.7–22.8
Intercompartmental clearance (Q)	mL/day ^a	404 (26.7)	441 (8.31)	372–514	129 (44.1)	110 (10.8)	102–125
Peripheral volume (V_3)	mL ^a	2,220 (28.6)	2,120 (7.94)	1,820–2,430	57.7 (41.7)	57.7 (1.54)	56.8–58.6
Bioavailability (F)	%	0.402 (8.13)	0.408 (4.22)	0.375–0.439	80.7 (34.3)	86 (18.1)	73.4–101
First order absorption rate (K_a)	day ^{-1a}	0.42 (6.89)	0.39 (3.07)	0.37–0.42	57.6 (40.4)	32.8 (15.2)	30.1–39.5
Duration of zero order absorption (D1)	day	0.153 (0.653)	0.153 (0)	0.153–0.153	79.7 (42.5)	79.6 (11.7)	74.6–92.7
Endogenous EPO (eEPO)	ng/mL	0.193 (5.39)	0.196 (1.25)	0.191–0.201	45.9 (37.7)	50 (17)	45.1–60.6
σ_{PK}	%	–	–	–	31.8 (6.48)	38.5 (4.53)	35.1–41.7

%RSE: relative standard error, defined as the standard error of estimation/estimated value $\times 100\%$

^aThese units are for a 70 kg subject

results of a random dichotomization implemented by the MIXTURE subroutine in NONMEM are compared with the results of an arbitrary dichotomization implemented by stratifying by age (*i.e.*, child < 18 years or adult \geq 18 years). However, here we proposed a parametric bootstrap approach to compare the pharmacokinetic parameter distribution between adults and children. Briefly, the adult pharmacokinetic model was used to simulate data for one pediatric study, which then was analyzed using the adult pharmacokinetic model parameters as a prior information. This process was repeated 1,000 times using a different set of pharmacokinetic model parameters, obtained from a nonparametric bootstrap analysis of the adult data. The distribution of pediatric PK parameters obtained from this parametric bootstrap analysis was then compared with the estimated parameters in children using method C. The fixed effects parameters estimated using method C were within the 95% confidence interval of the parametric bootstrap, thus confirming the similarity of the pharmacokinetic parameter point estimates between adults and children (Table 14.3). However, although the between-subject variability in the volume of distribution of the central compartment, the intercompartmental clearance and the first-order absorption rate constant was 40, 17, and 75% larger in children compared to adults, the residual variability in darbepoetin alfa concentrations was 21% lower for children. These results demonstrate the utility of the proposed approach to detect differences in the distribution of pharmacokinetic parameters between adults and children.

The new pediatric European Union (EU) regulation and the need to balance the demand for pediatric studies with the ethical need for minimizing the burden of studies in children necessitate optimal techniques in the assessment of safety/efficacy and use of drugs in children. Modeling and simulation (M&S) is one way to circumvent some difficulties in developing medicinal products in children. The example presented illustrates how modeling and simulation techniques can be optimally used to integrate all available prior information, which will be helpful to optimize pediatric dose selection. As discussed in an exposure–response relationship guidance for industry from the US Food and Drug Administration (US FDA 2003), models developed using the PRIOR subroutine in NONMEM that have been properly evaluated can be used to plan future PK/PD studies for pediatric patients and optimize key study features such as sample sizes, sampling time points, or study duration. Other applications of M&S include selection of the pediatric drug dosing for clinical studies (especially in newborns, including the very-low-birth-weight premature newborns), pediatric product formulation, and labeling for pediatric doses and indications from a clinical pharmacology perspective.

References

- Agarwal AK, Silver MR, Reed JE, Dhingra RK, Liu W, Varma N, Stehman-Breen C (2006) An open-label study of darbepoetin alfa administered once monthly for the maintenance of haemoglobin concentrations in patients with chronic kidney disease not receiving dialysis. *J Intern Med* 260:577–585

- Agoram B, Heatherington AC, Gastonguay MR (2006) Development and evaluation of a population pharmacokinetic-pharmacodynamic model of darbepoetin alfa in patients with nonmyeloid malignancies undergoing multicycle chemotherapy. *AAPS J* 8:E552–E563
- Anderson BJ, Holford NH (2008) Mechanism-based concepts of size and maturity in pharmacokinetics. *Annu Rev Pharmacol Toxicol* 48:303–332
- Cella M, Gorter de Vries F, Burger D, Danhof M, Della Pasqua O (2010) A model-based approach to dose selection in early pediatric development. *Clin Pharmacol Ther* 87:294–302
- Doshi S, Chow A, Pérez-Ruixo JJ (2010) Exposure-response modeling of darbepoetin alfa in anemic patients with chronic kidney disease not receiving dialysis. *J Clin Pharmacol* 50:75S–90S
- Doshi S, Pérez-Ruixo JJ, Jang GR, Chow AT (2009) Pharmacokinetics of erythropoiesis-stimulating agents. In: Molineux G, Foote MA, Elliott S (eds) *Erythropoietins and erythropoiesis: molecular, cellular, preclinical, and clinical biology*, 2nd edn. Birkhäuser, Basel, Switzerland, pp 195–224
- US Food and Drug Administration (2000) Guidance for industry. E11 clinical investigation of medicinal products in the pediatric population. <http://www.fda.gov/downloads/RegulatoryInformation/Guidances/ucm129477.pdf>. Accessed 1 May 2010
- US Food and Drug Administration (2003) Guidance for industry. exposure–response relationships – study design, data analysis, and regulatory applications. <http://www.fda.gov/downloads/Drugs/GuidanceComplianceRegulatoryInformation/Guidances/UCM072109.pdf>. Accessed 1 May 2010
- Erickson-Miller CL, Pelus LM, Lord KA (2000) Signaling induced by erythropoietin and stem cell factor in UT-7/EPO cells: transient versus sustained proliferation. *Stem Cells* 18:366–373
- Hamrén B, Björk E, Sunzel M, Karlsson M (2008) Models for plasma glucose, HbA1c, and hemoglobin interrelationships in patients with type 2 diabetes following tesaglitazar treatment. *Clin Pharmacol Ther* 84:228–235
- Harker LA, Roskos LK, Marzec UM, Carter RA, Cherry JK, Sundell B, Cheung EN, Terry D, Sheridan W (2000) Effects of megakaryocyte growth and development factor on platelet production, platelet life span, and platelet function in healthy human volunteers. *Blood* 95:2514–2522
- Jolling K, Pérez-Ruixo JJ, Hemeryck A, Vermeulen A, Greway T (2005) Mixed-effects modelling of the interspecies pharmacokinetic scaling of pegylated human erythropoietin. *Eur J Pharm Sci* 24:465–475
- Krzyzanski W, Jusko WJ, Wacholtz MC, Minton N, Cheung WK (2005) Pharmacokinetic and pharmacodynamic modeling of recombinant human erythropoietin after multiple subcutaneous doses in healthy subjects. *Eur J Pharm Sci* 26:295–306
- Lazareno S, Birdsall NJM (1993) Estimation of competitive antagonist affinity from functional inhibition curves using the Gaddum, Schild and Cheng-Prusoff equations. *Br J Clin Pharmacol* 109:1110–1119
- Lerner G, Kale AS, Warady BA, Jabs K, Bunchman TE, Heatherington A, Olson K, Messer-Mann L, Maroni BJ (2002) Pharmacokinetics of darbepoetin alfa in pediatric patients with chronic kidney disease. *Pediatr Nephrol* 17:933–937
- Mager DE, Woo S, Jusko WJ (2009) Scaling pharmacodynamics from *in vitro* and preclinical animal studies to humans. *Drug Metab Pharmacokinet* 24(1):16–24
- Miller R, Ewy W, Corrigan BW, Ouellet D, Hermann D, Kowalski KG, Lockwood P, Koup JR, Donevan S, El-Kattan A, Li CS, Werth JL, Feltner DE, Lalonde RL (2005) How modeling and simulation have enhanced decision making in new drug development. *J Pharmacokinet Pharmacodyn* 32:185–197
- Olsson-Gislekog P, Jacqmin P, Pérez-Ruixo JJ (2007) Population pharmacokinetics meta-analysis of recombinant human erythropoietin in healthy subjects. *Clin Pharmacokinet* 46:159–173
- Olsson-Gislekog P, Karlsson MO, Beal SL (2002) Use of prior information to stabilize a population data analysis. *J Pharmacokinet Pharmacodyn* 29:473–505
- Pérez Ruixo JJ (2006) Optimizing the design of phase I studies of erythropoietin receptor agonist through mechanism-based PK/PD modeling and simulation. Population approach group in Europe meeting. <http://userpage.fu-berlin.de/~page/>. Accessed 1 May 2010

- Pérez-Ruixo JJ, Kimko HC, Chow AT, Piotrovsky V, Krzyzanski W, Jusko WJ (2005) Population cell life span models for effects of drugs following indirect mechanism of action. *J Pharmacokinetic Pharmacodyn* 32:767–793
- Pérez-Ruixo JJ, de Ridder F, Kimko H, Samtani M, Cox E, Mohanty S, Vermeulen A (2008a) Simulation in clinical drug development. In: Bertau M, Mosekilde E, Westerhoff HV (eds) *Biosimulation in drug development*. Wiley-VCH, Germany, pp 3–24
- Pérez-Ruixo JJ, Krzyzanski W, Bouman-Thio E, Miller B, Jang H, Bai SA, Zhou H, Yohrling J, Cohen A, Burggraaf J, Franson K, Davis H (2009) Pharmacokinetics and pharmacodynamics of the erythropoietin Mimetibody™ construct CNTO 528 in healthy subjects. *Clin Pharmacokinetic* 48:601–613
- Pérez-Ruixo JJ, Krzyzanski W, Hing J (2008) Pharmacodynamic analysis of recombinant human erythropoietin effect on reticulocyte production rate and age distribution in healthy subjects. *Clin Pharmacokinetic* 47:399–415
- Roskos LK, Lum P, Lockbaum P, Schwab G, Yang BB (2006) Pharmacokinetic and pharmacodynamic modeling of pegfilgrastim in healthy subjects. *J Clin Pharmacol* 46:747–757
- Sharma A, Ebling WF, Jusko WJ (1998) Precursor-dependent indirect pharmacodynamic response model for tolerance and rebound phenomena. *J Pharm Sci* 87:1577–1584
- Sheiner L, Wakefield J (1999) Population modelling in drug development. *Stat Methods Med Res* 8:183–193

Chapter 15

Model Based Development of an Agent for the Treatment of Generalized Anxiety Disorder

Peter A. Lockwood and Jaap W. Mandema

Abstract PD0332334 (PD334) is a novel beta amino acid analog of pregabalin (Pgb). Pregabalin has been previously studied in six clinical studies of general anxiety disorder (GAD). Because these compounds have similar pharmacology, certain features of their dose response relationships could be similar. Thus, data from the pregabalin GAD program was used to provide information about the safety (incidence of somnolence) and efficacy (reduction in Hamilton Anxiety Rating score) dose–response relationships for PD334 in GAD. This chapter illustrates the use of prior pregabalin data from other large-scale clinical studies to select the PD334 dose range to study in Phase 3, and the implementation of models based on assumptions of common PD334/pregabalin dose–response features that resulted from consideration of the comparative pharmacology. External validation of the PD334 dose–response model with Phase 3 data is demonstrated.

15.1 Introduction

The value of integrating pharmacologically based dose–response modeling into the drug development process is well recognized. This process facilitates important decision-making related to dose selection, trial design and development strategies. Lalonde *et al.* (2007) provide a succinct review of modeling and simulation in clinical drug development and discuss where assumption rich versus assumption minimal models are applicable in the development process, and how these elements fit together to inform development strategy and decision making. The authors emphasize that effective drug development integrates data across studies. Models are the tools for enabling this integration, reflecting what is understood and what is assumed, and which must be continually updated as new information becomes available.

P.A. Lockwood (✉)
Pfizer Global Research and Development, Clinical Pharmacology,
Primary Care Business Unit, New London, CT, USA
e-mail: peter.lockwood@pfizer.com

Mandema *et al.* (2005b) described how safety and efficacy data obtained from a number of clinical studies of drugs (statins) that lowered low-density lipoprotein cholesterol (LDL-C) or inhibited cholesterol absorption (ezetimibe) were integrated to evaluate the efficacy of gemcabene, a novel lipid-lowering agent that was to be given in combination with atorvastatin. The modeling demonstrated that gemcabene provided an additional LDL-C lowering benefit at low doses of atorvastatin, but almost no incremental benefit at high doses of atorvastatin. This was different from ezetimibe, which provided benefit across the entire atorvastatin labeled dose range. The model-based analysis provided an indirect quantitative comparison of the LDL lowering effect of atorvastatin/ezetimibe versus atorvastatin/gemcabene, which led to a decision to terminate gemcabene development.

Mandema and Wang (2003) presented a case study that illustrates how an integrated drug model derived from literature reports of seven dose-ranging clinical studies of the 5HT agonists sumatriptan, zolmitriptan, naratriptan, and rizatriptan, was used to optimize the Phase 2 dose-finding strategy for a new 5HT agonist indicated for the relief of moderate to severe migraine pain. Subsequent to this, the dose–response relationship of sumatriptan and eletriptan for patients that achieve migraine pain relief up to 4 h after treatment was reported based on an integrated analysis of results from 19 randomized clinical trials (Mandema *et al.* 2005a).

Noteworthy in these examples is that the models used to support decision-making were not highly complex, were easy to comprehend by non-modeling experts and could be derived and applied quickly to influence decisions made by the development team. In this manuscript we describe how data from a compound with the same mechanism-of-action (pregabalin) was integrated to derive models characterizing the dose–response relationship for both efficacy and tolerability of a novel $\alpha_2\delta$ ligand (PD334) being developed for generalized anxiety disorder (GAD). The application of these models to select doses for Phase 3 studies is described and the actual efficacy of the selected doses is compared to predicted outcomes after 6 weeks of treatment in a Phase 3 study.

GAD is a condition characterized by ongoing, excessive anxiety and worry that the affected individual finds difficult to control. The lifetime prevalence rate in the general population in the United States is approximately 5%, based on the Diagnostic and Statistical Manual of Mental Disorders (DSM) criteria for GAD. In the primary care setting, the prevalence rate is estimated to be approximately 8%, rendering GAD to be the most frequent anxiety disorder in primary care and the second most frequent psychiatric disorder after depression (Weisberg 2009; Wittchen and Hoyer 2001). Individuals with GAD can experience a considerable degree of impairment and disability, which leads to significant economic costs resulting from lost productivity and high medical resource use (Rickels and Rynn 2001). Pregabalin, an $\alpha_2\delta$ ligand like PD334, has been shown to be efficacious in GAD (Pande *et al.* 2003; Feltner *et al.* 2003; Rickels *et al.* 2005; Pohl *et al.* 2005; Montgomery *et al.* 2006).

The $\alpha_2\delta$ site is a subunit of voltage-gated calcium channels located in the central nervous system (CNS). Four $\alpha_2\delta$ subtypes have been identified, of which types 1 ($\alpha_2\delta$ -1) and 2 ($\alpha_2\delta$ -2) are bound by known $\alpha_2\delta$ ligands. The term “Ca²⁺ channel

$\alpha_2\delta$ ligands” has recently been applied to an evolving drug class that includes gabapentin (Neurontin[®]) and pregabalin (Lyrica[®]). Evidence indicates a relationship between $\alpha_2\delta$ subunit binding and the modulation of processes that result in the release of neurotransmitters. This modulation is characterized by a reduction of excessive neurotransmitter release that is observed in certain neurological and psychiatric disorders (Dooley *et al.* 2007). Ligands for $\alpha_2\delta$ subunits are a new class of compounds for the treatment of GAD. PD334, a high-affinity $\alpha_2\delta$ ligand considered to have a similar mechanism of action to pregabalin, shows approximately sevenfold selectivity for $\alpha_2\delta$ -1 over $\alpha_2\delta$ -2 (based on assays in membrane preparations from cells expressing recombinant porcine $\alpha_2\delta$ -1 or human $\alpha_2\delta$ -2 proteins; data on file). Pregabalin on the other hand shows similar selectivity for the two subunits. The increased selectivity of PD334 could result in an improved therapeutic window if efficacy and tolerability are mediated through the different subunits. Although the mechanism of action of PD334 is yet to be fully elucidated, results from studies in genetically modified mice with a mutation in the $\alpha_2\delta$ -1 gene, and with compounds that are structurally related to PD334, indicate that binding to the $\alpha_2\delta$ subunit is necessary for the anxiolytic effect of the drug. PD334 has shown activity in animal models of anxiety, and from preclinical studies, the projected daily dose effective in humans was expected to be around 500-mg (data on file).

The PD334 dose–response relationships for efficacy and tolerability were based on a simultaneous analysis of either the safety or the efficacy data obtained from a Phase 2 proof-of-concept (POC) study for this compound, and Phase 2 and 3 clinical studies of pregabalin. A simultaneous analysis with pregabalin was thought to be helpful to provide an indirect comparison of PD334 to pregabalin. Additionally, a simultaneous analysis could reduce the uncertainty in the dose–response relationship of PD334 because it was plausible that certain parameters, such as the shape and maximal effect of the dose–response relationship could be similar for the two compounds because of their similar mechanism of action. Modeling of preclinical data obtained in the Vogel water lick conflict studies (Vogel *et al.* 1971) in male Wistar rats (data on file) supported the assumption of a similar E_{\max} for the parent compounds. The Vogel water-lick conflict test is an animal model predictive of anxiety. Rats are deprived of water for 24-h, then allowed to drink by licking from a tube, then deprived of water for a further 24-h. When the rats are allowed to drink on a second occasion, they receive a 1-s 1-mA shock through the drink tube, after every ten licks. Thus, a conflict or anxiety-producing situation exists. Rats are motivated to drink, however they are inhibited by the shock. Anxiety is reflected by the low amounts of drinking. Standard anxiolytic drugs produce effects that allow rats to overcome this behavioral inhibition and drink despite the shock. Compounds that significantly increase the number of shock episodes over concurrently run controls are presumed to possess anxiolytic-like properties. Observing a similar E_{\max} for the clinical efficacy and tolerability of compounds with a similar mechanism of action is not unprecedented (Mandema *et al.* 2005a, b). Thus, data from the pregabalin GAD program could provide some information about the dose–response relationships for PD334.

15.2 Materials and Methods

15.2.1 Data

The combined dose–response analysis was undertaken using a database of 24 efficacy and tolerability observations across six pregabalin studies and one PD334 trial listed in Table 15.1. This database comprised observations from all Phase 2 and 3 trials of pregabalin in GAD. The endpoints analyzed were the least squares mean change from baseline HAM-A score at end of study (last observation carried forward (LOCF)) and incidence of somnolence. Somnolence was noted as the dominating adverse event in the pregabalin and PD334 clinical studies.

Table 15.1 Summary of studies included in the analysis

Study	Description	Doses and sample size
1007	A Phase 2, randomized, double-blind, placebo-controlled, parallel group, 5-week trial to assess the efficacy and safety of PD334 compared to placebo and alprazolam extended-release in patients with generalized anxiety disorder	PD334 250 mg BID, PD334 100-mg BID, placebo, alprazolam ER 1 mg BID
021	A placebo controlled study of pregabalin (Pgb) and lorazepam in patients with generalized anxiety disorder (Pande <i>et al.</i> 2003)	600 mg day Pgb, 150 mg day Pgb, placebo, 6 mg day lorazepam; 64 patients/trt, 4-weeks of trt: 1-week titration; TID regimen, 1-week taper
025	A placebo controlled study of pregabalin and lorazepam in patients with generalized anxiety disorder	600 mg day Pgb, 150 mg day Pgb, placebo, 6 mg day lorazepam; 64 patients/trt, 4-weeks of trt: 1-week titration; TID regimen; 1-week taper
026	A placebo-controlled study of pregabalin and lorazepam in patients with generalized anxiety disorder (Feltner <i>et al.</i> 2003)	600 mg day Pgb, 150 mg day Pgb, placebo, 6 mg day lorazepam; 64 patients/trt, 4-weeks of trt: 1-week titration; TID regimen; 1-week taper
083	A placebo-controlled study of pregabalin and alprazolam in patients with generalized anxiety disorder (Rickels <i>et al.</i> 2005)	600 mg day Pgb, 450 mg day Pgb, 300 mg day Pgb, placebo, 1.5 mg day alprazolam; 97 patients/trt, 4-weeks of trt: 1 week titration; TID regimen; 1-week taper
085	A placebo-controlled study of pregabalin dosed BID and TID in patients with generalized anxiety disorder (Pohl <i>et al.</i> 2005)	450 mg day Pgb (150 TID), 400 mg day Pgb (200 BID), 200 mg day (100 BID), placebo; 97 patients/trt, 6-weeks of trt: 1-week titration; 1-week taper
087	A placebo-controlled study of pregabalin and venlafaxine in patients with generalized anxiety disorder (Montgomery <i>et al.</i> 2006)	600 mg day Pgb (300 BID), 400 mg day Pgb (200 BID), venlafaxine 75 mg (37.5 BID), placebo, 97 patients/trt, 6-weeks of trt: 1-week titration; 1-week taper

trt :Treatment

15.2.2 Dose Response Analysis

When combining results from different trials, the random trial-to-trial differences in the patient populations must be taken into account. A trial-specific, random-effects model accounts for such heterogeneity by treating the model parameters as random variables. Therefore, dose–response models with both fixed and random effects (mixed effects models) were fit to the efficacy and safety data using maximum likelihood estimation methods implemented in S-Plus version 6.2.

The base model for the analysis of the efficacy and safety data assumed the following:

1. The dose–response relationship for both compounds was non-linear
2. The maximum HAM-A change from baseline (E_{\max}) and the maximum probability of somnolence were the same for pregabalin and PD334
3. The shape of the dose–response relationship for pregabalin and PD334 was similar for the efficacy and tolerability endpoints
4. The potency of pregabalin and PD334 with respect to efficacy and tolerability was different, allowing for a different therapeutic index between the two compounds
5. All heterogeneity in response across trials can be explained by variability in the placebo response

All assumptions were tested as described in the model selection section. If a certain assumption was rejected by the data, the model was changed accordingly.

15.2.2.1 Efficacy

The basic model, describing the HAM-A change from baseline score versus dose, is described in (15.1).

$$\text{HAM-A}_{ij} = E_0 + \frac{E_{\max} \cdot \text{Dose}^{\gamma}}{\text{Dose}^{\gamma} + \text{EDPgb}_{50}^{\gamma} \cdot P} + \eta_i + \varepsilon_{ij} \quad (15.1)$$

In this equation, HAM-A_{ij} is the estimated least squares mean HAM-A change from baseline score for the j th arm in the i th trial; E_0 is the placebo response; E_{\max} is the maximal drug effect, reflecting the maximal difference in response between placebo and active treatment; Dose is the dose in mg/day; EDPgb_{50} is the pregabalin dose to achieve 50% of E_{\max} ; P is the relative potency between PD334 and pregabalin ($P = 1$ for pregabalin administration); γ is the Hill coefficient for defining the shape and is equal to one unless specified otherwise, η_i is a trial specific random effect that is normally distributed with mean 0 and variance ω^2 that accounts for the trial-to-trial variability in placebo response. ε_{ij} is the residual variability with variance σ^2/N_{ij} . N_{ij} is the sample size for the j th arm in the i th trial and σ^2 is the between subject variance. The between subject variance was fixed to the computed weighted average that was based on the standard error and subject number reported for each arm in the seven trials.

The pregabalin and PD334 studies were of either 4 or 6 weeks duration, therefore the impact of time on the placebo response and the maximum drug effect was evaluated. Other models that were evaluated, incorporated sigmoidicity in the drug effect ($\gamma \neq 1$), a separate maximum drug effect (E_{\max}) for PD334 and pregabalin or trial specific random variation in E_{\max} to evaluate additional heterogeneity in the effects between trials.

15.2.2.2 Tolerability

Somnolence was noted as the dominating adverse event in the pregabalin and PD334 clinical studies. A logistic regression analysis was used to characterize the dose–response relationship for the probability of somnolence [$P(\text{Som})$] and the base model is displayed in (15.2).

$$\text{logit}(P(\text{Som})_{ij}) = E_0 + \frac{E_{\max} \cdot \text{Dose}}{\text{Dose} + \text{EDP}_{\text{gb}_{50}} \cdot P} + \eta_i \quad (15.2)$$

In this equation, $P(\text{Som})_{ij}$ represents the probability of a patient having a somnolence event in the j th treatment arm of the i th trial; E_0 is the placebo response; E_{\max} is the maximal drug effect, reflecting the maximal difference in response between placebo and active treatment; Dose is the dose in mg/day; $\text{EDP}_{\text{gb}_{50}}$ is the pregabalin dose to achieve 50% of E_{\max} ; P is the relative potency between PD334 and pregabalin and η_i is a trial specific random effect that is normally distributed with mean 0 and variance ω^2 that accounts for the trial-to-trial variability in placebo response. The number of patients with a somnolence event out of the total number of patients N_{ij} in the j th treatment arm of the i th trial was assumed to follow a binomial distribution according to the probability predicted by the model above. Models that incorporated the considerations listed previously (*e.g.*, a separate maximum drug effect (E_{\max}) for PD334 and pregabalin) were evaluated.

15.2.2.3 Model Selection

Model selection was based on the Log Likelihood criterion. The difference in two times the Log of the Likelihood for a full and reduced model (likelihood ratio) is approximately asymptotically χ^2 distributed, with degrees of freedom equal to the difference in number of parameters between the two models. Therefore, an additional parameter in the model would be declared as statistically significant if the difference was greater than the critical value of 3.841 at the 5% level of significance.

15.2.2.4 Model Uncertainty

A bootstrap analysis was used to characterize the uncertainty in the model parameter estimates. A total of 1,000 “new” efficacy data sets were generated from the original data by sampling the mean HAM-A change from baseline from the distribution

characterized by the observed least squares mean and standard error for each treatment arm in each trial. Similarly, 1,000 new safety data sets were generated from the original data by sampling from a binomial distribution characterized by the observed somnolence incidence and sample size for each treatment arm in the trial. Model parameters were estimated for each “new” data set. If the final model failed to converge, an alternative model was selected to ensure that all of the bootstrapped data sets contributed to the estimation of the uncertainty in the dose response. The alternative models were as follows:

1. Dose independent response for PD334, E_{\max} dose response model for pregabalin
2. Dose independent response for pregabalin, E_{\max} dose response model for PD334
3. Dose independent response for pregabalin and PD334
4. Linear dose response model for PD334, E_{\max} dose response model for pregabalin
5. Linear dose response model for pregabalin, E_{\max} dose response model for PD334
6. Linear dose response model for pregabalin and PD334

The model selection was based on a comparison of the log likelihood value. The preferred alternative model in all non-convergence instances was a linear dose response model for PD334 and an E_{\max} dose response model for pregabalin.

The HAM-A change from baseline or the probability of somnolence was predicted with each set of parameters over a dose range of 0 to 800-mg. This yielded a collection of dose–response curves that characterized the uncertainty about the pregabalin and PD334 mean dose–response relationship. Plots of the expected dose–response together with 80% confidence intervals were constructed and responses at 100, 200, 300, 400, 500, 600, 700, and 800 mg were tabulated. Confidence intervals were constructed by calculating percentiles of the distributions of efficacy and safety outcomes at each dose. For example, 80% confidence intervals were constructed using the 10th and 90th percentiles.

15.2.3 Dose Selection for Phase 3 Studies

Based on the dose–response relationship for the HAM-A change from baseline or the probability of somnolence, the joint probabilities of achieving a target profile were derived for different doses of PD334 and a dose range was selected for Phase 3 that maximized the probability of achieving the target profile. For PD334, the target profile was an improvement (*i.e.*, reduction in HAM-A score) over placebo in the HAM-A score of at least two units and a placebo adjusted incidence of somnolence of less than 25%. A two-point change (*i.e.*, reduction) in HAM-A score is considered clinically significant. The probability of achieving the target profile, *i.e.*, the probability of technical success, was calculated assuming that one, two or three doses would be taken forward to Phase 3. The joint probabilities were derived assuming the efficacy and safety endpoints were independent – *i.e.*, there was no correlation between HAM-A and somnolence scores. The upper limit of the dose range was constrained to 600 mg because of concerns about manufacturing costs for higher doses.

15.2.4 Model Validation

Three doses that covered the desired dose range for Phase 3 studies, according to the target profile, were subsequently evaluated in a Phase 3 trial. The Phase 3 study was a randomized, double blind, placebo-controlled, fixed-dose, parallel group, multi-site study in 520 outpatients with generalized anxiety disorder. Subjects (130/treatment arm) were randomized to either a placebo arm or one of three active treatment groups – 175 mg BID, 225 mg BID or 300 mg BID. The study consisted of a 7–14 day screening phase; an 8-week double-blind treatment phase; and a 2-week double-blind dose-tapering follow-up phase. The subjects enrolled were men and women ages 18–65 who meet DSM-IV criteria for generalized anxiety disorder with a preponderance of anxious symptoms over depressive symptoms. Each of the doses studied was titrated to the desired dose for 1 week. Efficacy measurements were obtained at weeks 1, 2, 4, 6, and 8. To validate the PD334 efficacy model, a dose–response relationship for the HAM-A change from baseline endpoint was predicted for this trial on basis of the Phase 2 model. The predictions included the uncertainty in the estimated dose–response relationship and sample size based uncertainty. Clinical HAM-A change from baseline outcomes for each of the doses evaluated in the Phase 3 study were then compared to the model prediction. Week 6 outcomes of the clinical study were selected for model validation because the model was derived using data from studies of either 4 or 6 weeks duration.

15.3 Results

15.3.1 Efficacy

The change in HAM-A was best described by an E_{\max} dose–response relationship that assumed a similar E_{\max} between pregabalin and PD334. Adding a different E_{\max} for PD334 did not improve the fit. A sigmoid E_{\max} model did not significantly improve the fit ($p = 0.15$) compared to the E_{\max} model. The ED_{50} ($p = 0.78$) and E_{\max} ($p = 0.98$) were not significantly different after taking the trial duration differences (*i.e.*, 4 and 6 weeks) into account. There was no significant additional between trial heterogeneity in E_{\max} . As expected, there was a significant increase in placebo response at 6 weeks compared to 4 weeks ($p = 0.008$). Figure 15.1 displays the goodness of fit of the model to the HAM-A dose–response data for the individual pregabalin and PD334 (study 1007) clinical studies, and illustrates the variability in the placebo response. The figure shows that the HAM-A effect is well predicted for each dose after accounting for the trial-to-trial variability in placebo response. Parameter estimates and 80% confidence intervals for the fixed and

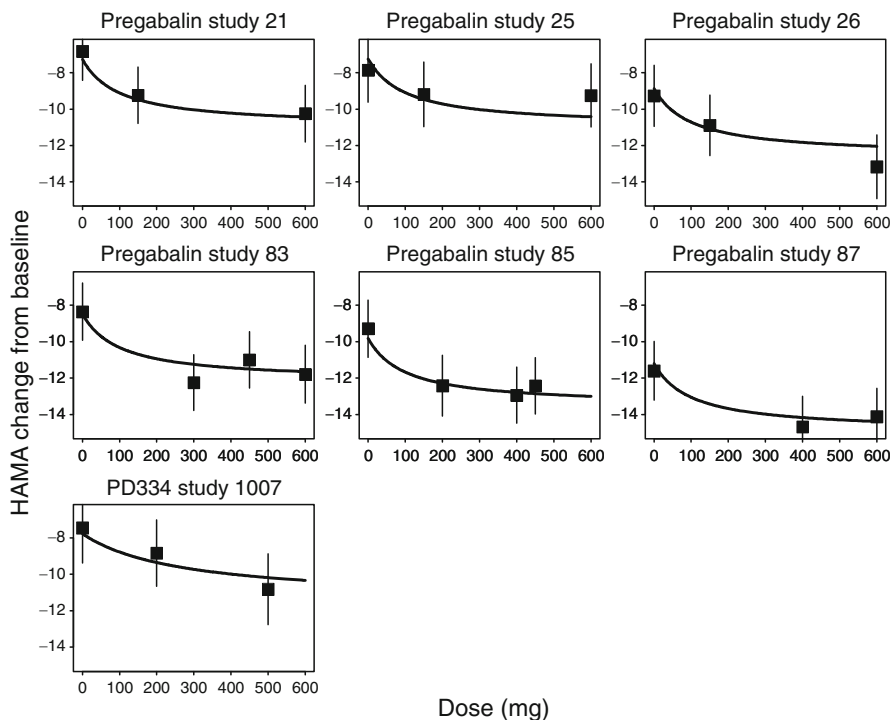


Fig. 15.1 Observed vs. predicted HAM-A change from baseline relative to dose for each study. The *symbols* and *bars* represent the observed last observation carried forward (LOCF) mean and 95% confidence interval. The *solid line* is the model prediction HAM-A change from baseline

Table 15.2 Estimates of fixed and random effects derived from HAM-A dose–response model

Parameter	Estimate	80% confidence interval
E_{\max} (HAM-A units)	−3.71	−5.07 to −3.07
ED_{50} pregabalin (mg)	100	36 to 271
ED_{50} PD334 ₅₀ (mg)	268	101 to 797
Relative potency	2.68	0.80 to 9.58
$E_{0-4 \text{ week}}$ (HAM-A units) ^a	−7.92	−8.34 to −7.47
$E_{0-6 \text{ week}}$ (HAM-A units) ^b	−10.51	−11.0 to −9.93
ω (between study SD in placebo response)	0.78	0.56 to 1.08
σ (between subject SD) ^c	7.21	

SD standard deviation (HAM-A units)

^aMean placebo effect at 4-weeks

^bMean placebo effect at 6-weeks

^cThis parameter was fixed to a weighted average observed across all studies

random effects are displayed in Table 15.2. The maximum effect mediated by either drug is a 3.7-point change in the HAM-A score. The ED_{50} for pregabalin is 100 and 268-mg for PD334.

15.3.2 Tolerability

The somnolence incidence was best described by an E_{\max} dose–response relationship that assumed a similar E_{\max} between pregabalin and PD334. Adding a different E_{\max} for PD334 did not improve the fit. A sigmoid E_{\max} model did not significantly improve the fit ($p = 0.07$) compared to the E_{\max} model. The placebo response ($p = 0.053$), ED_{50} ($p = 0.38$), and E_{\max} ($p = 0.13$) were not significantly different between 4 and 6 weeks follow-up. There was no significant additional between trial heterogeneity in E_{\max} . Figure 15.2 displays the goodness-of-fit of the model to the incidence of somnolence data for the individual pregabalin and PD334 clinical studies. The figure shows that the incidence of somnolence is well predicted for each dose after accounting for the trial-to-trial variability in the placebo response. The error bar reflects a 95% confidence interval for the observation. Parameter estimates and 80% confidence for the fixed and random effects are displayed in Table 15.3. The placebo effect of somnolence for a typical trial is 11.5% (10.2–13.7%; 80% CI). The maximal total incidence of somnolence is estimated to be 44.8% (32.1–75.6) with a maximal absolute difference from placebo of 33.3% (21.9–56.9%).

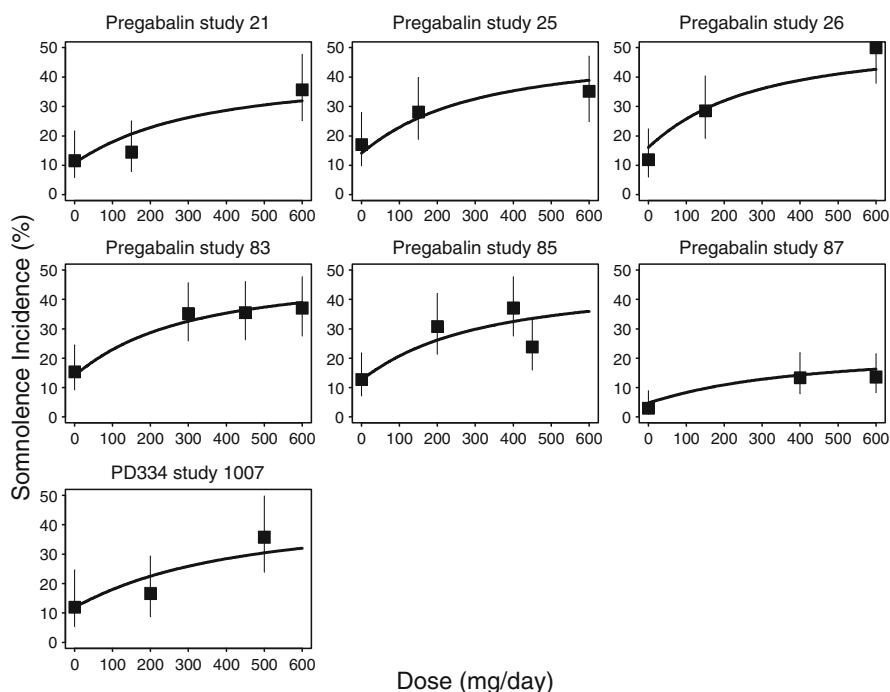


Fig. 15.2 Observed vs. predicted incidence of somnolence vs. dose for each study. The symbols and bars represent the observed incidence and 95% confidence interval. The solid line is the model prediction of the incidence of somnolence vs. dose

Table 15.3 Estimates of fixed and random effects derived from pregabalin and PD334 somnolence probability dose–response model

Parameter	Estimate	80% confidence interval
E_{\max}	1.83	1.41 to 2.96
ED ₅₀ pregabalin (mg)	208	91 to 731
ED ₅₀ PD334 (mg)	277	141 to 879
Relative potency	1.34	0.60 to 3.71
E_0	−2.04	−2.18 to −1.84
ω (between study SD in placebo response)	0.44	0.36 to 0.55

SD standard deviation

Note that E_0 and E_{\max} are reported in the logit domain

15.3.3 Simulation Results

Figure 15.3 displays the placebo adjusted mean HAM-A change from baseline score versus dose and 80% confidence intervals for pregabalin and PD334. Figure 15.4 displays the incidence of somnolence versus dose and 80% confidence intervals for pregabalin and PD334. Confidence intervals are narrower for pregabalin in Figs. 15.3 and 15.4 because of the availability of more data for pregabalin compared to PD334.

Figure 15.5 displays the joint probability that the improvement (*i.e.*, reduction) from placebo in HAM-A score will be more than 2 (characterized as less than −2) and the somnolence incidence difference from placebo will be less than 25%, as a function of dose.

Based on the joint probability, doses of 400 to 600 mg have the highest and very similar (approximately 66%) chance of demonstrating a profile that is consistent with the desired target profile. Even though doses greater than 600 mg also have a high likelihood of success, the upper limit of the dose range was constrained to 600 mg because of concerns about manufacturing costs for higher doses. Inspection of the probability dose–response curve indicates that there is more than a 50% chance that a 350 mg dose will demonstrate an improvement (reduction) of two HAM-A units, whereas a 200 mg dose has a small chance (28%) of demonstrating the desired safety and efficacy properties. The chances of success continue to increase up to 600 mg after which, there is a decrease in the probability of success due to the higher likelihood of somnolence. A dose of about 550mg has the highest probability of 68% of reaching the target profile. If one dose were to be selected for Phase 3, this dose would maximize the probability of demonstrating a HAM-A reduction of more than two points and an incidence of somnolence less than 25% (*i.e.*, technical success). The probability of achieving technical success can be increased to 76% if two doses (300 and 600 mg) are selected. The 76% chance is the probability, based on the uncertainty in the dose response relationships, that at least one of the two doses can achieve technical success. The maximal probability of technical success at 78% is achieved if three doses (300, 450, and 600 mg) are

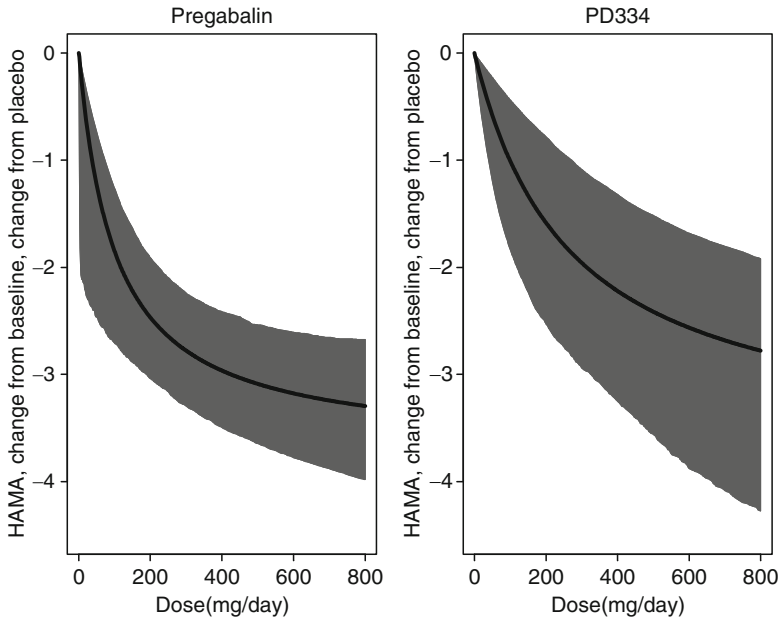


Fig. 15.3 Pregabalin and PD334 HAM-A dose–response relationships (difference from placebo) with 80% confidence intervals

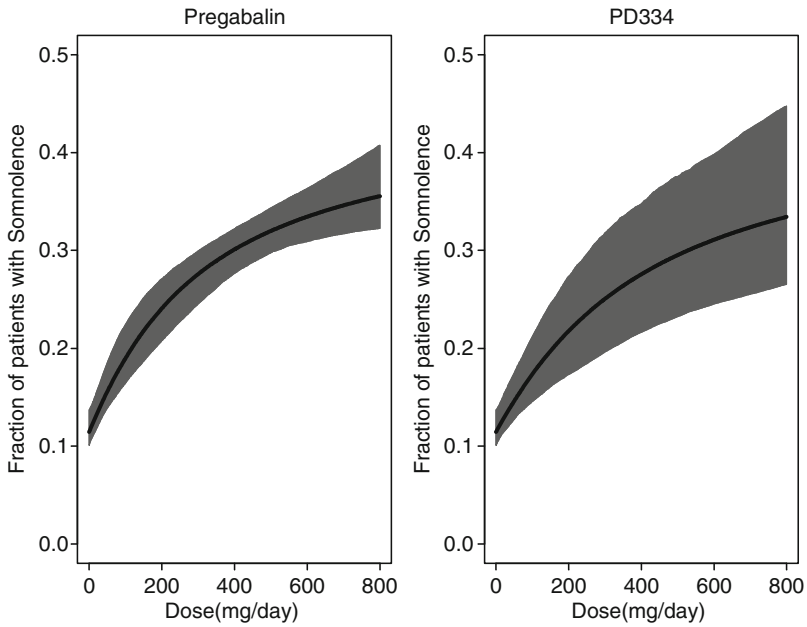


Fig. 15.4 Pregabalin and PD334 dose–response relationships and 80% confidence intervals for incidence of somnolence

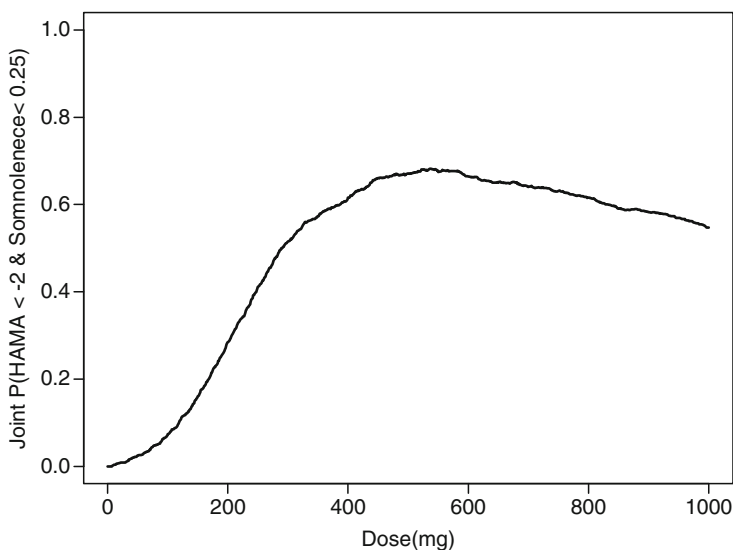


Fig. 15.5 The joint probability that the mean HAM-A improvement (reduction) from placebo score will be more than 2 and the difference from placebo incidence of somnolence will be less than 25% with increasing doses of PD334. Negative HAM-A sign reflects a two-point reduction from baseline score

selected. In fact, there is only a 79% chance that the target profile would be met if the whole dose range was taken forward and evaluated. This suggests that the chance of Phase 3 success is maximized by taking two or three doses forward.

15.3.4 Comparison of Week 6 Phase 3 Outcome and Model Prediction

The mean predicted HAM-A change from baseline at week 6, 80% prediction interval (gray region) and observed responses (black squares) for the PD334 Phase 3 study are displayed in Fig. 15.6. The observed responses at the 350, 450, and 600-mg daily dose are well within the region of uncertainty.

15.4 Discussion

This chapter describes how efficacy and safety data were integrated using simple models to generate dose response–probability curves that were a composite of the safety and efficacy data. This relationship was used to identify the optimal dose range, *i.e.*, the dose range that had the highest probability of achieving a predefined target profile and inform dose selection for Phase 3 studies for a compound being developed for generalized anxiety disorder. Several Phase 3 studies were initiated

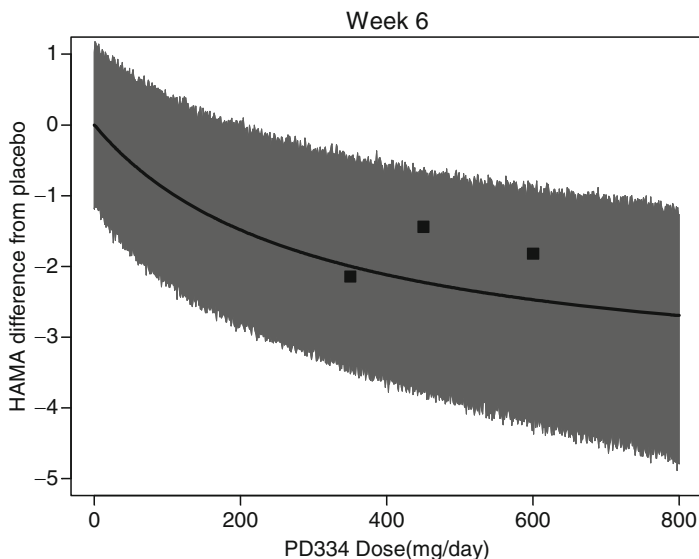


Fig. 15.6 Predicted mean HAM-A change from baseline (solid line), 80% prediction interval (gray region) for the Phase 3 study. Observed outcomes shown as solid squares

that evaluated doses in the range of 150 to 600 mg. The results for one of the Phase 3 trials were available and the outcomes were compared to model predictions.

This exercise highlights the use of prior (pregabalin) data from other large-scale clinical studies, and the building of assumptions about common features of compounds from the same class, based on considerations of the comparative pharmacology. The assumption of a similar E_{\max} relationship between dose and response for pregabalin and PD334 with the two compounds having a common E_{\max} but differing ED_{50} was critical. It provided a realistic sense of the relationship between dose and response for PD334 and precluded any unrealistic expectations by the development team about the compound efficacy at doses higher than what was studied in Phase 2A (500 mg). The common E_{\max} assumption was considered reasonable because *in vitro* studies had demonstrated both compounds to bind to the same sites and *in vivo* studies demonstrated comparable maximum effect in the Vogel water-lick model. The alternative development strategy of ignoring the pregabalin data and studying additional doses and patients would have significantly contributed to the cost and execution time of the development program that would have been hard to justify given the similar pharmacology.

The assumption of the E_{\max} relationship and joint modeling improved the precision of the estimate of the PD334 effect compared to the analysis of just the PD334 Phase 2 data alone. The standard error reported for the placebo adjusted HAM-A change from baseline score at the 200 and 500-mg active doses in the PD334 POC study (1007) was 1.33 based on 53 subjects and 1.37 based on 53 subjects, respectively. The standard error for the difference in the change from

baseline effect from placebo for 500 mg PD334 is about 0.83 on basis of the E_{\max} model from the joint analysis with Pregabalin (Fig. 15.3). Based on the relationship between standard error and sample size, this means that between 130 and 140 patients per treatment group, *i.e.*, about 80 additional patients per treatment arm, would have been required in the POC study to obtain a similar precision as that yielded by the model based analysis. The efficacy model was used to predict the outcome of one completed Phase 3 study. The observed week 6 data was well within the region of predicted uncertainty thus suitably validating the efficacy model with an external data source.

The analysis allowed for the therapeutic index (TI), defined by the ratio of the ED_{50} for safety and efficacy, to be different between pregabalin and PD334. This was carried forward in the simulations, despite the result from a joint analysis of both of the efficacy and safety endpoints, showing no statistically significant difference between a model assuming different relative potencies and a model assuming the same relative potency across endpoints ($p = 0.78$). This nonsignificant difference in the two models was not considered consistent with the pharmacology that supports the “unique therapeutic index for each compound” concept. The two compounds had different selectivity for the receptor subtypes and therefore it was quite possible that differences in affinity and intrinsic efficacy could manifest different TI's for either compound. Based on the results of the analysis, the TI of PD 334 was estimated to be smaller than the TI of Pregabalin, which was an unexpected result given the preclinical hypothesis of superior receptor subtype selectivity. However, the ratio of the TI of PD334 and Pregabalin was not significantly different from one, suggesting the two compounds could be therapeutically equivalent.

One of the advantages of this analysis is that it was not complex and could be easily understood by members of the development team who did not have a background in modeling and simulation. The analysis used LS mean end of study HAM-A data based on LOCF imputation, which were the data that were first officially reported. This facilitated timely modeling and reporting to the development team, which in turn led quickly to discussions of the central issues, which were: (1) what is the target therapeutic profile; (2) what is the dose range that would meet the target and; (3) how many doses should be considered for the Phase 3 program. These discussions were greatly enhanced by the availability of the integrated (*i.e.*, safety and efficacy) dose–response curve.

References

- Dooley JD, Taylor CP, Donevan S, Feltner D (2007) Ca^{2+} channel $\alpha_2\delta$ ligands: novel modulators of neurotransmission. *Trends Pharmacol Sci* 28:75–82
- Feltner DE, Crockatt JG, Dubovsky SJ, Cohn CK, Shrivastava RK, Targum SD et al (2003) A randomized, double blind, placebo-controlled, fixed-dose, multicenter study of pregabalin in patients with generalized anxiety disorder. *J Clin Psychopharmacol* 23:240–249

- Lalonde RL, Kowalski KG, Hutmacher MM, Ewy W, Nichols DJ, Milligan PA, Corrigan BW, Lockwood PA, Marshall SA, Benincosa LJ, Tensfeldt TG, Parivar K, Aantea M, Glue P, Koide H, Miller R (2007) Model-based drug development. *Clin Pharm Ther* 82:21–32
- Mandema JW, Wang W (2003) Use of modeling and simulation to optimize dose-finding strategies. In: Kimko HC, Duffull SB (eds) *Simulation for designing clinical trials*, vol 127, *Drugs and the pharmaceutical sciences series*. Marcel Dekker, New York, pp 289–312
- Mandema JW, Cox E, Alderman J (2005a) Therapeutic benefit of eletriptan compared to sumatriptan for the acute relief of migraine pain – results of a model-based meta-analysis that accounts for encapsulation. *Cephalalgia* 25:715–725
- Mandema JW, Hermann D, Wang W, Sheiner T, Milad M, Bakker-Arkema R, Hartman D (2005b) Model-based development of Gemcabene, a new lipid-altering agent. *AAPS J* 7(3): E513–E522. Article 52 <http://www.aapsj.org>. Accessed Aug 2009
- Montgomery SA, Tobias K, Zornberg GL, Kasper S, Pande AC (2006) Efficacy and safety of pregabalin in the treatment of generalized anxiety disorder: a 6-week, multicenter, randomized, double blind, placebo-controlled comparison of pregabalin and venlafaxine. *J Clin Psychiatry* 67:771–782
- Pande AC, Crockatt JC, Feltner DE, Janney CA, Smith WT, Weisler R et al (2003) Pregabalin in generalized anxiety disorder: a placebo controlled trial. *Am J Psychiatry* 160:533–540
- Pohl RB, Feltner DE, Fieve RR, Pande AC (2005) Efficacy of pregabalin in the treatment of generalized anxiety disorder: double blind, placebo-controlled comparison of BID versus TID dosing. *J Clin Psychopharm* 25:151–158
- Rickels K, Rynn MA (2001) What is generalized anxiety disorder. *J Clin Psychiatry* 62 (suppl 11):4–12
- Rickels K, Pollack MH, Feltner DE, Lydiard RB, Zimbroff DL, Bielski RJ et al (2005) Pregabalin for treatment of generalized anxiety disorder: a 4-week, multicenter, double blind, placebo-controlled trial of pregabalin and alprazolam. *Arch Gen Psychiatry* 62:1022–1030
- Vogel JR, Beer B, Clody DE (1971) A simple and reliable conflict procedure for testing antianxiety agents. *Psychopharmacologia* 21:1–7
- Weisberg RB (2009) Overview of generalized anxiety disorder: epidemiology, presentation and course. *J Clin Psychiatry* 70(suppl 2):4–9
- Wittchen H-U, Hoyer J (2001) Generalized anxiety disorder: nature and course. *J Clin Psychiatry* 62(suppl 11):15–19

Chapter 16

Balancing Efficacy and Safety in the Clinical Development of an Atypical Antipsychotic, Paliperidone Extended-Release

Filip De Ridder and An Vermeulen

Abstract The clinical outcomes of three pivotal clinical trials with paliperidone ER, an atypical antipsychotic were prospectively predicted with a model using a limited amount of paliperidone ER pharmacokinetic data, human *in vivo* D₂-receptor occupancy data and the generally accepted D₂-receptor derived therapeutic window hypothesis. The latter was further substantiated using historical risperidone safety data. Model predictions guided the selection of the dose range for clinical trials, particularly with regards to the extremes of the dose range studied.

16.1 Introduction

Schizophrenia is a severe, chronic mental illness that affects approximately 1% of the worldwide population. Clinical symptoms are apparent relatively early in life, generally emerging during adolescence or early adulthood. The symptoms of schizophrenia include the presence of hallucinations, delusions and disorganized thoughts, which are absent in healthy subjects and thus are labeled as “positive symptoms.” Patients also show symptoms such as social withdrawal, diminished affect, poverty of speech and the inability to experience pleasure, which are labeled as “negative symptoms.” In addition, schizophrenic patients suffer from mood symptoms and cognitive deficits, such as impaired attention and memory.

Current pharmacological treatment of schizophrenia is based on the blockade of cortical dopamine D₂-receptors (Pani *et al.* 2007). Over the past decades, a large number of D₂-antagonists have been developed for the treatment of schizophrenia, starting with the discovery of chlorpromazine in 1952, followed by the so-called conventional antipsychotics (*e.g.*, haloperidol). These first-generation antipsychotics helped relieve the positive symptoms of the disease, but were associated with safety

F. De Ridder (✉)

Janssen Research & Development, a division of Janssen Pharmaceutica NV,
Biostatistics & Programming, Beerse, Belgium
e-mail: fdridder@its.jnj.com

and tolerability issues, including extra-pyramidal symptoms (EPS) and cognitive impairment. In the 1990s, second-generation antipsychotics, called atypicals, were introduced (*e.g.*, risperidone, olanzapine). Although these antipsychotics represented a significant improvement, there is still a need for new antipsychotic drugs that target undertreated aspects of the disorder, such as cognitive impairment and social functioning, and have a better safety profile.

In a recent review, Nucci *et al.* (2009) discuss the opportunities for model-based drug development in schizophrenia. Drug development in schizophrenia can gain a lot from a model-based approach, as there is a large variety of data sources available to work with, such as preclinical and clinical pharmacokinetics, biomarkers (imaging) and clinical data of both new as well as marketed compounds.

In this chapter, we will illustrate the use of an integrated PK/PD-modeling approach during the clinical development of paliperidone ER. Paliperidone ER was designed to provide a controlled delivery of the active metabolite of risperidone over a 24-h period, which was expected to lead to an improved therapeutic window. Currently, paliperidone ER is approved for the acute and maintenance treatment of schizophrenia and the acute treatment of schizoaffective disorder as mono- or adjunctive therapy.

The objective of the modeling and simulation (M&S) project was to inform the design of the clinical phase 3 program in the treatment of acute schizophrenia. More specifically, the question was to identify a dose range to be studied that would provide the best balance between clinical efficacy (symptom and functional improvement) and safety (*e.g.*, extra-pyramidal side effects). The project was carried out in 2003 prior to the execution of the clinical trials. In the meantime, data that was used in the M&S exercise as well the results of the phase 3 studies have been published and can be compared with the predictions made back in 2003.

16.2 Rationale

Data from imaging studies, which allow quantifying the striatal D₂-receptor occupancy *in vivo* in humans, started to accumulate in the 1990s. In a series of papers, recently reviewed by Pani *et al.* (2007), receptor occupancy levels of a range of antipsychotic drugs at their therapeutic dose levels as used in the clinic, were reported. These reports led to the hypothesis that the D₂-receptor occupancy in the striatum should lie between 65 and 80% to achieve an acceptable efficacy–safety balance: the lower threshold is required for clinical efficacy, whereas exceeding the higher threshold leads to an increased risk of side effects; in particular, EPS. Based upon this rationale, the following strategy was developed: (1) predict the distribution of D₂-receptor occupancy in a population of patients treated with paliperidone ER and (2) determine the doses at which D₂-receptor occupancy is within the 65 and 80% D₂-receptor range in most of the to-be-treated patients.

This approach relies on the generally accepted 65–80% D₂-receptor occupancy “window” hypothesis (Pani *et al.* 2007). Risperidone was one of the first D₂-receptor

antagonists, for which imaging data were collected, which helped to empirically derive this hypothesis (Nyberg *et al.* 1999). As paliperidone is the active metabolite of risperidone, this hypothesis was expected to be valid for paliperidone ER as well. However, to further substantiate this relationship, PK/PD-models were attempted, linking D_2 -receptor occupancy levels with symptom improvement (measured by the PANSS) and incidence of EPS using historical risperidone data. Unfortunately, a workable model for the relationship between plasma concentrations and symptom improvement for the risperidone data was not achieved.

16.3 Methods and Data

16.3.1 *D₂-Receptor Occupancy as a Biomarker for Efficacy and Safety*

16.3.1.1 *D₂-Receptor Occupancy Model*

As for most D_2 -antagonists, the relationship between plasma concentrations of the antagonist and striatal D_2 -receptor occupancy can be described by a hyperbola:

$$RO = RO_{\max} \frac{C}{K_d + C}$$

where RO is the receptor occupancy, C the plasma concentration and K_d , the apparent equilibrium dissociation constant, which is the plasma concentration at which 50% D_2 -receptor occupancy is observed. RO_{\max} is the maximal receptor occupancy that can be achieved. This model has been shown to apply for most antipsychotics with RO_{\max} equal to 100% (Nucci *et al.* 2009).

When RO_{\max} is assumed to be 100%, this model can be parameterized using a logit transformation of RO:

$$\log \frac{RO}{1 - RO} = -\log K_d + \log C$$

The advantage of this parameterization is that it constrains RO expressed as percentage to 0–100%.

Data of PET-studies are restricted to a few observations per subject, in order to limit exposure to radiation. Usually only two or three data points per subject are available. In most applications, these data points are all treated as independent observations and the receptor occupancy model is a simple regression model. In this way, all sources of variability are collapsed into the residual error. However, residual error comprises the sum of inter-individual variability in RO among subjects given their concentration, and pure measurement error, as well as model

misspecification. Nyberg *et al.* (1996) reported a difference in receptor occupancy of 3.2% between two measurements taken 2.5-h apart in schizophrenic patients treated with a long-acting injectable (haloperidol decanoate). This suggests that roughly half of the residual variation reported in PET-studies is due to measurement error and the other half due to other factors, including inter-individual variation. However, we assumed in the current project that the estimate of residual variation entirely reflects interindividual variation.

At the start of the project, D_2 -receptor occupancy after oral administration of paliperidone had been investigated in two healthy volunteer studies: (1) a study with a single dose of 1-mg oral solution (three subjects, one post-dose scan at the expected C_{\max}) and (2) a study with 6 mg of the paliperidone ER formulation (four subjects, two post-dose scans). K_d was estimated to be 6.4 ng/mL in the first study and 4.45 ng/mL in the second. A pooled analysis of all individual data of both studies yielded an estimate of 4.9 ng/mL (Karlsson *et al.* 2005). As there were only one or two measurements per subject, only a residual error component was estimated. The standard deviation was estimated to be 0.36 on the logit scale, which corresponds to a standard deviation of about 8% at a mean receptor occupancy level of 70%. In the following simulation work, it is assumed that the estimate of residual variation entirely reflects inter-individual variation.

16.3.1.2 Population PK-Model for Paliperidone ER

A population pharmacokinetic model was developed using the data observed in a four-way crossover trial in 32 healthy subjects, comparing the single dose PK of the experimental controlled-release formulations with an oral solution. At this stage, these were the only available data of paliperidone ER pharmacokinetics in humans. In the study, only one dose of paliperidone ER (4-mg) was employed. In subsequent simulations, dose-proportionality was assumed.

The pharmacokinetics of paliperidone ER was modeled according to a two-compartment model with sequential zero-order (with a lag time) and first-order absorption. Post-estimation model diagnostics were acceptable and interindividual variability (IIV) was estimated for most parameters. Inter-individual variability of the bioavailability of the solid dose formulations relative to oral solution was the most important factor determining IIV in plasma exposure at a given dose (Cirincione *et al.* 2007).

16.3.1.3 Prediction of D_2 -Receptor Occupancy

The population PK model was used to predict plasma concentration–time profiles during multiple dosing of paliperidone ER in a typical population of patients. The key assumptions that are made here were dose-proportionality over the dose range considered and similarity of model parameters (both typical values as well as the IIV) between patients and healthy subjects.

For a virtual population of 2,000 subjects, full 24-h interdose plasma concentration–time profiles (at hourly intervals) at steady state of once daily dosing regimens of 3, 6, 9, 12, 15, and 18-mg were simulated. Each subject’s simulated plasma concentration time-profile was converted into a D_2 -receptor occupancy time course using the hyperbola equation, where residual error was included to represent inter-individual variability. From the D_2 -receptor occupancy-time course of each virtual patient, the peak (at peak plasma concentrations) as well as the average D_2 -occupancy over all 24 predicted values was calculated. For each virtual patient, the lowest dose, which would result in a trough D_2 -receptor occupancy above 65% and a peak D_2 -receptor occupancy below 85%, was determined. This can be considered an individually optimized dose. Thus, the key drivers determining this dose are pharmacokinetic as well as pharmacodynamic variability.

16.3.2 Extrapyramidal Symptoms

16.3.2.1 Pharmacokinetic/Pharmacodynamic (PK/PD)-Model

The safety outcome of interest was the incidence of spontaneously reported EPS-related adverse events. EPS-related adverse events included side effects mapping to the following WHOART dictionary terms: hyperkinesia, dystonia, parkinsonism, bradykinesia, dyskinesia, dyskinesia tardive, dystonia, extrapyramidal disorder, hyperkinesia, hypertonia, hypokinesia, muscle contractions involuntary, oculogyric crisis, tongue paralysis, and tremor. The PK/PD-model was developed using data of a study with long-acting injectable RISPERDAL CONSTA[®] (Kane *et al.* 2003). In this 12-week, multicenter, double blind, randomized study, 400 patients received intramuscular injections of placebo or long-acting risperidone (25, 50, or 75 mg) every 2 weeks. In this study, the incidence of spontaneously reported adverse events attributed to EPS were similar in the placebo (13%) and the 25-mg risperidone (10%) groups, with higher rates in the 50 (24%) and 75-mg (29%) groups (Kane *et al.* 2003). Up to 11 blood samples at several occasions during the 12-week treatment period were collected for the determination of risperidone active moiety concentrations (risperidone + paliperidone). These data were used to develop a population pharmacokinetic model that was subsequently used to obtain average steady-state plasma concentration (C_{ss}) of the active moiety in each patient.

The time from the start of the double-blind treatment phase to the first treatment-emergent EPS-related event was modeled using hazard models. Hazard models provide a flexible framework to describe the risk for certain events happening to subjects in a clinical trial as a function of covariates, which might be either time-constant or time varying. In a hazard model, the time component is explicitly present, which can take into account different durations of treatment between patients (because of dropout) as well as differences in duration between studies. Cox *et al.* (1999) have introduced this approach in PK/PD-modeling.

For a more recent application of this approach to adverse event data, see Ito *et al.* (2008). Hazard models can also be used to describe the dropout process (Lindsey 2000).

The hazard (λ), the probability of observing an event at time t , given that it had not occurred before time t , is modeled as a function of covariates, including time, as follows:

$$\log \lambda(t, c_i) = f(t) + g(c_i)$$

where λ indicates the hazard for subject i at time t , t indicates the time since trial start, and c_i indicates a covariate.

The hazard function is composed of two parts. The first part, $f(t)$, sometimes called the disease progression model component, does not depend on treatment and describes how the hazard changes over time during a clinical trial in a population of patients assigned to the placebo group. The second part, $g(c_i)$, is the drug effect and is a function of an individual measure of drug exposure. Note that this model is a proportional hazards model as the drug effect is added to the placebo-time course hazard on the log scale. Nonproportional hazard models were also explored, but these did not give a better fit than the simpler model.

Typically, the EPS-related adverse events hazard decreases over time. This can be caused by a genuine decrease of the risk over time (*e.g.*, tolerance) or because of the heterogeneity between patients in their individual risk. In the latter case, patients with a high individual risk will experience the event earlier in the trial as compared to patients with a low individual risk. Consequently, as time progresses, only patients with a lower individual risk are still at risk for the event, thus decreasing the population-averaged hazard. These two cases cannot be separated when only one event per subject is considered. The functional form of $f(t)$ was explored graphically using Kaplan–Meier estimates of the cumulative hazard over time for placebo patients. These revealed that the decrease of the hazard over time was best described by a linear function:

$$f(t) = \beta_0 + \beta_1 t$$

As an individual measure of exposure, the average steady-state plasma concentration (C_{ss}) of active moiety (risperidone + paliperidone) over a dosing interval was used. Patient-specific C_{ss} was estimated using the dose, dosing interval, and the empirical Bayes estimate of CL/F. The latter was obtained from a population PK-model (unpublished results). For a limited number of patients (8.5%), no estimate of the individual clearance was available because they had been excluded from the population PK analysis. Note that this exposure measure is constant over time. In patients treated with long-acting injectable risperidone, plasma concentrations of the active moiety gradually increase during the first 2–4 weeks after the first injection (Gefvert *et al.* 2005). Therefore, the individual C_{ss} is an overestimation of the true exposure during the first few weeks of treatment.

Candidate functional forms of $g(c_i)$ were explored graphically by dividing all risperidone-treated patients into five exposure categories defined by their individual

C_{ss} and then relating the incidence of events within each category to exposure, a procedure known as evaluating the scale of the covariate (Hosmer *et al.* 2008). Based on this, a three-parameter logistic model was selected:

$$g(c_i) = \frac{\theta_1}{1 + \exp\left(\frac{\theta_2 - c_i}{\theta_3}\right)}$$

where θ_1 indicates the maximal effect, θ_2 is the EC_{50} , and θ_3 is a scale parameter (steepness).

In addition, also a threshold model was considered:

$$g(c_i) = \begin{cases} 0 & \text{if } c_i \leq \theta_1 \\ \theta_2 & \text{if } c_i > \theta_1 \end{cases}$$

where θ_1 indicates the threshold and θ_2 is the log risk increase.

A similar hazard model was developed for drop out. The probability to drop out decreased with time and was larger in the placebo group than in the risperidone arms. Patients were censored with respect to the occurrence of EPS if they dropped out or completed the trial without the occurrence of the event.

Parameter estimates were obtained using maximum likelihood estimation. The likelihood was explicitly derived from the hazard function, taking censoring into account (Kalbfleish and Prentice 2002). The likelihood contribution of a subject experiencing the event at time T is:

$$L = \left(\prod_{t=1}^{T-1} (1 - \lambda(t)) \right) \lambda(T)$$

where $\lambda(t)$ is the hazard at time t .

The likelihood contribution of a subject not experiencing the event during the trial and thus censored at time T , the last day in the trial, is

$$L = \prod_{t=1}^T (1 - \lambda(t))$$

Maximum likelihood estimates and their standard errors were obtained using SAS 8.2 (PROC NLMIXED). The reliability of the standard errors on the parameter estimates reported by NLMIXED was assessed by constructing a likelihood profile for each of the model parameters.

16.3.2.2 PK/PD-Simulation

EPS-incidence in the planned clinical trials with oral paliperidone ER was predicted using a simulation model with three different submodels (Fig. 16.1):

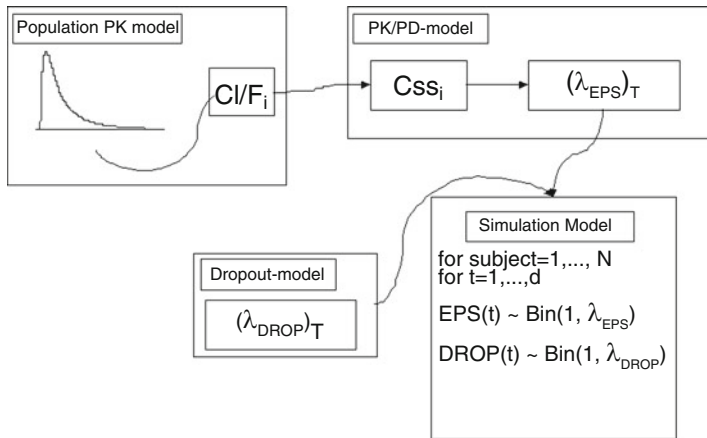


Fig. 16.1 Schematic representation of the clinical trial simulation model

1. *Exposure model*: subject-specific values for the apparent clearance (CL/F) were sampled from a lognormal distribution with mean and variance derived from the population PK model (see Sect. 16.3.1.2). Average steady-state concentration was then calculated as follows: $C_{ss,i} = CL_i/F * 1,000/\text{dose}/24 \text{ h}$.
2. *EPS-model*: generates the hazard of developing EPS at time t as a function of the subject specific $C_{ss,i}$. The risk is converted into an event using a binomial probability model.
3. *Dropout model*: generates the hazard of discontinuation at time t as a function of time and treatment. The risk is converted into an event using a binomial probability model.

For each study, 120 subjects, the planned number of patients per arms, were simulated for a treatment duration of 6 weeks (1,000 replicates).

The key assumptions of this simulation model are the following:

1. Risperidone active moiety has the same potency (EC_{50}) as paliperidone for increasing the EPS risk. The PET-data that were available at the time of the project suggested a lower EC_{50} value (4.95-ng/mL) (Karlsson *et al.* 2005) for paliperidone than for risperidone active moiety (9.9-ng/mL) (Gefvert *et al.* 2005). Therefore, two scenarios were considered: one with the EC_{50} estimated from the risperidone data and one with an EC_{50} reduced by 50%.
2. Average concentrations determine the risk for EPS.
3. For the exposure model, the same assumptions as before were applied, namely dose proportionality and similarity of parameters in healthy volunteers and patients.
4. Conditional on time and plasma concentration, EPS and dropout are independent events.

16.4 Results

16.4.1 Predicting Efficacy and Safety using D_2 -Receptor Occupancy as a Biomarker

The predicted distribution of peak and average steady state D_2 -receptor occupancy in the virtual patient population is summarized in Fig. 16.2 for doses ranging from 3 to 18-mg. At any given dose, this distribution reflects differences between patients in D_2 -receptor occupancy. The degree of variation is determined by interindividual

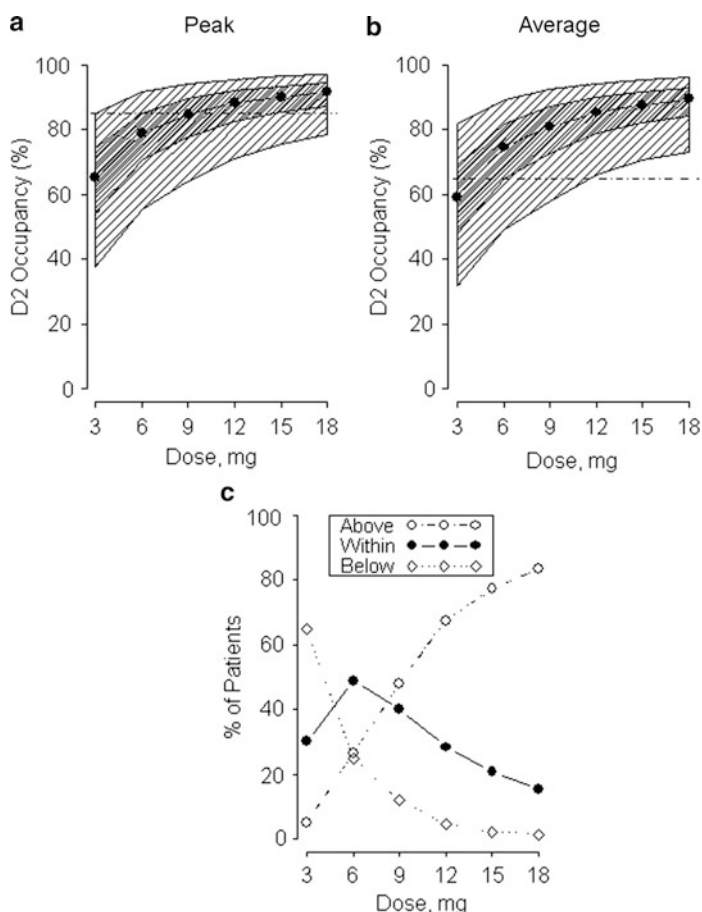


Fig. 16.2 Predicted distribution of steady-state D_2 -receptor occupancy in a population of patients treated with paliperidone ER as a function of dose: (a) Peak D_2 -occupancy at C_{max} , (b) average D_2 -occupancy over the dosing interval. Shaded areas indicate the 5th, 95th percentile range (comprising 90% of patients) and the 25th, 75th range (50% of patients), (c) percentage of patients below, within or above the therapeutic D_2 -occupancy range

differences in pharmacokinetics as well as IIV in D_2 -occupancy given plasma concentrations. Quantitatively, both sources of variability were equally important.

With 3-mg dosing, the predicted average steady state D_2 -occupancy was less than 65% in the majority of patients (Fig. 16.2). With increasing doses, the proportion of patients reaching the efficacy threshold increases, with the largest increase between 3 and 9-mg. At the same time, the proportion of patients exceeding the safety threshold gradually increases. On average, doses beyond 12-mg do not offer much gain in terms of the efficacy/safety trade-off. The proportion of patients within the therapeutic window is highest at 6 mg. The impact of the uncertainty of K_d was investigated by repeating the simulation with a K_d at its lower and upper 95% confidence limit, respectively (Fig. 16.3). The prediction that most patients are within the therapeutic range with 6 mg is not changed. The largest impact is seen for the 3-mg dose, which is clearly an ineffective dose for the high K_d and becomes similar to 6 mg for the low K_d .

For most patients, the individually optimized dose, defined as the lowest dose for which the peak D_2 -receptor occupancy falls below 85% and the average D_2 -occupancy exceeds 65%, was predicted to be 6 mg (Fig. 16.4). In addition, for the majority of patients (85%) the individually optimal dose would be 3, 6, or 9-mg.

It was concluded that 3 mg could be a noneffective or minimal effective dose, whereas an optimal efficacy balance might be achieved in the 6–12-mg range. In three subsequent clinical trials, the dosages in this range (6, 9, and 12-mg) were

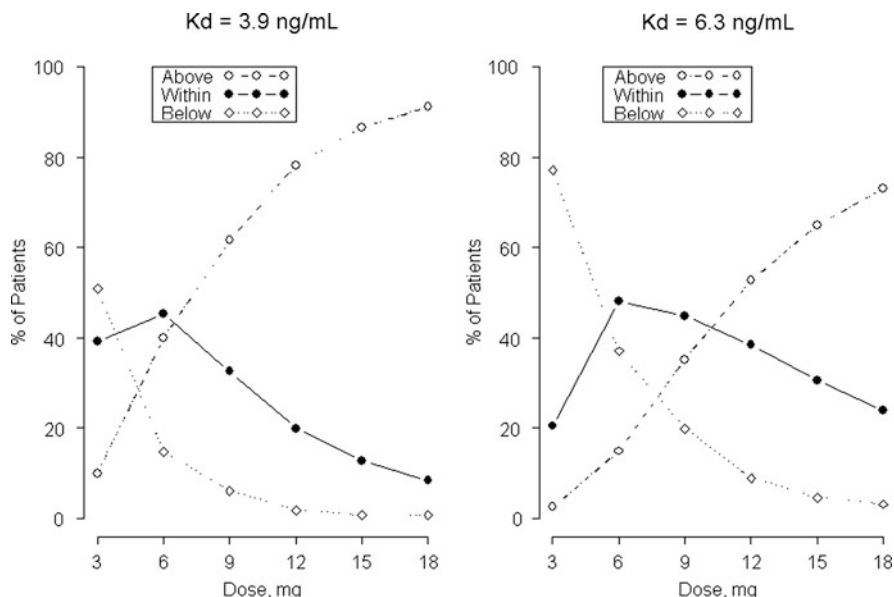
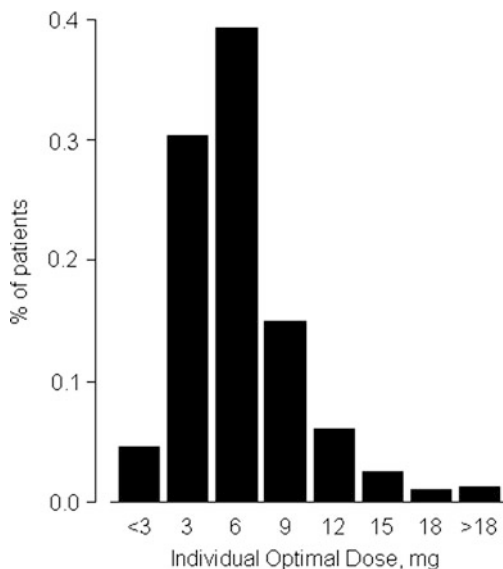


Fig. 16.3 Predicted distribution of steady state D_2 -receptor occupancy in a population of patients treated with paliperidone ER as a function of dose: percentage of patients below, within or above the therapeutic D_2 -occupancy range at the lower respectively upper 95% confidence limit of the estimate of K_d

Fig. 16.4 Distribution of the individually optimized dose (lowest dose achieving an average D_2 -occupancy above 65% and a peak D_2 -occupancy below 85%)



replicated in two trials, and 3 and 15-mg dosages were investigated in one trial: Study 1: 6, 9 and 12 mg; Study 2: 6 and 12 mg, and Study 3: 3, 9, and 15-mg.

The results of the clinical trials demonstrated that all doses tested showed a larger symptom improvement compared to placebo (Meltzer *et al.* 2008). The effect was smallest for 3 mg and only a modest further increase of symptom improvement could be observed with 12 and 15 mg doses. At doses of 3 and 6 mg, the profiles of EPS signs and symptoms were similar to placebo, whereas doses of 9 mg and higher were associated with elevated rates of EPS. Based on these data, 6 mg was considered to offer a good balance between safety and efficacy and is the approved recommended starting dose (Meltzer *et al.* 2008).

16.4.2 Predicting EPS-Incidence

16.4.2.1 PK/PD Model for EPS-Incidence

In the 12-week study with a long-acting injection of risperidone, the hazard for EPS-related adverse events was related to average steady-state plasma concentrations (Fig. 16.5). Below 35-ng/mL, the risk to develop EPS is similar to placebo. Above 35-ng/mL, a steep increase of the hazard is observed. During the first 2 weeks of treatment, there is no clear separation between exposure groups. This could be because during this period, plasma concentrations are still gradually increasing (Gefvert *et al.* 2005). Models with plasma concentration as time-varying

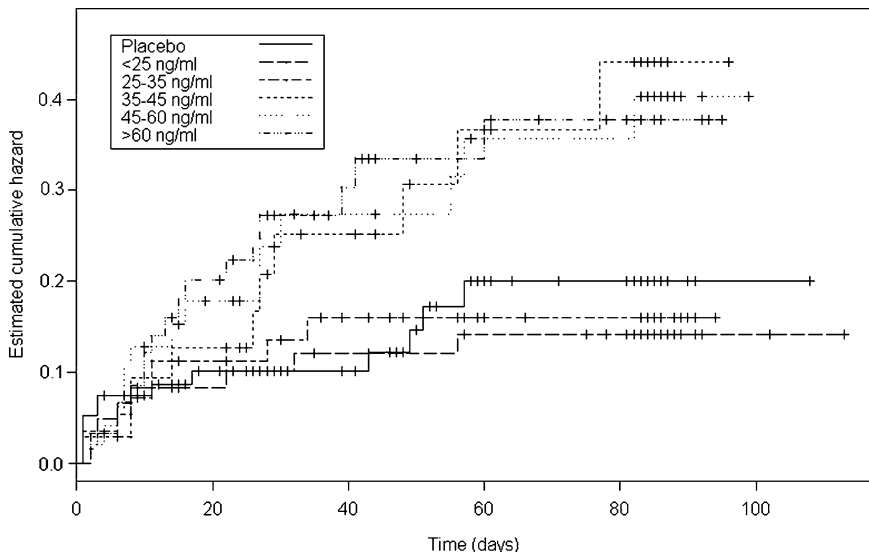


Fig. 16.5 Kaplan–Meier estimates of the cumulative hazard function for time to first extra-pyramidal symptoms (EPS)-related adverse event by exposure groups defined by the average steady-state active moiety plasma concentrations ($N = 35$ – 63 per group, $N = 98$ for placebo)

covariate did not provide a better fit, most likely because the total number of events during this period was too low.

When the three-parameter logistic model was fitted to the data, the scale parameter (θ_3) was not estimable. Inspection of the log likelihood profile for θ_3 indicated that this was because of the steepness of the relationship as decreasing values of θ_3 increased the likelihood. The scale parameter was therefore fixed to a value of 1, which gave a fit similar to the threshold model. The final model was checked by a posterior predictive check. An external validation was done by fitting the model to data of another study with long-acting risperidone (Chue *et al.* 2005), which had not been used for model building. These data gave very similar estimates for the drug model parameters, but the intercept of the placebo-submodel was lower in study 2, indicating an overall lower EPS-incidence in this study. The final model was fitted to the pooled data of both studies, allowing for a different intercept (Table 16.1).

The exposure–response relationship is illustrated in Fig. 16.6. For average steady-state plasma concentrations below 30-ng/mL, the ratio of the hazard for developing EPS over the hazard in the placebo-treated patients is close to 1, indicating no increased risk. At higher plasma concentrations, there is a steep increase of the risk, reaching a plateau of about 2.8 (log hazard ratio was estimated to be 1.02) with plasma concentrations over 40-ng/mL. In the right panel of Fig. 16.6, the exposure–response relationship is translated into a D_2 -receptor occupancy–risk relationship. Plasma concentrations were converted to D_2 -receptor occupancy using a K_d of 9.9-ng/mL (Gefvert *et al.* 2005). The risk for EPS increases when the average steady state D_2 -occupancy goes beyond 70% and reaches a plateau from 80% onwards.

Table 16.1 Parameter estimates of the final PK/PD model

Parameter		Estimate	Standard error	CV (%)
Time dependency				
β_1	Intercept – Study 1	-5.32	0.21	4
	Intercept – Study 2	-6.07	0.26	4
β_2	Common slope	-0.029	0.005	17
Drug effect				
θ_1	Maximum effect	1.02	0.21	20
θ_2	EC ₅₀ (ng/mL)	32.1	1.17	4
θ_3	Scale	1	Fixed	-

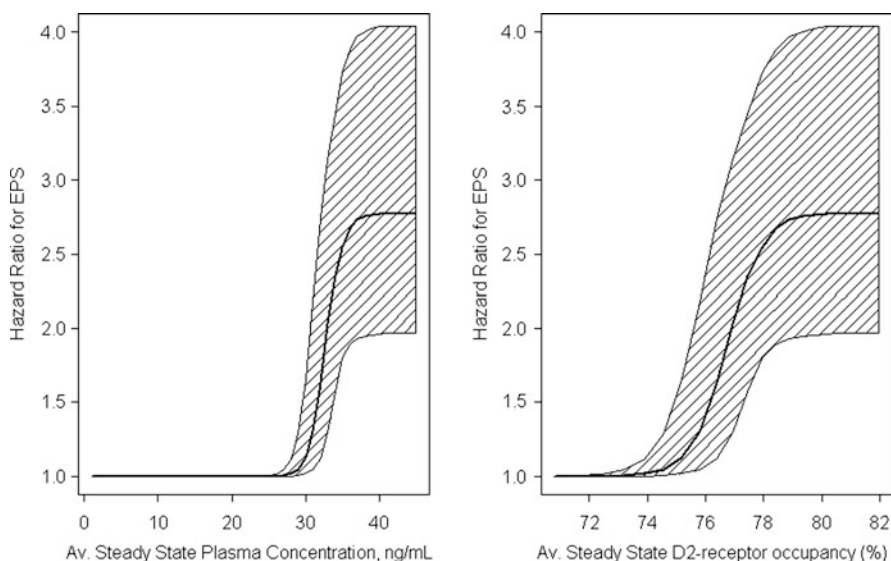


Fig. 16.6 Final PK/PD-model relating the risk for EPS-related adverse events to risperidone exposure in clinical trials with a long-acting injection expressed as average steady-state plasma concentrations (*left*) and D₂-receptor occupancy (*right*). *Shaded area* represents 95% uncertainty band due to model parameter uncertainty

A hazard model for dropout was developed, which included a time component (drop out risk decreased with time on study) and a treatment-dependent intercept. Dropout risk was higher for placebo-treated patients, but there was no relationship with dose or exposure in the risperidone-treated patients.

16.4.2.2 PK/PD Simulation for EPS-Incidence

The predicted dose–response for the EPS-incidence in the planned clinical trials with paliperidone ER is shown in Fig. 16.7. The shape of the dose–response curve depends on the assumption about the D₂-receptor affinity of paliperidone ER. The observed incidence for the doses that were replicated in the clinical trials shows a

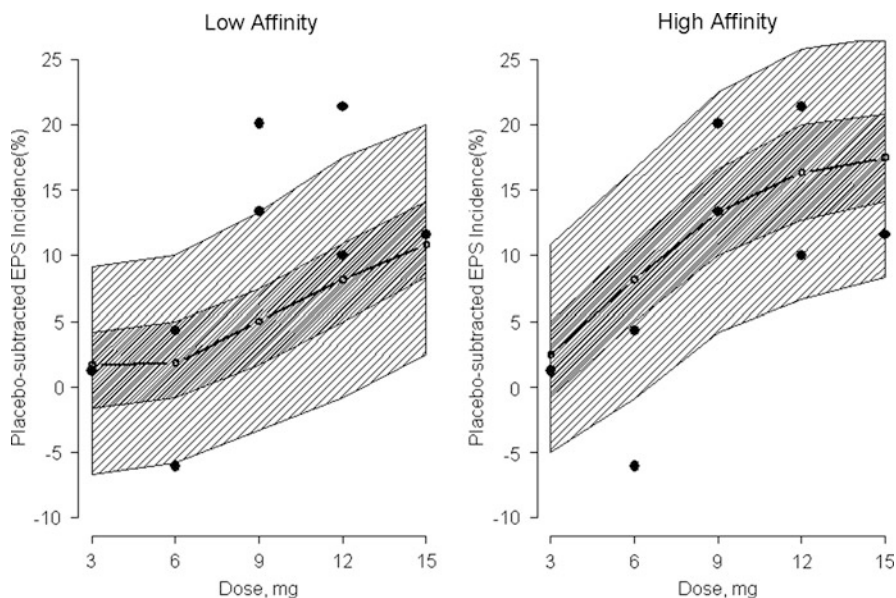


Fig. 16.7 Clinical trial simulation of the incidence of EPS-related adverse events for paliperidone ER for two scenarios of K_d (low affinity: $K_d = 9.9$ ng/mL, high affinity: $K_d = 4.95$ ng/mL). Shaded areas indicate the 5th, 95th and 2.5th, 97.5th percentiles of the distribution of expected trial outcomes. The dots indicate the observed values in the trials that were subsequently conducted. Data are represented as placebo-subtracted incidences to account for differences in placebo incidence between trials

large variability between trials, in line with the expected variability because of sampling, variability in the pharmacokinetic characteristics of patients, as well as the stochastic nature of the EPS occurrence. Either scenario captured the general pattern of the observed incidence of EPS-related adverse events in the three paliperidone ER clinical trials, although the low affinity scenario underpredicted the EPS incidence for 9 and 12 mg, whereas the high affinity scenario overpredicted the incidence for 6 mg. Interestingly, when the PK/PD-model was retrospectively fitted to the paliperidone ER data, the EC_{50} was estimated at 24 ng/mL, an intermediate value in between both scenarios (unpublished results).

16.5 Discussion

The outcomes of several planned clinical trials with paliperidone ER were prospectively predicted using a simple model relating plasma concentrations to D_2 -receptor occupancy levels. This model was based on a limited amount of data on the pharmacokinetics of paliperidone ER (24 healthy subjects) and human *in vivo* D_2 -receptor occupancy characteristics (seven healthy subjects). It used the generally

accepted hypothesis that at least 65% receptor occupancy is required for efficacy and that, at or above 80% receptor occupancy, the risk of developing side effects increases. Predictions of the model guided the dose choice for pivotal clinical trials with paliperidone ER, particularly concerning the extremes of the dose range studied. The lowest dose (3 mg) was included because it was likely to be a minimally effective dose, whereas the 18-mg dose, which was likely not to give any gain in terms of the efficacy/safety balance, was discarded.

Population simulations predicted 6 mg to be the dose with the most optimal balance between efficacy and safety. At the same time, the population simulations allowed to assess the amount of inter-individual variability in receptor occupancy levels. These results suggested that most patients would achieve an optimal efficacy/safety balance with 6 mg, which was also the case for a fair proportion of patients at 3 and 9 mg. These predictions agreed well with the results of the three clinical studies that were subsequently run.

To further substantiate the D₂-receptor occupancy theory, attempts were made to construct PK/PD-models for clinical efficacy and safety using historical risperidone data. Unfortunately, a longitudinal PK/PD model for clinical efficacy of risperidone could not be established. In a recent review, Mauri *et al.* (2007) concluded that the relationship between plasma concentrations and efficacy has not been unequivocally established for many atypical antipsychotics. Usually, one explores the relationship between a clinical endpoint and concentrations or doses, using simple regression or correlation models. More elaborate PK/PD models using the longitudinal nature of symptom scores can potentially have merit as they allow to deal with some of the inherent complexities of running schizophrenia clinical trials, notably the placebo response and dropout. This is illustrated in the case studies of Kimko *et al.* (2000) and Friberg *et al.* (2009). The failure to establish an exposure–response relationship using a longitudinal PK/PD-model for risperidone was probably because the lowest doses studied already had a substantial therapeutic effect. Ortega *et al.* (2010) retrospectively developed a longitudinal dose–response model using data of the three paliperidone ER clinical trials. They were not able to establish a dose–response relationship as the effect at the lowest dose (3-mg) was already substantial.

A PK/PD-model for the hazard of developing EPS-related side effects was developed using average steady-state plasma concentrations as input. A steep exposure–response relationship was established, which supported the D₂-hypothesis as the risk was increased when the average steady-state concentration yielded a D₂-occupancy of more than 80%. This agrees well with the analysis presented by Medori *et al.* (2006).

The case study presented in this chapter illustrates that with limited data on the human pharmacokinetics and a biomarker, and some realistic assumptions based on prior knowledge, model-based predictions of the outcome of clinical trials can be achieved. It is clear, however, that the validity of the biomarker is a key requirement. Over the past decades, data supporting the D₂-receptor occupancy window hypothesis have been accumulated for many antipsychotics, including risperidone. It is thus not unexpected that the receptor occupancy window hypothesis holds for the extended

release formulation of its active metabolite. Although all current antipsychotics share D_2 -antagonism as a key pharmacological characteristic, each drug also possesses its unique fingerprint related to other receptor interactions or other features of the D_2 -receptor interaction (Pani *et al.* 2007). The approach described here can be easily extended to other biomarkers, offering unique opportunities for a more widespread use of model-based drug development (Nucci *et al.* 2009).

References

- Chue P, Eerdeken M, Augustyns I, Lachaux B, Molcan P, Eriksson L, Pretorius H, David AS (2005) Comparative efficacy and safety of long-acting risperidone and risperidone oral tablets. *Eur Neuropsychopharmacol* 15:111–117
- Cirincione BB, Redman ML, Fiedler-Kelly J, Ludwig EA, Vermeulen A (2007) Population pharmacokinetics of paliperidone ER in healthy subjects and schizophrenia patients. *Clin Pharmacol Ther* 81(1 suppl):S19
- Cox EH, Veyrat-Follet C, Beal SL, Fuseau E, Kenkare S, Sheiner LB (1999) A population pharmacokinetic-pharmacodynamic analysis of repeated measures time-to-event pharmacodynamic responses: the antiemetic effect of ondansetron. *J Pharmacokinet Biopharm* 27:625–644
- Friberg LE, de Greef R, Kerbusch T, Karlsson M (2009) Modeling and simulation of the time course of asenapine exposure response and dropout patterns in acute schizophrenia. *Clin Pharmacol Ther* 86(1):84–91
- Gefvert O, Eriksson B, Persson P, Helldin L, Bjorner A, Mannaert E, Remmerie B, Eerdeken M, Nyberg S (2005) Pharmacokinetics and D_2 receptor occupancy of long-acting injectable risperidone (Risperdal ConstaTM) in patients with schizophrenia. *Int J Neuropsychopharmacol* 8:27–36
- Hosmer DW, Lemeshow S, May S (2008) Applied survival analysis: regression modeling of time to event data, Wiley series in probability and statistics. Wiley, New York
- Ito K, Hutmacher MM, Liu J, Qiu R, Frame B, Miller R (2008) Exposure-response analysis for spontaneously reported dizziness in pregabalin-treated patients with generalized anxiety disorder. *Clin Pharmacol Ther* 84(1):127–135
- Kalbfleish JD, Prentice RL (2002) The statistical analysis of failure time data, Wiley series in probability and statistics. Wiley, New York
- Kane JM, Eerdeken M, Lindenmayer J-P, Keith SJ, Lesem M, Karcher K (2003) Long-acting risperidone: efficacy and safety of the first long-acting atypical antipsychotic. *Am J Psychiatry* 160:1125–1132
- Karlsson P, Dencker E, Nyberg S, Mannaert E, Boom S, Talluri K, Rossenu S, Eriksson B, Eerdeken M, Farde L (2005) Pharmacokinetics and dopamine D_2 and serotonin 5-HT_{2A} receptor occupancy of paliperidone in healthy subjects. *Eur Neuropsychopharmacol* 15(suppl 3):S386
- Kimko HC, Reece SSB, Holford NHG, Peck CC (2000) Prediction of the outcome of a phase 3 clinical trial of an antischizophrenic agent (quetiapine fumarate) by simulation with a population pharmacokinetic and pharmacodynamic model. *Clin Pharmacol Ther* 68(5):568–577
- Lindsey JK (2000) Dropouts in longitudinal studies: definitions and models. *J Biopharm Stat* 10:503–526
- Mauri MC, Volonteri LS, Colasanti A, Fiorentini A, De Caspari IF, Bareggi SR (2007) Clinical pharmacokinetics of atypical antipsychotics. *Clin Pharmacokinet* 45(5):359–388
- Medori R, Mannaert E, Gruender G (2006) Plasma antipsychotic concentration and receptor occupancy, with special focus on risperidone long-acting injectable. *Eur Neuropsychopharmacol* 16:233–240

- Meltzer HY, Bobo WV, Nuamah IF, Lane R, Hough D, Kramer M, Eerdeken M (2008) Efficacy and tolerability of oral paliperidone extended release tablets in the treatment of acute schizophrenia: pooled data from three 6-week, placebo-controlled studies. *J Clin Psychiatry* 69(5):817–829
- Nucci G, Gomeni R, Poggesi I (2009) Model-based approaches to increase efficiency of drug development in schizophrenia: a can't miss opportunity. *Expert Opin Drug Discov* 4(8):837–856
- Nyberg S, Farde L, Halldin C (1996) Test-retest reliability of central [¹¹C]raclopride binding at high D₂ receptor occupancy. *Psychiatry Res* 67:163–171
- Nyberg S, Eriksson B, Oxenstierna G, Halldin C, Farde L (1999) Suggested minimal effective dose of risperidone based on PET-measured D₂ and 5-HT_{2A} receptor occupancy in schizophrenic patients. *Am J Psychiatry* 156(6):869–875
- Ortega I, Perez-Ruixo JJ, Stuyckens K, Piotrovsky V, Vermeulen A (2010) Modeling the effectiveness of paliperidone ER and olanzapine in schizophrenia: meta-analysis of 3 randomized, controlled clinical trials. *J Clin Pharmacol* 50:293–310
- Pani L, Pira L, Marchese G (2007) Antipsychotic efficacy: relationship to optimal D₂-receptor occupancy. *Eur Psychiatry* 22:267–275

Part IV
Expanded Applications of M&S

Chapter 17

Application of Modeling and Simulation in the Development of Protein Drugs

Lorin K. Roskos, Song Ren, and Gabriel Robbie

17.1 Introduction

As defined by the United States Food and Drug Administration (FDA) (<http://www.fda.gov/AboutFDA/CentersOffices/CBER/ucm133077.htm>), “biological products include a wide range of products such as vaccines, blood and blood components, allergenics, somatic cells, gene therapy, tissues, and recombinant therapeutic proteins. Biologics can be composed of sugars, proteins, or nucleic acids or complex combinations of these substances, or may be living entities such as cells and tissues. Biologics are isolated from a variety of natural sources – human, animal, or microorganism – and may be produced by biotechnology methods and other cutting-edge technologies.” The focus of this chapter is on PK-PD modeling and clinical trial simulation of therapeutic and prophylactic proteins from discovery through clinical development.

Protein drugs include hormones, growth factors, cytokines, antibodies, and proteins conjugated to small molecule drugs, toxins, or radionuclides. The proteins can be endogenous proteins or novel constructs generated by molecular engineering. The drugs can function as agonists, antagonists, cytotoxins, coagulation factors, enzymes, and can also recruit immune effector functions. Although protein drugs have a wide variety of biological functions and molecular and pharmacokinetic characteristics, they share several important attributes, differing uniquely from most small molecule drugs, that must be considered when conducting PK-PD analyses for model-based drug discovery and development. These attributes and the implications for PK-PD modeling are listed in Table 17.1. Protein drugs can exhibit target-mediated drug disposition (TMDD); likewise, the kinetics of the target are frequently altered and drug-mediated target disposition is commonly observed. Special physiological barriers exist to absorption and biodistribution of proteins.

L.K. Roskos (✉)
Pharmacokinetics, Pharmacodynamics & Bioanalysis, Translational Sciences,
MedImmune, Inc., One MedImmune Way, Gaithersburg, MD 20878, USA
e-mail: RoskosL@MedImmune.com

Table 17.1 Unique pharmacokinetic and pharmacodynamic attributes of protein drugs that should be considered when conducting PK-PD modeling

Attribute	Consequence and modeling approach
Target frequently affects the kinetics of the drug	Dose-dependent PK Apply TMDD models
Drug frequently affects the kinetics of the target	Time-dependent PK Change in target concentration Change in number and phenotype of targeted cell populations Apply PK-PD model to describe change in target concentration, cell populations, and effects of target on PK
Physiological barriers exist to rate and extent of absorption and biodistribution	Model feasibility of extravascular dosing Apply PBPK modeling techniques for absorption and biodistribution kinetics
High specificity for human target can decrease the relevance of animal models	Apply PK-PD modeling to account for differences in specificity Evaluate PK-PD collected using surrogate molecules or transgenic animals
Drug can be used to elicit effects secondary to target interaction	Model PK-PD properties secondary to ADCC, CDC, or conjugation to drugs, toxins, or radionuclides
Dose-limiting toxicities are often not observed	Optimal biological dose determined by PK-PD is more often used for dose-selection than maximum tolerated dose Apply model-based approach for clinical dose selection
Drug can sometimes induce mechanism-related cytokine release Highly potent molecules with long half-lives can be generated	PK-PD modeling can be used to establish a MABEL starting dose for first-in-human studies where appropriate
Protein drugs can be immunogenic	Evaluate antidrug antibody (ADA) and titer as potential covariates in data analyses Consider exclusion of ADA-positive subjects from data analyses Incorporate PD endpoints in studies to evaluate neutralization of drug by ADA
Kinetics of drug and target are highly dependent on format of the bioanalytical method	Choose reagents appropriately Understand what the assay is measuring before conducting PK-PD modeling

Protein drugs, particularly monoclonal antibodies, can exhibit high specificity for the human target, which must be considered when conducting translational PK-PD modeling of animal data for human dose estimation. PK-PD modeling to predict human exposure-response relationships can be critical. Dose-limiting toxicities are frequently not observed, so the selection of an optimal biological dose level, rather than identification of a maximum tolerated dose (as traditionally determined for

small molecule cytotoxic drugs in oncology), might be necessary. Some proteins can exhibit safety risk factors, such as the potential for severe acute cytokine release, which could warrant a first-in-human starting dose determined by simulation of a minimum anticipated biologic effect level (MABEL). Protein drugs can be immunogenic in animals and humans, and the antidrug antibody responses can affect drug concentration and activity, which has to be considered while evaluating PK-PD relationships. Finally, the bioanalytical methods used to quantify protein drug levels and PD biomarkers can be highly dependent on the assay format; therefore, the PK-PD modeler must have a good understanding of the assay and what is being measured.

The protein drug targets are not only involved in the pharmacological or toxicological effects, but also can represent an important elimination pathway for the drug. The elimination of biologics is typically mediated by two major pathways: the nonspecific protein elimination pathway and the specific target-mediated pathway. At low dose levels, the target-mediated pathway may be predominant. At high dose levels, the target-mediated pathway is usually saturated and the nonspecific protein elimination pathway may predominate. A mechanism-based PK-PD model that includes target binding and turnover kinetics can accurately describe the PK profile for protein drugs that are subject to target-mediated disposition.

Throughout this chapter, the implications of these protein attributes on PK-PD modeling approaches are discussed: first, through a review of the essential PK-PD properties of proteins; and second, through examples of applied PK-PD modeling at different stages of drug discovery and development.

17.2 PK-PD Models of Protein Drugs

PK-PD models of protein drugs should incorporate the unique absorption, biodistribution, and clearance characteristics of the protein, and for the relationship of exposure to target modulation, downstream PD effects, and clinical endpoints. The pharmacokinetic profile can be profoundly affected by binding of the drug to the target, binding of the drug to specific binding proteins (nontarget), and target-mediated clearance. The PK profile can also be affected by the conditions and procedures of the bioanalytical method, and by whether the assay measures unbound drug, partially bound drug, or total drug levels. Because the PK can be influenced by target binding, not only can protein drugs elicit pharmacodynamic effects, the pharmacodynamic effects can also affect the pharmacokinetics; thus, the PK and PD properties of protein drugs often are intricately linked.

17.2.1 *Absorption and Bioavailability*

Most proteins must be administered parenterally, because nonparenteral bioavailability is usually poor because of mucosal barriers to absorption or because

of local degradation. Absolute bioavailability by intranasal dosing or inhalation is usually acceptable only for small peptides. For these reasons, subcutaneous (SC) administration is the most common extravascular route of protein administration.

Following SC administration, absorption can occur via the lymphatic system or blood capillaries. Lymphatic absorption has been associated with substantially slower absorption rates (as observed in systemic circulation sampling) compared to absorption via blood capillaries (Toon *et al.* 1996). A positive correlation between lymphatic absorption and molecular weight has been reported (Supersaxo *et al.* 1988, 1990). The cumulative recovery of human recombinant interferon alpha-2a (MW: 19 kDa) via the lymphatic system was 60%. The absolute bioavailability and absorption rate of protein drugs can also be influenced by dose and concentration differences, which can additionally complicate absorption models (Woo and Jusko 2007). Larger proteins, such as monoclonal antibodies, undergo predominantly lymphatic absorption. Absorption rate after SC dosing tends to decrease with increasing molecular weight; however, absolute bioavailability is variable between molecules and might be affected more by differences in susceptibility to local degradation than by differences in molecular weight. Monoclonal IgG antibodies have an absolute bioavailability of around 60–70% despite a very slow absorption rate, which has been attributed to protection (salvaging) of IgG from catabolism by the neonatal Fc receptor, FcRn (Wang *et al.* 2008).

The SC absorption kinetics via the vascular and lymphatic pathways can be modeled by two parallel, first-order absorption processes with different absorption rates. This method is applicable for protein drugs with very different absorption rates and absolute bioavailability. The vascular absorption is often modeled as a first-order absorption process. The lymphatic absorption can be modeled as first-order absorption with a lag time before absorption. The lag time can be modeled as an absolute delay (a discontinuous or change point model, in which the lag time for a subject is assumed to have zero variance) or a variable delay. The variable lag time is typically modeled by a series of transit compartments that precede the first-order absorption compartment; methods for implementation of the compartmental delay and the effect on the resolution or variance of the lag time have been described (Savic *et al.* 2007).

Modeling of the SC absorption of filgrastim (MW: 18.8 kDa) and the monoclonal antibody, CAT-354 (MW: 150 kDa) by a dual absorption model are illustrated in Fig. 17.1 (Wang *et al.* 2001; Oh *et al.* 2010). The models used for the absorption process for filgrastim and CAT-354 were the same, although the clearance models were different (nonlinear for filgrastim and linear for CAT-354). Although the T_{max} values were very different (approximately 5 h for filgrastim and 5 days for CAT-354), the dual absorption models provided good descriptions of the absorption kinetics. Consistent with observations that a higher molecular weight is associated with a greater fraction of dose absorbed through the lymphatic system, the fraction of dose absorbed through the delayed absorption route was 57–67% for filgrastim and 85% for CAT-354.

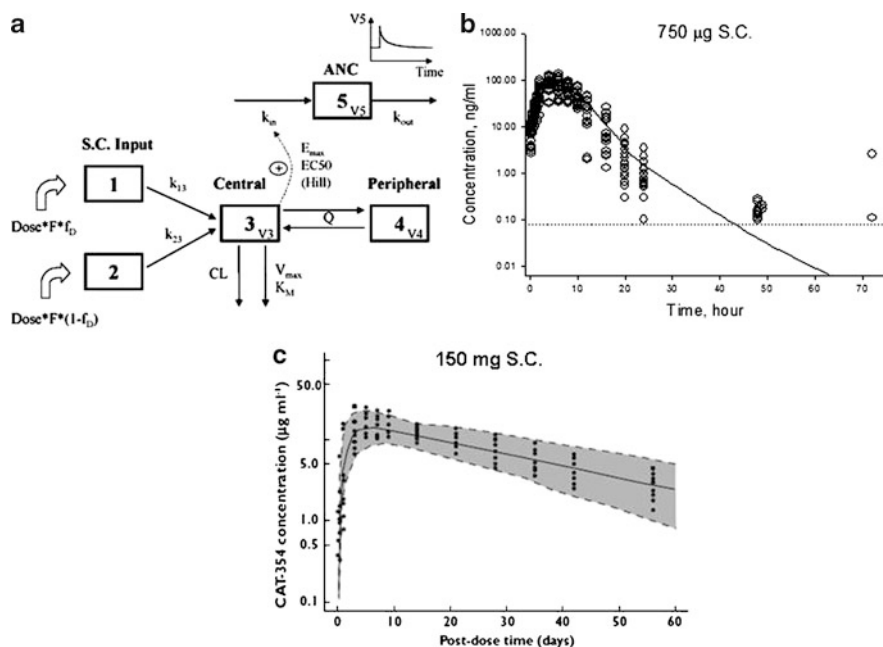


Fig. 17.1 Modeling the subcutaneous (SC) absorption kinetics of protein drugs: (a) A PK-PD model of filgrastim after SC dosing; filgrastim is absorbed from the SC site by two parallel pathways; (b) parallel absorption model in panel A fitted (*solid line*) to filgrastim PK data from healthy subjects after a single SC dose (Wang *et al.* 2001); (c) parallel absorption PK model for CAT-354 fitted to PK data from healthy subjects following a single SC dose (Oh *et al.* 2010)

17.2.2 Bimolecular Interaction of Drug with Target

The obligatory first step of the PK-PD relationship is interaction of drug with the target. For protein drugs, modeling of a bimolecular interaction can be essential to understanding the PK-PD relationship when binding reduces free concentrations of drug (increases apparent volume of distribution), contributes to total clearance of drug, or alters the kinetics and total concentrations of the target. As described later in this chapter, the bimolecular model can be a theoretical basis for establishing affinity, potency, and pharmacokinetic properties of an engineered protein drug prior to lead generation and optimization. The same model can be used and refined during drug development to model and characterize PK-PD relationships in animal models and humans.

A bimolecular interaction model of drug (C) with receptor (R) is shown in Fig. 17.2, and its implications for TMDD will be discussed further in Sect. 17.2.4. While this model structure can be applied to TMDD, we emphasize that Fig. 17.2 represents a general model of a bimolecular interaction that has several PK-PD applications for protein drugs:

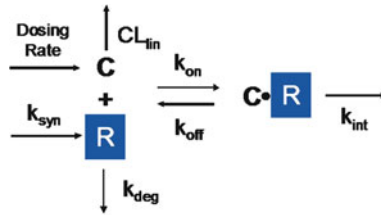


Fig. 17.2 Model of reversible drug (C) binding to a receptor (R), with subsequent endocytosis of the drug-receptor complex ($C\bullet R$). k_{syn} zero-order synthesis rate of receptor; k_{deg} first order degradation rate of receptor; k_{on} association rate constant; k_{off} dissociation rate constant; k_{int} internalization rate constant of drug-receptor complex

1. *Off-target protein binding:* Some protein drugs have specific binding proteins that can affect disposition and clearance.
2. *Enzyme kinetics:* The model structure is identical to the Michaelis–Menten model of enzyme kinetics; if the protein drug is an enzyme, *e.g.*, asparaginase, the model could be used to describe metabolism of the substrate.
3. *TMDD:* The model can describe pharmacokinetic effects of the target on the volume of distribution and clearance of the drug.
4. *Drug-mediated target disposition:* The model can describe changes in total target concentrations that occur when the clearance of the drug-target complex is different than for the free target; this effect is commonly observed with binding of drug to soluble targets. The model can also incorporate downstream changes in target concentration, *e.g.*, changes in number and phenotype of cell populations that express the target.
5. *Ligand displacement:* If the drug competes with binding of an endogenous ligand to the target, a competitive binding model can be developed to describe effects on ligand concentrations and kinetics.
6. *Pharmacodynamics:* The model can describe changes in free, total, or drug-target complex concentrations as PD models of target occupancy or suppression. With a transduction function related to target occupancy or suppression, the model can describe effects on downstream PD biomarkers or clinical endpoints.

17.2.3 Biodistribution

Protein drugs undergo limited distribution in body water. Most proteins initially distribute into a central volume of distribution equal to plasma volume (~40 mL/kg). Proteins do not cross cell membranes unless they are internalized by a receptor or undergo phagocytosis or pinocytosis. In most cases the internalization process will result in transport of the protein to the lysosomes where the protein will be catabolized. For these reasons, the steady-state volume of distribution (V_{ss}) is usually less than or equal to extracellular water (ECW~200 mL/kg).

For example, the steady-state volume of distribution of CAT-354 (MW: 150 kDa), an IgG4 monoclonal antibody to IL-13, is 64 mL/kg in healthy subjects. Smaller proteins can distribute more rapidly and extensively than larger proteins; however, the V_{ss} is usually less than ECW. Anakinra (MW: 17 kDa) has a reported V_{ss} of 10.1 L (~144 mL/kg for a 70 kg subject) (Gueorguieva *et al.* 2008). The low V_{ss} relative to ECW does not mean that the protein does not distribute throughout ECW; the low V_{ss} is caused by limited partitioning to some tissues. In particular, proteins have little permeability across tight junctions (*e.g.*, blood-brain barrier and placental barrier) unless they are transported. Partitioning of protein drugs to cerebrospinal fluid is approximately 0.2% relative to serum (Gueorguieva *et al.* 2008; Wang *et al.* 2008). Although the placental barrier is relatively impermeable to many proteins, IgG antibodies are efficiently transported across the placenta when the neonatal Fc receptor (FcRn) is expressed during the second and third trimester of pregnancy (Pentsuk and van der Laan 2009).

Binding of the protein drug to specific binding proteins and soluble receptors can affect the biodistribution of the drug. If the PK assay measures unbound drug, then the apparent volume of distribution could exceed ECW if the unbound fraction is small. In such cases, modeling of the bimolecular interaction with specific binding proteins can provide insight into the biodistribution and disposition of the drug. Insulin-like growth factor 1 (IGF-1, MW 7.6 kDa) is an endogenous growth factor that is highly protein bound by specific binding proteins. Figure 17.3 shows modeling of free IGF-1 (measured by radioimmunoassay) and bound IGF-1 (calculated from total IGF-1 measured by radioimmunoassay after acid/ethanol extraction) using a bimolecular interaction model of IGF-1 with circulating IGF binding proteins, with incorporation of linear and receptor-mediated (Michalis–Menten) elimination following administration of IGF-1 to healthy volunteers (Mizuno *et al.* 2001). Applying the protein-binding model with one-compartment distribution for the free and bound IGF-1, the volume of distribution was 168 mL/kg for free IGF-1 and 54.8 mL/kg for bound IGF-1. The lower volume for the bound form

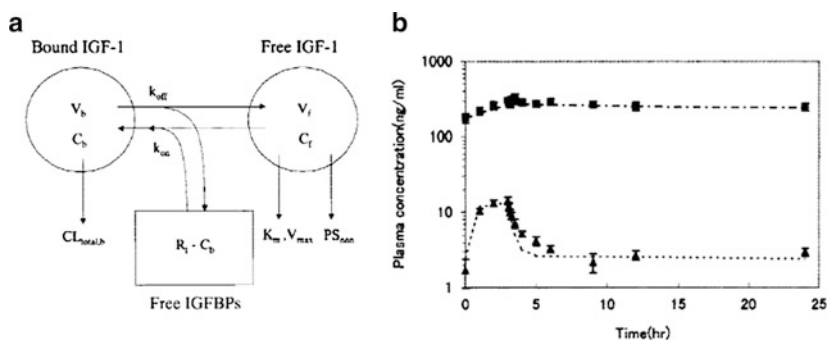


Fig. 17.3 (a) Bimolecular model describing the PK of IGF-1 in healthy subjects, with reversible binding to IGF binding proteins (IGFBP) in plasma; (b) fitting of model (*dashed lines*) to free IGF-1 (*triangles*) and IGFBP-bound IGF-1 (*squares*) plasma levels following an IV infusion of IGF-1 (Mizuno *et al.* 2001)

was attributed to the higher molecular weight of the IGF-1 and binding protein complexes (~50–150 kDa), which restrict biodistribution.

Physiologically based pharmacokinetic (PBPK, see Chap. 22) models can be used to model the time-course of drug in tissues. PBPK models for monoclonal antibodies in mice have described disposition into various healthy tissues and tumor (Ferl *et al.* 2005; Davda *et al.* 2007; Garg and Balthasar 2007; Urva *et al.* 2010). The PBPK models can provide useful information on the partitioning and kinetics of distribution into tissue; however, such models are experimentally challenging and time-consuming to establish (Poulin and Theil 2000, 2002). A focused analysis of biodistribution into a particular tissue of interest can be a more practical approach to PBPK modeling. For example, a relatively simple and practical model for the distribution of anakinra into the CSF of patients following subarachnoid hemorrhage has been described (Gueorguieva 2008). Biodistribution of proteins into tumors has been a controversial area of research. Modeling of distribution into tumor nodules supported the idea that a binding site barrier might restrict drug penetration into the tumor (Weinstein and van Osdol 1992). A single-dose study of the penetration of monoclonal antibody scFv fragments in a mouse xenograft model suggests that a higher affinity of the antibody to the target might limit distribution into the tumor, consistent with the binding site barrier hypothesis (Adams *et al.* 2001). Recent modeling of equilibrium distribution kinetics suggests that higher affinity antibodies are more effective at target binding in tumors and that the major barriers to antibody penetration are slow diffusion and convective flow, interstitial pressure, and high target expression and internalization rate that create a local sink and limit antibody penetration (Ackerman *et al.* 2008).

17.2.4 Clearance

Protein drugs can be cleared by multiple, parallel elimination pathways. The elimination pathways include renal clearance, elimination by the reticuloendothelial system (RES), target-mediated endocytosis, and nonspecific proteolysis and degradation. Formation of protein complexes, such as drug and soluble target complexes or antidrug antibody complexes, can also contribute to elimination of the drug presumably through more efficient clearance by the RES. Catabolism by extracellular proteases can contribute, in some cases, to elimination of the molecule.

Renal clearance is an important elimination pathway for proteins that are small enough to undergo glomerular filtration. The ability of the protein to be filtered depends on physical factors such as molecular weight, structure, charge, and water of hydration that contribute to the overall hydrodynamic radius of the molecule. Proteins greater than 70 kDa are not filtered. Generally some impediments to renal filtration exist for molecules larger than approximately 7 kDa (Lote 2000).

Clearance by the RES contributes to the elimination of all protein drugs; however, the importance of this elimination pathway depends on the relative magnitude of the other clearance processes. RES clearance mechanisms include phagocytosis by

macrophages and Kupffer cells and also fluid phase pinocytosis by endothelial cells. RES clearance, which is usually represented by the residual clearance of the protein when no renal or target-mediated clearance occurs, appears to be a relatively slow process associated with elimination half-lives of hours to weeks depending on whether the protein is salvaged from catabolism by FcRn. When IgG antibodies or Fc fusion proteins undergo pinocytosis or phagocytosis by cells expressing FcRn, the acidic pH (~6) of the early endosome allows binding of the Fc domain to FcRn (Roopenian and Akilesh 2007). The protein is then recycled to the cell surface and released in the extracellular, pH 7.4 environment, which salvages the molecule from lysosomal catabolism. Salvaging by FcRn is responsible for the 3 week elimination half-life of wild-type, human IgG antibodies in humans. Mutation of the FcRn binding domain that increase affinity of IgG antibodies to FcRn at pH 6, but not pH 7.4, have led to the successful engineering of antibodies with lower clearance and longer elimination half-lives than wild-type IgG, which could permit more convenient dosing regimens for some antibodies and Fc fusion proteins (Dall'Acqua *et al.* 2002).

Clearance of protein drugs by their target can cause dose-dependent and time-dependent pharmacokinetics. The PK profile, in some cases, can be dramatically affected by the PD response, or by disease states and comedications (*e.g.*, cytotoxic chemotherapy) that alter expression of the target or the number of cells that express the target. Because of the potential complexity of PK-PD models that describe TMDD, the approaches to modeling TMDD are reviewed in detail in Sect. 17.2.4.1.

Modeling of protein drug pharmacokinetics allows a quantitative evaluation of various parallel elimination pathways and implications for human dosing. In Fig. 17.4, the contribution of different clearance pathways to the elimination of filgrastim and pegfilgrastim (filgrastim conjugated to polyethylene glycol) was assessed by modeling the PK in rats receiving a bilateral nephrectomy compared to sham operated controls (Yang *et al.* 2004). Filgrastim and pegfilgrastim were dosed at 5 and 100 $\mu\text{g}/\text{kg}$. The contribution of renal clearance was evaluated by simultaneously modeling the PK collected from the nephrectomized rats and the sham controls. In Fig. 17.4b, the contribution of renal clearance to filgrastim (MW: 18.8 kDa) elimination when receptor-mediated elimination is saturated by the high dose of filgrastim is clearly observed by the lower AUC in sham controls relative to nephrectomized rats. In Fig. 17.4d, the higher hydrodynamic size of pegfilgrastim (MW: 38.8 kDa) prevented renal clearance, as indicated by the overlapping PK curves for the nephrectomized rats and sham controls following the high dose. Modeling of the data indicated that in absence of receptor-mediated clearance (as would occur in patients with chemotherapy-induced neutropenia), renal clearance accounts for over 75% of filgrastim clearance.

Filgrastim, which is used to treat chemotherapy-induced neutropenia, must be dosed subcutaneously daily to maintain effective concentrations because of high renal clearance; by contrast, pegfilgrastim can be dosed once per cycle of chemotherapy as a single SC injection. This is an example of rational engineering of a protein drug: prospective, preclinical modeling and simulation predicted that pegfilgrastim levels, following a single dose, would be sustained during neutropenia and

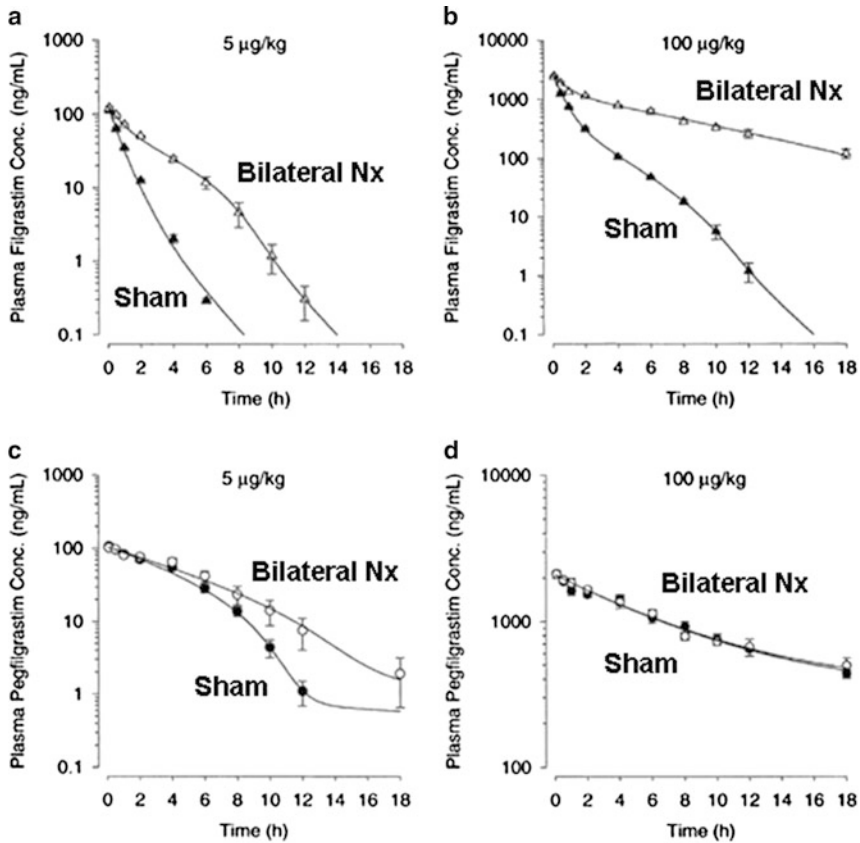


Fig. 17.4 Modeling multiple clearance pathways (renal, reticuloendothelial, and receptor-mediated) of protein drugs. Observed (*symbols*) and modeled (*solid line*) drug concentration-time profiles after intravenous administration of filgrastim or pegfilgrastim in sham-operated (*closed symbols*) and bilateral nephrectomized (*open symbols*) rats following single doses of (a) 5 $\mu\text{g}/\text{kg}$ filgrastim, (b) 100 $\mu\text{g}/\text{kg}$ filgrastim, (c) 5 $\mu\text{g}/\text{kg}$ pegfilgrastim, or (d) 100 $\mu\text{g}/\text{kg}$ pegfilgrastim (Yang *et al.* 2004)

would wash out rapidly after neutrophil recovery (Galluppi *et al.* 2001). The PK-PD properties of pegfilgrastim that were predicted by modeling and simulation were confirmed in a well-designed phase 1 study by a head-to-head comparison of filgrastim and pegfilgrastim in cancer patients before and after chemotherapy (Johnston *et al.* 2000).

17.2.4.1 Target-Mediated Drug Disposition

The importance of TMDD for describing the PK-PD of many protein drugs has led to a number of publications in recent years about the appropriate ways to model TMDD.

Table 17.2 Pharmacokinetic models of target-mediated drug clearance

Clearance model	Simplifications	Target-mediated clearance	References
Target-mediated drug disposition	None	$k_{on}, k_{off}, k_{int}, k_{deg}, R_{tot}(0)$	Mager and Jusko (2001)
Quasi-steady-state approximation	$k_{on} * C * R - (k_{off} + k_{int}) * RC = 0$	$K_{ss},^a k_{int}, k_{deg}, R_{tot}(0)$	Gibiansky <i>et al.</i> (2008)
Rapid-binding approximation	$k_{int} \ll k_{off}$ $k_{on} * C * R - k_{off} * RC = 0$	$K_D,^b k_{int}, k_{deg}, R_{tot}(0)$	Mager (2005) and Marathe <i>et al.</i> (2009)
Michaelis–Menten approximation	$C_{free} \sim C_{total}^c$ $k_{on} * C * R - (k_{off} + k_{int}) * RC = 0$	V_{max}, k_M^d	Segel (1993), Gibiansky (2008), and Yan <i>et al.</i> (2010)

$$^a K_{ss} = (k_{off} + k_{int})/k_{on}$$

$$^b K_D = k_{off}/k_{on}$$

$$^c R_{tot} K_D / (K_D + C)^2 \ll 1$$

$$^d V_{max} = k_{int} * R_{tot}, k_M = (k_{off} + k_{int})/k_{on}$$

Several different methods have been proposed and used to model the TMDD of protein drugs. Although the theoretical papers that support these models are rigorous and insightful, the topic can be confusing to those who are new to PK-PD modeling of protein drugs and are not familiar with the various models and terminology. In this section we attempt to provide some clarification of the various TMDD models and their differences and applications.

The four major TMDD models are summarized in Table 17.2. In order from the most complicated to the most simplified, the models are:

1. TMDD model (full model)
2. Quasi-steady-state approximation
3. Rapid-binding or quasi-equilibrium approximation
4. Michaelis–Menten approximation

Models 1–3 can accommodate the condition in which binding of drug to the target, per se (prior to clearance), can affect the PK time-course of unbound drug. In other words, binding to the target can affect the apparent volume of distribution of the drug. Model 4, the Michaelis–Menten approximation, assumes that the effect of target on the PK is due only to clearance. In this case, the unbound concentration of drug after target binding is still approximately equal to the total (unbound plus target-bound) concentration. As shown in Table 17.2, the more complex models have a larger number of parameters that must be supported by data.

Target-Mediated Drug Disposition Model

The full TMDD model for interaction of drug concentration (C) with a targeted receptor (R) is illustrated in Fig. 17.2. Although the publications on TMDD

modeling have been presented using a two-compartment distribution model for drug, for simplicity the model is presented in this chapter as a one-compartment PK-model. The system of equations describing this interaction, for an IV bolus of drug, is as follows:

$$\frac{dC}{dt} = k_{\text{off}}RC - k_{\text{on}}C * R - \text{CL}_{\text{lin}}C \quad (17.1)$$

$$\frac{dRC}{dt} = k_{\text{on}}C * R - (k_{\text{off}} + k_{\text{int}})RC \quad (17.2)$$

$$\frac{dR}{dt} = k_{\text{syn}} - k_{\text{deg}}R - k_{\text{on}}C * R + k_{\text{off}}RC \quad (17.3)$$

The benefits of the full TMDD model are that it allows for: (1) changes in drug concentration related to rapid or slow binding to target, (2) clearance by the target, and (3) time-dependent PK related to up-regulation or down-regulation of the target when the rate constant for internalization of the drug-receptor complex (k_{int}) is different from the baseline turnover rate constant of the receptor (k_{deg}). The limitations are that the five TMDD parameters in the model might not be identifiable by the PK time-course alone. For example, the rates of drug association and dissociation from the receptor can be much faster than other processes of drug disposition *in vivo*. Also, a time-dependent change in receptor expression related to drug binding might occur in a rapid time frame relative to the drug half-life; therefore, k_{deg} and k_{int} might not be identifiable by PK modeling unless direct measurements of total receptor concentration or drug-receptor complex are possible. Dramatic changes in receptor expression can also occur on a much longer time-scale because of downstream effects of target modulation, *e.g.*, by increasing or decreasing the number of receptor-bearing cells; such a change is not accounted for by the TMDD model alone.

Experimental values for some parameters can be determined *in vitro* and fixed in the model; however, such an approach should be done cautiously. The value of k_{on} and k_{off} can be determined *in vitro*, in many cases by surface plasmon resonance; but for some membrane targets a soluble form is not available and on-cell affinity must be determined, which yields an equilibrium binding constant (rather than association and dissociation rate constants) that can be affected by receptor density and avidity (Roskos *et al.* 2007). Also other system processes, such as distribution of drug to the receptor, can be rate limiting, and fixing association or dissociation constants might not be appropriate. An estimate of k_{int} can be determined by confocal imaging of the internalization kinetics of the drug-receptor complex, which can be used to stabilize the model or provide a practical check for the parameter value determined by model fitting. Also, if receptor or drug-receptor complex concentrations are not directly measurable, then a

simplification can be made to make k_{deg} equal to k_{int} if supported experimentally or by the PK profile.

Quasi-Steady-State (QSS) and Rapid Binding (RB) Approximations

The QSS and rapid binding (RB) approximations make a simplification that allows the number of parameters in the full TMDD model to be reduced by one: the free receptor, free drug levels, and drug-receptor complex are assumed to be in rapid equilibrium. In this case, the simplified TMDD model can be expressed in terms of an apparent equilibrium constant (K_{ss} or K_{D}) rather than using the rate constants k_{on} and k_{off} . Otherwise, the advantages and limitations of the QSS and RB models are the same as described for the full TMDD model. The primary difference between the QSS and RB models is that the RB model assumes that the k_{int} is smaller than the k_{off} ; thus, the equilibrium constant in the RB model is described by the ratio of k_{off} to k_{on} . The QSS model acknowledges that the k_{int} can be greater than or equal to the k_{off} . From a standpoint of data fitting, the models are identical as the QSS and RB are both parameterized using an apparent equilibrium binding constant.

For both models, the effect of target binding on unbound drug concentration is assumed to be instantaneous. This assumption would be manifested as a dose-dependent central volume of distribution, in which the V_c decreases with increasing dose. Such an observation could justify use of the QSS or RB models; however, other factors that could influence V_c should be ruled out. For example, soluble receptor, a specific binding protein, or a pre-existing antidrug antibody could cause this same effect. In such a case, the structural PK model would be different than described by the QSS, RB, or full TMDD model. Target binding and associated volume of distribution changes can also be manifested in the shape of the terminal phase, as drug concentrations drop to levels that are influenced by target binding; however, the terminal phase can also be influenced by other factors, including soluble binding proteins and even matrix interference as the levels approach the limit of quantitation of the PK assay. Discrimination and selection among QSS, RB, and full TMDD models, therefore, should usually not be based on goodness of fit criteria alone.

Michaelis–Menten Approximation

The Michaelis–Menten approach is the most commonly used modeling method to describe TMDD effects on protein drug clearance, and has been used successfully for many different drugs (Bauer *et al.* 1994, 1999; Kuwabara *et al.* 1996; Wang *et al.* 2001; Roskos *et al.* 2006). Unfortunately, a perception seems to exist that the Michaelis–Menten model is empirical and not mechanistic like the more highly parameterized TMDD models. As pointed out by Gibiansky *et al.*, the Michaelis–Menten model is mechanistic; but as with all models, the assumptions of the model must be valid (Gibiansky *et al.* 2008). As mentioned above, the major assumption is that target binding, per se, has a negligible effect on unbound drug concentration

and volume of distribution, but primarily affects drug clearance. If this assumption is met, the target-mediated clearance can be expressed as:

$$CL_{\text{target}} = \frac{k_{\text{int}}R_{\text{total}}}{\frac{k_{\text{off}} + k_{\text{im}}}{k_{\text{on}}} + C} \quad (17.4)$$

This equation can be further simplified to:

$$CL_{\text{target}} = \frac{V_{\text{max}}}{k_{\text{M}} + C} \quad (17.5)$$

where k_{M} is the Michaelis constant, which is equivalent to K_{ss} in the QSS model. Importantly, this model reduces to two parameters, as opposed to four parameters in the QSS and RB models and five parameters in the full TMDD model. As described by Yan *et al.*, the RB model reduces to the Michaelis–Menten approximation when:

$$R_{\text{total}} \left(\frac{k_{\text{off}}}{k_{\text{on}}} \right) / \left(\frac{k_{\text{off}}}{k_{\text{on}}} + C \right)^2 \ll 1 \quad (17.6)$$

This describes the situation in which drug is either partially saturating the target or the ratio of total receptor concentration to the equilibrium affinity constant is low, *i.e.*, conditions in which target binding is not influencing free drug concentration. We note also that because the V_{max} term is proportional to the total receptor concentration, time-dependent nonlinearity can be modeled by this equation when changes in receptor expression or the number of cells expressing the target can be measured. This approach has been successfully applied to the PK-PD relationship for pegfilgrastim (Roskos *et al.* 2006) as described below in the section on cytokinetics, and for PK-PD relationships for MEDI-551 after B-cell depletion and reconstitution following recruitment of antibody dependent cellular cytotoxicity (Lau *et al.* 2010).

The success of the Michaelis–Menten approximation for most cases of TMDD has probably been caused by limitations of bioanalytical method sensitivity that might be inadequate to characterize PK at very low concentrations of drug that can be influenced by target binding, and that during drug development, usually relatively little data are collected at drug concentrations producing minimal target engagement (yielding conditions described by equation 17.6). However, the development of more sensitive bioanalytical methods, highly potent drugs effective at low levels of receptor occupancy, and application of MABEL starting doses (see Sect. 17.3.2) for some drugs, might create more cases in which the more highly parameterized TMDD models have a distinct advantage over the Michaelis–Menten approximation.

In summary, the simplest TMDD model should be used that is supported by the data and meets the purpose of the modeling or simulation exercise. As in all models, there is elegance in simplicity, and the law of parsimony also applies to TMDD models.

17.2.5 Interactions of Drug and Soluble Target

The bimolecular interaction of a drug with a soluble target can be described using the same equations used for the full TMDD, QSS, or RB models. However, there are some notable differences from membrane target interactions that should be considered. Protein drugs that interact with soluble targets present in low concentrations generally exhibit linear pharmacokinetics when the total drug concentrations are measured. However, because the soluble target can bind drug in serum and accumulate after dosing, it is essential to know if the PK assay measures unbound or total drug levels. If the assay measures free drug levels, then the PK profile can mimic a TMDD clearance process, even when binding of the drug to the soluble target does not affect clearance. Depending on the assay format, the drug levels can be modeled either as the free levels, or the sum of the free and bound drug concentrations. Also, binding of drug to the soluble target can have a dramatic effect on the total target concentrations, especially when administering monoclonal antibodies. Because of the very low clearance of the antibody drug relative to the clearance of the soluble target, the binding of the antibody to the target can greatly decrease target clearance, resulting in an increase in total target levels that can be several logs greater than baseline levels.

Often, assays can be established to measure free drug, free target, total drug, total target, or drug-target complexes. The significance is that the parameters for the full TMDD, RB, and QSS models can be more readily estimated. In particular, the parameters for k_{deg} of the soluble target at baseline and the k_{int} (usually called k_{complex} in a soluble target model) can be estimated. Sometimes characterization of the kinetics of the target can be precisely estimated if the target can be administered in relevant animal models, or if target PK data are available from the literature. The PK-PD of omalizumab (Hayashi *et al.* 2007) and an antibody to Dkk-1 (Betts *et al.* 2010) are excellent examples of modeling antibody and soluble target interactions. In both cases, the antibody-target complex was cleared faster than the unbound antibody. These models successfully described effects of drug on free and total target levels, in addition to nonlinear PK related to clearance of the complex. Mechanisms of enhanced clearance of an antibody to a soluble target could include crosslinking of multimeric targets with enhanced elimination by the RES or impaired binding of target-bound antibody to FcRn.

17.2.6 Cytokinetics

Many protein drugs can affect cell populations by altering the proliferation rate or lifespan of the population. Hematopoietic growth factors are good examples of drugs that increase proliferation of blood cell lineages. Monoclonal antibodies that deplete target cells through antibody dependent cellular cytotoxicity and complement dependent cytotoxicity are good examples of drugs that decrease the

survival of targeted cell populations. PD models that describe these effects should incorporate appropriate mathematical representations of cell proliferation and survival. If the cell population expresses the drug target and the drug is subject to TMDD, alteration in cell numbers can produce a profound, time-dependent effect of the PK of the drug. In this case, the model must incorporate feedback regulation of PK by the PD response. Examples of models for cell lifespan, proliferation, maturation, and feedback regulation of PK are described in the subsequent sections.

17.2.6.1 Cell Lifespan

Unlike drug molecules, most cells are not eliminated randomly. The cells persist until they die from senescence or apoptosis, or die prematurely from a random or drug induced event. The lifespan in absence of random destruction is the intrinsic longevity of the cell. Some cell types, *e.g.*, neutrophils, are eliminated randomly from circulation and the loss of the cells can be described by a first-order elimination rate constant and half-life. Cytokinetic models should incorporate the concepts of intrinsic longevity and random destruction to model the overall lifespan of the cell. Modeling of cell lifespan is not new: models of cell lifespan were developed over 50 years ago to describe radioisotopic tracer studies and blood cell transfusions (Dornhorst 1951; Eadie and Brown 1953). More recently, these same concepts have been applied to the PD effects of protein drugs on cell populations. Recent manuscripts have described various approaches to PK-PD modeling of cell lifespan (Krzyzanski *et al.* 1999, 2005).

The first example of modeling the exposure-response relationship for a hematopoietic growth factor was conducted for hemodialysis patients receiving erythropoietin, and was conducted as a population dose-response analysis (Uehlinger *et al.* 1992). The modeling included parameterization of the lifespan of the erythrocyte. Although the model assumed zero variance for intrasubject erythrocyte lifespan (all erythrocytes entering the circulation at the same time die at the same time), this simplification is usually valid for the modeling of erythrocyte kinetics. The authors noted that the time to reach a new steady-state hematocrit after initiation of therapy was equal to the erythrocyte lifespan. The reason is that when erythrocyte production rate steps to a higher value, the erythrocytes continue to accumulate until the first erythrocytes that entered circulation after start of therapy reach the end of their lifespan; at that time the death rate of erythrocytes becomes equal to the new production rate and steady-state is attained.

A generalized model of cell lifespan should incorporate cell longevity, the variance of longevity, and random destruction. The first application of a generalized cell lifespan model to the PK-PD of a hematopoietic growth factor described the effects of PEG-rhuMGDF on platelet kinetics (Roskos *et al.* 1997; Harker *et al.* 2000). This model (Fig. 17.5), which was applied to peripheral platelet counts and the kinetics of autologous platelet tracers following administration of the thrombopoietin analog to healthy volunteers, accounted for the concentration-response relationship for stimulation of precursor cells, delays in the emergence of new

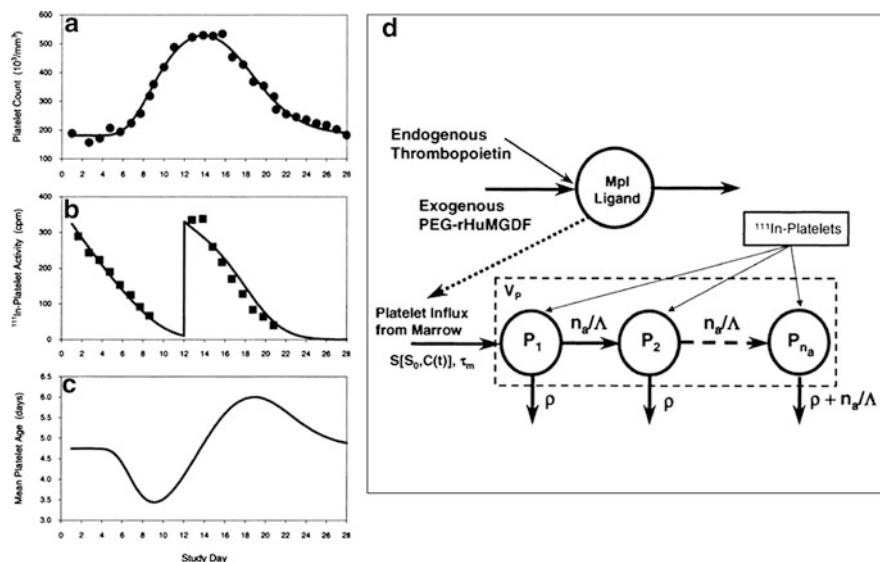


Fig. 17.5 Pharmacokinetic-pharmacodynamic modeling of the thrombopoietic effects of a thrombopoietin analog (PEG-rHuMGDF) in healthy volunteers following a single SC dose. (a) Modeled PD effects on platelet counts in blood; (b) simultaneous modeling of the kinetics of an autologous radiolabeled platelet tracer in blood; and (c) theoretical changes in mean platelet age in blood calculated by the PK-PD model. (d) The PK-PD model describes the intrinsic longevity of platelets (Λ), nonlinear random destruction of platelets (ρ), and the intra-subject variability of intrinsic platelet longevity (controlled by n , the number of catenary-linked transit compartments) are represented by the model. Simultaneous modeling of autologous radiolabeled platelet tracers allowed analysis of effects of drug on platelet survival (Harker *et al.* 2000)

platelets from marrow, random destruction of platelets (because of endothelial use), and the intrasubject variability of platelet lifespan (Harker *et al.* 2000). The design of this clinical pharmacology study was rigorous, as autologous platelet tracer kinetics were evaluated at four different time points, because the authors recognized prospectively that the single dose of the protein would produce a time-dependent change in the mean age of platelets in circulation, which would alter the cell lifespan estimate derived from the platelet tracer; simultaneous PK-PD modeling of endogenous platelets and autologous tracer was used to account for this kinetic complexity. The modeling accurately predicted an approximately 2-day difference in the mean lifespan of the platelets when the average age of the cells in circulation was the youngest (between baseline and the peak in platelet counts, in which the proportion of new platelets in circulation was the highest) compared to when the mean age was the oldest (between the peak and the return of platelet counts to baseline, in which the proportion of senescent platelets in circulation was the highest). Additionally, parameters for platelet intrinsic longevity and random destruction rate derived from modeling the nonstationary system were consistent with literature values.

Modeling the cell count as the sum of a series of transit compartments, in which the cell lifespan is represented by the mean transit time through the compartments, imparts a gamma distribution to variance of the intrasubject cell lifespan; the variance can be decreased by increasing the number of transit compartments. The same model architecture can be applied readily to other cytokinetic models. The random destruction element is important; as mentioned earlier, a decreased cell lifespan related to the cytotoxic effects of a drug can readily be incorporated (Lau *et al.* 2010).

17.2.6.2 Cell Proliferation, Maturation, and Feedback Regulation of PK

Protein drugs that affect cell populations can affect proliferation rates and maturation of progenitor cells, in addition to effects on mature cells. A change in the total number of cells expressing the drug target, in turn, can affect the PK of the drug. PK-PD modeling of the granulopoietic effects of pegfilgrastim demonstrates how a PK-PD model can account for pluripotent effects of a protein drug on a cell lineage, and how time-dependent changes in PK can be accommodated by the model (Roskos *et al.* 2006). In Fig. 17.6, modeling is illustrated of the dose- and time-dependent PK of pegfilgrastim and the time-course of effects on blood band cells and mature neutrophils. The model incorporated effects on progenitor cell production rate, maturation times of precursor cells in marrow, early release of band cells and neutrophils from marrow, and margination of blood neutrophils. The TMDD of pegfilgrastim was modulated by changes in precursor cell and neutrophil mass in blood and marrow. A modified Michaelis–Menten model was used to describe the TMDD. Because the V_{\max} of the Michaelis–Menten model is proportional to total receptor number, the V_{\max} was assumed to be proportional to the precursor cell and neutrophil cell mass. This simplified TMDD approach, linked to a mechanistic PD model, provided a good description of the complex exposure-response relationship.

17.3 Applied Modeling and Simulation from Discovery Through Clinical Development

Model-based drug discovery and development have important applications from the earliest stages of drug discovery through clinical development of the drug. Figure 17.7 highlights the major PK-PD activities that are conducted at various stages of discovery and development. In this section, the application of modeling and simulation to the discovery, preclinical development, and clinical development of protein drugs are described by example.

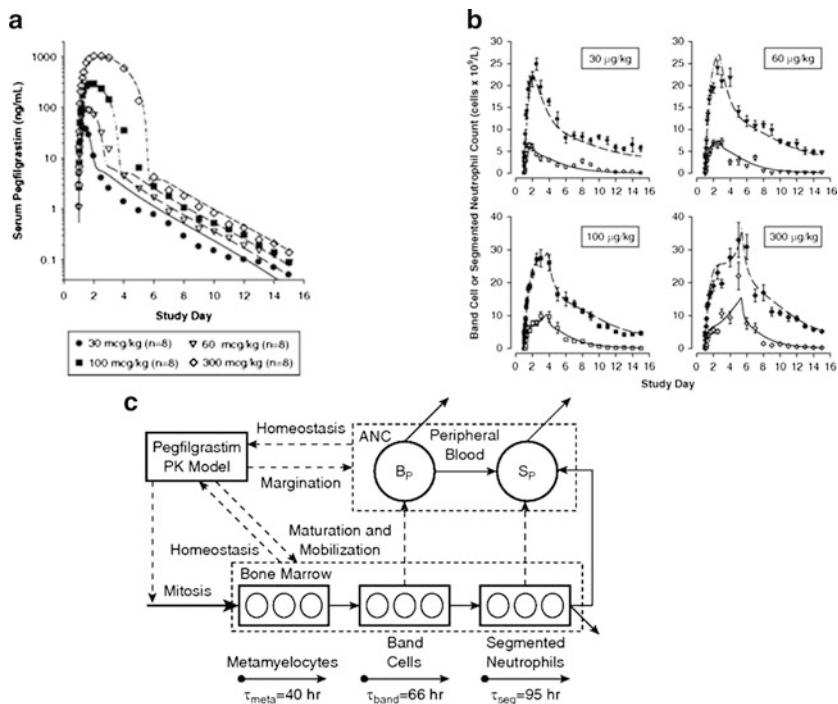


Fig. 17.6 PK-PD modeling of the effects of pegfilgrastim on neutrophil counts in the blood of healthy subjects, with homeostatic regulation of pegfilgrastim clearance by changing neutrophil and precursor cell mass in blood and marrow. **(a)** Modeled (*lines*) and observed (*symbols*) pegfilgrastim serum concentrations after single SC doses; **(b)** modeled (*lines*) and observed mean band cell (*open symbols*) and segmented neutrophil (*closed symbols*) counts in peripheral blood; **(c)** pharmacodynamic model describing the granulopoietic effects of pegfilgrastim. Serum concentrations of pegfilgrastim stimulate mitosis and mobilization of band cells and segmented neutrophils in bone marrow, decrease maturation times for postmitotic cells in marrow, and affect margination of the peripheral blood band cell (B_p) and segmented neutrophil (S_p) populations, the sum of which is the total absolute neutrophil count (ANC). Changes in neutrophil counts in peripheral blood provide feedback regulation of pegfilgrastim clearance (Roskos *et al.* 2006)

17.3.1 Drug Discovery: Target Evaluation and Lead Drug Optimization and Selection

During drug discovery, a major difference between small molecules and protein drugs is that for small molecules, many rounds of lead drug optimization can be conducted quickly and inexpensively. Thus, it is relatively easy to compare pharmacological, safety, metabolism, and PK properties of small molecule drug candidates. Proteins are more time consuming and expensive to produce. Also, because of the costs and difficulties of GMP manufacturing, carrying more than one potential lead drug into GLP safety studies and phase 1 is usually not feasible. Therefore, the design and selection of the best lead protein drug must be conducted during early discovery;

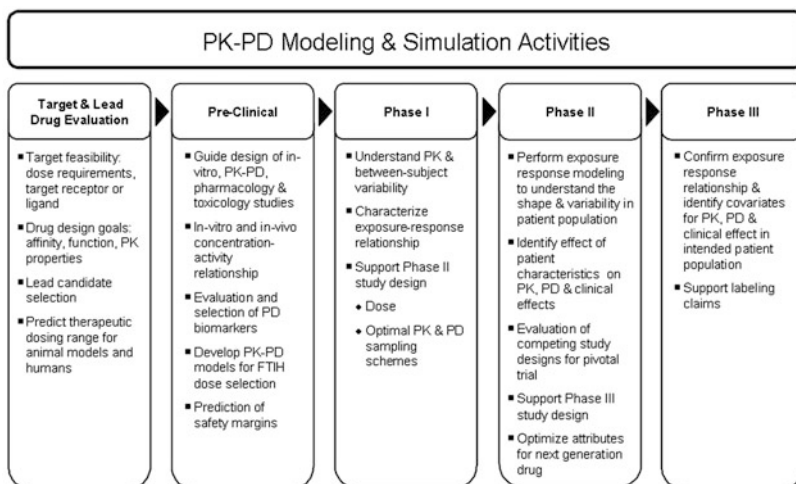


Fig. 17.7 Application of PK-PD modeling and simulation at various stages of drug discovery and development

incorrect selection of a lead protein, even if corrected during late discovery or preclinical development, can set back a project by many years. Therefore, PK-PD modeling and simulation is often “front-loaded” to help ensure that the best protein drug candidate is engineered and selected early in the discovery process.

Theoretical PK-PD simulations can be conducted to evaluate the feasibility of modulating a specific target. For example, simulations can help address whether targeting a ligand or the receptor could be advantageous, depending on the levels of ligand and receptor and the theoretical potential for TMDD. If significant concerns exist regarding the ability to modulate the target, an early PK-PD study might be conducted in relevant animal models, using a commercially available surrogate molecule or a potential lead drug. An excellent example of a discovery PK-PD evaluation was described for an antibody to Dkk-1 (Betts *et al.* 2010). In this early evaluation, the authors characterized the PK-PD of the antibody in two species and the PK of the target (to provide more robust characterization of the antibody-target interaction). They conducted allometric scaling of antibody and target PK for human dose estimation. When major concerns about the target do not exist, this type of rigorous evaluation is generally reserved until after lead selection and before GLP safety studies. Usually only theoretical evaluations are conducted before lead optimization.

Modeling and simulation are important when establishing protein engineering objectives for potency and PK properties. For example, simulations can be conducted to predict the optimum affinity of a protein for the target (Roskos *et al.* 2007). Examples of these simulations are shown in Fig. 17.8 for an antibody to a soluble target (Fig. 17.8a) and a cell-membrane target (Fig. 17.8b, c). As illustrated by the simulations, improvements in affinity of an antibody to a soluble target are

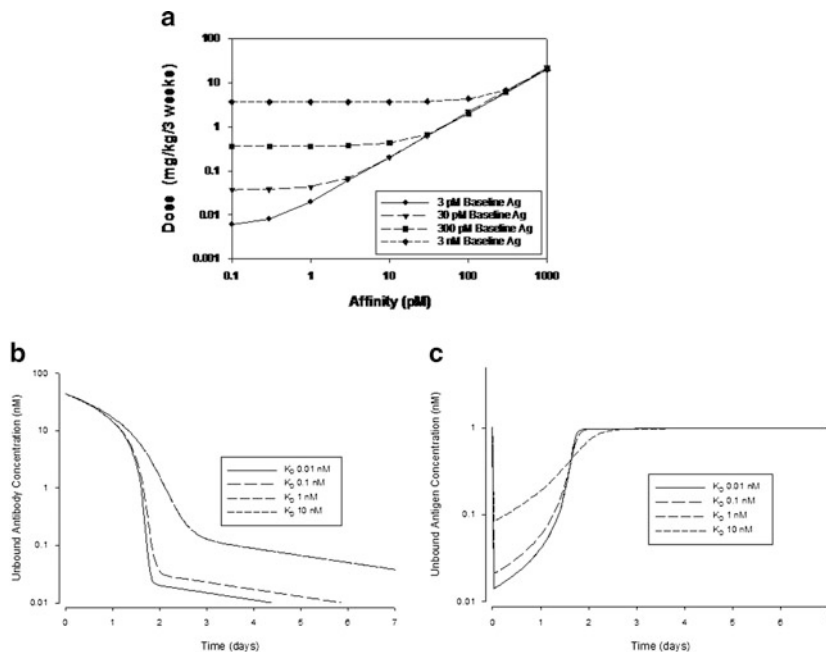


Fig. 17.8 Theoretical effect of antibody affinity to target (equilibrium dissociation constant, K_D) on potency for soluble and cell membrane targets. (a) Simulation of the maintenance dose of antibody required to suppress unbound concentrations of a soluble antigen in serum *in vivo* by 90% at steady-state prior to the next maintenance dose as a function of antibody affinity and baseline antigen (Ag) concentration. Simulated effect of antibody affinity on (b) antibody pharmacokinetics and (c) unbound antigen levels for an antibody targeting an internalizing, cell membrane receptor (Roskos *et al.* 2007)

expected to improve potency, but with decreasing returns as affinity is increased further; also level and turnover of the target are important considerations. For a membrane target, the optimum affinity can be a more complex problem when TMDD is predicted. Higher affinity can result in more rapid elimination of drug at subsaturating concentrations; if the effective concentrations are achieved at low levels of receptor occupancy, then the potential advantage of higher affinity could be offset by more rapid clearance of the drug. Also, simulations can help determine if the PK properties should be optimized: for example, by mutation of the Fc domain of an antibody to decrease clearance and extend half-life.

17.3.2 Preclinical Development

PK-PD modeling and simulation have many applications during preclinical development. Modeling and simulation can help design *in vitro*, PK-PD, pharmacology, and toxicology studies. Modeling provides important characterization of *in vitro* and

in vivo concentration-activity relationships. Because of the high specificity of many protein drugs for the human target, sometimes surrogate molecules (homologous proteins) or transgenic animals must be used to characterize the biology of the target and the pharmacology of the drug; PK-PD modeling can help account for differences in potency, PK, and target expression to allow simulation of the expected effects of the lead drug in humans. Pharmacodynamic biomarkers, which can provide valuable information during the early development of many drugs, are usually not well-characterized at the preclinical stage. Preclinical PK-PD modeling can help characterize and select biomarkers for potential application in clinical studies.

One of the most important applications of modeling and simulation for protein drugs during preclinical development is for human dose estimation, prediction of safety margins from toxicokinetic and safety data collected from GLP toxicology studies, and justification of the starting dose in the first-in-human phase 1 study. The critical importance of this modeling function was highlighted by the tragic phase 1 study of TGN1412, in which the starting dose of 0.1 mg/kg in healthy subjects produced full receptor occupancy of the CD28 costimulatory molecule, which triggered T-cell activation and life-threatening cytokine release (Suntharalingam *et al.* 2006). The event led to the recommendation of a MABEL starting dose for high risk molecules; the application of PK-PD modeling to starting dose selection for biologics has been reviewed (Tabrizi and Roskos 2007; Agoram 2009; Lowe *et al.* 2010).

Allometric scaling of nonclinical PK data to humans is an essential part of human exposure estimation for a first-in-human trial. A good overview of scaling principles and their application is provided in the FDA guidance document, *Estimating the Maximum Safe Starting Dose in Initial Clinical Trials for Therapeutics in Adult Healthy Volunteers* (2005). For protein drugs, the linear clearance pathways are generally expected to scale allometrically; however, there are exceptions for intact monoclonal antibodies and fusion proteins. Species differences exist in the binding of the human Fc-domain to animal FcRn, particularly in rodents (Ober *et al.* 2001), which result in differences in PK that are not accurately predicted by allometry. For intact, wild-type monoclonal antibodies, we recommend using the expected PK of endogenous IgG in humans to predict the linear clearance and distribution kinetics of an IgG drug; we currently use the PK parameters determined for CAT-354 for this purpose (Oh *et al.* 2010). However, Fc-fusion proteins should be evaluated in animals and potentially scaled, as the protein fused to the Fc-domain could potentially affect FcRn binding and clearance. The TMDD component of clearance must also be accounted for when predicting human exposures. Differences in affinity to target, expression in humans, and turnover rate must be considered in the translational PK-PD model.

17.3.3 Clinical Development

With the background on protein drugs discussed in previous sections, one can frame the design and objectives of the clinical studies of these molecules. The objectives

of phase I trials for protein drugs are similar to small molecules, that is to assess safety, tolerability, and PK. A special safety objective is to evaluate the immunogenic potential of the molecule by assessing the presence of antidrug antibodies. When feasible, PD or preliminary clinical activity at single or multiple ascending doses are assessed in a small number of subjects.

In contrast to small molecules, proteins have some special features that need to be considered. The target receptor for the pharmacological effect also plays a critical role in the elimination of biologics, especially at low concentration levels. because of this reason, nonlinear PK is often observed. A wide range of doses covering nonsaturating and saturating ranges should be tested in a phase I trial to fully characterize the PK by allowing one to estimate nonlinear PK parameters reliably. In addition to IV doses, SC doses are often tested in phase I trials to determine the SC bioavailability. Whenever possible, PD samples should also be collected to provide valuable information for both the receptor-mediated clearance and the pharmacological effect. It is also desirable to measure free and total drug concentrations, as well as free and total target concentrations over time, which is required to build a mechanism-based PK-PD model.

From a clinical operations perspective, phase I studies of protein drugs are frequently much longer than those of small molecules because of the long half-life. Because the presence of high drug concentrations may interfere with the detection of antidrug antibodies and can lead to false negative results of immunogenicity, it is important to follow the decline in serum drug concentrations to very low levels to accurately assess immunogenicity. This leads to extended PK sampling over long periods of time (several months).

PK and PD data obtained from the wide range of phase I doses can enable identification and characterization of biological activity of the molecule using PK-PD modeling and simulation. PK-PD modeling of monoclonal antibodies after phase I may need to rely on preclinical *in vitro* and *in vivo* information such as binding affinity, target turnover, target-antibody complex internalization kinetics, animal disease model efficacy results to guide dose selection and study design in subsequent phase II/III trials.

In many cases, product development teams get their first view of clinical activity of a molecule in the intended patient population in phase II trials. Phase II trials usually evaluate multiple dose levels and regimens to explore the dose-concentration-response relationship for efficacy and safety in the target patient population. Although patient numbers in these Phase II trials are large, the information is generally not sufficient to clearly understand the concentration-clinical effect relationship and associated variability, making it difficult to select one particular dose or dosing regimen for phase III trials. This can happen for various reasons; primarily, the effect is of a size that will require large numbers to decisively evaluate a particular dose, which is only possible in a phase III study, or, because the large sample size is usually split to evaluate different dose levels. This is done so the results of a phase II clinical trial can provide information across a dose range allowing one to look for trends in clinical activity, to assess if multiple dose cohorts show signs of clinical activity or lack thereof. The purpose of this is to

enable the project team to conclusively establish that there is no clinical activity and to stop proceeding to a phase III trial rather than identifying a particular dose level or regimen. Therefore, in many instances the dose-concentration-effect relationship hypothesized from phase II data can only be evaluated conclusively for the first time in a phase III trial in a large enough and broad enough setting.

Modeling of phase III data allows for development of a robust PK-PD-clinical endpoint model and confirmation of dose-concentration-effect relationship with adequate numbers of patients, evaluation of differential effects in any particular subgroup, or assessment of the impact of concomitant therapy or disease severity on clinical activity. Because of this, the regulatory agencies require drug developers to understand phase III clinical data by modeling to confirm that the optimal dose has been studied and has been proposed as the therapeutic dose in the product label. Although all of the above is not unique to biologics but is applicable to small molecules, this is particularly relevant to protein drugs because of the long clinical trials and as well long dosing intervals (weeks to months).

17.3.3.1 Utility of PK-PD Models in a Clinical Setting

The utility of developing a PK-PD model can be many, such as:

- Elucidation of mechanism of action
- Prediction of optimal dose regimens
- Analysis of disease progression
- Provision of the rationale for clinical trial observations in phase III trials in regulatory interactions for approval
- Justification of dose in product label as the optimal dose to regulatory agencies
- Evaluation of particular covariates to understand if any dose modifications are needed for a subgroup of patients
- Demonstration of similarity of concentration-effect relationship between different patient populations
- Provision of support for switching to alternate route of administration, dosage form or dosing regimen
- Evaluation of the effects of organ dysfunction
- Guidance for development of next generation compounds

Examples of PK-PD modeling of protein drugs to support the above applications are presented below.

17.3.3.2 Selection of Phase II/III Doses

In phase I, safety, PK, and sometimes PD or preliminary clinical activity are assessed in a small number of healthy subjects or patients. These data, together with efficacy results from animal disease models if available, can be used to select phase II/III doses.

The practical application of PK-PD modeling is illustrated by the example of HuHMFG1 (AS1402), a humanized monoclonal human milk fat globule-1 antibody that targets the immunodominant epitope of the MUC1 gene product. It has been tested in a phase I study of 26 breast cancer patients receiving doses ranging from 1 to 16 mg/kg (Royer *et al.* 2010). Intensive PK data were analyzed by a linear two-compartment population PK model using nonlinear mixed effects modeling (NONMEM[®]). Covariate analysis of the potential impact of demographics on PK indicated that body weight did not influence clearance or volume of distribution, suggesting the use of fixed dose instead of body weight-based dose of HuHMFG1 in future trials. Fixed dosing is preferred over body weight-based dosing because the simplified dosing leads to decreased dosing errors and improves dosing convenience. A limited PK sampling strategy was selected based on the model, in which one sample is collected immediately before the start of an infusion and the second is taken at the end of infusion. This sampling schedule is usually acceptable in phase II/III trials.

The next example shows the application of integrated PK-PD model in clinical trials to understand clinical activity and to identify target therapeutic concentrations when PD biomarker data is available. Otelixizumab is an aglycosylated chimeric/humanized monoclonal antibody directed to human CD3 ϵ . A population PK-PD model was fit to pooled data from three phase I/II studies in subjects with either type 1 diabetes or psoriasis (Wiczling *et al.* 2010). The PD biomarkers were changes in CD4+ and CD8+ T-cell counts, and modulation and saturation of CD3/T-cell receptors (TCR) after IV administration of otelixizumab. Otelixizumab PK was described by monoexponential decline with Michaelis–Menten elimination. Non-linearity was manifested at high concentrations ($K_m = 0.968 \mu\text{g/mL}$). Lymphocyte dynamics were captured by a direct inhibition model. In diabetic subjects, the otelixizumab serum concentration producing a 50% decrease in peripheral blood counts was 0.0187 $\mu\text{g/mL}$ for CD4+ T cells and 0.0120 $\mu\text{g/mL}$ for CD8+ T cells. Corresponding values for psoriatic subjects were much lower: 0.000533 $\mu\text{g/mL}$ for CD4+ T cells and 0.000269 $\mu\text{g/mL}$ for CD8+ T cells. Total (sum of unbound and otelixizumab-bound) CD3/TCR was approximately equal to unbound CD3/TCR, suggesting that there were few otelixizumab-(CD3/TCR) complexes at the T-cell surface. Down-modulation of CD3/TCR was described by direct inhibition. Otelixizumab concentrations producing 50% reduction in free CD3/TCR sites was similar for diabetes and psoriasis, 0.0144 and 0.0162 $\mu\text{g/mL}$. This integrated PK/PD model was successfully applied to describe otelixizumab pharmacokinetics, the time course of lymphocyte redistribution in blood, and modulation and saturation of CD3/TCR at the T-cell surface. This model described the PK-PD data reasonably well and can be used to guide dose selection in future clinical studies.

17.3.3.3 Characterization of the Dose-Concentration-Effect Relationship

In phase II, drugs are tested in the target patient population at a range of doses to evaluate the initial efficacy and safety and to find the minimum effective dose. Mathematical tools have been applied to the quantitative analyses of phase II data

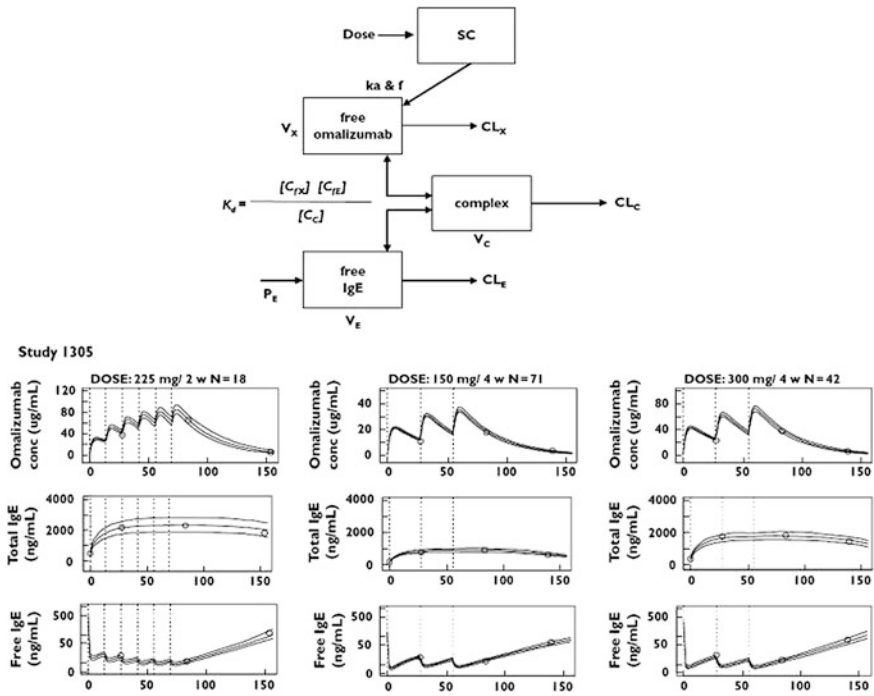


Fig. 17.9 Population PK-PD modeling of the effects of omalizumab on free and total IgE levels in asthma patients (Hayashi *et al.* 2007)

in many aspects. In particular, dose-concentration-effect relationships can be described by mechanistic PK-PD models with the ultimate goal to project the optimal dose for phase III studies.

The omalizumab PK-PD model showcases the use of PK-PD modeling and simulation in drug development (Fig. 17.9). Omalizumab is an anti-IgE antibody approved for the treatment of allergic asthma. An omalizumab-IgE binding model has been reported for omalizumab (Hayashi *et al.* 2007; Lowe *et al.* 2009). This model fits total serum omalizumab concentration, free and total serum IgE concentration data well. Because clinical efficacy is associated with serum free IgE levels, an individualized dosing strategy was developed to maintain serum free IgE below the target level required for efficacy. This model can be used to simulate serum free IgE concentrations at different dose regimens for different patient populations to recommend the optimal dose regimen to be tested in phase III studies.

17.3.3.4 Demonstration of the Similarity of PK-PD Relationship Between Different Patient Populations

An example of the use of modeling to demonstrate similarity of PK-PD relationship between different patient populations, Japanese and Caucasians, and pediatric and

adult populations, is illustrated by omalizumab. A mechanism-based binding model was developed (Hayashi *et al.* 2007) to characterize omalizumab and IgE concentrations in 202 Japanese patients and to compare these values to 531 Caucasian patients with evaluable trough concentration in two registration trials, Study 008 and 009, of 52-week duration and a short term 8-week study, Study 007. The population PK model was a one-compartment model with body weight as a significant covariate on clearance and volume of distribution of omalizumab. The PK-PD model indicated that both production rate and clearance of free IgE were positively correlated with baseline IgE values in Japanese patients. For a 61-kg patient with baseline IgE of 482 ng/ml, estimated clearance of free omalizumab and free IgE were 7.32 and 71 mL/h, respectively; estimated clearance of omalizumab-IgE complex was 5.9 mL/h; estimated half-life for omalizumab and IgE were 23 and 2.5–2.7 days, respectively. The PK-PD model developed from Japanese patients was used to predict omalizumab and IgE values in Caucasian patients from Studies 007, 008, and 009. Based on the overlap of observed omalizumab, free IgE and total IgE concentrations in Caucasian patients to predicted values, the PK and PD of omalizumab and IgE were inferred to be similar between the two populations.

The mechanism-based PK-PD model developed in adolescents and adults with minor modifications was used to evaluate omalizumab PK and PD in pediatric patients between 6 and 12 years of age, to support a pediatric sBLA. Baseline IgE values in pediatric patients was higher than adults, which was shown to correlate with clinical outcome of asthma. The model was used to demonstrate similarity of pediatric PK and PD parameters with adults and was used to develop a dosing table in pediatric patients (from FOI clinical pharmacology review of omalizumab pediatric supplement by the FDA).

17.3.3.5 Evaluation of Demographic or Disease Covariates to Determine the Need of Dose Modifications for Subpopulations

One example in which population PK modeling was used to demonstrate appropriateness of the dose for the entire patient population is presented for motavizumab (Zhao *et al.*), a humanized monoclonal antibody that binds to the highly conserved F-protein of respiratory syncytial virus (RSV) and is being tested as prophylaxis in preterm infants and high-risk full term infants at risk of RSV disease. The phase III clinical trial studied five monthly intramuscular doses of 15 mg/kg in preterm infants of different gestational ages (GAs) with and without chronic lung disease and term infants at risk of RSV disease. Only trough serum concentrations could be collected in this pediatric population. Motavizumab trough concentrations exhibited modest interindividual variability in these pediatric patients. The patient population in the phase III study was diverse with respect to GA, chronological age (CA), body weight, race, and the presence or absence of chronic lung disease. The appropriateness of body weight-based dosing and contribution of demographic variables to observed variability in trough serum concentrations was evaluated by

population PK modeling. In addition to the trough concentration data from the phase III clinical trial, simultaneous modeling of intensive serum concentration data from adults and sparse serum concentration data with information on peak concentrations and terminal phase concentrations from five other pediatric studies was performed.

Typical of a monoclonal antibody molecule exhibiting linear kinetics, a two-compartment model fit motavizumab serum concentration data best. The two-compartment model scaled for body weight from infants to adults using allometry exponents of 0.75 for CL and 1.0 for volume of distribution (V_d) resulted in underestimation of adult CL values and overestimation of adult V_d values because of lower than “mature” CL in infants and higher than expected V_d values based on body weight. The lower CL in infants was attributable to immature elimination mechanisms. Elimination mechanisms mature and CL approaches values based on allometric scaling alone as infants age (Fig. 17.10).

Similarly, the higher V_d value in infants compared to adults has been documented in the literature (Anderson *et al.* 2000; Anderson and Holford 2008). Rapid changes in body water distribution in early life because of neonatal body composition has been documented (Anderson *et al.* 2000; Anderson and Holford 2008). This indicated that changes in body weight alone do not adequately explain the changes in CL and V_d in pediatric patients. Age was an important variable to be considered in addition to body weight. Two age descriptors GA and CA are relevant in the motavizumab patient population. To account for the continuum in

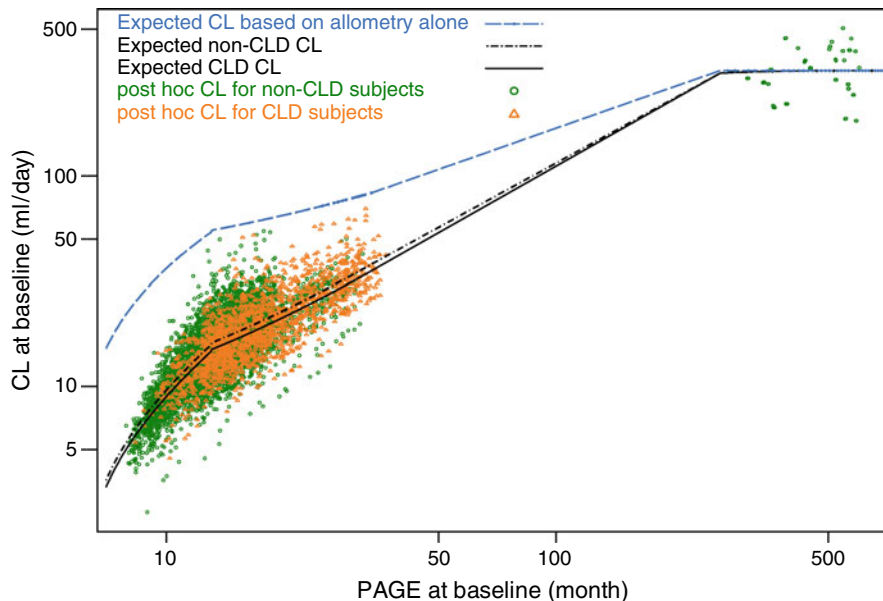


Fig. 17.10 Comparison of post hoc clearance (CL) estimates of motavizumab in healthy adult subjects and infants with or without chronic lung disease (CLD) as a function of PAGE (chronological age plus gestational age [GA]). Body weight and simple allometry alone did not adequately explain differences in clearance between subjects

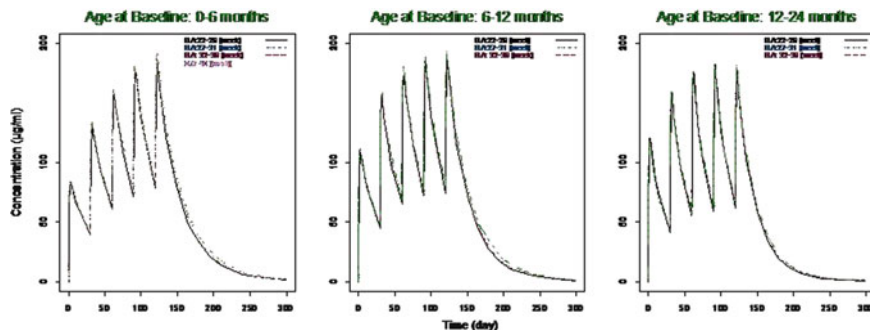


Fig. 17.11 Simulated motavizumab concentrations in infants of different chronological and GAs. The effect of demographic covariates other than body weight were not found to be clinically significant and the simulations confirmed the adequacy of body weight-based dose for the entire pediatric patient population receiving motavizumab

maturation of clearance during gestation and post birth, a new variable PAGE, which is the sum of GA and CA, was considered (Anderson *et al.* 2000; Anderson and Holford 2008; Allegaert *et al.* 2004). Of the two age components in PAGE, the effect of CA on CL and V_d was much greater than GA. Although, age was an important covariate for scaling CL and V_d from infants to adults, the results of the population PK model indicated that serum concentrations are primarily governed by body weight in the intended population of premature infants and high-risk pediatric subjects in the first 2 years of life. Because the phase III dose of motavizumab is based on body weight, simulations were performed using demographic characteristics of the phase III study to evaluate comparability of serum concentrations across a range of subpopulations differing in GA and CA. The results of the simulation demonstrated comparable motavizumab concentrations following 15 mg/kg dosing across ten different subpopulations differing in GA and CA. The effect of demographic covariates other than body weight were not found to be clinically significant and confirmed the adequacy of body weight-based dose for the entire pediatric patient population receiving motavizumab (Fig. 17.11).

17.3.3.6 Evaluation of Drug–Drug Interactions

Unlike small molecule drugs, few PK-based drug–drug interactions have been reported for protein drugs. This is because of differences in the mechanisms involved in absorption, distribution, metabolism, and excretion of the two classes of molecules. For proteins, the most common route of administration is not oral, it is usually by intravenous, SC, or intramuscular injections. For small molecules, oral administration is often the preferred route, especially for chronic indications. Therefore, interaction of protein drugs on small molecule bioavailability are not expected. Although proteins are not metabolized by CYP450, in unusual cases they might inhibit or induce CYP450 and potentially affect the clearance of small molecules.

Several PK-based drug-drug interaction examples are discussed below. Cytokines (interleukin-1 β , interleukin-4, interleukin-6, tumor necrosis factor- α , and interferon- γ) have been shown to inhibit CYP450 at both the mRNA and protein levels (Mahmood and Green 2007). Interferon- α decreased the clearance of cyclophosphamide by 63% in patients. Clearance of basiliximab, an anti-IL-2R α antibody, was reduced by 22 and 51% when coadministered with azathioprine and mycophenolate mofetil, respectively. Serum concentration of trastuzumab, an anti-HER2 antibody, was increased by 150% when coadministered with paclitaxel. The apparent clearance of adalimumab, an anti-TNF α antibody, was reduced by 29–40% when coadministered with methotrexate. In some cases, the reduction in antibody drug clearance in combination with small molecules, as observed with adalimumab in combination with methotrexate, could be due to immunosuppression and a decrease in the incidence and titer of anti-drug antibody responses. The exposure of SN38, the active metabolite of irinotecan, was increased by 33% when coadministered with bevacizumab, an anti-VEGF antibody (Zhou and Davis 2009). Recent reports in conference proceedings have described an effect of tocilizumab, an antibody to the IL-6 receptor, on CYP450 activities in rheumatoid arthritis patients; and these potential effects are described in the prescribing information. Chronic upregulation of IL-6 in RA patients is believed to have down-regulated expression of some CYP450 enzymes; after treatment with tocilizumab, the AUC of CYP3A4 substrates (simvastatin, omeprazole, and dextropropofol) and a CYP2C19 substrate (omeprazole) were decreased by up to 57%. Because of this finding, a regulatory expectation might be established for conducting formal drug interaction studies in patients receiving cytokines or cytokine-modulating drugs.

The drug-drug interaction potential of proteins can be assessed by population PK modeling or by formal *in vivo* drug-drug interaction studies. Of course, the importance of drug-drug interaction depends on the therapeutic index and the scheduling of combination therapies. Although a few examples of drug interactions with protein drugs have been described, we emphasize that a clinically-relevant, PK-based drug-drug interaction with a protein drug has not been reported.

17.3.3.7 Comparison of Fixed Dosing vs. Body Size-Based Dosing

At the end of phase II, many decisions must be made before phase III studies can be well designed. One important question is dosing strategy. For biotherapeutics, body size-based doses are usually tested in phase I and II studies. However, in adult patient population, fixed dosing is preferred for drugs with wide therapeutic index mainly because of convenience.

A simulation study published recently compared the performance of fixed dosing vs. body size-based dosing for 12 monoclonal antibodies in adult patients (Wang *et al.* 2009). It was found that the difference in the population distribution

curves of AUC and C_{\max} between the two dosing regimens was small and neither dosing approach showed clear advantage in reducing intersubject variability in PK exposure.

The potential effect of body size on PK, PD, efficacy and safety should be evaluated based on phase I and phase II data. If body size is identified as a significant covariate for PK or PD, then simulations can be performed to calculate drug exposure or PD response following fixed dose and body size-based dose. Many times, body size only explains a small proportion of the overall intersubject variability in PK and PD even though it is a statistically significant covariate for PK parameters. Body size-based dose should only be recommended if it is warranted such as for drugs with narrow therapeutic index in which the margin between the therapeutic and toxic concentrations is small, if body-size contributes greatly to intersubject variability, or when dosing pediatric patients.

17.3.3.8 Provision of Support for Switching to Alternative Route of Administration, Dosage Form, or Dosing Regimen

PK PD modeling to support switch to an alternate dosing regimen is illustrated using trastuzumab. Trastuzumab is a humanized monoclonal antibody against the extracellular domain of human epidermal growth factor receptor 2 (HER-2) and is indicated for treatment of HER-2 positive metastatic breast cancer. A population PK approach was used to characterize the PK of trastuzumab by simultaneously modeling intensive PK data from 16 patients in a phase I study and sparse weekly peak and trough concentration data from 460 patients in phase II and III studies (Bruno *et al.* 2005). The final PK model was a two-compartment model. Significant covariates that affected trastuzumab clearance and volume of distribution were level of shed extracellular domain of HER-2 receptor and body weight with a modest increase in clearance in patients with four or more metastatic sites. The population PK model predicted a mean steady state peak concentration of 110 $\mu\text{g/mL}$ and trough concentration of 66 $\mu\text{g/mL}$ following weekly maintenance dose of 2 mg/kg. An intensive loading dose schedule followed by administration of maintenance dose every 3 weeks was anticipated to achieve higher serum concentrations of trastuzumab early and also synergize administration of trastuzumab with standard chemotherapy. Simulations were performed using the population PK model to compare trough concentrations after 6 mg/kg every 3 weeks or after 2 mg/kg every week. Simulations indicated higher peak and slightly lower mean trough concentration with 80% of patients achieving target level of 20 $\mu\text{g/mL}$ following 6 mg/kg every 3 weeks dose compared to 90% with the 2 mg/kg every week dose. This alternate dosing schedule was later evaluated in a phase I/II study in 72 patients (Leyland-Jones *et al.* 2010). Trastuzumab was administered at 6 mg/kg weekly for 3 weeks followed by a maintenance dose of 6 mg/kg every 3 weeks. As predicted by the model, the observed mean trough concentration 3 weeks after the fourth dose was similar to that observed with weekly maintenance dose of 2 mg/kg.

17.3.3.9 Provision of Rationale for Clinical Observations in Phase III Trials in Regulatory Interactions for Approval

Ustekinumab is a human monoclonal antibody that binds and neutralizes cytokines IL-12 and IL-23, which have been implicated in psoriasis. Population PK of ustekinumab was characterized in 1,937 psoriasis patients from two phase III studies, PHOENIX 1 and 2 (Zhu *et al.* 2009). Patients received SC administration of either placebo, 45 or 90 mg ustekinumab on weeks 0 and 4 followed by dosing active treatment every 12 weeks. A one-compartment model was chosen as the structural model and various covariates such as demographic, disease characteristics, concomitant medication, smoking status, and alcohol use were evaluated using data from the PHOENIX 2 trial. Data from PHOENIX 1 trial was used as an external validation data set. Body weight was found to be a significant covariate impacting both SC clearance (CL/F) and SC volume of distribution (V/F), with patients weighing 100 kg or more having an approximately 55% higher CL/F and 37% higher V/F, resulting in 30% lower steady state trough concentrations. None of the other demographic covariates were significant except for minor observations of a 5.9% higher CL/F in females and 11% lower V/F in non-Caucasian patients, which were not considered clinically significant. Interestingly, CL/F and V/F were higher by 29 and 13%, respectively, in diabetes patients. The final model was used to simulate the combined effect of body weight and diabetes on expected ustekinumab steady state exposures, which were predicted to be 40–50% lower in diabetes patients weighing 100 kg or more. This population PK model was subsequently used to characterize the exposure-response relationship between ustekinumab exposures to the efficacy endpoint Psoriasis Area and Severity Index (PASI) in the two PHOENIX trials. The PASI scores were modeled using an indirect response model with drug concentrations inhibiting formation rate of psoriatic skin lesions followed by evaluation of covariates. A trend toward higher exposures and lower CL/F was seen in responders and partial responders compared to nonresponders. More importantly, the modeling identified a bimodal distribution in IC₅₀, with a 30-fold higher IC₅₀ value in partial responders compared to responders, indicating different sensitivity to ustekinumab in psoriasis patients. The PK-PD modeling of ustekinumab helped relate drug exposures to the clinical endpoint and helped identify interindividual sensitivity to ustekinumab to explain the intersubject differences in clinical response.

17.4 Conclusions

PK-PD modeling and simulations have many important applications in the development of protein drugs. Application of PK-PD modeling can improve the engineering of protein drugs, contribute to the selection of the best lead drug candidate, and improve the probability of successful development. For modeling of protein PK-PD, a thorough understanding of the biology of the target and the pharmacology

of the drug is required. Unlike small molecules, the PK properties of protein drugs are often intricately linked to the biology of the target. Mechanistic, biologically based models should be established to describe exposure-response relationships. Model assumptions should be carefully based on experimental data where feasible. PK-PD modelers should also be proactive: appropriate PK and PD assays should be established as early in development as possible; and the modeler should understand the characteristics of the assays and what the assays are measuring. The effects of antidrug antibodies, which can affect pharmacokinetics, efficacy, and safety, should also be considered when conducting PK-PD modeling. Although this chapter has provided a general overview of PK-PD approaches to modeling and simulation of protein drugs, successful PK-PD modeling of novel proteins must be founded on innovation: every case is different.

References

- Ackerman ME, Pawlowski D, Wittrup KD (2008) Effect of antigen turnover rate and expression level on antibody penetration into tumor spheroids. *Mol Cancer Ther* 7:2233–2240
- Adams GP, Schier R, McCall AM, Simmons HH, Horak EM, Alpaugh RK et al (2001) High affinity restricts the localization and tumor penetration of single-chain fv antibody molecules. *Cancer Res* 61:4750–4755
- Agoram BM (2009) Use of pharmacokinetic/pharmacodynamic modelling for starting dose selection in first-in-human trials of high-risk biologics. *Br J Clin Pharmacol* 67:153–160
- Allegaert K, Anderson BJ, Naulaers G, de Hoon J, Verbesselt R, Debeer A et al (2004) Intravenous paracetamol (propacetamol) pharmacokinetics in term and preterm neonates. *Eur J Clin Pharmacol* 60:191–197
- Anderson BJ, Holford NH (2008) Mechanism-based concepts of size and maturity in pharmacokinetics. *Annu Rev Pharmacol Toxicol* 48:303–332
- Anderson BJ, Woollard GA, Holford NH (2000) A model for size and age changes in the pharmacokinetics of paracetamol in neonates, infants and children. *Br J Clin Pharmacol* 50:125–134
- Bauer RJ, Gibbons JA, Bell DP, Luo ZP, Young JD (1994) Nonlinear pharmacokinetics of recombinant human macrophage colony-stimulating factor (M-CSF) in rats. *J Pharmacol Exp Ther* 268:152–158
- Bauer RJ, Dedrick RL, White ML, Murray MJ, Garovoy MR (1999) Population pharmacokinetics and pharmacodynamics of the anti-CD11a antibody hu1124 in human subjects with psoriasis. *J Pharmacokinet Biopharm* 27:397–420
- Betts AM, Clark TH, Yang J, Treadway JL, Li M, Giovannelli MA et al (2010) The application of target information and preclinical pharmacokinetic/pharmacodynamic modeling in predicting clinical doses of a Dickkopf-1 antibody for osteoporosis. *J Pharmacol Exp Ther* 333:2–13
- Bruno R, Washington CB, Lu JF, Lieberman G, Banken L, Klein P (2005) Population pharmacokinetics of trastuzumab in patients with HER2+ metastatic breast cancer. *Cancer Chemother Pharmacol* 56:361–369
- Dall'Acqua WF, Woods RM, Ward ES, Palaszynski SR, Patel NK, Brewah YA et al (2002) Increasing the affinity of a human IgG1 for the neonatal Fc receptor: biological consequences. *J Immunol* 169:5171–5180
- Davda JP, Jain M, Batra SK, Gwilt PR, Robinson DH (2008) *Int Immunopharmacol* 8(3):401–413
- Dornhorst AC (1951) The interpretation of red cell survival curves. *Blood* 6:1284–1292

- Eadie GS, Brown IW Jr (1953) Red blood cell survival studies. *Blood* 8:1110–1136
- Ferl GZ, Wu AM, DiStefano JJ III (2005) A predictive model of therapeutic monoclonal antibody dynamics and regulation by the neonatal Fc receptor (FcRn). *Ann Biomed Eng* 33:1640–1652
- Galluppi GR, Rogge MC, Roskos LK, Lesko LJ, Green MD, Feigal DW Jr et al (2001) Integration of pharmacokinetic and pharmacodynamic studies in the discovery, development, and review of protein therapeutic agents: a conference report. *Clin Pharmacol Ther* 69:387–399
- Garg A, Balthasar JP (2007) Physiologically-based pharmacokinetic (PBPK) model to predict IgG tissue kinetics in wild-type and FcRn-knockout mice. *J Pharmacokinet Pharmacodyn* 34:687–709
- Gibiansky L, Gibiansky E, Kakkar T, Ma P (2008) Approximations of the target-mediated drug disposition model and identifiability of model parameters. *J Pharmacokinet Pharmacodyn* 35:573–591
- Georguieva I, Clark SR, McMahon CJ, Scarth S, Rothwell NJ, Tyrrell PJ et al (2008) Pharmacokinetic modelling of interleukin-1 receptor antagonist in plasma and cerebrospinal fluid of patients following subarachnoid haemorrhage. *Br J Clin Pharmacol* 65:317–325
- Harker LA, Roskos LK, Marzec UM, Carter RA, Cherry JK, Sundell B et al (2000) Effects of megakaryocyte growth and development factor on platelet production, platelet life span, and platelet function in healthy human volunteers. *Blood* 95:2514–2522
- Hayashi N, Tsukamoto Y, Sallas WM, Lowe PJ (2007) A mechanism-based binding model for the population pharmacokinetics and pharmacodynamics of omalizumab. *Br J Clin Pharmacol* 63:548–561
- Johnston E, Crawford J, Blackwell S, Bjurström T, Lockbaum P, Roskos L et al (2000) Randomized, dose-escalation study of SD/01 compared with daily filgrastim in patients receiving chemotherapy. *J Clin Oncol* 18:2522–2528
- Krzyzanski W, Ramakrishnan R, Jusko WJ (1999) Basic pharmacodynamic models for agents that alter production of natural cells. *J Pharmacokinet Biopharm* 27:467–489
- Krzyzanski W, Jusko WJ, Wacholtz MC, Minton N, Cheung WK (2005) Pharmacokinetic and pharmacodynamic modeling of recombinant human erythropoietin after multiple subcutaneous doses in healthy subjects. *Eur J Pharm Sci* 26:295–306
- Kuwabara T, Kobayashi S, Sugiyama Y (1996) Pharmacokinetics and pharmacodynamics of a recombinant human granulocyte colony-stimulating factor. *Drug Metab Rev* 28:625–658
- Lau Y, Wang B, Faggioni R, Lu H, Gross R, Wang Y *et al* (2010) Mechanistic pharmacokinetic-pharmacodynamic modeling of MEDI-551, a humanized IgG1 against CD19, for first-in-human starting dose recommendation. *Clin Pharmacol Ther* 87(Suppl 1):S58
- Leyland-Jones B, Colomer R, Trudeau ME, Wardley A, Latreille J, Cameron D et al (2010) Intensive loading dose of trastuzumab achieves higher-than-steady-state serum concentrations and is well tolerated. *J Clin Oncol* 28:960–966
- Lote CJ (2000) Principles of renal physiology, 4th edn. Kluwer Academic Publishers, London
- Lowe PJ, Tannenbaum S, Gautier A, Jimenez P (2009) Relationship between omalizumab pharmacokinetics, IgE pharmacodynamics and symptoms in patients with severe persistent allergic (IgE-mediated) asthma. *Br J Clin Pharmacol* 68:61–76
- Lowe PJ, Tannenbaum S, Wu K, Lloyd P, Sims J (2010) On setting the first dose in man: quantitating biotherapeutic drug-target binding through pharmacokinetic and pharmacodynamic models. *Basic Clin Pharmacol Toxicol* 106:195–209
- Mager DE, Jusko WJ (2001) General pharmacokinetic model for drugs exhibiting target-mediated drug disposition. *J Pharmacokinet Pharmacodyn* 28:507–532
- Mager DE, Krzyzanski W (2005) Quasi-equilibrium pharmacokinetic model for drugs exhibiting target-mediated drug disposition. *Pharm Res* 22:1589–1596
- Mahmood I, Green MD (2007) Drug interaction studies of therapeutic proteins or monoclonal antibodies. *J Clin Pharmacol* 47:1540–1554

- Marathe A, Krzyzanski W, Mager DE (2009) Numerical validation and properties of a rapid binding approximation of a target-mediated drug disposition pharmacokinetic model. *J Pharmacokinet Pharmacodyn* 36:199–219
- Mizuno N, Kato Y, Iwamoto M, Urae A, Amamoto T, Niwa T et al (2001) Kinetic analysis of the disposition of insulin-like growth factor 1 in healthy volunteers. *Pharm Res* 18:1203–1209
- Ober RJ, Radu CG, Ghetie V, Ward ES (2001) Differences in promiscuity for antibody-FcRn interactions across species: implications for therapeutic antibodies. *Int Immunol* 13:1551–1559
- Oh CK, Faggioni R, Jin F, Roskos LK, Wang B, Birrel C et al (2010) An open-label, single-dose bioavailability study of the pharmacokinetics of CAT-354 after subcutaneous and intravenous administration in healthy males. *Br J Clin Pharmacol* 69:645–655
- Pentsuk N, van der Laan JW (2009) An interspecies comparison of placental antibody transfer: new insights into developmental toxicity testing of monoclonal antibodies. *Birth Defects Res B Dev Reprod Toxicol* 86:328–344
- Poulin P, Theil FP (2000) A priori prediction of tissue: plasma partition coefficients of drugs to facilitate the use of physiologically-based pharmacokinetic models in drug discovery. *J Pharm Sci* 89:16–35
- Poulin P, Theil FP (2002) Prediction of pharmacokinetics prior to in vivo studies. II. Generic physiologically based pharmacokinetic models of drug disposition. *J Pharm Sci* 91:1358–1370
- Roopenian DC, Akilesh S (2007) FcRn: the neonatal Fc receptor comes of age. *Nat Rev Immunol* 7:715–725
- Roskos LK, Stead R, Harker L, Cheung EN (1997) A cytokinetic model of platelet production and destruction following administration of peg-rhuMGDF. *Blood* 90:171
- Roskos LK, Lum P, Lockbaum P, Schwab G, Yang BB (2006) Pharmacokinetic/pharmacodynamic modeling of pegfilgrastim in healthy subjects. *J Clin Pharmacol* 46:747–757
- Roskos LK, Klakamp S, Liang M, Arends R, Green L (2007) Molecular engineering II: antibody affinity. In: Dubel S (ed) *Handbook of therapeutic antibodies*, 1st edn. Wiley-VCH, Weinheim, pp 145–170
- Royer B, Yin W, Pegram M, Ibrahim N, Villanueva C, Mir D et al (2010) Population pharmacokinetics of the humanised monoclonal antibody, HuHMF61 (AS1402), derived from a phase I study on breast cancer. *Br J Cancer* 102:827–832
- Savic RM, Jonker DM, Kerbusch T, Karlsson MO (2007) Implementation of a transit compartment model for describing drug absorption in pharmacokinetic studies. *J Pharmacokinet Pharmacodyn* 34:711–726
- Segel IH (1993) *Enzyme kinetics: behavior and analysis of rapid equilibrium and steady state enzyme systems*. Wiley, New York
- Suntharalingam G, Perry MR, Ward S, Brett SJ, Castello-Cortes A, Brunner MD et al (2006) Cytokine storm in a phase 1 trial of the anti-CD28 monoclonal antibody TGN1412. *N Engl J Med* 355:1018–1028
- Supersaxo A, Hein W, Gallati H, Steffen H (1988) Recombinant human interferon alpha-2a: delivery to lymphoid tissue by selected modes of application. *Pharm Res* 5:472–476
- Supersaxo A, Hein WR, Steffen H (1990) Effect of molecular weight on the lymphatic absorption of water-soluble compounds following subcutaneous administration. *Pharm Res* 7:167–169
- Tabrizi MA, Roskos LK (2007) Preclinical and clinical safety of monoclonal antibodies. *Drug Discov Today* 12:540–547
- Toon S (1996) The relevance of pharmacokinetics in the development of biotechnology products. *Eur J Drug Metab Pharmacokinet* 21(2):93–103
- Uehlinger DE, Gotch FA, Sheiner LB (1992) A pharmacodynamic model of erythropoietin therapy for uremic anemia. *Clin Pharmacol Ther* 51:76–89
- Urva SR, Yang VC, Balthasar JP (2010) Physiologically based pharmacokinetic model for T84.66: a monoclonal anti-CEA antibody. *J Pharm Sci* 99:1582–1600

- Wang B, Ludden TM, Cheung EN, Schwab GG, Roskos LK (2001) Population pharmacokinetic-pharmacodynamic modeling of filgrastim (r-metHuG-CSF) in healthy volunteers. *J Pharmacokinet Pharmacodyn* 28:321–342
- Wang W, Wang EQ, Balthasar JP (2008) Monoclonal antibody pharmacokinetics and pharmacodynamics. *Clin Pharmacol Ther* 84:548–558
- Wang DD, Zhang S, Zhao H, Men AY, Parivar K (2009) Fixed dosing versus body size-based dosing of monoclonal antibodies in adult clinical trials. *J Clin Pharmacol* 49:1012–1024
- Weinstein JN, van Osdol W (1992) The macroscopic and microscopic pharmacology of monoclonal antibodies. *Int J Immunopharmacol* 14:457–463
- Wiczling P, Rosenzweig M, Vaickus L, Jusko WJ (2010) Pharmacokinetics and pharmacodynamics of a chimeric/humanized anti-CD3 monoclonal antibody, oteelixumab (TRX4), in subjects with psoriasis and with type 1 diabetes mellitus. *J Clin Pharmacol* 50:494–506
- Woo S, Jusko WJ (2007) Interspecies comparisons of pharmacokinetics and pharmacodynamics of recombinant human erythropoietin. *Drug Metab Dispos* 35:1672–1678
- Yan X, Mager DE, Krzyzanski W (2010) Selection between Michaelis–Menten and target-mediated drug disposition pharmacokinetic models. *J Pharmacokinet Pharmacodyn* 37:25–47
- Yang BB, Lum PK, Hayashi MM, Roskos LK (2004) Polyethylene glycol modification of filgrastim results in decreased renal clearance of the protein in rats. *J Pharm Sci* 93:1367–1373
- Zhao L, Roskos L, Griffin P, Losonsky GA, Groothuis JR, Jallal B, Robbie GJ (2010) Population pharmacokinetics analysis of motavizumab in children at risk for RSV infection. Pediatric Academic Societies (PAS) annual meeting, Vancouver, Canada
- Zhou H, Davis HM (2009) Risk-based strategy for the assessment of pharmacokinetic drug-drug interactions for therapeutic monoclonal antibodies. *Drug Discov Today* 14:891–898
- Zhu Y, Hu C, Lu M, Liao S, Marini JC, Yohrling J et al (2009) Population pharmacokinetic modeling of ustekinumab, a human monoclonal antibody targeting IL-12/23p40, in patients with moderate to severe plaque psoriasis. *J Clin Pharmacol* 49:162–175

Chapter 18

Modeling and Simulation in Pediatric Research and Development

Jeffrey S. Barrett

Abstract Pediatric research and development is typically poorly funded in both academic and industrial settings creating greater incentive for optimized trial designs with high degree of technical success. Likewise, the application of modeling and simulation approaches is extremely valuable in the evaluation of pediatric trial design. Beyond bridging adult dose-exposure relationships, pediatric clinical trial simulation models must accommodate relevant developmental, maturational, and size relationships on both PK and PD expressions. Design considerations that address sample size per age strata, the probability of achieving adult exposure-response targets, and assumptions regarding PD response vs. outcomes are especially valuable in the support of pediatric drug development and/or dosing guidance.

18.1 Introduction

The typical child is remarkably healthy and the occasion to treat them with medicine is usually precipitated only by infection, fevers associated with bacterial or viral infections, and sedation requirements on the unfortunate visit to the ER. Not surprisingly, antibiotics, acetaminophen, and sedatives such as propofol and midazolam are among the most highly used medicines in children in an in-patient setting (Barrett *et al.* 2008a, b). The marketplace attests to the economic reality that children are not the “target population” for most new molecular entities (NMEs) in drug development. This reality, in part, motivated the assignment of pediatrics as a “special population” in the recent past. On face value this is not an apparently egregious term to associate with the study of children. However, the notion that a single study design will be sufficient to extend the data generated in adults to pediatrics is flawed even if the adult and pediatric indications are similar. Although

J.S. Barrett (✉)

Department of Pediatrics, The Children’s Hospital of Philadelphia,
Division of Clinical Pharmacology and Therapeutics,
University of Pennsylvania Medical School, Philadelphia, PA, USA
e-mail: barrettj@email.chop.edu

opinions differ regarding the upper age boundary for pediatrics, the age window from birth to 17, 18, or 21 years is wide and represents approximately one-fourth of the average human life expectancy. Of course there are subcategories (neonates, infants, children, adolescents, etc.) that further differentiate this general classification, but the key notion and the basis for much of the current pediatric study design requirements, at least from a regulatory perspective, is that pediatrics represents a developmental continuum over which younger individuals mature into fully developed adults. Although clinical experience over the entire continuum is sought, the value of information collected across this continuum is not equal in that earlier age ranges (younger populations) tend to be more dynamic and require more consideration for dosing requirements. Likewise, pediatric clinical trial designs should consider variation in both PK and PD behavior, which may vary separately or in conjunction along nonlinear developmental and/or maturational trajectories.

Unlike the typical child, the critically ill child often manifests additional factors beyond age, size, and development that need to be considered when prescribing medicines (Zuppa and Barrett 2008). Assumptions regarding the consistency of pharmacokinetic behavior and linearity over time, dose, and condition may not be guaranteed in these children. Both the class and number of pharmaceutical agents administered are also likely at issue for critically ill children. Cancer, infectious disease, and neurologic conditions all represent therapeutic areas where polypharmacy exists in children and where risk of drug interactions is greater.

There are several key questions addressed in this chapter as we consider the strategy and implementation of clinical trial simulation (CTS) in the study of pediatric populations. These include the following:

- Who performs pediatric research and, more specifically, clinical trials in children and why?
- What are the objectives of the various studies and how are these objectives aligned with study designs?
- To what extent does (or can) modeling and simulation facilitate the design of pediatric trials?
- How specifically is CTS implemented to advance pediatric research in the various settings where these investigations occur?

To deal with these questions we must also consider one additional matter that affects all others as well as the underlying assumptions that frame pediatric research in general. Assuming that CTS performed for pediatric trials is fundamentally the same as in adults, what are the key differences (between adults and pediatrics) and how do we address them in the design and implementation of pediatric CTS?

Although there are few published examples of CTS focused in pediatrics, the occasion to consider CTS has increased dramatically largely motivated by regulatory considerations from the European Medical Agency (EMA) and the Food and Drug Administration (FDA). The most common application is the standard PK/safety trial employed when adult and pediatric indications are perceived to be similar and there is information/data to support such assumptions. The primary goal in this setting is to ensure an adequate sample size and an informative sampling

scheme that considers the potential shift in PK across age strata or temporal changes in PD response. More uncommon but perhaps increasing is the interest in pediatric efficacy trials.

Drug developers and pediatric caregivers have different objectives when it comes to evaluating the relevant clinical pharmacologic principles that underlie their query. The drug developer ultimately must contend with the dosing of the “typical” pediatric patient, keeping in mind that a recipe for dosing within the usual constraints of an otherwise normal developing child must be provided in the labeling. The caregiver must address the individual patient, regardless of how the patient presents. Thus, although the typical patient may represent the normal scenario (hopefully) for caregivers, the critically ill child, the child on extracorporeal membrane oxygenation (ECMO), the hypothermic child, the obese child, and the child on multiple medications with some degree of interaction potential must all be treated with the best medical judgment the caregiver can provide. Hence, the availability of source data in these categories is invaluable to the caregiver. When data are not available some level of extrapolation occurs (usually empirically). Although not trial simulation per se, individual patient forecasting (simulation based on prior knowledge and perhaps some individual patient data) is becoming a desirable tool for the caregiver.

Differences between children and adults with respect to PK and PD are often influenced by physiologic factors such as body composition, total body water, protein binding, cytochrome P450 ontogeny, gastrointestinal motility and pH, and organ (*e.g.*, renal and hepatic) function, all of which can produce significant influences on absorption, distribution, metabolism, and elimination throughout childhood. Likewise, knowledge of pediatric clinical pharmacology is essential to the design and conduct of informative pediatric trials. More than ever, pharmaceutical sponsors are encouraged to plan for the pediatric investigation as an essential part of their clinical development plans, especially with the reissuance of the Product Research and Equity Act (PREA) (Ward and Kauffman 2007). For older drugs on the market, NIH administers the appropriation of funds that support pediatric research for off-patent drugs through the Best Pharmaceuticals for Children Act (BPCA) (Ward and Kauffman 2007) with guidance on the research scope and protocol design from the FDA. In both cases (PREA and BPCA studies), access to pediatric patients is commonly attained through networks of pediatric centers of excellence. For clinical pharmacology studies encompassing PK, PD, safety and efficacy in a limited sense, the Pediatric Pharmacology Research Units (PPRU, <http://ppru.org>) have had a longstanding history for supporting trials resulting in labeling for children. More recently, the Obstetrics Pharmacology Research Unit (OPRU, <http://opru.rti.org/>) has focused on maternal and newborn trials. Specific indication networks also exist and are essential in the identification and enrollment of often critically ill patients and patients with chronic and/or life-threatening disease. Table 18.1 lists many of the available pediatric clinical research networks along with their website URL (if available) aligned with the supporting NIH institution.

Table 18.1 Pediatric clinical research networks sponsored by the National Institute of Health (NIH)

Funding institution	Specific network (and website if available)
NICHD	Obstetric-Fetal Pharmacology Research Units (OPRU) http://www.nichd.nih.gov/research/supported/opru_network.cfm NICHD Domestic and International Pediatric and Maternal HIV Studies Network www.nichd.nih.gov/research/supported/pphsn.cfm Pediatric Research in Office Settings (PROS) http://www.aap.org/pros/ The National Collaborative Pediatric Critical Care Research Network (CPCCRN) http://www.cpccrn.org/ Maternal Fetal Medicine Units Network (MFMU) http://www.bsc.gwu.edu/mfmu/ Stillbirth Collaborative Research Network http://scrn.rti.org/ Diabetes Research in Children Network (DirecNet) http://www.nichd.nih.gov/research/supported/directnet.cfm
NHLBI	Cincinnati Pediatric Research Group (CPRG) http://www.cincinnatichildrens.org/research/project/cprg/ Pediatric Heart Network (PHN) http://www.pediatricheartnetwork.org/ NHLBI Pediatric Cardiology Network www.pediatricheartnetwork.org Pediatric Asthma Clinical Research Network PICU Network (Pediatric Critical Network) http://pedscm.org/ The NHLBI Acute Respiratory Distress Syndrome Network http://www.ardsnet.org/
NCI	Pediatric Brain Tumor Consortium (PBTC) http://www.pbtc.org/ Cooperative Human Tissue Network (CHTN) Pediatric Division http://www.chtn.ims.nci.nih.gov/ Childhood Cancer Research Network http://www.cancer.gov/cancertopics/factsheet/Sites-Types/childhood New Approaches to Neuroblastoma Therapy Consortium (NANT) http://www.nant.org/ COG (Children's Oncology Group) http://www.childrensoncologygroup.org/
NIAID	Cooperative Clinical Trials in Pediatric Transplantation (CCTPT) https://www.cctptstudies.org/ Vaccine and Treatment Evaluation Units (VTEUs) http://www.niaid.nih.gov/factsheets/vteu.htm Collaborative Antiviral study group – NIAID/DMID ^a http://www.casg.uab.edu/
NCRR	Glaser Pediatric Research Network http://www.gprn.org/ CF Foundation Therapeutic Development Network (CF TDN) http://www.cff.org/ Clinical and Translational Science Awards (CTSA) Consortium http://ctsaweb.org/upenn.html
NEI	Pediatric Eye Disease Investigator Group (PEDIG) http://public.pedig.jaeb.org/ Studies of the Ocular Complications of AIDS (SOCA) network http://www.jhucct.com/soca/
NIMH	Pediatric Practice Research Group (PPRG) Research Units on Pediatric Psychopharmacology Autism Network (RUPP)
NIDDK	Biliary Atresia Research Consortium (BARC) http://www.barcnetwork.org/ The Environmental Determinants of Diabetes in the Young (TEDDY) http://teddy.epi.usf.edu/

(continued)

Table 18.1 (continued)

Funding institution	Specific network (and website if available)
NINDS	INCLIN TRUST (INCLIN) http://www.inclitrust.org/ American Spinal Muscular Atrophy Randomized Trials Consortium http://www.smafoundation.org/links.asp
NIAMS	Childhood Arthritis & Rheumatology Research Alliance (CARRA) http://www.arthritis.org/carra.php
Multiple institutes	Neonatal Research Network (NRN) – NICHD, NHLBI https://neonatal.rti.org/about/mls_background.cfm Pediatric AIDS Clinical Trials Group (PACTG)/International Maternal Pediatric Adolescent AIDS Clinical Trials (IMPAACT) Group – NIAID, ^a NICHD http://pactg.s-3.com/ Blood and Marrow Transplant (BMT) Clinical Trials Network (CTN) – NHLBI, NCI https://web.emmes.com/study/bmt/ Cooperative International Neuromuscular Research Group (CINRG) – NICHD, NCRR http://www.cinrgresearch.org/ Type 1 Diabetes TrialNet (Trial Net) – NIDDK, ^a NIAID, NICHD http://www.diabetestrialnet.org/tnet1.html Global Network for Women’s and Children’s Health – NICHD, ^a NCI, NIDCR, NCCAM http://gn.rti.org/ Southern California Permanente Clinical Trials – NIA, NCI, NEI, NINDS, NIDDK, NHLBI http://xnet.kp.org/clinicaltrials/ Pediatric HIV/AIDS Cohort Study (PHACS) – NICHD, NIAID, NIMH, NIDA, NIDCD, NHLBI https://phacs.nichdclinicalstudies.org/overview.asp Clinical Trials Network of Columbia U, Cornell U, and NY Presbyterian Hospital (CTN) – NHLBI, NIA, NEI, NIMH, NCI, NIND http://www.clinicaltrialnetwork.com/

^a Primary funding source

Several academic and industry-based contract research organizations (CROs) offer services for the conduct of pediatric trials but most of these are focused on providing trial management and infrastructure for multicenter trials as well as a data coordinating center. More recently the NIH has solicited applications for a pediatric trials network in an effort to further improve the efficiency of contractual arrangements and the conduct of trials that support the BPCA. Hence, although the recent past was fraught with difficulty in the conduct of pediatric clinical trials, these obstacles have less to do with the availability of trial infrastructure and more to do with the availability of the population and/or the ethics of a particularly study design.

18.2 Methods for Modeling and Simulation Applications

In discussing methodologies to support modeling and simulation applications in pediatrics, we address the types of study designs that are typically employed and also pediatric patients as a subpopulation. The actual pharmacometric methodologies

are not different than those employed in adult settings but considerations for how the pediatric condition is quantitatively identified from the human continuum can vary.

18.2.1 *Common Trial Designs for Pediatrics*

As discussed previously, pediatric investigation typically ensues only after substantial data is available in adults. Although the FDA and EMA have provided some guidance in the planning of pediatric investigations via a decision tree approach that is based on common dose-exposure and exposure-response expectations, the most common clinical evaluation involves (a) a confirmation of the PK and safety, (b) some level of PK/PD correlation with adults, (c) justification of dose selection, or (d) a Phase III trial in the event pediatric market exclusivity is sought. Currently, the timing of the pediatric investigation plan (PIP) required by the EMA is earlier than that the pediatric written request reply expected by FDA (roughly the end of phase I for the EMA/PIP vs. the end of phase II for the FDA). Some sponsors feel that the EMA PIP requirement occurs too early to know if they have a viable drug candidate. On a practical basis, this difference in timing also implies that the amount and nature of data available to decision makers varies. This has resulted in additional choices in the types of modeling and simulation approaches used to support the PIP as opposed to the FDA interaction. Principally, it has created an awareness and necessity to consider so-called “bottom-up” approaches to project pediatric dose-exposure relationships. These are discussed in detail later in this chapter.

Regarding differences in trial designs between adult and pediatric drug development programs, most of the differences reflect the compression in scope in the pediatric setting. The reality is that a single study often suffices for each phase of development; often only for phase I (PK/safety) if the pediatric and adult indications are the same and the PK/PD is similar. The PREA (Ward and Kauffman 2007) has created some financial incentive for pharmaceutical sponsors to pursue Phase III trials, but these have not always yielded meaningful results. A recent review of pediatric antihypertensive trials by FDA and academic scientists found some glaring trends in the study failures (Benjamin *et al.* 2008). The paper states, “We found poor dose selection, lack of acknowledgement of differences between adult and pediatric populations, and lack of pediatric formulations to be associated with failures. More importantly, our ability to combine data across trials allowed us to evaluate and potentially improve trial design.” Many of these were certainly avoidable and will be addressed in this chapter; it is also clear that the regulators see the merit in encouraging quality trial designs in order to limit study failures. This is especially relevant in pediatrics as there is seldom an opportunity to repeat a trial if the design was perceived as flawed or for some other reason that would support success from a modified design.

Table 18.2 provides a comparison of some common designs employed in both adult and pediatric settings. There is concern to minimize pediatric exposures and limit both noneffective treatments (doses) as well as doses outside the likely

Table 18.2 Comparison of basic trial designs utilized to support pediatric drug development with reference to adult counterparts

Design	Adult construct	Pediatric considerations
Phase I: PK/safety	Typically separate single and multiple dose trials with broad dose ranges supported by animal toxicology data and the desire to define the MTD	Usually single or multiple dose trial (typically single dose)
	Alternating panel, rising dose design common (three actives and one placebo per cohort)	Fewer dose groups bracketed around the doses likely to achieve adult exposures
	Sample size not based on hypothesis testing; exploratory PK used as initial estimates	Safety collected and examined relative to exposure but not with the intent of describing MTD (except in oncology)
	Dense sampling for PK (non-compartmental analysis [NCA])	Sample size based on power to detect a difference (<i>e.g.</i> 30%) in clearance between adjacent age strata and adults Sparse sampling; sampling designs altered in lower age/weight strata
Phase II: dose ranging PK/PD	Two to four doses with or without placebo are common	More than two doses is rare; often the dose range is narrow and difficult to separate based on exposure profiles
	Occasionally powered for efficacy; consideration as the supportive PK/PD trial coupled with a traditional Phase III trial at one of the same doses studied	Emphasis on confirming dose selection; sample size usually driven by available population and requirement for sample size minimums within age strata
	Duration usually consistent with the expected standard of care but shortened if proof-of-concept is sought	Occasionally extended to accumulate chronic safety but mostly short duration
Phase III: parallel group (control)	Parallel-group	Parallel-group
	Treatment vs. placebo or active control	Treatment vs. placebo (less common) or active control
	Sample size based on power to detect a difference with control	Sample size based on power to detect a difference with control but guided by available population
	Design can vary with claim intention (equivalence vs. superiority vs. non-inferiority)	Design seldom focuses on claims; seeks “positive” outcome
Effect-control (titration)	Basis for approval (primary endpoints) defined a priori by sponsor and FDA	Often a conflict between adult vs. pediatric outcomes as well as regulatory “buy in.”
	Titration study	Titration study
	Achievement of sustained surrogate thresholds consistent with well-managed patient vs. active or placebo	Thresholds often based on adult targets without challenge to pediatric PK/PD relationships
	Sample size based on power for comparison	Sample size based on power for comparison; guided by comparison across age strata as well

recommended range for pediatrics. Sampling is also conducted in a sparse manner and reliant on population model-based approaches for analysis even in the phase I setting. Although less of an issue in older children, this becomes a necessity in infants and neonates where the typical investigational review board (IRB) requirements limited the total blood collected on study to 3 mL/kg. Safety too is viewed somewhat differently. There is certainly a special emphasis on understanding the exposure risks of dosing children, particularly developmental risks. This does not come at the expense of defining the full dose-response curve in children however. The target dose range of interest is typically a subset of what has been studied in adults except of course in pediatric oncology settings where toxicity is still often a marker for efficacy. Likewise, the emphasis of safety evaluation is based on assessing whether the nature and severity of safety signals are similar in children vs. adults at the doses targeted for pediatric use, not necessarily at defining the therapeutic window exclusively from pediatric investigation.

18.2.2 Converting the Developing Child into the In Silico Child

Historically, dosing in children has been viewed as a scaling exercise with a simple normalization of body weight (BW) for the intended age (or weight) of a child (*P*, pediatric) applied to the adult (*A*) dose.

$$\text{Dose}_P = \text{Dose}_A \times \frac{\text{BW}_P}{\text{BW}_A}$$

In this manner, we need not understand the source of PK difference in the developing child, trusting only that the linear scaling of BW is a reasonable means to adjust dose. This approach tends to under-predict dose requirements across the pediatric continuum though it is not equally bad in all age/weight ranges (Johnson 2008). Substituting body surface area (BSA) for BW in a similar manner is used quite extensively in pediatric oncology settings under the assumption that similar “geometry” can be achieved with this transformation.

$$\text{Dose}_P = \text{Dose}_A \times \frac{\text{BSA}_P}{\text{BSA}_A}$$

It has also been reported that this expression under-predicts infant and neonate dosing requirements (Johnson 2007). Allometric or power models are used in various biological settings to adjust for size dependencies of growing/developing systems. The value of the exponent (“*b*”) in the equation below varies with the type of biologic variable being scaled. In the PK sense it is common to associate an allometric exponent of 0.75 for clearance-related variables and 1 for volume of distribution. There is certainly no consensus on the numeric validity of these generalized constants.

$$Y = a \times BW^b \begin{cases} b = 0.25, \text{ time-related variables} \\ b = 0.75, \text{ metabolic variables} \\ b = 1, \text{ anatomical variables} \end{cases}$$

It is relevant however that we recognize that the adjustments are focused on size and not the more complex biology of a whole living system. If we apply this approach to dose adjustment for children recognizing the relationship between clearance, volume of distribution and dose, we arrive at the following expression, which overpredicts dose requirements in children less than 1 year of age although it is superior to BSA in this age range (Johnson 2007).

$$\text{Dose}_P = \text{Dose}_A \times \left(\frac{\text{BW}_P}{\text{BW}_A} \right)^{0.75}$$

Thus there is no one simple way to generalize dose adjustment in pediatric populations from an adult dosage. This should really not be surprising given that the adult continuum over which fixed dosing is often recommended typically excludes elderly and obese populations treating them as “special” as well. A pharmacokinetic model is required to serve as the backbone of such consideration. There are choices with respect to compartmental vs. physiologic model with respect to the PK characterization; these are essentially driven by the availability of data from which these models can be constructed. In either case, expressions for dealing with the ontogeny of enzyme systems involved with drug metabolism and for describing the maturation process of organs involved with drug clearance is essential to account for the systematic deviations described above regardless of the structural model choice. As it is the most common situation, we will describe these relationships from the standpoint of a compartmental model structure under the assumption that we are describing the PK in children with some prior knowledge of adult PK.

Broadly speaking, we can target systemic clearance as a key population parameter from which both maturation (MF) and organ function (OF) require consideration when adjusting for pediatric populations. Consider the generalized population expression for clearance below:

$$\text{CL}_P = \text{CL}_A \times \left(\frac{\text{BW}}{70} \right)^{0.75} \times \text{MF} \times \text{OF}$$

Maturation is generally considered a continuous function (MF), which achieves an asymptote at the adult value (MF=1) at some finite point in development. Usually, the MF is derived from a time index related to birth. Expressions for MF based on postconceptual age (PCA), postmenstrual age (PMA), postnatal age (PNA), and gestational age (GA) have all been considered (Anderson and Holford 2008). Inconsistent use of terminology has limited the accurate interpretation of data on health outcomes for newborn infants, especially for those born preterm or conceived using assisted reproductive technology (Engle 2004) so one must be

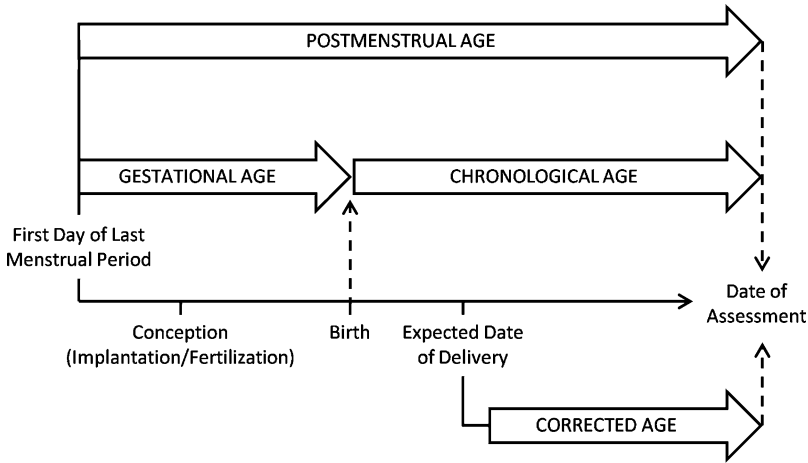


Fig. 18.1 Age terminology during perinatal period adopted from the American Academy of Pediatrics policy statement (Engle 2004)

careful when trying to derive these relationships from the literature. Figure 18.1 illustrates the relationship between the various age indices. “Gestational age” or “menstrual age” is the time elapsed between the first day of the last normal menstrual period and the day of delivery. “Chronological age” or “postnatal” age is the time elapsed after birth (Fig. 18.1). PMA is the time elapsed between the first day of the last menstrual period and birth (GA) plus the time elapsed after birth (chronological age). “Corrected age” (or “adjusted age”) is a term used to describe children up to 3 years of age who were born preterm (Fig. 18.1). Corrected age is calculated by subtracting the number of weeks born before 40 weeks of gestation from the chronological age. Corrected age and chronological age are not synonymous in preterm infants. “Conceptional age” is the time elapsed between the day of conception and the day of delivery.

For the purpose of modeling a key requirement is that the same time index be used when pooling data and that the accurate transformations of time are ensured. MF expressions vary from very simple relationships (Tod *et al.* 2008) as below

$$MF = \frac{PCA^s}{PCA_{50}^s + PCA^s}$$

to more complex expressions in which estimate the time to maturation (TM) as a parameter (Potts *et al.* 2009) with a cutoff point that designates a different slope on the MF (Hill_A vs. Hill_B).

$$\begin{cases} MF = \frac{1}{1 + [PMA/TM_{50}]^{Hill_A}}, & PMA \leq TM_{50} \\ MF = \frac{1}{1 + [PMA/TM_{50}]^{Hill_B}}, & PMA > TM_{50} \end{cases}$$

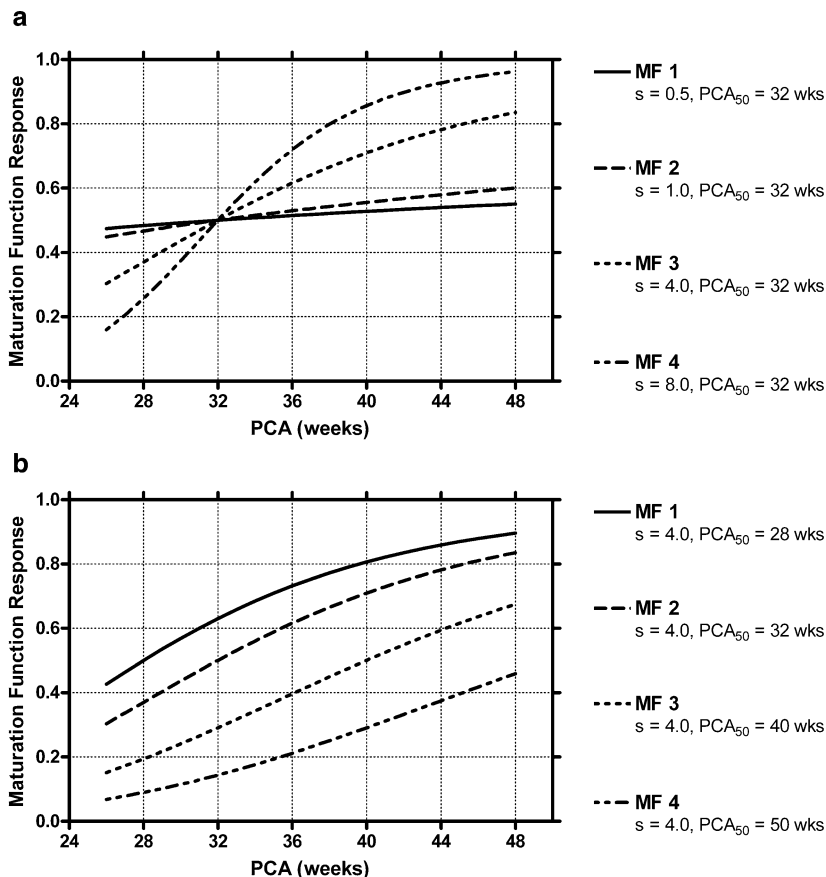


Fig. 18.2 Influence of slope factor (a) and maturation time (estimated by PCA_{50} in this example) (b) on maturation functions ($MF = PCA^S / PCA_{50}^S + PCA^S$) vs. age index (PCA in this example) used to adjust clearance in a developmental PK model

Based on these expressions it is clear that the most common MFs are empirically and not physiologically defined. Necessarily, their predictive value is closely linked to range of the observed data from which they are defined. As more of these relationships are reported for various drug attributes, it may be possible to generalize these empirical relationships. An important future consideration will be the extent to which these functions align with more physiologically-based relationships (*i.e.*, so-called “bottom-up” approaches). The shape of the general MF is shown in Fig. 18.2.

An OF value of 1 is associated with healthy children but can be higher or lower for critically ill children. These relationships are typically expressed as sigmoidal or hyperbolic functions employing a biomarker of OF (*e.g.*, serum creatinine or creatinine clearance for kidney function) but these factors can also be treated as covariates of clearance as either continuous or dichotomous variables depending on the target population. Often a more immediate consideration is the necessity of

addressing the age-dependent expression of metabolizing enzyme activity. Much is now known about the ontogeny of many of the cytochrome P450 family of enzymes (Kearns *et al.* 2003; Stevens *et al.* 2008) and recent efforts have incorporated ontogenic functions into drug clearance expressions (Johnson *et al.* 2006, 2008). As complementary data become available for phase II metabolism and transporters, these too can be employed when relevant. The manner in which ontogeny relationships are accommodated in the clearance expressions is similar to that defining MFs. Specifically, age-related functions that define the fraction of adult enzyme expression are factored into the overall clearance expression. Many of these (ontogeny functions, OF) have been defined for the P450 family (Johnson *et al.* 2006). A generalized expression would look like the following:

$$OF = \frac{a \times \text{Age}}{TM_{50} + \text{Age}} + b$$

Variations of this generalized expression are used for some enzymes; these typically involve the addition of a power function (exponent) on Age. It should be appreciated that even within the P450 family of enzymes there is great variability in the half-time of adult expression ranging from 3.5 days for hepatic CYP2C9 to 2.4 years for gut CYP3A (Johnson *et al.* 2006) as well as the functional level at birth. This is especially relevant when dealing with drugs that have multiple elimination pathways and/or involve multiple enzymes for drug clearance. Some functional expressions derived by Johnson *et al.* (2006) are shown in Fig. 18.3.

The appropriate incorporation of developmental influences is an active area of research for many engaged in pediatric clinical pharmacology research. As the experimental data is generated it is likewise important that model-based approaches evolve to accommodate the new knowledge. Important gaps exist in phase II metabolic pathways (Blake *et al.* 2005) and transporter ontogeny considerations although research in these areas looks promising (Ge *et al.* 2007; Strolin Benedetti and Baltes 2003).

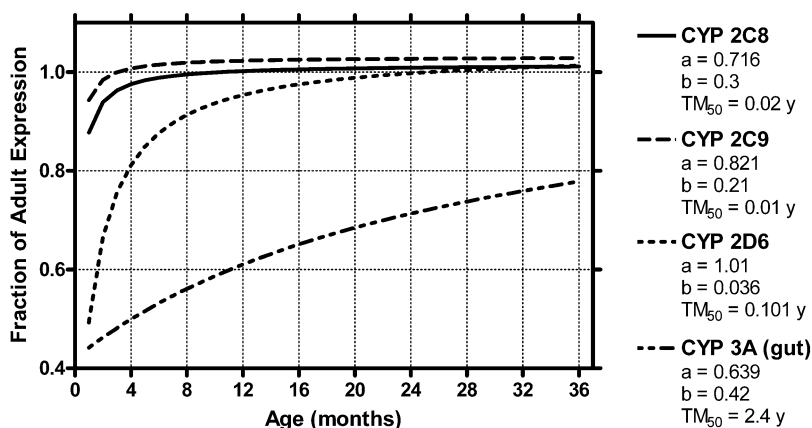


Fig. 18.3 Ontogeny-based functions for common CYP P450 enzymes used to adjust estimates of drug clearance

An important parallel effort involves the derivation of physiologic relationships that reflect important developmental processes. Current physiologically based pharmacokinetic (PBPK) models incorporate age/size dependencies that permit “scaling” of dose in a manner analogous to compartmental approaches. An important milestone in this process has been the development of the underlying physiologic parameter databases that permit such age-dependent projections. The extension of PBPK models beyond adjusting for size likewise must incorporate developmental and age-dependent physiologic factors to further improve their generalizability and utility for individualizing exposure prediction beyond the plasma compartment (Ginsberg *et al.* 2004; Yang *et al.* 2006). Table 18.3 lists several known relationships between age-dependent physiologic parameters and pharmacokinetic attributes and parameters. Additional detail is provided in Sect. 18.5.1.

Although the relationship between developing physiology and pharmacokinetic attributes is generally at least qualitatively appreciated, far less emphasis has been placed on the relationships between developmental changes and pharmacologic pathways. As these represent the target mechanisms of beneficial action and/or the off-target affects that lead to toxicity, they are often critical in the assessment of the pediatric therapeutic window. These relationships likewise have been absent in the discussion of pediatric development plans and decision trees used to define regulatory expectations for such plans. Table 18.4 shows several examples of systems known to exhibit age-dependent physiologic factors that are postulated to account for differences between pediatric and adult exposure targets or expectations in clinical response.

Table 18.3 Physiologic changes that correlate with the time course of PK attributes (ADME)

Pharmacokinetics		Physiologic considerations	
Attributes	Parameters	Time course	Relationships
Absorption	K_a , F_{abs} , F , MRT_{abs} , C_{max} , T_{max}	Typically occurs rapidly; gastric emptying changes with age	Mucosa changes with age Length/surface area changes with age Ontogeny of pre-systemic enzymes/transporters
Distribution	V_d ($V_{d_{\text{ss}}}$, etc.), f_u , BBB, RBC partition	Changes are rapid during the first weeks and months of life	Fat, water partition changes with age/development Change in protein composition and concentration with age Permeability changes with age/developmental status; lung capacity; skin penetration
Metabolism	CL , CL_m , formation rate constants	Varied time to near adult expression ranging from <1 months (CYPs 2C9 and 2C8) to >2 years (gut 3A4) (Johnson <i>et al.</i> 2008)	Ontogeny of systemic and organ-specific enzymes/transporters
Excretion	CL , CL_r	Varied time to adult function (Rodman 1994)	Kidney function maturation and ontogeny of renal transporters

BBB blood brain barrier, RBC red blood cell

Table 18.4 Examples of developmental influences on physiologic processes that may affect the pharmacodynamics of selected drug classes

Pathway or system	Developmental considerations	Drug classes potentially affected	PD response
Coagulation	Changes in hemostatic response – number and nature of platelet membrane receptors, clotting factors (Revel-Vilk and Chan 2003)	Antithrombotics, antiplatelet agents, vitamin K antagonists	Antifactor-Xa activity, IPA (%), bleeding rate and extent, etc.
Pulmonary system	Vascular wall composition of pulmonary and systemic capacitance vessels and their intravascular pressure changes through development (Belik <i>et al.</i> 2000)	Corticosteroids, calcium channel blockers, prostacyclins, endothelin-1 inhibitors	Collagen, major growth factors (TGF-beta, IGF-2, and bFGF), and cytokine gene expression
Immune system	Development of the immune system is a partial explanation for the increase in the incidence of infectious sequelae (Clapp 2006)	Antibiotics, anti-infectives, antiretrovirals, etc.	MIC determination, cell-kill curves, etc.
Cutaneous system	Newborns have an immature cellular immune defense system that leads to increased susceptibility to infections (Dorschner <i>et al.</i> 2003)	Topical antibacterials	Infection susceptibility
Brain stem	Developmental aspects of phasic sleep parameters, REM density and body movement, and the executive system (Kohyama and Iwakawa 1990)	Drugs which promote loss of sleep as side effect or agents to treat disorders such as ADHD	Correlation of sleep parameters with age likely reflects brain-stem maturation

18.3 The Pediatric CTS Model

The basic construct for a trial simulation model has been defined in other chapters of this book. As previously stated, the general framework is the same for pediatric application, though designs, age/developmental considerations, population characteristics, and the time course of study evaluation (and likewise disease progression) need to be defined specifically for the proposed pediatric setting. With these checkpoints in

mind, Table 18.5 illustrates the issues that the pediatric clinical pharmacologist and pharmacometrician must consider within the framework of a trial simulation model as defined by Holford (2006) for the adult scenario.

Table 18.5 Elements of a CTS model with consideration for differences between adult and pediatric components and model elements based on nomenclature described by Holford *et al.* (2000)

Components and elements	Considerations for pediatrics
I/O model	
PK	Models must accommodate size, organ maturation and developmental factors that affect the various underlying PK processes (see Table 18.2)
PD	Models must consider physiologic factors which affect target exposure requirements, or exposure sensitivities which otherwise imply a different therapeutic window from adults (see Table 18.3)
Disease progression	The time scale over which a disease progresses in children relative to adults or independent of adults (in the case of pediatric-specific indications) must be defined relative to the window of clinical investigation. The impact of state of disease progression on enrollment criteria may be important for study completion/subject availability
Placebo response	Value of adult priors questionable; pediatric-specific expectations should be defined; may require input from thought leaders for new indications
Parameter covariate	Plausibility of pediatric-specific covariates needs to be evaluated as would justification for previously-defined adult covariates which may not be relevant in pediatric populations
Parameter variability	Consideration for potential differences with adult variance estimates or model-based expressions
Residual	Consideration for residual vs. inter-occasion variability and potential confounding with progression from developmental stage
Pharmacoeconomics	Consideration for scenarios with and without pediatric formulation should be made; should consider off-patent use and distribution in developing countries (compassionate use)
Covariate distribution model	
Demographics	Potential for site differences (confounding response) in demographics may be relevant; subpopulations where genetic linkages are plausible can be relevant (<i>e.g.</i> , sickle cell and SMA)
Distribution and covariance	Impact of sample size on distributional assumptions (type) and inflation of covariance
Trial execution model	
Nominal design	Duration, dose range and observation windows represent key design parameters; sampling time and density with respect to age strata very relevant
Deviations from nominal design	Must address the necessity of certain sample size minimums in order to enroll subpopulations if they represent a target group; must consider stopping rules and rescue therapy in certain indications

The emphasis of many pediatric CTS exercises is the evaluation of drug performance over the age continuum or at least the FDA-defined age strata with the primary concern to ensure that adequate numbers of pediatric subjects within these age strata are enrolled and administered a dose that yields comparable exposures to adults (unless a pediatric therapeutic exposure has been defined). Equally important is that a sampling design is proposed to ensure that the primary PK/PD parameters of interest can be obtained from the proposed trial design. This outcome is attained usually through a compromise between optimal design and clinical practicality. Considering the weight range of premature newborns, this can present a major challenge even if the bioanalytical method has been refined to cope with small sample volumes. In many situations, it is simply not possible to sample more than 2–3 occasions because of such constraints. A commonly employed strategy is to randomize subjects to different (two or more) sampling schemes so that the pooled dataset contains the information content required to estimate key parameters. Several of the examples provided at the end of the chapter illustrate this approach and a more detailed discussion of the analysis stages for the common PK/safety design is discussed in the Sect. 18.3.2.

Hence, the pediatric CTS objectives are commonly focused on the dose-sample size-sampling scheme interface. This can become very complex depending on the PK attributes of the target species as mentioned previously but also based on biopharmaceutic issues and formulation requirements. For example, as children under the age of six are typically unable to swallow tablets/capsules effectively, liquid or granule (sprinkles) formulations are often sought and hence equivalence becomes a concern. Assumptions regarding the outcome of adult food effect trials may not be valid in these settings. Moreover, dealing with fixed dose multiples may present challenges to scaling (both from a manufacturing and clinical perspective). An important output then for these efforts is to provide the likelihood that the proposed design yields the desired milestones. This is obviously the impetus behind using CTS in this setting as it necessitates replication within scenario and under various assumptions regarding the certainty of parameter estimates – usually defined by the prior probabilities that such estimates reflect reality.

18.3.1 Priors for Pediatric CTS

Priors are an essential part of modeling and simulation. In the Bayesian context they help define the expectation from a proposed experimental design as well as its outcomes. Priors do not have equal value however and the proximity of the prior to our intended setting will improve the validity of our simulations and predictions. One of the more challenging aspects of supporting CTS approaches in pediatrics is the identification of reliable priors from which parameter and covariate distributions can be considered.

We can obtain priors from many sources based on the availability of data. These include studies in older children, pediatric populations that differ from the target

indication, adults, animals, *in vitro* experiments, and physiochemical properties of the target agent itself. Of course, it is possible to select priors from multiple sources as long as one recognizes the uncertainty in applying the prior and the methodological approach(s) necessary to connect the data/models together. Figure 18.4 shows the hierarchy of data potentially available as priors for pediatric CTS along with the techniques used to connect the various data and model elements. Figure 18.4 also illustrates the data used in the “top-down” vs. “bottom-up” approaches discussed later in the chapter.

While the prior may serve as a bridge, one aspect of the trial simulation will require the projection of dose-exposure, exposure-response and/or response-outcome relationships onto realistic normal or critically ill pediatric population. Distributions can certainly be defined to fulfill this requirement, but resampling from actual pediatric populations will always provide more confidence in these relationships particularly if they are indexed against potentially plausible covariates (age, weight, BMI, gender, race, genotype, phenotype, etc.) where covariance can more easily be established.

The usual starting point is the actual pediatric population of interest. Depending on the indication, foundations or consortiums may exist that assemble patient registries where such data can be requested. This is the case for the children’s oncology group (COG), the spinal muscular atrophy (SMA) foundation and the Pediatric AIDS Clinical Trials Group (PACTG). Additional online resources are becoming available as well. Table 18.6 lists some available resources from which pediatric priors can be obtained. Of interest, the Lexi-Comp online system provides text-based summaries of many pediatric PK and PK/PD studies from which dosing guidance is supported. Many of these are not described in the drug monograph. The

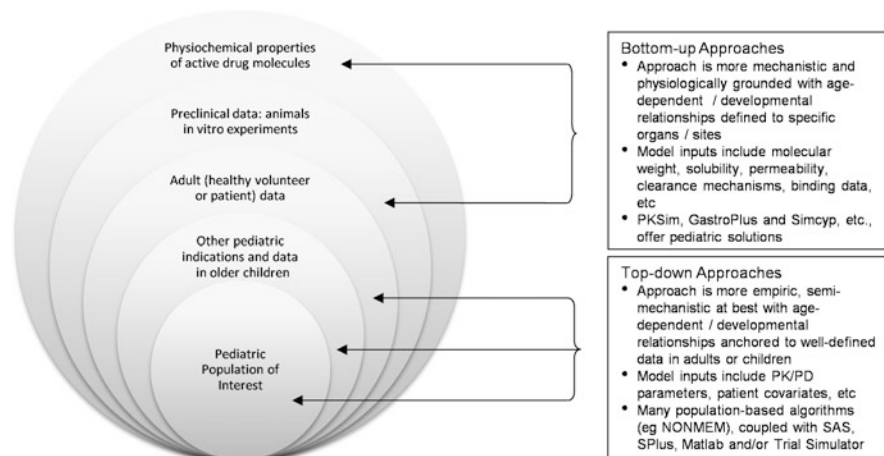


Fig. 18.4 Data hierarchy for identification of priors used in various pediatric modeling and simulation applications with corresponding approaches used to construct the simulation model

Table 18.6 Pediatric-specific data repositories

Data source	Access	Data elements available
National Health and Nutrition Examination Survey (NHANES)	Researchers worldwide; survey data available on the internet and on CD-ROM (http://www.cdc.gov/nchs/surveys.htm)	Demographic, socioeconomic, dietary, and health-related questions. The examination component consists of medical, dental, and physiological measurements
Pediatric Health Information System (PHIS) through the Child Health Corporation of America (~40 institutions)	Member institutions can register at www.chca.com and select PHIS as requested site for access	Member-specific standardized data on demographics, diagnoses, procedures, interventions, and outcomes for patients admitted to participating institutions
Lexi-Comp on-line. Internet-based drug information platform for multi-user groups in a networked system (http://webstore.lexi.com/ONLINE)	Available to individuals or institutions via license agreement. Database tables that are compatible with Oracle [®] , SQL Server [®] , and MySQL [®]	Drug interactions, allergies, therapeutic duplication, dose range, indications, cross reactivity, side effects, pharmacology, pregnancy and lactation precautions, warnings, references, flat text dosing, common prescriptions, drug disease interactions
National Institute of Child Health and Development (NICHD) PeDAR (PPRU)	Under development. Access granted to participating PPRU sites; broader access likely in the future	Data elements derived from pediatric clinical pharmacology studies conducted by the PPRU (PK and some PD)

NHANES data is very helpful with respect to demographic data in children, particularly age, weight, gender, etc. that can be used to sample from as opposed to creating distributions for each of these covariates. This is particularly helpful when considering age or weight criteria for dose adjustments across pediatric subpopulations or consideration for BSA vs. allometric (weight-based) expressions for adjusting dose or expressing PK parameter-size functionality.

An additional concern for the valuation of priors is the potential problem that data pooling can create particularly when the design, population, dosing (route and regimen) and/or formulations vary across studies. Specifically, the diversity of the underlying data used to define models that generate parameter estimates (priors) can necessitate a structural and/or covariate model, which is not relevant to the intended pediatric CTS model. For example, during the development of an adult drug product, different formulations are likely to have been evaluated in healthy volunteers or patients. Pooling PK data across formulations with varied absorption profiles particularly when bioavailability may be correlated with formulation or when food effects vary by formulation may require a more complex structural model to describe such formulation-dependent shifts in PK

attributes. Most importantly, the inclusion of studies describing early formulation development in adults may be irrelevant to the pediatric setting. In many cases the most straightforward approach is to eliminate the data that does not extrapolate to the likely pediatric use. In other situations, one can use a more complex model with refined expectation about the pediatric formulation (*e.g.*, generalized expressions about drug release relative to age dependency on absorption parameters), especially if it is not yet developed. In any case, pooling adult data in an effort to guide expectations about pediatric PK, PK/PD, or PD-outcome relationships should be based on criteria that at least qualitatively judge the relevance to the pediatric clinical setting.

18.3.2 Typical Workflow

There is a typical progression of modeling and simulation activities to support the development and use of a pediatric CTS model. Although the CTS model is inherently based on constructing simulation schemes that test the sensitivity of design, population, and conduct factors against a well specified model that encompasses the variability in the target population, PK, PK-PD, and/or PD-outcome relationships, there is a flow for the creation of objectives and construction that typically represents a team-based exercise. Figure 18.5 illustrates the general stages of a pediatric CTS project. Though the details of the stages are necessarily project specific, this schematic depicts the common stages along with the deliverables by stage.

An essential component of the exercise is the effective communication of the results along with their interpretation. It is growing increasingly common to include the results of the modeling and simulation exercise into regulatory documents as well as the transfer of the entire simulation model so that regulatory authorities may also gain confidence with the recommendations of the sponsor. The regulatory agencies in the United States and Europe have become increasingly interested in the use of CTS in pediatrics particularly on the use of adult priors to leverage the design of pediatric trials (Abernethy and Burckart 2010; Holford 2010; Madabushi *et al.* 2010).

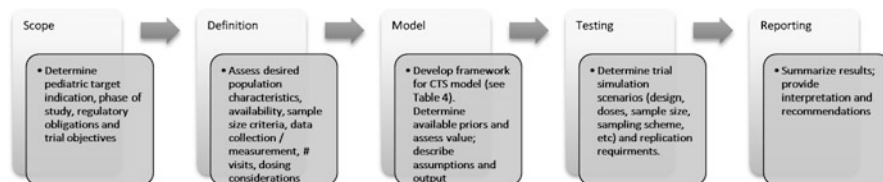


Fig. 18.5 Schematic representing the typical workflow for a pediatric CTS project

18.4 Examples

Several examples of modeling and simulation approaches applied in varied pediatric settings have been provided to illustrate the techniques discussed previously. Emphasis is placed on showing the connectivity of the objectives to the proposed workflow as well as the interpretation of results and recommendations for trial design or dosing considerations.

18.4.1 Safety/PK Trial to Fulfill Regulatory Requirements – Low Molecular Weight Heparin

The use of low molecular weight heparin (LMWH) in children represents an example where pediatric use is different from that in adults where the data attesting to their safety and efficacy resides. In general, LMWHs are used in both prophylactic and treatment deep vein thrombosis (DVT) settings with clinical evaluation occurring predominantly post hip or knee replacement surgery. This is not the case in children where the primary clinical evaluation has occurred in children at risk for thromboembolism (TE) usually because of either congenital or acquired prothrombotic disorders. Congenital disorders consist of protein C, protein S, antithrombin, plasminogen and/or Factor V Leiden, prothrombin gene defect, or dysfibrinogenemia. The most predominant acquired prothrombotic risk factor is the presence of a central venous line. Positive outcomes for pediatric trials are based in part on the demonstration of successful management of LMWH administration in the target pediatric patient population. Although multiple disease foci are relevant, LMWH therapy in these patients is often judged based on the ability to keep a patient's anti-Xa activity within a perceived therapeutic window. An important objective of these trials is the investigation of the PK/PD behavior of the LMWH in question (dalteparin) with the goal of characterizing dose-exposure and exposure-response relationships.

For a proposed prospective trial, the basis for the simulations was a population-based, PK/PD model developed from an open-label, dose-finding trial in children (>36 weeks GA, 16 years) with objectively confirmed TE. A total of 43 children were enrolled in the study, 9 patients were incomplete, 4 had a thrombotic event requiring therapeutic heparin and 5 withdrew voluntarily, 34 received drug, and 31 contributed PK data. The population PK/PD model that described the time course of anti-Xa activity was based on a two-compartment PK model with first-order absorption with allometrically scaled clearance (CL and Q) and central and peripheral compartment volume of distribution with a proportional CV error model and endogenous anti-Xa activity as a baseline parameter. The first-order conditional method (FOCE) with η - ε interaction was used for method/estimation of final parameter estimates. Preliminary analysis suggests that the median maintenance

dose to achieve the target anti-Xa level was varied and correlated with indices of body size (age and weight).

The clinical results of the study (Mitchell *et al.* 2007) and the results of the population analysis (Barrett *et al.* 2008a, b) have been previously reported. The primary assumption relevant to the prospective trial was that the PK/PD response to dalteparin in children with TE is similar to the planned target population, principally children with cancer. As the target age range (neonates to 18 years) was similar, demographic alignment is expected as well. Hence, the final population model and parameter estimates were used to construct simulation scenarios to evaluate the impact of sampling scheme (timing of blood sample collection for anti-Xa activity) and sample size within and across age strata. There were two primary objectives for the simulation exercise:

- Evaluate sample size: a total N of 10–50 pediatric patients ($N = 2, 4, 6, 8, 10$ per age strata)
- Evaluate sampling schemes to ensure accurate assessment of key parameters: single and two-point sample densities and impact of randomization across strata

Single-point designs were analyzed during the pilot coding of the simulation solution and performed poorly with an unacceptable number of trial evaluations (based on the simulated sampling) unable to converge in NONMEM upon estimation of the simulated designs regardless of sample size. Two-point designs with different sampling windows (Design 1 = 1–3, 5–8 h or Design 2 = 3–5, 8–12 h) were proposed by the study steering committee. Each of the 10 scenarios (5 sample size categories \times 2 sampling schemes) was evaluated with 100 trial simulations per design examined. Each of the ten sampling scheme/sample size combinations required a unique dataset to be created. Matching population demographics (age, weight, gender, etc.) were obtained from the original population dataset from the pediatric TE trial in order to mimic the “to-be-evaluated” target population.

The basic process involved refitting each of the 100 simulated trials using the historical population model. Comparison of the population parameter estimates from the simulated data with the original model parameters used to generate the source data was made to examine if the scheme and sample size was adequate. The calculation of bias is based on these deviations was calculated on a percentage scale. The entire workflow for the simulation analysis is described in Fig. 18.6. Batch processing of the NONMEM simulation jobs was accomplished via PERL scripts and the calculation of bias for key parameters (CL, V, and K_a) was performed in SAS. The precision of the scenario about each parameter is obtained by examining the distribution of the individual deviations about the expected value of 0% bias. Box-n-whisker plots of the bias and precision were generated using SPLUS.

The single-point designs (4, 7, 12, 24 h) had difficulty with respect to run convergence in NONMEM and yielded unacceptable bias in CL and/or Vd when convergence was attained as previously discussed. It was also suggestive of age-specific bias because of shifts in absorption (with age) resultant from the single

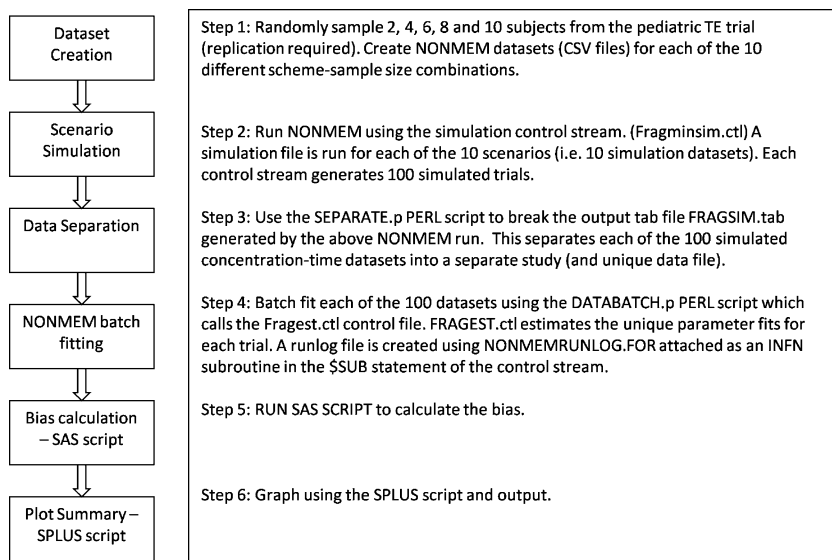


Fig. 18.6 Workflow for simulation execution to evaluate sample size and sampling scheme considerations for the pediatric LMWH trial

point sample collection within age strata. Box-n-whisker plots showing the precision and bias about key parameters generated from the simulated datasets for each of the two-point – sample size designs are shown in Fig. 18.7a–f.

In all cases, when evaluating the 2, 6 and 4, 10 vs. 3, 8 and 5, 12 randomized two-sample designs, the 3, 8 and 5, 12 design performed more efficiently with respect to estimation of CL and V. The 2, 6 and 4, 10 design was better for estimation of K_a . The choice of designs clearly favors the 3, 8 and 5, 12 design reflective of the 3–5, 8–12 h sampling window proposed in the protocol as there is a clear priority for CL over other parameters. Likewise, the sample size of 50 is well supported by the analysis as gains in precision even from a sample size increment of 40–50 are evident. Figure 18.7b shows the bias and precision from the recommended two-sample design and sample size. The interquartile range (indicated as a box height) for each of the key parameters evenly brackets the 0% bias designation and is within 20% bias for CL.

The results of the modeling and simulation exercise confirmed the appropriateness of the proposed sampling density and sample size to permit the assessment of potential age-dependent changes in dalteparin pharmacodynamics. The resultant population PK/PD analysis will permit (a) the determination of study-specific PK/PD parameters in the target population, (b) an examination of exposure-response (clinical endpoints) by age strata, and (c) dosing guidance and monitoring recommendations. These results will also allow re-examination of the pediatric TE Pop-PK/PD analysis (external validation) and assess the generalizability of the dalteparin dosing guidance across populations.

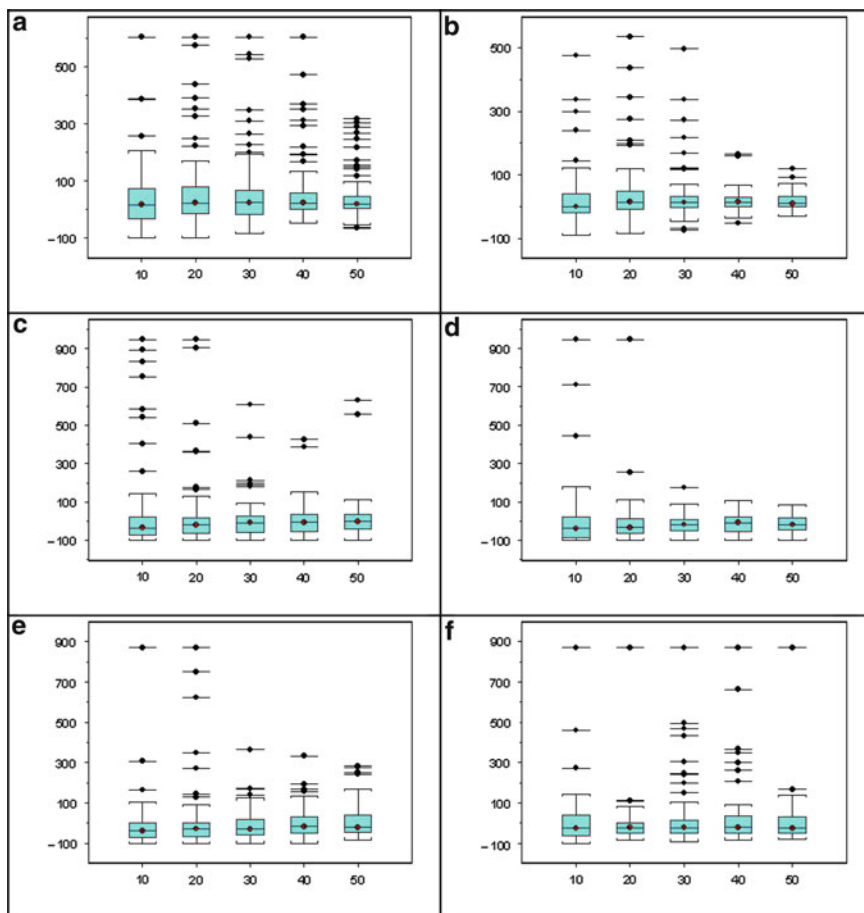


Fig. 18.7 Bias and precision of key PK parameters from simulation scenarios ($N = 100$ trials/scenario) of Dalteparin exposure resultant from different sampling designs and varied within age strata sample size ($N = 10-50$; 2-10 subjects/5 age strata): Clearance – design 1 (a), Clearance – design 2 (b), Volume of distribution – design 1 (c), Volume of distribution – design 2 (d), Absorption rate constant – design 1 (e), Absorption rate constant – design 2 (f). *Y*-axis represents % deviation from population estimates

18.4.2 BPCA Trial: Written Request for Actinomycin-D and Vincristine in Children with Cancer

Although actinomycin-D (AMD) and vincristine (VCR) have been used for the treatment of childhood rhabdomyosarcoma and Wilms tumor for over 40 years, there is virtually no PK information from which safe and appropriate age-based pediatric dosing can be derived. When treated with equivalent body-weight adjusted doses of AMD and VCR, infants and young children experience higher

toxicity rates than older children. For example, children with rhabdomyosarcoma under the age of 36 months who receive AMD VCR, and cyclophosphamide have a 15% risk of hepatopathy compared with a 4% risk in older children (Arndt *et al.* 2004). The current dosing paradigm for AMD and VCR administration to children less than 1 year of age dictates that doses should be reduced by 50% to avoid hepatic and neurotoxicity. It is not known whether this increased incidence of toxicity is due to differences in drug disposition or to pharmacological differences.

In an effort to define the AMD and VCR dose-exposure relationships and to quantify the effects of maturation on drug disposition, a modeling and simulation approach was undertaken to support a grant awarded to the COG through the BPCA. The goals of the clinical project were to propose a study design that would accurately describe disposition of both drugs in pediatric patients, and to appropriately power the study. This consisted of (1) development of suitable actinomycin and VCR pediatric population PK models from limited data, (2) proposal of feasible clinical trial designs, (3) employment of the population PK model to simulate trial results given current knowledge and stated assumptions, (4) evaluation of trial design performance, and (5) selection of a suitable trial design based on the ability to accurately describe dose-exposure relationships.

A nonlinear mixed-effects model was constructed for actinomycin using pharmacokinetic data from 33 patients from ages 1.6 to 20.3 years old (Mondick *et al.* 2008). Demographic data (age, weight, and gender) were examined as covariates for the ability to explain interindividual variability in AMD pharmacokinetics (PK). A three-compartment model with first-order elimination was chosen as the structural model with allometric expressions incorporating BW to describe the effects of body size on AMD PK. Age and gender had no discernable effects on AMD PK in the population studied. The VCR population PK model consisted of a two compartment model with linear scaling of parameters to BW, which was constructed from PK studies that were reported in the literature (Crom *et al.* 1994; de Graaf *et al.* 1995; Gidding 1999; Groninger *et al.* 2002; Sethi and Kimball 1981).

Various limited sampling schemes were evaluated to assess study design performance. Based on discussions with the project team, it was decided that patients could be available for PK sampling up to 6 h following actinomycin administration on the first study day. Additionally, 25% of patients could return to the clinic for an additional PK sample 1–4 days after the initial dose. It was also proposed that each patient could supply three to four PK samples for a given cycle. Based on the simulation results, a study design was chosen where patients (age range of <1–17 years) were randomized to one of two sampling schemes: Schedule 1: 5, 10 min, 2–3, 24–28, and 48–96 h; Schedule 2: 5 min, 0.75–1.5, 5–6, 24–28, and 48–96 h. This sampling scheme was found to be robust across the uncertainty in exposure metrics for both agents.

An analysis was then performed to examine the effect of maturational clearance changes in infants on exposure. Because there is no information available regarding the PK of AMD or VCR in this population, a range of effects was assumed, spanning a range of no difference in children under one to a fourfold decrease in clearance at an age of 3 months old. The design was then tested for the ability to

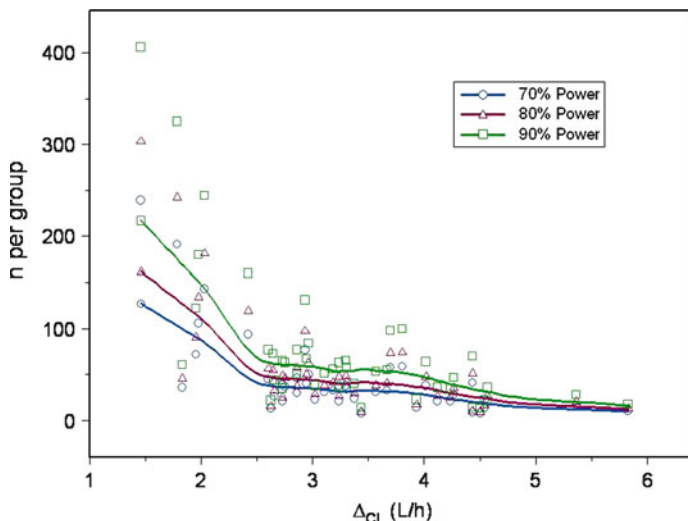


Fig. 18.8 Power – sample size analysis required to detect a 30% change in clearance in children under the age of one based on trial simulation model. Individual curves for 70, 80 and 90% power shown. The x -axis refers to the actual difference in Actinomycin clearance (Δ_{CL}) between children less than and greater than or equal to 1 year of age

suitably characterize this decrease in clearance. A power analysis was performed to determine the number of children less than 1 year needed to sufficiently estimate possible age effects, and the results of the power analysis were then confirmed via simulation. Our analyses suggest that a sample size of 35 patients in each age group would be sufficient to capture differences in clearance across age brackets (<1 year, ≥ 1 to <3 years, ≥ 3 to <12 years, and ≥ 12 to <17 years) (see Fig. 18.8).

A feasible and informative trial design was identified for the simultaneous evaluation of AMD and VCR pharmacokinetics in pediatric patients with Wilms' tumor or rhabdomyosarcoma. This design was modified to be robust across the uncertainty in key exposure metrics and probable maturational changes in young children. Results of this effort have been incorporated into a prospective trial protocol to be conducted through the COG Phase I Consortium that is still enrolling patients at the present time (due to complete enrollment by early 2011).

18.4.3 Exploratory PK/PD Trial: Topiramate Dose Finding in Post Surgical Neonates

Cerebral white matter (WM) injury has been considered the primary form of brain injury and the cause of long-term motor, cognitive, and behavioral disabilities in the preterm infant. Similar WM injury is seen in term infants requiring newborn heart surgery for serious congenital heart defects (CHD). Approximately 30,000 infants

with CHD are born in the United States each year, with at least a third needing surgical intervention in early infancy. Thus, about 11,000 heart operations are conducted annually. Advances in cardi thoracic surgical and anesthetic techniques, including cardiopulmonary bypass (CPB) and deep hypothermic circulatory arrest (DHCA), have substantially decreased mortality, expanding the horizon to address functional neurologic and cardiac outcomes in long-term survivors (Bellinger *et al.* 1991, 2003; Benson 1989; Ferry 1990; Wernovsky 2006). Basic science research in rat pups has identified that topiramate (TPM) can prevent WM injury by blocking developmentally regulated AMPA receptors, responsible for injury to vulnerable precursors of oligodendroglia (Cha *et al.* 2002; Follett *et al.* 2000, 2004).

In an effort to provide guidance to the design and conduct of the proposed oral TPM studies in newborns undergoing modified ultrafiltration (MUF) and CPB, simulations were undertaken to examine (a) the expected dose-exposure relationship, (b) the sampling scheme for the timing of blood collections, and (c) the sample size requirements. As this trial is novel in design and population with respect to TPM, much of the prior knowledge used in this exercise is contained in previous published experience with oral TPM in older children (Battino *et al.* 2005; Dahlin and Ohman 2004; Glauser *et al.* 2005; Mikaeloff *et al.* 2004), recent preclinical experiments with TPM in the pig and the previous experience with drug milrinone in children undergoing CPB and MUF (Zuppa *et al.* 2006). The primary focus of the proposed study was to verify the PK behavior of TPM in the newborn undergoing CPB and MUF as part of their standard of care. Results from this study will be used guide clinical investigation in anticipation of an IV formulation (under development). An important aspect of this initial trial is to confirm the pharmacokinetics of TPM during MUF/CPB and post-procedure during recovery. Investigations to explore design dependencies are reliant on nonlinear mixed-effect modeling and Monte Carlo simulation.

The underlying structural pharmacokinetic model for topiramate was a two-compartment disposition model with an additional MUF compartment to reflect the increased volume of distribution available during this phase. Because both V_d and CL are changing dynamically owing to the time-dependent application of vascular circuitry, fluid removal and filtration, and renal impairment as shown in Fig. 18.9, the simulation model must likewise be informed. Complicating these known fixed, nonrandom effects, are patient-specific random effects that dictate the individual differences in patient response. These effects are evident in the time to regain equilibrium in the pharmacokinetics on MUF/CPB. Based on the design of the trial, the drug kinetic model is defined by three distinct phases as below (Table 18.7):

- Phase I (baseline): Patients are dosed with 12.5 mg/kg BID (25 mg/kg/day) for 3 days. Normal drug kinetics applies and there is no additional dosing beyond this phase of the study. Two samples per day are to be collected. The scheme is relatively random except that consideration for late night sampling is given.
- Phase II (MUF/CPB): Procedure lasts 30 min. Samples are taken just before, during and immediately off bypass. It is assumed that the volume of distribution is doubled during this phase and that drug clearance is negligible.

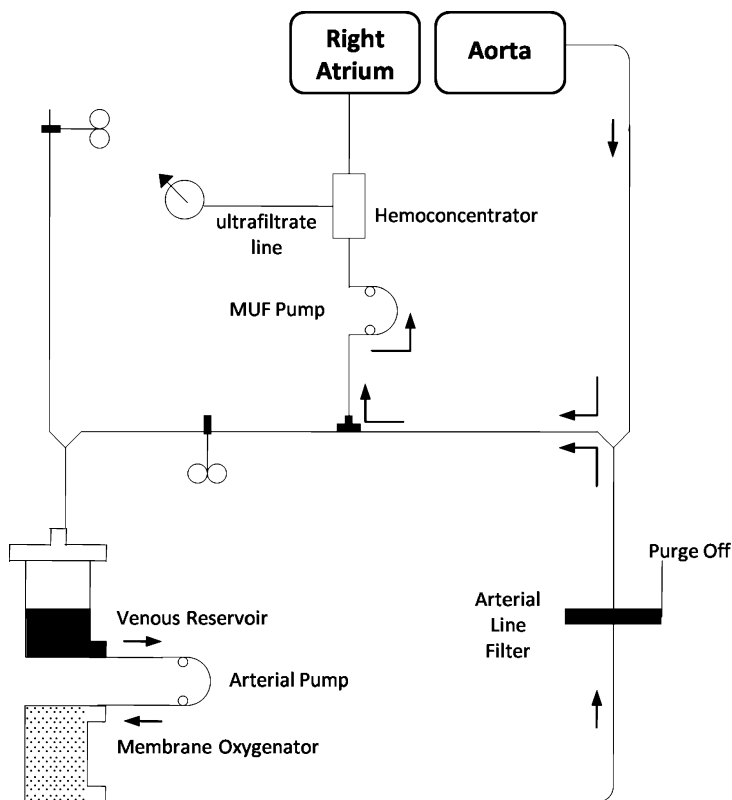


Fig. 18.9 Circuitry schematic illustrating the volume and clearance components to be accounted for in newborns receiving topiramate post surgery and during MUF/CPB and post procedure during recovery

Table 18.7 Pharmacokinetic parameter assumptions/priors used in the topiramate CPB/MUF pediatric (newborn post surgery) simulation model

Parameter	Phase I ^a	Phase II	Phase III
CL/F (L/h)	1.8	0.1	1.0
V/F (L)	8.0	16.0	8.0
Q/F (L/h)	0.5	0.5	0.5
V _{periph} /F (L/h)	1.0	1.0	1.0
K _a (h ⁻¹)	0.18 ^c	0.18 ^c	0.18 ^c

^aFrom $V = CL/K$ and published parameters (Mikaeloff *et al.* 2004)

^bInter-subject variance estimates on all parameters assumed at 35% CV; combined additive and proportional residual error model assumed: additive = 0.37 ng/mL SD with 35% CV proportional error

^cBased on the observed T_{max} between 1.4 and 4.3 h in adults

- Phase III (post-surgery): Two-days of postoperative recovery are used to observe the patient and examine the patient. This phase often discriminates patients based on renal function as many don't urinate well during this phase. Two samples per day for 2 days are obtained to monitor exposure and examine the recovery of drug clearance. It is assumed that only 60% recovery is obtained on average during this phase.

Simulations were generated to mimic the exposure of toprimate following the administration of 12.5 mg/kg BID and the procedures outlined previously. The population-PK model constructed from the priors and assumptions listed above was used to generate simulated patients based on the likely sampling windows and at various sample sizes. The criteria used to judge the adequacy of the proposed sampling scheme and study sample size is based on the examination of bias and precision around key parameters generated by refitting the simulated values to the original population model. The investigation will provide proof-of-concept for the dosing of TPM in neonates on MUF/CPB at doses which will yield target exposures. The sampling scheme proposed for the trial and evaluated in the simulations is based on sampling windows around each dose in Phase I, critical clinical endpoints in Phase II and at set intervals to examine drug elimination in Phase III. Table 18.8 shows the target sample allocation to phase with the actual value used in the initial simulation set.

For the purposes of sample size consideration, sample sizes of 10, 25, and 40 were considered. A sample size of 40 ensured that model parameters will be well-estimated for each of the targeted clinical phases. As the sampling density varies by phase, it is essential to obtain samples during phase II as projected to assess the impact of bypass on the pharmacokinetics. The mean prediction error in target PK parameters based on the model described above following 100 simulated trials ($N = 40/\text{trial}$) outperformed the sample sizes of 10 and 25 and verified the sample design as defined above.

Table 18.8 Sampling targets relative to phase and actual collection times used in the simulation exercise

Phase	Sampling window	Value of sample	Simulated time (post study start, h)
I	4–12 h	Elimination, dose 1	8
	12–24 h	Intrasubject var., baseline	14
	24–36 h		28
	36–48 h		42
	48–60 h		54
	60–72 h		63
	Pre-surgery/bypass	Effect of bypass	72
II			84
			84.25
	Immediately off bypass		84.42
III	Off-bypass – 96 h	Recovery time course	96
	96–108 h		108
	108–120 h		120
	120–132 h		132 h

18.5 Other Considerations

18.5.1 *The Role for “Bottom-Up” Approaches*

The use of a compartmental structural model to describe the pharmacokinetics of drugs in pediatric populations is somewhat limiting because of the nonphysiologic parameters that define such models. This is, in part, why nonphysiologic expressions for developmental and maturational effects are more commonly employed on a backbone of a compartmental-based structural model. “Bottom-up” approaches have the benefit of more physiologically based relationships to represent their structural models. Likewise, such model structures can more easily accommodate more physiologic-based maturational and developmental factors. Even so, we have not benefited from improved precision from these models largely because we do not yet have the quantitative understanding of the pathophysiologic factors that best define these phases in the developing child. Data from which these relationships could be defined would likely be invasive and otherwise difficult to obtain, though translational studies are filling in some of these gaps (Gittes 2009; Savidge *et al.* 2001).

More importantly, as the regulatory request for earlier pediatric development plans supersedes the generation of complimentary data in adults, these approaches have become more familiar to regulators and will certainly represent an important application of modeling and simulation to support pediatric development plans. Early experience (Gupta *et al.* 2006) suggests that these not only agree with “top down” approaches (reliant on adult data) for the typical child, but also that they allow additional consideration for simulation scenarios that address food and formulation effects (Kuentz *et al.* 2006; Parrott *et al.* 2009; Willmann *et al.* 2003) and drug interaction potential (Jamei *et al.* 2009).

18.5.2 *Pediatric Outcomes*

With the incentive provided by PREA regarding the extension of patent exclusivity for sponsors conducting efficacy trials in pediatric populations, the occasion to consider pediatric outcome trials has grown substantially. Several factors are often problematic in the design of such trials:

- Pediatric patients are not as easily identified, recruited or enrolled in many situations; often the available pool of patients for target indications is far less than the adult counterpart population (if one exists).
- Pediatric outcomes are often undefined in the context of what would represent the basis for clinical comparison to adults or as a response to be compared to placebo or active control groups.
- Most importantly, adult outcomes are not the same as pediatric outcomes for many indications. There is an acceptance of poor assumptions in this regard in

past pediatric trials and somewhat in current regulatory guidance in an effort to promote such trials even in the absence of portability of the adult outcome response to pediatric populations.

Regarding the issue of sample size for such studies, again simulation studies offer the ability to manage expectations for design and sample size considerations. It may be reasonable to relax the necessity of inference testing in certain pediatric populations, however, as in the case of the guidance for geriatrics:

The geriatric subpopulation should be represented sufficiently to permit the comparison of drug response in them to that of younger patients. For drugs used in diseases not unique to, but present in, the elderly, a minimum of 100 patients would usually allow detection of clinically important differences. For drugs to treat relatively uncommon diseases, smaller numbers of the elderly would be expected – Guideline for Industry.

Studies in Support of Special Populations: Geriatrics [ICH/E7 1994]

18.5.3 Pediatric Disease Progression

Disease progression models seek to define quantitatively the natural history of disease progression. One benefit to their construction is that the effectiveness of various treatment modalities can be judged against the patient status at various stages of disease. The construction of such models implies that the disease biology → clinical manifestation of disease → disease progression linkages are well-established and that longitudinal data within individuals exists to characterize the patient time course. Again, pediatrics represent a new challenge in this endeavor as the developmental and maturational factors must be understood if they confound or mask disease progression. In addition, the time course of pediatric disease relative to adults must be understood especially if a continuation to adult disease status is expected. While little has been done in the area of pediatric disease progression modeling, this is an active area of research for several groups and will likely form the backbone of pediatric CTS models in the future.

References

- Abernethy DR, Burckart GJ (2010) Pediatric dose selection. *Clin Pharmacol Ther* 87(3):270–271
- Anderson BJ, Holford NH (2008) Mechanism-based concepts of size and maturity in pharmacokinetics. *Annu Rev Pharmacol Toxicol* 48:303–332
- Arndt C, Hawkins D, Anderson JR, Breitfeld P, Womer R, Meyer W (2004) Age is a risk factor for chemotherapy-induced hepatopathy with vincristine, dactinomycin, and cyclophosphamide. *J Clin Oncol* 22(10):1894–1901
- Barrett JS, Patel D, Jayaraman B, Narayan M, Zuppa A (2008a) Key performance indicators for the assessment of pediatric pharmacotherapeutic guidance. *J Pediatr Pharmacol Ther* 13:141–155

- Barrett JS, Mitchell LG, Patel D, Cox P, Vegh P, Castillo M et al (2008b) A population-based analysis of dalteparin pharmacokinetics in pediatric patients at risk for thromboembolic events. *J Clin Pharmacol* 48(9):1107
- Battino D, Croci D, Rossini A, Messina S, Mamoli D, Perucca E (2005) Topiramate pharmacokinetics in children and adults with epilepsy: a case-matched comparison based on therapeutic drug monitoring data. *Clin Pharmacokinet* 44(4):407–416
- Belik J, Karpinka B, Hart DA (2000) Pulmonary and systemic vascular tissue collagen, growth factor, and cytokine gene expression in the rabbit. *Can J Physiol Pharmacol* 78(5):400–406
- Bellinger DC, Wernovsky G, Rappaport LA, Mayer JE Jr, Castaneda AR, Farrell DM et al (1991) Cognitive development of children following early repair of transposition of the great arteries using deep hypothermic circulatory arrest. *Pediatrics* 87(5):701–707
- Bellinger DC, Wypij D, duDuplessis AJ, Rappaport LA, Jonas RA, Wernovsky G et al (2003) Neurodevelopmental status at eight years in children with dextro-transposition of the great arteries: the Boston Circulatory Arrest Trial. *J Thorac Cardiovasc Surg* 126(5):1385–1396
- Benjamin DK Jr, Smith PB, Jadhav P, Gobburu JV, Murphy MD, Hasselblad V et al (2008) Pediatric antihypertensive trial failures: analysis of end points and dose range. *Hypertension* 51(4):834–840
- Benson DW (1989) Changing profile of congenital heart disease. *Pediatrics* 83:790–791
- Blake MJ, Castro L, Leeder JS, Kearns GL (2005) Ontogeny of drug metabolizing enzymes in the neonate. *Semin Fetal Neonatal Med* 10(2):123–138
- Cha BH, Silveira DC, Liu X, Hu Y, Holmes GL (2002) Effect of topiramate following recurrent and prolonged seizures during early development. *Epilepsy Res* 51(3):217–232
- Clapp DW (2006) Developmental regulation of the immune system. *Semin Perinatol* 30(2):69–72
- Crom WR, de Graaf SS, Synold T, Uges DR, Bloemhof H, Rivera G et al (1994) Pharmacokinetics of vincristine in children and adolescents with acute lymphocytic leukemia. *J Pediatr* 125(4):642–649
- Dahlin MG, Ohman IK (2004) Age and antiepileptic drugs influence topiramate plasma levels in children. *Pediatr Neurol* 31(4):248–253
- de Graaf SS, Bloemhof H, Vendrig DE, Uges DR (1995) Vincristine disposition in children with acute lymphoblastic leukemia. *Med Pediatr Oncol* 24(4):235–240
- Dorschner RA, Lin KH, Murakami M, Gallo RL (2003) Neonatal skin in mice and humans expresses increased levels of antimicrobial peptides: innate immunity during development of the adaptive response. *Pediatr Res* 53(4):566–572
- Engle WA (2004) Age terminology during the perinatal period. *Pediatrics* 114(5):1362–1364
- Ferry P (1990) Neurologic sequelae of open-heart surgery in children: an irritating question. *Am J Dis Child* 144:369–373
- Follett P, Koh S, Volpe J, Jensen F (2000) Protective effects of topiramate in a rodent model of periventricular leukomalacia. *Ann Neurol* 48:527
- Follett PL, Deng W, Dai W, Talos DM, Massillon LJ, Rosenberg PA et al (2004) Glutamate receptor-mediated oligodendrocyte toxicity in periventricular leukomalacia: a protective role for topiramate. *J Neurosci* 24:4412–4420
- Gaynor JW (1998) Use of modified ultrafiltration after repair of congenital heart defects. *Semin Thorac Cardiovasc Surg Pediatr Card Surg Annu* 1:81–90
- Ge Y, Haska CL, LaFiura K, Devidas M, Linda SB, Liu M et al (2007) Prognostic role of the reduced folate carrier, the major membrane transporter for methotrexate, in childhood acute lymphoblastic leukemia: a report from the Children's Oncology Group. *Clin Cancer Res* 13(2 Pt 1):451–457
- Gidding CE, Meeuwssen-de Boer GJ, Koopmans P, Uges DR, Kamps WA, de Graaf SS (1999) Vincristine pharmacokinetics after repetitive dosing in children. *Cancer Chemother Pharmacol* 44(3):203–209
- Ginsberg G, Hattis D, Miller R, Sonawane B (2004) Pediatric pharmacokinetic data: implications for environmental risk assessment for children. *Pediatrics* 113(4 Suppl):973–983

- Gittes GK (2009) Developmental biology of the pancreas: a comprehensive review. *Dev Biol* 326(1):4–35
- Glauser TA, Watemberg N, Mikaeloff Y, Nye JS (2005) Use of topiramate in very young children with refractory infantile spasms or refractory epilepsy. *Epilepsia* 46:200
- Groninger E, Meeuwse-de Boer T, Koopmans P, Uges D, Sluiter W, Veerman A et al (2002) Pharmacokinetics of vincristine monotherapy in childhood acute lymphoblastic leukemia. *Pediatr Res* 52(1):113–118
- Gupta M, Edgington AN, Willmann S, Adamson PC, Galinkin JL, Barrett JS (2006) Model-based approaches to investigate pharmacogenetic and developmental sources of variation in the pharmacokinetics of Midazolam after oral administration in children. *AAPS J* 8(S2):W4078
- Holford N (2010) Dosing in children. *Clin Pharmacol Ther* 87(3):367–370
- Holford NH, Kimko HC, Monteleone JP, Peck CC (2000) Simulation of clinical trials. *Annu Rev Pharmacol Toxicol* 40:209–234
- Jamei M, Dickinson GL, Rostami-Hodjegan A (2009) A framework for assessing inter-individual variability in pharmacokinetics using virtual human populations and integrating general knowledge of physical chemistry, biology, anatomy, physiology and genetics: a tale of “bottom-up” vs “top-down” recognition of covariates. *Drug Metab Pharmacokinet* 24(1):53–75
- Johnson TN (2008) The problems in scaling adult drug doses to children. *Arch Dis Child* 93(3):207–211
- Johnson TN, Thomson M (2008) Intestinal metabolism and transport of drugs in children: the effects of age and disease. *J Pediatr Gastroenterol Nutr* 47(1):3–10
- Johnson TN, Rostami-Hodjegan A, Tucker GT (2006) Prediction of the clearance of eleven drugs and associated variability in neonates, infants and children. *Clin Pharmacokinet* 45(9):931–956
- Johnson TN, Tucker GT, Rostami-Hodjegan A (2008) Development of CYP2D6 and CYP3A4 in the first year of life. *Clin Pharmacol Ther* 83(5):670–671
- Kearns GL, Robinson PK, Wilson JT, Wilson-Costello D, Knight GR, Ward RM et al (2003) Cisapride disposition in neonates and infants: *in vivo* reflection of cytochrome P450 3A4 ontogeny. *Clin Pharmacol Ther* 74(4):312–325
- Kohyama J, Iwakawa Y (1990) Developmental changes in phasic sleep parameters as reflections of the brain-stem maturation: polysomnographical examinations of infants, including premature neonates. *Electroencephalogr Clin Neurophysiol* 76(4):325–330
- Kuentz M, Nick S, Parrott N, Rothlisberger D (2006) A strategy for preclinical formulation development using GastroPlus as pharmacokinetic simulation tool and a statistical screening design applied to a dog study. *Eur J Pharm Sci* 27(1):91–99
- Madabushi R, Cox DS, Hossain M, Boyle DA, Patel BR, Young G, et al (2010) Pharmacokinetic and pharmacodynamic basis for effective argatroban dosing in pediatrics. *J Clin Pharmacol*, in press
- Mikaeloff Y, Rey E, Soufflet C, d’Athis P, Echenne B, Vallee L et al (2004) Topiramate pharmacokinetics in children with epilepsy aged from 6 months to 4 years. *Epilepsia* 45(11):1448–1452
- Mitchell LG, Barrett JS, Cox P, Vegh P, Patel D, Castillo M, et al (2007) Pharmacokinetics and dose-finding of fragmin in pediatric patients at risk for thromboembolic events. In: International society for thrombosis and haemostasis meeting, Geneva
- Mondick JT, Gibiansky L, Gastonguay MR, Skolnik JM, Cole M, Veal GJ et al (2008) Population pharmacokinetic investigation of actinomycin-D in children and young adults. *J Clin Pharmacol* 48(1):35–42
- Parrott N, Lukacova V, Fraczekiewicz G, Bolger MB (2009) Predicting pharmacokinetics of drugs using physiologically based modeling – application to food effects. *AAPS J* 11(1):45–53
- Potts AL, Anderson BJ, Warman GR, Lerman J, Diaz SM, Vilo S (2009) Dexmedetomidine pharmacokinetics in pediatric intensive care – a pooled analysis. *Paediatr Anaesth* 19(11):1119–1129
- Revel-Vilk S, Chan AK (2003) Anticoagulation therapy in children. *Semin Thromb Hemost* 29(4):425–432

- Rodman JH (1994) Pharmacokinetic variability in the adolescent: implications of body size and organ function for dosage regimen design. *J Adolesc Health* 15(8):654–662
- Savidge TC, Lowe DC, Walker WA (2001) Developmental regulation of intestinal epithelial hydrolase activity in human fetal jejunal xenografts maintained in severe-combined immunodeficient mice. *Pediatr Res* 50(2):196–202
- Sethi VS, Kimball JC (1981) Pharmacokinetics of vincristine sulfate in children. *Cancer Chemother Pharmacol* 6(2):111–115
- Stevens JC, Marsh SA, Zaya MJ, Regina KJ, Divakaran K, Le M et al (2008) Developmental changes in human liver CYP2D6 expression. *Drug Metab Dispos* 36(8):1587–1593
- Strolin Benedetti M, Baltes EL (2003) Drug metabolism and disposition in children. *Fundam Clin Pharmacol* 17(3):281–299
- Tod M, Jullien V, Pons G (2008) Facilitation of drug evaluation in children by population methods and modelling. *Clin Pharmacokinet* 47(4):231–243
- Ward RM, Kauffman R (2007) Future of pediatric therapeutics: reauthorization of BPCA and PREA. *Clin Pharmacol Ther* 81(4):477–479
- Wernovsky G (2006) Current insights regarding neurological and developmental abnormalities in children and young adults with complex congenital cardiac disease. *Cardiol Young* 16:92–104
- Willmann S, Schmitt W, Keldenich J, Dressman JB (2003) A physiologic model for simulating gastrointestinal flow and drug absorption in rats. *Pharm Res* 20(11):1766–1771
- Yang F, Tong X, McCarver DG, Hines RN, Beard DA (2006) Population-based analysis of methadone distribution and metabolism using an age-dependent physiologically based pharmacokinetic model. *J Pharmacokinet Pharmacodyn* 33(4):485–518
- Zuppa AF, Barrett JS (2008) Pharmacokinetics and pharmacodynamics in the critically ill child. *Pediatr Clin North Am* 55(3):735–755, xii
- Zuppa AF, Nicolson SC, Adamson PC, Wernovsky G, Mondick JT, Burnham N et al (2006) Population pharmacokinetics of milrinone in neonates with hypoplastic left heart syndrome undergoing stage I reconstruction. *Anesth Analg* 102(4):1062–1069

Part V
Evolving Methodologies in M&S

Chapter 19

Disease Progression Analysis: Towards Mechanism-Based Models

Stephan Schmidt, Teun M. Post, Massoud A. Boroujerdi, Charlotte van Kesteren, Bart A. Ploeger, Oscar E. Della Pasqua, and Meindert Danhof

Abstract Sustained disturbances of the biological homeostasis can result in chronic progressive diseases. The respective disease status as well as the corresponding effect of drug treatment on disease progression can be characterized at different levels of complexity, ranging from data-driven and descriptive to fully mechanistic approaches. Most of the currently employed disease progression models are mechanism-based and represent a mixture of these two extremes. Conceptually, mechanism-based disease progression models consist of three distinct parts: (1) a pharmacokinetic model to predict target exposure, (2) a pharmacodynamic model to characterize target binding, target activation, and transduction (receptor theory; dynamical system analysis), and (3) a disease model to characterize placebo response and disease progression. Once identified and validated, mechanism-based disease progression models can help understanding the behavior of the underlying disease system and, subsequently, support the identification of optimal dosing regimens using optimized clinical trial designs.

19.1 General Concepts

The objective of pharmacokinetic-pharmacodynamic (PKPD) modeling and simulation is to characterize and predict the effect of drugs in living organisms under physiological and pathophysiological conditions (Breimer and Danhof 1997; Danhof *et al.* 2005). In recent years, PKPD modeling has evolved from a descriptive, empirical discipline to a mechanistic science that has been increasingly employed in all phases of drug development as the theoretical basis for: (1) the selection of drug candidates, (2) lead optimization, and (3) the optimization of early proof-of-concept clinical trials (Derendorf *et al.* 2000; Miller *et al.* 2005; Danhof *et al.* 2007; Wang *et al.* 2008).

M. Danhof (✉)

Leiden-Amsterdam Center for Drug Research, Division of Pharmacology,
Leiden University, Leiden, The Netherlands
e-mail: m.danhof@lacdr.leidenuniv.nl

Mechanism-based PKPD models differ substantially from descriptive models as they contain specific expressions characterizing, in a strictly quantitative manner, processes on the causal path between drug administration and effect (Danhof *et al.* 2005). As a result, mechanism-based models have improved properties for extrapolation and prediction of clinical outcome and have become important tools for a more effective evaluation of the efficacy and safety of novel candidates during the drug development/approval process (FDA 2004; Danhof *et al.* 2005; Zhang *et al.* 2006; Lalonde *et al.* 2007; Bies *et al.* 2008; Ploeger *et al.* 2009). Despite these achievements, further advancement in this model-based strategy is necessary as current approaches often focus on the pharmacology of drugs rather than on the interaction between the drug, the biological system, and the disease process. It has become evident that to develop effective drug treatments, sufficient understanding of drug properties, the biological system, and the underlying disease processes is required. This concept has been applied in the area of disease progression modeling by combining models for the pharmacology of drugs with those for disease. Although substantial progress has been made in recent years in characterizing the pharmacology of drugs, such as in the areas of target exposure (PBPK) (Rowland *et al.* 2004), target binding and activation (receptor theory) (Danhof *et al.* 2007; Ploeger *et al.* 2009), and transduction and homeostatic feedback (dynamical systems analysis) (Zuideveld *et al.* 2001; Butcher *et al.* 2004; Butcher 2005), disease modeling is much less evolved. This is partly due to the fact that the etiology and the pathophysiology of most diseases are not fully understood. Lack of understanding of the natural course of disease, including underlying processes and progression, may result in underestimation of the importance of disease trajectory on the effect of drugs as well as of the implication of treatment effect (s) on the trajectory of a disease. This may lead to a poor rationale for treatment selection, dose range and, ultimately, limit disease management.

In conventional PKPD analyses the status of the biological system is generally assumed to be invariable with time and considered constant at baseline (Post *et al.* 2005; Danhof *et al.* 2007). This assumption does not hold for progressive, chronic diseases where biological functions deteriorate over time. Such deterioration usually manifests itself as clinical signs and symptoms that are characteristic for the underlying disease. For example, from a clinical perspective, degenerative diseases, such as Alzheimer's disease, rheumatoid arthritis, and osteoporosis progress in a somewhat continuous manner, whereas disorders, such as epilepsy, migraine, and depression show typically periodical patterns.

The predictive value of mechanism-based PKPD and disease progression modeling also relies on the analysis of biomarker response. Within this context, biomarkers are defined as strictly quantitative measures of processes that are located on the causal path between drug administration and effect (Danhof *et al.* 2005). To allow a closer distinction between the different process levels within this causal chain, a new classification system for biomarkers has been proposed (Danhof *et al.* 2005). According to this classification system, biomarkers can be separated into seven different groups: type 0, genotype/phenotype determining drug response; type 1, concentration of drug or drug metabolite; type 2, molecular target occupancy; type 3, molecular target activation; type 4, physiological measures; type 5,

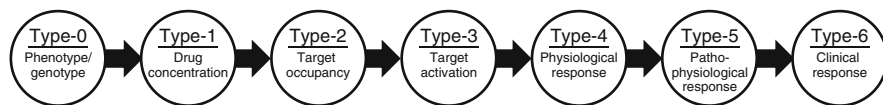


Fig. 19.1 Schematic representation of the concept of a cascading PKPD model for prediction of *in vivo* drug effects on the basis of intermediary biomarker responses. Figure and legend from Danhof *et al.* (2005)

pathophysiological measures; and type 6, clinical rating scales, as shown in Fig. 19.1 (Danhof *et al.* 2005). In combination, type 0–6 biomarkers provide comprehensive information on the interaction between the drug, the biological system, and the disease. This framework can be used as a qualitative and quantitative input for mechanism-based disease progression models (Lesko and Atkinson 2001; Danhof *et al.* 2005; Rolan *et al.* 2007). Once established and validated, these models allow studying (complex) dynamical systems and can be invaluable for understanding the differences between new and existing treatments during the course of a disease as well as for predicting clinical outcome (Danhof *et al.* 2005). Although the pertinent information on biomarker response vs. clinical response is either missing or available only at the end of phase 3 clinical trials for most investigational drugs, obtained data can be used to study the dynamics of the disease system, for the identification of targets and, subsequently, for the development of new drug candidates. Mechanism-based PKPD modeling and simulation approaches can support this process by serving as the scientific basis for selection, evaluation and validation of respective biomarkers (Danhof *et al.* 2005). Yet, the use of biomarkers, especially those used for regulatory purposes, remains restricted to drugs with a known mechanism of action and a well-established clinical effect (Lesko and Atkinson 2001; Danhof *et al.* 2005).

The presented biomarker classification system can be further expanded at levels 5 and 6 when taking into account the different levels, at which disease and the effect of drugs intervening with disease processes can be observed (Fig. 19.2) (Post *et al.* 2005). The most comprehensive description of the disease process can be derived by evaluating changes of a biological system at the molecular level (level I). Disturbances of the complex network between genetic, transcription-mediated and receptor-mediated events will eventually compromise biological functioning at the next level (level II; cellular level). Imbalances at the cellular level may result in alterations of organ function, which can then cause clinical symptoms or changes in clinical rating scales (level III). Ultimately, a sustained disturbance of homeostasis at levels I–III may result in an increased morbidity and mortality. In some cases, such as infectious diseases, an additional level of complexity is necessary as the functionality of the human organism is impaired by disease-causing pathogens. Three main features characterise the changes in biological function observed in each level, namely, the magnitude of time (rates), reversibility and the dimensionality of events.

The objective of this chapter is to provide a systematic overview of the concepts employed in disease progression modeling. First, an outline of the structural

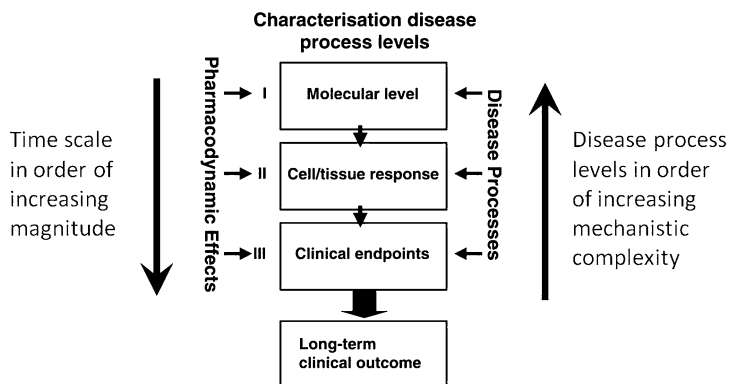


Fig. 19.2 Disease processes and pharmacodynamic effects can be observed at different levels of complexity. Changes of biological functions at the molecular (level I) and/or at the cellular (level II) can result in disturbances in a biological system's homeostasis, which is ultimately reflected in changes in clinical endpoints or rating scales (level III). Information obtained from all of these levels can be used to evaluate the progression of a disease and to predict clinical outcome. Figure and legend modified from Post *et al.* (2005)

models used to characterize disease progression at various levels of complexity will be provided, starting with descriptive models. Second, the qualitative as well as quantitative impact of therapeutic interventions on disease progression will be evaluated at each of these levels and will be illustrated with clinically relevant examples from various therapeutic areas. Finally, some of the challenges that typically arise during the development and validation process of disease progression models will be highlighted and approaches of how these challenges can be met will be presented.

19.2 Overview of Disease Process and Disease Progression Models

19.2.1 Descriptive Models

In theory, the progression of a disease, as well as the effect of drugs on the disease process, can be analyzed at each of the previously mentioned levels (Post *et al.* 2005). The first disease progression models were established based on clinical endpoints, clinical chemistry biomarkers, or rating scales (Chan and Holford 2001). For instance, changes in glomerular filtration rate in diabetic neuropathy (Bjorck *et al.* 1992; Gall *et al.* 1993; Lewis *et al.* 1993; Parving *et al.* 1995; Bakris *et al.* 1996; Crepaldi *et al.* 1998), Alzheimer disease cognitive assessment scale in Alzheimer's disease (Holford and Peace 1992), and Brief Psychiatric Rating Scale in schizophrenia (Kimko *et al.* 2000) were described using longitudinal linear

regression models (19.1). In these models, $S(t)$ represents the disease status at time t , S_0 the disease status at baseline, and α the rate of natural disease progression (Mould *et al.* 2007).

$$S(t) = S_0 + \alpha \cdot t \quad (19.1)$$

In (19.1), S_0 is a constant but can be modified to represent time-dependent functions, such as circadian rhythm. For some diseases, such as Parkinson's disease, more complex functions have been used to characterize the nonlinear change of disease status over time (Holford and Sheiner 1982; Chan and Holford 2001; Holford and Nutt 2008). Although untreated diseases usually progress in characteristic patterns, therapeutic interventions, including placebo, may have various effects on the trajectory of a disease.

In general, treatment effects can be classified into two different types: symptomatic and disease modifying. For both types of effect, the disease status is changed as a function of treatment ($f(T)$), which is comprised of active drug as well as placebo effects. Although the altered disease status is the result of a shift in baseline for symptomatic treatments (19.2), disease modifying interventions (19.3) affect the rate of disease progression as shown in Fig. 19.3a.

$$S(t) = (S_0 + f(T)) + \alpha \cdot t \quad (19.2)$$

$$S(t) = S_0 + (f(T) + \alpha) \cdot t \quad (19.3)$$

When drug treatment is discontinued, the disease will revert to its natural progression rate α , regardless of the type of treatment effect. However, the overall effect on disease status for symptomatic drugs is different from that of disease modifying drugs. Although the disease status of patients who had received symptomatic treatment is indistinguishable from that of untreated patients after treatment cessation, a disease modifying drug will result in a permanent improvement of the disease status compared to untreated patients (Fig. 19.3a).

Symptomatic treatments are believed to have a fast onset of effect compared to disease modifying effects, which take typically longer before they become noticeable. Symptomatic treatment effects can only reduce the severity of clinical signs and symptoms or change the biomarker response, whereas disease modifying treatments can slow, halt, or even reverse the progression of a disease (Chan and Holford 2001; Post *et al.* 2005). It should be noted that a combination of both symptomatic and disease modifying treatment effects also exists (Chan and Holford 2001). A clear distinction between the two types of effect based on clinical endpoints/biomarker response is difficult if the dominant effect masks the less pronounced one (Chan and Holford 2001) or if symptomatic interventions have a very slow onset of effect (Ploeger and Holford 2009). In the latter case, both symptomatic and disease modifying treatments seem to change the rate of disease progression and a differentiation between the two is not possible when solely based on visual inspection of the effect-time course (Fig. 19.3b). Instead, information on the nature of a treatment

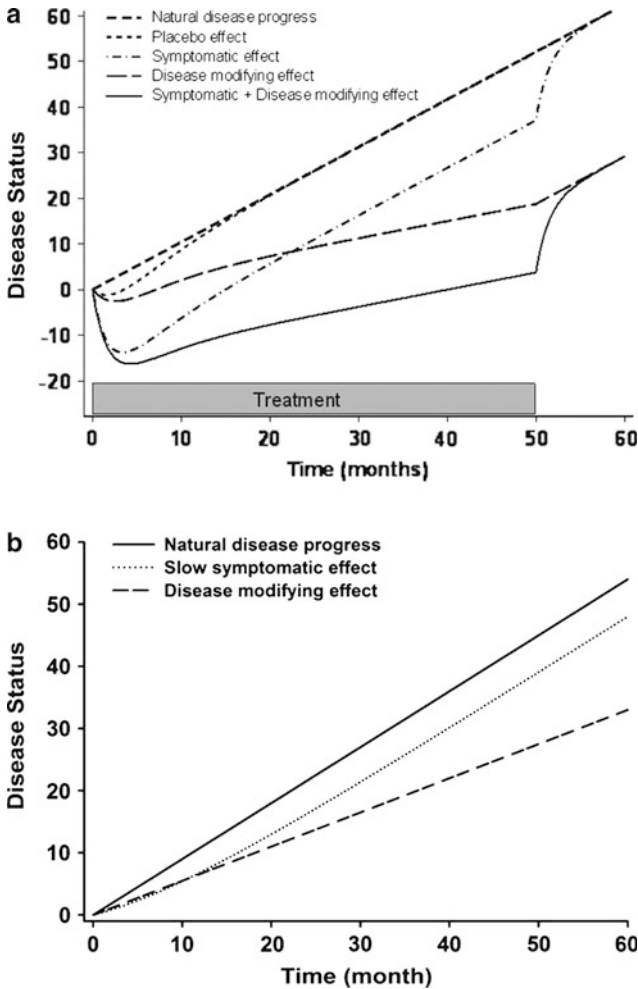


Fig. 19.3 (a) Changes in disease status of linearly progressing diseases following symptomatic, disease modifying or symptomatic + disease modifying treatment over a period of 60 month compared to natural disease progression. Treatments start at 0 and stop at 50 month. (b) Changes in disease status over a period of 60 months following treatment with drugs that have a very slow symptomatic or disease modifying effect compared to natural disease progression. On a strictly observational level, it is impossible to separate these two treatment effects during the first 12 months

effect can be obtained using a mechanism-based modeling approach (Post *et al.* 2005) and/or an optimized study design (Ploeger and Holford 2009).

Descriptive disease progression models have been successfully applied in various therapeutic areas to characterize changes in clinical endpoints and/or biomarkers. For example, changes in fasting plasma glucose (FPG) levels of patients with type 2

diabetes mellitus (T2DM) receiving once daily sustained-release gliclazide were assessed using a linear disease progression model (Frey *et al.* 2003).

$$\text{FPG}(t) = \text{FPG}_0 + \alpha \cdot t - f(T) \quad (19.4)$$

In this model, glucose-lowering effects were assumed to be symptomatic and driven by gliclazide plasma exposure. A mixture model was applied to account for differences between responders and nonresponders (Frey *et al.* 2003). The final model was externally qualified and could adequately predict changes in FPG of patients receiving gliclazide for up to 1 year (Frey *et al.* 2003). Although the Frey model provided an adequate description of the data, it should be considered that T2DM is a multifaceted, multiorgan disease characterized by a progressive loss of glycemic control as a result of disturbances in the glucose-insulin homeostasis (LeRoith 2002). These disturbances are caused by a chronic, progressive loss of insulin sensitivity in liver, muscle, and fat tissues, which are initially compensated by an increased insulin production in β -cells (LeRoith 2002). Rising insulin concentrations enhance glucose uptake into muscle and fat and decrease glucose production by the liver. Yet, the continuously increasing need for insulin eventually exhausts the capacity of β -cells resulting in progressive β -cell failure and chronically elevated plasma glucose levels (LeRoith 2002).

A comprehensive evaluation of the complex, multilevel (disease) processes involved in T2DM requires a more mechanism-based approach rather than a purely descriptive disease progression model. This is due to the fact that the deterioration of a biological system is summarized in a hybrid parameter in this descriptive model (19.4), the disease progression rate constant α . This hybrid parameter provides little information about the underlying pathophysiological processes and its value may change over time as the disease becomes more severe. A more encompassing analysis of the interaction between drug, biological system, and underlying disease processes can be obtained by exploring the underlying relationships within the biological system and combining them with the relevant disease processes in a mechanism-based modeling approach.

19.2.2 Mechanism-Based Models

A key feature of mechanism-based models is that they contain both drug-specific (*e.g.*, receptor affinity, intrinsic efficacy) and biological system-specific parameters (Danhof *et al.* 2007). While drug-specific parameters describe the interaction between the drug and the biological system, system-specific parameters describe the functioning of the underlying biological system (Danhof *et al.* 2007). The distinction between drug- and system-specific parameters becomes important when predicting the drug/treatment effect *in vivo* (Danhof *et al.* 2007).

19.2.2.1 Turnover Models

Earlier in this chapter, disease was defined as the disturbance of a biological system's homeostasis. In accordance with this definition, the rate of change of disease status (dS/dt) can be described in a more mechanistic way as the imbalance between synthesis (k_{in}) and elimination ($k_{out} \cdot S$) using a turnover model (19.5) (Dayneka *et al.* 1993; Post *et al.* 2005).

$$\frac{dS}{dt} = k_{in} - k_{out} \cdot S \quad (19.5)$$

The use of turnover models allows the differentiation of the source of disturbance being assigned to synthesis and/or elimination processes. In theory, multiple scenarios can be distinguished, of which the decrease in synthesis rates and the decrease in elimination rates are most relevant for disease progression (Post *et al.* 2005). The change in synthesis (dk_{in}/dt) and elimination rates (dk_{out}/dt) over time can be characterized according to (19.6),

$$\frac{d(k_{in}, k_{out})}{dt} = f_{dp}(k_{in}, k_{out}, t) \quad (19.6)$$

where $f_{dp}(k_{in}, k_{out}, t)$ is a time-dependent function characterizing the rate of change in synthesis and elimination rates (Post *et al.* 2005). In theory, this function can be defined in multiple ways, but will be constrained to first-order processes in this chapter (19.7).

$$f_{dp}(k_{in}, k_{out}, t) = -r_{dp,kin,out} \cdot k_{in,out} \quad (19.7)$$

As a result, k_{in} and k_{out} decrease exponentially with their respective disease progression rate constants (r_{dp}).

In case of therapeutic intervention, treatment effects can be classified according to the qualitative impact of drugs on disease progression (symptomatic vs. disease modifying effect). Both symptomatic and disease modifying effects can be dependent or independent of the disease (Post *et al.* 2005). The dependence of the treatment effect on the disease is determined by the mechanisms and mode of drug action. For instance, in Parkinson's disease, a degenerative disorder of the central nervous system, the signal transduction of dopaminergic neurons in the substantia nigra is reduced due to cell death resulting in slowed movements (bradykinesia), tremor, and other central as well as peripheral symptoms (Gallagher and Schapira 2009). According to the previously introduced classifications, the effect of dopamine agonists in Parkinson's disease is, in principle, a symptomatic and disease-independent therapeutic intervention. This is due to the fact that the achieved effect is independent of the number of functional dopaminergic neurons. In comparison, treatment of Parkinson's disease with drugs stimulating the release of dopamine from its neurons is a disease-dependent, symptomatic intervention. On the other hand, drugs stimulating the generation/survival of dopaminergic

neurons in the substantia nigra are expected to have a disease modifying effect that is independent of the disease, whereas that of drugs reducing the rate of cell death is disease-dependent and disease modifying.

A clear distinction between these various treatment effects is not possible and can even be misleading if solely based on visual inspection of the effect-time course. For example, when simulating the effect of drugs inhibiting the elimination of dopamine by blocking its enzymatic breakdown (k_{out}), obtained profiles must be interpreted with great care (Fig. 19.4). Given that after an initial improvement, the disease status following treatment declines faster than that of untreated patients, one may falsely conclude that these inhibitors actually accelerate the progression of Parkinson’s disease. However, this conclusion is incorrect as it neglects the

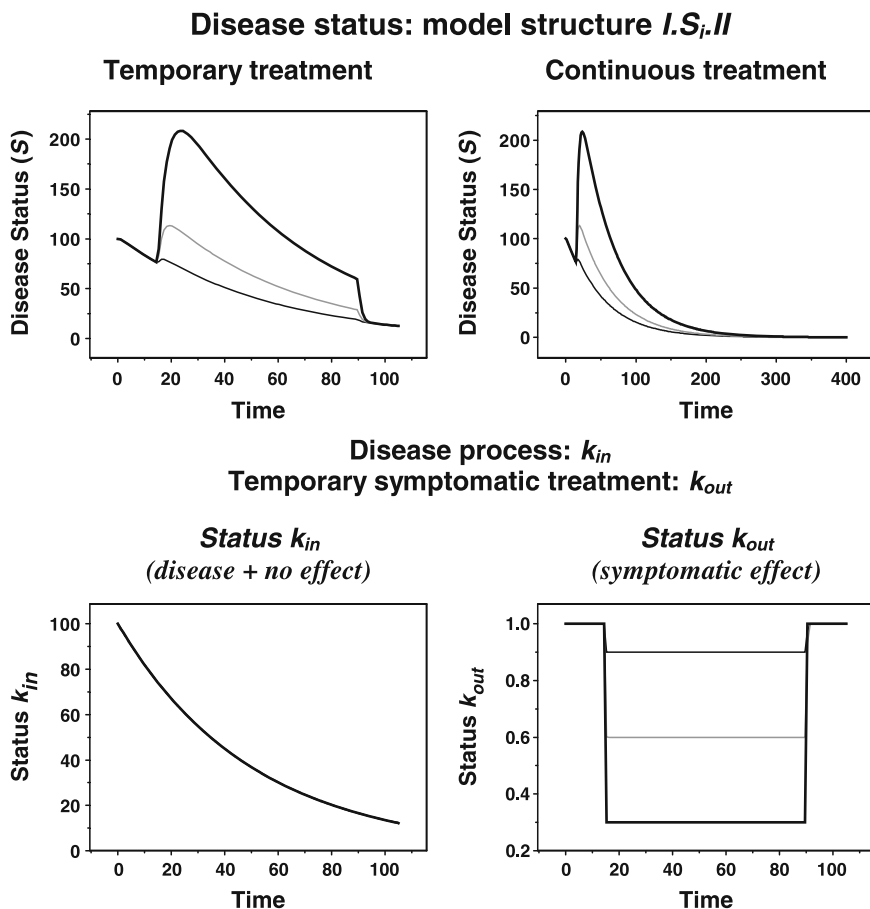


Fig. 19.4 Time course of disease status (S) for temporary, symptomatic and disease-independent treatment (*top left*) resulting from an exponentially decreasing synthesis (k_{in} , *bottom left panel*) together with three different effect levels (small: *thin black line*, intermediate: *thin gray line*, and high: *bold black line*) on the output parameter (k_{out} , *bottom right panel*). *Top right*: Time course of the disease status (S) without treatment cessation. Figure and legend modified from Post *et al.* (2005)

underlying mechanism of Parkinson's disease. The observed decline in disease status is primarily caused by continuous deterioration of dopaminergic neurons resulting in a decreased dopamine production (k_{in}) rather than disease accelerating treatment effects. The perpetual decrease in k_{in} also serves as an explanation of why these symptomatic treatment effects seem to wear off as the disease progresses. As a result, disease system analysis based on mechanism-based modeling and simulation approaches is superior to descriptive approaches when making inferences about the effect of treatment on disease progression.

19.2.2.2 Cascading Turnover Models

The concepts derived so far for mechanism-based turnover models have been based on single biomarker/clinical endpoint data. However, underlying pathophysiological processes of most diseases are more complex and cannot be sufficiently described by single endpoint measures. A more appropriate description of the disease system can be obtained using data on multiple biomarkers or endpoints on the causal path between drug exposure and effect. Once determined, this information can be used to evaluate the interdependence of these factors and to develop comprehensive models that ultimately allow the prediction of long-term disease progression and of treatment effects. For instance, chronic loss of insulin sensitivity in liver, muscle, and fat tissues, resulting in a disturbance of the glucose-insulin homeostasis, is regarded as a primary reason for developing T2DM (LeRoith 2002). The disturbance of this system cannot sufficiently be characterized by isolated measures of either glucose or insulin. Instead, information on the interaction between both is needed to characterize the underlying homeostatic feedback mechanisms and, subsequently, disease progression. Data can be obtained by challenging the system with either insulin infusions (*e.g.*, hyperinsulinemic euglycemic clamp) or glucose infusions (*e.g.*, frequently sampled intravenous glucose tolerance test) and measuring subsequent changes in both biomarkers (Monzillo and Hamdy 2003).

Knowledge of this feedback mechanism further allows evaluating drug effects on the glucose-insulin homeostasis. For example, glucose production in the liver can be stimulated by β_2 -adrenergic receptor agonists, such as terbutaline (Lima *et al.* 2004). Subsequent changes in FPG and fasting serum insulin (FSI) levels from baseline (FPG₀ and FSI₀) and reestablishment of homeostasis can be modeled using (19.8),

$$\begin{aligned}
 \frac{dFPG}{dt} &= k_{in1} \cdot (1 + S_1 \cdot C_p) - k_{out1} \cdot (1 + S_3 \cdot [FSI - FSI_0]) \cdot FPG \\
 k_{in1} &= k_{out1} \cdot FPG_0 \\
 \frac{dFSI}{dt} &= k_{in2} \cdot (1 + S_2 \cdot [FPG - FPG_0]) - k_{out2} \cdot FSI \\
 k_{in2} &= k_{out2} \cdot FSI_0
 \end{aligned}
 \tag{19.8}$$

where k_{in1} is the glucose production rate, k_{out1} is the disposition rate constant for glucose, k_{in2} is the insulin production rate, k_{out2} is the disposition rate constant for insulin, and C_p is the terbutaline concentration in plasma (Lima *et al.* 2004). In this homeostatic feedback model, production of FPG is stimulated by S_1 (terbutaline effect on glucose production), production of FSI is stimulated by S_2 (glucose effect on insulin production), and elimination of FPG is stimulated by S_3 (insulin-mediated glucose removal from plasma). Although this model has helped to improve the understanding of the feedback mechanisms involved in the glucose-insulin homeostasis, this approach has two main limitations. First, the long-term progression of T2DM may not be sufficiently predicted by biomarkers, such as FPG or FSI, that quickly respond to drug treatment. Second, loss of insulin-sensitivity and gradual degradation of β -cell function, as the primary drivers for the progression of T2DM, have not been included in this model.

An extension of the previously introduced cascading turnover model was proposed by de Winter *et al.* (2006), where the effect of three drugs with different mechanisms of action (pioglitazone: insulin-sensitizer; metformin: decrease of hepatic glucose production, and gliclazide: stimulation of insulin secretion from β -cells) on the disease progression in T2DM patients was evaluated. In this extended disease progression model, a link between changes in three markers (FPG, FSI, glycosylated hemoglobin A_{1c} [HbA_{1c}]) and the progressive loss of β -cell function, as well as insulin sensitivity (de Winter *et al.* 2006), was established using three interrelated turnover models as shown in 19.9 (de Winter *et al.* 2006).

$$\begin{aligned} \frac{dFSI}{dt} &= EF_B \cdot B \cdot (FPG - 3.5) \cdot k_{in,FSI} - k_{out,FSI} \cdot FSI \\ \frac{dFPG}{dt} &= \frac{k_{in,FPG}}{EF_S \cdot S \cdot FSI} - k_{out,FPG} \cdot FPG \\ \frac{dHbA_{1c}}{dt} &= FPG \cdot k_{in,HbA_{1c}} - k_{out,HbA_{1c}} \cdot HbA_{1c} \end{aligned} \quad (19.9)$$

The cascading character of this turnover model is determined by a feedback relationship between FSI and FPG as well as a feed-forward relationship between FPG and HbA_{1c} on the corresponding production rates. In this disease progression model, the production rate of FSI is directly proportional to FPG concentrations, corrected for an empirically determined FPG-stimulated FSI production threshold of 3.5 mmol/L (Matthews *et al.* 1985). On the other hand, the production rate of FPG is inversely proportional to FSI concentrations.

The effect of disease progression on the FPG-FSI- HbA_{1c} homeostasis was addressed by linking FSI production to the remaining β -cell function (B) and FPG production to the remaining insulin sensitivity (S). B and S are system-specific parameters that decrease nonlinearly over time as the disease progresses. Their values range from one (full, normal functionality) to zero (complete loss of functionality) and can be computed in various ways. In this model, the authors assumed an asymptotic decline in B and S , which was expressed according to 19.10,

$$B = \frac{1}{1 + \exp(b_0 + r_B \cdot t)}$$

$$S = \frac{1}{1 + \exp(s_0 + r_S \cdot t)} \quad (19.10)$$

where r_B and r_S define the rate of change in B and S (de Winter *et al.* 2006). To account for differences in function at baseline, b_0 and s_0 were introduced into the system. Large values of b_0 and s_0 indicate that patients have a longer T2DM history resulting in an advanced disease state at the start of the study. On the other hand, EF_B and EF_S are drug-specific parameters that characterize the effect of symptomatic therapeutic interventions on B and S (de Winter *et al.* 2006). In this context, EF_B values greater than one represent the stimulation of insulin secretion by gliclazide, whereas EF_S values greater than one represent the inhibition of hepatic glucose production by pioglitazone and metformin (de Winter *et al.* 2006).

The proposed cascading turnover model was found appropriate to characterize the time-courses of FPG and HBA_{1c} of 2,048 treatment-naïve T2DM patients (de Winter *et al.* 2006). When using the model of de Winter (19.8 and 19.9) and that of Frey 19.4 to simulate changes in FPG over 10 years, similar results were obtained for both models (Fig. 19.5). However, the mechanism-based model by

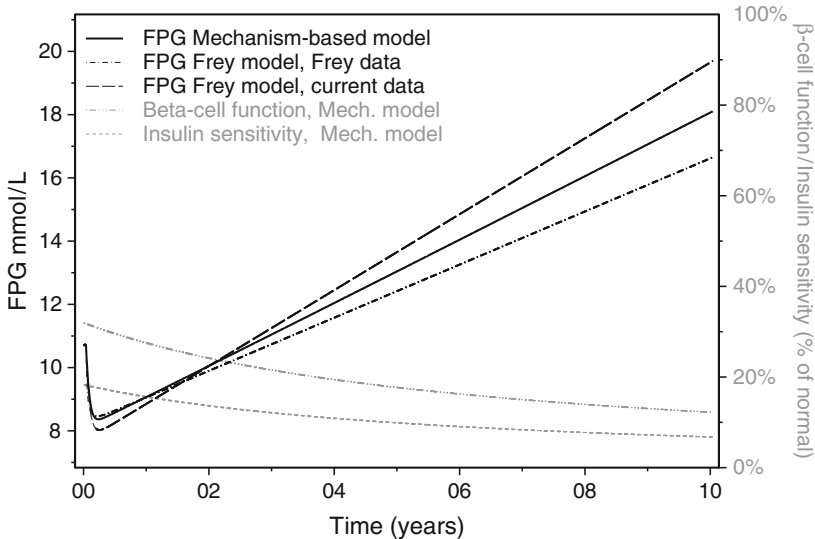


Fig. 19.5 Predicted time-course of fasting plasma glucose (FPG) for 10 years of gliclazide therapy (black lines, left y-axis) by the mechanism-based model (solid line), the Frey model on the current data (dashed) and the Frey model as published (dashed-dotted). The gray lines (right y-axis) show the non-linear time-courses of β -cell function (dashed-dotted) and insulin sensitivity (short dash) predicted by the mechanism-based model for 10 years of gliclazide therapy. Figure and legend from de Winter *et al.* (2006)

de Winter provides a promising conceptual advance for the study of disease progression in T2DM as it allows to also evaluating the impact of treatment on the loss of β -cell function and insulin sensitivity, independent from immediate antihyperglycemic effects (de Winter *et al.* 2006). Future modeling approaches may also take into account that the elimination of both glucose and insulin is concentration-dependent rather than constant as implemented in the previously introduced T2DM models (Jones *et al.* 1984; Boroujerdi *et al.* 1995).

19.2.3 Systems Pharmacology

Disease progression models discussed so far in this chapter are data-driven, starting at a clinical observation level, and have become increasingly more complex to better understand the (patho)physiology of the system and the implications of treatment interventions. Alternatively, disease processes can also be characterized based on a complete mechanistic description of the biological system, starting at the molecular/tissue level (Hunter and Nielsen 2005; Ploeger *et al.* 2009). Several physiology-based modeling platforms, such as the IUPS Physiome Project (Hunter and Nielsen 2005) or Archimedes (Eddy and Schlessinger 2003), have been set up aiming to develop an infrastructure for linking models of biological structure and function across multiple levels of spatial organization and multiple time scales (Hunter *et al.* 2005). The span of these models ranges from describing genes to whole organisms and eventually leads to very complex approaches (Bassingthwaight 2000; Hunter and Nielsen 2005; Hunter *et al.* 2005). At present, the development and validation of such models is still restricted by the free accessibility of data on the different spatial/temporal levels, the identifiability of model parameters as well as the availability of appropriate software tools that allow to run and visualize these models based on widely accepted modeling standards (Hunter and Nielsen 2005). Furthermore, given the focus on the anatomical and (patho)physiological properties, a current drawback in these models is the lack of an appropriate parameterization of the drug effects. Yet, multiple groups have been intensively working on overcoming these limitations by making model libraries as well as software tools for running and visualizing these models freely available on the World Wide Web (Hunter and Nielsen 2005).

In some cases, compromises with respect to model complexity have been made by combining the principles of systems pharmacology with those of mechanism-based models resulting in physiology-based approaches. For example, an integrated system of differential equations has been identified that links current knowledge on systemic calcium homeostasis with present understanding of bone biology (Peterson and Riggs 2010). This physiology-based approach combines elements on hormonal regulation, absorption, and elimination processes in gut and kidneys as well as bone remodeling processes into a single model as shown in Fig. 19.6 (Peterson and Riggs 2010). Clinical data on patients with varying degrees of renal insufficiency (Rix *et al.* 1999), anabolic therapy, and antiresorptive bone therapy

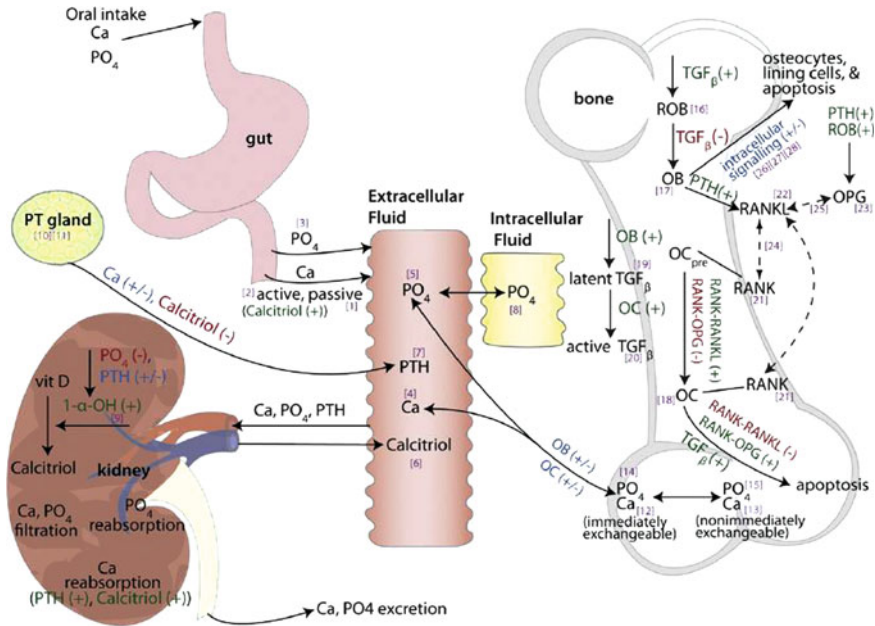


Fig. 19.6 Schematic of physiological system model to describe calcium homeostasis and bone remodeling. Effects: (+) stimulatory; (-) inhibitory; (±) bidirectional; → fluxes; - - - binding effects; [#] differential equation number; *Ca* calcium; *ECF Ca* extracellular fluid calcium; *OC* osteoclast; *OC_{pre}* OC precursor; *OB* osteoblast; *ROB* responding OB; *OPG* osteoprotegerin; *PO₄* phosphate; *PTH* parathyroid hormone; *RANK* receptor of NF-Kappa B; *RANKL* RANK, ligand; *TGFβ* transforming growth factor beta; *1-α-OH* 1 alpha hydroxylase. Figure and legend from Peterson and Riggs (2010)

(McClung *et al.* 2006; Lewiecki *et al.* 2007) were used to identify and estimate parameters sensitive to investigated system interventions (Peterson and Riggs 2010). The final model was found appropriate to simultaneously describe calcium homeostasis and bone remodeling in the presence of various diseases and/or therapeutic interventions using a single set of parameters within a single set of mathematical equations (Peterson and Riggs 2010).

As models become more complex, challenges in identifying system components may arise, which makes model parameterization rather difficult. Although identifiability determines whether unique drug- and system-specific parameters can be found, statistical properties, characterizing accuracy and precision, have to be considered when estimating these system parameters. One way of addressing this issue is to mathematically reduce these models by combining parameters into dimensionless variables without oversimplifying the system. The goal of this mathematical reduction is to capture the rate-limiting steps within the system (system behavior) rather than its complexity. This concept has been used in a number of

PKPD models (Zuideveld *et al.* 2001, 2004) and has also been successfully applied for modeling the progression of osteoporosis in healthy, postmenopausal women receiving the selective estrogen receptor modulator tibolone (Post 2009). In the latter approach, a previously proposed bone homeostasis model (Lemaire *et al.* 2004) was mathematically reduced and allowed describing the changes in several different bone formation and resorption markers as well as bone mineral density measures during the course of tibolone treatment. In this reduced model, two disease components were identified representing the onset of estrogen deficiency following menopausal transition and the subsequent establishment of a new homeostasis within the system (shift in the ratio between bone resorption and bone formation). This approach further allowed characterizing the different time scales relevant for changes in the different bone turnover markers as well as bone mineral density. Ultimately, the reduced model could also be used to distinguish between tibolone effects on both turnover markers and bone mineral density. Although tibolone had symptomatic effects on bone turnover markers, disease modifying effects were determined for bone mineral density. This finding adds a new dimension to the modeling of disease progression as it shows that different qualitative treatment effects can be observed for different types of markers within one comprehensive system. Extensions of this model may be used in the future to link dynamic changes in bone biology to the corresponding fracture risk.

19.3 Practical Challenges and Implementations

There are a number of factors that have to be considered during the development and validation of disease progression models for prospective use in drug development and therapeutics, of which some of the key aspects are highlighted in the following section.

One of the main challenges remains the assessment of the predictive value of a model for novel targets. The identifiability of drug- and disease-specific parameters depends on the data and current knowledge about the biological system. Given that mechanism-based modeling provides access not only to experimentally accessible, but also to hidden or inaccessible components of the biological system, model performance may be heavily influenced by the experimental conditions upon which data is generated. In physics, the influence that the observer and experimental setting may have on experimental results has long since been accepted. In medical research such acceptance has yet to come. Optimal design concepts are often ignored in investigational protocols, response data are not available following withdrawal of treatment and the effect of variable dosing regimens and treatment duration are usually limited by clinical, ethical, or experimental reasons. The evaluation of design-related factors in conjunction with model validation represents therefore an important step in the development of disease progression models. Evidence shows

that even models validated for parameter accuracy and bias may not necessarily be sufficient for simulation purposes.

Understanding of the role of experimental design factors is particularly important for the development of disease models and their subsequent use in clinical trial simulations. Yet, the majority of publications in which mechanism or physiology-based disease models are used, exclude the potential impact of experimental factors. In addition, from a statistical perspective, the exposure-response relationship in a PKPD analysis is evaluated primarily by testing the null hypothesis in the presence and absence of drug. This approach often yields biased results as it neglects important information on the interaction between drug, biological system, and disease processes. To appropriately consider these factors, advanced analysis techniques as well as innovative study designs have to be used (Santen *et al.* 2009a, b). For example, in the area of antidepressant drug research, chances of identifying a statistically significant drug effect, even for marketed compounds with known efficacy, are limited (Khan *et al.* 2002). This unsatisfactory outcome is caused by a number of factors, which can be categorized as: drug-, disease-, and trial-related factors (Santen *et al.* 2009a). Drug-related factors are pharmacokinetic variability, difficulties in dose selection, and poor compliance. Disease-related factors include large variability in (placebo) response, heterogeneity of patient populations, and difficulties of measuring the severity of the disease in an objective and meaningful manner (Santen *et al.* 2009a). Trial design-related factors are inadequate study size, suboptimal inclusion criteria, and the use of insufficient endpoints and/or statistical methods. All of these factors are usually closely related and should, therefore, be evaluated in a single comprehensive approach. Although the conventional approach of testing the null hypothesis in the presence and absence of drug is still considered as the most conservative method for confirming the existence of drug effects, a model-based evaluation allows studying the (causal) dynamics of the underlying disease system including drug-, disease-, and clinical trial-related factors.

Missing values and dropout constitute another important factor that may lead to model misspecification and bias in drug-specific and disease-specific parameter estimates. For instance, dropout is common in late clinical trials and has been dealt with using various methods, such as carrying the last observation forward or classifying this data record as missing (Hu and Sale 2003). However, if subjects leave a study because of a lack of efficacy, caused by side effects, or because of worsening of the disease conditions, ignoring this information yields biased estimates for treatment effects as well as associated variability. To appropriately address these issues, a distinction between the different types of dropouts has to be made. In general, dropout processes can be categorized as: completely random, random, and informative (Hu and Sale 2003). Although completely random dropouts may be ignored during the model building process, random dropouts can be modeled separately, whereas informative dropouts have to be jointly modeled with disease as well as drug-related effects (Hu and Sale 2003; Karlsson and Holford 2008).

The nature and magnitude of placebo response in an experimental protocol also plays an important role in disease progression modeling. For example, it has been shown for schizophrenia that placebo response can be highly variable and often declines with time (Welge and Keck 2003; Friberg *et al.* 2009). One way of addressing this issue would be to extend the trial duration. However, study prolongation is in many cases not feasible because: (1) ethical issues arise when active treatment is retained from patients for an extended period of time and (2) the probability of patients dropping out of the study increases as the trial duration increases.

To overcome these limitations, innovative trial designs are needed. In many cases, a fixed design, such as the placebo-controlled parallel group design, is not sufficient to enable identification of drug- and/or disease-specific parameters (Santen *et al.* 2009a, b). For example, attempts to distinguish between symptomatic and disease modifying effects may fail if both effects exist at the same time. Such a distinction would require a different trial design, including treatment arms with different durations and availability of data on response after treatment completion. Furthermore, it has been demonstrated that mathematical modeling and simulation approaches can be used to optimize trial design and, subsequently, support the claim of symptomatic and/or disease modifying effects (Ploeger and Holford 2009). In a recent investigation, the outcome of two different trial designs, wash-out and delayed start, was simulated using a disease progression model for Parkinson's disease with identical drug effects, study population, duration, and sample size (Ploeger and Holford 2009). In the washout design, active treatment is started right away and discontinued after 13.6 months allowing for a 3-month washout period and compared with placebo treatment for the full period. On the other hand, in the delayed start design active treatment is started after 6 month of placebo treatment and compared to active treatment for the full period (Fig. 19.7). Simulations also accounted for the possibilities of higher dropout rates for placebo treated patients as well as a potential increase in dropout in the washout period. Results from these simulations indicate that upon termination of the treatment, the washout design was superior compared to the delayed start design for distinguishing different treatment effect types as shown in Fig. 19.7 (Ploeger and Holford 2009).

Finally, it should be noted that a sufficient understanding of time in the disease process is crucial when evaluating treatment effects because a change in biological system parameters frequently results in an altered response to drug therapy over time (de Winter *et al.* 2006; Holford and Nutt 2008). As a consequence, a stronger consideration of the different time domains, such as time since the start of disease, in model-based drug development will help to further increase our understanding of the variability associated with the clinical data and to more appropriately select respective study populations. It should further be noted that understanding of the time scale or dimensionality in disease processes may help to identify fast-responding biomarkers early on and allow accurate prediction of the long-term treatment effects. In addition, identification and validation of such biomarkers would significantly

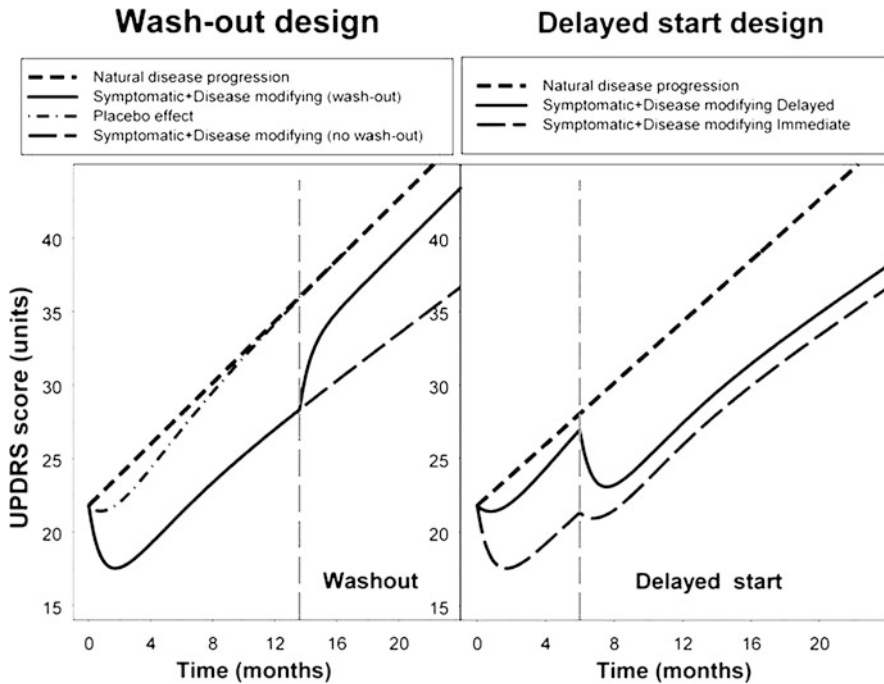


Fig. 19.7 Predicted change in the Unified Parkinson's disease rate scale (UPDRS) over time for a drug with symptomatic and disease modifying effects compared with placebo in a parallel group design with and without washout (*left hand plot*), and to a delayed start design (*right hand plot*). In the delayed start design one group receives placebo treatment first and will then be switched to active treatment, whereas the other group receives active treatment immediately. The vertical dashed line indicates the start of washout for the washout design or the start of delayed treatment for the delayed start design. Figure and legend from Ploeger and Holford (2009)

improve the chances for a successful therapeutic intervention. This could be achieved by choosing suitable doses or dosing regimens for patients initiating drug treatment at different stages in the disease process. It is important to note that different biomarkers can represent different qualitative responses to treatment as shown for postmenopausal osteoporosis. In this example, symptomatic treatment effects were identified for fast responding bone turnover markers, whereas disease modifying effects were determined for slower responding but more clinically meaningful bone mineral density measures (Post 2009). Nevertheless, within the context of dynamic disease system analysis, it is still feasible to obtain information from short term markers to predict long term changes. As a consequence, the selection of an appropriate study design, including the effects of dropout and of differences in patient population (disease status) are critically important aspects. They should be carefully evaluated before attempting to quantitatively characterize the effects of treatment on disease processes.

19.4 Summary

1. In conventional PKPD analyses, the status of the biological system is generally assumed to be invariable with time and considered constant at baseline. This assumption does not hold for progressive, chronic disorders where biological functions change over time. The change of biological functions and subsequent changes in treatment response can be characterized by disease progression modeling.
2. Disease progression modeling is an advanced analysis tool that allows characterizing the interaction between drug, biological system and disease by combining models for the pharmacology of drugs with those for disease processes.
3. Disease progression models can be established at different levels of complexity using two opposing approaches: top-down or bottom-up. Top-down approaches are usually data-driven, starting at a clinical observation level, and becoming increasingly more complex to better understand the system. In contrast, bottom-up approaches are based on a complete mechanistic description of the biological system, starting at the molecular level. Both approaches have advantages and disadvantages. Although a descriptive disease progression model may not predict the clinical outcome beyond the data on which it was established, a full system approach may face problems with the identifiability of model parameters. Mechanism-based disease progression models represent a mixture of these two extremes.
4. Conceptually, a mechanism-based disease progression model consists of three distinct parts: a pharmacokinetic model to predict target exposure, a pharmacodynamic model to characterize target binding, target activation and transduction (receptor theory; dynamical system analysis), and a disease model to characterize placebo response and disease progression.
5. Mechanism-based disease progression models often require information on multiple biomarkers/clinical endpoints, taking into account the underlying disease processes as well as feedback and feed-forward mechanisms associated with the etiology and (patho)physiology.
6. A distal-proximal classification system has been proposed for biomarkers, which can be used as basis for disease modeling, providing comprehensive information on the interaction between the drug, the biological system, and the disease.
7. Two basic types of qualitative treatment effects can be distinguished: symptomatic and disease modifying. Symptomatic treatments typically have a fast onset of effect but can only reduce the severity of clinical symptoms or change the biomarker response, whereas disease modifying treatments can slow, halt, or even reverse the progression of a disease.
8. A mechanism-based modeling approach can be used in conjunction with optimized study designs to separate symptomatic from disease-modifying effects. These differences are not evident from visual inspection, or simple regression of the time course of response.

9. The selection of an appropriate study design, including the effects of dropout and of differences in patient population (disease status) are critically important aspects that should be carefully evaluated before attempting to quantitatively characterize the effects of treatment on disease processes.

References

- Bakris GL, Copley JB, Vicknair N, Sadler R, Leurgans S (1996) Calcium channel blockers versus other antihypertensive therapies on progression of NIDDM associated nephropathy. *Kidney Int* **50**:1641–1650
- Bassingthwaighte JB (2000) Strategies for the physiome project. *Ann Biomed Eng* **28**:1043–1058
- Bies RR, Gastonguay MR, Schwartz SL (2008) Mathematics for understanding disease. *Clin Pharmacol Ther* **83**:904–908
- Bjorck S, Mulec H, Johnsen SA, Norden G, Aurell M (1992) Renal protective effect of enalapril in diabetic nephropathy. *BMJ* **304**:339–343
- Boroujerdi MA, Umpleby AM, Jones RH, Sonksen PH (1995) A simulation model for glucose kinetics and estimates of glucose utilization rate in type 1 diabetic patients. *Am J Physiol* **268**:E766–E774
- Breimer DD, Danhof M (1997) Relevance of the application of pharmacokinetic-pharmacodynamic modelling concepts in drug development. The “wooden shoe” paradigm. *Clin Pharmacokinet* **32**:259–267
- Butcher EC (2005) Can cell systems biology rescue drug discovery? *Nat Rev Drug Discov* **4**:461–467
- Butcher EC, Berg EL, Kunkel EJ (2004) Systems biology in drug discovery. *Nat Biotechnol* **22**:1253–1259
- Chan PL, Holford NH (2001) Drug treatment effects on disease progression. *Annu Rev Pharmacol Toxicol* **41**:625–659
- Crepaldi G, Carta Q, Deferrari G, Mangili R, Navalesi R, Santeusano F, Spalluto A, Vanasia A, Villa GM, Nosadini R (1998) Effects of lisinopril and nifedipine on the progression to overt albuminuria in IDDM patients with incipient nephropathy and normal blood pressure. The Italian Microalbuminuria Study Group in IDDM. *Diabetes Care* **21**:104–110
- Danhof M, Alvan G, Dahl SG, Kuhlmann J, Paintaud G (2005) Mechanism-based pharmacokinetic-pharmacodynamic modeling – a new classification of biomarkers. *Pharm Res* **22**:1432–1437
- Danhof M, de Jongh J, De Lange EC, Della Pasqua O, Ploeger BA, Voskuyl RA (2007) Mechanism-based pharmacokinetic-pharmacodynamic modeling: biophase distribution, receptor theory, and dynamical systems analysis. *Annu Rev Pharmacol Toxicol* **47**:357–400
- Dayneka NL, Garg V, Jusko WJ (1993) Comparison of four basic models of indirect pharmacodynamic responses. *J Pharmacokinet Biopharm* **21**:457–478
- de Winter W, DeJongh J, Post T, Ploeger B, Urquhart R, Moules I, Eckland D, Danhof M (2006) A mechanism-based disease progression model for comparison of long-term effects of pioglitazone, metformin and gliclazide on disease processes underlying Type 2 Diabetes Mellitus. *J Pharmacokinet Pharmacodyn* **33**:313–343
- Derendorf H, Lesko LJ, Chaikin P, Colburn WA, Lee P, Miller R, Powell R, Rhodes G, Stanski D, Venitz J (2000) Pharmacokinetic/pharmacodynamic modeling in drug research and development. *J Clin Pharmacol* **40**:1399–1418
- Eddy DM, Schlessinger L (2003) Archimedes: a trial-validated model of diabetes. *Diabetes Care* **26**:3093–3101
- FDA (2004) Innovation or stagnation: challenge and opportunity on the critical path to new medical products. March 2004 In: Challenges and opportunities report - March 2004.

- Available at: <http://www.fda.gov/downloads/ScienceResearch/SpecialTopics/CriticalPathInitiative/CriticalPathOpportunitiesReports/UCM113411.pdf>. Accessed: 12 October 2010.
- Frey N, Laveille C, Paraire M, Francillard M, Holford NH, Jochemsen R (2003) Population PKPD modelling of the long-term hypoglycaemic effect of gliclazide given as a once-a-day modified release (MR) formulation. *Br J Clin Pharmacol* **55**:147–157
- Friberg LE, de Greef R, Kerbusch T, Karlsson MO (2009) Modeling and simulation of the time course of asenapine exposure response and dropout patterns in acute schizophrenia. *Clin Pharmacol Ther* **86**:84–91
- Gall MA, Nielsen FS, Smidt UM, Parving HH (1993) The course of kidney function in type 2 (non-insulin-dependent) diabetic patients with diabetic nephropathy. *Diabetologia* **36**:1071–1078
- Gallagher DA, Schapira AH (2009) Etiopathogenesis and treatment of Parkinson's disease. *Curr Top Med Chem* **9**:860–868
- Holford N, Nutt JG (2008) Disease progression, drug action and Parkinson's disease: why time cannot be ignored. *Eur J Clin Pharmacol* **64**:207–216
- Holford NH, Peace KE (1992) Methodologic aspects of a population pharmacodynamic model for cognitive effects in Alzheimer patients treated with tacrine. *Proc Natl Acad Sci USA* **89**:11466–11470
- Holford NH, Sheiner LB (1982) Kinetics of pharmacologic response. *Pharmacol Ther* **16**:143–166
- Hu C, Sale ME (2003) A joint model for nonlinear longitudinal data with informative dropout. *J Pharmacokinet Pharmacodyn* **30**:83–103
- Hunter P, Nielsen P (2005) A strategy for integrative computational physiology. *Physiology (Bethesda)* **20**:316–325
- Hunter P, Smith N, Fernandez J, Tawhai M (2005) Integration from proteins to organs: the IUPS Physiome Project. *Mech Ageing Dev* **126**:187–192
- Jones RH, Sonksen PH, Boroujerdi MA, Carson ER (1984) Number and affinity of insulin receptors in intact human subjects. *Diabetologia* **27**:207–211
- Karlsson MO, Holford N (2008) A tutorial on visual predictive checks. PAGE, Marseille
- Khan A, Leventhal RM, Khan SR, Brown WA (2002) Severity of depression and response to antidepressants and placebo: an analysis of the Food and Drug Administration database. *J Clin Psychopharmacol* **22**:40–45
- Kimko HC, Reele SS, Holford NH, Peck CC (2000) Prediction of the outcome of a phase 3 clinical trial of an antischizophrenic agent (quetiapine fumarate) by simulation with a population pharmacokinetic and pharmacodynamic model. *Clin Pharmacol Ther* **68**:568–577
- Lalonde RL, Kowalski KG, Hutmacher MM, Ewy W, Nichols DJ, Milligan PA, Corrigan BW, Lockwood PA, Marshall SA, Benincosa LJ, Tensfeldt TG, Parivar K, Amantea M, Glue P, Koide H, Miller R (2007) Model-based drug development. *Clin Pharmacol Ther* **82**:21–32
- Lemaire V, Tobin FL, Greller LD, Cho CR, Suva LJ (2004) Modeling the interactions between osteoblast and osteoclast activities in bone remodeling. *J Theor Biol* **229**:293–309
- LeRoith D (2002) Beta-cell dysfunction and insulin resistance in type 2 diabetes: role of metabolic and genetic abnormalities. *Am J Med* **113(Suppl 6A)**:3S–11S
- Lesko LJ, Atkinson AJ Jr (2001) Use of biomarkers and surrogate endpoints in drug development and regulatory decision making: criteria, validation, strategies. *Annu Rev Pharmacol Toxicol* **41**:347–366
- Lewiecki EM, Miller PD, McClung MR, Cohen SB, Bolognese MA, Liu Y, Wang A, Siddhanti S, Fitzpatrick LA (2007) Two-year treatment with denosumab (AMG 162) in a randomized phase 2 study of postmenopausal women with low BMD. *J Bone Miner Res* **22**:1832–1841
- Lewis EJ, Hunsicker LG, Bain RP, Rohde RD (1993) The effect of angiotensin-converting-enzyme inhibition on diabetic nephropathy. The Collaborative Study Group. *N Engl J Med* **329**:1456–1462
- Lima JJ, Matsushima N, Kisson N, Wang J, Sylvester JE, Jusko WJ (2004) Modeling the metabolic effects of terbutaline in beta2-adrenergic receptor diplotypes. *Clin Pharmacol Ther* **76**:27–37

- Matthews DR, Hosker JP, Rudenski AS, Naylor BA, Treacher DF, Turner RC (1985) Homeostasis model assessment: insulin resistance and beta-cell function from fasting plasma glucose and insulin concentrations in man. *Diabetologia* **28**:412–419
- McClung MR, Lewiecki EM, Cohen SB, Bolognese MA, Woodson GC, Moffett AH, Peacock M, Miller PD, Lederman SN, Chesnut CH, Lain D, Kivitz AJ, Holloway DL, Zhang C, Peterson MC, Bekker PJ (2006) Denosumab in postmenopausal women with low bone mineral density. *N Engl J Med* **354**:821–831
- Miller R, Ewy W, Corrigan BW, Ouellet D, Hermann D, Kowalski KG, Lockwood P, Koup JR, Donevan S, El-Kattan A, Li CS, Werth JL, Feltner DE, Lalonde RL (2005) How modeling and simulation have enhanced decision making in new drug development. *J Pharmacokinet Pharmacodyn* **32**:185–197
- Monzillo LU, Hamdy O (2003) Evaluation of insulin sensitivity in clinical practice and in research settings. *Nutr Rev* **61**:397–412
- Mould DR, Denman NG, Duffull S (2007) Using disease progression models as a tool to detect drug effect. *Clin Pharmacol Ther* **82**:81–86
- Parving HH, Rossing P, Hommel E, Smidt UM (1995) Angiotensin-converting enzyme inhibition in diabetic nephropathy: ten years' experience. *Am J Kidney Dis* **26**:99–107
- Peterson MC, Riggs MM (2010) A physiologically based mathematical model of integrated calcium homeostasis and bone remodeling. *Bone* **46**:49–63
- Ploeger BA, Holford NH (2009) Washout and delayed start designs for identifying disease modifying effects in slowly progressive diseases using disease progression analysis. *Pharm Stat* **8**:225–238
- Ploeger BA, van der Graaf PH, Danhof M (2009) Incorporating receptor theory in mechanism-based pharmacokinetic-pharmacodynamic (PK-PD) modeling. *Drug Metab Pharmacokinet* **24**:3–15
- Post TM (2009) Disease system analysis: between complexity and (over) simplification. *Department of Pharmacology, Leiden University, Leiden*, pp 148–189
- Post TM, Freijer JJ, DeJongh J, Danhof M (2005) Disease system analysis: basic disease progression models in degenerative disease. *Pharm Res* **22**:1038–1049
- Rix M, Andreassen H, Eskildsen P, Langdahl B, Olgaard K (1999) Bone mineral density and biochemical markers of bone turnover in patients with predialysis chronic renal failure. *Kidney Int* **56**:1084–1093
- Rolan P, Danhof M, Stanski D, Peck C (2007) Current issues relating to drug safety especially with regard to the use of biomarkers: a meeting report and progress update. *Eur J Pharm Sci* **30**:107–112
- Rowland M, Balant L, Peck C (2004) Physiologically based pharmacokinetics in drug development and regulatory science: a workshop report (Georgetown University, Washington, DC, May 29–30, 2002). *AAPS Pharm Sci* **6**:E6
- Santen G, Horrigan J, Danhof M, Della Pasqua O (2009a) From trial and error to trial simulation. Part 2: an appraisal of current beliefs in the design and analysis of clinical trials for antidepressant drugs. *Clin Pharmacol Ther* **86**:255–262
- Santen G, van Zwet E, Danhof M, Della Pasqua O (2009b) From trial and error to trial simulation. Part 1: the importance of model-based drug development for antidepressant drugs. *Clin Pharmacol Ther* **86**:248–254
- Wang Y, Bhattaram AV, Jadhav PR, Lesko LJ, Madabushi R, Powell JR, Qiu W, Sun H, Yim DS, Zheng JJ, Gobburu JV (2008) Leveraging prior quantitative knowledge to guide drug development decisions and regulatory science recommendations: impact of FDA pharmacometrics during 2004–2006. *J Clin Pharmacol* **48**:146–156
- Welge JA, Keck PE Jr (2003) Moderators of placebo response to antipsychotic treatment in patients with schizophrenia: a meta-regression. *Psychopharmacology (Berl)* **166**:1–10
- Zhang L, Sinha V, Forgue ST, Callies S, Ni L, Peck R, Allerheiligen SR (2006) Model-based drug development: the road to quantitative pharmacology. *J Pharmacokinet Pharmacodyn* **33**:369–393

- Zuideveld KP, Maas HJ, Treijtel N, Hulshof J, van der Graaf PH, Peletier LA, Danhof M (2001) A set-point model with oscillatory behavior predicts the time course of 8-OH-DPAT-induced hypothermia. *Am J Physiol Regul Integr Comp Physiol* **281**:R2059–R2071
- Zuideveld KP, Van der Graaf PH, Newgreen D, Thurlow R, Petty N, Jordan P, Peletier LA, Danhof M (2004) Mechanism-based pharmacokinetic-pharmacodynamic modeling of 5-HT_{1A} receptor agonists: estimation of *in vivo* affinity and intrinsic efficacy on body temperature in rats. *J Pharmacol Exp Ther* **308**:1012–1020

Chapter 20

Using a Systems Biology Approach to Explore Hypotheses Underlying Clinical Diversity of the Renin Angiotensin System and the Response to Antihypertensive Therapies

Arthur Lo, Jennifer Beh, Hector De Leon, Melissa K. Hallow, Ramprasad Ramakrishna, Manoj Rodrigo, Anamika Sarkar, Ramesh Sarangapani, and Anna Georgieva

Abstract In this chapter, we discuss how a systems biology approach can be used in drug development, by presenting an example of building and parameterizing a model of the renin angiotensin system (RAS) pathway. The RAS plays a pivotal role in regulating blood pressure (BP) and kidney function. We introduce a mathematical representation of the pathway in the systemic circulation and describe how we derived the parameters of the model from available clinical measurements and inferences about the homeostatic nature of the physiological system. The chapter includes a brief introduction to the implementation of RAS-modulating therapies, model validation and variability at the pathway level. The chapter also describes the process of extending the model from the systemic circulation to the kidney and the process by which the two models were connected. The work presented here is part of one regulatory pathway in a larger physiological model of BP regulation and renal function (in both healthy and disease states) that is used to generate and test hypotheses of the underlying physiology to investigate a range of clinical scenarios.

20.1 Introduction

The appeal of an integrated model of human physiology in drug discovery and development is the ability to investigate the interactions among multiple biological systems as a whole rather than as individual pieces. Just as the actions of a therapeutic agent extend beyond the binding kinetics at a target site, a systems biology approach to

A. Lo (✉)
Entelos, Inc., 110 Marsh Drive, Foster City, CA, USA, 94404
e-mail: lo@entelos.com

modeling disease can reveal subtleties of the entire physiological system that may not be apparent in a model based on the individual physiological components. By extending the focus of the integrated model to encompass both a detailed representation of the mechanism of action and the functional change measured in the clinic, the systems biology approach can provide both meaningful and practical insights to further guide and optimize the process of drug discovery and development.

The current model of the renin angiotensin system (RAS) pathway is part of a larger model that has been developed to investigate different hypotheses about the role of angiotensin II (Ang II) in the physiological function of the kidney, in addition to its recognized role in blood pressure (BP) regulation. In particular, hypertensive patients receiving therapies that suppress or down regulate the RAS may experience a delay in the onset of glomerulosclerosis, interstitial and tubulofibrosis (Brenner *et al.* 2001). The larger model is a powerful tool for quickly testing multiple hypotheses about the physiology that can help answer a wide range of drug development questions. For instance, it can be used to predict the expected changes in BP for specific therapies in clinical trials, or to identify patient types that are most likely to benefit from RAS therapies based on specific characteristics or biomarkers (and thus enrich a clinical trial). It can be used to test mechanistic hypotheses that are infeasible or impractical to test clinically, or to test the impact of known or hypothesized drug characteristics (*e.g.*, localization in the kidney, ability to access specific receptors) on end-organ protection, possibly providing support for drug development and differentiation claims.

Moreover, pathway models are increasingly being used in drug discovery and in clinical development to address a range of circumstances in which characterizing the efficacy or safety of a drug effect is dependent on perturbations at the molecular and cellular level. While the variability in drug response among patients can be linked to characteristics routinely collected in demographic surveys, including gender and race, some variability can be traced to different protein expression levels, gene expression levels, and mutations in relevant biological entities such as drug target receptors or metabolizing enzymes. To this end, mathematical models of signaling and metabolic pathways have been used to elucidate the dynamic behavior of the biological system of interest (Michelson 2006).

The utility of mathematical models in drug development have included: (1) identifying and optimizing drug targets within complex pathways via mechanistic dynamic simulations (Aksenov *et al.* 2005; Rullmann *et al.* 2005; Michelson *et al.* 2006); (2) identifying combinations of therapies that would achieve efficacy without interfering with the biological function of the drugs' targets in normal tissue, thus limiting toxicity (FitzGerald *et al.* 2006; Christopher *et al.* 2004); (3) characterizing the role that mutations in the drug target have on the overall clinical efficacy (Liu *et al.* 2007); (4) reconciling seemingly contradictory experimental data by showing that different protein expression levels in cell lines and tissues can lead to a largely different behavior of the same signaling network (Schoeberl *et al.* 2006); and (5) translating animal data into usable interventions for a corresponding response in human patients (Shoda *et al.* 2005).

20.2 Overview

The regulation of BP involves multiple (and not necessarily independent) pathways that affect different physiological systems to maintain homeostasis. In this chapter, we introduce a clinical data-based approach to developing and validating a mathematical representation of one biological pathway that has been shown to play a pivotal role in cardiovascular pathophysiology. We investigate the functional effect of the RAS pathway at the level of the systemic circulation and at the level of an organ. At the end of the chapter, we provide a description for the procedure to integrate the RAS pathway into a larger physiological model of BP regulation. While our focus is on the RAS and its role in hypertension, we believe this approach can be generalized to other pathways and diseases. Our goal is to demonstrate that relevant clinical insights can be achieved by modeling at the pathway level through a representation of the normal physiological state and the physiological perturbations that lead to disease, and by modeling at the integrated level of the larger physiological system.

In what follows, we will briefly discuss hypertension, introduce the RAS pathway, describe previous modeling efforts of BP regulation and acquaint the reader with the process of pathway modeling and how it has been used to answer clinical research questions.

20.2.1 *Epidemiology and Pathophysiology of Hypertension*

Hypertension, the medical condition of elevated BP, is a public health problem that affects both developed and developing nations. The American Heart Association states that hypertension is the most important risk factor for heart disease and stroke in the United States. Despite substantial improvements in public awareness, clinical diagnosis, and treatment, the number of patients diagnosed with hypertension that successfully respond to medications is below optimal (27%) (Hajjar and Kotchen 2003). Hypertension has been long recognized to confer increased risk to patients with diabetes, atherosclerotic, and atherothrombotic cardiovascular disease leading to an increased likelihood of myocardial infarction (MI), stroke, peripheral vascular disease (PVD), renal failure and heart failure (HF). Other risk factors contributing to the complex etiology of hypertension include age, weight, race/ethnicity, diabetes and dietary sodium intake.

20.2.2 *Role of the RAS Pathway in Modulating Arterial Pressure*

The etiologies of elevated BP are varied and difficult to characterize in any specific patient or clinical subject. Hypertension is postulated to result from numerous

pathophysiological mechanisms including increased peripheral resistance, increased sympathetic nerve system activity, overproduction of sodium-retaining factors and vasoconstrictors (*e.g.*, Ang II and endothelin), increased sodium reabsorption by the kidneys, deficiencies of vasodilators such as atrial natriuretic peptide (ANP), nitric oxide (NO) and prostacyclin (PGI₂), or from an imbalance in the regulation of glomerular pressure. These mechanisms all lead to hypertension, but a single mechanism is difficult to identify in any individual patient. Ang II has been the focus of intensive research aimed at elucidating its role in the control of BP, extracellular fluid and electrolyte homeostasis as shown in Fig. 20.1. Ang II is a peptide with potent vasoconstricting effects that is part of the RAS pathway, a cascade of bioactive peptides and regulatory enzymes. The classical systemic RAS pathway has been described to start with the synthesis and release of angiotensinogen (AGT) into the systemic circulation by the liver. Renin, a proteolytic enzyme synthesized by the juxtaglomerular cells in the kidney, cleaves AGT to form the decapeptide angiotensin I (Ang I). Angiotensin-converting enzyme (ACE) cleaves Ang I to form Ang II, which is the octapeptide hormone that regulates BP by the modulation of sodium reabsorption in the kidney and by effecting central and peripheral nervous system activity to increase cardiac output and systemic vascular resistance.

RAS-modulating therapies directly manipulate this pathway to alter the levels of Ang II in the systemic circulation to reduce BP. Three classes of RAS-modulating pharmacological therapies are currently available on the market: direct renin inhibitors (DRIs) target renin activity; ACE inhibitors (ACEI) block the conversion from Ang I to Ang II; and angiotensin-receptor blockers (ARBs) prevent the binding of Ang II to the angiotensin II receptor type I (AT1). All three reduce the

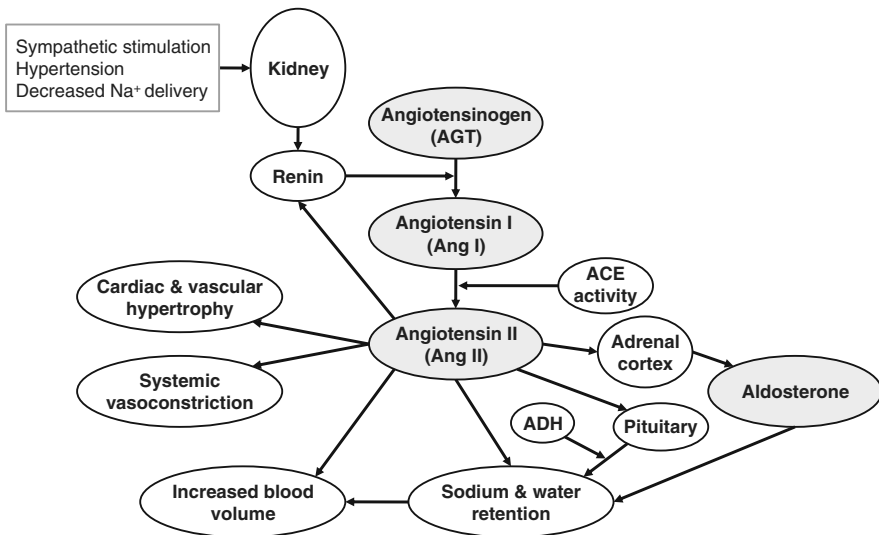


Fig. 20.1 A diagrammatic representation of the role of Ang II in regulating blood pressure

systemic activity of Ang II, which leads to vasodilation, decreased renal sodium reabsorption and reduced secretion of vasopressin (from the brain) and aldosterone (from the adrenal cortex).

20.2.3 Modeling Approaches to Long-Term Regulation of Blood Pressure

Computational approaches to modeling BP regulation were pioneered by Guyton and Coleman in 1972. These authors published the first model that provided the foundation toward our understanding of the relationship between venous return, cardiac output and the vasculature (Guyton *et al.* 1972a, b). The original and updated versions of the model focus on the role of the kidney in long-term BP regulation and the effect of blood volume regulation in the development of hypertension, but have been noted to underestimate the influence of the sympathetic nervous system (SNS) (Osborn *et al.* 2009). In addition, the representation of the RAS pathway in this model is oversimplified. The Guyton/Coleman (GC) model does not include vascular remodeling and its effects on vascular geometry and hemodynamics as significant contributors to increased peripheral vascular resistance (Korner and Angus 1997; Korner *et al.* 1992). To address the under-representation of the SNS, Karaaslan *et al.* (2005) published a modified version of the GC model that added the influence of the renal sympathetic nerve activity (rSNA) on the synthesis and release of renin and the afferent arteriolar tone.

20.2.4 Creating a Model of Hypertension Incorporating the RAS Pathway

Our goal was to develop a model that captures current knowledge of the pathophysiology of hypertension and incorporates the RAS pathway to predict the effects of RAS-modulating therapies on BP regulation and renal function in subjects with essential hypertension or compromised renal function. The Guyton/Karaaslan models for normal BP regulation provided a starting point with the following extensions:

1. Changes in the physiology were represented by different parameter values in the model to capture the transition from normal to diseased states.
2. Addition of a detailed mechanistic representation of renal function (glomerular filtration rate and albuminuria), incorporating concepts from existing models (Lazzara and Deen 2007; Smithies 2003; Drumond 1994).
3. Inclusion of a detailed representation of the concentration of the systemic circulating RAS-related peptides including intermediates such as angiotensin I (Ang I) and angiotensin (1–7) (Ang(1–7)) and a separate representation of intrarenal RAS.
4. Incorporation of the effects of Ang II in hypertension and the pharmacological actions of RAS-modulating therapies on the RAS pathway.

The focus of this chapter lies in the following two sections to demonstrate the application of the RAS pathway model in the context of clinical pharmaceutical research.

20.3 Model of Systemic RAS

In our model, the representation of the RAS pathway incorporates the synthesis and conversion of AGT to Ang I, Ang II and downstream metabolites such as Ang(1–7). The activity of enzymes including renin, ACE, a chymase-like enzyme, and neutral endopeptidase (NEP) were included in the model in addition to the binding rates of Ang II to the two Ang II receptors (AT1 and AT2). The inclusion of these peptides and enzymes allows for the investigation of antihypertensive therapies that target the RAS. Figure 20.2 is a diagrammatic representation of the pathway model.

20.3.1 Model Structure

The model that describes the dynamics of the RAS (Fig. 20.2) is represented using a system of ordinary differential equations (20.1)–(20.7). Each biochemical reaction has zeroth-order components of production (k_n) and first order degradation kinetics expressed through half-life parameters (h_n). We have assumed that binding or enzymatic reactions can be expressed as first-order reactions with

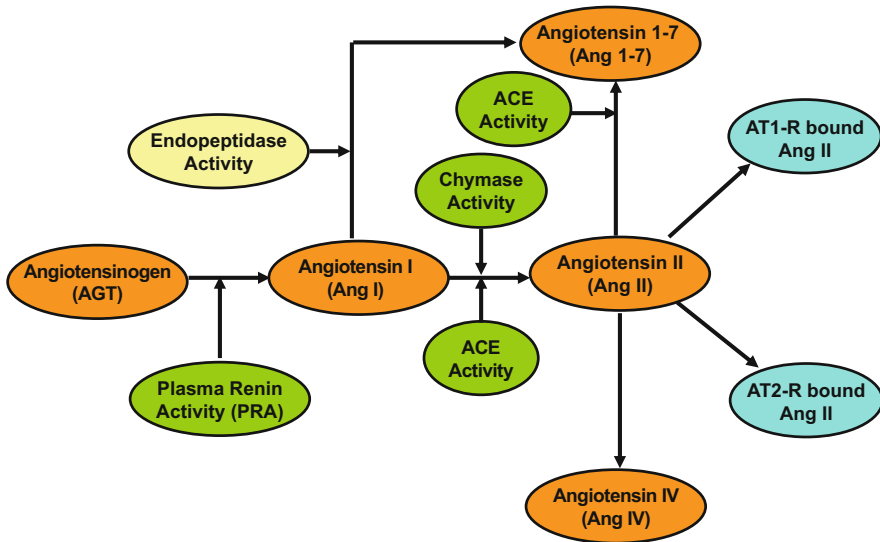


Fig. 20.2 The renin-angiotensin pathway that is represented in the model describes the precursors and metabolites of Ang II

parameters (c_n). A justification for this simplification is provided later in the text. A feedback function, f , relating plasma renin activity (PRA) to AT1-bound Ang II is also included in the model.

$$\text{PRA} = \frac{V_{\max}[\text{AGT}]}{[\text{AGT}] + [\text{AGT}]_0} * f([\text{AT1} - \text{bound AngII}]) \quad (20.1)$$

$$\frac{d[\text{AGT}]}{dt} = k_{\text{AGT}} - \text{PRA} - \frac{\ln(2)}{h_{\text{AGT}}} [\text{AGT}] \quad (20.2)$$

$$\frac{d[\text{AngI}]}{dt} = \text{PRA} - (c_{\text{ACE}} + c_{\text{Chym}} + c_{\text{NEP}})[\text{AngI}] - \frac{\ln(2)}{h_{\text{AngI}}} [\text{AngI}] \quad (20.3)$$

$$\begin{aligned} \frac{d[\text{AngII}]}{dt} &= (c_{\text{ACE}} + c_{\text{Chym}})[\text{AngI}] - (c_{\text{ACE2}} - c_{\text{AngII}=\text{AngIV}} - c_{\text{AT1}} - c_{\text{AT2}}) \\ &\quad \times [\text{AngII}] - \frac{\ln(2)}{h_{\text{AngII}}} [\text{AngII}] \end{aligned} \quad (20.4)$$

$$\frac{d[\text{Ang}(1-7)]}{dt} = c_{\text{NEP}}[\text{AngI}] + c_{\text{ACE2}}[\text{AngII}] - \frac{\ln(2)}{h_{\text{Ang}(1-7)}} [\text{Ang}(1-7)] \quad (20.5)$$

$$\frac{d[\text{AngIV}]}{dt} = c_{\text{AngII}=\text{AngIV}}[\text{AngII}] - \frac{\ln(2)}{h_{\text{AngIV}}} [\text{AngIV}] \quad (20.6)$$

$$\frac{d[\text{AT1} - \text{bound AngII}]}{dt} = c_{\text{AT1}}[\text{AngII}] - \frac{\ln(2)}{h_{\text{AT1}}} [\text{AT1} - \text{bound AngII}] \quad (20.7)$$

$$\frac{d[\text{AT2} - \text{bound AngII}]}{dt} = c_{\text{AT2}}[\text{AngII}] - \frac{\ln(2)}{h_{\text{AT2}}} [\text{AT2} - \text{bound AngII}] \quad (20.8)$$

A range of feasible values for the enzyme activity rates in humans was determined from the available data in the published literature. When a specific range of data could not be found, an assumption was made about the steady-state equilibrium for the angiotensin peptide concentrations to calculate the rates of the remaining unknown parameters. For example in (20.2) a steady-state approximation yields:

$$k_{\text{AGT}} = \left(\text{PRA} + \frac{\ln(2)}{h_{\text{AGT}}} \right) \text{AGT}^* \quad (20.9)$$

As the degradation rate (h_{AGT}) of AGT and a range of baseline PRA rates are known, we selected a steady-state equilibrium value for AGT (AGT^*) from the range known in literature to obtain a value for the rate of AGT synthesis (k_{AGT}).

The variables and parameters with their reported ranges from clinical studies are summarized in Table 20.1, as are the parameters where the values are not reported or known.

Table 20.1 List of definitions and values of various physiological rates and parameters in the systemic RAS module

Parameter	Units	Reported range	Reference
[AGT]	pmol/ml	4.8–4,50,000	Katsurada <i>et al.</i> (2007)
[Ang I]	fmol/ml	3.9–22.9	Nussberger <i>et al.</i> (2002)
[Ang II]	fmol/ml	2.2–7.3	Nussberger <i>et al.</i> (2002)
[Ang(1–7)]	fmol/ml	3.1–31.7	Chappell <i>et al.</i> (1998)
[Ang IV]	fmol/ml	?	
[AT1-bound Ang II]	fmol/ml	?	
[AT2-bound Ang II]	fmol/ml	?	
AGT $t^{1/2}$ (h_{AGT})	h	16	Hyp primer
Ang I $t^{1/2}$ (h_{AngI})	min	0.5	Schalekamp <i>et al.</i> (1989)
Ang II $t^{1/2}$ (h_{AngII})	min	0.5	van Kats <i>et al.</i> (1997)
Ang(1–7) $t^{1/2}$ ($h_{Ang(1-7)}$)	min	29	Iusuf <i>et al.</i> (2008)
Ang IV $t^{1/2}$ (h_{AngIV})	min	?	
AT1 and AT2 Ang II $t^{1/2}$	min	?	
AGT synthesis rate (k_{AGT})	fmol/ml/h	?	
PRA	ng/ml/h	0.34–1.45	Nussberger <i>et al.</i> (2007)
ACE (c_{ACE})	1/h	?	
Chymase (c_{Chym})	1/h	?	
NEP (Ang I-Ang(1–7)) (c_{NEP})	1/h	?	
ACE2 (c_{ACE2})	1/h	?	
Ang II to Ang IV ($c_{AngII-AngIV}$)	1/h	?	
Ang II AT1 binding rate (c_{AT1})	1/h	?	
Ang II AT2 binding rate (c_{AT2})	1/h	?	
Regulatory feedback on PRA (f)	n/a	?	

The question marks indicate parameters where the data was difficult to find from the literature or not known

20.3.2 Systemic RAS Model Assumptions

A complete parameterization of the model rate constants based upon experimental measurements was not available in the literature. Thus, multiple assumptions about the physiology were made to complete the parameterization of the model structure, as follows.

1. The baseline PRA is the rate of AGT conversion to Ang I in healthy subjects. The rate of substrate conversion can change in response to the circulating concentration of AGT and in response to the feedback function f from a change in AT1-bound Ang II.
 - These assumptions are based on the detailed kinetic studies in human plasma conducted by Poulsen (1973).
 - PRA is assumed to be proportional to the concentration of its substrate, AGT, because the concentration of AGT is comparable to the Michaelis-Menten constant (K_m).

2. The activity of ACE and chymase (C_{ACE} , C_{chym}) in converting Ang I to Ang II is assumed proportional to the concentration of the substrate (Ang I).
 - ACE and chymase activity in the vasculature were determined to have V_m values of 222 and 154 pmol/ml/h, respectively, which was considerably greater than rates (~ 0.3 pmol/ml/h) measured in humans (Takai *et al.* 1997; Meng *et al.* 1995).
3. ACE was assumed to be responsible for $>95\%$ of the conversion of Ang I to Ang II.
 - Human and animal data support the hypothesis of ACE being the primary enzyme responsible for Ang I to Ang II conversion in normotensive humans (Saris *et al.* 2000; Wei *et al.* 2002; Schuijt *et al.* 2002).
 - ACE expression and systemic conversion of AGT to Ang I take place primarily in the pulmonary circulation.
4. 10% of Ang II was assumed to be converted to Ang(1–7) and 90% to Ang IV.
 - Since no quantitative data in the literature is available, this assumption was based on measured circulating activity of ACE2, the primary pathway for the conversion of Ang II to Ang(1–7) compared to the rate of Ang II degradation to Ang IV (van Kats *et al.* 1997).
5. The instantaneous amount of Ang II bound to membrane AT1 and AT2 receptors is a small fraction of circulating Ang II.
 - This assumption is based upon the geometric relationship between the volume of the blood and the surface area of the vasculature.
6. Ang II binds preferentially to AT1 than AT2 receptors.
 - Data from human smooth muscle cells and renal tissue indicate that AT2 receptors are expressed at lower levels compared to AT1 receptors (Haulica *et al.* 2005).
7. Ang I and Ang II have half lives of approximately 30 s in the systemic circulation (Schalekamp *et al.* 1989; van Kats *et al.* 1997).
8. For Ang IV, the model assumes a half-life of 10 min, which is between the reported half lives of Ang II and Ang(1–7).
9. The concentrations of Ang IV and Ang(1–7) in the systemic circulation were calculated based on the solution of the steady-state equilibrium equations.
10. PRA increases via a regulatory feedback mechanism in response to a reduction in BP, in a relationship that reflects a reduction in Ang II binding to the AT1 receptors.
 - An analysis of clinical data from trials testing therapies that modulate the RAS pathway suggests a rapid increase in PRA 24 h posttreatment, which correlates with the reductions in Ang II bound to AT1 receptors and BP (LeFebvre *et al.* 2007; Maillard *et al.* 1999; Gainer *et al.* 1998; Delacretaz *et al.* 1995; Burnier *et al.* 1995).

20.3.3 Parameterization of a Representative Normotensive Virtual Patient (VP)

To our knowledge, no studies have incorporated both known and hypothesized activity rates for the RAS pathway cascade into a single dynamic system. Based upon the aforementioned assumptions about the enzyme activities and the existence of a steady-state equilibrium, a single parameterization of this system of equations was derived such that the resulting numerical solution described a feasible normotensive patient (Table 20.2). It is important to note that the ranges of measured Ang I and Ang II concentrations in normotensive and hypertensive patients are assumed identical and that there is no obvious way to distinguish between normal and elevated BP solely on these concentrations (Matsui et al. 1999). The steady-state solution of the system described of ordinary differential equations (20.1)–(20.8) is shown in Table 20.3 (results derived by numerical methods). This parameter set

Table 20.2 Representative parameter set describing a feasible normotensive virtual patient (VP)

Parameter	Units	Normotensive VP
AGT $t^{1/2}$	h	10
Ang I $t^{1/2}$	min	0.5
Ang II $t^{1/2}$	min	0.66
Ang(1-7) $t^{1/2}$	min	30
Ang IV $t^{1/2}$	min	0.5
AT1 and AT2 Ang II $t^{1/2}$	min	12
AGT synthesis rate	fmol/ml/h	34,620
PRA	ng/ml/h	0.97
ACE	1/h	54.1
Chymase	1/h	1.1
NEP (Ang I-Ang(1-7))	1/h	1.1
ACE2	1/h	2.4
Ang II conversion to Ang IV	1/h	23.5
Ang II AT1 binding rate	1/h	11.8
Ang II AT2 binding rate	1/h	3.9
Regulatory feedback on PRA	n/a	1

A solution was obtained by solving the equilibrium solution of the system at steady state. Shaded rows show parameters that were determined by the steady state solution of the system of equations

Table 20.3 The steady-state values of the system described by equations (1) to (8) describing one feasible normotensive patient

States	Units	Normotensive VP
[AGT]	pmol/ml	483.9
[Ang I]	fmol/ml	7.5
[Ang II]	fmol/ml	4.75
[Ang(1-7)]	fmol/ml	14
[Ang IV]	fmol/ml	1.29
AT1-bound Ang II	fmol/ml	16.2
AT2-bound Ang II	fmol/ml	5.4

Shaded rows show the values determined by the steady state solution of the system of equations

describes one hypothetical subject or virtual patient (VP), and is the foundation of a framework for conducting hypothesis testing of this physiological system, as described by Friedrich and Paterson (2004).

20.4 Model Validation

20.4.1 Angiotensin Peptide Infusion Experiments

A validation of any model consists of the agreement between model predictions and one or more experimental data sets that were not used to determine the initial parameterization of the model. For this model of the RAS pathway, a validation of the model parameters describing the VP was conducted using a series of published radio-labeled angiotensin peptide infusion experiments (Danser *et al.* 1998; Admiraal *et al.* 1993). The published studies quantified the rates of systemic and tissue Ang II production and clearance by using a constant infusion of radio-labeled ^{125}I -Ang I and ^{125}I -Ang II. Based upon the known specific radioactivity of ^{125}I -Ang I and ^{125}I -Ang II, the plasma and tissue concentrations of Ang I and Ang II could be separated by their source (locally synthesized or exogenously delivered). In five human subjects where ^{125}I -Ang I was directly infused at a constant rate, blood samples taken between 5 and 10 min after the start of the infusion had constant levels of both ^{125}I -Ang I and ^{125}I -Ang II, which implied that the system reached a steady state within 5 min (Danser *et al.* 1998).

The infusion experiment was reproduced by modifying (20.3) with the addition of a term $k_2 = 23.1 \text{ fmol/ml/h}$ to represent a constant infusion rate of ^{125}I -Ang I consistent with the experimental protocol based upon the measures of radioactivity. Figure 20.3

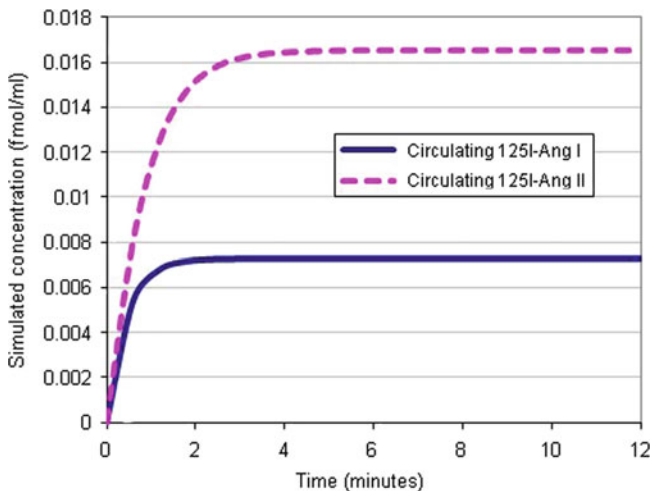


Fig. 20.3 The simulated change in radio-labeled ^{125}I -Ang I and ^{125}I -Ang II following an infusion at time 0. The model results are consistent with experimental observations

shows the simulated time course of both ^{125}I -Ang I and ^{125}I -Ang II as a steady state is reached in the normotensive VP within 5 min, thus confirming the set of chosen parameters.

Similar simulation experiments were conducted to reproduce the study by Admiraal *et al.*, in which arterial and venous levels of ^{125}I -Ang I and ^{125}I -Ang II across a number of vascular beds were measured to determine the local tissue metabolism and production of Ang II (Admiraal *et al.* 1993). In this study, tracer doses of ^{125}I -Ang I and ^{125}I -Ang II were infused in hypertensive patients and the study found that equilibrium was achieved within 8 min. To reproduce these experiments, (20.3) and (20.4) were modified with the additional terms $k_2 = 26.9$ fmol/ml/h and $k_3 = 21.8$ fmol/ml/h respectively.

In both simulations described above, a steady state was reached within 8 min, reinforcing the hypothesis that the chosen parameters in the model that describe a feasible VP are consistent with the behavior of a normotensive patient in the clinic. It is important to note that though the comparison was made between measurements in hypertensive patients and model simulations represented normotensive human subjects, the comparison is still justifiable based on data not showing differences between normal and patient populations (Matsui *et al.* 1999).

20.4.2 Representation and Parameterization of Antihypertensive Therapies

Additional testing of the model parameterization was conducted by incorporating the effects of the three main RAS-modulating therapies in the model and comparing the resulting simulated angiotensin peptide concentrations with data. ACEIs were simulated by changing the effect of the rate constant c_{ACE} , ARBs were simulated by modulating the effects of the rate constant c_{AT1} , and DRIs were simulated by altering the overall rate PRA. In (20.1)–(20.3) and (20.6) the therapeutic inhibitory effects of ACEI, ARB and DRI were implemented via the use of fractional reductions in enzyme activity, α , β and δ , respectively. For example, (20.6) becomes:

$$\frac{d[\text{AT1} - \text{bound AngII}]}{dt} = (1 - \beta)c_{\text{AT1}}[\text{AngII}] - \frac{\ln(2)}{h_{\text{AT1}}} \times [\text{AT1} - \text{bound AngII}] \quad (20.10)$$

AT1 receptors mediate the majority of Ang II actions involved in the regulation of BP and blood volume. Mazzolai *et al.* (1999) showed a 90% reduction ($\beta = 0.9$) in Ang II bound to AT1 receptors 4 h after a 150-mg dose of irbesartan, an ARB, administered to normotensive patients. ACEI blocks the action of ACE competitively and thus the conversion of Ang I to Ang II, thereby reducing circulating and local levels of Ang II. Data from Manhem *et al.* (1985) demonstrated a 96%

reduction ($\alpha = 0.96$) in ACE activity 4 h following a 20-mg dose of ramipril, an ACEI. Similarly, Nussberger *et al.* (2007) measured a 60–70% reduction in PRA 4 h after an 80-mg dose of aliskiren, a DRI, was administered to normotensive patients. Finally, the calibration of the regulatory feedback function f was based on observations from the literature showing that PRA increases in response to ACEI, ARB and DRI therapy (Luque *et al.* 1996). The reactive increase in PRA was hypothesized to be related to the reduction in AT1-bound Ang II based on the comparable increase observed in ACEI therapy (reduced Ang II) and ARB therapy (increased Ang II but reduced Ang II binding to AT1 receptors).

20.4.3 Validation of Antihypertensive Therapies in the Model

A comparison of the change in angiotensin peptide concentrations between the model and the literature was used to validate the implementation and parameterization of the antihypertensive therapies. The summary of this comparison is presented in Table 20.4.

ACEI therapy is associated with a decrease in Ang II, a reactive increase in plasma renin activity (PRA) and an increase in plasma Ang I. The reactive increase in PRA was also observed in response to ARB and DRI therapy. The simulated ACEI in the model predicted increased concentrations of Ang I and Ang(1–7) and decreased concentrations of Ang II, consistent with reported clinical data (Manhem *et al.* 1985). The time course of the Ang I and Ang II response predicted an equilibration in the angiotensin peptide concentrations after 5 h, in agreement with short-term measurements taken in the studies highlighted in Table 20.4.

Since ARBs act by blocking the binding of Ang II to the AT1 receptor rather than by inhibiting Ang II synthesis, their use results in an increase in plasma Ang II levels. The blockade of AT1 receptors increases renin activity and the corresponding concentration of plasma Ang I. The simulated effect of ARBs in the model predicts increased concentrations of circulating Ang I, Ang II, Ang(1–7) and PRA, consistent with published clinical data (Christen *et al.* 1991).

Table 20.4 Simulated vs. measured changes in circulating peptides and PRA following therapy (4 h)

		Ang I (%)	Ang II (%)	Ang(1–7) (%)	PRA (%)	Reference
ACE inhibition	Simulation	↑474	↓71	↑160	↑293	Luque <i>et al.</i> (1996)
	Measurement	↑480	↓76	↑100	↑370	
Renin inhibition	Simulation	↓56	↓55	↓55	↓62	Nussberger <i>et al.</i> (2007, 2002)
	Measurement	↓64	↓50		↓67	
AT1 block	Simulation	↑232	↑276	↑258	↑259	Christen <i>et al.</i> (1991)
	Measurement		↑320		↑370	

DRIs have a significant and sustained effect on PRA to reduce the concentration of both Ang I and Ang II in the circulation. The simulated effect of DRIs in the model predicts a decreased concentration of circulating Ang I, Ang II and Ang (1–7), consistent with results reported in clinical studies (Nussberger *et al.* 2007).

20.4.4 Representation of Variability Across Different Clinical Populations

Table 20.1 summarized the wide range of reported clinical values of enzyme activities in the RAS pathway cascade to reflect the intrinsic variability between human subjects. The values summarized in Table 20.2 described only one set of parameters for the system of equations that yields a feasible solution. To capture physiological variability observed in the clinic, the parameter values in Table 20.1 can be changed within the observed ranges to generate a new VP hypothesis. Although changing the parameters may yield a mathematically correct steady state solution for a new VP, the combination of parameter values may not result in steady state concentrations or enzyme activity rates that are consistent with the physiological data. For example, decreasing the rate of Ang II clearance from the circulation will increase the time it takes for Ang II to reach an equilibrium. If the resulting Ang II concentration at equilibrium increases significantly beyond physiological range determined by the infusion studies, then the chosen set of parameters for the VP is considered invalid. The verification of the simulated results against plausible data is an essential step during the process of model building.

A collection, or cohort, of multiple feasible VPs can be generated using a systematic process to explore the parametric space and a method for testing the feasibility criteria of each parameterization (Michelson *et al.* 2006). Table 20.5 summarizes one such method for exploring the parametric space that varies the half lives and enzyme activity rates around the nominal values of the first virtual patient

Table 20.5 A range of values that define the parametric space to explore the physiological variability of the biology

Parameter	Units	VP1	Nominal range (%)
AGT $t^{1/2}$	h	10	20–400
Ang I $t^{1/2}$	min	0.5	20–400
Ang II $t^{1/2}$	min	0.66	20–400
Ang(1–7) $t^{1/2}$	min	30	20–400
Ang IV $t^{1/2}$	min	0.5	20–400
AT1 and AT2 Ang II $t^{1/2}$	min	12	20–400
PRA	ng/ml/h	0.97	20–400
ACE	1/h	55.8	20–400
Chymase	1/h	0.56	20–400
NEP (Ang I-Ang(1–7))	1/h	1.1	20–400
ACE2	1/h	2.4	20–400

A patient hypothesis may be generated by simulating using different parameters within the nominal range where the value of 100% is equal to the values chosen for the first virtual patient

Table 20.6 The published range of angiotensin peptide concentrations that describe the criteria for a physiologically feasible normotensive patient

States	Units	Normotensive VP range
[AGT]	pmol/ml	75–480
[Ang I]	fmol/ml	3.9–21
[Ang II]	fmol/ml	2.2–17
[Ang(1–7)]	fmol/ml	3.1–31
[Ang IV]	fmol/ml	0.6–4.8

(VP1). Table 20.6 summarizes a set of feasibility criteria for the concentration of angiotensin peptides based on a survey of the literature.

The cohort of feasible VPs can be modified depending on the criteria used to describe a particular disease phenotype. For example, the feasibility criteria for PRA can be increased accordingly in patients that exhibit exaggerated renal production of renin leading to increased concentrations of plasma renin. It is important to note that the cohort of VPs may not follow the same distribution as the clinical population and additional refinement of the patient-generation procedure may be required.

20.4.5 Insights from Model Simulations

- In the range of parameter values of the systemic RAS pathway described in Table 20.5, the long half life of AGT (h_1) compared to Ang I and Ang II (h_2 and h_3) indicates a slower rate of AGT turnover compared to Ang I and Ang II.
 - As a result, the concentration of AGT is susceptible to larger changes resulting from increases or decreases in PRA compared to Ang I or Ang II. Changes in the circulating concentration of AGT may be easier to measure and may function as a better marker of changes to the RAS pathway than Ang II.
- ACE is the primary enzyme for the conversion of Ang I to Ang II in the systemic circulation.
 - Chymase is another enzyme that can convert Ang I to Ang II. Therapy that focuses on the inhibition of ACE activity does not affect the continued conversion of Ang I to Ang II by chymase.
 - Based on the clinically measured changes in circulating Ang I and Ang II and the assayed reduction in ACE activity in response to moderate doses of ACEI, the model predicts that ACE is responsible for greater than 95% of Ang II synthesis in the representative normotensive patient.
 - If the role of ACE in the synthesis of Ang II was reduced to <95%, the model was unable to reproduce the clinically measured reduction in Ang II.
- PRA increases in response to ARB or ACEI therapy can be represented by establishing a relationship between decreased Ang II binding to AT1 receptors and PRA.

20.5 Modeling RAS Within the Kidney

20.5.1 Introduction

In recent years, there has been additional focus on the role of local tissue-specific RAS in the development of cardiovascular and renal disease. In particular, the kidney possesses all the RAS components and enzymatic machinery required for the local tissue generation of Ang II and other RAS-related peptides. Here, we briefly address our approach of constructing and quantifying the renal RAS pathway and connecting it together with the systemic circulation of the angiotensin peptides. We will mention how uncertainty and lack of data are addressed and the application of the resulting model to test a variety of hypotheses on the potential effects of renal RAS.

20.5.2 Model Development

The model divides the kidney into two regions: the renal vasculature compartment, comprised of all vascular structures within the kidney (including the blood volume within those structures); and the renal tissue compartment, comprised of all tissue external to vascular structures (including the tubules and interstitial tissue) Fig. 20.4. The model makes the following assumptions and simplifications:

- RAS peptides are arterially delivered from the circulation to the renal vascular compartment at concentrations equal to systemic levels, and the peptides flow out of the renal vascular compartment back to the systemic circulation at concentration equal to renal vasculature levels.
- All angiotensin peptides and all enzymes in the RAS pathway are also produced locally within each compartment, although the rates of production and enzymatic conversion can vary greatly from those in systemic circulation, as discussed below. A concentration gradient exists between the renal tissue and renal vasculature, such that RAS peptides produced in the renal tissue diffuse into the

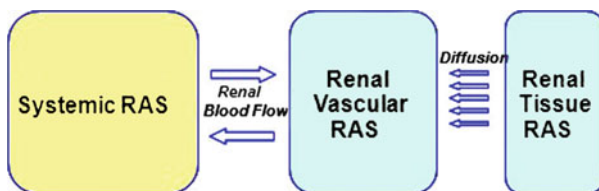


Fig. 20.4 The intrarenal RAS is compartmentalized into two regions: the renal vasculature and renal tissue. RAS peptides flow freely between the systemic circulation and renal vasculature. RAS peptides diffuse from the renal tissue to the renal vasculature due to the higher tissue concentrations

renal vasculature. Biopsy data shows that renal tissue levels of Ang I and Ang II are 10- to 100-fold higher than circulating levels (Navar *et al.* 2002; Metzger *et al.* 1999; Navar and Nishiyama 2004).

- Ang IV and Ang(1-7) levels in the kidney were not specifically modeled because of the limited availability of data. Instead, rates of conversion of Ang I and Ang II to Ang(1-7) and Ang IV were assumed to be incorporated into the degradation rates of Ang I and Ang II.
- Since limited data is available on any changes in the concentrations of AGT and renin within the renal tubules and interstitium, the rate of Ang I synthesis in the renal tissue compartment was assumed to be at equilibrium levels.

Thus, in modeling RAS concentrations within the renal vasculature compartment, we accounted for: (1) arterially delivered Ang I and Ang II peptides and return of these peptides to the systemic circulation; (2) production and utilization of Ang I and Ang II in the renal vascular bed (Navar *et al.* 2002; Metzger *et al.* 1999); (3) diffusion of Ang I and Ang II from the renal tissue into the renal vasculature; and (4) binding of Ang II to its receptors. For the model angiotensin peptide concentrations within the renal tissue compartment, we considered: (1) production and utilization of Ang I and Ang II in the renal tissue (Danser *et al.* 1998); (2) diffusion of locally produced peptides into the renal vasculature, and (3) binding of Ang II to its receptors.

Equations (20.11)–(20.14) for the renal vascular RAS are shown below. These equations are almost identical to those for systemic RAS, but the rates are specific for the renal circulation, include additional terms to describe the flow of angiotensin peptides in and out of the the kidney at a rate F_k , and include the diffusion of angiotensin peptides from the renal tissue compartment to the renal vasculature at a rate of D_k .

$$\begin{aligned} \frac{d[\text{AngI}]_{rv}}{dt} &= k_{\text{AngI-}rv} - (c_{\text{ACE-}rv} + c_{\text{Chym-}rv})[\text{AngI}]_{rv} - \frac{\ln(2)}{h_{\text{AngI-}rv}}[\text{AngI}]_{rv} \\ &\quad + F_k([\text{AngI}]_{\text{circ}} - [\text{AngI}]_{rv}) + D_k([\text{AngI}]_{rt} - [\text{AngI}]_{rv}) \end{aligned} \quad (20.11)$$

$$\begin{aligned} \frac{d[\text{AngII}]_{rv}}{dt} &= (c_{\text{ACE-}rv} + c_{\text{Chym-}rv})[\text{AngI}]_{rv} - (c_{\text{AT1-}rv} + c_{\text{AT2-}rv})[\text{AngII}]_{rv} \\ &\quad - \frac{\ln(2)}{h_{\text{AngII-}rv}}[\text{AngII}]_{rv} + F_k([\text{AngII}] - [\text{AngII}]_{rv}) \\ &\quad + D_k([\text{AngII}]_{rt} - [\text{AngII}]_{rv}) \end{aligned} \quad (20.12)$$

$$\begin{aligned} \frac{d[\text{AT1 - bound AngII}]_{rv}}{dt} &= c_{\text{AT1-}rv}[\text{AngII}]_{rv} \frac{\ln(2)}{h_{\text{AT1-}rv}}[\text{AT1 - bound AngII}]_{rv} \\ &\quad + F_k([\text{AT1 - bound AngII}]_{\text{circ}} \\ &\quad - [\text{AT1 - bound AngII}]_{rv}) \end{aligned} \quad (20.13)$$

$$\begin{aligned} \frac{d[\text{AT2-bound AngII}]_{\text{rv}}}{dt} &= c_{\text{AT2-rv}}[\text{AngII}]_{\text{rv}} - \frac{\ln(2)}{h_{\text{AT2-rv}}}[\text{AT2-bound AngII}]_{\text{rv}} \\ &\quad + F_k([\text{AT2-bound AngII}]_{\text{circ}} - [\text{AT2-bound AngII}]_{\text{rv}}) \end{aligned} \quad (20.14)$$

Equations for RAS within the renal tissue compartment are as follows:

$$\begin{aligned} \frac{d[\text{AngI}]_{\text{rt}}}{dt} &= k_{\text{AngI-rt}} - (c_{\text{ACE-rt}} + c_{\text{Chym-rt}})[\text{AngI}]_{\text{rt}} - \frac{\ln(2)}{h_{\text{AngI-rt}}}[\text{AngI}]_{\text{rt}} \\ &\quad - D_k([\text{AngI}]_{\text{rt}} - [\text{AngI}]_{\text{rv}}) \end{aligned} \quad (20.15)$$

$$\begin{aligned} \frac{d[\text{AngII}]_{\text{rt}}}{dt} &= (c_{\text{ACE-rt}} + c_{\text{Chym-rt}})[\text{AngI}]_{\text{rt}} - (c_{\text{AT1-rt}} + c_{\text{AT2-rt}})[\text{AngII}]_{\text{rt}} \\ &\quad - \frac{\ln(2)}{h_{\text{AngII-rt}}}[\text{AngII}]_{\text{rt}} - D_k([\text{AngII}]_{\text{rt}} - [\text{AngII}]_{\text{rv}}) \end{aligned} \quad (20.16)$$

$$\frac{d[\text{AT1-bound AngII}]_{\text{rt}}}{dt} = c_{\text{AT1-rt}}[\text{AngII}]_{\text{rt}} - \frac{\ln(2)}{h_{\text{AT1-rt}}}[\text{AT1-bound AngII}]_{\text{rt}} \quad (20.17)$$

$$\frac{d[\text{AT2-bound AngII}]_{\text{rt}}}{dt} = c_{\text{AT2-rt}}[\text{AngII}]_{\text{rt}} - \frac{\ln(2)}{h_{\text{AT2-rt}}}[\text{AT2-bound AngII}]_{\text{rt}} \quad (20.18)$$

20.5.3 Parameterization of the Renal RAS Model

20.5.3.1 Renal Vascular Compartment

The parameterization of the RAS enzyme activities in the renal vascular bed was primarily constrained based on experiments conducted by Danser *et al.* (1998). In this study, radio-labeled Ang I was injected into the renal artery of five hypertensive patients while catheters in the abdominal aorta and renal vein were used to sample the concentration of radio-labeled and endogenous Ang I and Ang II. The constraints of the renal RAS pathway based upon the Danser study can be summarized as follows:

1. Of Ang I entering the kidney from the systemic circulation, 70% is degraded, 10% is converted to Ang II, and 20% exits unchanged.
2. 73% of Ang II entering the kidney is degraded, and the remainder exits unchanged.
3. The concentration of Ang I at the renal vein is approximately 50% higher than the concentration at the renal artery.
4. The concentration of Ang II at the renal vein is approximately 50% lower than the concentration at the renal artery.

Table 20.7 A comparison between the rates of RAS pathway enzyme activity in the renal vasculature and the systemic circulation

	Parameter	Units	Renal vasc. value	Systemic value
$h_{\text{ANGI-rv}}$	Ang I half life	s	0.62	30
$h_{\text{ANGII-rv}}$	Ang II half life	s	1.25	30
$C_{\text{ACE-rv}}$	ACE activity	1/h	500	43
$k_{\text{Ang I-rv}}$	Ang I synthesis	fmol/ml/h	1,080	1,080

The following assumptions regarding the renal vascular RAS pathway were made to satisfy these constraints:

1. The rate of blood flow to the kidney (F_k) is ~ 1 L/min at rest and the blood volume of the kidney is 70 ml, equivalent to a residence time of 4 s.
2. The rate of local Ang I and Ang II degradation in the kidney is significantly increased over the systemic degradation rate to account for the high rate of angiotensin peptide removal in the renal circulation.
3. Since the concentration of Ang I leaving the renal circulation is 50% higher than Ang I entering the renal circulation, we assumed a large amount of endogenous Ang I formation. This endogenous Ang I was assumed to be generated in the renal tissue and to diffuse into the renal vasculature.
4. The rate of ACE activity is significantly higher in the renal circulation than the systemic circulation, in order to convert 10% of Ang I entering the kidney to Ang II.

Based upon these constraints and assumptions, the following parameters (Table 20.7) were calculated as one possible behavior for the renal RAS pathway based on the dynamic system that satisfies the constraints.

The chosen parameters yielded a solution for the dynamical system that satisfied the known constraints of the renal vascular bed. The renal vascular parameters with the same value as their systemic counterpart are not listed in the Table 20.7.

20.5.3.2 Renal Tissue Compartment

The RAS pathway within the renal tissue was implemented in a similar fashion as the renal vascular RAS, with identical enzymes, peptides and receptors. Although the concentration and activities of the enzymes were assumed different, there is minimal quantitative data for these rates in the published literature. The primary constraint for the renal tissue RAS is the assumption that the renal tissue should function as a source of Ang I and Ang II that enters into the renal vasculature. Therefore, the parameters describing the activity of the renal tissue RAS pathway was parameterized such that: (1) the equilibrium concentrations of the angiotensin peptides in the tissue pathway were a source of Ang I and Ang II in the renal vascular compartment; and (2) the constraints on Ang I and Ang II concentrations measured by Danser, 1998, were satisfied.

20.5.4 Hypothesis Testing and Other Applications of the Renal RAS Model

Since it is difficult to directly measure the peptide concentrations and enzyme activities of the RAS within different regions of the kidney, there is a considerable amount of uncertainty around the rates and concentrations of various RAS components. Our model of renal RAS provides the ability to hypothesize the effects of different scenarios and to determine the sensitivity of renal and systemic AT1-bound Ang II levels to changes in different model parameters. This approach to hypothesis testing can yield relevant insights on therapy targets that are more likely to result in renal protection, and help in interpreting results of experimental studies. For instance, we have used the model to show that changes in renal RAS peptide concentrations are not strongly reflected in changes in the concentration of systemic angiotensin peptides. In turn, this suggests that the measured levels of PRA, Ang I or Ang II in response to therapy in systemic circulation may not fully capture the changes that occur within the renal tissue, even though local concentrations of Ang II have a greater effect on renal function than systemic concentrations. In addition, we can test the effects of different enzyme rates on AT1-bound Ang II-induced damage to different compartments within the kidney by adding a model of renal disease progression dependent on the effects of local tissue concentrations of Ang II. Our model may also be used to understand how enhanced localization of RAS-modulating therapies can selectively affect renal vs. systemic targets and affect the rate of renal disease progression.

20.6 RAS Pathway Model Application in Drug Development

The detailed model of systemic and renal RAS pathways presented in this chapter is the foundation of a platform to investigate the response of this system to multiple RAS-modulating therapies. In particular, after careful parameterization and validation of model behavior with available clinical biomarker data, the model can be used to predict the relative effects of the different therapies on entities that are difficult to measure clinically. Further more, it can be used to predict the response to combination therapies for which clinical data is not available. The model also highlights any differences between circulating and renal RAS peptide concentrations, and how therapies that localize in the renal tissue may have different effects than therapies that remain only in the systemic circulation. The predicted concentrations of renal RAS peptides may also yield insight into the changes in local Ang II in response to therapies without requiring invasive and difficult tissue sampling. In addition, the model can be used to investigate questions around the effect of therapies on local tissue Ang II that, in turn, has an effect on renal function.

Using combinations of different classes of RAS-modulating therapies to treat hypertension is of interest in drug development. Since none of the currently prescribed therapies can block 100% of Ang II activity, it is thought that inhibiting the

RAS pathway at two points may provide a more complete blockade and have a better effect on reducing BP. While there is a large body of RAS biomarker data available for monotherapies, there is less complete data on the corresponding biomarker response to combination therapy due to a lack of resources to pursue all potential combinations and the cost factor of clinical trials. To further compound the problem of quantitation, AT1-bound Ang II is the actual effector of the RAS pathway and is not measured in the clinic. Instead, the changes in upstream biomarkers are used to estimate and compare the effectiveness of different classes of RAS modulating therapies. In particular, PRA and Plasma renin concentration (PRC) are typically measured in clinical trials but different classes of RAS drugs affect these biomarkers in different ways (*e.g.*, DRIs reduce PRA, while ARBs and ACEI increase PRA). This makes it difficult to compare the relative level of the reduction in AT-1 bound Ang II achieved by different mono and combination therapies.

The model presented above can be used to fill this gap, by predicting the relative % change in AT1-bound Ang II (*i.e.*, the effector of downstream changes in BP, glomerular filtration rate, end-organ protection, etc.) for different monotherapies and for combination therapies even in the absence of clinical biomarker data. To accomplish this analysis, the model was rigorously calibrated with biomarker data (PRA and PRC) from a large number of studies for a range of RAS-modulating monotherapies (*e.g.*, aliskiren, valsartan, losartan, irbesartan, enalapril, ramipril). The predicted changes in the RAS biomarkers by the model were subsequently validated using a smaller set of biomarker data from available combination studies (Fig. 20.5). In particular:

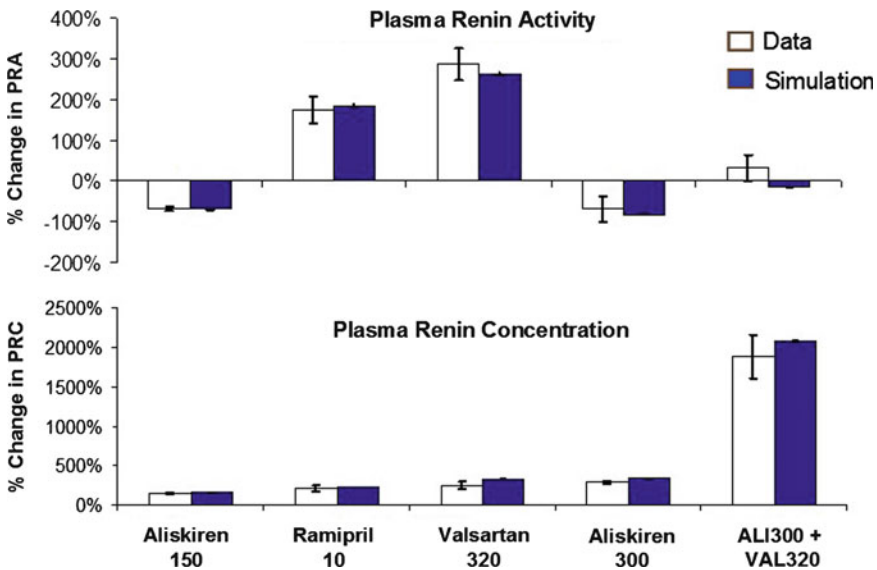


Fig. 20.5 Comparison between observed and predicted PRA and PRC response for a range of therapies

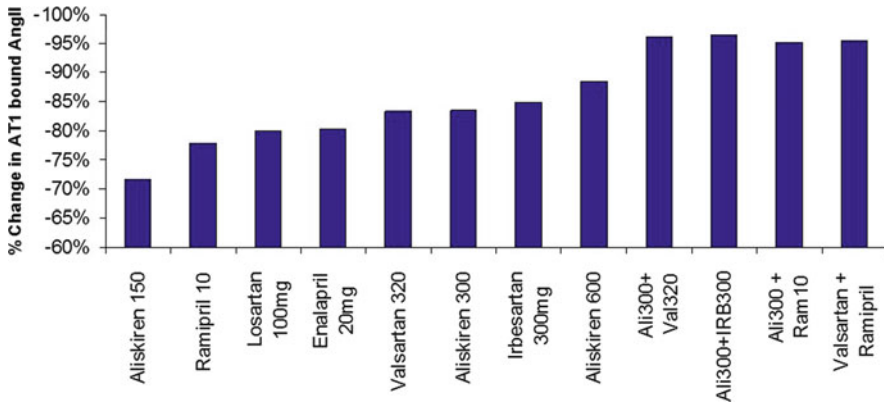


Fig. 20.6 Model prediction of the relative % change in AT-1 bound Ang II in response to a range of therapies

1. Studies of different doses of aliskiren (a DRI) monotherapy provided data on the reduction in PRA as well the corresponding reactive rise in PRC for each dose. This data was used to calibrate a pharmacodynamic (PD) curve relating aliskiren dose to % inhibition of PRA, and was used to calibrate the shape and strength of the feedback on renin with changes in AT1-bound Ang II (f) in Eq. 20.1.
2. After parameterization of this feedback relationship (f), the model was able to capture the PRA/PRC response to ARB and ACEI therapy using only changes in calibration of the % inhibition of AT1 binding rate or ACE activity, respectively. No additional changes in the model, including the feedback from AT1 to PRA, were needed.
3. The model was able to predict the biomarker (PRA/PRC) response to combinations of RAS drugs for which data was available, (e.g., aliskiren + valsartan), with no additional changes in model parameters.

The model can be used with confidence to predict the change in biomarkers for different combination therapies when sufficient biomarker data is not available to us (Fig. 20.6). For example, it has been used to predict the biomarker response for aliskiren 300 mg + ramipril 10 mg. In addition, the model predicts the relative % inhibition of AT1-bound Ang II for the different doses and types of RAS-modulating therapies. The strength of this integrated model lies in the prediction of AT1-bound Ang II levels, a valuable measure of the primary effector of the downstream response of the RAS pathway that is difficult to measure *in vivo*, and even more difficult to measure in the tissue.

20.7 Conclusion

In this chapter, we have briefly introduced our approach to building and calibrating a model of the RAS pathway in the systemic circulation and renal tissue. This model

then becomes part of a larger physiology model of BP regulation and kidney function. After creating the fundamental mathematical structure for the pathway, we presented our approach to parameterizing the model, either directly from available clinical measurements or inferred from steady-state assumptions. We then discussed our approach to representing the effects of RAS-modulating therapies in the model and validated the model behavior with data not used for its calibration.

We touched upon ways to include clinical variability in the model and concluded with a description of how the RAS pathway model was extended from the systemic circulation to the kidney. While a larger degree of uncertainty around the parameter values in the renal RAS pathway model may appear as a limiting factor, capturing the basic biology and physiology allows the model to be used for hypothesis testing and sensitivity analysis. Finally, we hope that this work will encourage the reader to find out more details of (1) how the RAS pathway model was linked to the model of BP regulation and renal functions, (2) include the effects of aldosterone, another peptide that regulates sodium and water reabsorption, (3) how the model was modified to capture the pathophysiology of hypertension and renal disease and (4) how the combined model was used to test various clinical hypothesis around RAS-modulating therapies in different patient phenotypes.

The goal of a model is to speed up the development process along the drug development pipeline. Novel therapies can be prioritized based on efficacy early in the drug development process, with multiple dosing regimens and protocols tested and simulated results returned prior to recruiting the first patient in a clinical trial. Combination therapies can also be evaluated in the model to look for potential nonadditive effects, and to identify the most potent approach in lowering BP in patients with multiple disease etiologies. A set of biomarkers could be determined that can identify the best responders to different therapeutic approaches for treating hypertension. Ultimately, the model is a versatile tool for pharmaceutical research and development to optimize current approaches to drug development, and provides new insight into the physiology to reduce the time to bring an effective novel therapy to the market.

Acknowledgements The authors would like to acknowledge Drs. Gabriel Helmlinger, Jeff Trimmer and Don Stanski for guidance on the methodology development, as well as critically reviewing the manuscript. The work presented here could not be completed without the scientific and clinical guidance of Drs. Deborah Keefe, Alan Charney, Bill Dole, Marion Dahlke, David Feldman. The authors would like to acknowledge the technical contributions of Alex Bangs and Dr. Kortney Leabourne to this manuscript.

References

- Admiraal PJ, Danser AH, Jong MS, Pieterman H, Derx FH, Schalekamp MA (1993) Regional angiotensin II production in essential hypertension and renal artery stenosis. *Hypertension* 21:173–184

- Aksenov SV, Church B, Dhiman A, Georgieva A, Sarangapani R, Helmlinger G, Khalil IG (2005) An integrated approach for inference and mechanistic modeling for advancing drug development. *FEBS Lett* **579**(8):1878–1883
- Brenner BM, Cooper ME, de ZD K, WF MWE, Parving HH, Remuzzi G, Snapinn SM, Zhang Z, Shahinfar S (2001) Effects of losartan on renal and cardiovascular outcomes in patients with type 2 diabetes and nephropathy. *N Engl J Med* **345**:861–869
- Burnier M, Hagman M, Nussberger J, Biollaz J, Armagnac C, Brouard R, Weber B, Brunner HR (1995) Short-term and sustained renal effects of angiotensin II receptor blockade in healthy subjects. *Hypertension* **25**:602–609
- Chappell MC, Pirro NT, Sykes A, Ferrario CM (1998) Metabolism of angiotensin-(1-7) by angiotensin-converting enzyme. *Hypertension* **31**:362–367
- Christen Y, Waeber B, Nussberger J, Porchet M, Borland RM, Lee RJ, Maggon K, Shum L, Timmermans PB, Brunner HR (1991) Oral administration of DuP 753, a specific angiotensin II receptor antagonist, to normal male volunteers. Inhibition of pressor response to exogenous angiotensin I and II. *Circulation* **83**:1333–1342
- Christopher R, Dhiman A, Fox J, Gendelman R, Haberitcher T, Kagle D, Spizz G, Khalil IG, Hill C (2004) Data-driven computer simulation of human cancer cell. *Ann N Y Acad Sci* **1020**:132–153
- Danser AH, Admiraal PJ, Derckx FH, Schalekamp MA (1998) Angiotensin I-to-II conversion in the human renal vascular bed. *J Hypertens* **16**:2051–2056
- Delacretaz E, Nussberger J, Biollaz J, Waeber B, Brunner HR (1995) Characterization of the angiotensin II receptor antagonist TCV-116 in healthy volunteers. *Hypertension* **25**:14–21
- Drumond MC, Kristal B, Myers BD, Deen WM (1994) Structural basis for reduced glomerular filtration capacity in nephrotic humans. *J clin invest* **94**(3):1187–1195
- FitzGerald TJ, Aronowitz J, Giulia CM, Fisher G, Kadish S, Lo YC, Mayo C, McCauley S, Meyer J, Pieters R, Sherman A (2006) The effect of radiation therapy on normal tissue function. *Hematol Oncol Clin North Am* **20**(1):141–163
- Friedrich CM, Paterson TM (2004) In silico predictions of target clinical efficacy. *Drug Discovery Today: Targets* **3**:216–222
- Gainer JV, Morrow JD, Loveland A, King DJ, Brown NJ (1998) Effect of bradykinin-receptor blockade on the response to angiotensin-converting-enzyme inhibitor in normotensive and hypertensive subjects. *N Engl J Med* **339**:1285–1292
- Guyton AC, Coleman TG, Cowley AW Jr, Liard JF, Norman RA Jr, Manning RD Jr (1972a) Systems analysis of arterial pressure regulation and hypertension. *Ann Biomed Eng* **1**:254–281
- Guyton AC, Coleman TG, Granger HJ (1972b) Circulation: overall regulation. *Annu Rev Physiol* **34**:13–46
- Hajjar I, Kotchen TA (2003) Trends in prevalence, awareness, treatment, and control of hypertension in the United States, 1988–2000. *JAMA* **290**:199–206
- Haulica I, Bild W, Serban DN (2005) Angiotensin peptides and their pleiotropic actions. *J Renin Angiotensin Aldosterone Syst* **6**:121–131
- Iusuf D, Henning RH, Van Gilst WH, Roks AJ (2008) Angiotensin-(1-7): pharmacological properties and pharmacotherapeutic perspectives. *Eur J Pharmacol* **585**:303–312
- Karaaslan F, Denizhan Y, Kayserilioglu A, Gulcur HO (2005) Long-term mathematical model involving renal sympathetic nerve activity, arterial pressure, and sodium excretion. *Ann Biomed Eng* **33**:1607–1630
- Katsurada A, Hagiwara Y, Miyashita K, Satou R, Miyata K, Ohashi N, Navar LG, Kobori H (2007) Novel sandwich ELISA for human angiotensinogen. *Am J Physiol Renal Physiol* **293**:F956–F960
- Korner PI, Angus JA (1997) Vascular remodeling. *Hypertension* **29**:1065–1066
- Korner PI, Bobik A, Angus JJ (1992) Are cardiac and vascular “amplifiers” both necessary for the development of hypertension? *Kidney Int Suppl* **37**:S38–S44
- Lazzara MJ, Deen WM (2007) Model of albumin reabsorption in the proximal tubule. *Am J Physiol Renal Physiol* **292**:F430–F439

- LeFebvre J, Shintani A, Gebretsadik T, Petro JR, Murphey LJ, Brown NJ (2007) Bradykinin B(2) receptor does not contribute to blood pressure lowering during AT(1) receptor blockade. *J Pharmacol Exp Ther* **320**:1261–1267
- Liu Y, Purvis J, Shih A, Weinstein J, Agrawal N, Radhakrishnan R (2007) A multiscale computational approach to dissect early events in the Erb family receptor mediated activation, differential signaling, and relevance to oncogenic transformations. *Ann Biomed Eng* **35**(6):1012–1025
- Luque M, Martin P, Martell N, Fernandez C, Brosnihan KB, Ferrario CM (1996) Effects of captopril related to increased levels of prostacyclin and angiotensin-(1-7) in essential hypertension. *J Hypertens* **14**:799–805
- Maillard MP, Mazzolai L, Daven V, Centeno C, Nussberger J, Brunner HR, Burnier M (1999) Assessment of angiotensin II receptor blockade in humans using a standardized angiotensin II receptor-binding assay. *Am J Hypertens* **12**:1201–1208
- Manhem PJ, Ball SG, Morton JJ, Murray GD, Leckie BJ, Fraser R, Robertson JI (1985) A dose-response study of HOE 498, a new non-sulphydryl converting enzyme inhibitor, on blood pressure, pulse rate and the renin-angiotensin-aldosterone system in normal man. *Br J Clin Pharmacol* **20**:27–35
- Matsui T, Tamaya K, Matsumoto K, Osajima Y, Uezono K, Kawasaki T (1999) Plasma concentrations of angiotensin metabolites in young male normotensive and mild hypertensive subjects. *Hypertens Res* **22**(4):273–277
- Mazzolai L, Maillard M, Rossat J, Nussberger J, Brunner HR, Burnier M (1999) Angiotensin II receptor blockade in normotensive subjects: a direct comparison of three AT1 receptor antagonists. *Hypertension* **33**:850–855
- Meng QC, Balcells E, Dell'Italia L, Durand J, Oparil S (1995) Sensitive method for quantitation of angiotensin-converting enzyme (ACE) activity in tissue. *Biochem Pharmacol* **50**:1445–1450
- Metzger R, Bohle RM, Pauls K, Eichner G, Alhenc-Gelas F, Danilov SM, Franke FE (1999) Angiotensin-converting enzyme in non-neoplastic kidney diseases. *Kidney Int* **56**:1442–1454
- Michelson S (2006) The impact of systems biology and biosimulation on drug discovery and development. *Mol Biosyst* **2**(6–7):288–291
- Michelson S, Sehgal A, Friedrich C (2006) In silico prediction of clinical efficacy. *Curr Opin Biotechnol* **17**(6):666–670
- Navar LG, Harrison-Bernard LM, Nishiyama A, Kobori H (2002) Regulation of intrarenal angiotensin II in hypertension. *Hypertension* **39**:316–322
- Navar LG, Nishiyama A (2004) Why are angiotensin concentrations so high in the kidney? *Curr Opin Nephrol Hypertens* **13**:107–115
- Nussberger J, Gradman AH, Schmieder RE, Lins RL, Chiang Y, Prescott MF (2007) Plasma renin and the antihypertensive effect of the orally active renin inhibitor aliskiren in clinical hypertension. *Int J Clin Pract* **61**:1461–1468
- Nussberger J, Wuerzner G, Jensen C, Brunner HR (2002) Angiotensin II suppression in humans by the orally active renin inhibitor Aliskiren (SPP100): comparison with enalapril. *Hypertension* **39**:E1–E8
- Osborn JW, Averina VA, Fink GD (2009) Current computational models do not reveal the importance of the nervous system in long-term control of arterial pressure. *Exp Physiol* **94**:389–396
- Poulsen K (1973) Kinetics of the renin system. The basis for determination of the different components of the system. *Scand J Clin Lab Invest* **31**:3–86
- Rullmann JA, Struemper H, Defranoux NA, Ramanujan S, Meeuwisse CM and van EA (2005) Systems biology for battling rheumatoid arthritis: application of the Entelos PhysioLab platform. *Syst Biol (Stevenage)* **152**(4):256–262
- Saris JJ, van Dijk MA, Kroon I, Schalekamp MA, Danser AH (2000) Functional importance of angiotensin-converting enzyme-dependent in situ angiotensin II generation in the human forearm. *Hypertension* **35**:764–768
- Schalekamp MA, Admiraal PJ, Derckx FH (1989) Estimation of regional metabolism and production of angiotensins in hypertensive subjects. *Br J Clin Pharmacol* **28**(Suppl 2):105S–113S

- Schoeberl B, Pace E, Howard S, Garantcharova V, Kudla A, Sorger PK, Nielsen UB (2006) A data-driven computational model of the ErbB receptor signaling network. *Conf Proc IEEE Eng Med Biol Soc* **1**:53–54
- Schuijt MP, de VR S, PR SMA, Danser AH (2002) Vasoconstriction is determined by interstitial rather than circulating angiotensin II. *Br J Pharmacol* **135**:275–283
- Shoda LK, Young DL, Ramanujan S, Whiting CC, Atkinson MA, Bluestone JA, Eisenbarth GS, Mathis D, Rossini AA, Campbell SE, Kahn R, Kreuwel HT (2005) A comprehensive review of interventions in the NOD mouse and implications for translation. *Immunity* **23**(2):115–126
- Smithies O (2003) Why the kidney glomerulus does not clog: a gel permeation/diffusion hypothesis of renal function. *Proc Natl Acad Sci USA* **100**:4108–4113
- Takai S, Shiota N, Sakaguchi M, Muraguchi H, Matsumura E, Miyazaki M (1997) Characterization of chymase from human vascular tissues. *Clin Chim Acta* **265**:13–20
- van Kats JP, de Lannoy LM, Jan Danser AH, van M Jr, Verdouw PD and Schalekamp MA (1997) Angiotensin II type 1 (AT1) receptor-mediated accumulation of angiotensin II in tissues and its intracellular half-life *in vivo*. *Hypertension* 1997 Jul 42–49
- Wei CC, Tian B, Perry G, Meng QC, Chen YF, Oparil S, Dell'Italia LJ (2002) Differential ANG II generation in plasma and tissue of mice with decreased expression of the ACE gene. *Am J Physiol Heart Circ Physiol* **282**:H2254–H2258

Chapter 21

Recent Developments in Physiologically Based Pharmacokinetic Modeling

Vikash Sinha and Holly H.C. Kimko

Abstract Physiologically based pharmacokinetic (PBPK) modeling is a mechanism based mathematical modeling technique to predict and integrate drug absorption, distribution, metabolism and excretion (ADME) of a compound in animals and human. A PBPK model maps the transfer of drug through different “organ” compartments and accounts for anatomical, physiological, physical, and chemical properties that influence ADME processes. Thus, application of PBPK has been of great interest lately in various phases of drug discovery and development. However, until recently PBPK based approaches could not be frequently applied within pharmaceutical industry because of the complexity of the model and the difficulty in obtaining necessary input parameters for a PBPK model, such as labor intensive tissue-to-plasma partition coefficient. In recent years, further improvement of *in vitro*, *ex vivo*, and *in silico* methods to provide input variable information has significantly increased the applicability of the PBPK based approach. In addition, several software programs have incorporated relevant PBPK equations and have made its application more widespread and simpler. More recently, the support of regulatory agencies for use of PBPK based methods has also encouraged drug developers to apply this technique in drug development. This chapter describes whole-body PBPK modeling methodology and its various applications in pharmaceutical industry.

21.1 Introduction

Selection of drug candidates with optimal pharmacokinetic (PK) parameters in early drug discovery is essential for convenient dosing regimens and effective therapy in patients. During drug discovery, considerable resources are required to assess the PK properties of potential drug candidates via *in vivo* and *in vitro* preclinical studies. Traditionally, the pharmaceutical industry has relied on empirical approaches such

V. Sinha (✉)

Janssen Research & Development, a division of Janssen Pharmaceutica NV, Beerse, Belgium
e-mail: vsinha@its.jnj.com

as allometry for predicting human PK before first-in-man studies. However, in recent years, there has been a growing interest in methods that improve predictions of human PK via mechanistic understanding of the underlying processes impacting drug's PK disposition.

PBPK approach has been intensively discussed as a tool to improve drug development process (Rowland *et al.* 2004, 2011; Peck 2010; Nestorov 2003; Theil *et al.* 2003). The concept of PBPK modeling was first described in the seminal work of Teorell (1937a, b), in which a set of differential equations for absorption, distribution and elimination of a drug was provided to describe pharmacokinetics. However, in the 1930s when the concept was developed, the computational power was not sufficient to solve the sets of equations to easily apply the concept of PBPK modeling in drug development. Therefore, simpler empirical models (*e.g.*, sums of exponential expressions) representing a small number of nonphysiological body compartments were used to describe the pharmacokinetics in the human body.

PBPK models employ *in vitro* and/or *in silico* data inputs, some of which are described in this chapter, to predict concentration vs. time profiles in plasma and tissues. The physiological framework provided by a PBPK model can integrate all input data and aid in understanding PK characteristics of potential drug candidates. An important differentiating feature is that, unlike empirical approaches, PBPK based approaches are derived from an understanding of the underlying anatomy and physiology of the species. Hence, the basic model equations representing anatomy and physiology are not drug specific but common to mammalian species, thereby facilitating interspecies scaling.

The Critical Path Opportunities Report issued by FDA in March 2006 states that: "The findings from *in silico* testing (computer simulation, rather than laboratory or animal testing) could reduce the risk and cost of human testing by helping product sponsors make more informed decisions on how to proceed with product testing and when to remove a product from further development." Application of mathematical modeling and simulation is being extensively used in drug development (Holford *et al.* 2000; Kimko and Duffull 2003), and simulation via PBPK certainly has a special niche in predicting human testing results by integration of information of physiology and physicochemical properties of an investigational drug. In addition, the support from the FDA in the use of PBPK approach is noteworthy: recently, scientists at the FDA have published the cases in which results from PBPK approach were used in supporting claimed contents regarding drug–drug interaction in the submissions by pharmaceutical companies during the period of August 2008 and August 2009 (Zhao *et al.* 2010; Rowland *et al.* 2011).

PBPK modeling starts from the understanding of anatomy, physiology and pathology to set up a model, whereas compartmental PK modeling derives from the observation of a measured time course of concentrations. Regardless of the starting points, the predicted concentration can be used to predict the pharmacodynamic (PD) response of the compound by extending the PK model via a PD link model. The characterization of a drug's PK in a complex biological system can be described by assembling all ADME processes in one global model, for example, using whole-body physiologically (WB-PBPK) based models (Gerlowski and Jain 1983;

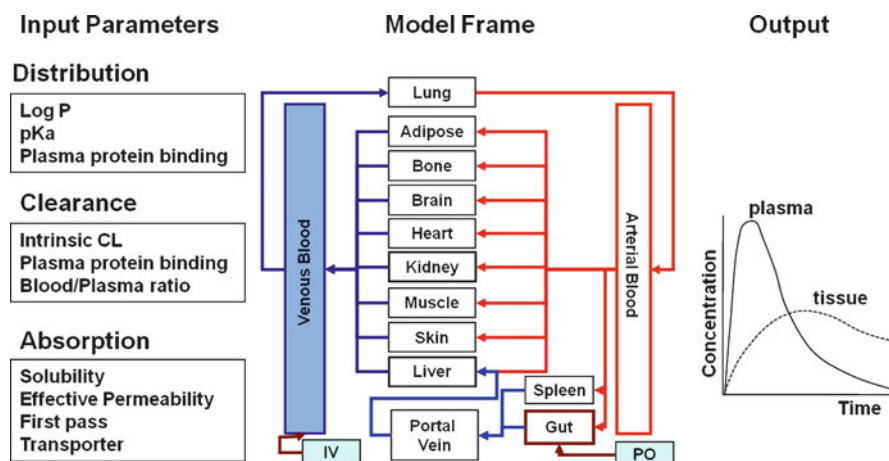


Fig. 21.1 Components of PBPK modeling approach

Nestorov 2003; Nestorov *et al.* 1998). WB-PBPK models map the complex drug transport scheme onto an anatomically correct and physiologically realistic compartmental structure, comprised of the organs of the body each perfused by and connected to the vascular system. The model is, therefore, predetermined and independent of the drug of interest. An example of a generic PBPK model is shown in Fig. 21.1. The most recent developments and applications of WB-PBPK have been reviewed in the literature (Nestorov 2007; Rowland *et al.* 2011).

Advances in the development of physiologically based prediction tools to assess the required input parameters such as tissue-plasma partition coefficient (P_{tp}), intrinsic clearance (CL_{int}), and rate and extent of absorption solely from *in vitro* data, together with the increasing availability of physiological data and user-friendly software interfaces (*e.g.*, GastroPlus[®], PKSim[®], SIMCYP[®]) has now greatly extended the application of WB-PBPK. An interesting feature of WB-PBPK models is allowance of linking of data from various sources (*in vitro* and *in vivo*) into a single mechanistic framework, making full use of all drug-related information available at each stage of the drug discovery process. As mentioned before, another major advantage is that, unlike empirical modeling, WB-PBPK models are not purely descriptive but may also account for the mechanistic basis of the observed data. For example, prediction failures with preclinical species can guide experimental efforts to understand the compound's properties and achieve a higher level of prediction accuracy before first-in-human studies. Sometimes more complex models that take into account factors such as involvement of active transporters may be required. The validation of model assumptions in a preclinical PBPK model such as rat or a dog may help in mechanistic understanding of pharmacokinetic behavior of a drug before first-in-human studies.

Figure 21.1 depicts the framework of WB-PBPK modeling approach. In the sections below, the concepts and applications of relevant *in vitro* based prediction procedures that can be used to predict drug clearance, tissue distribution and rate

and extent of absorption are introduced. The ability of these prediction tools to predict plasma and tissue concentration time profiles, when placed within a generic WB-PBPK model, is also briefly discussed.

21.2 Input Parameters for PBPK Modeling

21.2.1 Prediction of Hepatic Drug Clearance

For many drugs, the major organ of drug metabolism is the liver. Hence, prediction of hepatic drug clearance (CL_H) has received much attention in physiologically based modeling. The representative models available for CL_H predictions are well-stirred model, parallel tube model and dispersion models and are described below briefly:

- (a) *Well-stirred model*: The “well-stirred” model of hepatic drug clearance was first proposed by Gillette (1971) and established by Rowland *et al.* (1973) and Wilkinson and Shand (1975). This model assumes that the liver as well-stirred compartment and therefore the drug concentration in the hepatic sinusoids is assumed to be equal to that in the hepatic vein (Pang and Rowland 1977). In the commonly used form, net hepatic drug clearance based on whole-blood drug concentration ($CL_{H,B}$) is derived as a function of hepatic blood flow ($Q_{H,B}$), the free fraction of drug in blood ($f_{u,B}$), and the intrinsic metabolic clearance in the liver based on unbound drug concentration ($CL_{u,int,H}$):

$$CL_{H,B} = \frac{(Q_{H,B} \times CL_{u,int,H} \times f_{u,B})}{(Q_{H,B} + CL_{u,int,H} \times f_{u,B})} \quad (21.1)$$

This model assumes that the drug is distributed instantly and homogeneously throughout liver water and that the unbound concentrations in plasma and liver water are identical. Effectively, this means that drug distribution into the liver is perfusion-limited with no diffusion delay and that no active transport systems are involved.

A key feature of this model is that it equates whole-blood drug clearance, rather than plasma drug clearance, to liver blood flow, because the organ is potentially capable of extracting the drug from both plasma and blood cells. Most reported clearance values are referenced to plasma rather than blood, because it is more common to measure drug concentration in plasma. If plasma drug clearance (CL_H) is to be estimated, then (21.1) must be modified to take into account the free fraction in plasma (f_u) and the total blood to total plasma drug concentration ratio (C_B/C_P):

$$CL_H = \frac{(Q_{H,B} \times CL_{u,int,H} \times f_u)}{(Q_{H,B} + CL_{int} \times f_u)/(C_B/C_P)} \quad (21.2)$$

- (b) *Parallel tube model*: The parallel tube model assumes that the liver is composed of a collection of identical and parallel tubes, along which drug concentration decreases progressively in the direction of the hepatic blood flow (Pang and Rowland 1977).
- (c) *Dispersion model*: This is another commonly used but mathematically more complex model, which describes the hepatic uptake metabolic processes in terms of convective flow, axial dispersion (mixing of blood) and disappearance of drugs by elimination (Roberts and Rowland 1985, 1986a).

The well-stirred and parallel tube models are functionally equivalent if the hepatic extraction ratio (E_H) is low (<0.5), but differ at high E_H (Pang and Rowland 1977). For compounds with intermediate and high E_H , the well stirred model gives a lower CL_H than the parallel tube model (Pang and Rowland 1977; Jansen 1981; Pond and Tozer 1984; Iwatsubo *et al.* 1996, 1997; Houston 1994). The dispersion model has been shown to be superior to the well-stirred and parallel tube models for highly extracted drugs in rats (Roberts and Rowland 1986b). CL_{int} values from an *in vitro* microsomal study and an *in vivo* PK study in a preclinical species may be compared for the different models to select the right model for a particular compound.

21.2.2 Prediction of In Vivo CL from In Vitro CL

This is a two step process: firstly determination of intrinsic CL in microsomes or hepatocytes, and secondly scaling of *in vitro* CL to *in vivo* CL. In-depth reviews can be found in the literature describing this methodology (Iwatsubo *et al.* 1996, 1997; Houston 1994). Some of the basic principles are described below.

A drug's CL_{int} is defined as the ratio of the maximum metabolic rate (V_{max}) and the substrate concentration at the half-maximal velocity (K_m) of all enzymes involved in its metabolism, provided that the substrate concentration is well below the K_m of the metabolizing system (Iwatsubo *et al.* 1996). A simpler and commonly used approach is to estimate the CL_{int} directly from the rate of disappearance of parent drug at various substrate concentrations in a defined metabolizing system such as microsomal fraction of the organ of interest. This method is referred to as the *in vitro* half-life method. The CL_{int} is described then by the relationship $CL_{int} = 0.693/\text{in vitro half-life}$. Although both V_{max}/K_m and *in vitro* half-life approach have been shown to provide accurate estimation of *in vivo* CL (Obach *et al.* 1997), caution must be exercised with *in vitro* half-life approach which requires the substrate concentration to be well below the K_m value of each of the relevant enzymes involved in the metabolism. A saturable metabolism can yield to nonlinear kinetics and underestimation of CL_{int} (Iwatsubo *et al.* 1997). Also in some cases such as auto-activation and auto-inhibition, the classical V_{max}/K_m approach model cannot be applied (Houston and Kenworthy 2000).

21.2.3 *Scaling of In Vitro CL_{int} to In Vivo CL_{int}*

The CL_{int} data obtained from *in vitro* studies further requires scaling-up to obtain *in vivo* CL_{int}. The CL_{int} data obtained from *in vitro* studies is typically expressed as a function of microsomal protein concentration or on a per million hepatocyte basis. For the microsomal system, the scaling is performed based on the enzyme content of the microsomal system (*i.e.*, amount of microsomal protein per gram of liver). For hepatocytes, the scaling factor is determined by the hepatocyte content of the liver (*i.e.*, number of cells per gram of liver). The obtained CL_{int} is then scaled for a species-specific amount of liver (gram) per kilogram body-weight. The *in vivo* scaling of *in vitro* CL_{int} for both rat and human microsomes and hepatocytes has been recently reviewed by Barter *et al.* (2007).

The metabolic capacity of hepatocytes is because of full complement of drug-metabolizing enzymes, including phase I and II (*e.g.*, direct conjugation) metabolic processes and active transport systems contained within the hepatocyte cell. For these reasons, CL_{int} derived from hepatocytes have often been advocated to provide a better prediction of CL_H as compared with the microsomes extracted from hepatocytes (Brown *et al.* 2007; Miners *et al.* 2006; Lave *et al.* 1997). However, activity of metabolic enzymes in hepatocyte culture can vary extensively with time, culture conditions and the quality of liver donors (Lave *et al.* 1997; Blanchard *et al.* 2006; LeCluyse 2001). More recently, recombinant CYP systems have gained popularity to predict both inter-individual variability of drug CL within the population (Galetin *et al.* 2004; Rawden *et al.* 2005; Rostami-Hodjegan and Tucker 2007) and potential drug–drug interactions (Brown *et al.* 2005; Galetin *et al.* 2006).

21.2.4 *Factors Influencing Hepatic Clearance*

Inter-individual variability in hepatic clearance can be introduced by variability in liver abundance of cytochrome P450 enzymes (CYPs), microsomal protein per gram of liver (MPPGL), and liver weight. Also hepatic blood flow being a function of cardiac output is dependent on body surface area and age. Therefore, variability in these parameters can result in variability in hepatic blood flow (Johnson *et al.* 2006). The influence of extrinsic factors such as eating (Mathias 1990; Matheson *et al.* 2000), posture and physical activity (Bernardi *et al.* 1992; Edell *et al.* 1989; Ruckert and Juchems 1970; Wong *et al.* 1996) and diseases associated with significant hemodynamic changes may also be incorporated into the prediction of variability in drug clearance by allowing changes in hepatic blood flow (Rostami-Hodjegan and Tucker 2007).

The blood to plasma ratio is sometimes another important parameter influencing hepatic clearance. The fraction of drug unbound in blood (f_{uB}) is dependent on a drug's affinity for relevant plasma proteins and red cells, as well as the circulating concentrations of plasma proteins and the hematocrit. When the drug is unequally

distributed between red cells and plasma, the hematocrit also becomes a source of variability when predicting drug clearance. The population distribution of hematocrit values is well characterized, and the effects of age and sex, as well as many environmental influences, on the hematocrit are known (Rostami-Hodjegan and Tucker 2007).

Other factors that may influence hepatic clearance of drugs include active hepatic uptake and biliary transporters and their interplay with drug metabolizing enzymes. However, currently our knowledge on the abundance of specific transporters in the human liver and its associated variability is limited.

21.3 Physiologically Based Predictions of Tissue Distribution

Tissue distribution is another important determinant of the pharmacokinetics of drugs. In the WB-PBPK model, an important determinant of pharmacokinetic behavior is the affinity of drugs for specific tissues, which is characterized by the tissue-to-plasma partition coefficients (P_{tp}). These values can be determined at steady state, *i.e.*, when distribution equilibrium has been attained (Fichtl *et al.* 1991). Alternatively P_{tp} values can be determined *in vitro* using tissue homogenates, tissue slices or isolated perfused organs, all of which are steady state approaches (Post *et al.* 1978; Bickel and Gerny 1980; Bazil *et al.* 1987). However, these *in vitro* approaches are not always representative of the *in vivo* situation (Schuhmann *et al.* 1987). For example, basic drugs frequently distribute into lysosomes, which are disrupted by homogenization resulting in under-estimation of *in vivo* P_{tp} values in lysosomes-rich tissues such as lung, liver and kidney (MacIntyre and Cutler 1988).

Determination of P_{tp} values by drug infusion to animals and assay of blood and tissues is quite laborious, and therefore various methods have been proposed to predict P_{tp} from the physicochemical characteristics of the drug and the physiological composition of the tissues (Davis and Mapleson 1993; El Masri and Portier 1998; Poulin and Theil 2000, 2002; Poulin *et al.* 2001).

Volume of distribution in steady state (V_{ss}) is the volume of plasma (V_p) plus the sum of the apparent volumes of distribution of each tissue. These are determined by the drug's plasma to tissue partition coefficient (P_{tp}) multiplied by the tissue volume (V_t) (Sawada *et al.* 1984).

$$V_{ss} = V_p + \sum V_t \times P_{tp} = V_p + \sum V_t \times fu_p/fu_t \quad (21.3)$$

In vivo determination of P_{tp} is time consuming and not amenable to high throughput screening. To avoid the need for *in vivo* preclinical data, new approaches have investigated the correlation between human fu_t , (calculated from human V_{ss} and fu_p literature data) and physicochemical properties such as $\log D$, pK_a and fu_p (Lombardo *et al.* 2002, 2004). Thus by measuring *in vitro* parameters such as $\log D$, pK_a

and f_{up} , P_{tp} is calculated using tissue composition based equations as described in the sections below.

The equations reflecting a tissue composition based approach were first described by Poulin and coworkers and were applied to predict tissue partitioning of pharmaceutical acids, bases and neutrals. For a detailed description of derivation of these equations the readers should refer to their published work (Poulin and Theil 2000; Poulin *et al.* 2001). In brief, it is assumed that a drug distributes homogeneously into each tissue (and plasma) by passive diffusion. Consequently, the drug partitions between lipids and water and binds reversibly to common proteins present in plasma and tissue interstitial space:

$$P_{tp} = \frac{(P \times [V_{NLt} + 0.3 \times V_{PHt}] + [V_{Wt} + 0.7 \times VP_{PHt}]) \times f_{up}}{(P \times [V_{NLp} + 0.3 \times V_{PHp}] + [V_{Wp} + 0.7 \times VP_{PHp}]) \times f_{ut}} \quad (21.4)$$

The tissue composition input to (21.4) comprises the fractional tissue volume content (V) of neutral lipids (NL), phospholipids (PH), and water (W) in tissue (t) and plasma (p). The drug-specific input comprises the drug's lipophilicity (P , antilog of $\log P$) and macromolecular binding to common proteins present in plasma (f_{up}) and the tissue interstitial space (f_{ut}) (Poulin and Theil 2002). The main assumption implicit in these equations is that only passive diffusion governs tissue distribution of a drug, in which mainly two processes need to be accounted for: (a) reversible partitioning into tissue lipids and water; and (b) reversible binding to common proteins present in plasma and the interstitial space.

Poulin and Theil reported support for their equations with *in vivo* data of about 140 structurally diverse drugs obtained from the literature and found that 80% of all predicted V_{ss} were within a factor of two of the corresponding experimental values (Poulin and Theil 2002). The accuracy of P_{tp} predictions in adipose tissue (Poulin *et al.* 2001) as well as in nonadipose tissues has also been investigated (Poulin and Theil 2000). Overall, 85% of the predicted P_{tp} values differed from the mean experimental values by a factor of three ($n = 269$). Although considered generally successful by the authors, follow-up studies indicated that when applied to different data sets, the overall V_{ss} prediction accuracy of these equations was reduced (Jones *et al.* 2006; Parrott *et al.* 2005a). This may be explained by different physicochemical properties (Parrott *et al.* 2005b), as well as by distribution processes that are not covered in these equations, such as active transport, specific macromolecular binding, limitation for membrane permeation and ionic interactions (Poulin and Theil 2002).

A clear drawback of (21.4) is that P_{tp} predictions in lung and intestine, as well as the overall V_{ss} of moderate-to-strong bases, are less accurate, mainly as a result of under-predictions (Poulin and Theil 2000). The under predictions associated with moderate-to-strong bases have been thoroughly investigated by Rodgers *et al.* (Rodgers *et al.* 2005a, b) who showed that in the absence of other specialized mechanisms, electrostatic interactions with acidic membrane phospholipids will predominate for any basic compound that is sufficiently positively charged within tissue cells (Rodgers *et al.* 2005b). To accommodate the ionic interaction, Rodgers *et al.* have developed a new tissue composition-based approach and showed it to improve the predictability of P_{tp}

over the equations developed by Poulin and Theil (Rodgers *et al.* 2005a; Rodgers and Rowland 2006). More recently, De Buck *et al.* directly compared both approaches for their ability to predict rat and human V_{ss} on a data set mainly comprised of moderate-to-strong basic compounds. In both rat and humans the approach by Rodgers yielded more accurate predictions of V_{ss} ; however, prediction accuracy was better in rats (80% within twofold) as compared with human (80% within threefold) (De Buck *et al.* 2007a, b).

It should also be noted that, irrespective of the approach, under-predictions in lung and liver tissue were more pronounced than in other tissues (Poulin and Theil 2000; Rodgers *et al.* 2005a, b; De Buck *et al.* 2007a). This may be explained by the fact that distribution kinetics of lipophilic bases is also driven by sub cellular disposition kinetics, such as accumulation into acidic organelles and lysosomes (Yokogawa *et al.* 2002). A failure to account for such interactions may yield underpredictions and future approaches should be directed to incorporate these. Last but not least, overprediction of P_{tp} is a common issue with brain tissue, most probably because these approaches assume passive diffusion, and in comparison with other tissues, brain penetration is known to be more restrictive and selective (Berezhkovskiy 2004).

21.4 Prediction Models for Oral Absorption and Bioavailability

Oral administration is the most popular and convenient route of drug administration. Therefore, it is of particular interest to predict oral absorption in human from experimental *in vitro* data and biopharmaceutical properties. After oral administration, the drug will pass sequentially from the gastrointestinal lumen, through the intestinal wall and through the liver before entering the systemic circulation. Thus, oral bioavailability is defined as:

$$F_{\text{oral}} = F_a \times F_g \times F_h = F_a(1 - E_g)(1 - E_H) \quad (21.5)$$

where F_a is the net fraction of dose absorbed from the intestinal tract, F_g is the fraction of dose that escapes intestinal first-pass metabolism in enterocytes, F_h is the fraction of dose that escapes hepatic first-pass metabolism, E_g is the intestinal extraction ratio, and E_H is the hepatic extraction ratio. The oral bioavailability of a drug is dependent on physiological and drug specific parameters. Some of the important factors affecting these parameters are outlined below:

(a). *Factors affecting F_a :*

- Characteristics of the formulations such as drug particle size, shape, and excipients as they influence disintegration and dissolution
- Physicochemical properties of the drug such as solubility, lipophilicity, pK_a as they influence dissolution, permeability, and chemical stability
- Physiological and biochemical processes such as gastric emptying, intestinal transit time, GI fluid pH, intestinal blood flow, active transport, enterohepatic recirculation, presence of food and fluids

- (b). *Factors affecting F_g* include the abundance and location of enzymes and transporters in the gastrointestinal tract (GIT).
- (c). *Factors affecting F_h* has been discussed in more detail earlier in the clearance section.

In addition, age, sex, race and disease may have a role to play in the variability observed in the physiological factors affecting these parameters.

The interplay of parameters describing these processes determines the rate and extent of absorption. For more detailed information, the readers are referred to more in-depth review by (Rostami-Hodjegan and Tucker 2007; Jamei *et al.* 2009).

Different absorption models have been developed (Norris *et al.* 2000; Yu and Amidon, 1999) and incorporated in commercially available software tools – GastroPlus[®], SIMCYP[®], IDEA[®]. The commercially available models have not been published fully for proprietary reasons. In brief, these models are physiologically based transit models segmenting the GIT into different compartments, where the kinetics of transit, dissolution and uptake are described by sets of differential equations. For more details the reader are advised to refer to publications from Yu and Amidon (1999), Norris *et al.* (2000) and Jamei *et al.* (2009). Some of the basic elements of oral absorption models are discussed below.

The simulation models for oral absorption require a number of *in vitro* input parameters such as solubility, permeability, pK_a and dose to predict F_a . Simulation software such as SIMCYP[®] estimate the F_g using Q_{gut} model (Yang *et al.* 2007). The Q_{gut} model uses the form of “well-stirred” liver model of hepatic drug clearance to describe F_g but the flow term Q_{gut} is a hybrid of both permeability through the enterocyte membrane and villous blood flow (Yang *et al.* 2001; Rostami-Hodjegan and Tucker 2002).

$$F_g = \frac{Q_{gut}}{Q_{gut} + (fu_G \times CL_{u_{int,G}})} \quad (21.6)$$

where fu_G is the fraction of drug unbound in the enterocyte, and $CL_{u_{int,G}}$ is the net intrinsic metabolic clearance in the gut based on unbound drug concentration.

Operationally Q_{gut} model is based on the assumption that a higher permeability through enterocyte will decrease first-pass exposure to the enzyme, as will a higher blood flow-carrying drug away from the enterocyte. Details of how the parameters of both the well stirred and Q_{gut} model are determined and implemented in the model are discussed in the published work of Yang *et al.* (2007).

21.5 Applying Physiologically Based Approaches in Drug Development

PBPK based approaches are now commonly used in answering critical questions in early and late phases of drug development. The application of PBPK modeling may vary from early discovery to full clinical development of the compound depending on

the questions posed during the drug's development pathway. Some of the common uses are listed below:

- To estimate compound's physico-chemical properties and associated PK parameters based on chemical structure (such as V_{ss} , plasma protein binding, effective permeability, solubility, $\log P$, pK_a etc.)
- *In vivo* drug disposition in plasma and target tissues
- Human PK prediction for first-in human (FIH) study dose selection
- Drug–drug interaction potential
- Regional drug absorption and formulation evaluation
- Drug disposition in special populations
- Answering “what if questions” (*e.g.*, what if the particle size is reduced or dissolution profile of compound is changed, what will be its effect on PK properties)

In the absence of any clinical data (*i.e.*, pre-FIH phase), prediction of human PK can be made by first using *in vitro*/preclinical PK data as input for the models loaded into the simulation tools (Parrott *et al.* 2005b). PBPK modeling approach may involve the following steps, which is further illustrated in the example shown in Fig. 21.2:

1. Prediction of model parameters using established *in vitro* to *in vivo* scaling for clearance and mechanistic models of tissue distribution (described in the Sects. 21.2 and 21.3).
2. Simulation of the concentration vs. time profile of the compound in a preclinical species such as rat after an intravenous (IV) bolus dose, followed by comparison with observed IV profile. The model can be optimized using the observed IV profile, if needed.
3. Simulation of plasma concentration vs. time after an oral dose in a preclinical species using model parameters from the optimized IV model, followed by comparison with observed oral profile; further model optimization for absorption using the observed oral profile, if needed.
4. Prediction of human plasma concentration profile using the model parameters from the optimized preclinical PBPK model.

In the absence of experimentally measured input parameters (*e.g.*, early discovery projects), *in silico* predicted parameters (such as $\log P$, pK_a , Solubility, Permeability, Plasma protein binding etc.) using chemical structure of the compound can be used (Fig. 21.2a). However, one should be careful in predicting PK profile using *in silico* data only, as understandably the predictions may not be optimal (Fig. 21.2a). As more experimental input data become available during lead optimization stage, the predictions tend to become more reliable (Fig. 21.2b, c). It is recommended that human PK predictions are made after validation of model assumptions in at least one preclinical species.

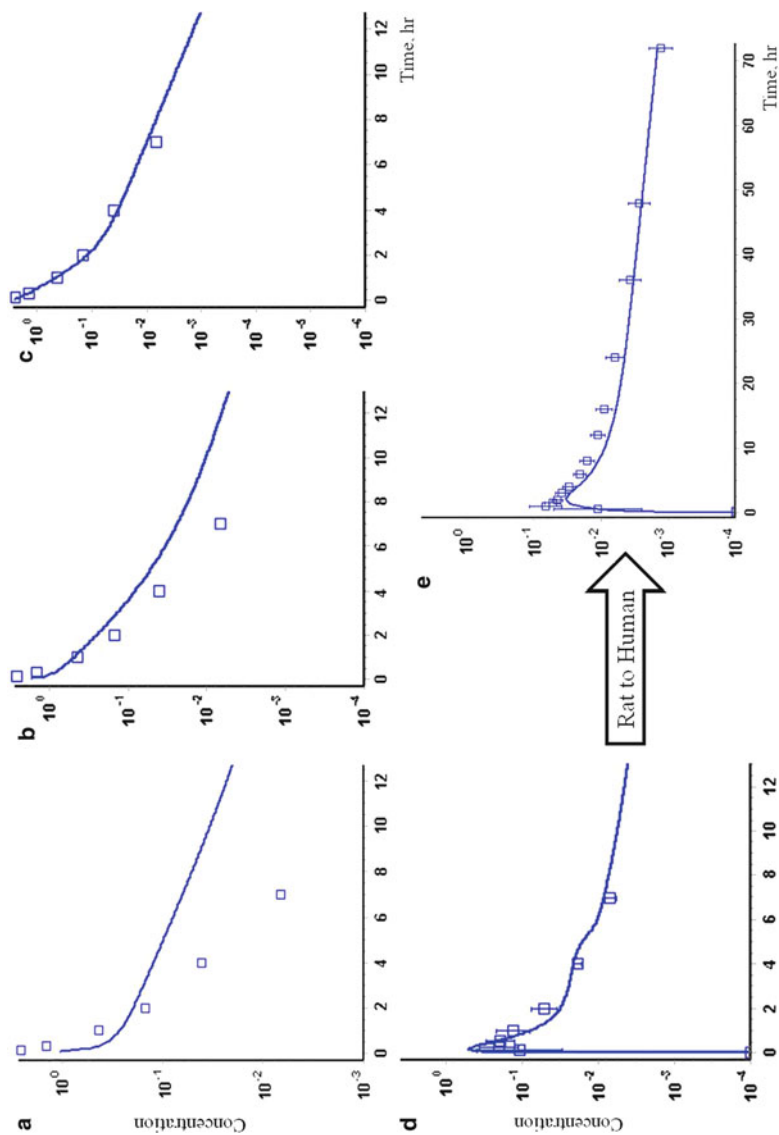


Fig. 21.2 Prediction of human PK from rat PK using PBPK approach: (a) IV rat PK profile prediction based on *in silico* input parameters derived from chemical structure and *in vitro* CL, (b) IV rat PK profile prediction with experimentally measured input parameters, (c) Optimized IV rat PK model after inclusion of K_p derived from rat tissue distribution study (d) PO rat PK profile predicted with the optimized model (e) PO PK profile prediction in human (the symbol represents observed PK)

21.6 Concluding Remarks

Physiologically based modeling offers an insight into the underlying mechanistic processes involved, hence have the potential to be more reliably predictive compared to the empirically based methods. This offers an opportunity to link various *in vitro* and *in vivo* data generated during different phases of discovery and pre-clinical development. Thus PBPK based modeling not only aids in the candidate selection very early on, but also allows answering “what if” questions in case a particular parameter needs to be changed (*e.g.*, by adjusting particle size).

The advances in computation capability have enabled simultaneous solutions from many differential equations that are necessary to calculate time courses of concentration in each physiological compartment. A few software that has been used for PBPK modeling includes Berkeley Madonna (University of California, Berkeley, <http://www.berkeleymadonna.com>), ADAPT (Biomedical Simulations Resource, University of Southern California, <http://bmsr.usc.edu>), SAAM II (SAAM Institute, Inc., <http://www.saam.com>), acsIX (Aegis Technologies Group, Inc., <http://www.acslsim.com>), SIMULINK (based on MATLAB, The Math Works, Inc. <http://www.mathworks.com>), MATHEMATICA (Wolfram Research, Inc., <http://www.wolfram.com>), STELLA (High Performance Systems, Inc. <http://www.hps-inc.com>), and so forth.

Using simulation software that is specifically designed for PBPK modeling such as GastroPlus[®], Simcyp[®] and PKSIM[®] can be used to improve preclinical and clinical study designs by enabling PK prediction in preclinical species and human. Some of these tools allow us to assess the effect of food on PK, drug–drug interaction potential, prediction of PK in children, inter-subject PK variability, and PK in special population such as renal failure or hepatic failure subjects. Despite its great potential, there are several scientific hurdles that need to be overcome for an optimal prediction using PBPK. Of particular concern are the inherent limitations and variability in some *in vitro* systems. These include the underprediction of hepatic clearance using microsomal systems or hepatocytes and the lack of *in vitro* assays for predicting renal and bilirubin clearance. Another hurdle is to integrate the *in vitro* data on active uptake and secretory transporters systems in a mechanistic way. The lack of physiological data on the abundance and variability of such transporters in human limits the possibility to evaluate the impact of transporters on drug’s disposition profile, but efforts are ongoing in this direction.

Prediction of the exposure of neonates, infants and children to a drug is also likely to be more successful using physiologically based pharmacokinetic models than simplistic allometric scaling, particularly in younger children, because of various organ maturation rates in the age groups. Such models require comprehensive information on the ontogeny of anatomical, physiological and biochemical variables, which is not easily available. Attempts to predict pharmacokinetics of drugs in several pediatric age groups, considering the ontogeny change in pediatrics, have been published (Bjorkman 2005; Ginsberg *et al.* 2004).

PBPK has significant potential to be an important component of model based drug development. A mechanistic approach integrating input data from various sources may lead to predictions that are more reliable, better-designed experiments and better selection of drug candidates. We predict that as more advanced *in vitro* tests and PBPK models are developed and validated, the level of confidence in PBPK based predictions will increase and improve its acceptance within the pharmaceutical industry and by regulatory agencies.

References

- Barter ZE, Bayliss MK, Beaune PH, Boobis AR, Carlile DJ, Edwards RJ, Houston JB, Lake BG, Lipscomb JC, Pelkonen OR, Tucker GT, Rostami-Hodjegan A (2007) Scaling factors for the extrapolation of *in vivo* metabolic drug clearance from *in vitro* data: reaching a consensus on values of human microsomal protein and hepatocellularity per gram of liver. *Curr Drug Metab* **8**:33–45
- Bazil CW, Raux ME, Yudell S, Minneman KP (1987) Equilibration of halothane with brain tissue *in vitro*: comparison to brain concentrations during anesthesia. *J Neurochem* **49**:952–958
- Berezhkovskiy LM (2004) Volume of distribution at steady state for a linear pharmacokinetic system with peripheral elimination. *J Pharm Sci* **93**:1628–1640
- Bernardi M, Di Marco C, Trevisani F, De Collibus C, Fornale L, Baraldini M, Andreone P, Cursaro C, Zaca F, Ligabue A et al (1992) The hemodynamic status of preascitic cirrhosis: an evaluation under steady-state conditions and after postural change. *Hepatology* **16**:341–346
- Bickel MH, Gerny R (1980) Drug distribution as a function of binding competition. Experiments with the distribution dialysis technique. *J Pharm Pharmacol* **32**:669–674
- Bjorkman S (2005) Prediction of drug disposition in infants and children by means of physiologically based pharmacokinetic (PBPK) modeling: theophylline and midazolam as model drugs. *Br J Clin Pharmacol* **59**:691–704
- Blanchard N, Hewitt NJ, Silber P, Jones H, Coassolo P, Lave T (2006) Prediction of hepatic clearance using cryopreserved human hepatocytes: a comparison of serum and serum-free incubations. *J Pharm Pharmacol* **58**:633–641
- Brown HS, Griffin M, Houston JB (2007) Evaluation of cryopreserved human hepatocytes as an alternative *in vitro* system to microsomes for the prediction of metabolic clearance. *Drug Metab Dispos* **35**:293–301
- Brown HS, Ito K, Galetin A, Houston JB (2005) Prediction of *in vivo* drug-drug interactions from *in vitro* data: impact of incorporating parallel pathways of drug elimination and inhibitor absorption rate constant. *Br J Clin Pharmacol* **60**:508–518
- Davis NR, Mapleson WW (1993) A physiological model for the distribution of injected agents, with special reference to pethidine. *Br J Anaesth* **70**:248–258
- De Buck SS, Sinha VK, Fenu LA, Gilissen RA, Mackie CE, Nijssen MJ (2007a) The prediction of drug metabolism, tissue distribution, and bioavailability of 50 structurally diverse compounds in rat using mechanism-based absorption, distribution, and metabolism prediction tools. *Drug Metab Dispos* **35**:649–659
- De Buck SS, Sinha VK, Fenu LA, Nijssen MJ, Mackie CE, Gilissen RA (2007b) Prediction of human pharmacokinetics using physiologically based modeling: a retrospective analysis of 26 clinically tested drugs. *Drug Metab Dispos* **35**:1766–1780
- Edell ES, Cortese DA, Krowka MJ, Rehder K (1989) Severe hypoxemia and liver disease. *Am Rev Respir Dis* **140**:1631–1635

- El Masri HA, Portier CJ (1998) Physiologically based pharmacokinetics model of primidone and its metabolites phenobarbital and phenylethylmalonamide in humans, rats, and mice. *Drug Metab Dispos* **26**:585–594
- Fichtl B, Nieciecki A, Walter K (1991) Tissue binding versus plasma binding of drugs: general principles and pharmacokinetic consequences. *Adv Drug Res* **20**:117–166
- Galetin A, Brown C, Hallifax D, Ito K, Houston JB (2004) Utility of recombinant enzyme kinetics in prediction of human clearance: impact of variability, CYP3A5, and CYP2C19 on CYP3A4 probe substrates. *Drug Metab Dispos* **32**:1411–1420
- Galetin A, Burt H, Gibbons L, Houston JB (2006) Prediction of time-dependent CYP3A4 drug-drug interactions: impact of enzyme degradation, parallel elimination pathways, and intestinal inhibition. *Drug Metab Dispos* **34**:166–175
- Gerlowski LE, Jain RK (1983) Physiologically based pharmacokinetic modeling: principles and applications. *J Pharm Sci* **72**:1103–1127
- Gillette JR (1971) Factors affecting drug metabolism. *Ann N Y Acad Sci* **179**:43–66
- Ginsberg G, Hattis D, Russ A, Sonawane B (2004) Physiologically based pharmacokinetic (PBPK) modeling of caffeine and theophylline in neonates and adults: implications for assessing children's risks from environmental agents. *J Toxicol Environ Health A* **67**:297–329
- Holford NHG, Kimko HC, Monteleone JPR, Peck CC (2000) Simulation of clinical trials. *Annu Rev Pharmacol Toxicol* **40**:209–234
- Houston JB (1994) Utility of in vitro drug metabolism data in predicting in vivo metabolic clearance. *Biochem Pharmacol* **47**:1469–1479
- Houston JB, Kenworthy KE (2000) In vitro-in vivo scaling of CYP kinetic data not consistent with the classical Michaelis-Menten model. *Drug Metab Dispos* **28**:246–254
- Iwatsubo T, Hirota N, Ooie T, Suzuki H, Shimada N, Chiba K, Ishizaki T, Green CE, Tyson CA, Sugiyama Y (1997) Prediction of in vivo drug metabolism in the human liver from in vitro metabolism data. *Pharmacol Ther* **73**:147–171
- Iwatsubo T, Hirota N, Ooie T, Suzuki H, Sugiyama Y (1996) Prediction of in vivo drug disposition from in vitro data based on physiological pharmacokinetics. *Biopharm Drug Dispos* **17**:273–310
- Jamei M, Turner D, Yang J, Neuhoﬀ S, Polak S, Rostami-Hodjegan A, Tucker G (2009) Population-based mechanistic prediction of oral drug absorption. *AAPS J* **11**:225–237
- Jansen JA (1981) Influence of plasma protein binding kinetics on hepatic clearance assessed from a “tube” model and a “well-stirred” model. *J Pharmacokinetic Biopharm* **9**:15–26
- Johnson TN, Rostami-Hodjegan A, Tucker GT (2006) Prediction of the clearance of eleven drugs and associated variability in neonates, infants and children. *Clin Pharmacokinetic* **45**:931–956
- Jones HM, Parrott N, Jorga K, Lave T (2006) A novel strategy for physiologically based predictions of human pharmacokinetics. *Clin Pharmacokinetic* **45**:511–542
- Kimko HC, Duffull S (2003) Simulation for designing clinical trials. Marcel Dekker, New York
- Lave T, Dupin S, Schmitt C, Valles B, Ubeaud G, Chou RC, Jaeck D, Coassolo P (1997) The use of human hepatocytes to select compounds based on their expected hepatic extraction ratios in humans. *Pharm Res* **14**:152–155
- LeCluyse EL (2001) Human hepatocyte culture systems for the in vitro evaluation of cytochrome P450 expression and regulation. *Eur J Pharm Sci* **13**:343–368
- Lombardo F, Obach RS, Shalaeva MY, Gao F (2002) Prediction of volume of distribution values in humans for neutral and basic drugs using physicochemical measurements and plasma protein binding data. *J Med Chem* **45**:2867–2876
- Lombardo F, Obach RS, Shalaeva MY, Gao F (2004) Prediction of human volume of distribution values for neutral and basic drugs. 2. Extended data set and leave-class-out statistics. *J Med Chem* **47**:1242–1250
- MacIntyre AC, Cutler DJ (1988) The potential role of lysosomes in tissue distribution of weak bases. *Biopharm Drug Dispos* **9**:513–526
- Matheson PJ, Wilson MA, Garrison RN (2000) Regulation of intestinal blood flow. *J Surg Res* **93**:182–196

- Mathias CJ (1990) Effect of food intake on cardiovascular control in patients with impaired autonomic function. *J Neurosci Methods* **34**:193–200
- Miners JO, Knights KM, Houston JB, Mackenzie PI (2006) In vitro-in vivo correlation for drugs and other compounds eliminated by glucuronidation in humans: pitfalls and promises. *Biochem Pharmacol* **71**:1531–1539
- Nestorov I (2003) Whole body pharmacokinetic models. *Clin Pharmacokinet* **42**:883–908
- Nestorov I (2007) Whole-body physiologically based pharmacokinetic models. *Expert Opin Drug Metab Toxicol* **3**:235–249
- Nestorov IA, Aarons LJ, Arundel PA, Rowland M (1998) Lumping of whole-body physiologically based pharmacokinetic models. *J Pharmacokinet Biopharm* **26**:21–46
- Norris DA, Leesman GD, Sinko PJ, Grass GM (2000) Development of predictive pharmacokinetic simulation models for drug discovery. *J Control Release* **65**:55–62
- Obach RS, Baxter JG, Liston TE, Silber BM, Jones BC, MacIntyre F, Rance DJ, Wastall P (1997) The prediction of human pharmacokinetic parameters from preclinical and in vitro metabolism data. *J Pharmacol Exp Ther* **283**:46–58
- Pang KS, Rowland M (1977) Hepatic clearance of drugs. I. Theoretical considerations of a “well-stirred” model and a “parallel tube” model. Influence of hepatic blood flow, plasma and blood cell binding, and the hepatocellular enzymatic activity on hepatic drug clearance. *J Pharmacokinet Biopharm* **5**:625–653
- Parrott N, Jones H, Paquereau N, Lave T (2005a) Application of full physiological models for pharmaceutical drug candidate selection and extrapolation of pharmacokinetics to man. *Basic Clin Pharmacol Toxicol* **96**:193–199
- Parrott N, Paquereau N, Coassolo P, Lave T (2005b) An evaluation of the utility of physiologically based models of pharmacokinetics in early drug discovery. *J Pharm Sci* **94**:2327–2343
- Peck CC (2010) Quantitative clinical pharmacology is transforming drug regulation. *J Pharmacokinet Pharmacodyn* **37**(3)
- Pond SM, Tozer TN (1984) First-pass elimination. Basic concepts and clinical consequences. *Clin Pharmacokinet* **9**:1–25
- Post C, Andersson RG, Ryrfeldt A, Nilsson E (1978) Transport and binding of lidocaine by lung slices and perfused lung of rats. *Acta Pharmacol Toxicol (Copenh)* **43**:156–163
- Poulin P, Schoenlein K, Theil FP (2001) Prediction of adipose tissue: plasma partition coefficients for structurally unrelated drugs. *J Pharm Sci* **90**:436–447
- Poulin P, Theil FP (2000) A priori prediction of tissue: plasma partition coefficients of drugs to facilitate the use of physiologically based pharmacokinetic models in drug discovery. *J Pharm Sci* **89**:16–35
- Poulin P, Theil FP (2002) Prediction of pharmacokinetics prior to in vivo studies. 1. Mechanism-based prediction of volume of distribution. *J Pharm Sci* **91**:129–156
- Rawden HC, Carlisle DJ, Tindall A, Hallifax D, Galetin A, Ito K, Houston JB (2005) Microsomal prediction of in vivo clearance and associated interindividual variability of six benzodiazepines in humans. *Xenobiotica* **35**:603–625
- Roberts MS, Rowland M (1985) Hepatic elimination–dispersion model. *J Pharm Sci* **74**:585–587
- Roberts MS, Rowland M (1986a) A dispersion model of hepatic elimination: 1. Formulation of the model and bolus considerations. *J Pharmacokinet Biopharm* **14**:227–260
- Roberts MS, Rowland M (1986b) A dispersion model of hepatic elimination: 3. Application to metabolite formation and elimination kinetics. *J Pharmacokinet Biopharm* **14**:289–308
- Rodgers T, Leahy D, Rowland M (2005a) Physiologically based pharmacokinetic modeling 1: predicting the tissue distribution of moderate-to-strong bases. *J Pharm Sci* **94**:1259–1276
- Rodgers T, Leahy D, Rowland M (2005b) Tissue distribution of basic drugs: accounting for enantiomeric, compound and regional differences amongst beta-blocking drugs in rat. *J Pharm Sci* **94**:1237–1248
- Rodgers T, Rowland M (2006) Physiologically based pharmacokinetic modeling 2: predicting the tissue distribution of acids, very weak bases, neutrals and zwitterions. *J Pharm Sci* **95**:1238–1257

- Rostami-Hodjegan A, Tucker GT (2002) The effects of portal shunts on intestinal cytochrome P450 3A activity. *Hepatology* **35**:1549–1550
- Rostami-Hodjegan A, Tucker GT (2007) Simulation and prediction of in vivo drug metabolism in human populations from in vitro data. *Nat Rev Drug Discov* **6**:140–148
- Rowland M, Benet LZ, Graham GG (1973) Clearance concepts in pharmacokinetics. *J Pharmacokinet Biopharm* **1**:123–136
- Rowland M, Balant L, Peck C (2004) Physiologically based pharmacokinetics in drug development and regulatory science: a workshop report (Georgetown University, Washington, DC, May 29–30, 2002). *AAPS J* **6**(1):56–67
- Rowland M, Peck C, Tucker G (2011) Physiologically based pharmacokinetics in drug development and regulatory science. *Ann Rev Toxicol Pharm* **51**:45–73
- Ruckert KH, Juchems R (1970) Hemodynamics in posture changes. *Z Kreislaufforsch* **59**:685–698
- Sawada Y, Hanano M, Sugiyama Y, Harashima H, Iga T (1984) Prediction of the volumes of distribution of basic drugs in humans based on data from animals. *J Pharmacokinet Biopharm* **12**:587–596
- Schuhmann G, Fichtl B, Kurz H (1987) Prediction of drug distribution in vivo on the basis of in vitro binding data. *Biopharm Drug Dispos* **8**:73–86
- Teorell T (1937a) Kinetics of distribution of substances administered to the body. I. The extravascular modes of administration. *Arch Int Pharmacodyn* **57**:205–225
- Teorell T (1937b) Kinetics of distribution of substances administered to the body. II. The intravascular modes of administration. *Arch Int Pharmacodyn* **57**:226–240
- Theil FP, Guentert TW, Haddad S, Poulin P (2003) Utility of physiologically based pharmacokinetic models to drug development and rational drug discovery candidate selection. *Toxicol Lett* **138**:29–49
- Wilkinson GR, Shand DG (1975) Commentary: a physiological approach to hepatic drug clearance. *Clin Pharmacol Ther* **18**:377–390
- Wong F, Liu P, Allidina Y, Blendis L (1996) The effect of posture on central blood volume in patients with preascitic cirrhosis on a sodium-restricted diet. *Hepatology* **23**:1141–1147
- Yang J, Rostami-Hodjegan A, Tucker GT (2001) Prediction of ketoconazole interaction with midazolam, alprazolam and triazolam: incorporating population variability. *Br J Clin Pharmacol* **52**:472p–473p
- Yang J, Jamei M, Yeo KR, Tucker GT, Rostami-Hodjegan A (2007) Prediction of intestinal first-pass drug metabolism. *Curr Drug Metab* **8**:676–684
- Yokogawa K, Ishizaki J, Ohkuma S, Miyamoto K (2002) Influence of lipophilicity and lysosomal accumulation on tissue distribution kinetics of basic drugs: a physiologically based pharmacokinetic model. *Methods Find Exp Clin Pharmacol* **24**:81–93
- Yu LX, Amidon GL (1999) A compartmental absorption and transit model for estimating oral drug absorption. *Int J Pharm* **186**:119–125
- Zhao P, Zhang L, Lesko K, Huang SM (2010) Utility of physiologically based pharmacokinetic modeling and simulation in drug development and challenges in regulatory reviews. *Clin Pharm Therap* **87**(S1):S72

Chapter 22

Covariate Distribution Models in Simulation

Peter L. Bonate

Abstract The components of a clinical trial simulation consist of the input–output model, the covariate distribution model, and the trial execution model. The input–output model consists of submodels that incorporate the drug’s pharmacokinetics and pharmacodynamics, the disease progression during the trial, the trial endpoints, and the residual variability. Some of these submodels may include covariate influences on model parameters, which comprise the covariate distribution model. Appropriate simulation of clinical trials requires appropriate simulation of covariates because generation of covariates from an invalid probability distribution may result in an inadequate distribution of the simulation output. Basically, you need the right inputs to get the right outputs. This chapter will define covariate distribution models, will show how internal and external datasets may be used to define an appropriate probability distribution, and will demonstrate how to model covariate distributions.

22.1 Introduction

Modeling and simulation has use across all phases of drug development from scaling preclinical data for predicting the starting dose in a first-time-in-human study to simulating the statistical power of a clinical trial given a drug’s exposure-response relationship (Chien *et al.* 2005). The latter is referred to as clinical trial simulation, which has a principle goal of reducing drug development costs and timelines through the application of *in silico* “test-driving” study designs and study conditions before their actual implementation. Given what is already known about the drug, the idea is to maximize the probability of success of a future clinical trial through the application of modeling and simulation.

P.L. Bonate (✉)

Clinical Pharmacology, Modeling, and Simulation, GlaxoSmithKline,
Research Triangle Park, NC, USA
e-mail: peter.l.bonate@gsk.com

Holford *et al.* (2000) define the components of a clinical trial simulation as the input–output model, the covariate distribution model, and the trial execution model. The input–output model consists of submodels that incorporate the drug’s pharmacokinetics and pharmacodynamics, the disease progression during the trial, the trial endpoints, and the residual variability. Some of these submodels may include covariate influences on model parameters, which comprise the covariate distribution model. Basically, the input–output models are functions that map the set of inputs to the set of outputs. The covariate distribution model describes the distribution of the covariates and their intercorrelations. The trial execution model consists of the study design elements, and potential submodels for compliance, protocol deviations, and missing data.

In a population pharmacokinetics submodel, a set of doses and covariate influences are mapped to the concentrations through the pharmacokinetic model

$$\{\text{doses, covariates}\} \xrightarrow{\text{model}} \text{concentration}$$

Using the terminology just described, the set of doses and covariates are the inputs, whereas the resulting concentrations are the outputs. The input-output model may be a compartmental model (*e.g.*, a 1-compartment model with first-order absorption) or a physiologically based model. The dose and drug concentration observation or prediction event times are trial execution components. The covariates are the set of patient characteristics (*e.g.*, age, sex, weight, renal function, etc.) that may influence the pharmacokinetic parameters in the model. How these covariates are distributed and how they are correlated are defined in the covariate distribution model. The purpose of this chapter is to introduce covariate distribution models, explain how they are used in trial simulations, and show the roles of internal and external datasets and how they may be used in practice.

22.2 Covariate Distribution Models

Covariate distribution models will be illustrated by example. Bonate (2006) reported on the population pharmacokinetics of tobramycin using the dataset previously reported by Aarons *et al.* (1989). A two-compartment pharmacokinetic model best described the plasma concentration-time profile by incorporating a covariate submodel that linked drug clearance (CL) to the trial subject’s creatinine clearance (CrCL) and central volume of distribution (V1) to the trial subject’s weight. The final mean pharmacokinetic and covariate model parameter estimates follow:

$$\begin{aligned} \text{CL(L/h)} &= 7.47 \left(\frac{\text{CrCL in L/h}}{7.2 \text{ L/h}} \right) \\ \text{V1(L)} &= 17.4 \left(\frac{\text{weight in kg}}{67 \text{ kg}} \right) \\ \text{Q(L/h)} &= 1.50 \\ \text{V2(L)} &= 7.73 \end{aligned} \tag{22.1}$$

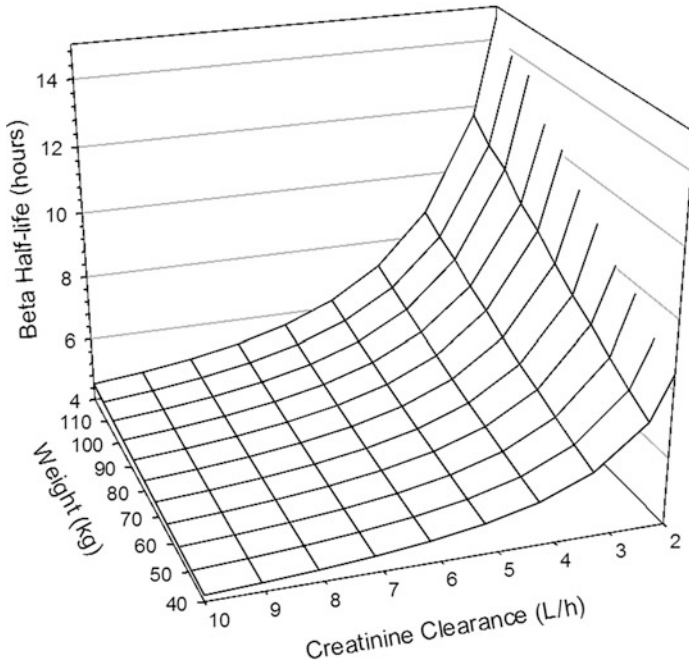


Fig. 22.1 Tobramycin β -half-life as a function of weight and CrCL under the 2-compartment model of Aarons *et al.* (1989). Reprinted from Bonate (2006)

where Q is intercompartmental clearance and V_2 is the peripheral volume of distribution. In order to simulate using this model, the dose, time, CrCL, and body weight data must be provided. Event times for dose(s) and concentrations are trial design elements that are specified by the trial design submodel. CrCL and body weight values must be provided in the course of simulating the concentration-time profiles. To illustrate the influence of the covariate submodel, Fig. 22.1 presents the results of a deterministic (non-stochastic) simulation of tobramycin β -half-life as a function of weight and CrCL. When CrCL is less than 5 L/h, elimination β -half-life appears to remain relatively constant regardless of weight. But when CrCL is decreased, such as during renal impairment, then β -half-life increases with increasing weight.

It should be noted that deterministic simulations have their place, but may be misleading for planning clinical trials. This is what Savage (2009) refers to as the “Flaw of Averages,” which states that plans based on average conditions may be wrong on-average. The Flaw of Averages is derived from Jensen’s Inequality (http://en.wikipedia.org/wiki/Jensen's_inequality, accessed March 2010) which simply states that the nonlinear transform of a mean is not equal to the mean after nonlinear transformation, *e.g.*, $\text{Ln}(\text{mean of } X) \neq \text{mean of } \text{Ln}(X)$. For linear functions, like a linear regression model, Jensen’s inequality does not apply, but modeling in pharmacokinetics and pharmacodynamics are usually in the nonlinear domain and the inequality applies.

Covariate influences and clinical trial simulations are most realistic when Monte Carlo simulation is used, rather than deterministic simulation. Monte Carlo simulation, which got its name from Ulam and von Neumann in the 1940s who invented the methodology during their work on the Manhattan project (Metropolis 1987), is based on random sampling of some or all of the model inputs from a proposed probability distribution function (pdf) that results in the generation of the outputs and can be summarized, for example, by its range and expected value. Returning to the tobramycin example, a Monte Carlo simulation would involve randomly selecting a patient's weight and CrCL from a realistic range of values, calculating his/her pharmacokinetic profile, and then estimating the half-life. When this process is repeated many times, a range and expected value can be derived from the distribution of simulated half-lives. Deterministic simulation yields that for a 60 kg person with a CrCL of 135 mL/min, the tobramycin half-life is 4.5 h. Clearly, not every person in the world weighing 60 kg and having a CrCL of 135 mL/min has a tobramycin half-life of 4.5 h. Some might be 5 h, some might be 3 h because of different covariates that are not identified in each person. The point is, in a realistic setting, for patients weighing 60 kg and having a CrCL of 135 mL/min, there is an expected *range* of half-lives, not a single value.

To obtain the expected value and probable range using Monte Carlo simulation, it is necessary to be able to simulate the model covariates – weight and CrCL in this case. To simulate these covariates, it is necessary to define the pdf of the covariates and their joint distribution. Once the joint covariate distribution model is defined, the covariate values can be realistically, stochastically simulated and used as the inputs to the model. It is still assumed that dose and time are fixed study design elements, but, if appropriate, it is possible to treat dose and time as stochastic elements as well.

To appreciate the complexity of a joint pdf, notice that CrCL can be calculated using the Cockcroft and Gault (1976) equation,

$$\text{CrCL} = \frac{(140 - \text{Age}) \times \text{Weight} \times (0.85 \text{ if female})}{72 \times \text{Scr}} \quad (22.2)$$

where Age is in years, Weight is in kg, and Scr is serum creatinine concentration in mg/dL. Thus, age, weight, sex, and Scr values are needed for each simulated subject, which results in a four-dimensional joint pdf. As the number of covariates increases, the dimensionality increases and it becomes increasingly difficult to define the joint pdf, as well as judging the impact any single covariate has on the dependent variable.

A number of assumptions may be made to simplify the construction of a joint pdf. One approach to defining the joint covariate distribution is to treat all covariates as independent. This was illustrated by Lowe *et al.* (2009). In their simulation, 1,000 subjects were simulated by randomly sampling from independent uniform distributions using the range of observed body weights and range of observed baseline IgE values. When the covariates are uncorrelated this is a perfectly valid approach. Sometimes though, covariate independence may lead to unrealistic

combinations of covariates. For example, in a simulation of children and adults, an adult with a weight of 5 kg might be simulated. Hence, treating the covariates as independent must be used with caution.

A different simplification is to treat the covariates as hierarchical and conditional in the sense that even though two covariates might be correlated, one covariate might be thought of as being predictive of the other such that if one covariate value is selected first, the other covariate can then be selected conditional on the first covariate. In this example, one might first randomly select the subject's gender followed by age, each independently of the other. Then weight could reasonably be selected conditional on sex and age. Lastly, Scr might be calculated based on age, weight, and sex. In this manner, all covariates are randomly selected according to realistic marginal and joint pdfs.

But what are these distributions? How does one determine what is the range or mean of covariates required in the simulation? Sometimes these are made using educated guesses, using only a range of realistic values. For example, in a study in adults, one might assume that age is uniformly distributed on the range 18–60 years old and that males and females are equally likely. Hence, one would first generate a random number from a uniform distribution on the interval (0, 1) and if the value is ≤ 0.5 , the patient is male, otherwise they are female. Then age can be simulated using the equation

$$\text{Age} = 18 + (60 - 18)U \quad (22.3)$$

where U is a different random number drawn from the Uniform (0,1) distribution. However, age and weight are correlated in a nonlinear manner, since as patients age they tend to get heavier, but when they become elderly, their weight tends to decline. How is weight then conditional on age? And once age, weight, and sex are selected, how is Scr dependent on these variables? Hence, conditional distributions become difficult to define. The only real answer to these more complicated conditional distributions is to use external or internal databases and develop the relationships through modeling or resampling.

22.2.1 Internal Databases

Biopharmaceutical companies often have clinical trial data, including covariate data, in internal databases from previous clinical trials undertaken by a company. For instance, a pdf of alanine aminotransferase (ALT) values, a marker of drug-induced liver injury, may be generated from a clinical trial that included adult patients with acute myelogenous leukemia (AML). From such a database, a software program that uses maximum likelihood to fit different pdfs can be used to find the optimal distribution that best fits the data. Examples of these software include Risk Solver (<http://solver.com>, accessed May 2010) or EasyFit (<http://www.mathwave.com/products/easyfit.html>, accessed May 2010). To illustrate, with EasyFit the program fits almost 60 different pdfs, *e.g.*, normal, log-normal, gamma, Weibull, Student's T -distribution, etc., to the data and determines which one is the best fit to the data using

goodness of fit criteria (Kolmogorov–Smirnov, Anderson–Darling, and Chi-squared test) yielding the maximum likelihood estimates for the parameters that define the distribution, *e.g.*, mean, shift, variance, etc. The resulting pdf using the estimated parameters can be randomly sampled from to generate covariate values from the distribution. When needed covariates are not independent, however, a model for the relationship between one covariate and another may be required, which will be discussed later in this chapter.

In a sense, when looking at data from other studies, this is a type of data mining problem and all the issues and problems regarding data mining apply. Many questions need to be asked in a data mining exercise, but foremost is how representative are the data to the population of interest since generating a covariate distribution model from a nonrepresentative dataset may invalidate an entire analysis. The data mining process may be thought of as follows: extract the data, model the data, and then interpret and use the results. Each step presents its own issues and challenges. In the dataset identification and extraction step, finding the data (where it is located, what is the directory structure) may be quite difficult. Once the data are located, it may need to be converted to a usable format. For example, if it is stored as a SAS[®] transport file, it may need to be converted to an Excel spreadsheet or an R-dataset. Once read into a usable dataset, the data may need to be cleaned. Missing values and outlier values may need to be dealt with. Clinical chemistry or hematology measurements derived from different sites may have reported different units in their data which will need to be standardized to a common unit across all sites.

Accepting a best fit pdf model presents its own challenges. What level of validation is needed at this stage? How well does the covariate pdf model need to fit the observed data to be useful? There are no guidelines here; the analyst must make his/her own decision, documenting assumptions, and justifications. Once the covariate pdf is accepted, obtaining random covariate values from that distribution may not be possible. For instance, suppose that the distribution that best described a covariate was a Nakagami distribution (a distribution related to the Gamma distribution). Many programs like SAS (SAS Institute, Cary, NC), R (www.r-project.org), and the Pharsight Trial Simulator 2 (Pharsight, Mountain View, CA) do not have built-in functionality to randomly select values from a Nakagami distribution, so it may be necessary to use a less well fitting distribution such as a Gamma distribution that can be easily used by available simulation software.

22.2.2 *External Databases*

22.2.2.1 **The United States Census of Demographic Characteristics of Americans**

The United States (US) census is commissioned by the US Department of Commerce to generate every decade a representative database of individual demographic characteristics of Americans. Every 10 years, questionnaire forms are mailed to every

household in the US that query many things, including the age, race, and number of people in the home. The information is used in many different government programs ranging from the number of congressional seats assigned to a state to how much money a state gets from the national government for education. It is a tremendous, costly effort. The last census was in 2010 with the next one planned in 2020.

The data from the census can be used to generate age, race, and sex pdfs that are representative of US citizens. A summary of the 2000 census can be found at http://www2.census.gov/census_2000/datasets/100_and_sample_profile/0_United_States/2kh00.pdf, accessed May 2010. Based on the results of the 2000 census, 49.1% of the population was male, 50.9% was female. The median age was 35 years with 28.7% of the population less than 19 years old and 12.4% being 65 years or older. The majority of the population was White (75.1%), followed Hispanic or Latino (12.5%), Black (12.3%), and Asian (3.6%). Assuming that similar demographic characteristics will be exhibited in future clinical trial subjects, demographic pdfs derived from this database can be used to generate general population demographic covariates that can then be used directly or for other higher level covariate assignments.

22.2.2.2 National Institutes of Health Databases

External databases are public domain databases and some of these can be an excellent source of covariate information. Most, if not all, of the useful ones are generated by governments or through government grants. Private companies do not readily share their data although there are efforts to persuade companies to release their placebo data from large clinical trials. The largest source of such external data is available from the US National Institutes of Health. Many of the Institutes release their clinical trial data after a period of time and make it available to researchers for free or for a nominal fee. In accordance with Health Insurance Portability and Accountability Act (HIPAA) regulations, all the public released data have been stripped of any type of identifiable features that could link a data record to a particular individual. Each institute has its own guidelines for access to the data and which data they make available to researchers. Although not all Institutes have made their data publicly available, Institutes that do allow data access are noted as follows:

- The National Institute of Allergy and Infectious Diseases (<http://www.aactg.org/clinical-trials/access-published-data>, accessed May 2010) allows access to AIDS Clinical Trials Group (ACTG) studies databases through the National Technical Information Services (<http://www.ntis.gov/>, accessed May 2010), which is a warehouse for data and documents issued by US government agencies. One problem with Institute-specific databases, such as the ACTG databases, is that they may not include all relevant covariate data for a particular clinical trial simulation project. For instance, most ACTG databases do not capture

electrocardiographic QT interval data. If these data are needed, a database from the National Heart Lung and Blood Institute (NHLBI) may be needed.

- The NHLBI has a number of epidemiological databases available for researchers (<https://biolincc.nhlbi.nih.gov/home/>, accessed May 2010), including the Framingham Heart Study, as well as a number of clinical trials. The Framingham Heart Study (<http://www.framinghamheartstudy.org>, accessed May 2010) is especially useful since it has studied patients every other year since 1949. Included in the database are weight, height, age, blood pressure, electrocardiogram, smoking history, alcohol consumption, as well as many cardiovascular laboratory tests. Most clinical studies are of short duration and the demographics in their database capture information that is limited to a brief period of a patient's life. If long-term weight or weight-derived metrics like body mass index or body surface area are needed, then the Framingham dataset may be more informative than brief, time-limited demographic data.
- The National Institute on Mental Health (NIMH) allows researchers who have authorization via a Data Use Certification (DUC) can access to NIMH databases (<http://www.nimh.nih.gov/health/trials/datasets/index.shtml>, accessed May 2010). A total of six studies in adults and two studies in pediatric patients were available at the end of 2009. The NIMH is limited by lack of documentation regarding the variables collected in each study. Industry access to this data might be problematic since the NIMH requires researchers to certify that their organization is covered by a Federal Wide Assurance issued by the Department of Health and Human Services Office of Human Research Protections assuring that privacy and distribution guidelines will be followed.
- The National Institute of Diabetes and Digestive and Kidney Diseases (NIDDK) has a large number of databases available to researchers (<https://www.niddkrepository.org/niddk/jsp/public/resource.jsp>, accessed May 2010), including data in African-Americans who are often underrepresented in clinical trials (<https://www.niddkrepository.org/niddk/jsp/public/AASK/AASKDesc.jsp>, accessed May 2010). The NIDDK warehouse allows on-line access but requires Institutional Review Board approval and completion of a DUC.

Sometimes, but not always, one can find a published clinical trial report with key covariate data concerning the population of interest in a particular therapeutic area. Using the baseline data or data from the placebo arm, one can generate the covariate distribution and how particular covariates are correlated with each other. From these databases, covariate pdfs can be developed from which to sample for a clinical trial simulation project.

22.2.2.3 The US National Health and Nutrition Examination Survey

One of the most useful of all databases is the National Health and Nutrition Examination Survey (NHANES) (U.S. Department of Health and Human Services and Health Statistics *et al.* 2007), which was initiated in the early 1960s and first

completed in 1971 to study the health and nutritional status of adults and children in the United States, and is available from the National Center for Health Statistics (www.cdc.gov/nchs/nhanes.htm, accessed May 2010). Originally conducted periodically, in 1999 the NHANES switched to a continuous survey with data updated more regularly. The most recent update was 2010 and the next update is planned in 2012. Also, with the NHANES III survey, select components, including clinical chemistry and hematology data, were assessed twice on the same patient so that this particular database is more longitudinal in nature and can be used to assess both between- and within-subject variability. The NHANES is freely available to the public without IRB approval or DUC and even has a tutorial on how to use and analyze their data.

The NHANES is a combination of interview-administered questionnaire and mobile physical examination that collects demographic, socioeconomic, medical, and laboratory data. The laboratory data collected, although not comprehensive, includes a wide variety of clinical laboratory test results including glucose, lipid panel, electrolytes, liver function tests, and hematology. Medical history data include blood pressure, body mass index, and some information on diseases the person might have, like diabetes. Demographic data include sex, race, age, weight, and height. Most of the covariates needed for pharmacokinetic-pharmacodynamic analyses can be found in the NHANES database. However, this database is a random sample of the US population irrespective of age and comprises a “snapshot” set of values. It is not limited to particular disease states. Thus, if the demographics of patients with AML were needed, this database may not be representative of that population because of differences between biochemistry and hematology values in cancer patients and the population in general.

Generating Covariate Probability Density Functions

The NHANES database is a good source upon which to use for generating covariates pdfs. In the tobramycin example, the goal was to simulate the tobramycin pharmacokinetic parameters, which required first assigning CrCL and weight values to each simulated patient. To calculate CrCL, randomly selected values of age, weight, sex, and Scr were needed. The NHANES III database was used for this purpose. The NHANES data that were needed are stored in various datasets, which must be downloaded from the NHANES website. It is a good practice to download the corresponding documentation with variable names and descriptors since the variable names are obscure at times, *e.g.*, DMARETHN corresponds to the variable name for race-ethnicity. Each dataset is stored as a SAS transport file that will have to be converted to a usable format if the analyst’s statistical analysis resources cannot directly read SAS transport files. In this case, SAS for Windows (Version 9.2) was used for the analysis. Fortunately, the NHANES website also has a SAS program that converts the SAS transport file to a usable SAS dataset where each column has the corresponding label identifier.

Table 22.1 Summary statistics for NHANES III database used for modeling and simulating CrCL

	Mean	Std dev	Min	Max
Age (years)	47.5	20.3	18	90
Weight (kg)	71.7	14.3	21.8	130.5
Scr (mg/dL)	1.07	0.24	0.50	3.00

After importing the data, summary statistics were used to characterize each variable. It was decided that only adult subjects 18 years or older with normal weight and Scr would be used in the analysis. Therefore, subjects with body mass index greater than 35 kg/m^2 and subjects with Scr greater than 3 mg/dL or less than 0.5 mg/dL were removed from the database. The dataset had 14,974 observations consisting of 7,682 females (51.3%) and 7,292 males (48.7%) with summary statistics presented in Table 22.1.

In the first step, the dataset was split into a pdf model development dataset consisting of ~90% of the data ($n = 13,503$) with the remainder assigned to be a model validation dataset ($n = 1,471$). Data splitting was done using a random uniform variable; if the variable was ≤ 0.90 the observation was assigned to the model development dataset, otherwise it was assigned to the model validation dataset. In the pdf model development dataset, weight was modeled as a function of sex and age, where sex was coded as “0” for males and “1” for females. A scatter plot of weight as a function of age indicated that a quadratic regression model was required and that males appeared to be generally heavier than females (Fig. 22.2). Robust regression using MM estimation (Yohai 1987) was used to fit the following model to weight since the methodology is not as sensitive to outliers and/or influential data than ordinary least squares methods

$$\text{Weight} = \theta_0 + \theta_1 \text{AGE} + \theta_2 \text{AGE}^2 + \theta_3 \text{SEX} \quad (22.4)$$

Examination of the residuals showed that the residual tails deviated from normality (data not shown) and that the assumption of normality might not be tenable. Hence, the model was refit using the Ln-transformation of Weight

$$\text{Ln}(\text{Weight}) = \theta_0 + \theta_1 \text{AGE} + \theta_2 \text{AGE}^2 + \theta_3 \text{SEX} \quad (22.5)$$

The model parameter estimates are presented in Table 22.2.

Figure 22.3 presents the goodness of fit plots to the model which showed that weight was adequately modeled using age and sex as predictors. When race was included in the model, it was not statistically significant at the 0.01 level (data not shown). Using the model validation dataset, the average prediction error was 1.02 kg with a standard deviation of 18.0 kg; the lower and upper deciles were -21.7 to 24.4 kg .

A predictive check was done to see how well the model predicted weight given sex and age based on a simulation of 10,000 subjects. First, a random value from a uniform (0, 1) distribution was chosen. If the value was less than 0.49, the subject

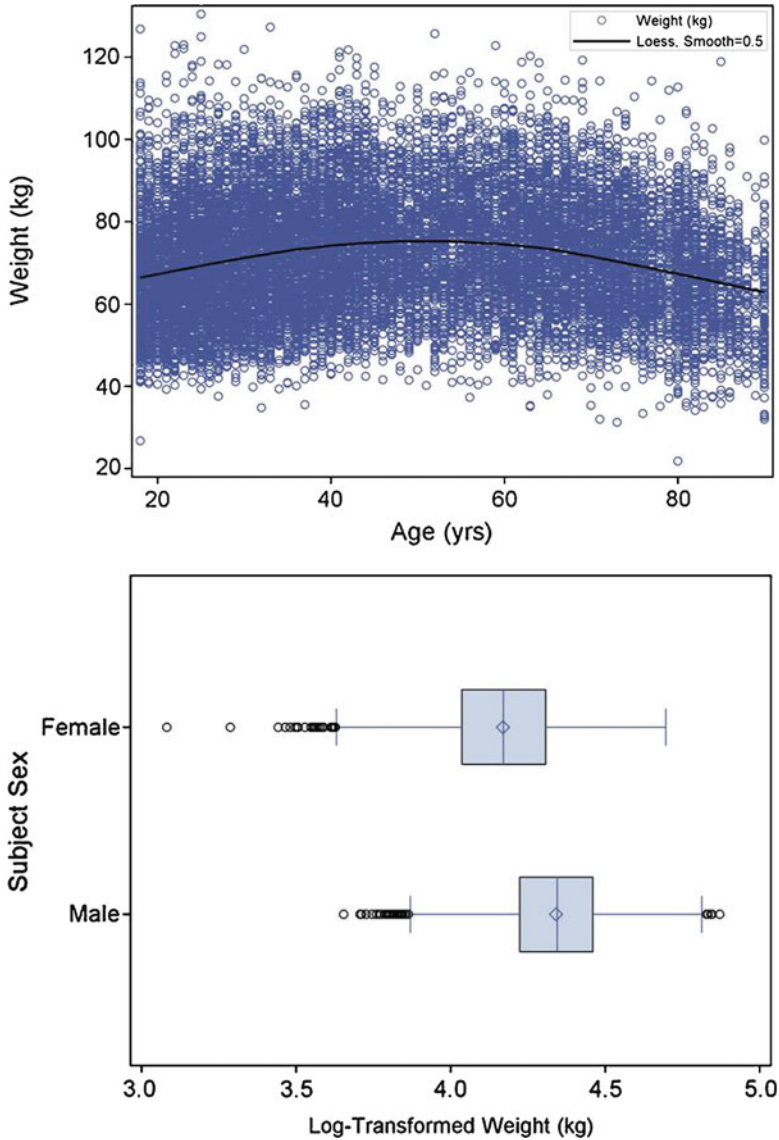


Fig. 22.2 Scatter plot of weight as a function of age in the NHANES III database (*top*) and box and whisker plot of weight as a function of subject sex. *Solid line* in *top* plot is the LOESS smooth using a 0.5 spanning proportion

was assigned to be male; otherwise the subject was assigned to be female. Next, the subject's age was randomly chosen using (22.3) with a lower limit of 18 years and an upper limit of 90 years. Given the subject's age and sex, his/her weight was then simulated using (22.5). The bottom right panel of Fig. 22.3 presents a kernel smoothed histogram of the simulated and observed values. The average simulated

Table 22.2 Model parameter estimates for (22.5)

Parameter	Estimate	Standard error
Intercept (θ_0)	4.025	0.0109
Age (θ_1)	0.0146	4.70×10^{-4}
(Age) ² (θ_2)	-1.452×10^{-4}	4.56×10^{-6}
Sex (θ_3)	-0.169	0.00330
Standard deviation	0.176	

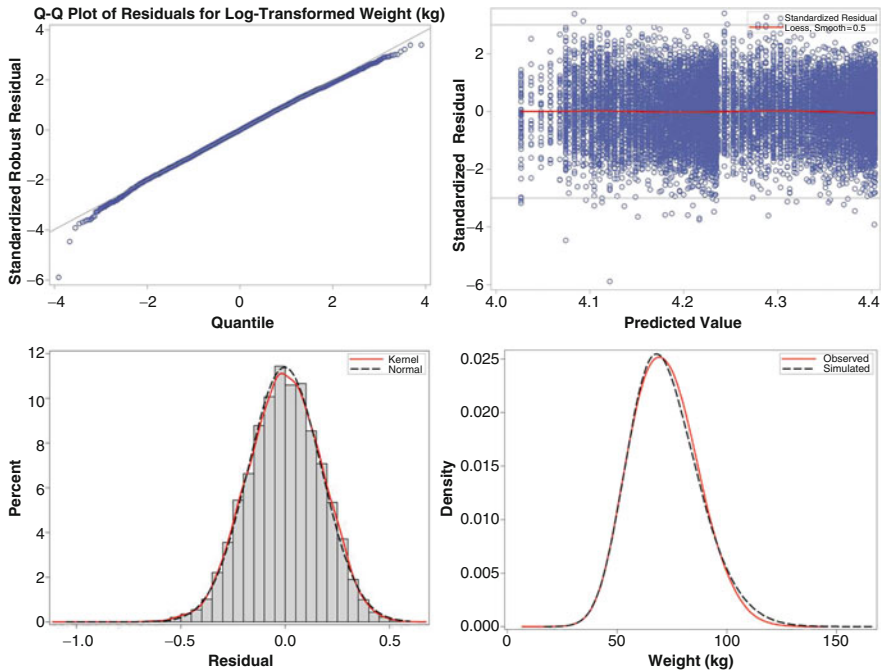


Fig. 22.3 Residual analysis of Ln-transformed weight as a function of age and sex based on (22.5). The *bottom right* plot is a kernel smooth histogram comparing the observed data with the simulated data given the final model in (22.6)

weight was 72.1 kg with upper and lower deciles of 54.2 and 92.0 kg, which was comparable with the observed mean weight of 71.7 kg and upper and lower deciles of 53.7 and 90.6 kg, respectively. Based on the results of the predictive check and residual analysis, the model was deemed credible.

A model for Scr was next developed as a function of age, weight, and sex. The same methodology was employed. The distribution of Scr values was right-skewed, so a log-transformation was used to make the data more close to a normal distribution (Fig. 22.4). Age and weight appeared to be slightly curvilinear with regards to Ln-transformed Scr and males tended to have higher Scr values than females

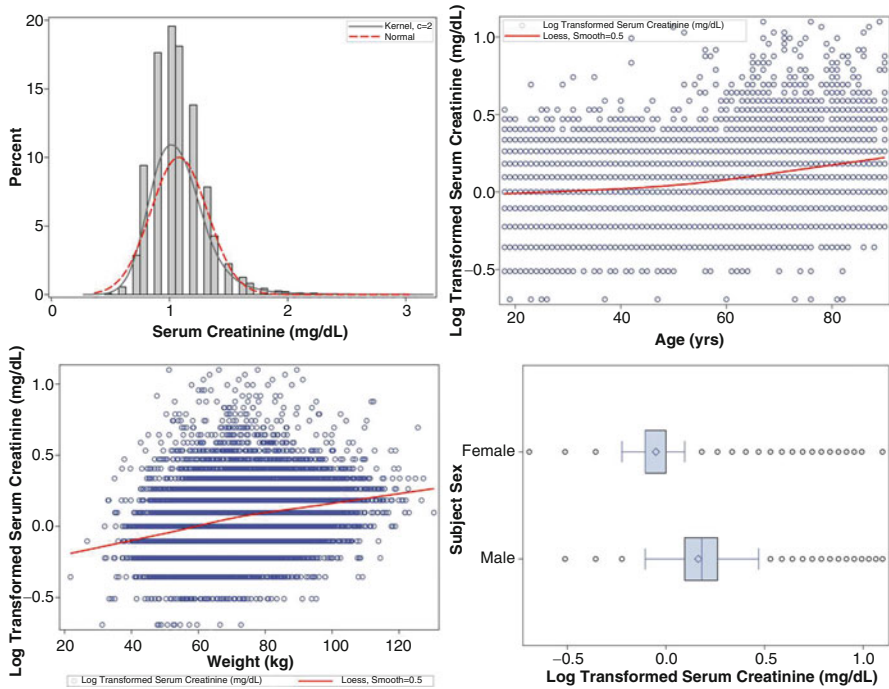


Fig. 22.4 Descriptive plots of Scr (*top left*) and Ln-transformed Scr as a function of AGE (*top right*), WEIGHT (*bottom left*), and SEX (*bottom right*)

(Fig. 22.4). Robust regression using MM estimation was used to estimate the following model to the Ln-transformed Scr data

$$\begin{aligned}
 Ln(Scr) = & \theta_0 + \theta_1 SEX + \theta_2 WEIGHT + \theta_3 AGE + \theta_4 (WEIGHT)(SEX) \\
 & + \theta_5 (AGE)(SEX) + \theta_6 (WEIGHT)(AGE) + \theta_7 (SEX)(AGE)(WEIGHT) \\
 & + \theta_8 WEIGHT^2 + \theta_9 AGE^2
 \end{aligned}
 \tag{22.6}$$

This model allowed for interactions between age, sex, and weight, and also for age and weight to be incorporated with quadratic terms. Examination of the goodness of fit plots shown in Fig. 22.5 revealed that the residuals were heavy-tailed on both sides of the mean. Thus, the assumption of normality did not appear appropriate in this case. Hence, the same linear model was refit but with the residual variance being modeled as a Student’s *T*-distribution where the degrees of freedom were estimated. The effect of sex was not significantly different than zero based on a *T*-test ($T = 0.57, p = 0.57$). However, when a model contains significant interactions and nonsignificant main effects, it is recommended to keep the main effects in the model (Kirk 1982). Thus, all the terms were kept in the model. The model parameter estimates are presented in Table 22.3.

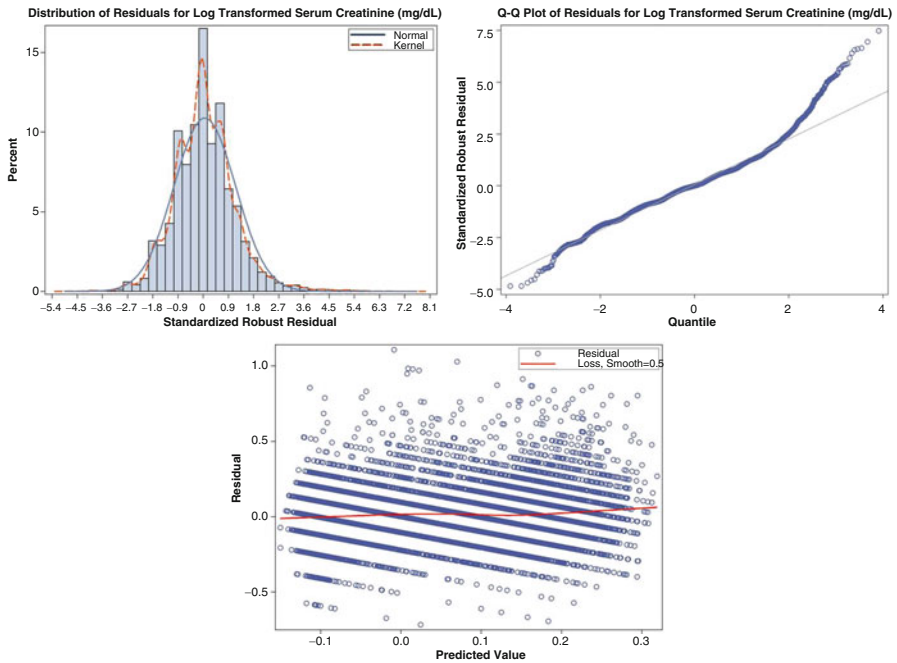


Fig. 22.5 Goodness of fit plots for Ln-transformed Scr as a function of age, weight, and sex using (22.6) with residual variability modeled as a Normal distribution

Table 22.3 Model parameter estimates for (22.6)

Parameter	Estimate	Standard error
Intercept (θ_0)	-0.127	0.0480
Sex (θ_1)	0.0113	0.0378
Weight (θ_2)	0.00544	0.00106
Age (θ_3)	-0.00280	6.79×10^{-4}
Sex \times Weight (θ_4)	-0.00349	5.35×10^{-4}
Sex \times Age (θ_5)	-0.00340	7.32×10^{-4}
Weight \times Age (θ_6)	2.12×10^{-5}	7.15×10^{-6}
Sex \times Weight \times Age (θ_7)	6.22×10^{-5}	1.04×10^{-5}
(Weight) ² (θ_8)	1.57×10^{-5}	6.01×10^{-6}
(Age) ² (θ_9)	6.45×10^{-5}	3.76×10^{-6}
Degrees of freedom	5.56	0.259
Standard deviation	0.0169	3.55×10^{-4}

The goodness of fit plots are shown in Fig. 22.6. Using the model validation dataset, the average prediction error was -0.007 mg/dL with a standard deviation of 0.24 mg/dL; the lower and upper deciles were -0.28 to 0.26 mg/dL.

A predictive check was done to see how well the model predicts Scr given sex, age, and weight based on a simulation of 10,000 subjects. First, a random variate from a uniform distribution was chosen. If the value was less than 0.49 , the subject

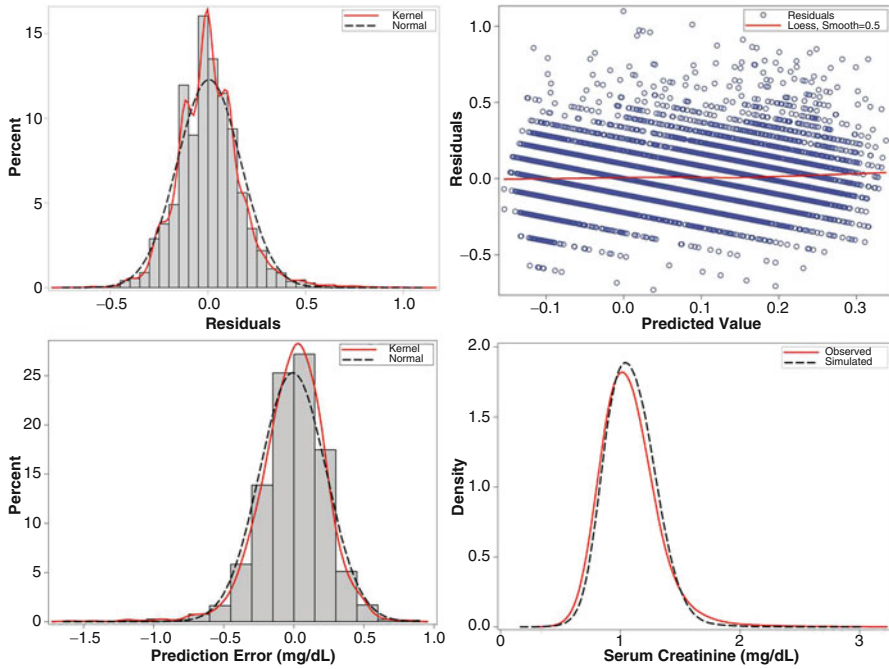


Fig. 22.6 Goodness of fit plots for Ln-transformed Scr as a function of age, weight, and sex using (22.6) with the residual variability modeled using Student’s T -distribution. The *bottom right* plot is a kernel smooth histogram comparing the observed data with the simulated data given the final model in (22.6). Note that QQ plots are unavailable with a Student’s T -distribution

was male; otherwise the subject was female. The subject’s age was then randomly chosen using (22.3) with a lower limit of 18 years and an upper limit of 90 years. Conditional on the subject’s age and sex, weight was then simulated using (22.5). Once his/her sex, age, and weight were simulated, their Scr was calculated using (22.6) with Student’s T -distribution and six degrees of freedom. The bottom right panel of Fig. 22.6 shows a kernel smooth histogram of the observed and simulated data. The average simulated Scr was 1.09 mg/dL with upper and lower deciles of 0.86 and 1.33 mg/dL, which compares to the observed mean of 1.08 mg/dL and upper and lower deciles of 0.80 and 1.40 mg/dL, respectively. Based on the results of the predictive check and residual analysis, the Scr model was deemed acceptable.

Given the models developed for weight and Scr, a simulation can now be developed to calculate individual CrCL values using the Cockcroft-Gault equation (22.2). A histogram of resulting simulated values is shown in Fig. 22.7. The average calculated CrCL was 76 mL/min with lower and upper deciles of 40 and 115 mL/min, which compares to the observed mean of 82 mg/dL and upper and lower deciles of 44 and 118 mL/min, respectively. The average CrCL was lower than the normal mean usually reported as 90 mL/min. However, the age range in this simulation was up to 90 years old and since CrCL decreases with increasing age, it would be expected that in a

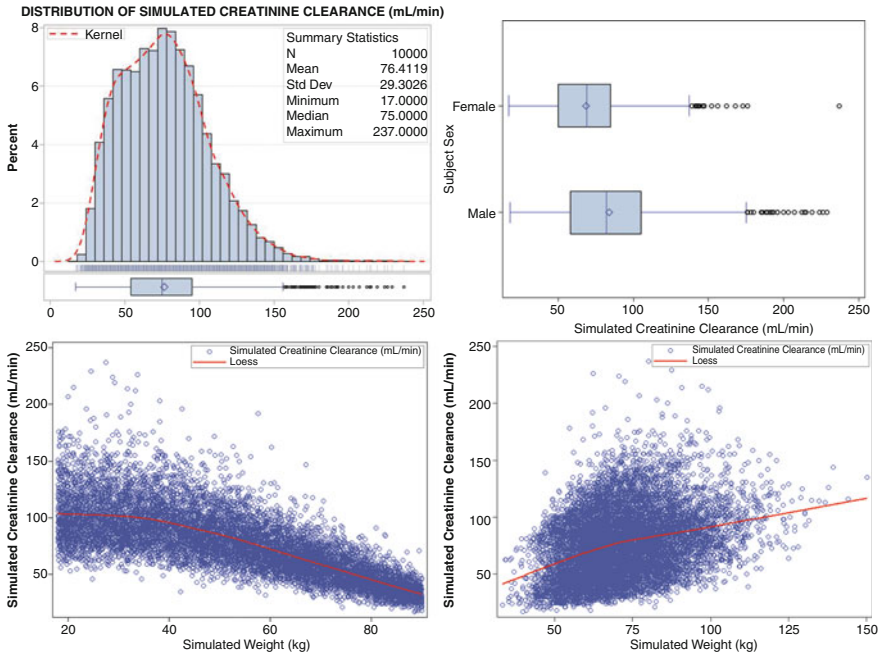


Fig. 22.7 Simulated CrCL values based on 10,000 randomly generated subjects (*upper left*), stratified by sex (*upper right*), and plotted against age (*lower left*) and weight (*lower right*)

simulation with a large proportion of elderly subjects, the average CrCL would be lower than derived from a database comprising mostly younger individuals. Hence, the parametric simulation model for CrCL was accepted.

In summary, the NHANES III database was used to develop a hierarchical model for CrCL based on a subject's sex, age, weight, and Scr. The modeled values for weight and Scr were practically identical to observed values. Calculated CrCL values derived from the sex, age, and weight pdfs were lower than observed values but this can be explained by difference in the ages of subjects in the two groups. Nevertheless, the simulated CrCL values were quite similar to the observed values. This approach can then be used to simulate the population pharmacokinetics of tobramycin.

Generating Laboratory Clinical Values

A second example of the use of the NHANES III database concerns generation of clinical laboratory values. Drug clearance or volume of distribution may be pathophysiologically related to clinical chemistry measurements like AST or ALT when the drug is subject to hepatic metabolism in health and disease. In this case, AST or

ALT database values are needed to generate pdfs for these covariate. The NHANES datasets are cross-sectional data and are not longitudinal, except for the NHANES III. In NHANES III, AST and ALT measurements were made a second time in a nonrandom subsample of $\sim 10\%$ of subjects. The participants in the second query were mainly adults equally split between 20 and 39 years of age and 40 years or older with an equal sex distribution. Lazo *et al.* (2008) used this dataset to show that elevated AST, ALT, and bilirubin concentrations would be reclassified as normal in more than 30% of retested subjects and that alkaline phosphatase and SGPT were more reliable with only 15% being reclassified as normal upon retesting.

With repeated measures data, the total variability in the data can be partitioned into a between-sample component (between-subject variability, BSV) and residual component (within-sample variability, WSV). In the CrCL example, the total variance represented a composite of between-, within-, and residual variability. With the repeated measures data, the residual variance represents residual variability and within-subject variability. In this example, AST activity was analyzed in an effort to find a suitable model to simulate baseline values in adults 18 years and older.

The NHANES III secondary measurement database was merged with the NHANES III primary database and only those subjects 18 years and older with both first and secondary measurements included. A total of 1,250 subjects were available with the average time between the first and second measurement being 17.5 days (range: 1–52 days). Figure 22.8 presents a kernel smooth of the AST values

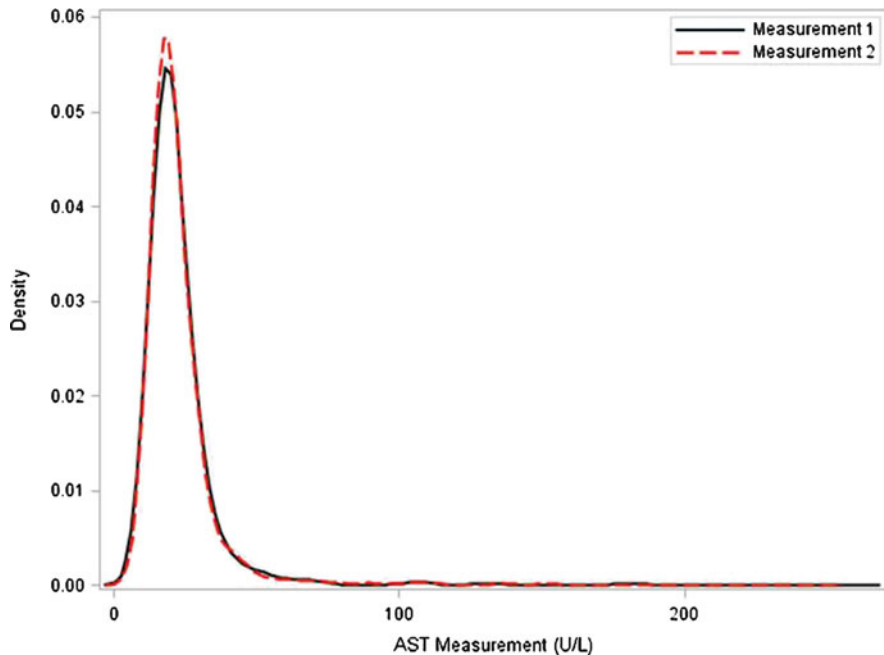


Fig. 22.8 Histogram of AST activity pooled from the time of the first and second measurements

at the time of the first and second measurement. The distribution of AST values for the first and second measurements were quite similar though both were highly skewed. To begin, a linear mixed effects model of the following form was estimated

$$\text{Ln}(AST) = \theta_0 + \theta_1(\text{SEX}) + \theta_2(\text{VISIT}) + \varepsilon \quad (22.7)$$

where VISIT refers to the first or second measurement and the residuals were assumed to be normally distributed. AST does not differ between males and females so sex was not included in the model. The goodness of fit of the residuals showed distinct deviations from normality, as might be surmised from such a highly skewed dataset. Further, a predictive check showed that the simulated values could not reproduce the upper range of AST observations (data not shown).

Next, a mixture model was estimated using the NLMIXED procedure in SAS where

$$\begin{aligned} \text{Ln}(AST) &= \theta_0 + \theta_2(\text{SEX}) + \theta_4(\text{VISIT}) + \varepsilon && \text{if Group 1} \\ \text{Ln}(AST) &= \theta_1 + \theta_2(\text{SEX}) + \theta_4(\text{VISIT}) + \theta_3\varepsilon && \text{if Group 2} \end{aligned} \quad (22.8)$$

In this model, subjects were assigned to Group 1 or Group 2 with probability p and each group was allowed to have a different mean and variance. Essentially what the model does is to test whether a better fit is obtained for each patient if they were Group 1 or Group 2. The visit effect (whether it was the first or second measurement) under this model was not statistically significant and the reduced model ($\theta_4 = 0$) was refit. With the reduced model, all parameters were precisely estimated with coefficients of variation $<50\%$ for all parameters (Table 22.4).

The residuals appeared to be normally distributed with no clear trends in the residual vs. predicted values (data not shown). Hence, a mixture model appeared to be a more appropriate model than a normal distribution. The model was then used to simulate results for 10,000 subjects. A kernel smooth to the simulated and observed data are shown in Fig. 22.9. A comparison of the simulated and observed summary statistics showed that the mean values were similar (23 U/L for the observed data and 22 U/L for the simulated data). Further, the ranges were similar (8–257 U/L for

Table 22.4 Model parameter estimates for (22.8)

Parameter	Estimate	Standard error
θ_0	3.072	0.0111
θ_1	3.459	0.0406
θ_2	-0.178	0.0154
θ_3	2.145	0.0944
Proportion in Group 1	0.897	0.0137
CV% BSV in Group 1	25.2	0.825
CV% BSV in Group 2	57.2	1.856
Residual variability %	12.7	0.317

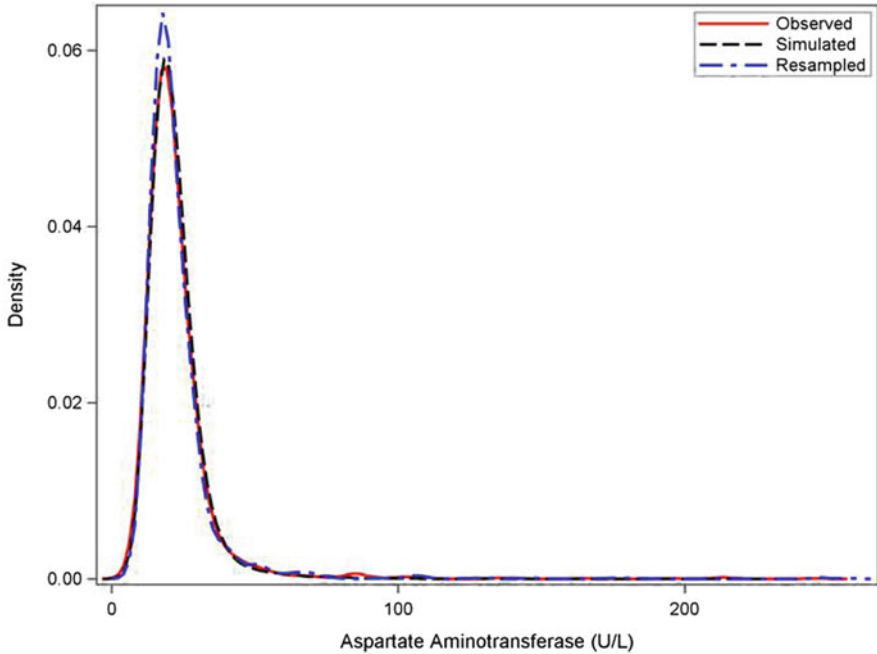


Fig. 22.9 Kernel smooth of simulated, resampled, and observed (*solid line*) AST values at baseline. Simulated values (*dashed line*) were generated from 10,000 simulated subjects. Resampled values (*dash-dot line*) were generated from 10,000 subjects

the observed data and 5–218 for the simulated data). The lower and upper deciles were even closer (14–32 U/L for the observed data and 14–31 U/L for the simulated data). Hence, given this model, an analyst can simulate baseline AST data in a random adult population.

The AST dataset was challenging to model because of the extreme skewness in the distribution. Luckily a parametric mixture model could be found to adequately describe the data. But suppose a parametric model could not be found, how then does one simulate the appropriate covariate distribution? One method is to resample from observed data using a random sampling with replacement approach. Figure 22.9 also shows the distribution from 10,000 resampled subjects compared to the simulated and observed distributions. The results are indistinguishable. The advantage of the resampling method is ease of programming. There is no modeling involved so the simulated values are easily obtained. Also, the dataset can be conditioned to obtain resample in certain subpopulations. For instance, Fig. 22.10 presents a kernel smooth of males 65 years and older whose ALT was normal (<33 U/L). The resampled data was indistinguishable from the observed data. The down-side to this method is that it requires a dataset of fairly large size such that the resampling does not result in multiple copies of the same observation.

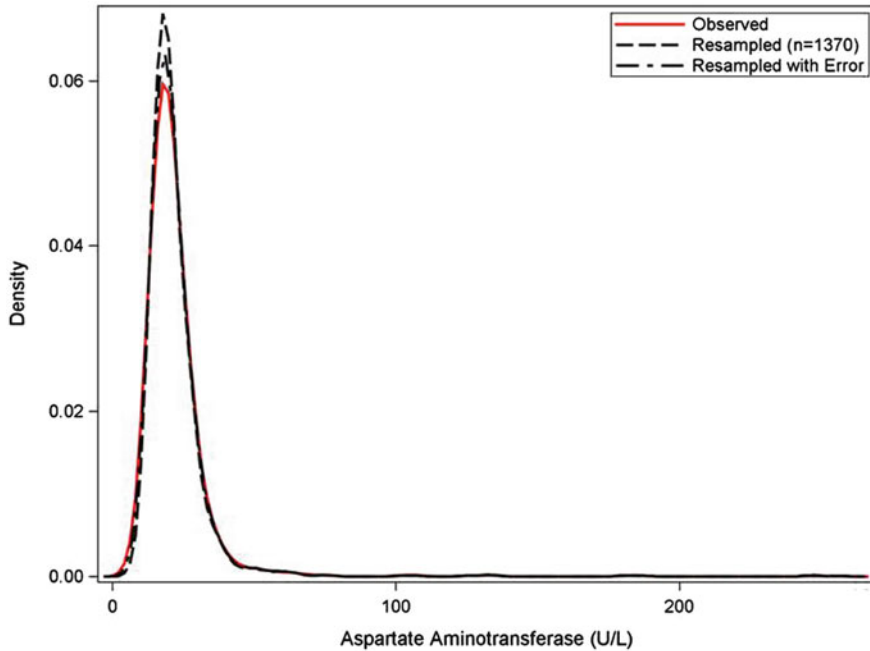


Fig. 22.10 Kernel smooth of resampled and observed AST values at baseline in males 65 years and older with normal ALT values (<33 U/L). Observed values (*solid line*) were based on 1,370 subjects. Resampled values (*dashed line*) and resampled with error (*dashed-dot line*) were generated from 10,000 subjects

A modification to the resampling method is to add some small degree of random error to the resampled values so that if the dataset being resampled is relatively small there won't be a large degree of copying the same values. So, if the resampled value were X , then $X^* = X + s$, where s is a normally distributed random variable with mean 0 and variance σ^2 . Figure 22.10 shows the resampled values when a normally distributed random error term was added with a standard deviation of 4 U/L. Again, the resampled values with error were indistinguishable from the observed data. The problem with this method is that if the random error term variance is too large then the resampled values might not approximate the observed data well, so some degree of fine-tuning may be needed on the variance estimate.

22.3 Future Perspectives

There is current debate in the literature about transparency of data. How much data should be made available after a study is completed? Pharmaceutical companies argue that data should be proprietary to maintain the intellectual property. But is it really necessary to keep placebo data or comparator data away from other

investigators that might find it useful? Right now there are some external data available to the public for building covariate distribution models, but not a lot. All of it seems to be from the United States; Japan, China, the European Union, none of them make data from their studies available. It can be expected though that as more data become available models for covariates will become available and be portable from study to study much like the current effort to develop disease progression models.

There is an effort in the pharmacometrics field to develop public-access, open-source disease progression models (see www.opendiseasemodels.org, accessed May 2010). The underlying hypothesis for this program is that these models, being open-source, will help facilitate their acceptance and increase their utilization. These same efforts should be applied for covariate distribution models. If someone needs to simulate the weight for a subject in some age range, the model used should not be dependent on the company where that person is employed. These models should be portable and applicable universally. It is hoped that these same organizations will expand their charters to include covariate distribution models.

In summary, covariate distribution models are just as important for simulation purposes as are pharmacokinetic-pharmacodynamic models. A poorly defined covariate distribution can invalidate the results from a simulation. Modelers cannot simply input a range of covariates and expect to achieve simulation results that are robust, representative, and reliable. Time and effort must be spent in developing and validating these models. Only then can the results from a simulation be confidently trusted.

Acknowledgments The author would like to thank Steve Weller at GlaxoSmithKline for his thoughtful comments.

References

- Aarons L, Vozeh S, Wenk M, Weiss P, Follath F (1989) Population pharmacokinetics of tobramycin. *Br J Clin Pharmacol* **38**:305–314
- Bonate PL (2006) *Pharmacokinetic-pharmacodynamic modeling and simulation*. Springer, New York
- Chien JY, Friedrich S, Heathman M, de Alwis DP, Sinha V (2005) Pharmacokinetics/pharmacodynamics and the stages of development: role of modeling and simulation. *AAPS J* **7**:E544–E559
- Cockcroft DW, Gault MH (1976) Prediction of creatinine clearance from serum creatinine. *Nephron* **16**:31–41
- Holford NHG, Kimko HC, Monteleone JPR, Peck CC (2000) Simulation of clinical trials. *Annu Rev Pharmacol Toxicol* **40**:209–234
- Kirk RE (1982) *Experimental design: procedures for the behavioral sciences*. Brooks/Cole Publishing Company, Belmont
- Lazo M, Selvin E, Clark JM (2008) Clinical implications of short-term variability in liver function test results. *Ann Intern Med* **148**:348–352

- Lowe PJ, Tannenbaum S, Gautier A, Jimenez P (2009) Relationship between omalizumab pharmacokinetics, IgE pharmacodynamics, and symptoms in patients with severe allergic (IgE-mediated) asthma. *Br J Clin Pharmacol* **68**:61–76
- Metropolis N (1987) The beginning of the Monte Carlo method. *Los Alamos Sci* **12**:125–130
- Savage S (2009) *The flaw of averages*. Wiley, New York
- U.S. Department of Health and Human Services, Center for Disease Control and Prevention, National Center for Health Statistics (2007) *National health and nutrition examination survey, 2007–2008*. http://www.cdc.gov/nchs/data/nhanes/nhanes_07_08/overviewbrochure_0708.pdf. Accessed May 2010
- Yohai VJ (1987) High breakdown point and high efficiency robust estimates for regression. *Ann Statist* **16**:642–656

Index

A

- ACE. *See* Angiotensin-converting enzyme
- ACE inhibitors (ACEI), 217, 460
- α 1-Acid glycoprotein (AAG), 302
- Adaptive designs (AD)
 - confirmatory studies
 - AD, 118–119
 - enrichment designs, 121–122
 - group sequential designs, 117–118
 - practical considerations, 122–123
 - sample size re-estimation, 119–120
 - treatment selection, 120–121
 - type I error rate, 117
 - definition, 109
 - dose escalation, 110
 - features, 110
 - learn phase
 - ADR approaches, 116
 - aMCP-Mod, 114
 - DcoD, 114
 - dose selection and response, 111–113
 - GADA, 113–114
 - IntR, 115
 - MULTOB, 115
 - t*-test adaptation, 115–116
 - U.S. FDA and EMEA, 111
 - simulation programs, 110–111
 - toolbox strategy, 128
 - and trial simulations
 - ADR approaches comparison, 124–127
 - operating characteristics, 123–124
- Adaptive dose-ranging (ADR) methods
 - aMCP-Mod, 114
 - DcoD, 114
 - GADA, 113–114
 - IntR, 115
 - MULTOB, 115
 - t*-test adaptation, 115–116
- Adaptive multiple comparison procedure-modeling (aMCP-Mod), 114
- Adaptive trial designs. *See* Adaptive designs (AD)
- Angiotensin-converting enzyme (ACE), 216, 460, 473, 479
- Anticancer therapeutic intervention strategy, 282, 283
- Anti-HIV inhibitors, 233
- Antihypertensive agents
 - modeling and simulation, 218–220
 - pharmacology, 216–218
- Antihypertensive therapies, 475–477
- Anti-inflammatory drug development
 - FDA's Critical Path Report, 150–151
 - information, knowledge, understanding, and wisdom paradigm, 154, 155
 - learn-confirm-learn process
 - noise ratio, 152
 - nonclinical to clinical development, 152
 - response surface, 151–152
 - scientific tools, 152–153
 - leveraging pharmacometrics
 - drug actions, 154–155
 - drug concentration *vs.* time, 157
 - FTIH study (*see* First-time in human (FTIH) study)
 - NDA reviews, 155–156
 - nonclinical information–knowledge translation, 157–158
- model-based approach
 - PGDD, 153
 - pharmacometric knowledge integration, 153–154
 - new chemical entities (NCEs), 150
- Antimicrobial chemotherapy
 - antiinfective therapies, 253
 - antimicrobial-resistant pathogens, 252

- Antimicrobial chemotherapy (*cont.*)
 bench-to-bedside piece-wise knowledge integration, 266–268
 clinical application
 biomarker, 268
 CART analysis, 273
 dichotomous clinical outcomes, 268
 dose recommendation decisions, 272
 logistic regression analysis, 270
 Monte Carlo simulation, 271, 272
 PK/PD indices, 268–270
 defensive and offensive approach, 251
 human evolution, 253
 microbiota, 253
 PK/PD model
 advantage, 255
 antimicrobial drug combinations, 262–264
 concentration vs. effect curves, 260–261
 Hill model, 261–262
 host defense submodel, 265–266
 in vivo thigh model, 264
 minimum inhibitory concentration (MIC), 257–258
 pharmaco-microbiological principles, 255–256
 resistance submodel, 265
 time-kill studies, 258–260
streptococcus pneumoniae, 252
- Antithrombus therapy
 anticoagulant agents
 modeling and simulation, 207–209
 pharmacology, 205–206
 thrombus formation, 204–205
- Aranesp[®] (darbepoetin alfa)
 anemia treatment, 318
 dosing schemes, 317
 maturation-structured cytokinetic model, 316
 mechanistic PK/PD model, 319
 pediatric subjects, 321, 324
 visual predictive check (VPC), 322
- Argatroban Injection[®] (argatroban), 50
 Atorvastatin, 330
- B**
- Best Pharmaceuticals for Children Act (BPCA), 405
 Between-subject variability (BSV), 81, 325, 525
 Bivariate normal distributions, 66–73
 Blood pressure (BP) regulation. *See also* Renin-angiotensin system (RAS)
 arterial pressure modulation, 467–469
 epidemiology and pathophysiology, 467
 GC model, 469
 Guyton/Karaaslan models, 469
 Bridion (sugammadex), 32. *See also* Celsentri (maraviroc); Keppra (levetiracetam)
- C**
- Canadian Neurological Scale (CNS), 209
 Cardiopulmonary bypass (CPB), 428
 Cardiovascular pharmacology
 adaptive dosing simulation techniques
 dosage limitations, 223
 pharmacokinetic/pharmacodynamic model, 221
 visual predictive check, 222, 223
 antithrombus therapy
 anticoagulant agents, 205–209
 thrombus formation, 204–205
 hypercholesterolemia
 characterization, 199–200
 cholesterol lowering agents, 201–204
 statin effects, 200–201
 hypertension
 antihypertensive agents, 216–220
 risk factors, 216
 stroke
 clinical trials, 209–210
 disease progression models, 210–214
 longitudinal model, nonmonotonic stroke scale data, 214–216
- Celebrex[®] (celecoxib), 50
 Celsentri (maraviroc), 31. *See also* Bridion (sugammadex); Keppra (levetiracetam)
- Classification and regression tree (CART) analysis, 273
- Clinical Utility IndexSM (CUISM)
 basic elicitation steps, 105
 Bayesian methods, 103
 conjoint analysis, 105–106
 construction and function
 attributes independency, 93
 basic linear formula, 91–92
 elicitation process, 92
 integrated CUI construction, 90–91
 Monte Carlo simulation, 91
 swing-weighting method, 92–93
 decision context setting
 decision-maker(s) perspective, 90
 go/no-go decisions, 89–90
 high-quality decision, 89
 dopahexadine (*see* Dopahexadine)

- Francis Anscombe's approach, 103
- index estimation, 88
- multiattribute decisions, 87
- multiplicative functions, 103–104
- publications
 - animal toxicity, 101
 - calcium channels comparison, 102
 - human efficacy and toxicity, 101
 - Korsan's publication, 101–102
 - multiattribute utility function, 100–101
- utility calculation
 - Effect 1, 93–95
 - Monte Carlo simulation, 94–96
 - single drug dose vs. comparator, 93, 94
- utility concept illustration, 87, 88
- CNS. *See* Canadian Neurological Scale
- Cockcroft-Gault equation, 523
- Combined D-and C-optimality (DcoD), 114
- Contract research organizations (CROs), 407
- Controlled ovarian stimulation (COS), 133–134
- Corifollitropin alfa
 - COS, 133–134
 - development program, 134–136
 - dose-response studies
 - aims, 136
 - development program, 135, 136
 - model framework, 136–137
 - NOoc, 139–140
 - probability of success, 138, 139
 - regression models, 137–138
 - simulations, 138, 139
 - dose selection
 - body weight, impact, 142–143
 - cancelation rate, 143, 144
 - drug exposure and NOoc, 143, 144
 - inhibin-B levels, 140–142
 - model framework, 140, 141
 - PK model, 142
 - regression models, 142
- COS. *See* Controlled ovarian stimulation
- Covariate distribution models
 - CrCL calculation, 512
 - demographic characteristics, 514–515
 - Flaw of Averages, 511
 - input–output model, 510
 - internal databases, 513–514
 - Monte Carlo simulation, 514
 - NHANES (*see* National Health and Nutrition Examination Survey (NHANES))
 - NIH databases, 515–516
 - parameter estimation, 510–511
 - pharmacokinetic-pharmacodynamic models, 529
 - placebo data/comparator data, 528–529
 - tobramycin β -half-life, 511
- Creatinine clearance (CrCL), 510–512, 524
- CTS and quantitative pharmacology
 - dose-response relationship, 1
 - in drug development, 7–8
 - EMA and FDA, 3–5
 - protocol deviation, 5
 - technical definition, 2
 - variable adherence, 5–7
 - virtual trial subjects, information sources, 2
- Cytochrome P450 (CYP) enzymes, 201, 496
- Cytokinetics
 - cell lifespan
 - erythrocytes, 382
 - PK-PD modeling, 382, 383
 - platelets, 383
 - cell proliferation and maturation, 384
- D**
- Data use certification (DUC), 516
- DcoD. *See* Combined D-and C-optimality
- Decision-making, drug development
 - Clinical Utility IndexSM (CUISM)
 - basic elicitation steps, 105
 - Bayesian methods, 103
 - conjoint analysis, 105–106
 - construction and function (*see* Clinical Utility IndexSM (CUISM))
 - decision context setting
 - decision-maker(s) perspective, 90
 - go/no-go decisions, 89–90
 - high-quality decision, 89
 - dopahexadine (*see* Dopahexadine)
 - Francis Anscombe's approach, 103
 - index estimation, 88
 - multiattribute decisions, 87
 - multiplicative functions, 103–104
 - publications (*see* Clinical Utility IndexSM (CUISM))
 - utility calculation
 - Effect 1, 93–95
 - Monte Carlo simulation, 94–96
 - single drug dose vs. comparator, 93, 94
 - utility concept illustration, 87, 88
 - model-based framework
 - diagnostic tests, 62
 - dose-response evaluation, 73–74
 - joint model, 81

- learning and confirming questions, 62
 - model-based framework, 63, 78–80
 - notation and terminology
 - Δ estimation, 63–64
 - PTV and $P(\text{Correct})$, 65, 66
 - target value (TV), 64
 - trial data, 64–65
 - truth vs. trial, 65
 - oncology, 303
 - operating characteristics, decision
 - criteria (*see* Model-based drug development framework)
 - predictive models, 80–81
 - Deep hypothermic circulatory arrest (DHCA), 428
 - Deep vein thrombosis (DVT), 422
 - DHCA. *See* Deep hypothermic circulatory arrest
 - Diabetes mellitus
 - biomarkers, 178
 - definition, 176
 - experimental techniques, 178–180
 - insulin, 176, 177
 - treatment option and drug class, 177
 - types, 176
 - Direct renin inhibitors (DRIs), 468, 476, 477
 - Disease process and progression models
 - cascading turnover models
 - β -cell function, 451
 - FPG and FSI, 451–452
 - Frey model, 452
 - glucose-insulin homeostasis, 450
 - descriptive models
 - drug treatment, 445
 - Frey model, 447
 - linearly progressing diseases, 446
 - symptomatic treatments, 445
 - drug and biological system, 447
 - systems pharmacology
 - bone homeostasis model, 454–455
 - physiological properties, 453
 - turnover models
 - Parkinson's disease, 448–449
 - symptomatic and disease-independent treatment, 449–450
 - synthesis/elimination processes, 448
 - Dispersion model, 495
 - Dopahexadine. *See also* Clinical Utility IndexSM (CUISM)
 - CUI attributes, 96, 97
 - efficacy, 96
 - literature data, 98
 - outcomes to utility translation, 97
 - predictive regression models, 98, 99
 - reformulation, 98–100
 - DRIs. *See* Direct renin inhibitors
 - Drug-disease models
 - benefit-risk assessments, 195
 - biologically based mathematical models, 187
 - clinical outcomes, 195
 - clinical trial simulations, 195
 - diabetes mellitus
 - biomarkers, 178
 - definition, 176
 - experimental techniques, 178–180
 - insulin, 176, 177
 - treatment option and drug class, 177
 - types, 176
 - disease progression, 196
 - dosing calculators and guidance tools, 195
 - drug development
 - categories, 187
 - concept and time-course response, 190–192
 - dose response and safety attributes, 192
 - dose selection, 193–194
 - estimating human potency, 189
 - human exposure prediction, 189
 - projecting human doses, 190
 - stage-dependent application, 188–189
 - FPG-HbA1c model, 184–185
 - glucose-insulin regulation, 180–181
 - incorporating disease progression, 185
 - indirect response models, 183–184
 - literature database, 185–187
 - regulatory considerations, 194–195
 - target prioritization, 195
 - time-course models, 181–183
 - DVT. *See* Deep vein thrombosis
- E**
- EMA. *See* European Medicines Agency
 - End-of-Phase 2a (EOP2a) meetings, 41
 - EPS. *See* Extrapyrarnidal symptoms
 - Erythropoietic stimulating agents (ESA)
 - cell production and cell loss, 312
 - dosing interval regimen
 - Aranesp[®] (darbepoetin alfa) (*see* Aranesp[®] (darbepoetin alfa))
 - dose adaptation algorithm, 316
 - dose adjustments, 318
 - hemoglobin concentrations, 319
 - RBC lifespan, 317
 - pediatric study design

- data analysis methods, 321–323
 - drug efficacy, 320
 - intravenous and subcutaneous dosing, 321, 322
 - parametric bootstrap approach, 325
 - population pharmacokinetic parameters, 322–325
 - PK/PD model
 - BFU-E cells, 313
 - human erythropoietin, 312, 313
 - PED, 314, 315
 - population-based interspecies allometric scaling, 313–314
 - risk-benefit assessment, 315
 - UT-7 cells proliferation assays, 314
 - RBC dynamics, 312
 - Etoposide, 294
 - European guideline, pharmacokinetic modeling, 18–24
 - European Medicines Agency (EMA), 3, 404
 - European regulatory bodies. *See also* U.S. Food and Drug Administration
 - applications, 15
 - documentation assessors, 33
 - guidelines
 - advanced techniques, 25
 - dose response and selection, 25
 - European guideline, 17–24
 - ICH and pediatric guidelines, 17
 - model-based drug development, 16
 - modeling documentation
 - Bridion (sugammadex), 32
 - Celsentri (maraviroc), 31
 - Keppra (levetiracetam), 29–31
 - regulatory decisions
 - clinical trial application, 26–27
 - marketing authorization approval, 28–29
 - Pediatric Investigation Plan, 26
 - scientific advice, 27–28
 - regulatory system and procedure, 16
 - short and long term perspectives, 33
 - Swedish Medical Product Agency, 16
 - Exposure-response modeling, 17–24, 27
 - Extensive metabolizers (EM), 210
 - Extracellular water (ECW), 372–373
 - Extrapyramidal symptoms (EPS)
 - disease progression model, 350
 - drug effect, 350
 - incidence prediction
 - exposure-response relationship, 356, 357
 - hazard, 355, 356
 - parameter estimates, 356, 357
 - PK/PD simulation, 357–358
 - plasma concentration, 355–356
 - intramuscular injections, 349
 - maximum likelihood estimation, 351
 - PK/PD-simulation, 351–352
 - population pharmacokinetic model, 349
 - three-parameter logistic model, 351
- F**
- Fasting plasma glucose (FPG), 178, 183, 446, 452
 - FDA. *See* U.S. Food and Drug Administration
 - FDA's Critical Path Opportunities Report, 492
 - FDA's Critical Path Report, 150–151
 - First-order conditional method (FOCE), 422
 - First-time in human (FTIH) study
 - clinical trial simulation vs. clinical outcome, 169–171
 - irreducible population model, 168–169
 - monocyte count, 168
 - nonclinical knowledge, 159–163
 - performance, 162
 - PK and PD data, 159, 162, 164
 - population pharmacokinetic analysis
 - drug concentration vs. time, 164, 165
 - Michaelis–Menten-type function, 164
 - parameter estimation, 166
 - population predicted vs. drug concentration, 164–166
 - response analysis, 167–169
 - TNF α -time data, 167
 - Flaw of Averages, 511
 - FPG. *See* Fasting plasma glucose
 - FPG-HbA1c model, 184–185
- G**
- Gabapentin, 331
 - Gaddum's equation, 314
 - General adaptive dose allocation (GADA), 113–114
 - Generalized anxiety disorder (GAD). *See* PD0332334 (PD334); Pregabalin
 - Gestational diabetes, 176
 - Glucose-insulin regulation, 180–181
 - Glycosylated hemoglobin (HbA1c), 178
 - Guyton/Coleman (GC) model, 469
 - Guyton/Karaaslan models, 469

H

- Haloperidol, 345
- hCG. *See* Human chorionic gonadotropin
- Hepatic drug clearance
 - parallel tube and dispersion model, 494
 - well-stirred model, 494
- Hepatitis C
 - drug efficacy value, 242
 - mechanistic simulations, 244
 - model structure, 242, 243
 - nonlinear mixed effects model, 242
 - pegylated interferon effects, 241
 - physiology of liver, 240
 - ribavirin effects, 241
 - RNA, 240
 - sustained virologic response, 239
 - therapy outcome, 239
 - viral load profiles, 243, 244
- Hill model, 261–262
- Host defense submodel, 265–266
- Human chorionic gonadotropin (hCG), 134, 294
- Human immuno virus (HIV)
 - anti-HIV drug effects, 231
 - anti-HIV inhibitors, 233
 - cell types, 230
 - dose and dosing schedule, 234–237
 - INH, 232
 - model parameters estimation, 237–239
 - PK-PD principles, 234
 - reproductive minimal inhibitory concentration, 233
 - viral load-time profiles, 233
- Hypercholesterolemia
 - characterization, 199–200
 - cholesterol lowering agents
 - clinical trials, 201
 - interarm variability, 204
 - K-PD model, 202
 - LDL time course, 202
 - meta-analysis, 203
 - model-based approach, 202
 - statin effects, 200–201
- Hypertension
 - antihypertensive agents
 - modeling and simulation, 218–220
 - pharmacology, 216–218
 - risk factors, 216

I

- IGF binding proteins (IGFBP), 373
- Indirect response models, 183–184
- Interesting region (IntR) of DR profile, 115

K

- KD₃ concept, 132–133
- Keppra (levetiracetam), 29–31. *See also* Bridion (sugammadex); Celsentri (maraviroc)
- Kidney
 - hypothesis testing and applications, 484
 - model development
 - Ang I and Ang II peptides, 481
 - renal tissue compartment, 481–482
 - renal vasculature, 481
 - parameterization
 - renal tissue compartment, 483
 - renal vascular compartment, 482–483

L

- Lotka-Volterra predator prey models, 228
- Low density lipoprotein (LDL)
 - cholesterol, 199
- Low molecular weight heparin (LMWH), 206, 422–425

M

- MABEL. *See* Minimum anticipated biologic effect level
- Mechanism-based models
 - biological functions, 442, 444
 - clinical trials, 443
 - disease process and progression models
 - cascading turnover models, 450–453
 - descriptive models, 444–447
 - drug and biological system, 447
 - systems pharmacology, 453–455
 - turnover models, 448–450
 - disease processes, 442
 - PKPD modeling
 - biological function deterioration, 442
 - biomarker response, 442–443
 - disease processes and pharmacodynamic effects, 443, 444
 - practical challenges and implementations
 - delayed and washout design, 457, 458
 - drug-related factors, 456
 - optimal design, 455
 - physiology-based disease models, 456
 - placebo treatment, 457
- MI. *See* Myocardial infarction
- Michaelis–Menten approximation, 379–380
- Microsomal protein per gram of liver (MPPGL), 496
- Minimum anticipated biologic effect level (MABEL), 369

- Minimum inhibitory concentration (MIC), 257–258
 - Model-based drug development framework
 - diagnostic tests, 62
 - dose-response evaluation, 73–74
 - joint model, 81
 - learning and confirming questions, 62
 - model-based framework, 63, 78–80
 - notation and terminology
 - Δ estimation, 63–64
 - PTV and $P(\text{Correct})$, 65, 66
 - target value (TV), 64
 - trial data, 64–65
 - truth vs. trial, 65
 - operating characteristics, decision criteria
 - based on dose estimated effect, 77–78
 - based on interval estimates, 70–73
 - based on point estimates, 67–70
 - based on relative potency, 74–75
 - based on relative potency and top dose, 75–77
 - theoretical calculation, 66–67
 - predictive models, 80–81
 - Modeling and simulation (M&S)
 - corifollitropin alfa (*see* Corifollitropin alfa)
 - fit-for-purpose approach, 147
 - interdisciplinary collaboration, 132
 - KD₃ concept, 132–133
 - learn-and-confirm cycles, 145
 - longitudinal modeling, 147
 - optimal synergy, 145, 146
 - Modeling and simulation studies contribution
 - European regulatory agencies
 - applications, 15
 - Bridion (sugammadex), 32
 - Celsentri (maraviroc), 31
 - clinical trial application, 26–27
 - documentation assessors, 33
 - guidelines (*see* European regulatory bodies)
 - Keppra (levetiracetam), 29–31
 - marketing authorization approval, 28–29
 - model-based drug development, 16
 - Pediatric Investigation Plan, 26
 - regulatory system and procedure, 16
 - scientific advice, 27–28
 - short and long term perspectives, 33
 - Swedish Medical Product Agency, 16
 - U.S. FDA
 - approval types, 43–45
 - approved doses, phase 3 trials, 50–52
 - confirmatory evidence, 52, 53
 - drug development and dose optimization, 54
 - model-based primary endpoints, 52, 54
 - pediatric dosing regimen, 48–50
 - pharmacokinetic review, 43–44
 - pharmacometrics (*see* Pharmacometrics)
 - regulatory impact, published cases, 44–48
 - standardization, 55
 - Modified ultrafiltration (MUF), 428
 - Monte Carlo simulation, 91, 94–96, 271, 272, 512
 - Multiple objectives (MULTOB), 115
 - Myocardial infarction (MI), 53, 467
- ## N
- National Health and Nutrition Examination Survey (NHANES)
 - analyses, 517
 - clinical laboratory values generation
 - AST activity, 524–525
 - first and second measurements, 526
 - Kernel smooth, 526, 527
 - residual vs. predicted values, 526
 - covariate pdfs generation
 - Cockcroft-Gault equation, 523
 - CrCL values, 523–524
 - fit plots, 522
 - Ln-transformed Scr data, 520, 521
 - quadratic regression model, 518
 - robust regression, 521
 - SAS program, 517
 - Scr values, 520, 521
 - National Heart Lung and Blood Institute (NHLBI), 516
 - National Institute of Diabetes and Digestive and Kidney Diseases (NIDDK), 516
 - National Institute on Mental Health (NIMH), 516
 - National Institutes of Health (NIH), 405–407, 515–516
 - National Institutes of Health Stroke Scale (NIHSS), 209
 - NDA and BLA submissions, 39
 - Neutral endopeptidase (NEP), 470, 472, 474, 478
 - New chemical entities (NCEs), 150, 152
 - New molecular entities (NMEs), 189, 403
 - NIH. *See* National Institutes of Health

NIHSS. *See* National Institutes of Health Stroke Scale
N-methyl-d-aspartate (NMDA) receptor, 210
 NSCLC disease model, 42–43

O

Obstetrics Pharmacology Research Unit (OPRU), 405
 Office of Generics Drugs (OGD), 5
 Oncology
 AAG, 302
 adverse event modeling and prediction
 hemoglobin dynamics, 299
 myelosuppressive effect, 301
 paclitaxel, 300
 red blood cells (RBC), 300
 risk-benefit ratio, 300
 trabectedin-induced neutropenia, 300, 301
 anticancer therapeutic intervention
 strategy, 282, 283
 antineoplastic agents, 302
 biomarkers *vs.* surrogate endpoints
 capecitabine *vs.* fluorouracil, 292
 etoposide, 294
 hCG, 294
 multivariate logistic models, 293
 second-line treatment strategies, 292
 tumor activity, 291
 tumor growth inhibition (TGI), 292, 293
 cellular kinetics, 282
 differential diagnosis, 303–304
 drug development, 302, 303
 mathematical modeling tool, 281, 282
 translational models
 anticancer drugs, 296
 anticancer treatments, 294
 cell death process, 295
 cMet phosphorylation and HGF receptor, 296, 297
 rituximab, 297
 time efficacy index (TEI), 296
 tumor growth
 angiogenesis and apoptosis, 288
 biological dynamic systems, 284
 cell cycle model, 285, 286
 cell proliferation, 289
 decay, 289–291
 dynamic, stable and unstable system models, 285
 k-stage multilevel Markov model, 288

metastasis, 288
 molecular clock, 287
 proliferative or circular models, 286
 time parameterization, 286

OPRU. *See* Obstetrics Pharmacology Research Unit

P

Paclitaxel, 300
 Paliperidone extended-release (Paliperidone ER)
 dose-response model, 359
 D₂-receptor occupancy
 advantage, 347
 healthy volunteer studies, 348
 plasma concentrations, 347
 population PK-model, 348
 prediction, 348–349
 efficacy and safety prediction, 353–355
 EPS (*see* Extrapyramidal symptoms (EPS))
 population simulations, 359
 rationale, 346–347
 schizophrenia, 345, 346
 Parallel tube model, 495
 Parkinson's disease, 42, 448
 PD0332334 (PD334)
 atorvastatin, 330
 data analysis, 332
 dose response analysis
 efficacy, 333–334
 model selection, 334
 model uncertainty, 334–335
 tolerability, 334
 dose-response curve, 339
 dose selection, 335
 drug development process, 329
 DSM-IV criteria, 336
 efficacy, 336–337
 E_{max} relationship, 342
 gabapentin, 331
 HAM-A dose-response relationships, 339, 340
 lipid-lowering agent, 330
 model validation, 336
 phase 3 study, 341, 342
 prevalence, 330
 somnia *vs.* dose, 339, 340
 therapeutic index (TI), 343
 tolerability, 338–339
 PED. *See* Pharmacological effective dose
 Pediatric dosing regimens, 48–50

- Pediatric Investigation Plan, 26
 - Pediatric Pharmacology Research Units (PPRU), 405
 - Pediatric research and development
 - actinomycin-D and vincristine
 - nonlinear mixed-effects model, 426
 - power-sample size analysis, 427
 - and VCR, 425–426
 - bottom-up approaches, 431
 - clinical pharmacology, 405
 - CTS model
 - components and model elements, 417
 - data hierarchy, 419
 - data repositories, 420
 - PK/PD, 420–421
 - typical workflow, 421
 - disease progression models, 432
 - drug developers, 405
 - exploratory PK/PD trial
 - CPB and MUF, 428, 429
 - drug kinetic model, 428–430
 - TPM, 428
 - WM injury, 427
 - implementation, 404
 - LMWH
 - Box-n-whisker plots, 424
 - clinical trials, 422
 - PK/PD analysis, 424
 - single-point designs, 423–424
 - two-point designs, 423
 - modeling and simulation applications
 - BSA, 410–411
 - common trial designs, 408–410
 - maturation function, 411
 - ontogeny-based functions, 414
 - PBPK models, 415
 - P450 family, 414
 - vs. physiologic model, 411
 - physiologic processes, 416
 - OF value, 413
 - various age indices, 412
 - NIH, 405–407
 - trial design factors, 431–432
 - Pegylated interferon, 241
 - Peripheral vascular disease (PVD), 467
 - Pharmacological effective dose (PED), 314, 315
 - Pharmacometrically-guided drug development (PGDD) program, 153
 - Pharmacometrics
 - division
 - EOP2a meetings, 41
 - knowledge management, 41–42
 - NDA and BLA submissions, 39
 - pediatric trials, 40–41
 - QT studies, 39–40
 - research and policy development, 42–43
 - vision and strategic goals, 38
 - drug development and dose
 - optimization, 54
 - history, 37–38
 - leveraging
 - drug actions, 154–155
 - drug concentration vs. time, 157
 - FTIH study (*see* First-time in human (FTIH) study)
 - NDA reviews, 155–156
 - nonclinical information–knowledge translation, 157–158
 - regulatory decisions
 - approval types, 43–45
 - approved doses, phase 3 trials, 50–52
 - confirmatory evidence, 52, 53
 - model-based primary endpoints, 52, 54
 - pediatric dosing regimen, 48–50
 - pharmacokinetic review, 43, 44
 - regulatory impact, published cases, 44–48
 - standardization, 55
- Physiologically based pharmacokinetic (PBPK) modeling
- applications, 493
 - components, 493
 - drug development, 500–502
 - input parameters
 - factors influencing hepatic clearance, 496–497
 - hepatic drug clearance, 494–495
 - in vitro CL to in vivo CL, 495
 - scaling, 496
 - mechanistic integration, 503
 - model based drug development, 504
 - oral absorption and bioavailability, 499–500
 - tissue distribution
 - plasma volume, 497
 - tissue composition-based approach, 498–499
- PK/PD models
- antimicrobial chemotherapy (*see* Antimicrobial chemotherapy, PK/PD model)
 - EPS-incidence, 355–357
 - EPS-related adverse events, 349–351
 - ESA, 312–315
 - mechanism-based models, 442–444

- PK/PD models (*cont.*)
 protein drugs (*see* Protein drugs, PK/PD models)
- Plasma renin activity (PRA), 471, 472, 477, 479, 485, 486
- Plasma renin concentration (PRC), 485, 486
- PPRU. *See* Pediatric Pharmacology Research Units
- PRA. *See* Plasma renin activity
- Pregabalin. *See also* PD0332334 (PD334)
 E_{\max} relationship, 342
 fixed and random effects, 339
 HAM-A dose–response relationships, 339, 340
 mechanism-of-action, 330
 phase 2 and 3 trials, 332
 somnolence, 334
 therapeutic index (TI), 343
- Product Research and Equity Act (PREA), 405
- Protein drugs
 application, 398
 biotechnology methods, 367
 clinical development model and simulation
 different patient populations, 392–393
 disease covariates, 393–395
 dose–concentration–effect, 391–392
 dosing regimen, 397
 drug–drug interactions, 395–396
 evaluation, 389–390
 fixed dosing vs. body size-based dosing, 396–397
 pharmacological effect, 389
 phase II/III doses, 390–391
 PK–PD models, 390
 rationale provision, 398
- drug discovery
 application, 386
 molecules and protein, 385
 PK–PD modeling, 386–387
- PK/PD models
 absorption and bioavailability, 369–371
 attributes and implications, 367, 368
 bimolecular interaction, 371–372
 biodistribution, 372–374
 cyto kinetics, 381–384
 drug and soluble target interaction, 381
 FcRn, 375
 filgratim and pegfilgrastim, 375–376
 Michaelis–Menten approximation, 379–380
 QSS and RB approximations, 379
 RES, 374–375
 TMDD, 376–379
- preclinical development, 387–388
 target evaluation, 385–387
 target-mediated pathway, 369
- Q**
- Quantitative pharmacology and CTS
 dose–response relationship, 1
 in drug development, 7–8
 EMA and FDA, 3–5
 protocol deviation, 5
 technical definition, 2
 variable adherence, 5–7
 virtual trial subjects, information sources, 2
- Quasi-steady-state (QSS) approximation, 379
- R**
- Rapid binding (RB) approximation, 379
- RAS. *See* Renin angiotensin system
- Regulatory review
 European regulatory bodies
 applications, 15
 Bridion (sugammadex), 32
 Celsentri (maraviroc), 31
 clinical trial application, 26–27
 documentation assessors, 33
 guidelines (*see* European regulatory bodies)
 Keppra (levetiracetam), 29–31
 marketing authorization approval, 28–29
 model-based drug development, 16
 Pediatric Investigation Plan, 26
 regulatory system and procedure, 16
 scientific advice, 27–28
 short and long term perspectives, 33
 Swedish Medical Product Agency, 16
- U.S. Food and Drug Administration
 drug development and dose optimization, 54
 pharmacometrics
 EOP2a meetings, 41
 history, 37–38
 knowledge management, 41–42
 NDA and BLA submissions, 39
 pediatric trials, 40–41
 QT studies, 39–40
 research and policy development, 42–43
 vision and strategic goals, 38
 regulatory decisions
 approval types, 43–45
 approved doses, phase 3 trials, 50–52

- confirmatory evidence, 52, 53
 - model-based primary endpoints, 52, 54
 - pediatric dosing regimen, 48–50
 - pharmacokinetic review, 43, 44
 - regulatory impact, published cases, 44–48
 - standardization, 55
 - Renal sympathetic nerve activity (rSNA), 469
 - Renin angiotensin system (RAS)
 - ACE activity, 479
 - AGT turnover, 479
 - angiotensin peptide infusion, 475–476
 - assumptions, 472–473
 - BP regulation
 - arterial pressure modulation, 467–469
 - epidemiology and pathophysiology, 467
 - GC model, 469
 - Guyton/Karaaslan models, 469–470
 - characteristics, 466
 - clinical populations, 478–479
 - drug development
 - model behavior, 484
 - vs. PRA and PRC, 485–486
 - kidney
 - hypothesis testing and applications, 484
 - model development, 480–482
 - parameterization, 482–483
 - mathematical models, 466
 - model structure
 - AGT synthesis, 471
 - first-order reactions, 470
 - physiological rates and parameters, 472
 - steady-state, 471
 - zeroth-order components, 470
 - physiology model, 487
 - representation and parameterization, 476–477
 - validation, antihypertensive therapies, 477–478
 - virtual patient (VP), 474–475
 - RePharmaCo. *See* Dopahexadine
 - Reproductive minimal inhibitory concentration (RMIC)
 - binary outcomes, 234
 - ECC_{ss}, 235, 236
 - model parameters, 233
 - R₀ value, 234
 - Reticuloendothelial system (RES), 374
 - Ribavirin, 241
 - Risperidone
 - D₂-receptor antagonists, 346–347
 - EPS-related adverse events, 355, 356
 - longitudinal PK/PD model, 359
 - steady-state plasma concentration, 350
 - Rituximab, 297, 298
- S**
- Schizophrenia, 345, 346
 - Spinal muscular atrophy (SMA), 419
 - Streptococcus pneumoniae*, 252
 - Stroke
 - clinical trials, 209–210
 - disease progression models
 - CYP2D6 gene activity, 210, 211
 - NIHSS, 211
 - NMDA receptors, 210
 - pharmacokinetic-pharmacodynamic analysis, 211
 - population pharmacodynamic parameters, 213
 - population pharmacokinetic parameters, 212
 - nonmonotonic stroke scale data, 214–216
 - Swedish Medical Product Agency. *See* European regulatory bodies
 - Sympathetic nervous system (SNS), 469
- T**
- Target-mediated drug disposition (TMDD), 367, 376–379
 - Thromboembolism (TE), 422, 423
 - TMDD. *See* Target-mediated drug disposition
 - Topiramate (TPM), 428–430
 - Trileptal® (oxcarbazepine), 50
 - t*-Test adaptation, 115–116
 - Type 1 diabetes, 177
 - Type 2 diabetes, 177
 - Type 2 diabetes mellitus (T2DM), 446–447, 451
- U**
- U.S. Food and Drug Administration. *See also* European regulatory bodies
 - Critical Path Opportunities Report, 492
 - Critical Path Report, 150–151
 - draft guidance, 111, 123
 - drug development and dose optimization, 54
 - pharmacometrics
 - EOP2a meetings, 41
 - history, 37–38
 - knowledge management, 41–42
 - NDA and BLA submissions, 39

- pediatric trials, 40–41
- QT studies, 39–40
- research and policy development, 42–43
- vision and strategic goals, 38
- regulatory decisions
 - approval types, 43–45
 - approved doses, phase 3 trials, 50–52
 - confirmatory evidence, 52, 53
 - model-based primary endpoints, 52, 54
 - pediatric dosing regimen, 48–50
 - pharmacokinetic review, 43, 44
 - regulatory impact, published cases, 44–48
- standardization, 55

V

- Variable adherence phenomena, 5–7

- Viral dynamic model

- chain reaction, 230

- free virions, 229

- hepatitis C

- drug efficacy value, 242

- mechanistic simulations, 244

- model structure, 242–243

- nonlinear mixed effects model, 242

- pegylated interferon effects, 241

- physiology of liver, 240

- ribavirin effects, 241

- RNA, 240

- sustained virologic response, 239

- therapy outcome, 239

- viral load profiles, 243–244

HIV

- anti-HIV drug effects, 231

- anti-HIV inhibitors, 233

- cell types, 230

- dose and dosing schedule, 234–237

- INH, 232

- model parameters estimation, 237–239

- PK-PD principles, 234

- reproductive minimal inhibitory

- concentration, 233

- viral load-time profiles, 233

- quantitative elements, 228

- Virtual patient (VP), 353, 474–475

- Visual predictive check (VPC), 222, 223

- Vogel water-lick model, 342

W

- Well-stirred model, 494

- Within-sample variability (WSV), 525

Z

- Zosyn[®] (piperacillin/tazobactam), 49